Contrails

Cleared February 1st, 1973
Clearing Authority: Air Force Flight Dynamics Laboratory

PARAMETRIC PERFORMANCE ANALYSIS OF CREW ESCAPE CONCEPTS IN THE VTOL AND CONVENTIONAL TAKE-OFF AND LANDING SITUATIONS

D. W. Brown
D. B. Standish

*** Export controls have been removed ***

This document is subject to special export controls and each transmittal to foreign governments or foreign nationals may be made only with prior approval of the AF Flight Dynamics Laboratory (FDFR), Wright-Patterson AFB, Ohio.

Approved for Public Release

Contrails

FOREWORD

This document is the final report of a parametric performance analysis of four crew escape concepts under Air Force Contract AF33(615)-5332, BPSN 6(631362-62405364) during the period from August 1966 through January 1968. The technical management of this effort was the responsibility of the Air Force Flight Dynamics Laboratory, Air Force Systems Command, Wright-Patterson Air Force Base, Ohio with funds provided by the Life Support Systems Program Office (System 412A), Aeronautical Systems Division, Wright-Patterson Air Force Base, Ohio. The effort was performed by the Los Angeles Division of North American Rockwell Corporation, International Airport, Los Angeles, California. (North American Rockwell Corporation report number NA-67-1053 has been assigned for company internal use only).

Air Force administrators were Mr. Thomas E. Bahan, Contracting Officer; Mr. Frank I. Toth, SEKNA, Buyer; Mr. Marvin C. Whitney, FDFR, Initiator; Mr. Richard J. Dobbek, FDFR, Technical Manager; Mr. James M. Peters, FDFR, Program Director; and Lt. Richard Van Hersett, SEG/SESC, Director of Computations.

North American Rockwell Corporation participating personnel were Mr. James F. Hegenwald, Jr., Crew Station and Escape Systems, Program Manager; Mr. Dean W. Brown, Project Engineer; Mr. David B. Standish, Computer Program Director; Mr. Donald E. Turner, Contracts and Pricing, Contracts Administrator; Mr. Garth Parker, Aerodynamics, Aerodynamic Data Development Director; Mr. Warren Osborn, Mathematician; Mr. James Carey, Mathematician; Mr. Robert A. Maier, Computing Technology, Supervisor; Mr. Roland R. Koehler, Programmer; Mr. Mark J. Killian, Computing Systems Analyst; and Mr. Steven G. Monroe, Programmer.

This manuscript was released by the authors in January 1968 for publication as an AFFDL Technical Report.

This technical report has been reviewed and is approved.

GEORGE A. SOLT, JR.
Chief, Recovery & Crew Station Branch
Vehicle Equipment Division
AF Flight Dynamics Laboratory

Approved for Public Release

Contrails

ABSTRACT

The results of a parametric, performance analysis of four crew escape concepts are described. This analysis embodies investigation of aircraft escape system and aerodynamic factors which influence the performance of crew escape concepts in the low altitude flight regime. A matrix of aircraft performance and maneuver conditions at the instant of emergency was developed from which representative ejection conditions were derived by allowing finite times for man-machine reactions. An existing six-degree-of-freedom computer program was modified to meet the study requirements and to conform to the Wright-Patterson Air Force Base computer and plotting system characteristics. The computer matrix consisted of 3328 ejection variations for each of the four escape concepts: A. Ejection Seat; B. Encapsulated Seat; C. Inset Capsule; and D. Nose Capsule. Of the total of 13,312 basic conditions, 1920 were conducted in three degrees of freedom and the remainder were in six degrees of freedom. The computer output consisted of both graphical and numerical data tapes. The graphical tapes were converted by a Stromberg-Carlson 4020 printer plotter, and FULFLO equipment produced cross plots of 42 output parameters for each six-degree-of-freedom run and 24 for each three-degree-of-freedom run. The numerical data tapes were analyzed by a computer program which determined the safe emergency altitude for each ejection condition and analyzed the effect of the accelerations imposed upon the crewman. A comprehensive investigation of the capabilities and limitations of the four escape concepts when subjected to the matrix ejection conditions was conducted.

This abstract is subject to special export controls and each transmittal to foreign governments or foreign nationals may be made only with the prior approval of the AF Flight Dynamics Laboratory (FDFR), Wright-Patterson AFB, Ohio.

Approved for Public Release

Contrails

Approved for Public Release

Contrails

TABLE OF CONTENTS

Section		Page
I	INTRODUCTION	1
II	PRELIMINARY INVESTIGATION	2
	1. AIRCRAFT FACTORS	2
	2. ESCAPE SYSTEM FACTORS	3
	3. MAN-MACHINE REACTION INTERVALS	19
	4. AERODYNAMIC FACTORS	28
	5. PROGRAM PARAMETERS	28
III	PARAMETRIC COMPUTER PROGRAM	34
	1. COMPUTER PROGRAM	34
	2. PROGRAM OUTPUT	41
IV	SUBROUTINES	45
	1. DIRECTIONAL AUTOMATIC REALIGNMENT OF TRAJECTORY (DART)	45
	2. GYRO-CONTROLLED VERNIER ROCKET STABILIZATION (STAPAC)	47
V	ANALYSIS	52
	1. SAFE EMERGENCY ALTITUDE ANALYSIS METHODS	52
	2. ACCELERATION ANALYSIS METHODS	53
	3. SAFE EMERGENCY ALTITUDE ANALYSIS	74
	4. ACCELERATION ANALYSIS	132
	5. DISCUSSION	143
APPENDIX	SAFE EMERGENCY ALTITUDE CROSS PLOTS	149
REFERENCES		358

Approved for Public Release

Contrails

LIST OF ILLUSTRATIONS

Figure	Title	Page
1	Open Ejection Seat - System A	4
2	Encapsulated Ejection Seat - System B	5
3	Inset Cabin Capsule - System C	7
4	Separable Nose Capsule - System D	8
5	C_DS vs Distance Traveled to Full Open - Drag Parachute - System A	9
6	C_DS vs Distance Traveled to Full Open - Drag Parachute - System C	10
7	C_DS vs Distance Traveled to Full Open - Recovery Parachutes - Systems A and B	11
8	C_DS vs Distance Traveled to Full Open - Recovery Parachute - System C	12
9	C_DS vs Distance Traveled to Full Open - Recovery Parachute - System D	13
10	Center of Gravity Location Versus Rocket Thrust Vector - System A	14
11	Center of Gravity Location Versus Rocket Thrust Vector - System B (Booms Stowed)	15
12	Center of Gravity Location Versus Rocket Thrust Vector - System B (Booms Extended)	16
13	Center of Gravity Location Versus Rocket Thrust Vector - System C	17
14	Center of Gravity Location Versus Rocket Thrust Vector - System D	18
15	System Weight to Crew Weight Ratio Versus CG Movement at 10 G	20
16	Rocket-Catapult Thrust Curves for System A	24
17	Rocket-Catapult Thrust Curves for System B	25
18	Rocket Thrust Curves for System C	26
19	Rocket Thrust Curves for System D	27
20	Man-Machine Reaction Time	29
21	Ejection Matrix for Each Escape Concept	31/32
22	Wind Axis, Stability Axis & Body Axis Reference System	35
23	Body Axis to Earth Axis Reference System	36
24	Parachute Attachment Geometry	42
25	DART System	46
26	Pitching Velocity Versus Time for System A With and Without "DART"	48
27	STAPAC Cutaway View	49
28	Pitching, Rolling and Yawing Velocity Versus Time for System C With and Without "STAPAC"	51
29	Human Reaction to Simple Tumbling - Center of Rotation at Iliac Crest	55
30	Acceleration ($\pm G_X$) Versus Δ Time	56
31	Acceleration ($\pm G_Y$) Versus Δ Time	57
32	Acceleration ($\pm G_Z$) Versus Δ Time	58
33	Point (A) Selection for System A	61
34	Point (A) Selection for System B	62

Approved for Public Release

Contrails

LIST OF ILLUSTRATIONS - Continued

Figure	Title	Page
35	Point (A) Selection for System C	64
36	Point (A) Selection for System D	65
37	"G" Coordinates Versus the Human Body for the Escape Concepts .	67
38	Vector Orientation for Angles Pertaining to Arbitrary Point "G".	68
39	Maximum Rate of Onset Limits - G_Z, G_X Plane	71
40	Maximum Rate of Onset Limits - G_Z, G_Y Plane	72
41	Maximum Rate of Onset Limits - G_Y, G_X Plane	73
42	System A Safe Emergency Altitude Versus α (γ = Zero Deg; q = Zero Deg/Sec; V = Zero KN)	75
43	System B Safe Emergency Altitude Versus α (γ = Zero; q = Zero Deg/Sec; V = Zero KN)	76
44	System C Safe Emergency Altitude Versus α (γ = Zero Deg; q = Zero Deg/Sec; V = Zero KN)	77
45	System D Safe Emergency Altitude Versus α (γ = Zero Deg; q = Zero Deg/Sec; V = Zero KN)	78
46	System A Safe Emergency Altitude Versus α (γ = Zero Deg; p = Zero Deg/Sec; V = Zero KN)	79
47	System B Safe Emergency Altitude Versus ϕ (γ = Zero Deg; p = Zero Deg/Sec; V = Zero KN)	80
48	System C Safe Emergency Altitude Versus ϕ (γ = Zero Deg; p = Zero Deg/Sec; V = Zero KN)	81
49	System D Safe Emergency Altitude Versus ϕ (γ = Zero Deg; p = Zero Deg/Sec; V = Zero KN)	82
50	System A Safe Emergency Altitude Versus α (γ = 10, -10, -30 and -60 Deg; q = Zero Deg/Sec; V = 100 KN)	83
51	System B Safe Emergency Altitude Versus α (γ = 10, -10, -30 and -60 Deg; q = Zero Deg/Sec; V = 100 KN)	84
52	System C Safe Emergency Altitude Versus α (γ = 10, -10, -30 and -60 Deg; q = Zero Deg/Sec; V = 100 KN)	85
53	System D Safe Emergency Altitude Versus α (γ = 10, -10, -30 and -60 Deg; q = Zero Deg/Sec; V = 100 KN)	86
54	System A Safe Emergency Altitude Versus α (γ = Zero Deg; q = Zero, 30 and 90 Deg/Sec; V = 100 KN)	87
55	System B Safe Emergency Altitude Versus α (γ = Zero Deg; q = Zero, 30 and 90 Deg/Sec; V = 100 KN)	88
56	System C Safe Emergency Altitude Versus α (γ = Zero Deg; q = Zero, 30 and 90 Deg/Sec; V = 100 KN)	89
57	System D Safe Emergency Altitude Versus α (γ = Zero Deg; q = Zero, 30 and 90 Deg/Sec; V = 100 KN)	90
58	System A Safe Emergency Altitude Versus γ (α = 15 Deg, q = Zero Deg/Sec; p = 60 Deg/Sec; V = 100 KN)	91
59	System B Safe Emergency Altitude Versus γ (α = 15 Deg, q = Zero Deg/Sec; p = 60 Deg/Sec; V = 100 KN)	92
60	System C Safe Emergency Altitude Versus γ (α = 15 Deg, q = Zero Deg/Sec; p = 60 Deg/Sec; V = 100 KN)	93
61	System D Safe Emergency Altitude Versus γ (α = 15 Deg, q = Zero Deg/Sec; p = 60 Deg/Sec; V = 100 KN)	94

Approved for Public Release

Contrails

LIST OF ILLUSTRATIONS - Continued

Figure	Title	Page
62	System A Safe Emergency Altitude Versus γ (α = -15 Deg; q = 30 Deg/Sec; p = 60 Deg/Sec; V = 100 KN)	95
63	System B Safe Emergency Altitude Versus γ (α = -15 Deg; q = 30 Deg/Sec; p = 60 Deg/Sec; V = 100 KN)	96
64	System C Safe Emergency Altitude Versus γ (α = -15 Deg; q = 30 Deg/Sec; p = 60 Deg/Sec; V = 100 KN)	97
65	System D Safe Emergency Altitude Versus γ (α = -15 Deg; q = 30 Deg/Sec; p = 60 Deg/Sec; V = 100 KN)	98
66	System A Safe Emergency Altitude Versus γ (α = -90 Deg; q = 90 Deg/Sec; p = 180 Deg/Sec; V = 100 KN)	99
67	System B Safe Emergency Altitude Versus γ (α = -90 Deg; q = 90 Deg/Sec; p = 180 Deg/Sec; V = 100 KN)	100
68	System C Safe Emergency Altitude Versus γ (α = -90 Deg; q = 90 Deg/Sec; p = 180 Deg/Sec; V = 100 KN)	101
69	System D Safe Emergency Altitude Versus γ (α = -90 Deg; q = 90 Deg/Sec; p = 180 Deg/Sec; V = 100 KN)	102
70	System A Safe Emergency Altitude Versus γ (ϕ = 90 and 180 Deg; p = 60 and 180 Deg/Sec; V = 100 KN)	103
71	System B Safe Emergency Altitude Versus γ (ϕ = 90 and 18 Deg; p = 60 and 180 Deg/Sec; V = 100 KN)	104
72	System C Safe Emergency Altitude Versus γ (ϕ = 90 and 180 Deg; p = 60 and 180 Deg/Sec; V = 100 KN)	105
73	System D Safe Emergency Altitude Versus γ (ϕ = 90 and 180 Deg; p = 60 and 180 Deg/Sec; V = 100 KN)	106
74	System A Safe Emergency Altitude Versus γ (q = 30 and 90 Deg/Sec; α = 90 and -90 Deg; V = 100 KN).	107
75	System B Safe Emergency Altitude Versus γ (q = 30 and 90 Deg/Sec; α = 90 and -90 Deg; V = 100 KN).	108
76	System C Safe Emergency Altitude Versus γ (q = 30 and 90 Deg/Sec; α = 90 and -90 Deg; V = 100 KN).	109
77	System D Safe Emergency Altitude Versus γ (q = 30 and 90 Deg/Sec/ α = 90 and -90 Deg; V = 100 KN).	110
78	System A Safe Emergency Altitude Versus γ (Ψ = Zero, 15 and 45 Deg; r = Zero and -90 Deg/Sec; V = 100 KN)	112
79	System B Safe Emergency Altitude Versus γ (Ψ = Zero, 15 and 45 Deg; r = Zero and -90 Deg/Sec; V = 100 KN)	113
80	System C Safe Emergency Altitude Versus γ (Ψ = Zero, 15 and 45 Deg; r = Zero and -90 Deg/Sec; V = 100 KN)	114
81	System D Safe Emergency Altitude Versus γ (Ψ = Zero, 15 and 45 Deg; r = Zero and -90 Deg/Sec; V = 100 KN)	115
82	System A Safe Emergency Altitude Versus γ (Ψ = 15 Deg; r = Zero Deg/Sec; V = 100 KN)	116
83	System B Safe Emergency Altitude Versus γ (Ψ = 15 Deg; r = Zero Deg/Sec; V = 100 KN)	117
84	System C Safe Emergency Altitude Versus γ (Ψ = 15 Deg; r = Zero Deg/Sec; V = 100 KN)	118

Approved for Public Release

Contrails

LIST OF ILLUSTRATIONS - Concluded

Figure	Title	Page
85	System D Safe Emergency Altitude Versus γ (ψ = 15 Deg; r = Zero Deg/Sec; V = 100 KN)	119
86	System A Safe Emergency Altitude Versus ϕ (γ = Zero, -10 and -30 Deg; p = Zero Deg/Sec; V = 100 KN)	120
87	System B Safe Emergency Altitude Versus ϕ (γ = Zero, -10 and -30 Deg; p = Zero Deg/Sec; V = 100 KN)	121
88	System C Safe Emergency Altitude Versus ϕ (γ = Zero, -10 and -30 Deg; p = Zero Deg/Sec; V = 100 KN)	122
89	System D Safe Emergency Altitude Versus ϕ (γ = Zero, - 10 and -30 Deg; p = Zero Deg/Sec; V = 100 KN)	123
90	Best Recovery Height vs Aircraft Condition for Total Matrix	124
91	Best Recovery Height vs Aircraft Condition for Total Matrix (V = 100 KN)	125
92	Safe Emergency Altitude Versus System (γ = Zero Deg; V = Zero, 100 and 800 KN, Time = 2.4 and 3.2 Seconds)	126
93	Safe Emergency Altitude Versus System (γ = -10 Deg; V = 100 and 800 KN; Time = 2.4 and 3.2 Seconds)	127
94	Safe Emergency Altitude Versus System (γ = -90 Deg; V = 100 KN; Time = 2.4 and 3.2 Seconds)	128
95	Weight Influence on SEA	129
96	Thrust Line Offset Influence on SEA	130
97	Impulse Influence on SEA	131
98	System Comparison of Total Acceleration Versus Velocity (p = Zero Deg/Sec; q = 90 Deg/Sec)	133
99	System Comparison of Total Acceleration Versus Velocity (p = Zero Deg/Sec; q = Zero Deg/Sec)	134
100	System Comparison of Total Acceleration Versus Velocity (p = 180 Deg/Sec; q = 90 Deg/Sec)	135
101	System Comparison of Total Acceleration Versus Velocity (p = 180 Deg/Sec; q = Zero Deg/Sec)	136
102	System A and B Total Phase I Acceleration Versus Velocity (Min Offset, Min and Max Impulse, 10,000 Ft)	137
103	System A and B Total Phase III Acceleration Versus Velocity (Min Offset, Min and Max Impulse, 10,000 Ft)	138
104	System C and D Total Phase III Acceleration Versus Velocity (Min Offset, Min and Max Impulse, 10,000 Ft)	139
105	System A and B Total Phase III Acceleration Versus Velocity (Max Impulse, Min and Max Offset, 10,000 Ft)	140
106	System C and D Total Phase III Acceleration Versus Velocity (Max Impulse, Min and Max Offset, 10,000 Ft)	141

Approved for Public Release

Contrails

LIST OF TABLES

Table	Title	Page
I	Summary of Mass Properties of Escape Systems A and B	.21
II	Summary of Mass Properties of Escape Systems C and D	.22
III	Maximum Values of Impulse, Thrust and "G" For The Four Escape System Concepts.	.23
IV	Computer Program Input Data.	.37
V	Program Output	.43
VI	Point (A) Locating Dimensions.	.66
VII	Acceleration Tolerance Ellipsoids.	.69

Approved for Public Release

Contrails

LIST OF ABBREVIATIONS AND SYMBOLS

A/C	Aircraft
Cat	Catapult
C_D	Coefficient of drag
CG	Center of gravity
℄	Centerline
C_l	Rolling moment coefficient
C_{l_p}	Damping in roll
C_{l_r}	Rolling moment due to yaw velocity
C_L	Coefficient of lift
C_m	Pitching moment coefficient
C_{m_q}	Damping in pitch
C_n	Yaw moment coefficient
C_{n_r}	Damping in yaw
C_{r_p}	Yawing moment due to rolling velocity
C_y	Side force coefficient
DART	Directional Automatic Realignment of Trajectory
Deg	Degrees
D_O	Normal parachute canopy diameter
F	Fahrenheit temperature
FRL	Fuselage Reference Line
FT	Feet
FULFLO	Reproduction process which utilizes the Fulton Processor for film development and the Xerox Copyflo machine for production of enlarged prints on bond or vellum
G	Acceleration due to gravity
Gx	Acceleration by force applied horizontally (+ forward)

Approved for Public Release

Contrails

G_y	Acceleration by force applied laterally (+ rightward)
G_z	Acceleration by force applied vertically (+ upward)
Kip	One thousand pounds
KN	Knots (True unless otherwise specified)
LB	Pounds
M	Mach number
p	Rolling velocity about the X body axis (degrees/second)
q	Pitching velocity about the Y body axis (degrees/second)
r	Yawing velocity about the Z body axis (degrees/second)
S	Drag area ($feet^2$)
SC-4020	Stromberg-Carlson cathode-ray tube plotter
Sec	Seconds
SEA	Safe emergency altitude
S.R.P.N.	Seat reference point - neutral
STAPAC	Gyro - controlled vernier rocket stabilization
V	Velocity (feet per second)
VTOL	Vertical takeoff and landing
X_B, Y_B, Z_B	Body axis
X_W, Y_W, Z_W	Wind axis
X_S, Y_S, Z_S	Stability axis
α	Angle of attack, measured from the X stability axis to the X body axis in the plane of symmetry (degrees)
β	Angle of side slip, measured from the X wind axis to the X stability axis (degrees)
γ	Flight path angle of aircraft; positive for climb (degrees)
θ	Angle between the X body axis and the line of intersection of the horizontal and vertical planes through the X body axis (degrees)

Approved for Public Release

Contrails

Φ	Angle between the Z body axis and the line of intersection of a vertical plane in which Φ is measured and a plane through the YZ body axis (degrees)
Ψ	Angle between the heading reference in the horizontal earth plane and the line of intersection of the horizontal plane and the vertical plane through the X body axis (degrees)

Approved for Public Release

Contrails

Approved for Public Release

Contrails

SECTION I

INTRODUCTION

The most hazardous regime of aircraft performance envelopes has proved to be that associated with low-level flight where velocities range from zero for the VTOL types to high speed for the low-level dash types of aircraft. Escape from an aircraft which encounters an emergency at low altitude becomes increasingly difficult as the attitude of the aircraft deviates from the upright and as sink rates are introduced.

The objective of this program was to determine the effects of adverse flight conditions on the performance of four crew escape concepts during low altitude escape: (A) the open ejection seat; (B) the encapsulated ejection seat; (C) the inset cabin capsule; and (D) the separable nose capsule. Even though the investigation was performed on escape concepts rather than specific systems, the computer program input data were derived from existing designs which have undergone considerable development.

A competitive comparison of the four escape concepts was not a study objective; in fact, a fair comparison is practicable only in the environment of a specific parent aerospace system with given mission, performance, and crew number. Nevertheless, the understanding of certain escape concept characteristics is enhanced by a concurrent knowledge of the relative attributes of dissimilar concepts. In order to present an equitable analysis of the performance of each of the escape configurations, the impulse of the propulsion system of each was adjusted so that all would reach terminal velocity under the full parachute at the same height when ejected at zero altitude - zero speed from an upright level aircraft. Thus the concepts were provided a significant common denominator to assure maximal impartiality.

Although each computer run time duration was less than twice that of the real time required for the ejection, economic considerations dictated that a selective program be devised to yield a maximal amount of data from only 3328 ejection conditions. Consideration of the volume of output data and its utilization in quantitative comparisons indicated the need for application of computerized analysis procedures wherever possible. The output data from the computer program therefore consisted of two IBM tapes, one to produce graphical representations of each of the output parameters via the Stromberg-Carlson 4020 printer plotter and FULFLO process, and the other to contain selected numerical data. A computer program scanned these data to define the safe emergency altitude for each escape concept for each matrix performance point, and to determine whether human tolerance to acceleration was exceeded. The computerized analysis and the graphical output established limitations of the crew escape concepts, associated problems, and areas in which increases in performance may be made.

Approved for Public Release

Contrails

SECTION II

PRELIMINARY INVESTIGATION

An investigation was conducted to determine the influences of various aircraft factors upon the selection, design and effectiveness of crew escape concepts; define the features of and derive aerodynamic data necessary for the analysis of each concept; and determine the flight conditions and escape system variables to be considered.

1. AIRCRAFT FACTORS

The selection of the crew escape configuration is dependent upon the aircraft performance envelope as well as the aircraft design features. The extreme conditions of the envelope generally determine whether the system will be an open or encapsulated escape device, based upon the environmental protection which the crew member must be provided during the escape. The extent of personnel clothing which can be worn by the crew member without degrading operational efficiency, will limit the open escape concept because of post-ejection exposure to great aerodynamic pressure and to the rarefied atmosphere.

The criteria for escape concept selection are established by reference 1 which states that the maximum limits of an open escape concept shall be a velocity of 600 knots and an altitude of 50,000 feet, that high performance aircraft must provide successful egress for the crew members over the entire mission profile of the aircraft, and that for medium performance aircraft, ground level escape capabilities must be offered at the minimum stall speed of the aircraft. No mention of the impact of mission profile on escape design is made regarding essentially low performance aircraft.

Particular emphasis should be applied to flight phases where emergencies may rapidly reach disastrous proportion since the time available for escape, the capability of the system and the size of the crew dictate the selection of either single or multiple escape configurations regardless of the requirement for environmental protection. Unless ejection paths are mechanically divergent, multiplace aircraft are vulnerable because sufficient time must be allowed between the ejections of single place escape units to avoid trajectory convergency among the several jettisoned or ejected components.

Although the mission profile of VTOL aircraft is similar to that of conventional takeoff and landing aircraft, the selection of the escape concept must not be based solely upon the upper limits of performance since the VTOL mode places the aircraft for relatively long periods in an inherently hazardous regime of flight at low speed, low altitude. Failure of the propulsion and/or stability system during the VTOL mode can cause the rapid development of high rates of sink, roll and pitch since the aircraft is dependent upon propulsion units to provide controllable rates of vertical lift and sink.

It cannot be overlooked that even though landing and takeoff modes for conventional aircraft are of considerably less time duration than those of VTOL types, hazardous conditions nevertheless develop rapidly at low altitude.

Approved for Public Release

Contrails

The aircraft's physical characteristics significantly affect the selection, design and utilization of the escape system. On multiplace aircraft the arrangement and numbers of crew stations are influential. Tandem positioning of the crew requires special consideration for sequencing of individual escape units and provisions for protection from the temperatures, pressures and toxic effluent from the escape propulsion devices. Multiplace capsules are affected by seating arrangement because the propulsion system must be located such that the line of thrust passes in close proximity to the center of gravity of the ejected mass. Thus a tandem seating arrangement may require additional aircraft depth to accommodate a rocket beneath the cabin, while a side-by-side arrangement may lend itself to location of the propulsion unit between the crew stations.

The separation direction for escape is dependent not only upon mission profile but upon the location of external features of the aircraft which present physical interference as well as aerodynamic effects upon escape. For VTOL and conventional aircraft, the takeoff and landing situations negate the application of the downward direction as a primary mode. On the other hand the low-altitude low-speed maneuver, control and accident potential characteristics of VTOL aircraft could conceivably justify provisions for alternate separation directions, possibly automatically sensed and initiated. High rates of attitude change during the separation phase of escape increase the hazards presented by the location of aircraft extremities such as wing tips, empennage and other external structure relative to the cockpit.

2. ESCAPE SYSTEM FACTORS

Escape system concepts chosen for this analysis are the open ejection seat (System A), the encapsulated ejection seat (System B), the inset cabin capsule (System C) and the separable nose capsule (System D). Optimized existing system configurations are studied in order to gain maximal advantage of previously developed data. Various features include stability, static and dynamic shifts of CG location, weight and inertia, variable thrust and impulse magnitudes and thrust direction, including variations during rocket burning and the characteristics of the recovery parachute. Since aircraft escape systems in current service are dependent upon the human for activation, man-machine reaction times are also established.

a. System Descriptions

The open ejection seat (A) (figure 1) of this study is typical of supersonic seats which are automatic once the initiation mechanism is manually activated. The configuration incorporates a stabilization parachute deployed at 0.12 seconds and a recovery parachute initiated at 2.0 seconds if below 15,000 feet. The stabilization chute incorporates a 4.4 foot Guide Surface canopy attached to the back of the seat, and the recovery parachute is a standard 28-foot diameter, flat circular.

The encapsulated ejection seat (B) (figure 2) is a compact equivalent of that developed for the XB-70A. The system is fully automatic after

Approved for Public Release

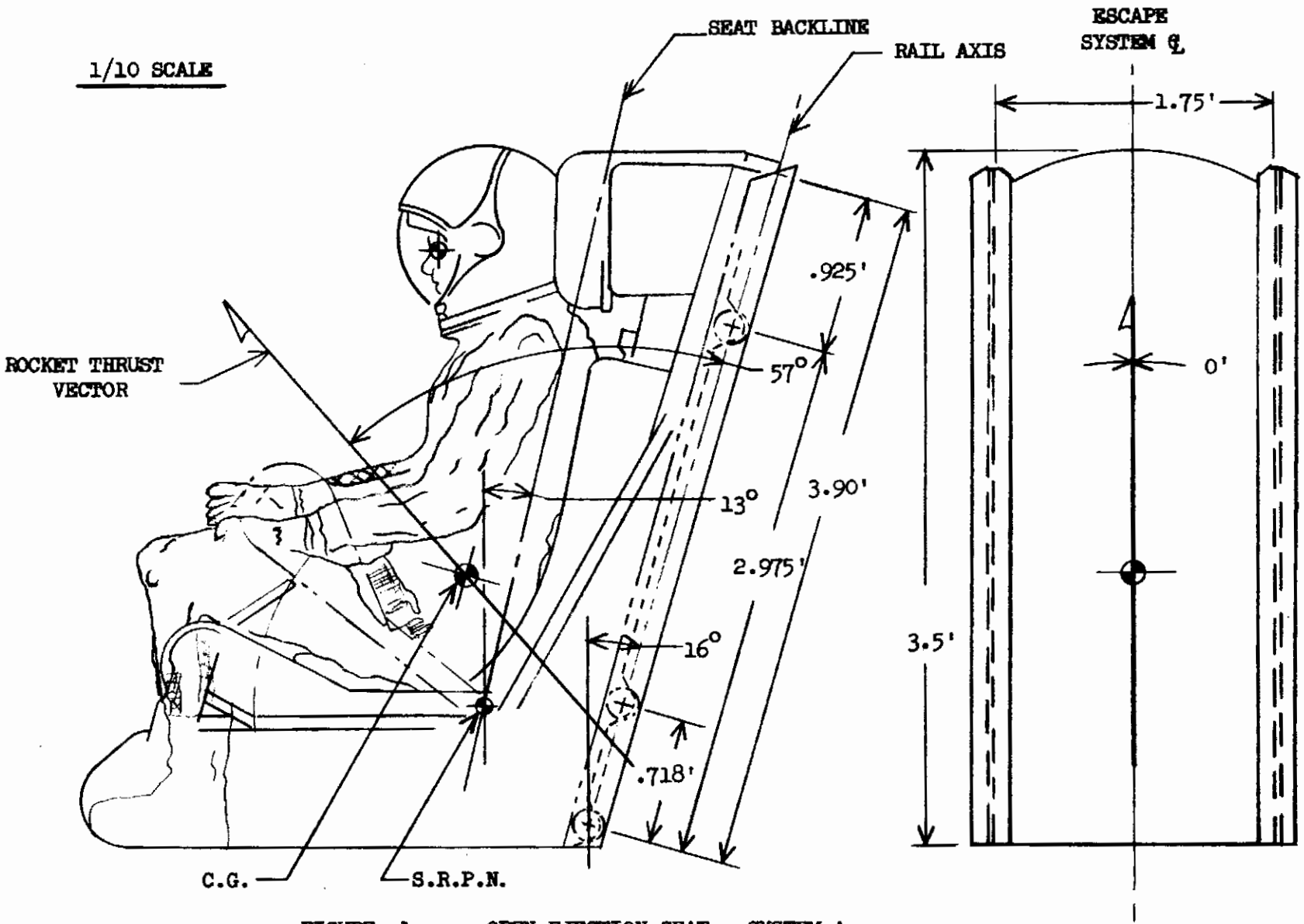

FIGURE 1 - OPEN EJECTION SEAT - SYSTEM A

Approved for Public Release

Contrails

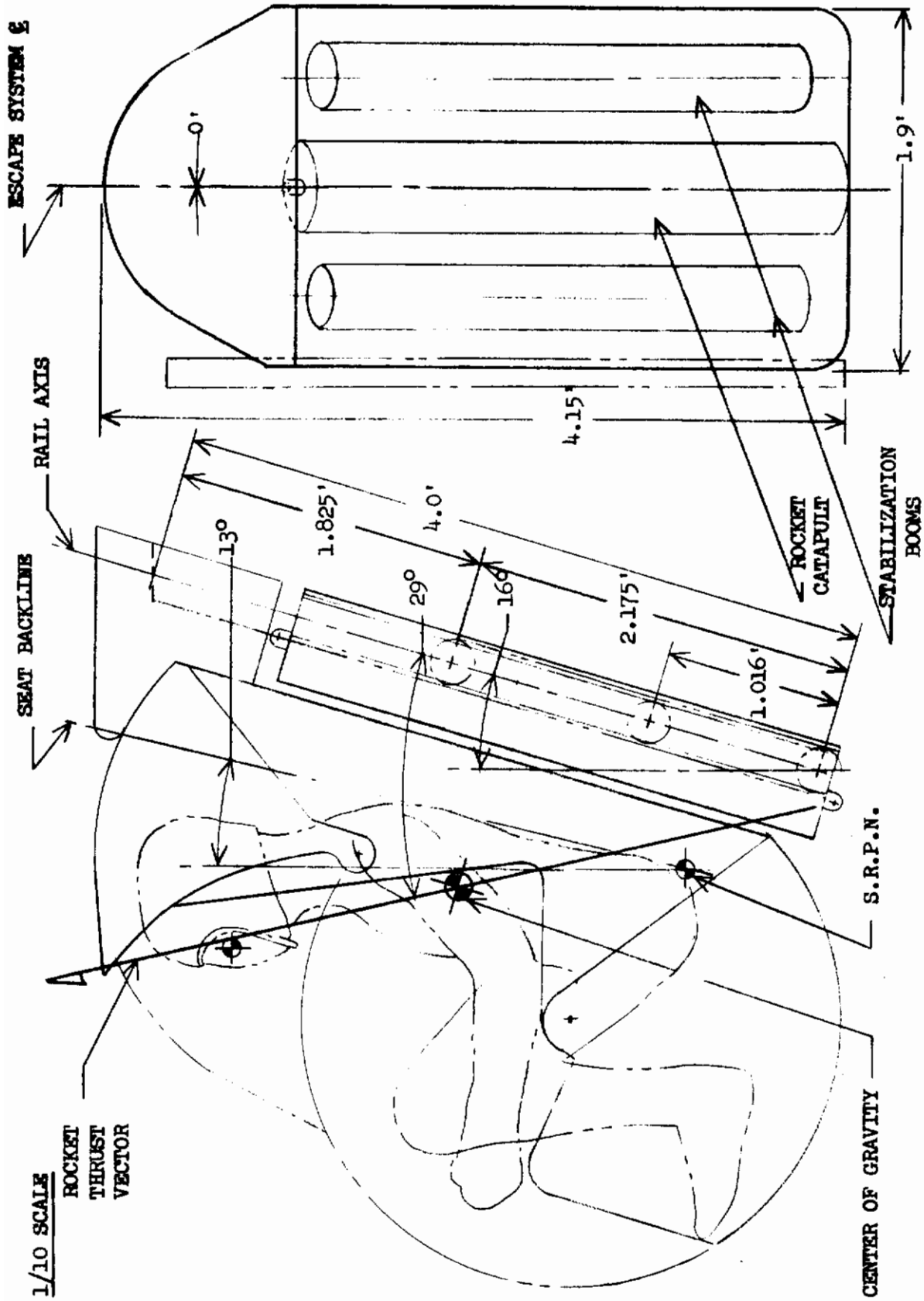

FIGURE 2 - ENCAPSULATED EJECTION SEAT - SYSTEM B

Approved for Public Release

Contrails

initiation and for stabilization employs telescoping booms actuated 0.14 seconds after ejection initiation and boom-attached chutes released 1.5 seconds later. The 34.5-foot diameter, 10% Extended Skirt recovery parachute is deployed at 2.25 seconds when below 15,000 feet.

The inset cabin capsule (C) (figure 3) provides simultaneous escape for all four of the crew members. The automatic sequence after manual initiation deploys two drag stabilization parachutes at 0.15 seconds and 1.5 seconds respectively, and main recovery parachutes are automatically deployed at 3.0 seconds below 15,000 feet. The drag parachutes are deployed in sequence to both reduce the velocity of the capsule under high speed ejection and to maintain stability. The first drag chute is a 8.7 foot diameter FIST Ribbon and the second is a 11.6 foot diameter Ribbed Guide Surface. The large weight of this capsule requires a recovery parachute drag area precluding application of a single parachute because of excessive opening time, requiring that a cluster of three 55-foot diameter Ringsail parachutes be incorporated.

The separable nose capsule (D) (figure 4) is similar to the single place F-104 ejectable nose concept. This system is also automatic after initiation, employs a three-vane stabilization feature and deploys the main recovery parachute at 2.2 seconds below 15,000 feet. The parachute is a 71.5-foot diameter Ringslot design.

b. Parachute Factors

Figures 5 through 9 show drag, stabilization and recovery parachute drag area versus distance curves used in the program. The drag characteristics of all parachutes are considered proportional to distance traveled. This relationship was reported in reference 2, and is based upon the theory that "a given parachute inflates in a fixed distance regardless of the velocity or altitude at which it is deployed and regardless of the weight that it carries." Certain assumptions are made, the first being that four times the chute diameter is allowed for line stretch and the second that the fixed distance allowed for a particular type parachute to open is derived from test data. The values applied are 4.5 D_0 for solid cloth canopies and 6.5 D_0 for Ringslot and Ringsail canopies.

c. Mass Properties

The data input to the computer program includes four conditions of CG thrust offset, shown pictorially in figures 10 through 14.

The determination of the dynamic CG shift during ejection (slump) is based upon the experimental work reported in references 3 and 4. These experiments are limited to seven test subjects varying in weight from 141 to 217 pounds. Based upon this work, it is determined that the average shift due to the CG change of the slumping crew member was 0.0336 inches per "G" in the horizontal direction and 0.02508 inches per "G" in the vertical direction. Relating the CG of the crew member(s) to the CG shift of the total ejected weight results in combined shifts which are quite small, especially for the

Approved for Public Release

Contrails

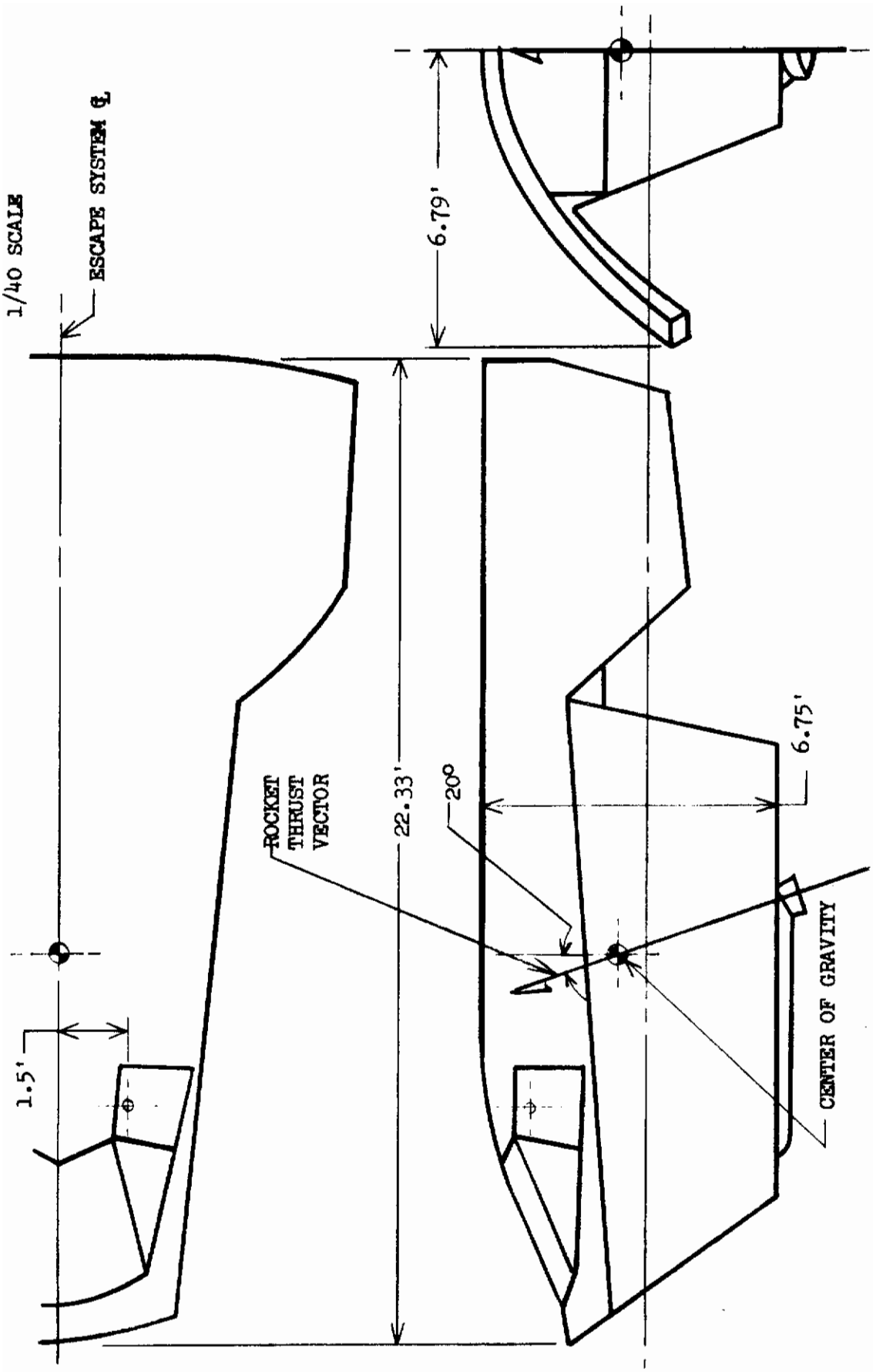

FIGURE 3 - INSET CABIN CAPSULE - SYSTEM C

Approved for Public Release

Contrails

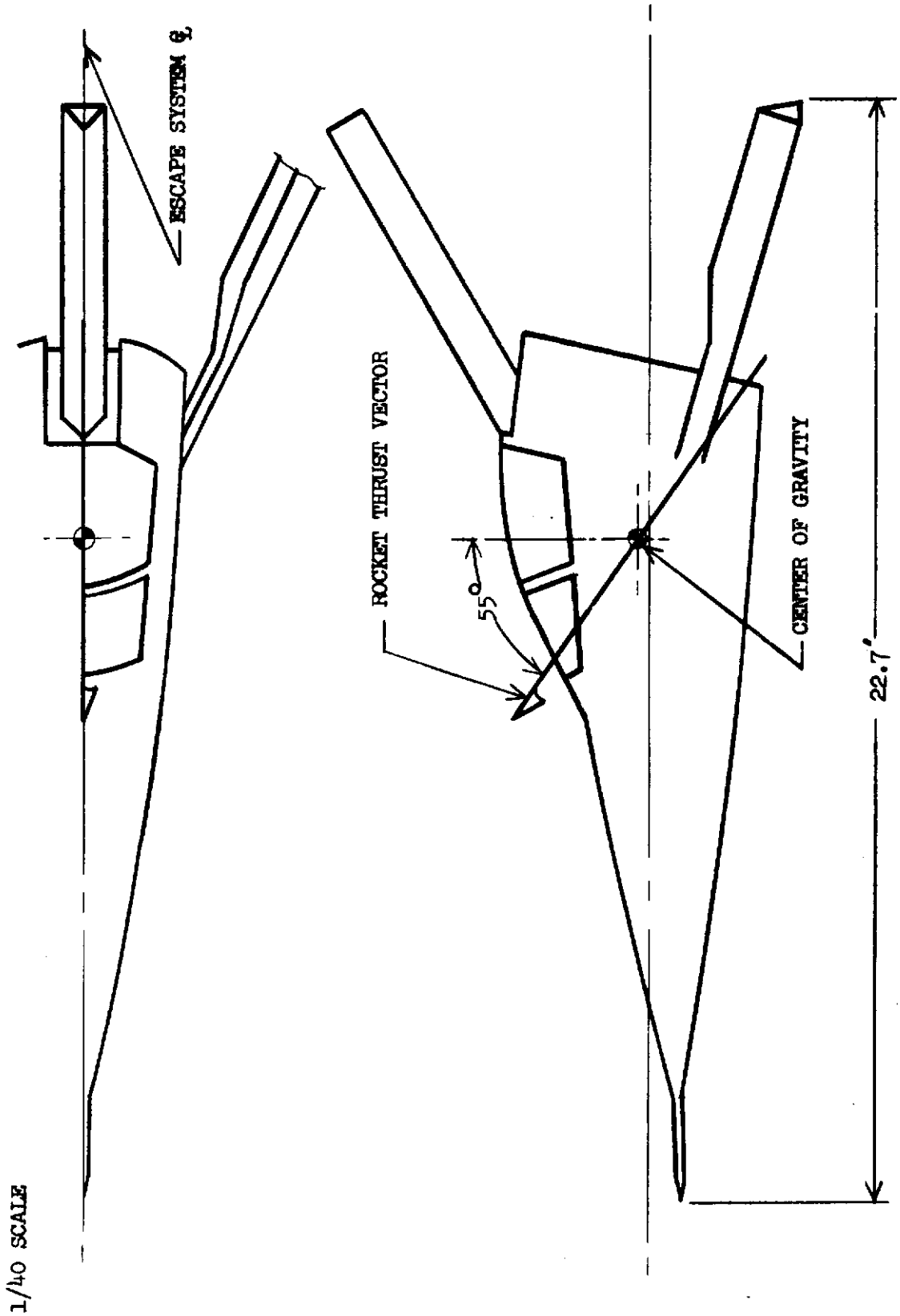

FIGURE 4 - SEPARABLE NOSE CAPSULE - SYSTEM D

Approved for Public Release

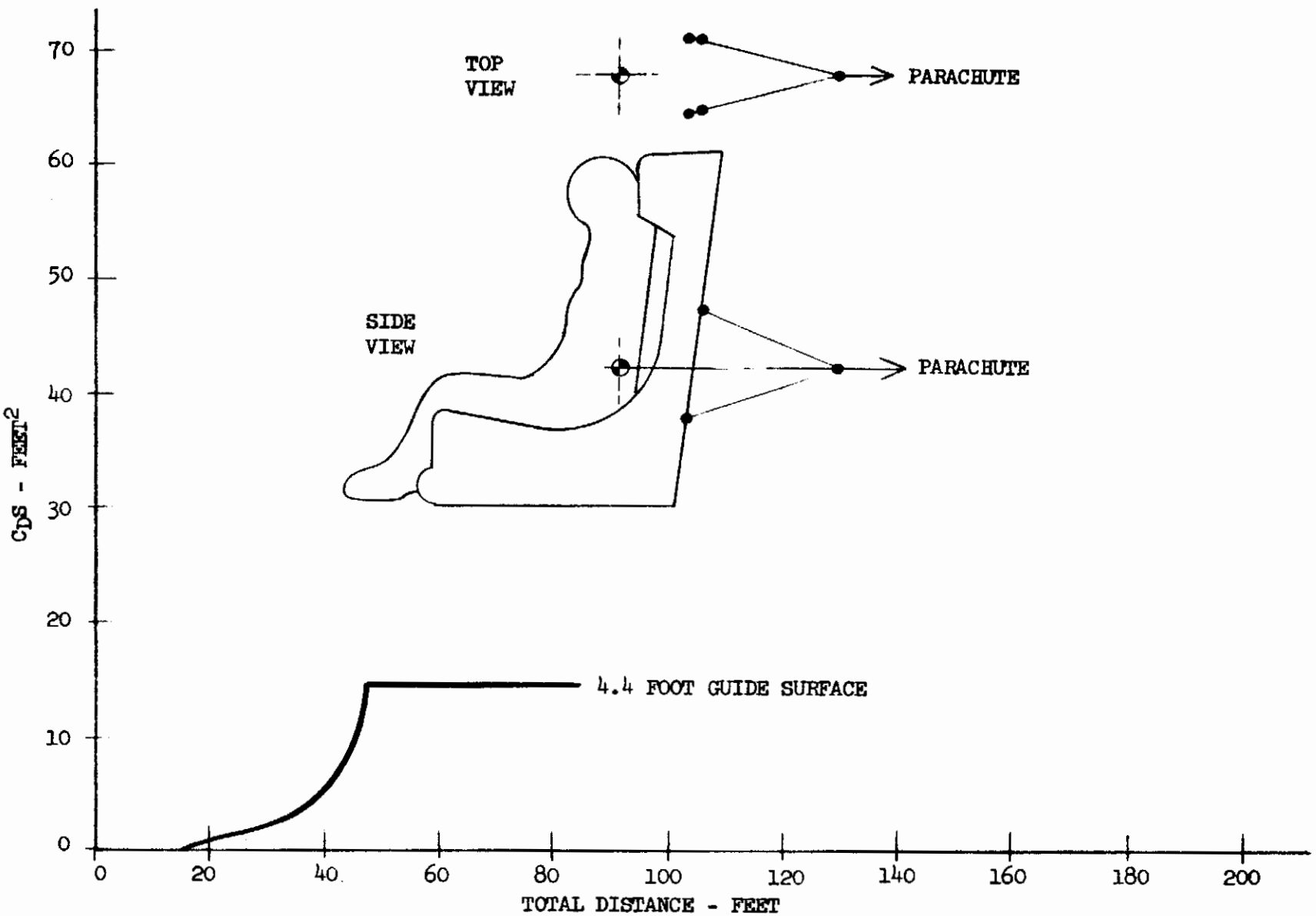

FIGURE 5 - C_DS VS DISTANCE TRAVELED TO FULL OPEN - DRAG PARACHUTE - SYSTEM A

Approved for Public Release

Contrails

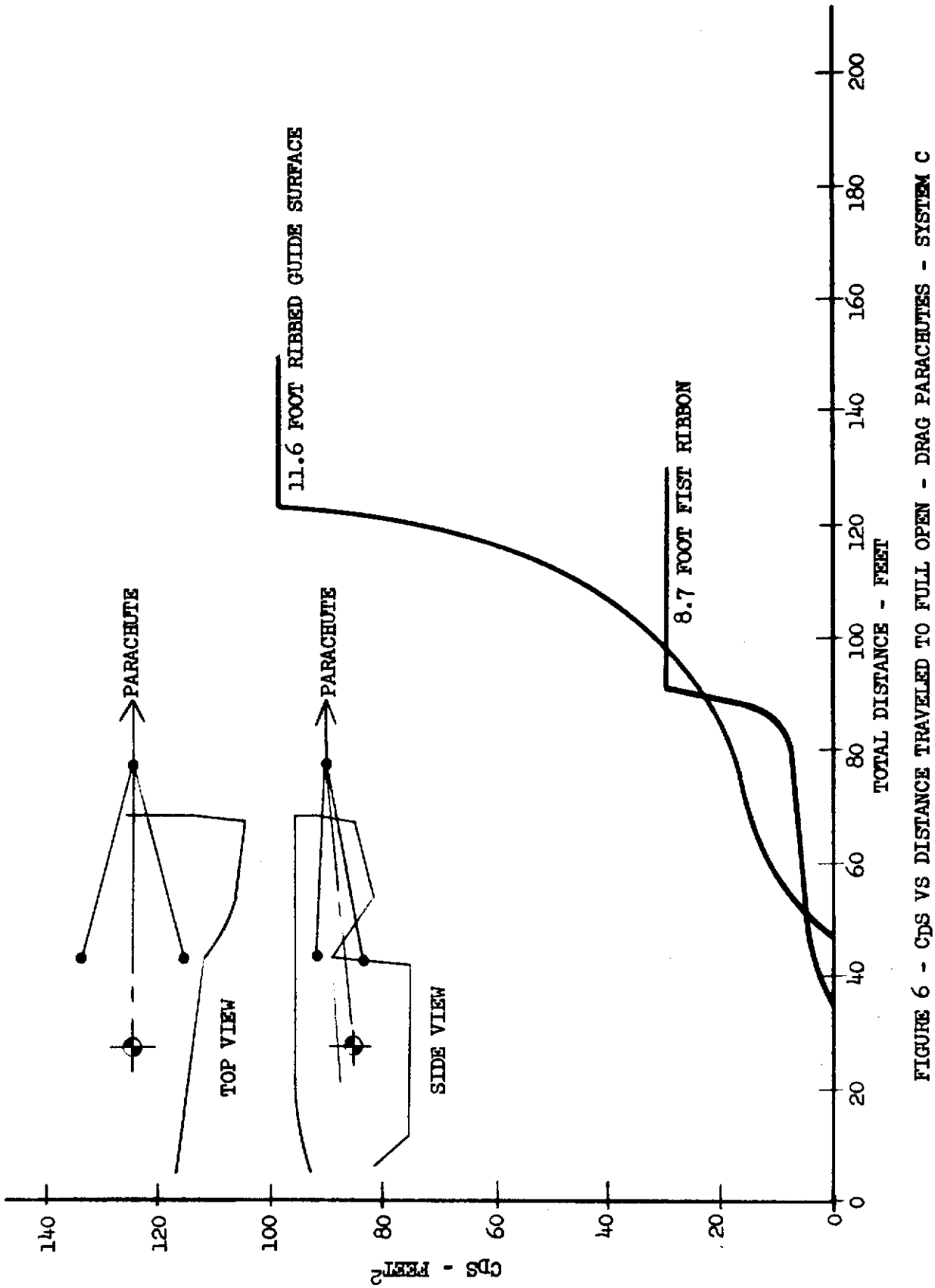

FIGURE 6 - CDS VS DISTANCE TRAVELED TO FULL OPEN - DRAG PARACHUTES - SYSTEM C

Approved for Public Release

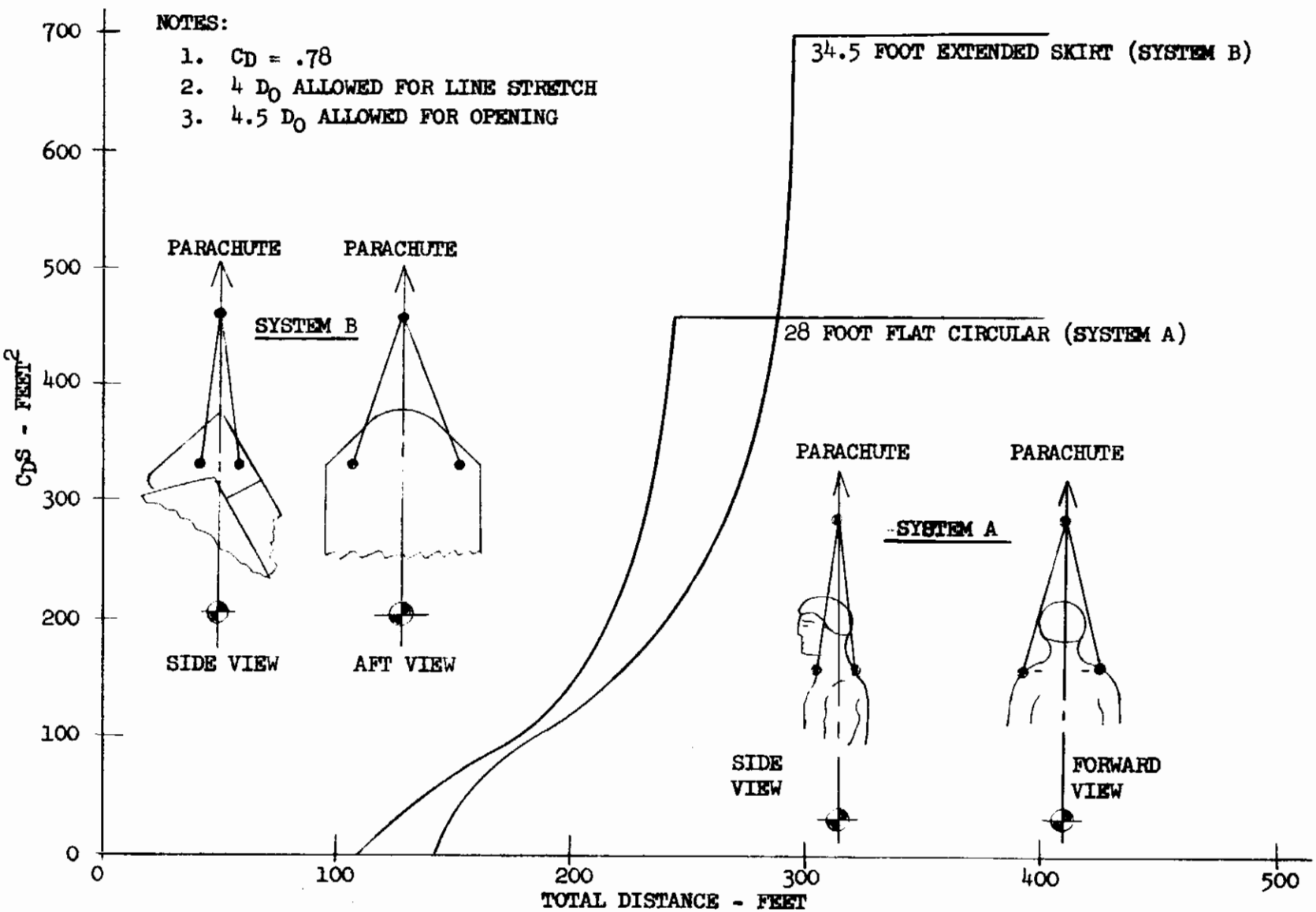

FIGURE 7 - C_DS VS DISTANCE TRAVELED TO FULL OPEN - RECOVERY PARACHUTE - SYSTEM A & B

Approved for Public Release

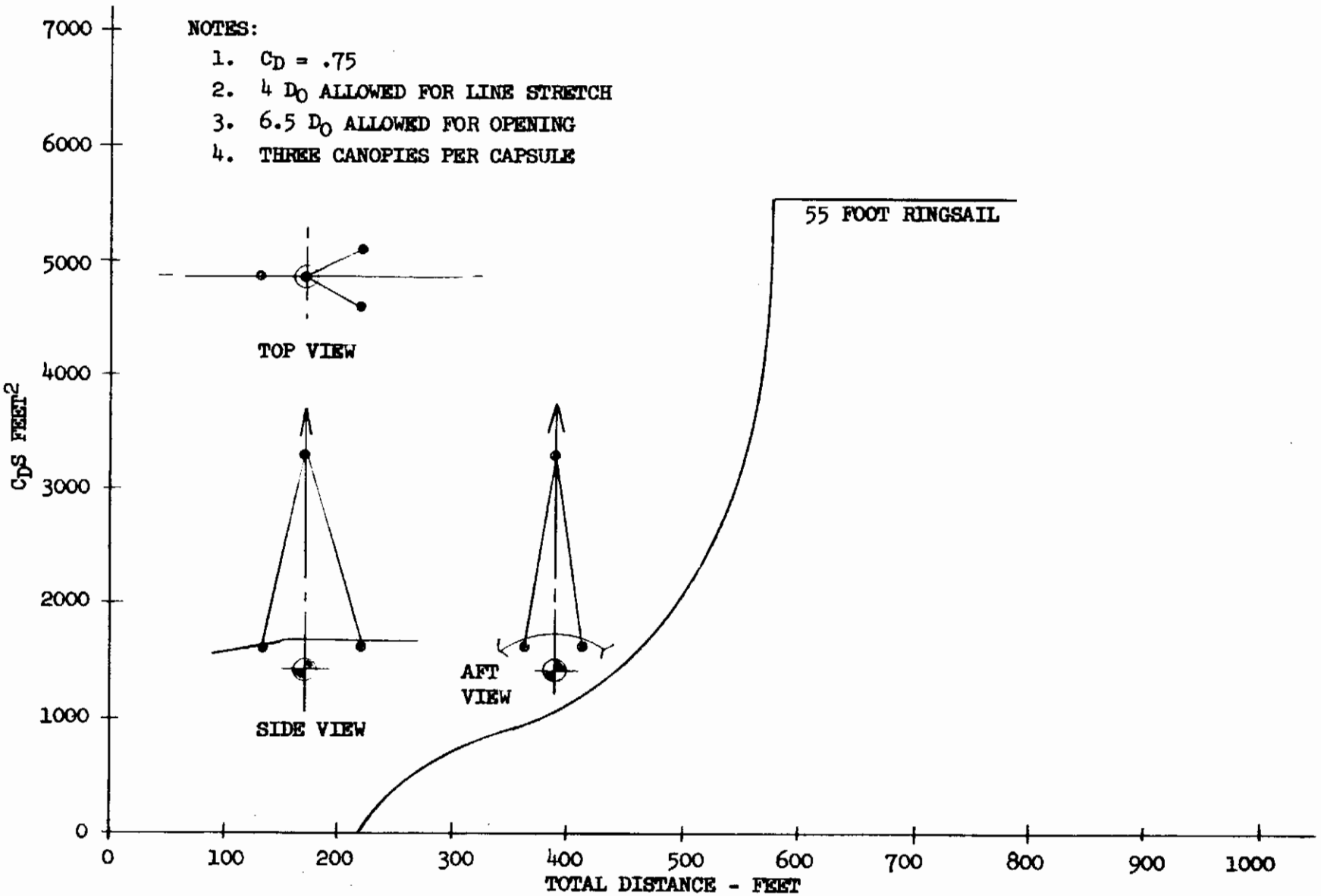

FIGURE 8 - C_DS VS DISTANCE TRAVELED TO FULL OPEN-RECOVERY PARACHUTE - SYSTEM C

Approved for Public Release

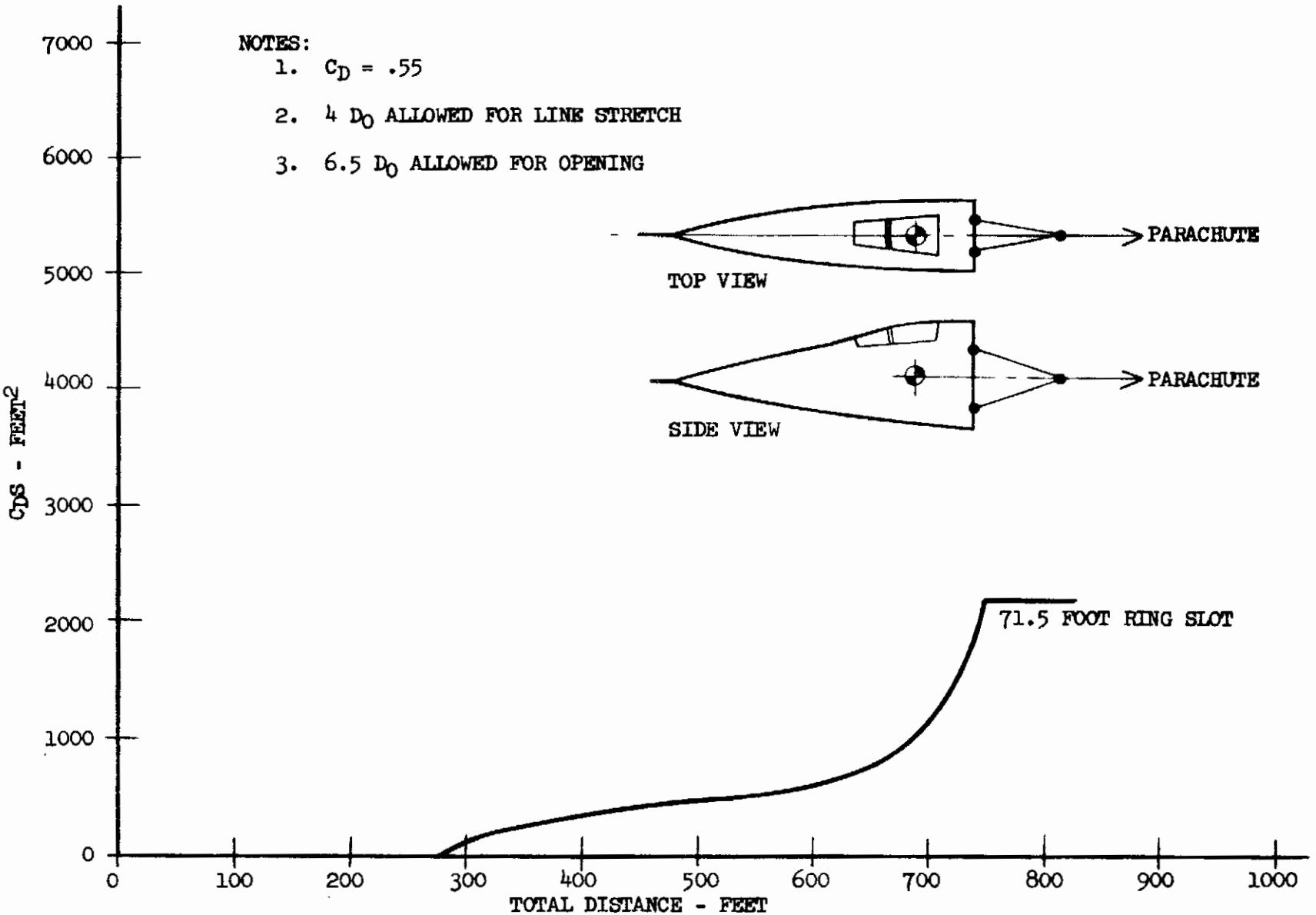

FIGURE 9 - C_DS VS DISTANCE TRAVELED TO FULL OPEN - RECOVERY PARACHUTE - SYSTEM D

Approved for Public Release

Contrails

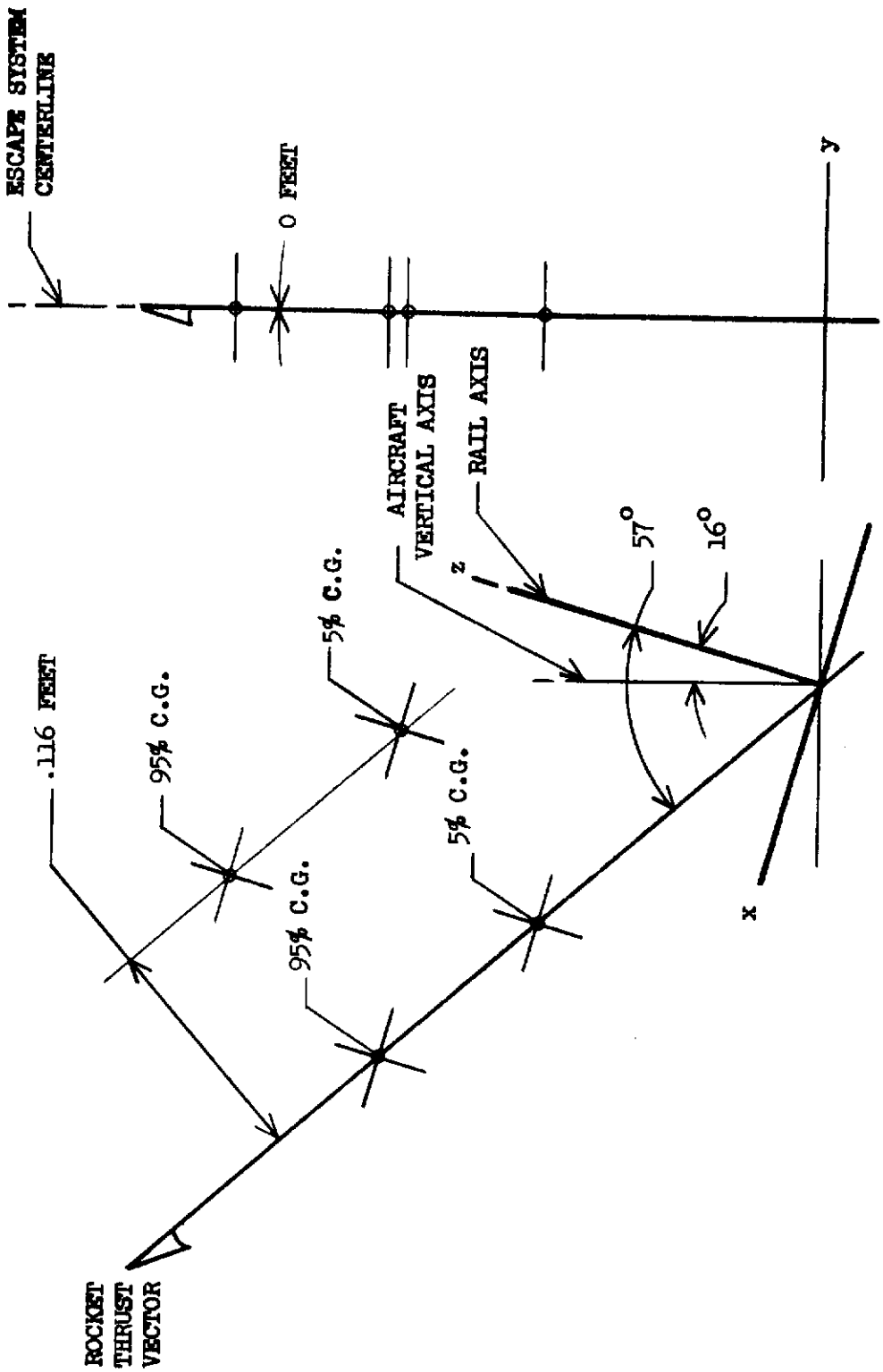

FIGURE 10 - CENTER OF GRAVITY LOCATION VERSUS ROCKET THRUST VECTOR-SYSTEM A

Approved for Public Release

Contrails

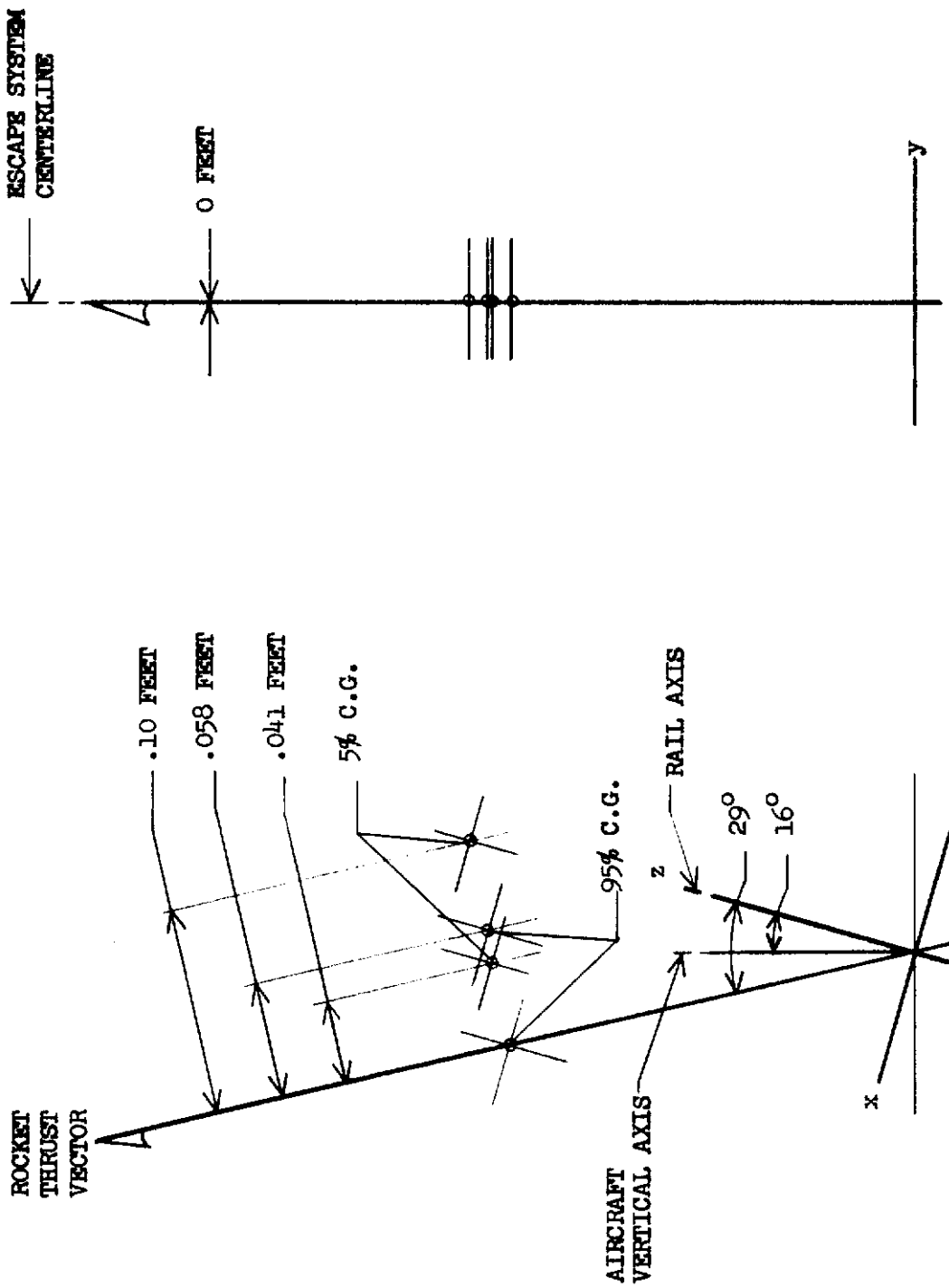

FIGURE 11 - CENTER OF GRAVITY LOCATION VERSUS ROCKET THRUST VECTOR-SYSTEM B (BOOMS STOWED)

Approved for Public Release

Contrails

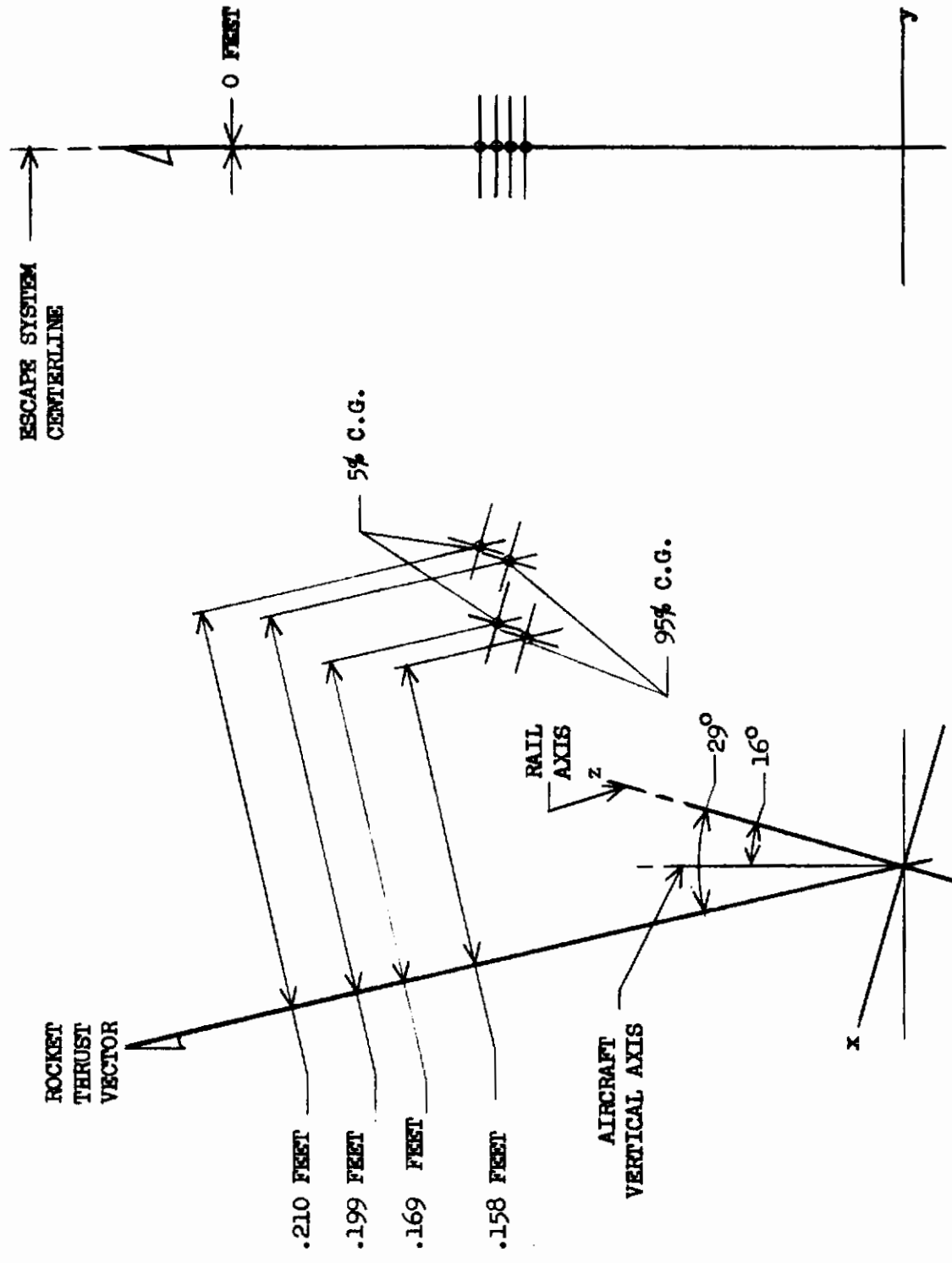

FIGURE 12 - CENTER OF GRAVITY LOCATION VERSUS ROCKET THRUST VECTOR - SYSTEM B (BOOMS EXTENDED)

Approved for Public Release

Contrails

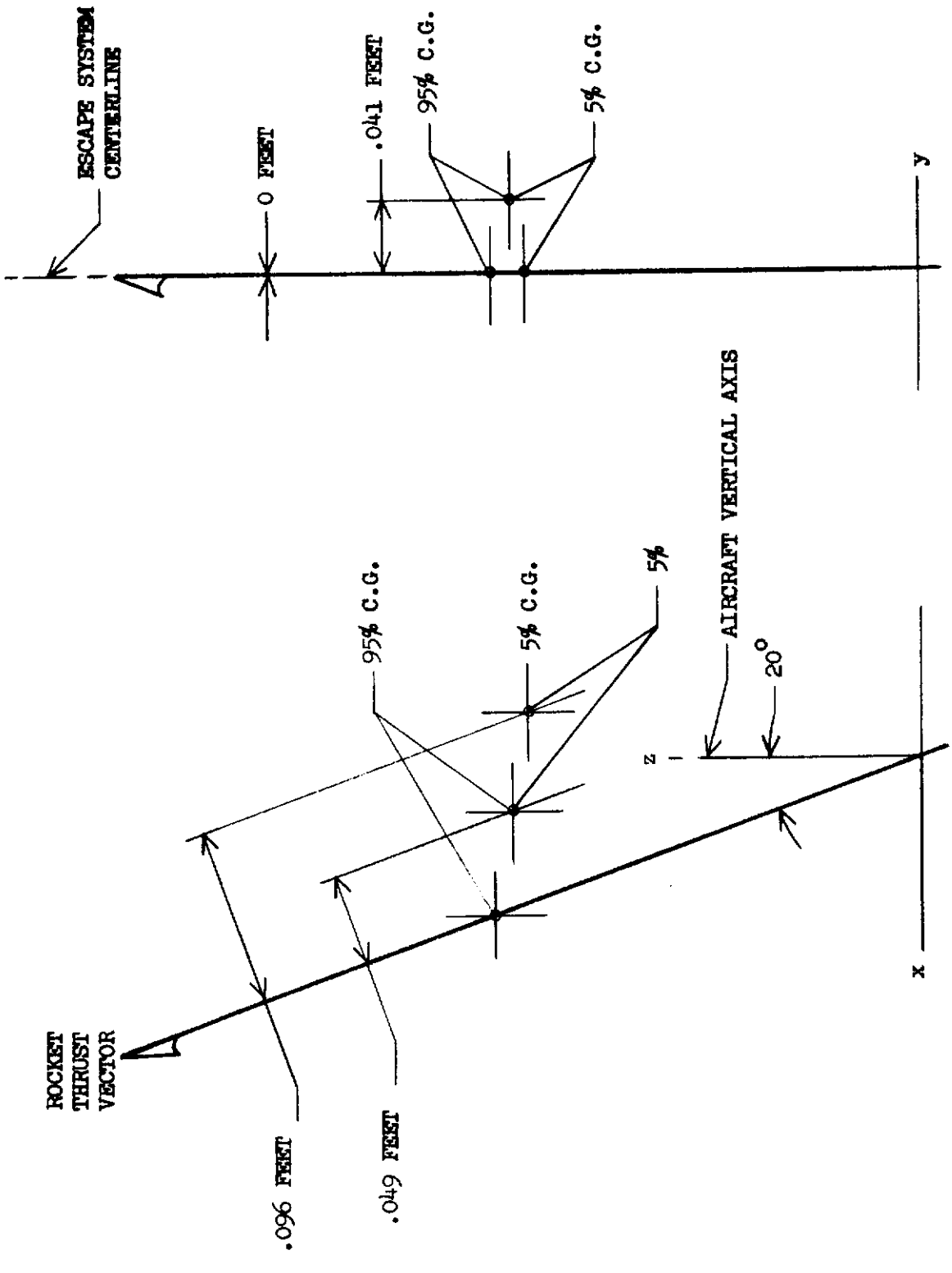

FIGURE 13 - CENTER OF GRAVITY LOCATION VERSUS ROCKET THRUST VECTOR - SYSTEM C

Approved for Public Release

Contrails

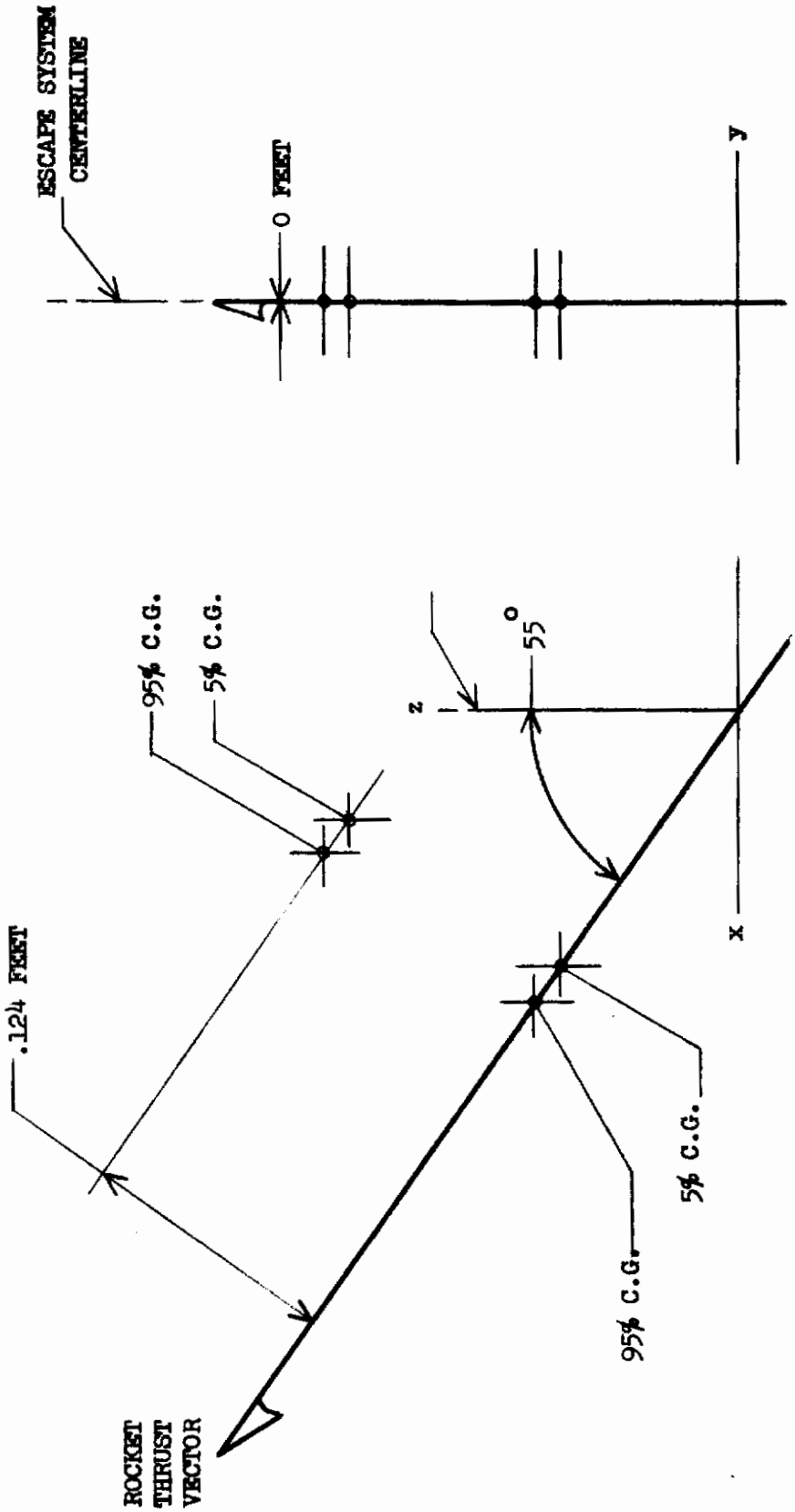

FIGURE 14 - CENTER OF GRAVITY LOCATION VERSUS ROCKET THRUST VECTOR - SYSTEM D

Approved for Public Release

Contrails

heavier systems. The relationship between the system-weight-to-crew-weight ratio versus the CG movement at 10 "G" is presented by figure 15.

Moment of inertia changes due to CG movements caused by slump were determined to be so minute in relation to the original moments that they were ignored.

The mass properties of the four escape concepts were developed for crews of both 5th and 95th percentile Air Force personnel. Where possible, the data were obtained from measurements of hardware. System A values are representative of current high-performance ejection seats, Systems B and C are based upon NAR/LAD in-house studies and System D figures are for the F-104 Ejectable Nose Capsule obtained from references 5 and 6. Summaries of the mass properties of all four systems are listed in Tables I and II.

d. Propulsion

Two types of escape system propulsion units are used, System A and B utilizing rocket-catapults and Systems C and D, pure rocket. The range of rocket nozzle angles is 13° to 55° forward of vertical, System A being 27°; System B, 13°; System C, 20°; and System D, 55°. The optimum angle for System A, B, and C is based on North American Rockwell Corporation work on similar systems. System D utilizes the angle (55°) applied during sled testing of the F-104 nose capsule. As the basis for reconciling the systems for comparison, the impulse of each is varied so that all systems attain terminal velocity under the full parachute at 100 feet altitude when ejected at zero velocity-zero altitude.

Table III lists the maximum values of impulse, thrust and "G" for the systems, and figures 16 through 19 show the curves for the individual propulsion systems after reconciliation.

3. MAN-MACHINE REACTION INTERVALS

The fact that current aircraft escape concepts are dependent upon the human for initiation prompts the input of maximum and minimum man-machine reaction times as variables in the program matrix. The ejection initiation time or time differential between the occurrence of a recognizable dire emergency and actuation of the escape device is input as 2.4 seconds minimum and 3.2 seconds maximum. This differential is based upon studies presented in reference 7 and is comprised of human response time and machine lag time.

It is assumed that the machine lag time or mechanical separation period is affected to only a minor degree by acceleration loads and is established as a constant 0.2 seconds. The human response time (1.4 seconds), composed of the human reaction and movement intervals and assumed to be unaffected by the acceleration range (0 to 8 G_z), consists of awareness, perception and decision. The awareness time (0.3 seconds) is the period required for the crewman to detect an unusual situation and focus on the object, instrument or advisory light. Perception time (0.6 seconds) is that consumed by the crewman in identifying and assessing the situation. Decision time (0.5 seconds) is the interval required to select a course of action.

Approved for Public Release

Contrails

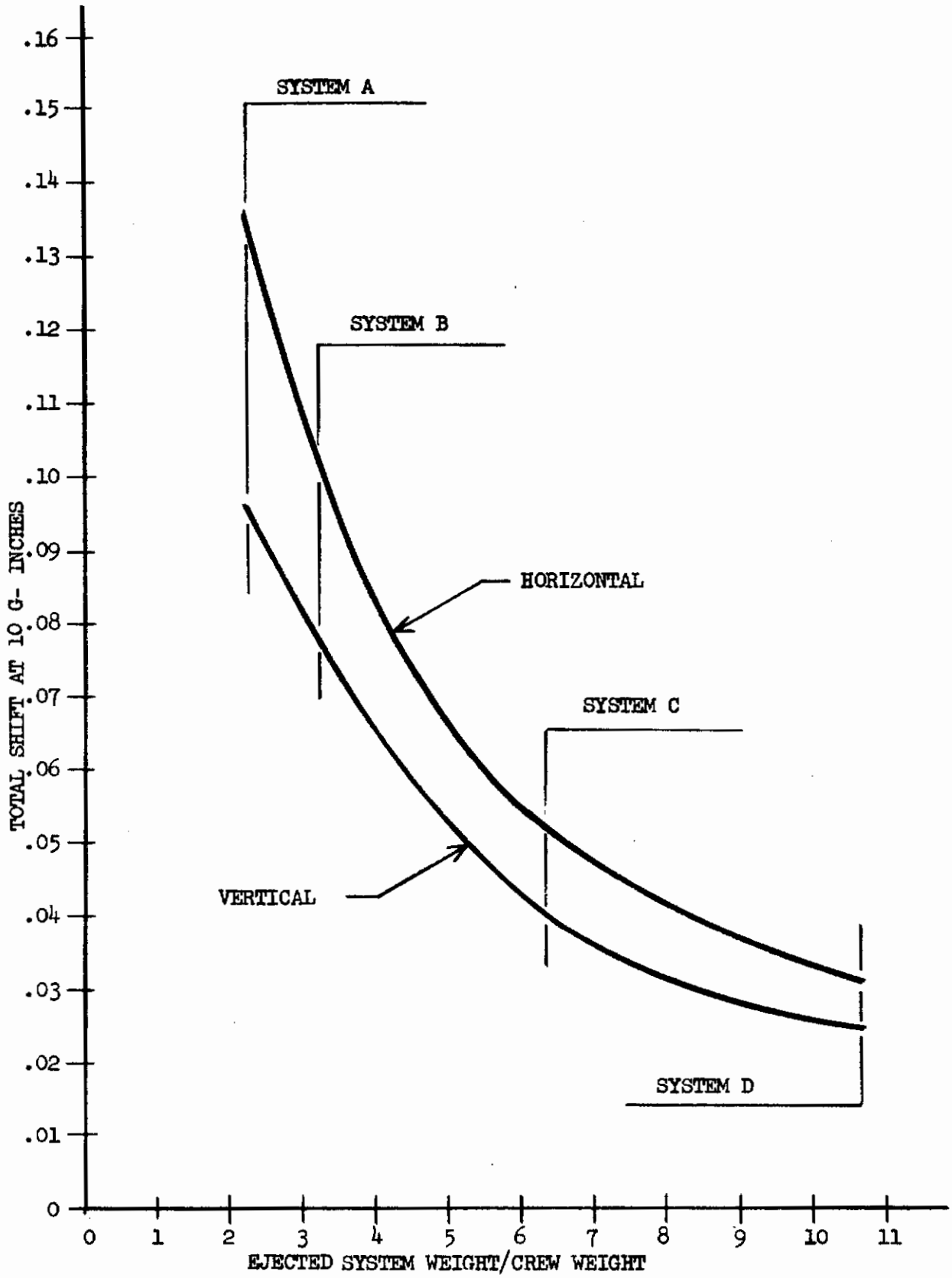

FIGURE 15-SYSTEM WEIGHT TO CREW WEIGHT RATIO VERSUS C.G. MOVEMENT AT 10 G

Approved for Public Release

Contrails

TABLE I

SUMMARY OF MASS PROPERTIES
OF ESCAPE SYSTEMS A AND B

	SYSTEMS							
	A *				B			
					BOOMS STOWED		BOOMS EXTENDED	
PERCENTILE CREWMEMBER	5		95		5	95	5	95
CG LOCATION (FEET)	MIN.	MAX.	MIN.	MAX.				
x (PERPENDICULAR TO RAIL AXIS)	.975	1.05	1.075	1.137	1.142	1.192	1.030	1.033
y (PERPENDICULAR TO SYSTEM ℄)	0	0	0	0	0	0	0	0
z (PARALLEL TO RAIL AXIS)	1.287	1.191	1.35	1.25	1.792	1.767	1.822	1.807
MOMENTS OF INERTIA (SLUG-FT^2)								
I_x	14.8	15.0	18.2	18.3	40	43	49	51
I_y	22.6	23.5	26.9	27.8	47	50	62	65
I_z	12.1	12.4	14.5	14.8	18	20	33	35
I_{xz}	-2.3	-2.4	-4.1	-4.2	-5	-8	-10	-7
REFERENCE POINT	SEE FIGURES 1 AND 2							

* For System A, Values Represent Measured Extremes for an Existing Seat.

Approved for Public Release

Contrails

TABLE II

SUMMARY OF MASS PROPERTIES
OF ESCAPE SYSTEMS C AND D

	SYSTEMS			
	C		D	
PERCENTILE CREWMEMBER(S)	5	95	5	95
CG LOCATION (INCHES)				
x (FUSELAGE STATION)	106.3	105	228.6	228.8
y (PERPENDICULAR TO SYSTEM $\mathcal{C}_L$)	0	0	0	0
z (FROM WATER LINE OF FWD EYE)	-24.1	-23.9		
z (WATER LINE)			103.1	103
MOMENTS OF INERTIA (SLUG-FT^2)				
I_x	1230	1258	240	243
I_y	3954	4030	1062	1065
I_z	4040	4137	1014	1015
I_{xz}	114	111	- 3	- 4
REFERENCE POINT	STATION AND EYE		STATION AND FUSELAGE PLANE	

Approved for Public Release

Contrails

TABLE III

MAXIMUM VALUES OF IMPULSE, THRUST AND "G" FOR THE FOUR ESCAPE SYSTEM CONCEPTS

PROPULSION		SYSTEM			
		A	B	C	D
MAXIMUM CURVE	IMPULSE/WEIGHT *	6.8	5.9	8.5	10.3
	MAX IMPULSE (LB-SEC)	2,812	3,659	44,000	22,942
	MAX THRUST (LB)	9,000	13,100	111,600	54,000
	MAX "G" PRODUCED BY THRUST	21.7	21.0	21.5	24.1
MINIMUM CURVE	IMPULSE/WEIGHT *	6.3	5.5	8.0	9.8
	MAX IMPULSE (LB-SEC)	2,597	3,447	41,650	21,712
	MAX THRUST (LB)	6,500	9,500	100,400	48,000
	MAX "G" PRODUCED BY THRUST	15.6	15.2	19.3	21.5

* MAXIMUM WEIGHT OF ESCAPE BODY

Approved for Public Release

Contrails

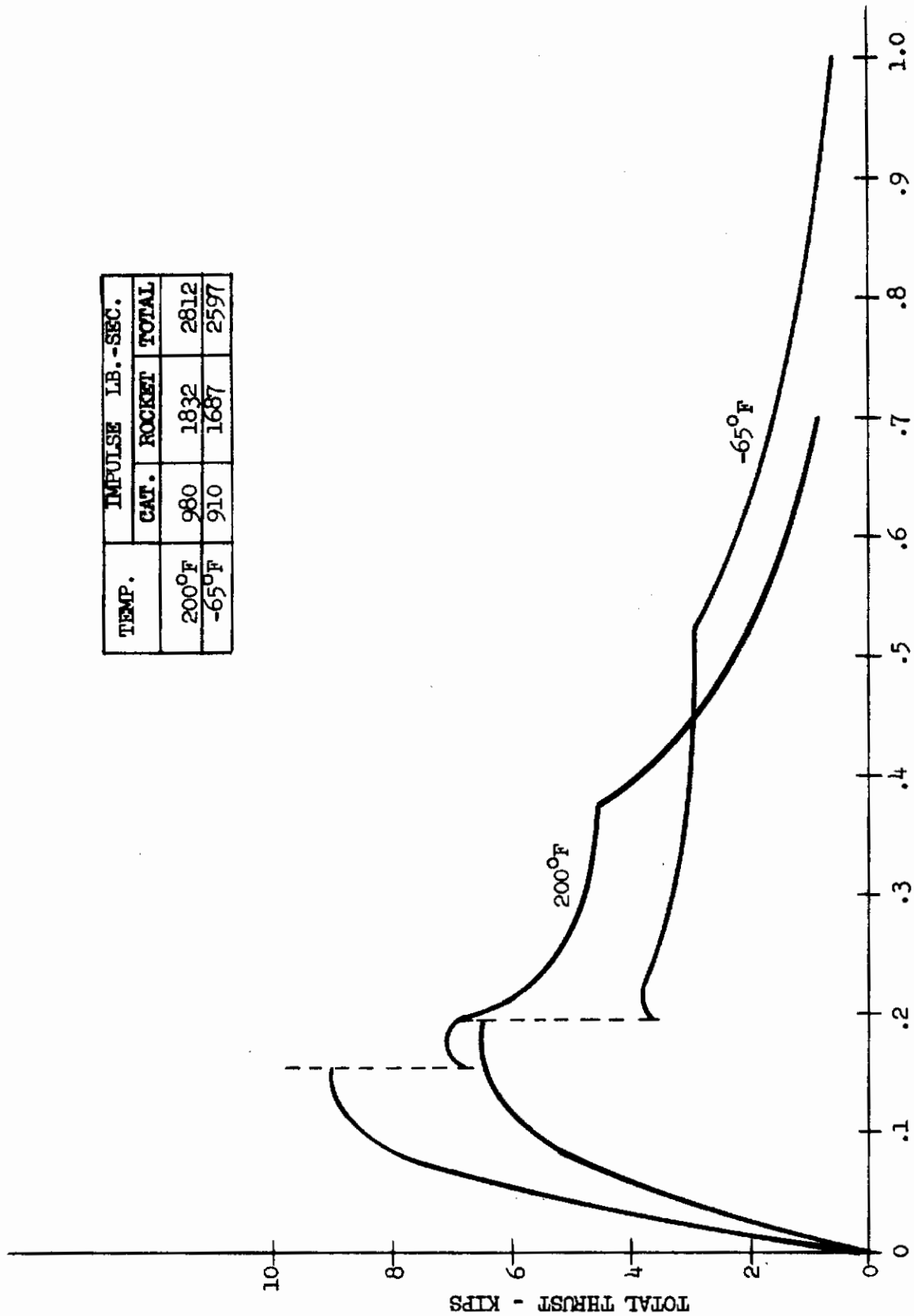

TEMP.	IMPULSE LB.-SEC.		
	CAT.	ROCKET	TOTAL
200°F	980	1832	2812
-65°F	910	1687	2597

FIGURE 16 - ROCKET-CATAPULT THRUST CURVES FOR SYSTEM A

Approved for Public Release

Contrails

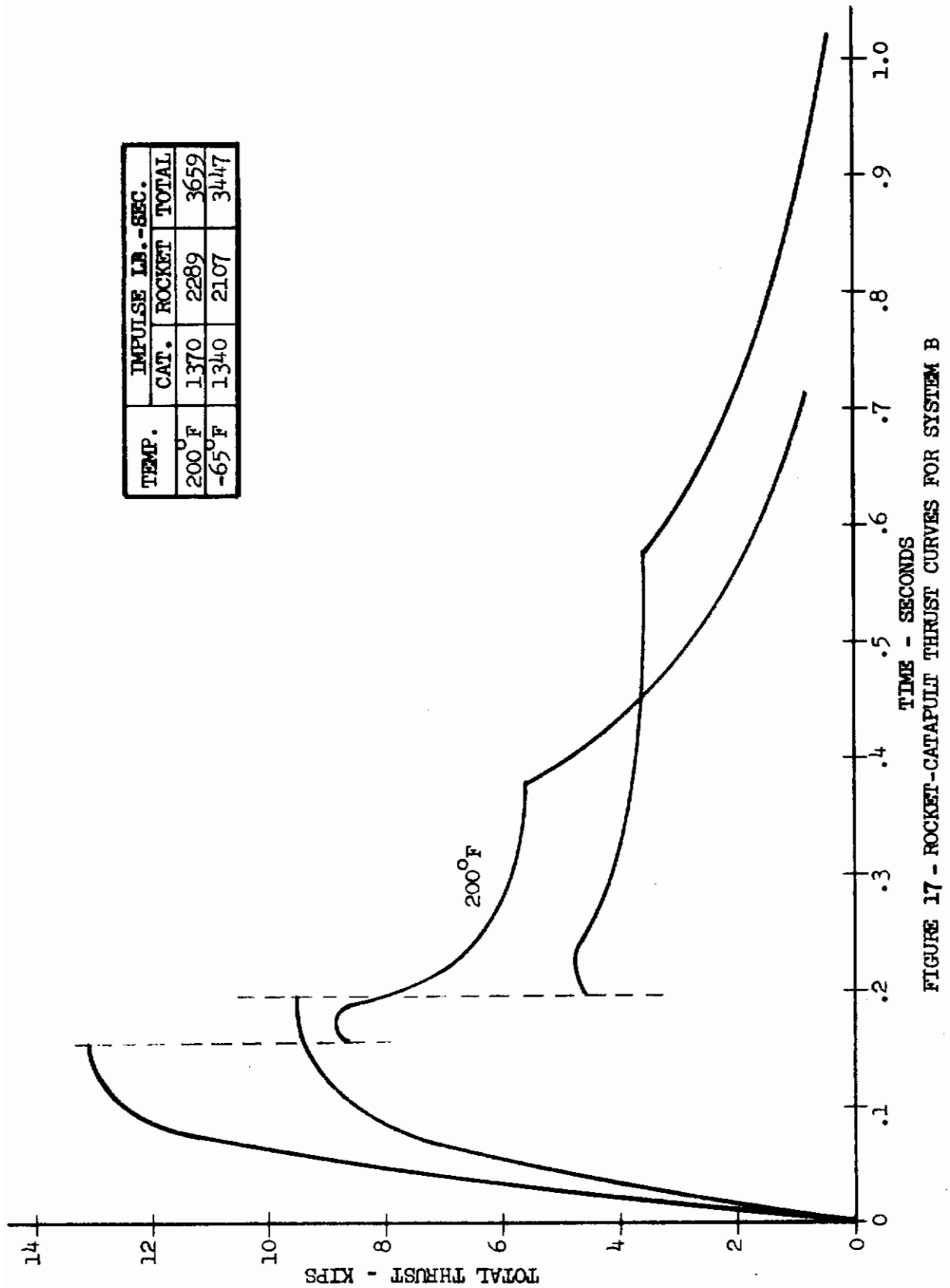

TEMP.	IMPULSE LB.-SEC.		
	CAT.	ROCKET	TOTAL
200°F	1370	2289	3659
-65°F	1340	2107	3447

FIGURE 17 - ROCKET-CATAPULT THRUST CURVES FOR SYSTEM B

Approved for Public Release

Contrails

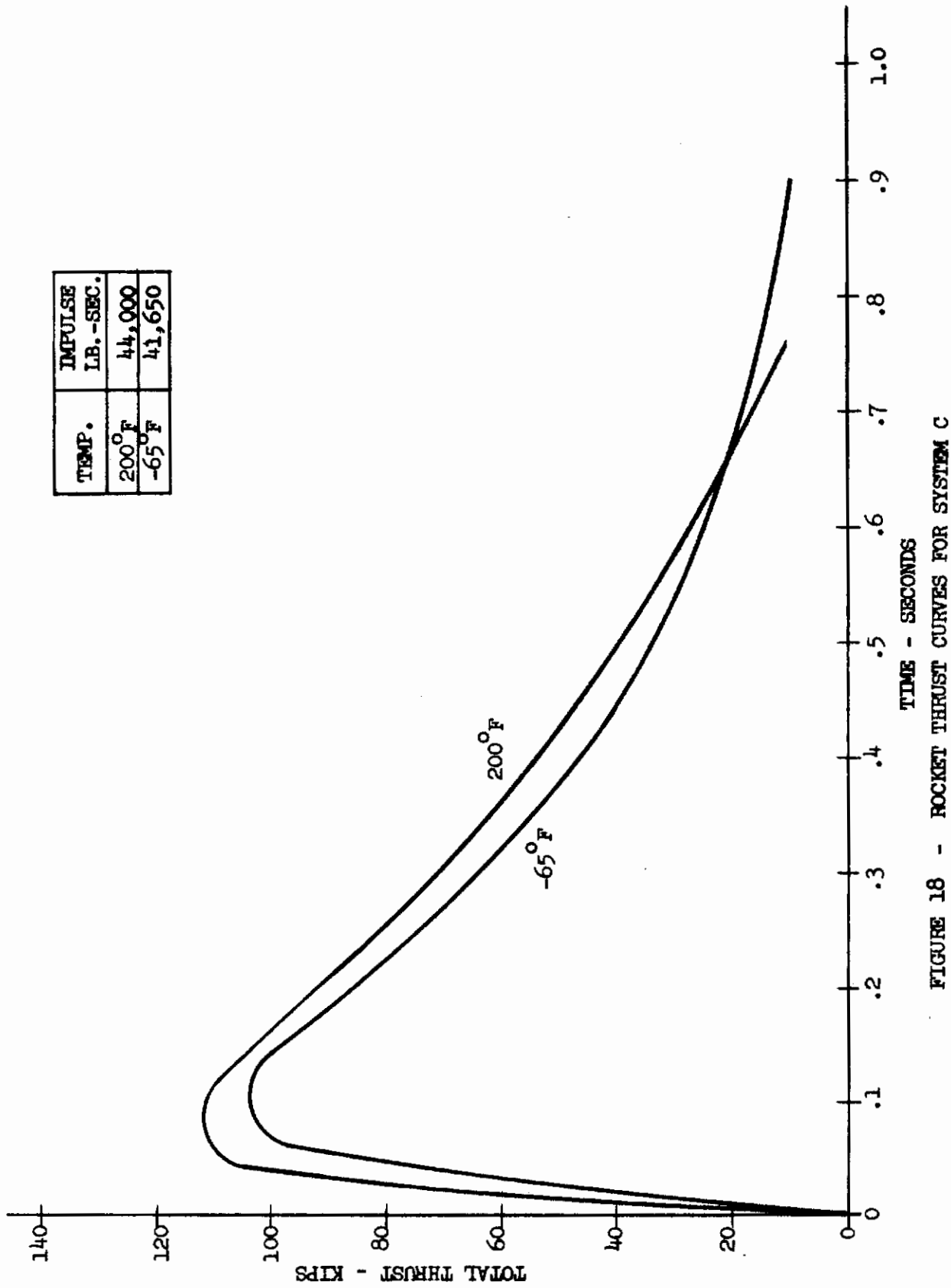

FIGURE 18 - ROCKET THRUST CURVES FOR SYSTEM C

Approved for Public Release

Contrails

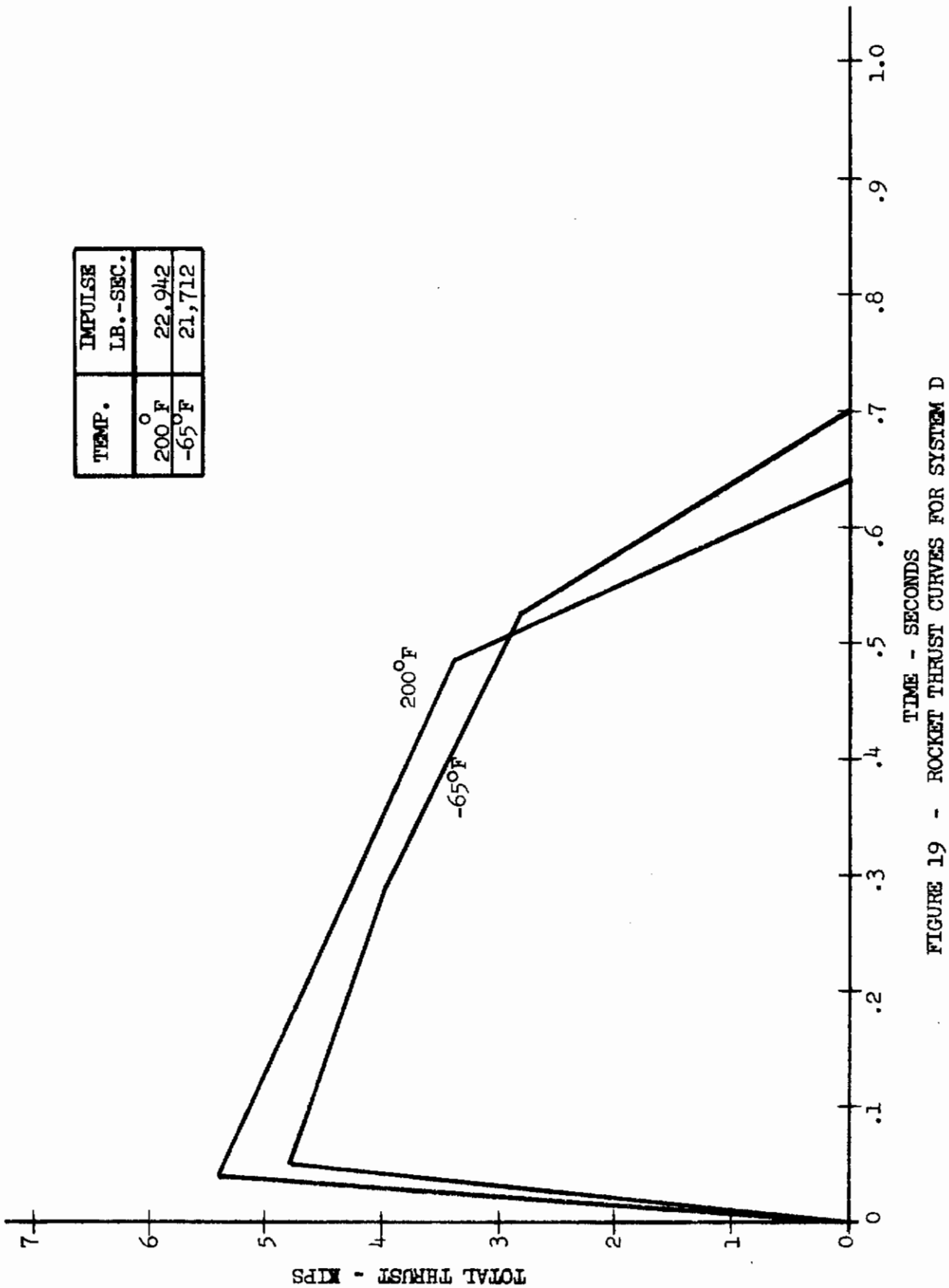

FIGURE 19 - ROCKET THRUST CURVES FOR SYSTEM D

Approved for Public Release

Contrails

The total human movement time is affected by acceleration (0.8 seconds for 0 to 1 G_z and 1.6 seconds for an 8 G_z environment) and is composed of response and control actuation. It is assumed that the crewman must reach 12 to 15 inches at right angle to the acceleration in order to position his hands on the ejection control. The response time is estimated at 0.5 seconds for 0 to 1 G_z and 1.3 seconds for 8 G_z. The control movement is in a direction parallel to the acceleration and is input as a constant 0.3 seconds. A graphical representation of the man-machine reaction times is conveyed by figure 20.

4. AERODYNAMIC FACTORS

Aerodynamic data were generated from existing system designs. Data for system A, the open ejection seat, are based upon the X-15 seat plus pilot (no fins or booms); system B, encapsulated ejection seat, upon a compact equivalent of the XB-70A capsule (with and without booms and stabilizing chutes); system C, the inset cabin capsule, upon an NAR in-house design study; and system D, the Lockheed-studied F-104 nose capsule with vanes.

The aerodynamic parameters, including rotary derivatives, were developed as dimensionless coefficients in the stability axes system for Mach numbers of 0.2 and 1.2 and were plotted versus angle of attack α, for three side slip angles β of 0°, 15° and 45°. The aerodynamic coefficient curves developed consisted of: (1) lift coefficient (C_L); (2) drag coefficient (C_D); pitching moment coefficient (C_m); rolling moment coefficient (C_l); yawing moments (C_n); side force coefficient (C_y); damping in pitch (C_{mq}); damping in roll (C_{lp}); damping in yaw (C_{nr}); rolling moment due to yawing velocity (C_{lr}); and yawing moment due to rolling velocity (C_{rp}). The data developed for M = .20 are considered applicable for M = .10 to .80 and the M = 1.2 data applicable for M = 1.05 to 1.4. Side slip data for β's between 0° and 15° and 15° and 45° were obtained by linear interpolation between data for $\beta = 0^\circ$ and 15° and $\beta = 15^\circ$ and 45°, respectively.

The aerodynamic coefficient curves are recorded in reference 8 and were estimated from references 6 and 9 through 22.

5. PROGRAM PARAMETERS

A matrix of flight and escape conditions (figure 21) yields maximal information regarding the four escape concepts. A total of 3328 case-conditions were selected, composed of 208 aircraft flight cases for each of 16 escape system features.

The aircraft flight cases are combinations of pitch (aircraft angle of attack) angles of 0°, 15°, 90°, -15°, and -90°; roll angles of 0°, 30°, 60°, 90°, and 180°; yaw angles of 0°, 15° and 45°; pitch rates of 0°/sec, 30°/sec, and 90°/sec; roll rates of 0°/sec, 60°/sec, and 180°/sec and yaw rates of 0°/sec and -90°/sec. Flight path angles of 0°, 10°, -10°, -30° and -90° are considered sufficient, when combined by interpolation with the other variables, to support a comprehensive analysis of escape limitations. Sink rate

Approved for Public Release

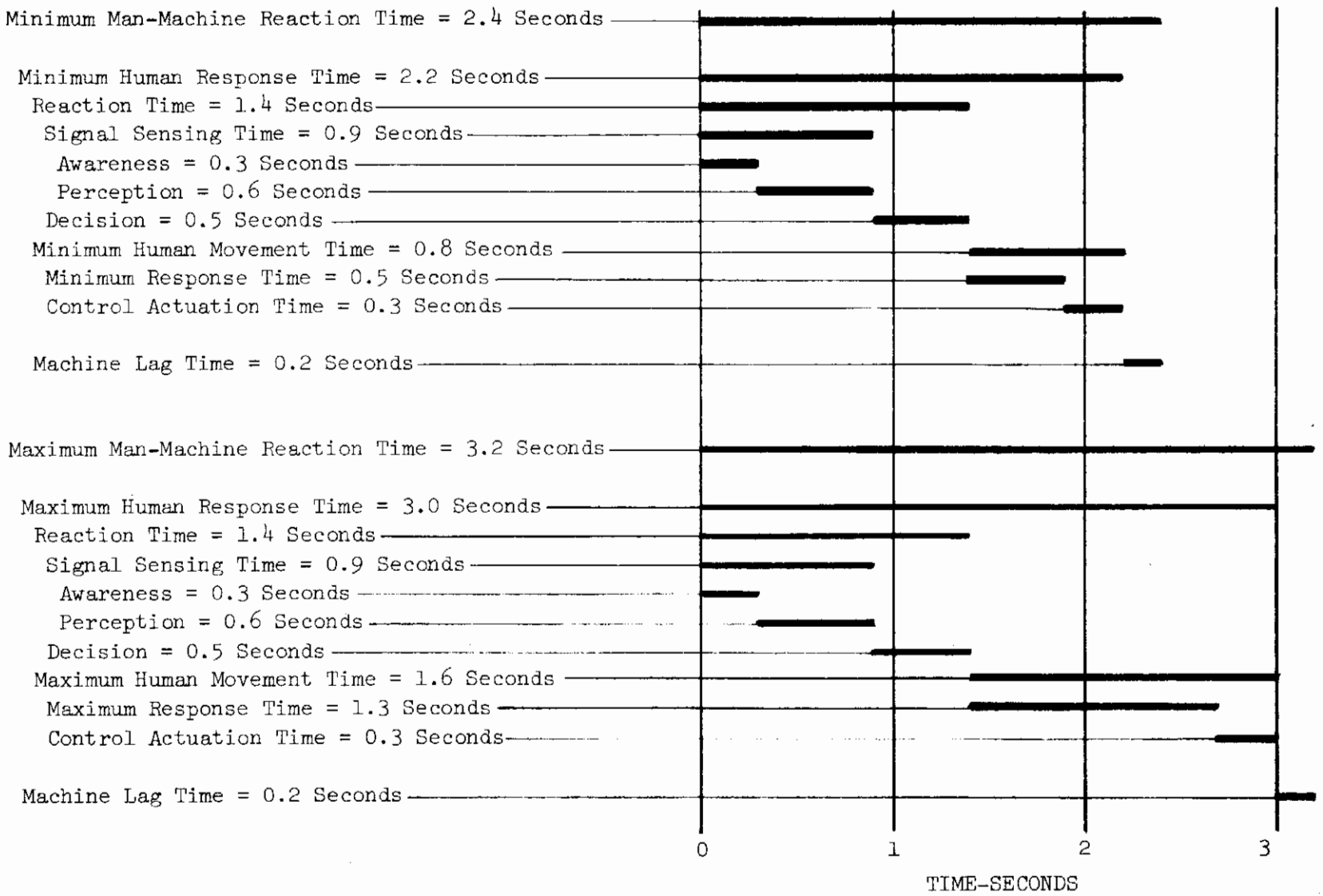

FIGURE 20 - MAN-MACHINE REACTION TIME

Approved for Public Release

Contrails

Approved for Public Release

Confidential

EJECTION MATRIX FOR EACH ESCAPE SYSTEM

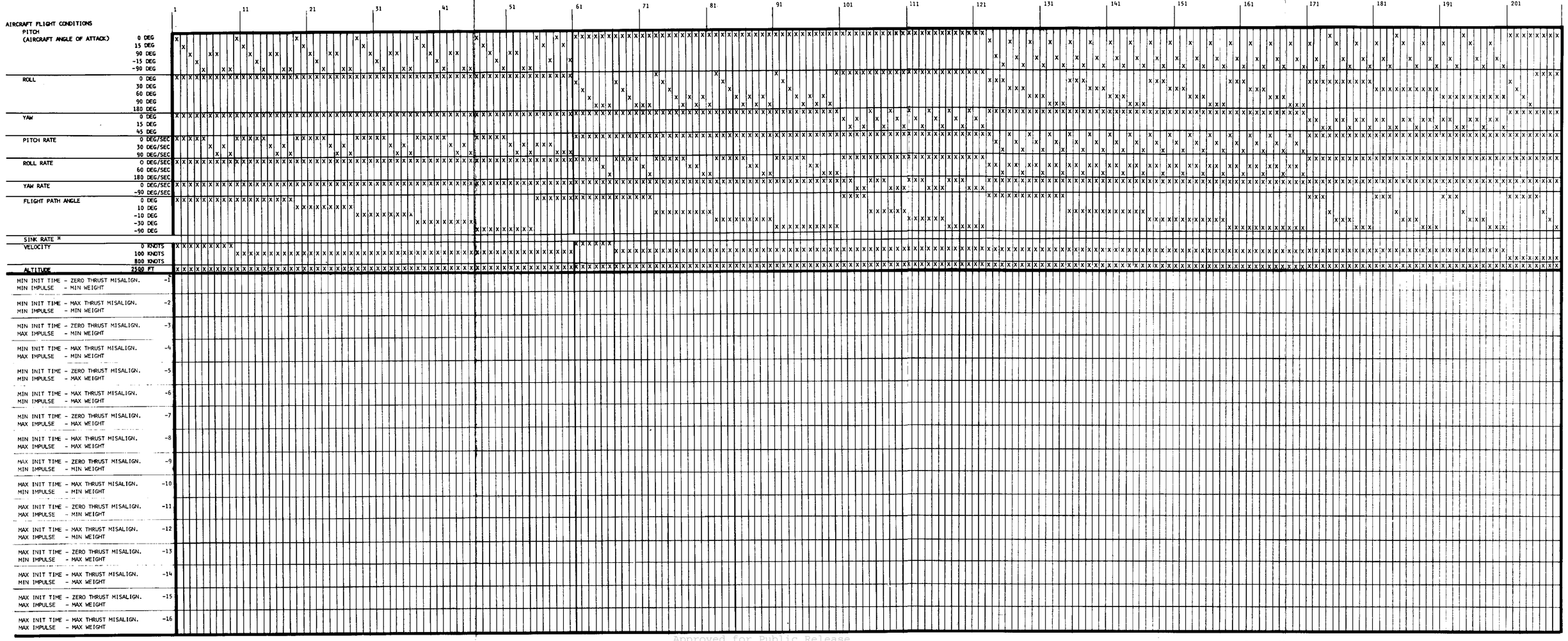

Approved for Public Release

Figure 21

Contrails

is treated as a combination of velocity and flight path angle. Aircraft velocities of 0, 100 and 800 knots are applied. Safe emergency altitudes are derived as explained in Section V after initiating the emergency in each case at 2500 ft.

Minimum and maximum values of four escape concept physical parameters are combined to define the sixteen conditions describing each system for each aircraft maneuver case. A maximum (3.2 seconds) and a minimum (2.4 seconds) value of the initiation time (man-machine reaction time) are applied. Rocket thrust and rocket burning time are input as maximum and minimum impulse curves, the maximum thrust-versus-time curve having the total impulse equivalent to a 200°F firing and the minimum thrust-versus-time curve equivalent to a -65°F firing. The CG - thrust vector static misalignment is introduced as both zero and maximum, the latter as tri-planar. While the offset is assumed to remain constant for the high mass inset cabin and nose capsules during the ejection process, except for rocket nozzle erosion, the offset for the individual ejection seat and encapsulated seat shifts as the occupant's body slumps and is displaced relative to the seat and rocket thrust vector. The vector shift (3°) caused by erosion of the rocket nozzle during firing is also accounted for. The weights of each escape concept are input as minima and maxima, which are sufficient to generate a comprehensive view of the differences in recovery parameters due to weight change.

Approved for Public Release

Contrails

SECTION III

PARAMETRIC COMPUTER PROGRAM

1. COMPUTER PROGRAM

NAR-PACEC is a six-degree-of-freedom computer program, written in FORTRAN IV language, that calculates the attitude and position-time history of a rigid body moving through three-dimensional space in accordance with the physical laws of motion. (Refer to figures 22 and 23). The program, reference 23, considers the forces produced by propulsive thrust, friction, aerodynamic characteristics, gravity and retardation devices, and is divided into five phases to facilitate calculation and to permit, with relative ease, modification to incorporate new ideas or concepts.

The program accommodates four different escape concepts and related aerodynamic tables, impulse curves and parachute data and is a successor to an older NAR machine language six-degree-of-freedom program. The present program allows the second escape concept a second set of aerodynamic tables for an escape body with stabilization devices erected following ejection. Input data for the program are listed in Table IV.

The Phase 0 condition encompasses aircraft motions prior to initiation of the ejection system. The time period extends from the instant of emergency until ejection initiation. The aircraft is assumed in steady-state, non-accelerative motion.

For structurally guided escape bodies only, Phase I commences at the initiation of escape and terminates when the middle pair of rollers of a three-pair set leaves the rails. The rails are assumed to be channels so that the reactions of the rollers may be in either of two directions perpendicular to the rail axis. Four combinations of reaction forces are possible. The combination generating the greatest friction (retarding force) is selected. A friction force attributable to lateral reactions on the rollers is also calculated. The emerging partial frontal area of the escape system is continually calculated by multiplying the total area by the ratio of the exposed instantaneous partial chord to the body total chord.

For structurally guided escape bodies only, Phase II begins as the middle pair of rollers leaves the rails and ends as the last pair departs. As in Phase I, the reaction force on the rollers may be in either of two directions perpendicular to the rail axis. The reaction force is computed first assuming it acts in the direction opposing the drag force. If the quantity computed is negative, then the reaction force is assumed to act in the opposite direction and the equations are changed accordingly. With one pair of rollers remaining in the rails during Phase II, the seat is free to rotate. If the fuselage-supported catapult tube is still attached to the seat, the bending moment is computed with change in pitch angle.

Phase III commences when the escape unit becomes free of the aircraft. For those escape bodies having rails and rollers, Phase III starts at the

Approved for Public Release

Contrails

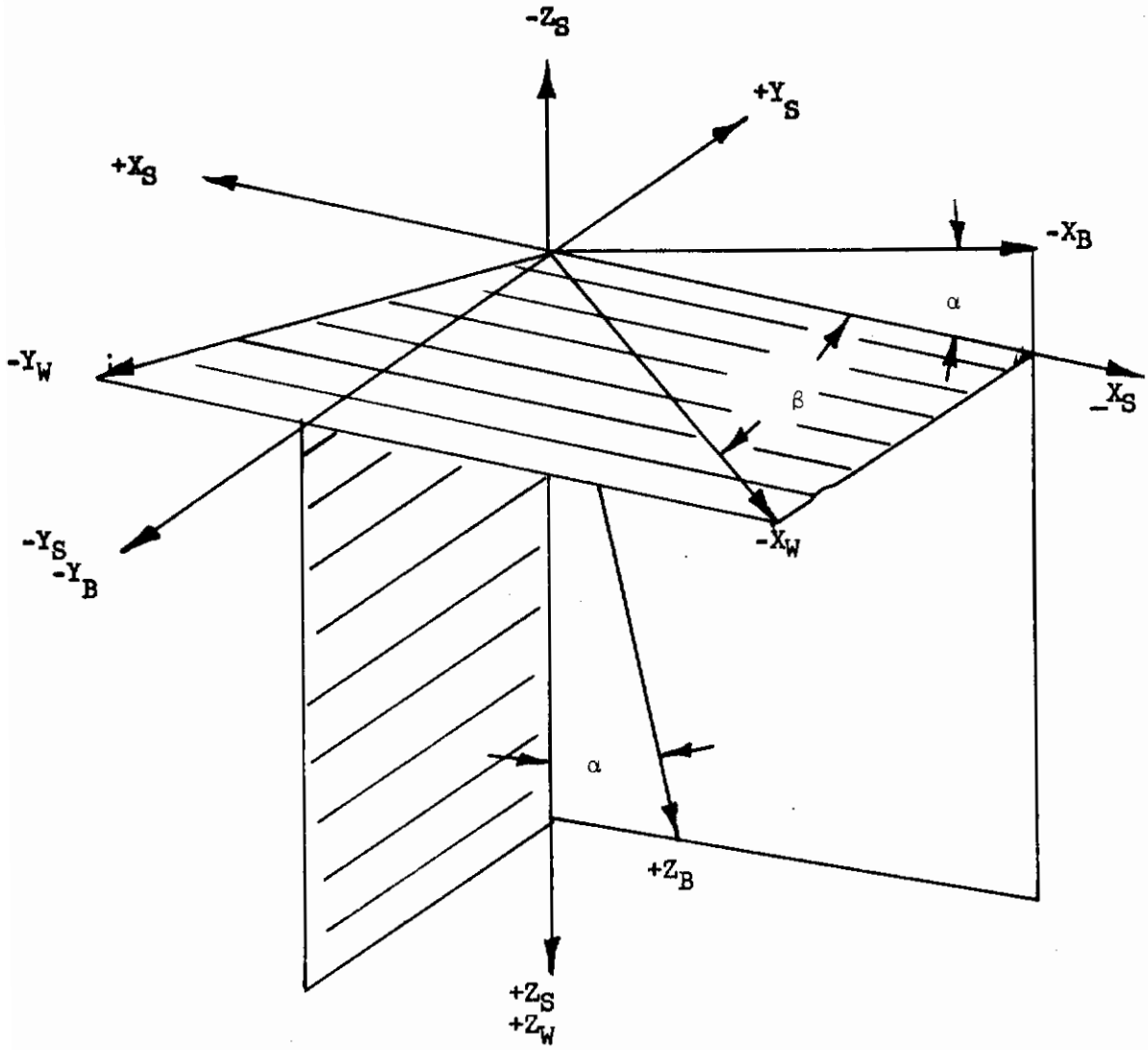

FIGURE 22 - WIND AXIS, STABILITY AXIS & BODY AXIS REFERENCE SYSTEM

Approved for Public Release

Contrails

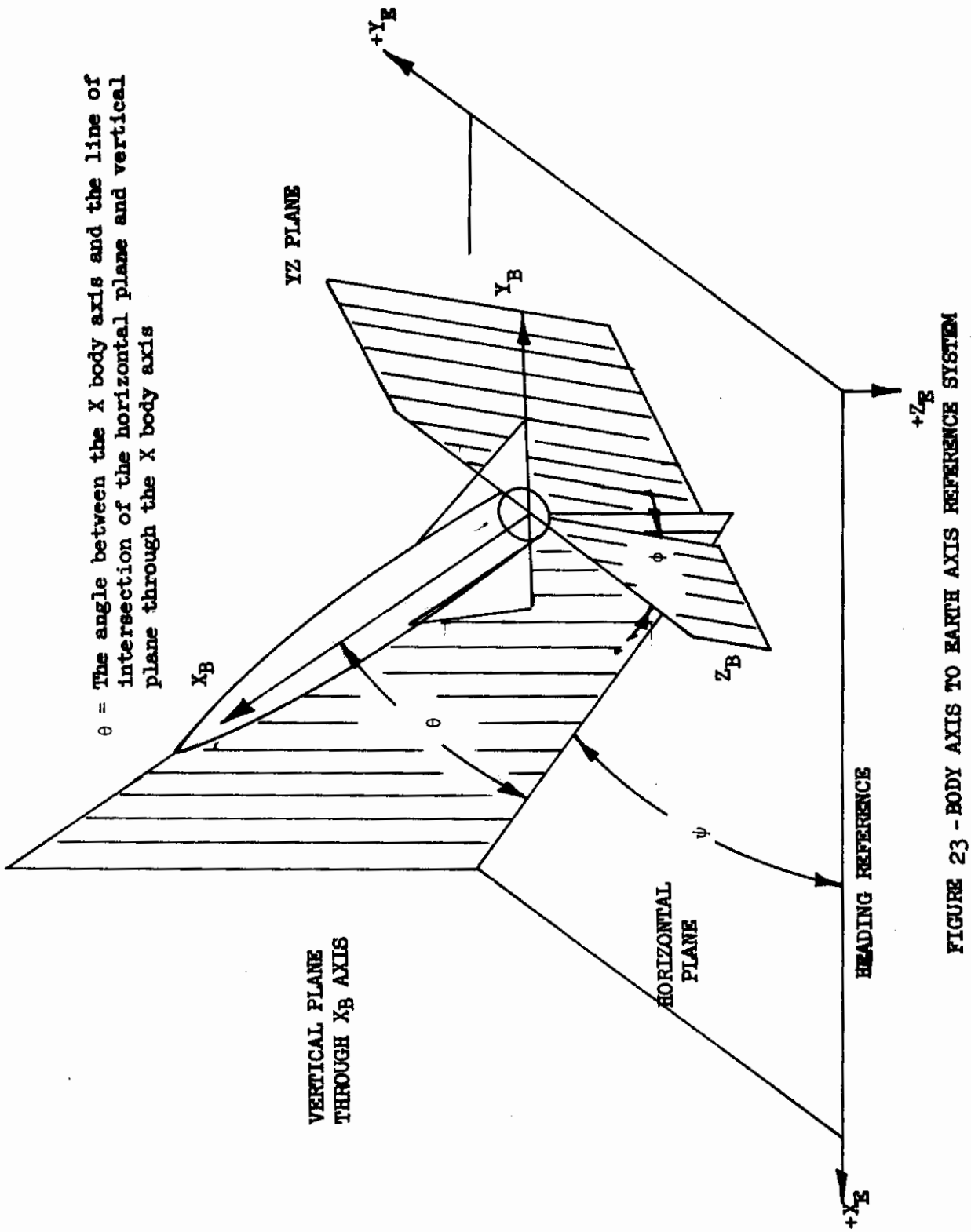

FIGURE 23 - BODY AXIS TO EARTH AXIS REFERENCE SYSTEM

Approved for Public Release

Contrails

TABLE IV

COMPUTER PROGRAM INPUT DATA

Main Program	Description
	Selection of three or six degrees of freedom
	Selection of no thrust misalignment or thrust misalignment
	Selection of no plot or plot
	Selection of no print or print
	Configuration now running 1, 2, 3, or 4
	Last configuration, this case
	Selection of minimum or maximum thrust
	Pitching velocity about the Y body axis - (q)
	Angle of attack - (α) (see figure 22)
	Flight path angle of A/C - (γ)
	Angle of side slip - (β) (see figure 22)
	The angle between the heading reference in the horizontal earth plane and the line of intersection of the horizontal plane and the vertical plane through the X body axis (ψ) (see figure 23)
	The angle between the Z body axis and the line of intersection of vertical plane in which θ is measured and a plane through the YZ body axis - (θ) (see figure 23)
	Rolling velocity about the X body axis
	Yawing velocity about the Z body axis
	Time differential between the occurrence of an emergency and actuation of the escape system
	Weight of ejected object prior to rocket burnout
	Weight of ejected object after rocket burnout
	Weight of ejected object at time of parachute deployment
	Time at which rocket thrust goes to zero
	Angle whose sine = parallel CG shift/perpendicular CG shift
	Distance CG shifts parallel to rail axis during stabilization system deployment
	Distance CG shifts perpendicular to rail axis during stabilization system deployment
	Moment of inertia with respect to the X axis before stabilization system deployment
	Moment of inertia with respect to the Z axis before stabilization system deployment
	Moment of inertia with respect to the Y axis before stabilization system deployment
	Moment of inertia with respect to the XZ axis before stabilization system deployment
	Moment of inertia with respect to the X axis after stabilization system deployment
	Moment of inertia with respect to the Z axis after stabilization system deployment
	Moment of inertia with respect to the Y axis after stabilization system deployment
	Moment of inertia with respect to the XZ axis after stabilization system deployment
	Moment of inertia with respect to X axis constant due to body slump

Approved for Public Release

Contrails

TABLE IV - Continued

Moment of inertia with respect to Z axis constant due to body slump
Moment of inertia with respect to Y axis constant due to body slump
Constant for sizing used in lift equation
Constant for sizing used in drag equation
Coefficient of friction between the rollers and the rails due to side load
Time at which stabilization device starts
Time of deployment of a stabilization device
Selection configuration symbol for plotting
Call for symbol to indicate termination of catapult thrust on plots
Call for symbol to indicate beginning of free fall in plots
Call for symbol to indicate termination of rocket thrust on plots
Call for symbol to indicate recovery parachute deployment on plots
Constant factor used to determine CG shift due to "G" forces
Constant factor used to determine CG shift due to "G" forces
Initial A/C altitude
Initial A/C velocity
Time at which program stops
Altitude at which program stops
Aerodynamic chord of ejected object
Aerodynamic span of ejected object
Distance parallel to rail axis from lower roller to initial CG of ejected object
Perpendicular distance from initial CG of ejected object to rail axis
Moment arm of catapult or rocket thrust
Distance of CG off sagittal plane
Distance between the CG and the thrust line perpendicular to the sagittal plane
Angle of catapult thrust forward of rail axis
Angle of rocket thrust forward of rail axis in sagittal plane
Angle of rocket thrust off sagittal plane
Angle of spine aft of A/C vertical axis
Angle of seat back aft of A/C vertical axis
Angle of rail axis aft of A/C vertical reference axis
Distance between top and bottom rollers
Distance from lower roller to middle roller
Distance from lower roller to top of rail
Distance from top roller to top of rail
Distance, parallel to rails, that ejected object moves before catapult stripoff
Reference area
Distance from Z axis to Point A perpendicular to Z axis
Distance from X axis to Point A perpendicular to X axis
Distance from X axis to Point A perpendicular to Y axis
Distance along Z axis between CG of aircraft and CG of escape system
Distance along X axis between CG of aircraft and CG of escape system
Selection of top or aft mounted parachute for first parachute
Selection of top or aft mounted parachute for second parachute
Selection of top or aft mounted parachute for third parachute
Selection of top or aft mounted parachute for fourth parachute
Coefficient of friction between the rollers and the rail
Load factor on A/C perpendicular to flight path

Approved for Public Release

Contrails

TABLE IV - Continued

Time at which first drag parachute is deployed
Time at which second drag parachute is deployed
Time at which recovery parachute is deployed
Automatic deployment altitude for main recovery parachute
Factor used to calculate bending of catapult tube
Bending moment of catapult tube when yield point has been exceeded
Incremental time during Phase 0
Incremental time during phase 1
Incremental time during phase 2
Incremental time during phase 3
Incremental time during phase 4
Thrust balancing factor
Code for three or six degree of freedom
Parachute attachment distance OE (figure 24)
Parachute attachment distance OK (see figure 24)
Parachute attachment angle OKL (see figure 24)
Parachute attachment distance FK (see figure 24)
Parachute attachment distance GK (see figure 24)
Parachute attachment distance OA (see figure 24)
Parachute attachment distance OI (see figure 24)
Parachute attachment distance OD (see figure 24)
Parachute attachment distance OF (see figure 24)
Parachute attachment distance OG (see figure 24)
Parachute attachment distance GC (see figure 24)
Parachute attachment distance EL (see figure 24)
Parachute attachment distance GE (see figure 24)
Parachute attachment distance FE (see figure 24)
Parachute attachment distance EI (see figure 24)
Parachute attachment angle $\alpha 1$ (see figure 24)
Parachute attachment angle $\alpha 2$ (see figure 24)
Parachute attachment angle $\beta 1$ (see figure 24)
Selection of no DART or DART subroutine
Selection of no STAPAC or STAPAC subroutine
Selection of no STAPAC or STAPAC subroutine in pitch plane
Selection of no STAPAC or STAPAC subroutine in roll plane
Selection of no STAPAC or STAPAC subroutine in yaw plane
Distance from A/C CG to A/C DART attach point along A/C X axis
Distance from A/C CG to A/C DART attach point along A/C Y axis
Distance from A/C CG to A/C DART attach point along A/C Z axis
Time delay from start of Phase III to start of STAPAC vernier rockets

DART Subroutine

An integer defining the system configuration
Angle between the seat X-axis and the radius to forward bridle pivot
Angle between seat X-axis and radius to apex of bridle
Angle between seat X-axis and radius to aft bridle pivot
Radius from seat origin to forward bridle pivot
Radius from seat origin to apex of bridle
Radius from seat origin to aft bridle pivot
An array describing DART brake line force versus length of line paid out

Approved for Public Release

Contrails

TABLE IV - Continued

	Attachment distance OE, OK, OKL, FK, GK, OA, OI, OD, OF, OG, GC, EL, GE, FE, EI, A1, A2 & B1 (similar to parachute attachment) - these 18 items required only when both bridles are flexible
STAPAC Subroutine	
	An array describing the vernier rocket thrust/time relationship
	An array describing the biasing spring torque about the gimbal axis
	An array describing the mechanical advantage of the gimbal/vernier rocket interconnecting linkage
	Angular position of the gyro gimbal relative to the caged position
	Angular velocity of the gyro gimbal
	Pitching angular velocity of the ejection seat
	Angular velocity of the gyroscope wheel about its spin axis
	Inertia of the gyroscope wheel about its spin axis
	Inertia of the wheel, gimbal and connecting linkage about the gimbal axis
	Inertia of the vernier rocket about its centerline of rotation prior to ignition
	Inertia of the vernier rocket about its centerline of rotation at the completion of rocket burning
	Angle at which the gimbal is stopped when rotating the vernier rocket toward the position of maximum aft pitching moment
	Angle at which the gimbal is stopped when rotating the vernier rocket toward the position of maximum forward pitching moment
	Factor of efficiency for a rotational collision with extremes of vernier rocket angular travel
	Load at which the rotational stop begins to yield
	Displacement of the rotational stop at load P
	Simulated thrust force at which rotational friction of the system has been measured
	The rotational friction of the system at simulated thrust
	The rotational friction of the system at zero vernier rocket thrust
	The effective misalignment of the vernier rocket thrust line relative to the rotational centerline of the vernier rocket
	Distance from the dynamic center of gravity of the ejected system to the centerline of the vernier rocket rotation
	Angle between the vernier rocket thrust line in the zero position and a line from the vernier rocket centerline of rotation to the dynamic center of gravity of the ejected system
	Angle between the horizontal seat reference plane and a line passing from the dynamic center of gravity to the vernier rocket centerline of rotation
	Flag to determine mode of interpolation for the biasing spring
	Flag to determine mode of interpolation for the vernier rocket thrust
	Flag to determine mode of interpolation for the linkage
	Flag to determine mode of interpolation for the gimbal angle
	Flag for determining rate sensitive only or rate and position sensitive

Approved for Public Release

Contrails

termination of Phase II. For escape systems with no rails and rollers, Phase III commences at the initiation of ejection. For convenience, Phase III terminates and Phase IV commences at the initiation of the final recovery parachute.

The program accommodates a maximum of three parachutes and if required can cause the last parachute, normally the recovery parachute, to shift from back-mounted to top-mounted. The initiation of parachute deployment for both drag and recovery parachutes may be introduced at any desired time.

Parachute drag area (C_DS) is input as a function of distance traveled through space. (See figures 5 to 9, Section II.) Vehicle attachment is simulated by a four-point geometrical system (figure 24) with the forces and moments calculated in a separate subroutine.

Thrusts for the catapult and rocket are individual curve inputs as time functions. (See figures 16 to 19, Section II.) The program accommodates two catapult and two rocket curves per system. For those systems utilizing both catapult and rocket, the catapult curve is read initially and terminates at strip-off. At this point in time the abscissa of the rocket curve is shifted and the rocket thrust is read until rocket cutoff time. For systems utilizing only the rocket, the distance that the ejected object moves parallel to the rails before catapult strip-off is set to a small negative value and only the rocket curve is read.

The program contains provisions for the total system CG to shift due to slump of the individual crew member. The shift is a function of the "G" forces and is assumed to be along the sagittal plane.

2. PROGRAM OUTPUT

A listing of the main program output may be found in Table V. For cases run in only three-degrees-of-freedom, the first 26 items are output; for six degrees, the entire listing is output. Those items appended by an asterisk (*) are oriented in the earth reference system.

The program provides for three methods of producing the output: (1) Numerical printout; (2) SC-4020 (cathode-ray tube); and (3) Benson-Lehner graphical.

The numerical printout is the standard operation mode and produces printed output that consists of a listing of the input and a time history output in standard decimal form. This output mode may be selected by input item 3. (Refer to Table IV.)

The SC-4020 output is optional and may be selected by input item 4. (Refer to Table IV.) Selection of this output mode produces an output tape which is utilized by the Stromberg-Carlson plotter (SC-4020) in projection of the data onto the face of a cathode-ray tube. The image produced can then be photographed by any of a number of cameras and the film utilized in the

Approved for Public Release

Approved for Public Release

POINTS A, B, C, AND D ARE LINE ATTACHMENTS
AND POINT E IS THE CONFLUENCE POINT.

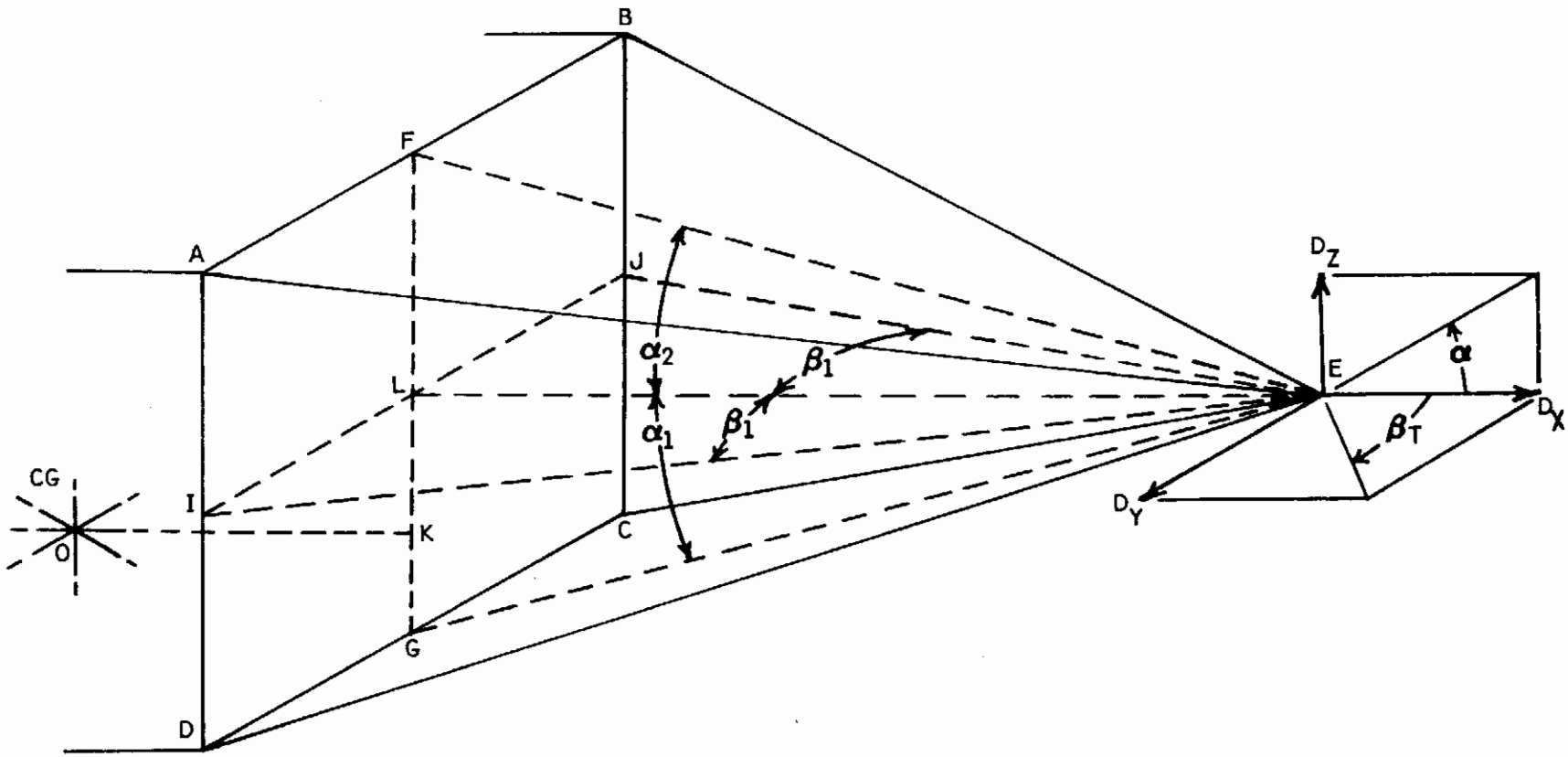

FIGURE 24 - PARACHUTE ATTACHMENT GEOMETRY

Confidential

Contrails

TABLE V

PROGRAM OUTPUT

Item	Description
1	Mach Number
2	Thrusting Moment (ft-lb)
3	Dynamic Pressure (lb/ft^2)
4	Total Velocity of Escape System (ft/sec)
5	Distance Along "X" Axis (ft) *
6	Velocity Along "X" Axis (ft/sec) *
7	Acceleration Along "X" Axis (ft/sec^2) *
8	Height Above Sea Level (ft) *
9	Velocity Along "Z" Axis (ft/sec) *
10	Acceleration Along "Z" Axis (ft/sec^2) *
11	Angle of Attack (deg)
12	Euler Angle Theta as Regards Body Direction (deg) *
13	Flight Path Angle (deg) *
14	Total Distance Traveled Along Flight Path (ft)
15	Acceleration of CG - "G"
16	Acceleration of Arbitrary Point - "G"
17	Pitching Velocity (deg/sec)
18	Pitching Acceleration (deg/sec^2)
19	Pitching Moment (ft-lb)
20	Damping Moment in Pitch (ft-lb)
21	Angle Theta as Regards "G" Force at CG (deg)
22	Angle Theta as Regards "G" Force of Arbitrary Point (deg)
23	Total Lift (lb)
24	Total Drag (lb)
25	Rolling Moment (ft-lb)
26	Damping Moment in Roll (ft-lb)
27	Angle Psi as Regards "G" Force at CG (deg)
28	Angle Psi as Regards "G" Force at Arbitrary Point (deg)
29	Rolling Velocity (deg/sec)
30	Rolling Acceleration (deg/sec^2)
31	Yawing Moment (ft-lb)
32	Yaw Damping Moment (ft-lb)
33	Angle Phi Regarding "G" Force at CG (deg)
34	Angle Phi Regarding "G" Force at Arbitrary Point (deg)
35	Yawing Velocity (deg/sec)
36	Yawing Acceleration (deg/sec^2)
37	Lateral Distance (ft) *
38	Velocity Along "Y" Axis (ft/sec) *
39	Acceleration Along the "Y" Axis (ft/sec^2) *
40	Side Slip Angle (deg)
41	Euler Angle Psi as Regards Body Direction (deg) *
42	Euler Angle Phi as Regards Body Direction (deg) *

* Denotes earth reference system (refer to figure 23).

Approved for Public Release

Contrails

production of the desired output print. The output consists of a title page, graphs and numerical data printout. Each page of the output contains a title strip which identifies the run conditions and two figures in the right margin of this title strip can also be utilized to identifying the particular run.

The title page for the SC-4020 lists the nine aircraft conditions at the time of the emergency (0.00 second) and at the time of initiation of ejection. The aircraft conditions listed are: Height; Velocity; Aircraft pitch; Aircraft pitch rate; Aircraft roll; Aircraft roll rate; Aircraft yaw; Aircraft yaw rate; Flight path angle and Time.

The graphical output consists of 24 graphs for three-degree-of-freedom computer runs or 42 graphs for six-degree-of-freedom computer runs. The abscissa of each of the graphs is time in seconds. The ordinate for the graph (refer to Table V) consists of items 1 through 24 for the three-degree-of-freedom runs and items 1 through 42 for the six-degree-of-freedom runs.

Data for each of the four escape concepts being analyzed appear on each of the graphs, providing individual concept information as well as comparison of all four if desired. Letters A through D identify plots for the four escape concepts, (A) ejection seat, (B) encapsulated ejection seat, (C) inset capsule, and (D) nose capsule.

The flight condition parameters of the aircraft between the time of the emergency (0.00 seconds) and the time of initiation of ejection are straight-line functions. In order to present the largest scale possible for the abscissa of the graphs, the aircraft conditions at the beginning and end of the period are plotted and the time span is removed from the graph. The number of parameters which are printed on each page can be varied from one to three.

The last portion of the SC-4020 output is composed of the numerical printout of the data. The frequency of printing time-point data within one condition can be varied from 1 to 200.

A link described in reference 24 may be appended to the program to read the output data to be plotted and prepare a magnetic tape in a form which can be used to control a Model J Benson-Lehner Plotter to yield the graph-sheet curves desired. This routine plots one straight-line sectional (linear point connection) curve per 8½-by-11-inch graph sheet, draws the axes, sequence-identifies, and numerically labels the axes.

Approved for Public Release

Contrails

SECTION IV

SUBROUTINES

1. DIRECTIONAL AUTOMATIC REALIGNMENT OF TRAJECTORY (DART)

The Stencel DART stabilization system, used on ejection seats, is a device which stabilizes the seat in pitch and roll. The system is composed of: (1) The "DART line" consisting of four braided nylon lines, the lower parts of which are encased in a nylon tube; (2) The bridle, consisting of an aluminum tube "V" frame, pivoted at the forward edge of the seat bottom and having an eye through which the DART line passes, and a steel cable which joins the eye of the forward bridle element to two points on the aft edge of the seat bottom; and (3) Two friction brake assemblies mounted on the seat bottom. (Reference 25)

Before ejection, the DART system is stowed, with the bridle folded up against the seat bottom and secured with a break line. The lower (covered) part of the DART line is attached by its fitting to the cockpit floor and stowed in the pockets of the stowage bag, which is attached to the DART line cover and inserted between the bridle and the seat bottom. The remainder of the DART line passes through the eye of the bridle, and divides, two lines going to each brake assembly. The lines pass through the brakes and the remaining length is stowed in pockets attached to the seat bottom.

Upon ejection, the bridle is extended and the lower part of the DART line (free length) is extracted from its stowage, without imposing any significant load on the seat. When the seat reaches a sufficient distance from the aircraft to completely withdraw the free length from its stowage, the line becomes taut and begins to be drawn through the brakes. These impose a load on the line, and, depending on the position of the seat, a correcting moment is applied to the seat. When the upper ends of the DART line are withdrawn from the brakes, the line separates from the seat.

In developing a DART configuration for a particular seat, the three parameters (1) Average DART force (combined brake load), (2) Free length, and (3) Runout length, are varied to obtain the desired combination of trajectory control and rotation rate. The DART system is depicted in figure 25.

The force and moment equations for the DART subroutine are as follows:

$$F_X = (XATTA - XATTB)(FD)/L \quad (1)$$

$$F_Y = (YATTA - YATTB)(FD)/L \quad (2)$$

$$F_Z = (ZATTA - ZATTB)(FD)/L \quad (3)$$

$$M_X = -F_Y(ZATTB) + F_Z(YATTB) \quad (4)$$

$$M_Y = F_X(ZATTB) - F_Z(XATTB) \quad (5)$$

$$M_Z = F_Y(XATTB) - F_X(YATTB) \quad (6)$$

Approved for Public Release

Contrails

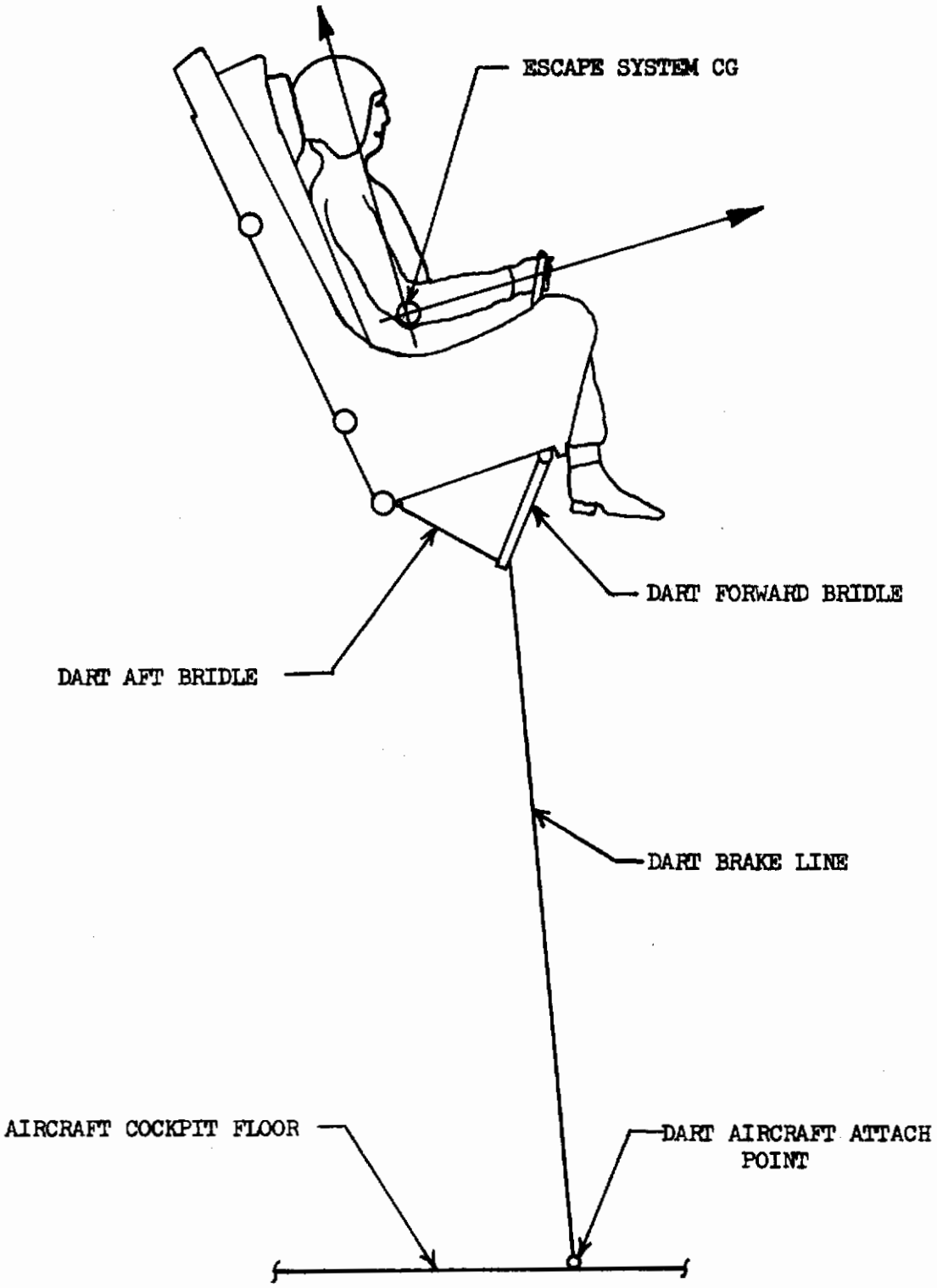

FIGURE 25 - DART SYSTEM

Approved for Public Release

Contrails

Where:

$$L = \sqrt{(XATTA - XATTB)^2 + (YATTA - YATTB)^2 + (ZATTA - ZATTB)^2}$$

FD is the DART brake force

XATTA, YATTA and ZATTA are the true distances in the escape system axis system between the escape system CG and the DART attach point on the A/C and are calculated by the main program

$$\delta 6 = \pi - \text{ARCTAN } (ZATTA - RC \text{ SIN } \delta_C)/(- XATTA + RC \text{ COS } \delta_C)$$

$$DD = \sqrt{(ZATTA - RC \text{ SIN } \delta_C)^2 + (- XATTA + RC \text{ COS } \delta_C)^2}$$

$$XATTB = XATTA - DD \text{ COS } \delta_6$$

$$ZATTB = ZATTA - DD \text{ SIN } \delta_6$$

YATTB = 0.0 = Bridle confluence point is on sagittal plane

For the specialized condition where both bridles are flexible, the force and moment equations are similar to those describing parachute attachment.

The effect of the DART system upon an ejection seat type of escape system is shown in figure 26. The aircraft conditions at emergency were: V = zero Kn, upright aircraft. The seat CG - rocket thrust offset was 0.16 ft. (Reference 25)

2. GYRO-CONTROLLED VERNIER ROCKET STABILIZATION (STAPAC)

A unique and simple system developed by the Douglas Aircraft Company and referred to as STAPAC, is utilized to stabilize an ejection seat against conditions of CG-main rocket thrust misalignment and aerodynamically induced pitching moments. It is operative from the time the seat leaves the guide-rails and burns for approximately 0.5 seconds. (Reference 25)

The system comprises a vernier rocket, a rate gyroscope, a spin-up/gimbal uncaging mechanism, a rocket ignition system, and interconnecting linkages and pneumatic lines. (Refer to figure 27.) The vernier rocket is ignited by a mechanically fired initiator.

The gyroscope is gimbaled about one axis only, providing a gyro which does not indicate position but is sensitive only to rotational rates. The rate gyro is mounted on the ejection seat with gyro wheel spin axis and gimbal axis oriented in a manner to sense only pitching motion of the ejection seat. The gyro inertia and design spin velocity are set to provide the required precessional torque to operate the vernier rocket. The rack which is used to spin the gyro up to speed also provides a gimbal caging function by indexing a slot in the gimbal structure. When the rack retracts to spin up the wheel, the gimbal is also uncaged. The mechanical linkage between the gyro and the vernier rocket transmits the rotational motion of the gimbal to the rocket. The pneumatic tubing channels gas from the spin-up mechanisms to the pin puller which actuates the rocket ignition system.

Approved for Public Release

Contrails

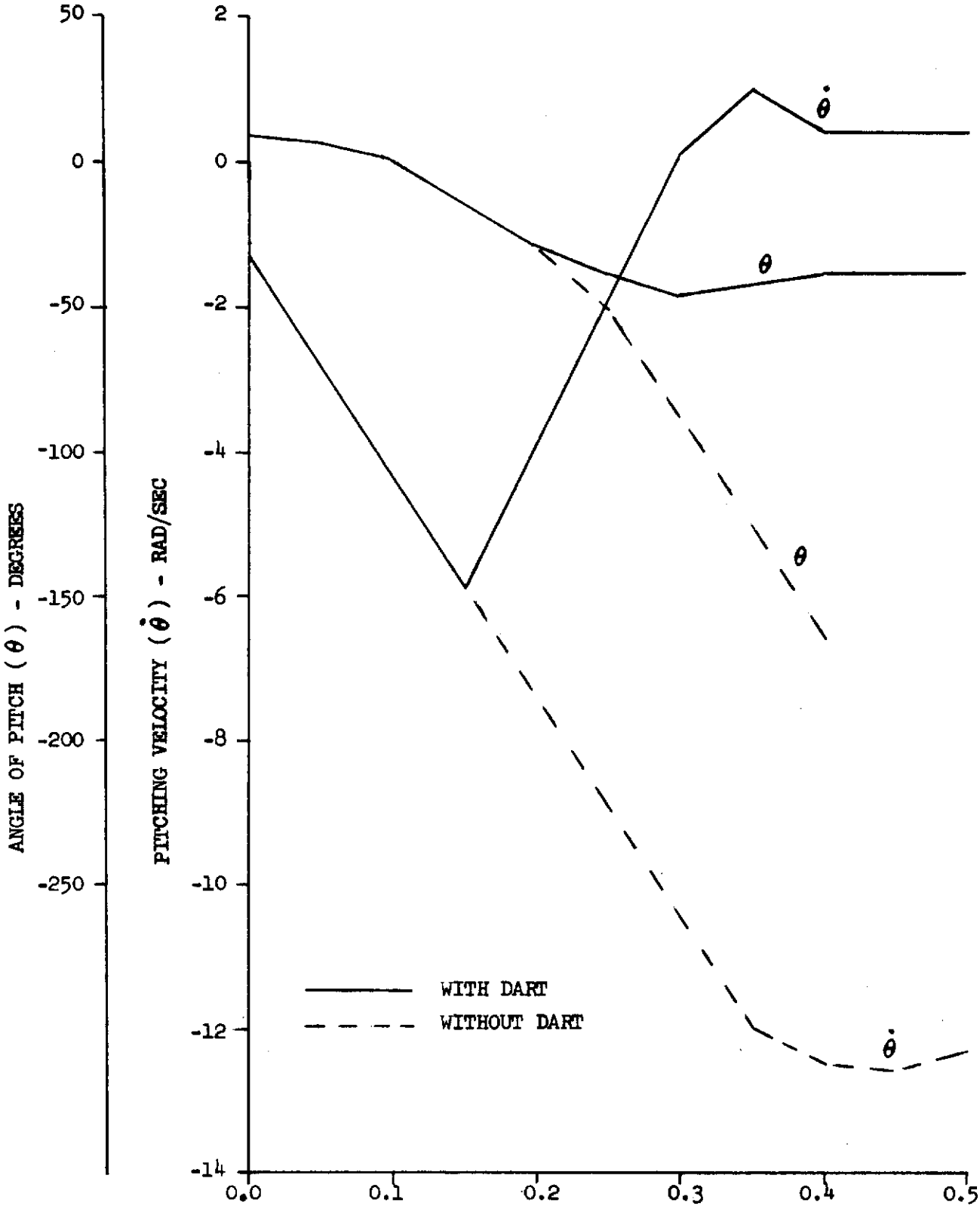

FIGURE 26. θ AND $\dot{\theta}$ VERSUS TIME FOR SYSTEM A WITH AND WITHOUT "DART"

Approved for Public Release

Contrails

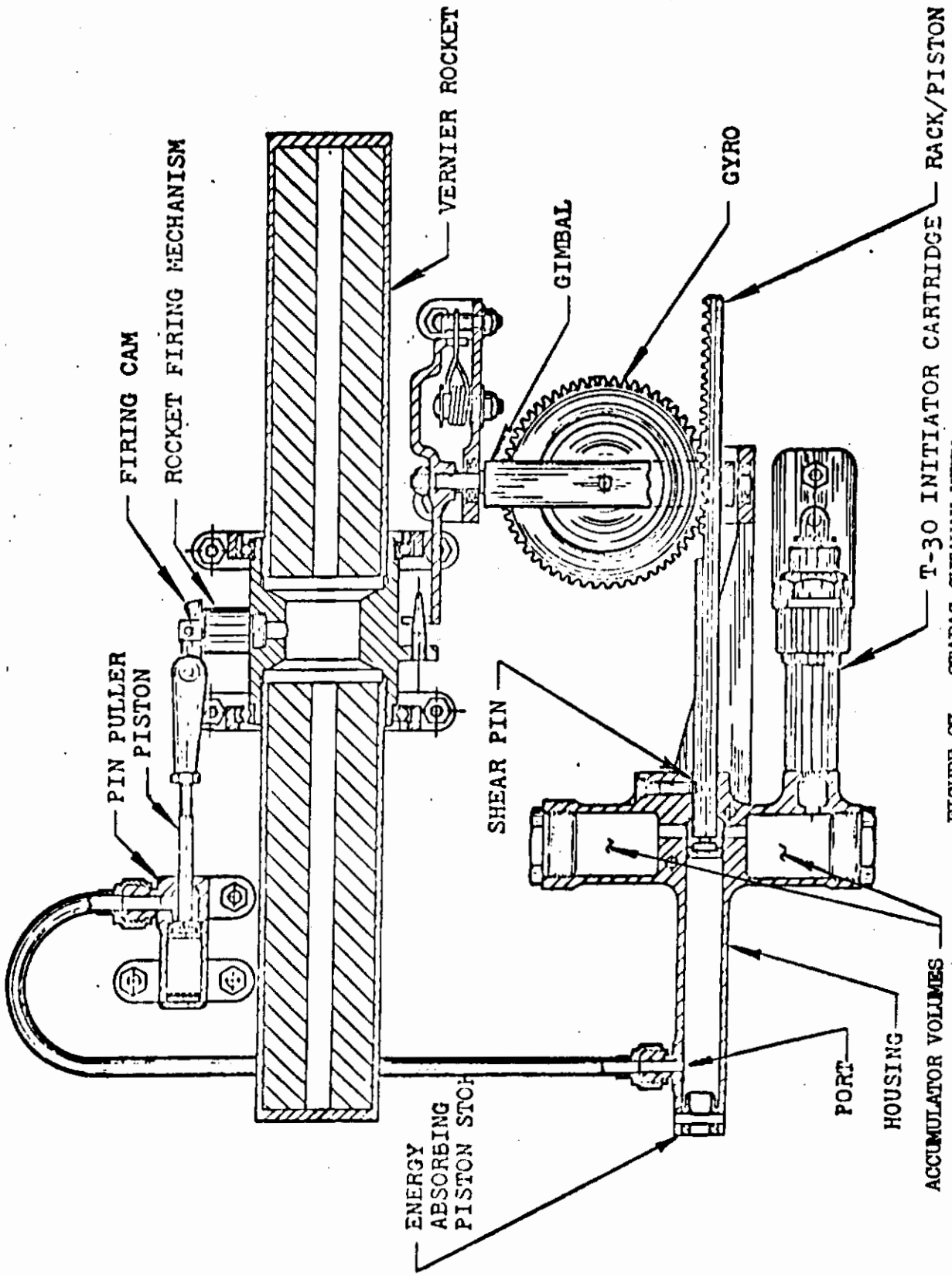

FIGURE 27 - STAPAC CUTAWAY VIEW

Approved for Public Release

Contrails

The NAR modified version included in this program provides for both rotational rates and escape system position, in all three axes. This is accomplished by providing a vernier rocket in each of three planes.

The force and moment equations for the STAPAC subroutine are as follows:

The STAPAC subroutine calculates two forces and one moment in a single plane.

$$F_X = FVAV \cos(THETA - PHIROC - \emptyset MEGO) \quad (13)$$

$$F_Z = FVAV \sin(THETA - PHIROC - \emptyset MEGO) \quad (14)$$

$$M_Y = (FVAV)(V_2)(\sin (PHIROC + \emptyset MEGO)) \quad (15)$$

Where:

FVAV = Vernier rocket thrust (16)

THETA, V_2 and ØMEGO are input variables and PHIROC is the angular position of the vernier rocket

Figure 28 compares the pitching, rolling and yawing velocities of an inset capsule with and without STAPAC under identical conditions. The initial aircraft conditions were q = 30 deg/sec; p = 30 deg/sec and V = 100 KN.

Approved for Public Release

Contrails

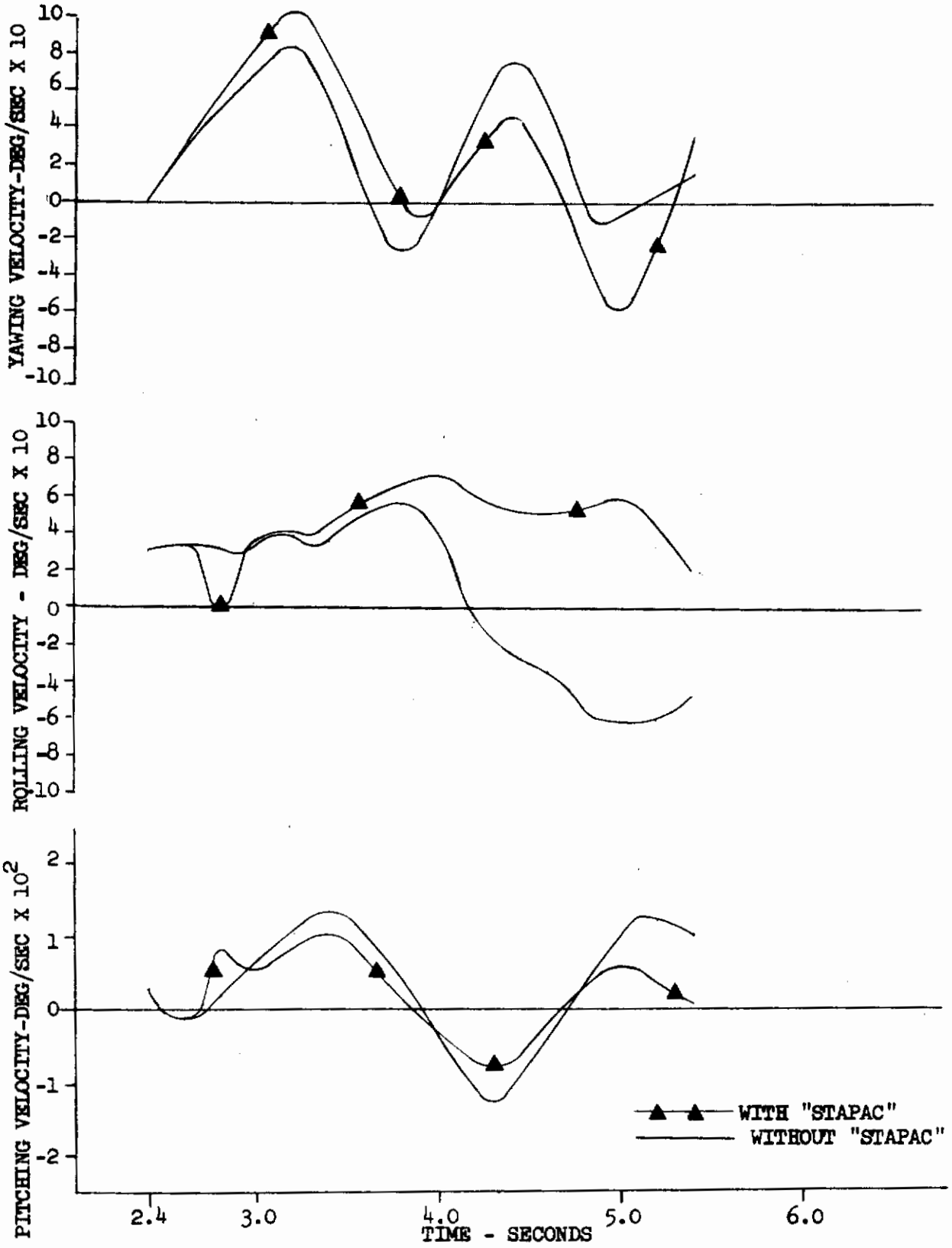

FIGURE 28 - PITCHING, ROLLING AND YAWING VELOCITY VERSUS TIME FOR SYSTEM C WITH AND WITHOUT "STAPAC"

Approved for Public Release

Contrails

SECTION V

ANALYSIS

1. SAFE EMERGENCY ALTITUDE ANALYSIS METHODS

The 3328 matrix ejections established the safe minimum altitude at which the aircraft may experience egress emergencies for each of the four escape concepts. Data for each of the 3328 ejections were scanned to determine the altitude (H_2) at which the recovery parachute descent velocity vector is $-90^\circ \pm 15^\circ$ and the vertical velocity for the escape body is less than five percent above the steady state terminal velocity of the parachute-escape body combination at the appropriate altitude. The minimum safe emergency altitude for the escape concept at a particular aircraft condition was established by finding the difference between the altitude at the emergency (2500 feet was selected for the computer program) and the altitude (H_2) which satisfies the escape body direction and velocity limits, and adding 100 feet, the selected minimum safe fully inflated parachute altitude. Safe Emergency Altitude = (Altitude at the Emergency - H_2) + 100 feet.

The computerized analysis program for determination of the Safe Emergency Altitude presented the following printed output:

Case

Condition

Concept

Safe Emergency Altitude

H_1 - Altitude at Ejection Initiation

α - Angle of Attack at Ejection Initiation

θ - Euler Angle of Ejection Initiation

ψ - Euler Angle of Ejection Initiation

ϕ - Euler Angle at Ejection Initiation

H_2 - Altitude at Descent Terminal Velocity

T - Time at H_2

X - Distance at T

Y - Distance at T

Total Distance Traveled to H_2

Terminal Velocity

Approved for Public Release

Contrails

2. ACCELERATION ANALYSIS METHODS

An analysis program (ANAL2) also examined whether human tolerance to acceleration is exceeded during the escape. The output is an IBM tape which is used by a Stromberg-Carlson 4020 printer plotter to convert the data to tabular and graphic plots. The tabular sheet presents the safe emergency altitude information previously listed and the following acceleration analysis information:

G Limits Not Exceeded

or

G Limits Exceeded

Time at Which Limits Were Exceeded

AXX - Acceleration, X Component

AYY - Acceleration, Y Component

AZZ - Acceleration, Z Component

AOS - Acceleration Limit, X Component

BOS - Acceleration Limit, Y Component

COS - Acceleration Limit, Z Component

Onset Limits Not Exceeded

or

Onset Limits Exceeded

Time at Which Limits Were Exceeded

AXX - Acceleration Onset, X Component

AYY - Acceleration Onset, Y Component

AZZ - Acceleration Onset, Z Component

AOS - Acceleration Onset Limit, X Component

BOS - Acceleration Onset Limit, Y Component

COS - Acceleration Onset Limit, Z Component

The graphical output of the analysis program contains crossplots of the four escape concepts for:

Acceleration of the Arbitrary Point - "G" Versus Time-sec

Approved for Public Release

Contrails

Euler Angle Theta Regarding "G" Force at Point Versus Time-sec

Euler Angle Psi Regarding "G" Force at Point Versus Time-sec

Euler Angle Phi Regarding "G" Force at Point Versus Time-sec

Acceleration of CG - "G" Versus Time-sec

Euler Angle Theta Regarding "G" Force at CG Versus Time-sec

Euler Angle Psi Regarding "G" Force at CG Versus Time-sec

Euler Angle Phi Regarding "G" Force at CG Versus Time-sec

a. Selection of Arbitrary Point (A)

The computer program determined the resultant acceleration at a point on or near the human body of the occupant or one of the occupants of the escape concept. The location of this point was accomplished as follows:

The experimentally determined tolerable limits of tumbling about the iliac crest as presented in reference 26 are shown in figure 29. This curve is a plot of revolutions per minute (rpm) versus duration (seconds) and established from 45 rpm for 600 seconds to 94 rpm for 3.2 seconds.

Tolerable limits of acceleration as presented in reference 27 are shown in figures 30, 31, and 32. These curves are plots of $\pm G_X$, $\pm G_Y$, and $\pm G_Z$ versus duration (seconds) and extend from .01 seconds to 2000 seconds.

It was desirable to select a point on or near the human body at which the acceleration limits alone could be used as a test of human tolerance. It was decided to compare the $-G_Z$ and rpm for like duration and select a point where application of the acceleration $-G_Z$ could result in a comparable rpm.

$$a = \frac{V^2}{(\text{radius})} = 32.2\ G \tag{17}$$

Therefore:

$$G = \frac{V^2}{(\text{radius})32.2} \tag{18}$$

Where:

$$V^2 = \left(\frac{2\pi(\text{radius})}{60}^2\ \text{rpm}^2\right) = .011(\text{radius})^2\ \text{rpm}^2 \tag{19}$$

Therefore:

$$G = \frac{.011(\text{radius})^2\text{rpm}^2}{(\text{radius})32.2} = .000341(\text{radius})\text{rpm}^2 \tag{20}$$

If we assume that the point lies along a line passing through the iliac crest and parallel to the spine then:

Approved for Public Release

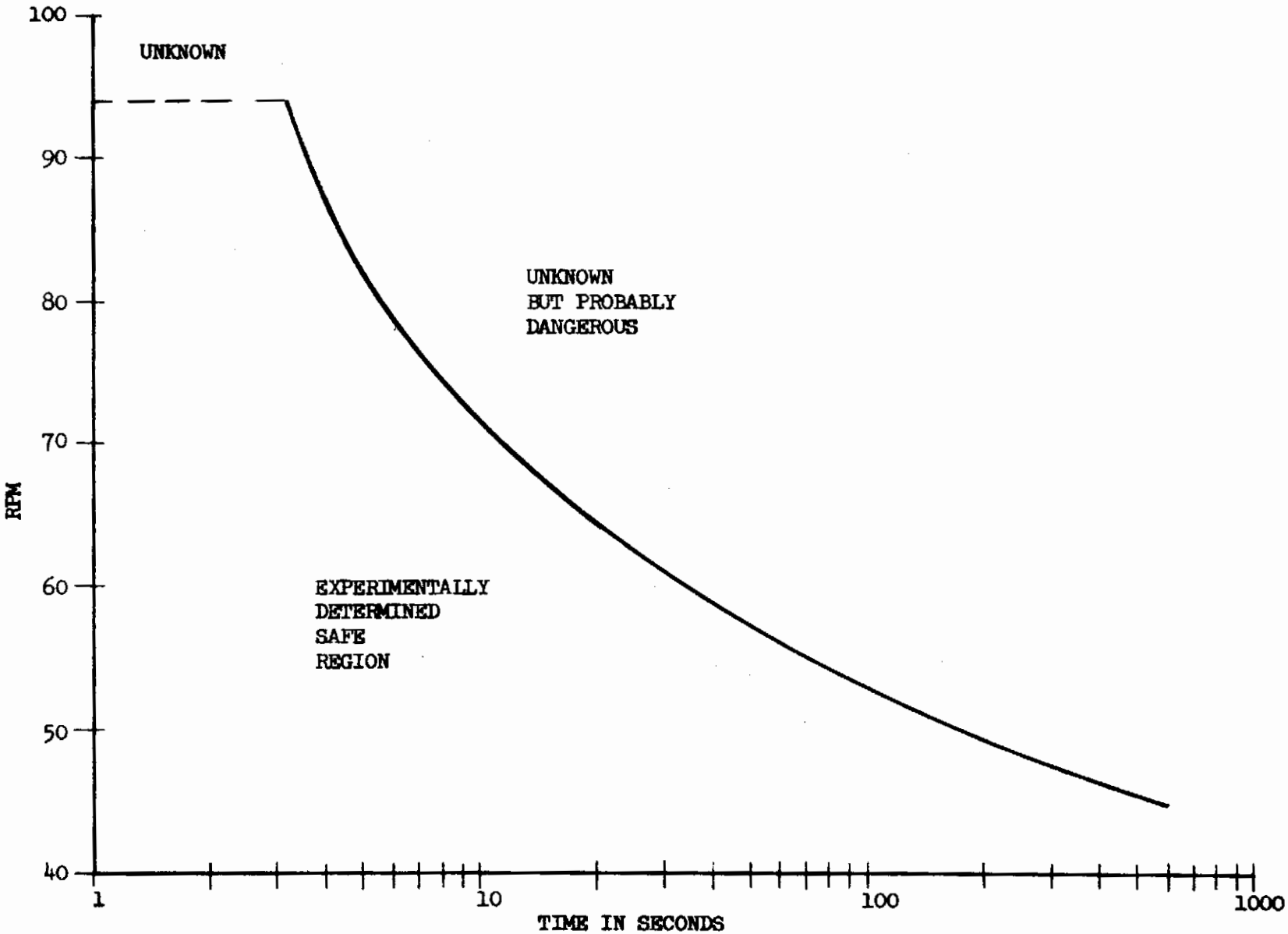

FIGURE 29 - HUMAN REACTION TO SIMPLE TUMBLING-CENTER OF ROTATION AT ILIAC CREST

Approved for Public Release

Contrails

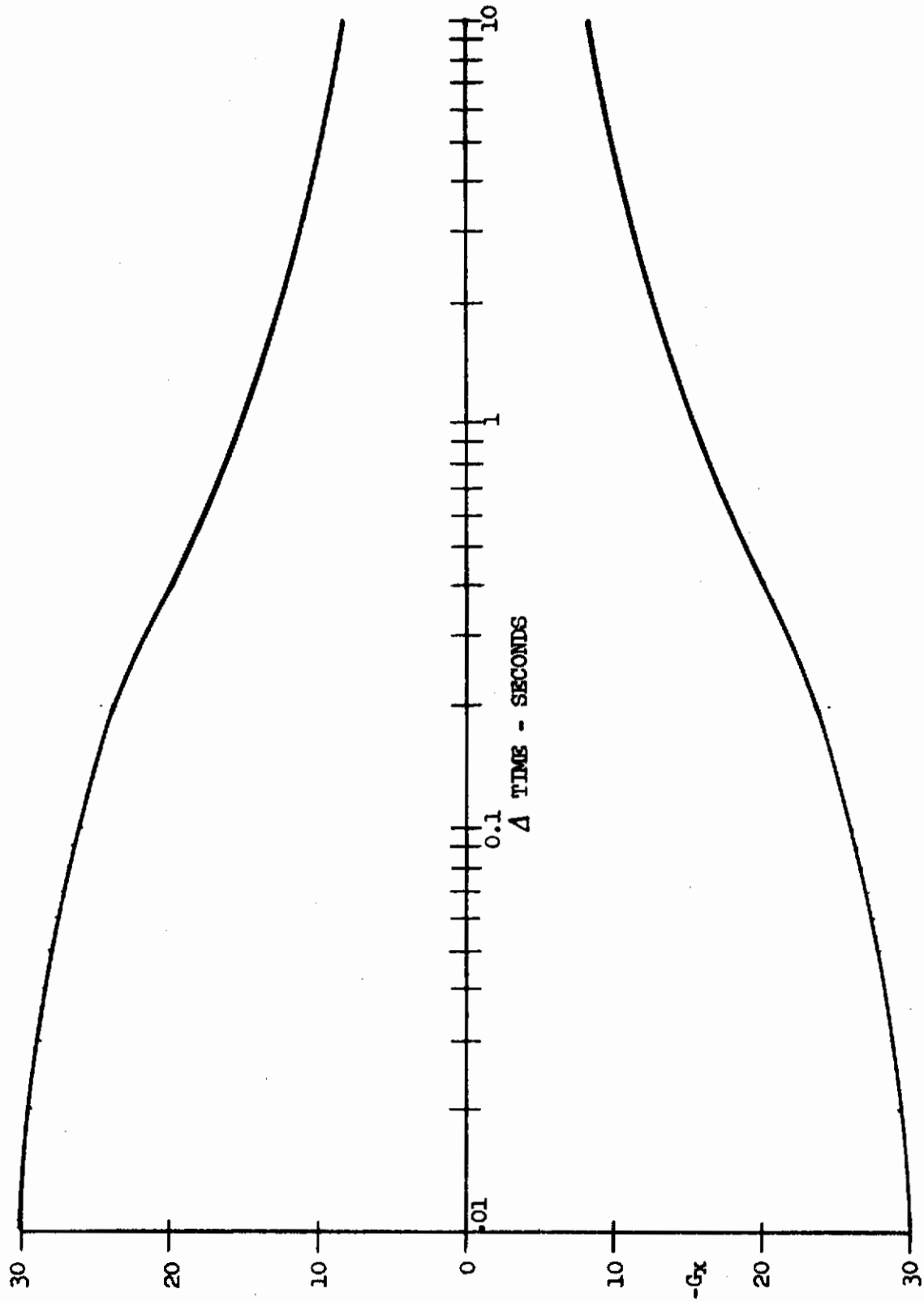

FIGURE 30 - ACCELERATION ($\pm G_x$) VERSUS Δ TIME

Approved for Public Release

Contrails

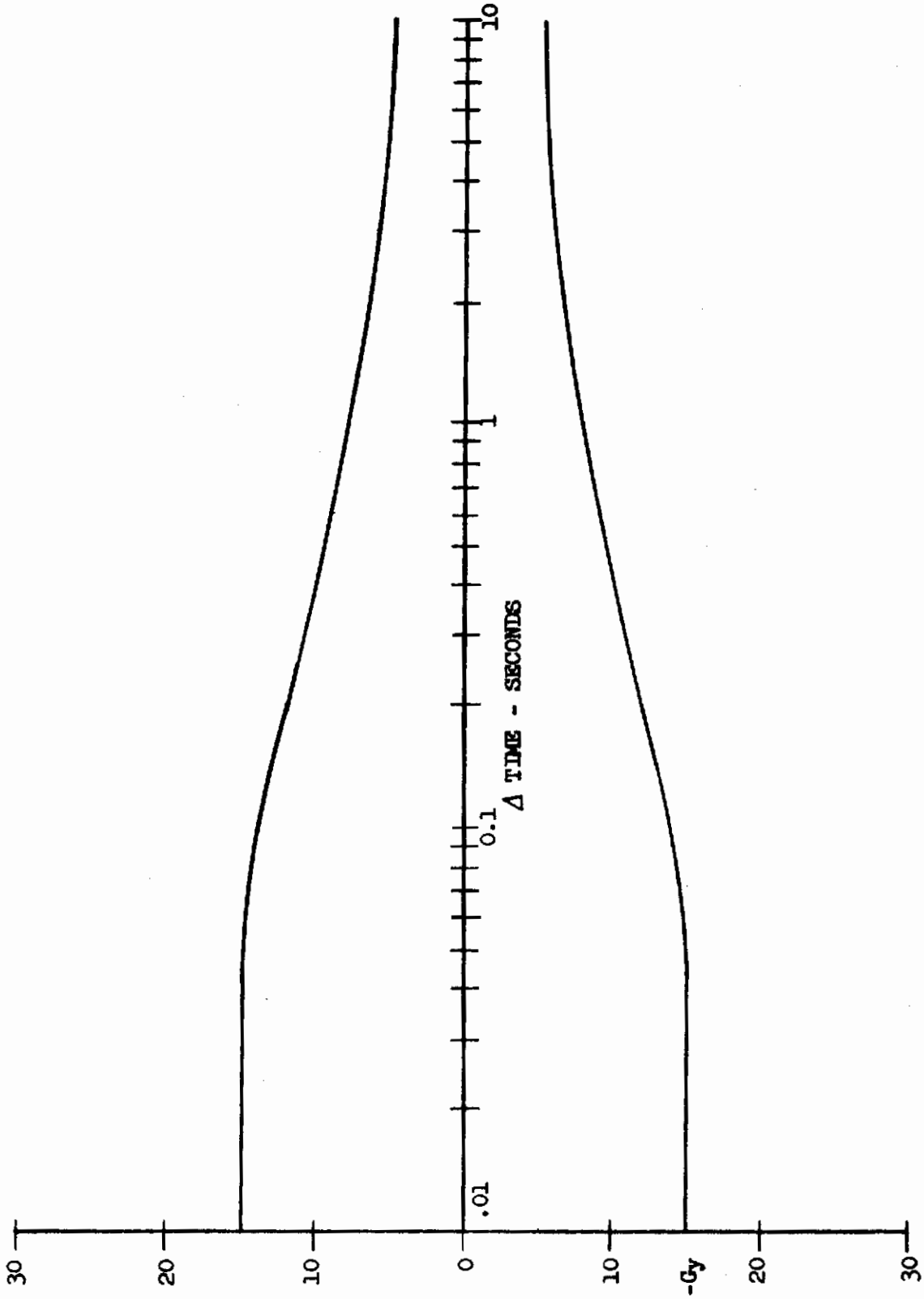

FIGURE 31 - ACCELERATION (±Gy) VERSUS Δ TIME

Approved for Public Release

Contrails

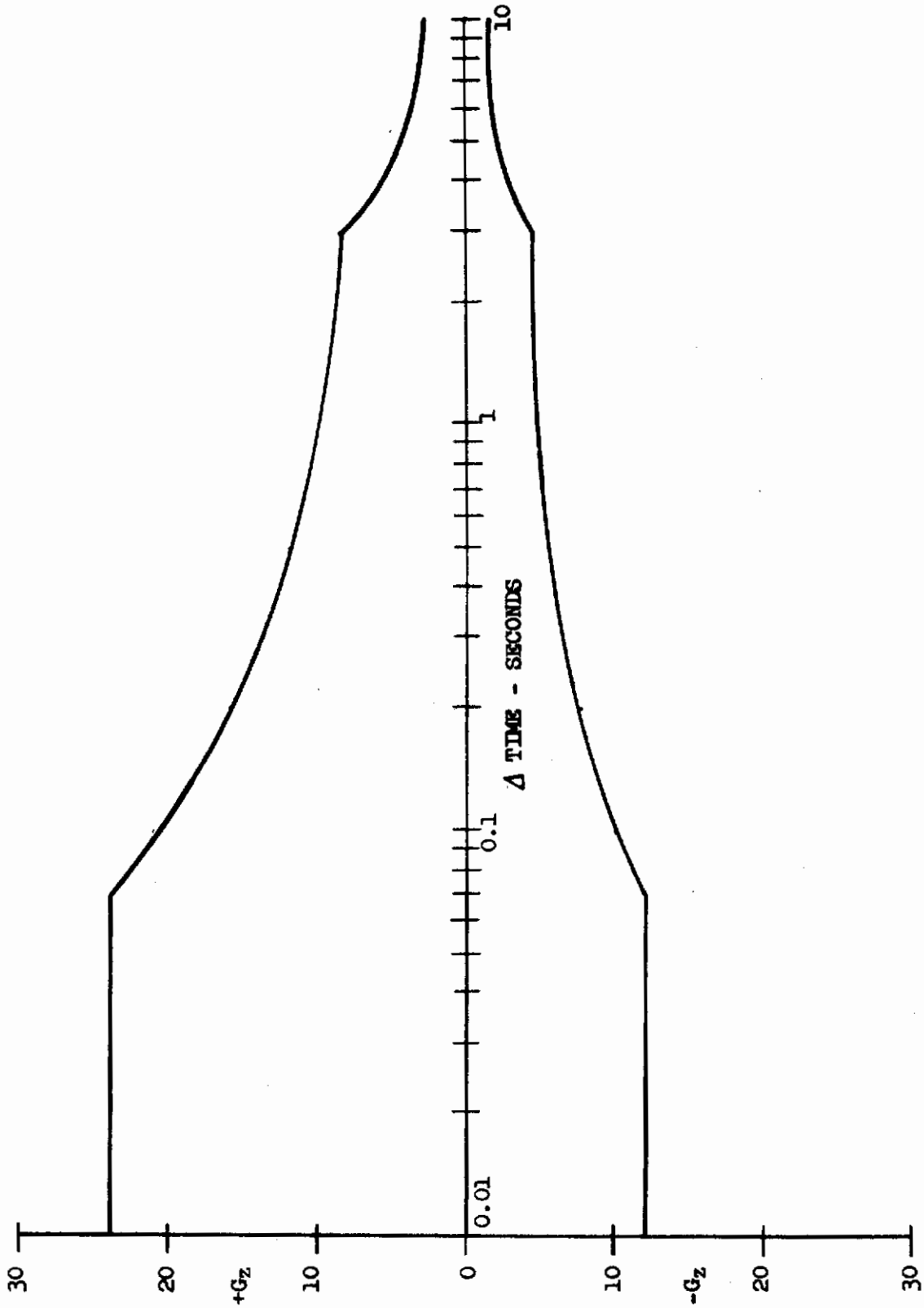

FIGURE 32 - ACCELERATION ($\pm G_z$) VERSUS Δ TIME

Approved for Public Release

Contrails

$$G = -G_Z = .000341(\text{radius})\text{rpm}^2 \quad (21)$$

$$\text{Radius} = 2932.55 \frac{-G_Z}{\text{rpm}^2} \text{ Feet} = 35190.6 \frac{-G_Z}{\text{rpm}^2} \text{ Inches} \quad (22)$$

Durations of 3.2 to 10 seconds were selected for comparison since at durations above 10 seconds the -GZ tolerance curve is constant and below 3.2 seconds the tolerance to tumbling curve is unknown. The locus of points fall in a 7.78 inch wide band which is perpendicular to the back line and located 8.13 inches above the iliac crest. Assuming that a distance is selected which is midway on this band, then (radius) is equal to approximately 12 inches. The resulting tumbling is compared to the limits of reference 27 in the following tables:

Duration (seconds)	Ref. 26 rpm	rpm^2	Ref. 27 $-G_Z$	$\frac{-G_Z}{\text{rpm}^2}$	Radius	rpm for Radius = 12
10.0	72	5184	1.2	.000231	8.13	59.32
8.0	74	5476	1.3	.000237	8.34	61.74
7.0	76	5776	1.4	.000242	8.52	64.07
6.0	78	6084	1.6	.000262	9.22	68.50
5.8	80	6400	1.7	.000265	9.32	70.60
5.0	82	6724	2.0	.000297	10.45	76.58
4.5	84	7056	2.2	.000311	10.94	80.32
4.1	86	7396	2.5	.000338	11.89	85.62
3.9	88	7744	2.8	.000361	12.70	90.62
3.7	90	8100	3.0	.000370	13.02	93.80
3.4	92	8464	3.5	.000413	14.53	101.30
3.2	94	8836	4.0	.000452	15.91	108.30

Certain ground rules which were established for determination of the location of the point are listed:

1. The point must lie on a line between the iliac crest and the eye.

2. It must be a minimum of 12 inches from the center of gravity of the escape concept.

3. It must be located such that the distance from the iliac crest to the point is a minimum.

4. The point must remain constant for each escape concept regardless of the variation in center of gravity location.

The data from reference 28 were used to determine the location of the iliac crest. Subject number 11 from this reference was selected as comparable to a 5th percentile subject by comparing certain vital dimensions to the criteria for 5th percentile given in "Anthropometry of Flying Personnel - 1950" reference 29.

Approved for Public Release

Contrails

	Reference 28	Reference 29
Weight	132.6 pounds	132.5 pounds
Sitting Height	33.3 inches	33.8 inches
Stature	62.7 inches	65.2 inches

Subject number 2 from reference 28 was selected as comparable to a 95th percentile subject because of the following comparison:

	Reference 28	Reference 29
Weight	203.2 pounds	200.8 pounds
Sitting Height	38.0 inches	38.0 inches
Stature	73.3 inches	73.1 inches

The iliac crest was assumed to be positioned at a distance equal to one-half the waist depth from the backline (back rest) and located from the top of the subject's head which is placed relative to the eye reference point. Utilizing the measurements of reference 28, the 5th percentile subject iliac crest is 3.9 inches from the backline and 28.3 inches below the top of the head. For the 95th percentile subject, the iliac crest is 4.95 inches from the backline and 31.8 inches below the top of the head. The eye is 10 inches forward of the backline and 4.2 inches below the top of the head; therefore in the seat reference coordinate system the iliac crest is located from the eye as follows: 5th percentile Z = -24.1 inches, X = -6.10 inches; and 95th percentile Z = -27.6 inches, X = -5.05 inches.

For System A the CG's (Table I) were positioned relative to an origin 2.5 inches below the seat reference point neutral. (Refer to figure 33.) The eye point and the iliac crests for the 5th and 95th percentile occupants were plotted and connected by lines. An arc of 12 inches radius was drawn from each CG location intersecting the corresponding iliac crest to eye line. Point (A) was selected as the midpoint of the resulting locus of points.

For System B the coordinate system is related to the rails and is measured vertically from the lower roller along the centerline of the rails and horizontally normal to the centerline of the rails. (Refer to figure 34.) The rails are canted 16 degrees back of vertical, the seat back angle is 13 degrees and the seat reference point neutral is located 6.25 inches above the lower roller and 5.125 inches forward of the rail centerline. The eye is located 10 inches forward of the backline and 31 inches vertically above the seat reference point neutral.

The 5th and 95th percentile iliac crest to eye lines were drawn as for System A. Center of gravity locations were plotted for the four conditions: 5th percentile with booms stowed; 5th percentile with booms extended; 95th percentile with booms stowed; and 95th percentile with booms extended. The 12 inch radii were drawn from each CG location. For each of the 95th percentile

Approved for Public Release

Contrails

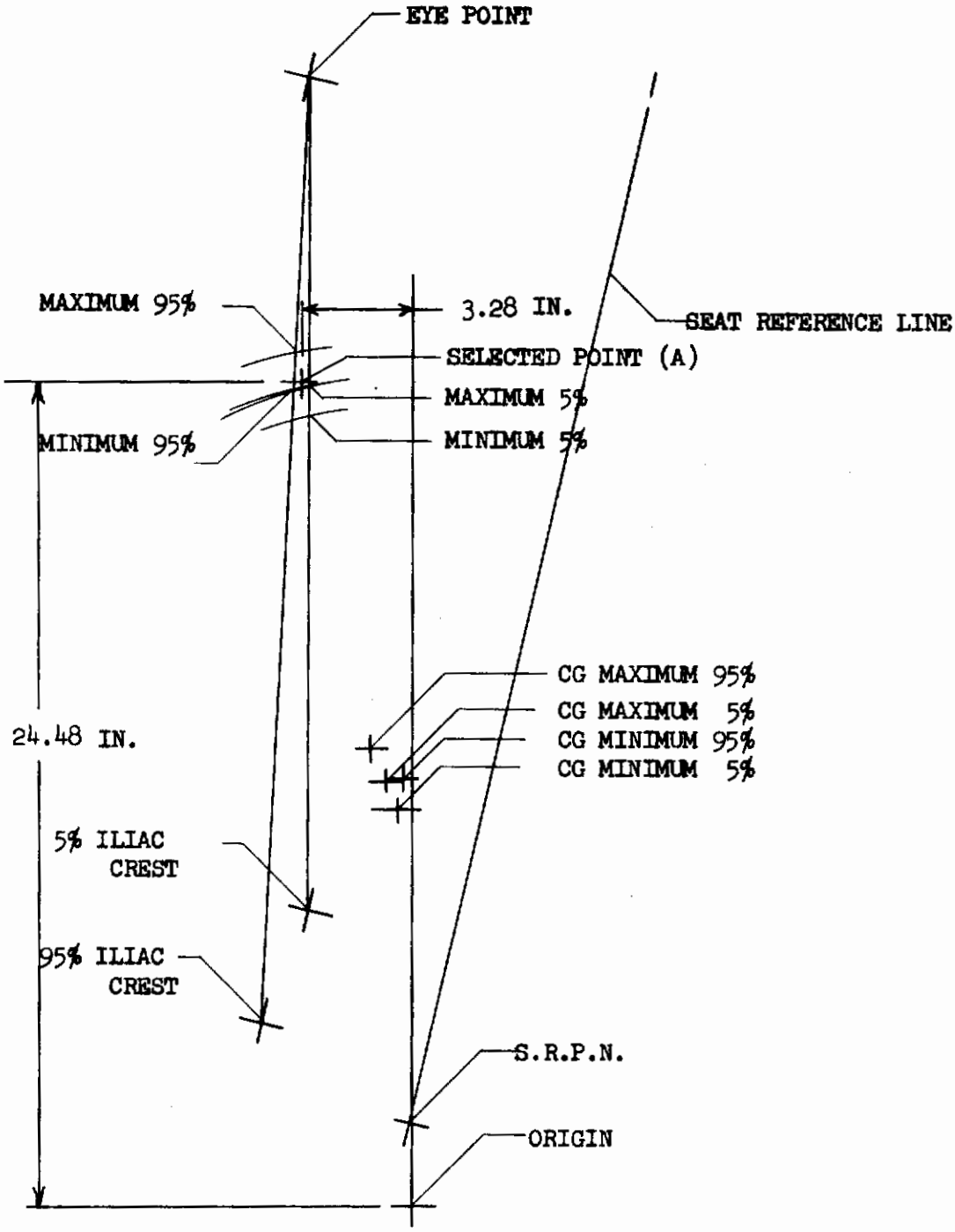

FIGURE 33 - POINT (A) SELECTION FOR SYSTEM A

Approved for Public Release

Contrails

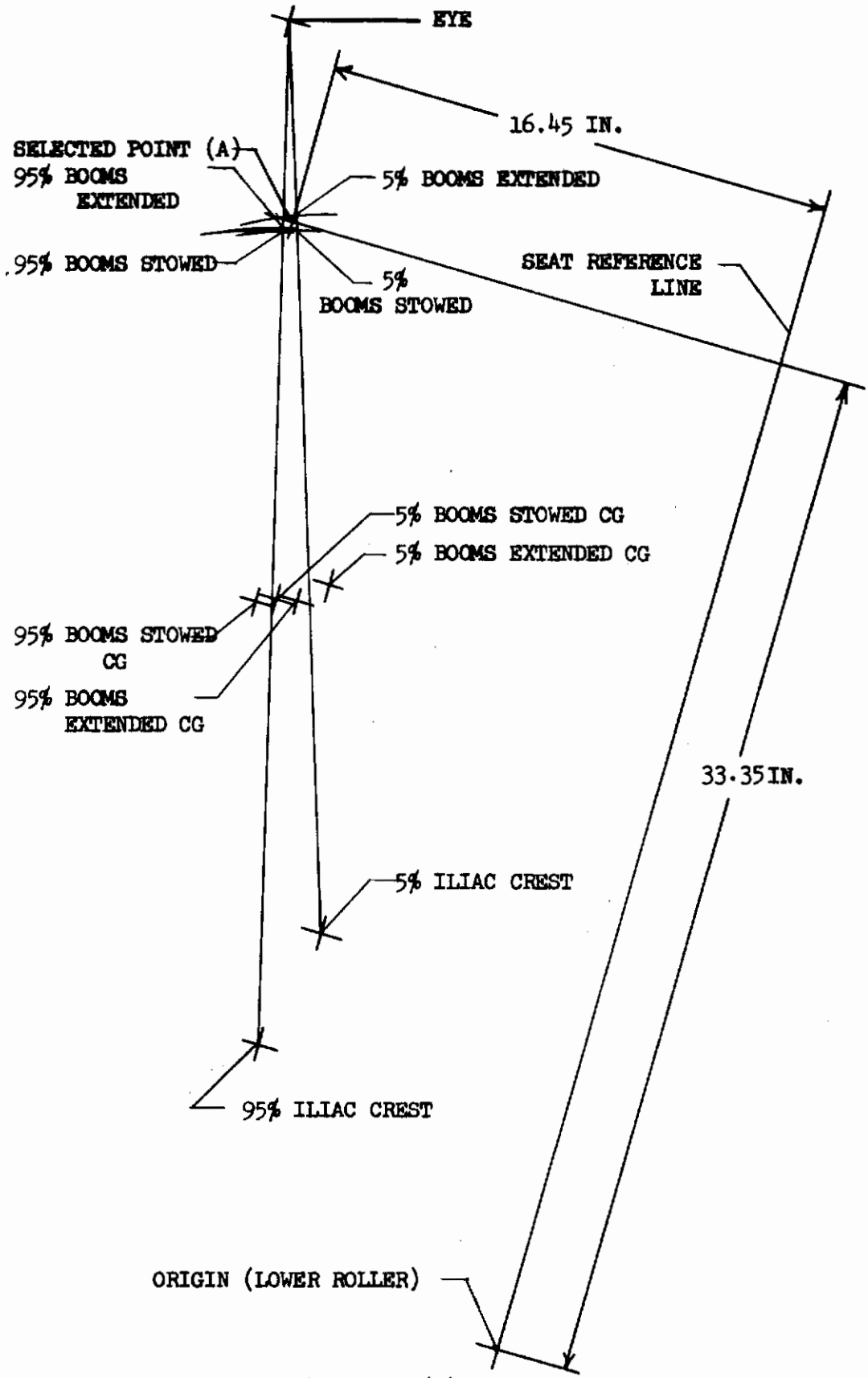

FIGURE 34 - POINT (A) SELECTION FOR SYSTEM B

Approved for Public Release

Contrails

CG locations two intersection points developed and, contrary to the rule that the distance from the iliac crest to point (A) should be a minimum, only the upper points were considered so that a locus of points consistent with the 5th percentile (A) points would be utilized.

For System C the coordinate system was related to the aircraft system with the Z coordinate measured vertically from the eye location and X given as a fuselage station. The eye position, 5th and 95th percentile CG's and iliac crests were plotted in figure 35. Lines were drawn between the iliac crests and the pilot's eye and a median point (A) was established.

For System D the eye location was estimated from reference 30 to be fuselage station 233.9 and water line 124.45. The 5th and 95th percentile centers of gravity, eye and iliac crests were plotted in figure 36 and the locations of point (A) were found by drawing arcs of 12 inch radius about the centers of gravity. The selected point (A) for System D was the midpoint of these two locations.

The locating dimensions (in system coordinates) for components used in the determination of point (A) are listed in table VI together with positions of the selected points (A) in the computer coordinate system. The selected points are shown in relationship to the human body in figure 37.

b. Acceleration Limits

For the analysis, four output parameters are considered: Acceleration of arbitrary point (G); Angle Theta as regards "G" force of arbitrary point (degrees); Angle Psi as regards "G" force at arbitrary point (degrees); and Angle Phi as regards "G" force at arbitrary point (degrees). For all three-degree-of-freedom runs only the first two parameters are generated. All four items are produced for each six-degree-of-freedom run. This information is shown graphically in figure 38.

Two sets of ellipsoids establish the limits of human tolerance to acceleration. (Reference 27.) The selection of ellipsoid set is based upon the orientation of the acceleration resultant. If angle Theta is positive, the ellipsoid set is defined by axes $A = 2G_X$; $B = 2G_Y$; and $C_1 = 2(+G_Z)$. When angle Theta is negative, the ellipsoid set is defined by the axes $A = 2G_X$; $B = 2G_Y$; and $C_2 = 2(-G_Z)$. Fifty-six ellipsoids are used to analyze the program output data and the acceleration tolerances at 28 time durations are applied.

Equations of ellipsoid, $X^2/A^2+Y^2/B^2+Z^2/C^2 = 1$, are appropriate where A, B and C (and C^1) are the axes of the 56 known ellipsoids and X, Y and Z are the values of the calculated axes. The limit ellipsoid data for the program are listed in table VII.

The coordinate system for the orientation of the resultant acceleration is related to the human spinal axis which is 13 degrees aft of escape body vertical for all four concepts.

Approved for Public Release

Contrails

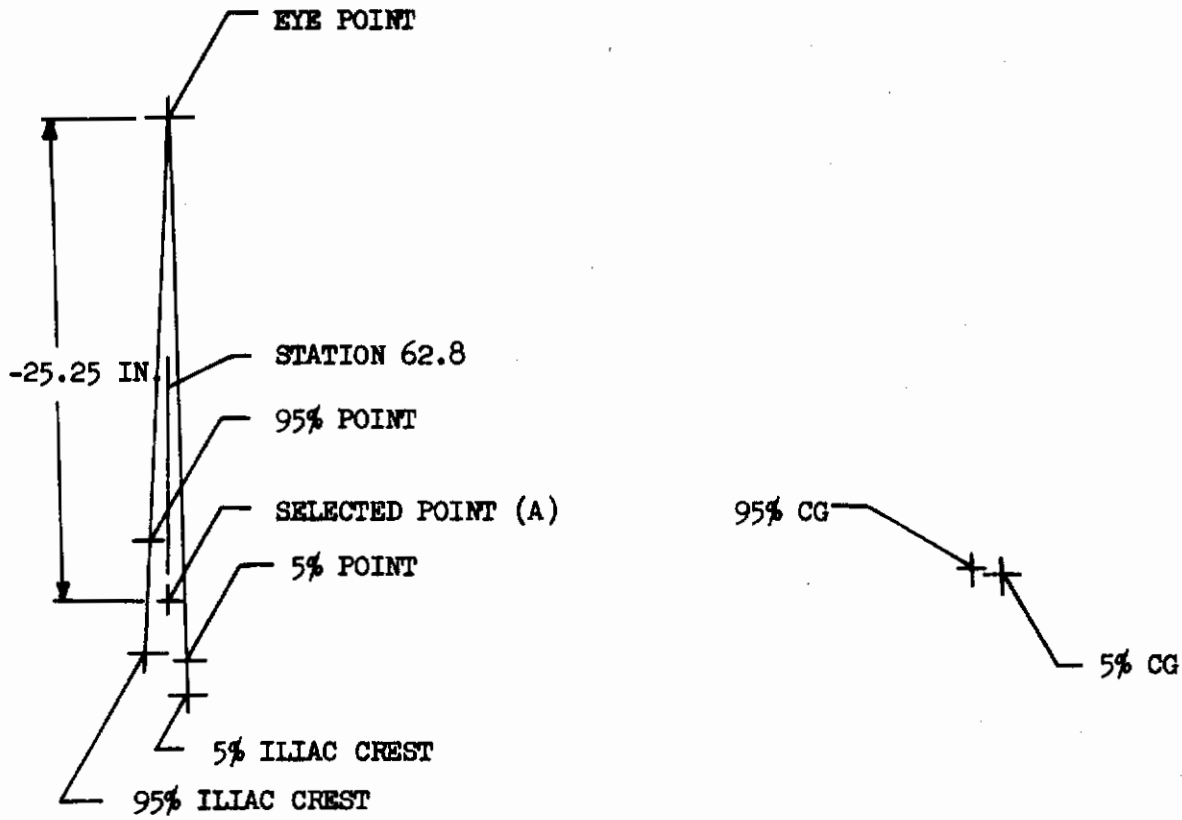

FIGURE 35 - POINT (A) SELECTION FOR SYSTEM C

Approved for Public Release

Contrails

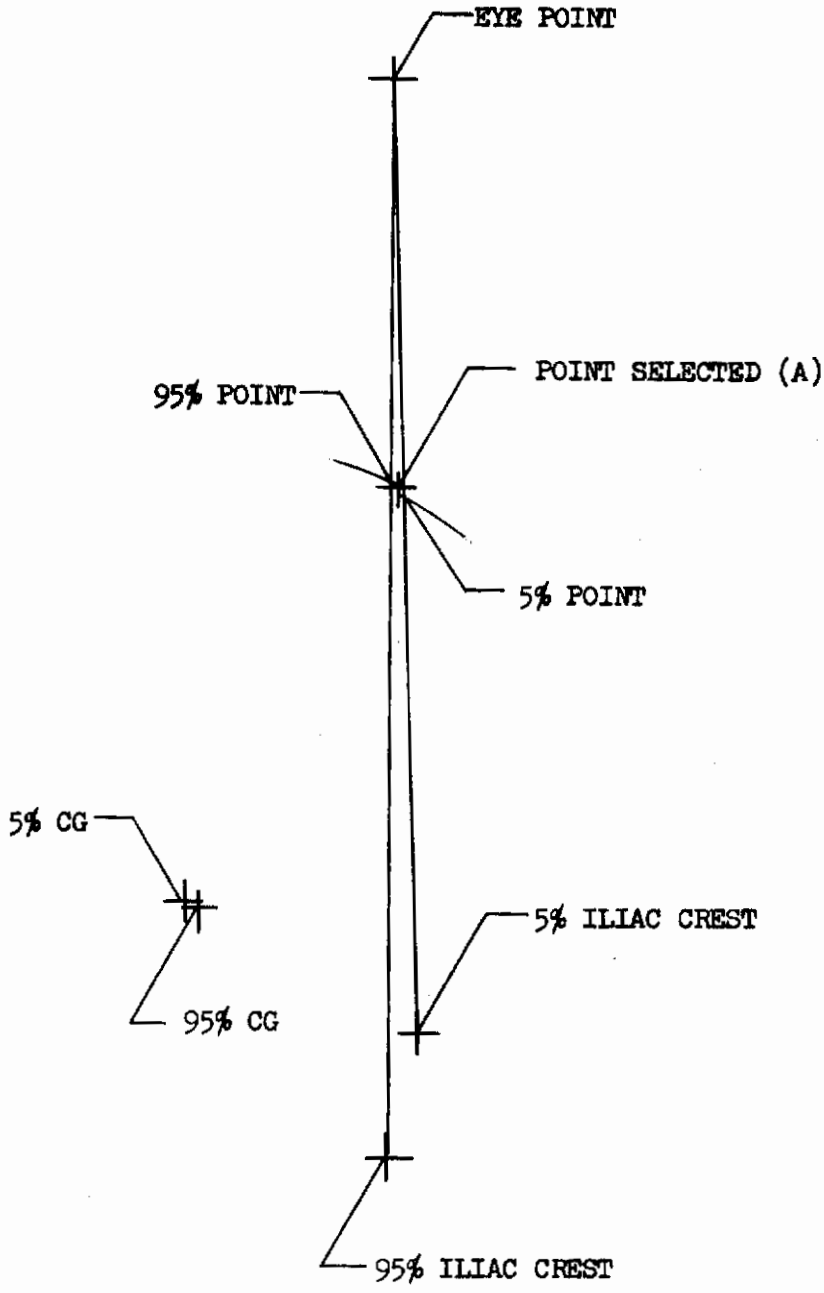

FIGURE 36 - POINT (A) SELECTION FOR SYSTEM D

Approved for Public Release

TABLE VI

POINT (A) LOCATING DIMENSIONS

	SYSTEM A						SYSTEM B						SYSTEM C			SYSTEM D		
	MINIMUM			MAXIMUM			BOOM STOWED			BOOMS EXTENDED								
	X	Y	Z	X	Y	Z	X	Y	Z	X	Y	Z	X	Y	Z	X	Y	Z
SYSTEM COORDINATES																		
EYE	3.1	0	33.5	3.1	0	33.5	18.4	0	39.6	18.4	0	39.6	63.0	-18.0	0	233.9	0	124.4
5th PERCENTILE ILIAC CREST	4.6	0	7.3	4.6	0	7.3	9.3	0	11.5	9.3	0	11.5	63.5	-18.0	-24.8	234.4	0	99.6
95th PERCENTILE ILIAC CREST	3.0	0	3.7	3.3	0	3.7	10.2	0	7.9	10.2	0	7.9	61.7	-18.0	-28.0	232.6	0	96.4
5% CENTER OF GRAVITY	0.4	0	11.8	0.7	0	12.6	13.7	0	21.5	12.2	0	21.9	106.3	0	-24.1	228.6	0	103.1
95% CENTER OF GRAVITY	0.2	0	12.7	1.2	0	13.6	14.3	0	21.2	13.0	0	21.6	105.0	0	-23.9	228.8	0	103.0
POINT A WITH:																		
5% CG	3.0	0	23.5	3.0	0	24.3	16.2	0	33.4	16.4	0	33.6	63.5	-18.0	-24.8	234.2	0	113.7
95% CG	5.5	0	24.3	3.4	0	25.4	16.6	0	33.0	16.6	0	33.0	44.1	-18.0	-22.2	233.9	0	114.0
SELECTED POINT (A)	3.3	0	24.5	3.3	0	24.5	16.4	0	33.4	16.4	0	33.4	62.8	-18.0	-25.2	234.0	0	113.8
REFERENCE POINT	SEAT REF. POINT LOW POSITION						℄ LOWER ROLLER						STATION & EYE			FUS. & STA. PLANE		
X COORDINATE	VERTICAL 13° FWD OF SEAT REF. LINE						VERTICAL - ℄ RAIL						VERTICAL - STATION LINE			VERTICAL-STATION LINE		
Z COORDINATE	HORIZONTAL NORMAL TO X						HORIZONTAL-NORMAL TO RAILS						WATER LINE			WATER LINE		
COMPUTER COORDINATES																		
5% CG TO POINT(A)	2.9	0	-12.7	2.6	0	-11.9	-6.2	0	-12.2	0.9	0	-12.2	43.5	-18.0	-1.2	-5.4	0	10.7
95%CG TO POINT A	3.1	0	-11.8	2.1	0	-10.9	-0.1	0	-12.3	0.1	0	-12.2	42.2	-18.0	-1.4	-5.2	0	10.8

Approved for Public Release

Contrails

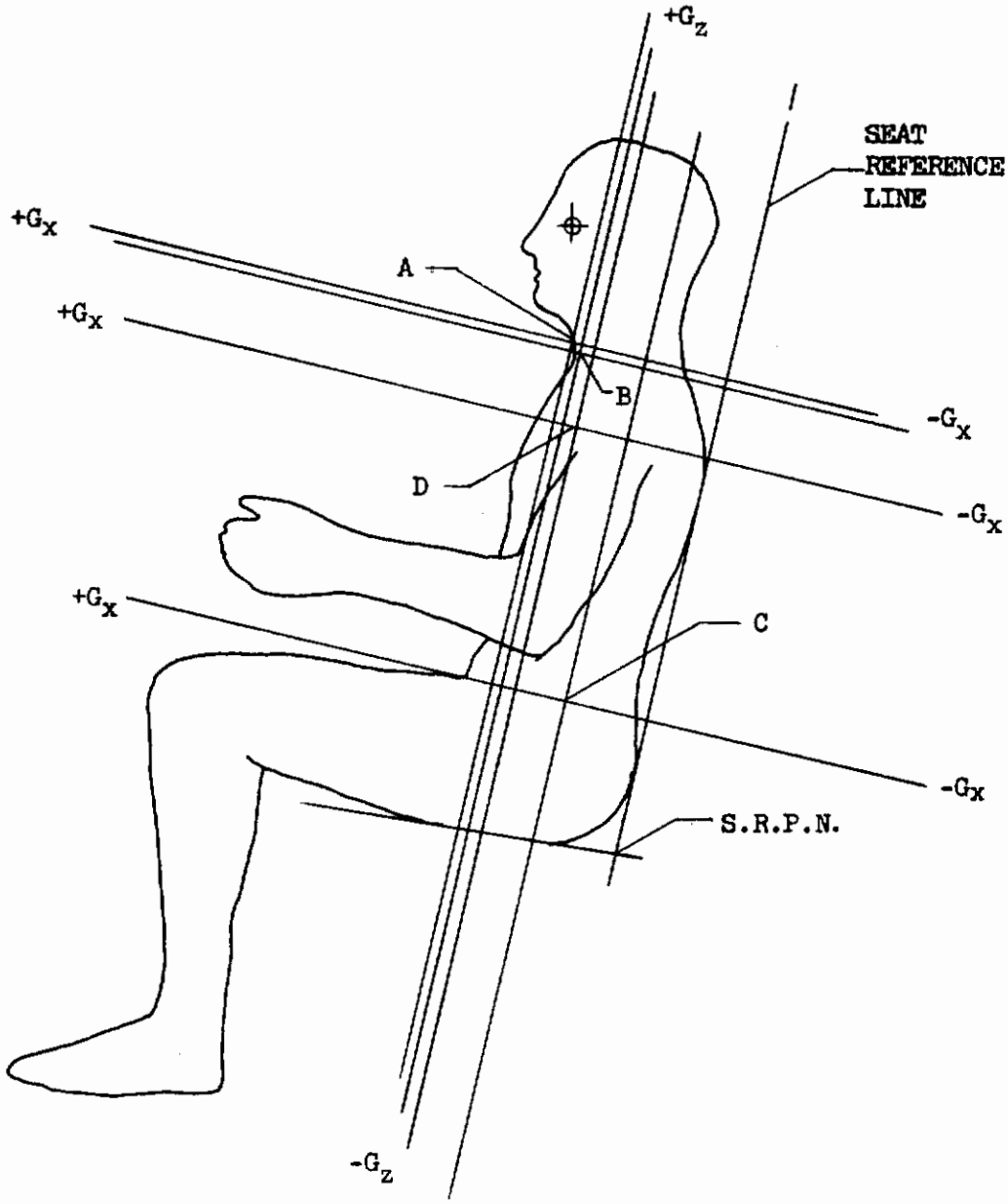

FIGURE 37 - "G" COORDINATES VERSUS THE HUMAN BODY FOR THE ESCAPE CONCEPTS

Approved for Public Release

Contrails

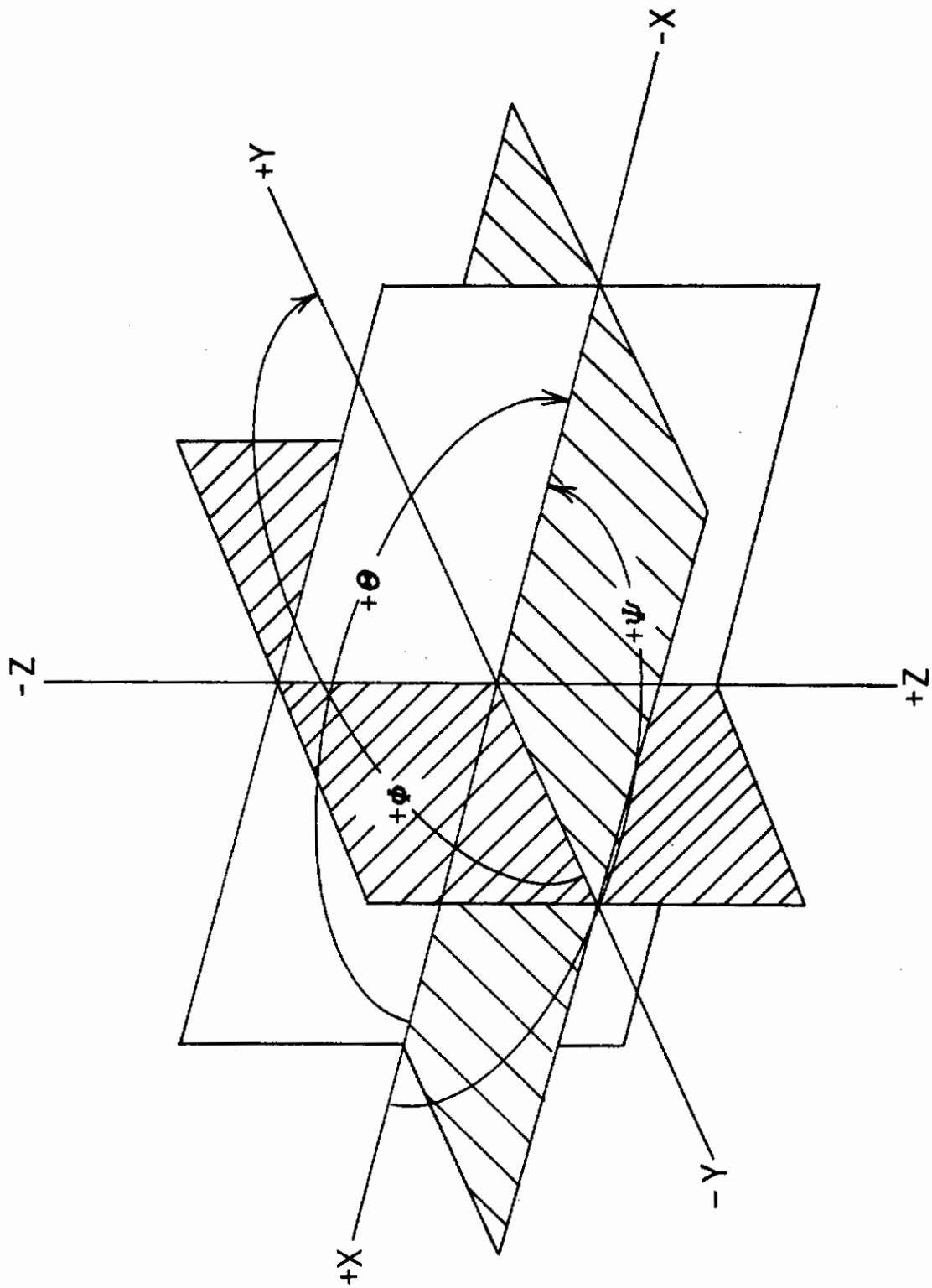

FIGURE 38 - VECTOR ORIENTATION FOR ANGLES PERTAINING TO ARBITRARY POINT "G"

Approved for Public Release

Contrails

TABLE VII

ACCELERATION TOLERANCE ELLIPSOIDS

DURATION (SECONDS)	ACCELERATION TOLERANCE ±G_x	±G_y	+G_z	-G_z	ELLIPSOIDS A	± B	+ C_1	- C_2
0.01	30.0	15.0	24.0	12.0	60.0	30.0	48.0	24.0
0.02	29.3	15.0	24.0	12.0	58.6	30.0	48.0	24.0
0.03	28.8	15.0	24.0	12.0	57.6	30.0	48.0	24.0
0.04	28.2	15.0	24.0	12.0	56.4	30.0	48.0	24.0
0.05	27.9	14.9	24.0	12.0	55.8	29.8	48.0	24.0
0.06	27.5	14.7	24.0	12.0	55.0	29.4	48.0	24.0
0.07	27.1	14.3	24.0	12.0	54.2	28.6	48.0	24.0
0.08	26.8	14.1	22.9	11.1	53.6	28.2	45.8	22.2
0.09	26.4	13.9	21.9	10.4	52.8	27.8	43.8	20.8
0.1	26.0	13.7	21.1	10.0	52.0	27.4	42.2	20.0
0.2	23.4	12.0	16.0	7.8	46.8	24.0	32.0	15.6
0.3	21.6	10.8	13.9	6.8	43.2	21.6	27.8	13.6
0.4	20.0	10.0	12.7	6.1	40.0	20.0	25.4	12.2
0.5	18.9	9.5	11.9	5.8	37.8	19.0	23.8	11.6
0.6	17.9	9.1	11.3	5.3	35.8	18.2	22.6	10.6
0.7	17.2	8.8	10.8	5.2	34.4	17.6	21.6	10.4
0.8	16.6	8.5	10.4	5.0	33.2	17.0	20.8	10.0
0.9	16.1	8.2	10.2	4.9	32.2	16.4	20.4	9.8
1.0	15.7	8.0	10.0	4.8	31.4	16.0	20.0	9.6
2.0	12.9	6.8	8.9	4.5	25.8	13.6	17.8	9.0
3.0	11.3	6.2	8.5	4.5	22.6	12.4	17.0	9.0
4.0	10.3	5.9	5.5	2.8	20.6	11.8	11.0	5.6
5.0	9.8	5.7	4.2	2.0	19.6	11.4	8.4	4.0
6.0	9.2	5.5	3.5	1.7	18.4	11.0	7.0	3.4
7.0	8.9	5.3	3.1	1.5	17.8	10.6	6.2	3.0
8.0	8.5	5.2	3.0	1.5	17.0	10.4	6.0	3.0
9.0	8.3	5.1	2.9	1.5	16.6	10.2	5.8	3.0
10.0	8.1	5.0	2.8	1.5	16.2	10.0	5.6	3.0

Approved for Public Release

Contrails

During the time from ejection initiation to 0.5 seconds past rocket burnout or second drag chute deployment whichever occurs last, the acceleration is checked at intervals of .02 seconds. The 56 tolerance ellipsoids are checked at each time step. This procedure analyzes the output data for acceleration versus duration.

c. Acceleration Rate of Onset Limits

The output is analyzed for rate-of-onset of acceleration by the ANAL2 computer program. The tolerance limit again is defined by two ellipsoids; when the resultant acceleration is orientated in the upper hemisphere (angle Theta positive), the ellipsoid is

$$\frac{X^2}{A^2} + \frac{Y^2}{B^2} + \frac{Z^2}{C^2} = 1 \qquad (23)$$

Where:

$$A = ((+G_X) + (-G_X)) = ((1000) + (1000)) = 2000 \text{ G/sec} \qquad (24)$$

$$B = ((+G_Y) + (-G_Y)) = ((300) + (300)) = 600 \text{ G/sec} \qquad (25)$$

$$C = ((2)(+G_Z)) = ((2)(300)) = 600 \text{ G/sec} \qquad (26)$$

When the resultant acceleration is orientated in the lower hemisphere (angle Theta negative), the ellipsoid is

$$\frac{X^2}{A^2} + \frac{Y^2}{B^2} + \frac{Z^2}{(C')^2} = 1 \qquad (27)$$

Where:

$$A = ((+G_X) + (-G_X)) = ((1000) + (1000)) = 2000 \text{ G/sec} \qquad (28)$$

$$B = ((+G_Y) + (-G_Y)) = ((300) + (300)) = 600 \text{ G/sec}$$

$$C' = ((2)(-G_Z)) = ((2)(200)) = 400 \text{ G/sec}$$

The three planes of the resultant tolerance limit to rate-of-onset of acceleration are depicted by figures 39, 40, and 41.

During the time from ejection initiation to 0.5 seconds past rocket burnout or second drag chute deployment, whichever occurs last, the rate-of-onset is checked at intervals of .02 seconds. One of the two tolerance ellipsoids is checked at each time step.

Approved for Public Release

Contrails

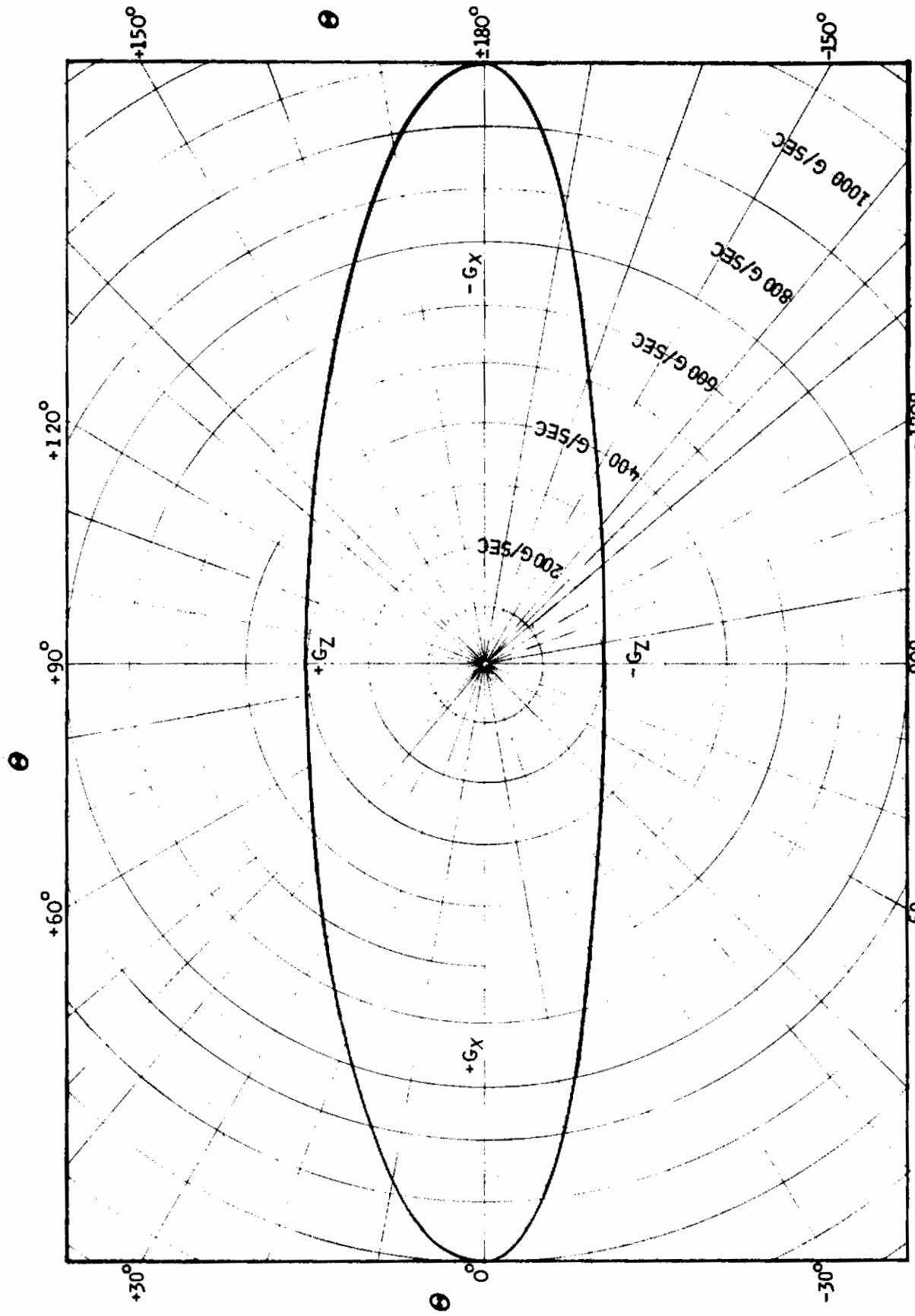

FIGURE 39 - MAXIMUM RATE OF ONSET LIMITS G_z, G_x PLANE

Approved for Public Release

Contrails

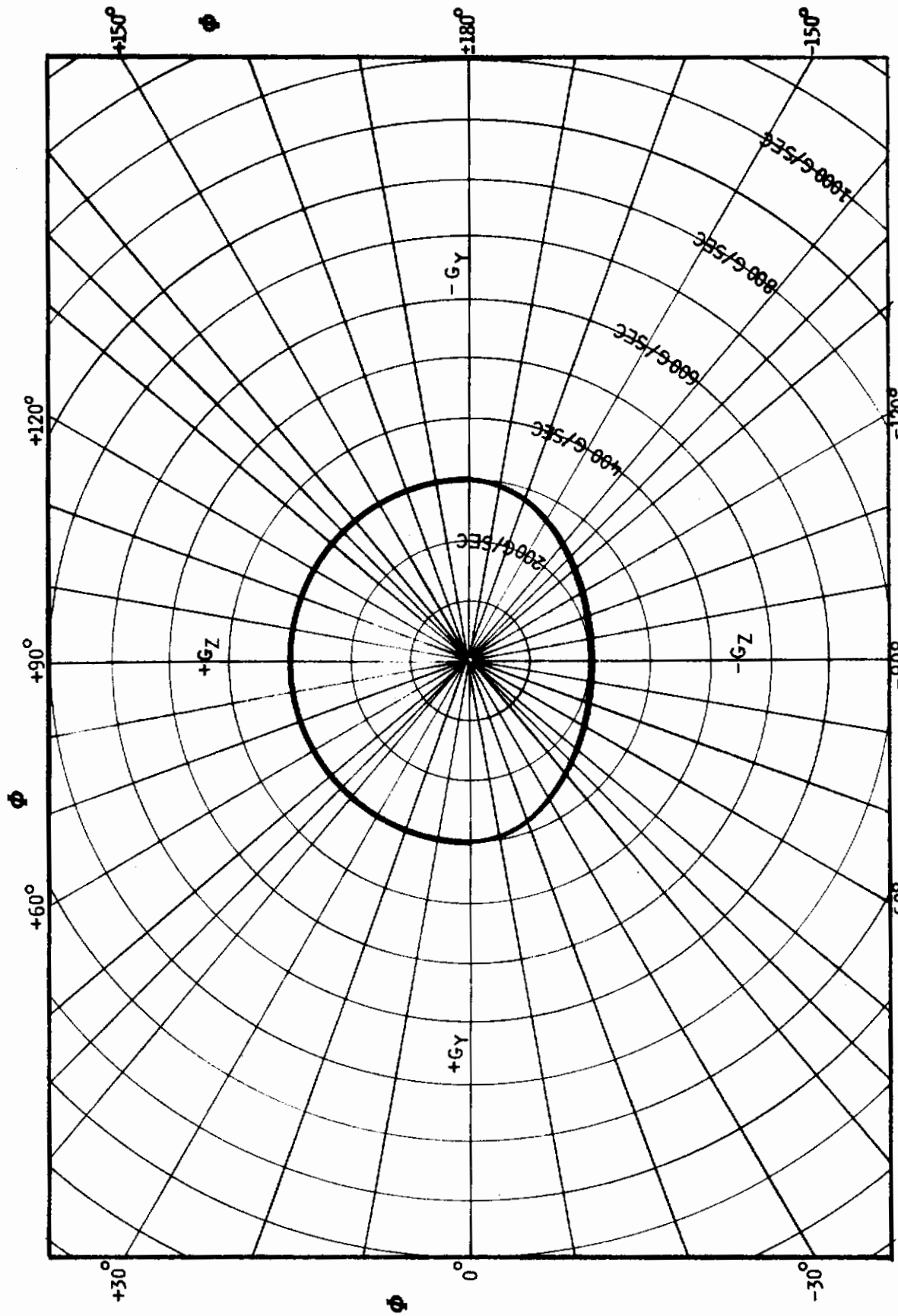

FIGURE 40 - MAXIMUM RATE OF ONSET LIMITS G_z, G_y PLANE

Approved for Public Release

Contrails

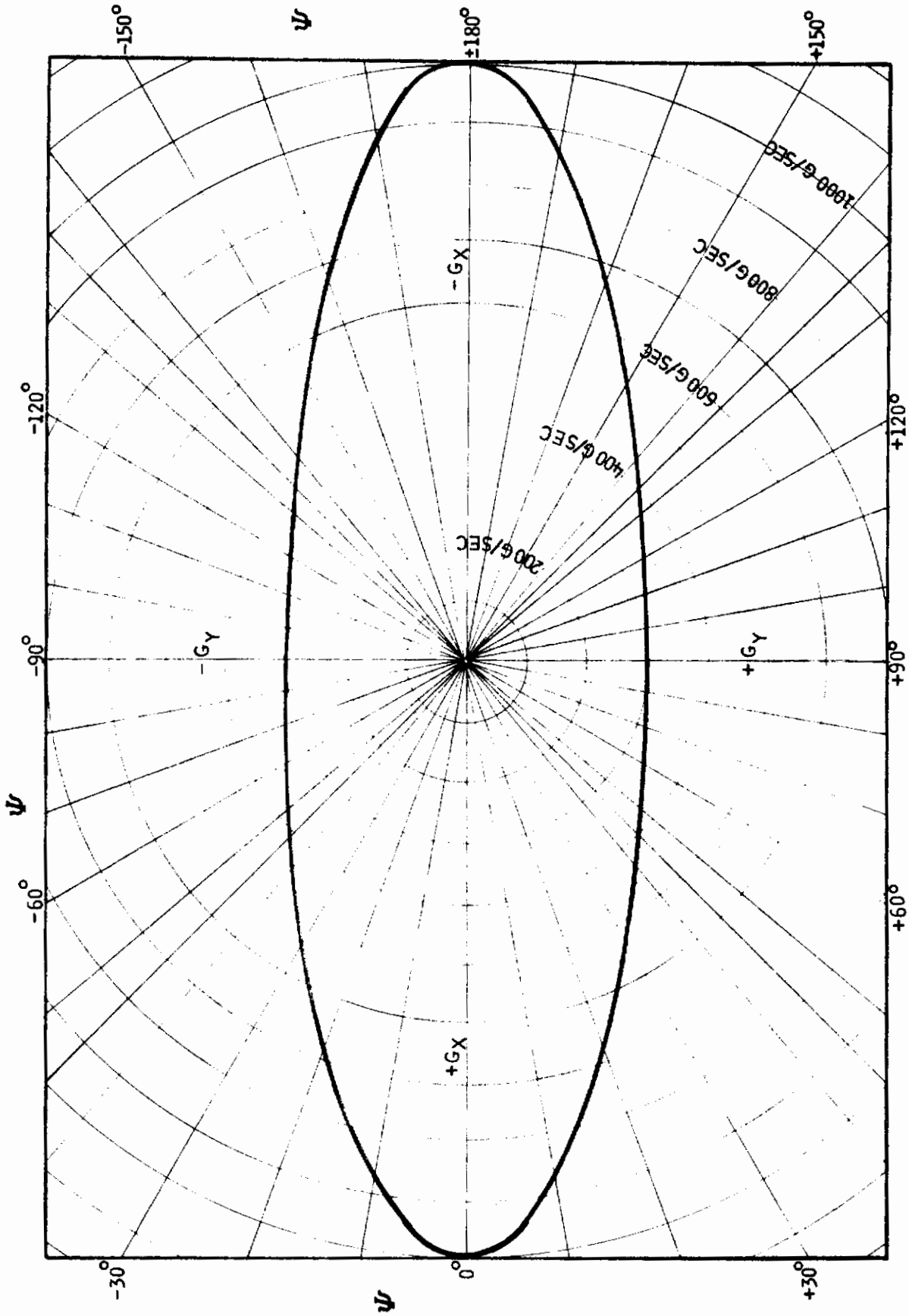

FIGURE 41 - MAXIMUM RATE OF ONSET LIMITS G_y, G_x PLANE

Approved for Public Release

Contrails

3. SAFE EMERGENCY ALTITUDE ANALYSIS (SEA)

In the Appendix are graphs of Safe Emergency Altitude (SEA) versus 16 escape system conditions for each of four systems for the 208 aircraft flight cases. Cross plots of these graphs, figures 42 through 97, show the SEA versus various initial aircraft attitudes, rotation rates, flight path angles, and ejection reaction times. On the cross plots, the highest SEA for each escape system condition in a given aircraft case dictates that system's plotted position.

Figures 42 through 45 show, for all systems, SEA versus aircraft angle of attack (α) for aircraft zero velocity, while figures 46 through 49 present SEA versus aircraft angle of roll (ϕ) for zero velocity. It can be seen that where α is the only variable, System D has both the lowest SEA, -230 feet at $\alpha = 15^{\circ}$, and the highest SEA, 1400 feet at $\alpha = -90^{\circ}$. Where ϕ is the only variable, System D has the lowest SEA, zero feet at ϕ = zero degree, and System C the highest, 1300 feet at $\phi = 180$ degrees.

SEA are plotted versus α for aircraft flight path angle (γ) of 10, -10, -30 and -60 degrees and for true velocity (V) = 100 knots, in figures 50 through 53. For these combinations, System D has the lowest SEA, -500 feet at $\gamma = 10^{\circ}$, and $\alpha = 15^{\circ}$, and also the highest, 2300 feet at $\gamma = -60^{\circ}$ and α = zero degree.

In figures 54 through 57, SEA are plotted versus α for pitching velocity (q) of zero, 30 and 90 °/sec. System C shows the lowest SEA, -200 feet at α = zero degree and q = zero °/sec, while System D shows the highest, 1450 feet at $\alpha = -90^{\circ}$ and q = 90 °/sec.

Figures 58 through 69 plot SEA versus γ for combinations of $\alpha = 15$, -15 and -90 degrees; q = zero, 30 and 90 °/sec, aircraft rolling velocity (p) of 60 and 180 °/sec, and aircraft angle of roll (ϕ) of 30, 60, 90 and 180 degrees. For conditions of $\alpha = 15^{\circ}$, q = zero °/sec and p = 60 °/sec, System B has the lowest SEA, 100 feet at γ = zero degrees and $\phi = 90^{\circ}$, while System D has the highest, 2100 feet at $\gamma = -90^{\circ}$ and $\phi = 30^{\circ}$. For conditions of $\alpha = -15^{\circ}$, q = 30 °/sec and p = 60 °/sec, the system having the lowest SEA is D with 220 feet at γ = zero degrees and $\phi = 180$ degrees, and again System D with the highest, 2100 feet at $\gamma = -90^{\circ}$ and $\phi = 90^{\circ}$. For conditions of $\alpha = -90^{\circ}$, q = 90 °/sec and p = 180 °/sec, System B has the lowest SEA, 475 feet at $\gamma = -30^{\circ}$ and $\phi = 90^{\circ}$, and System C has the highest, 1950 feet at $\gamma = -90^{\circ}$ and $\phi = 60^{\circ}$.

The influences of ϕ and p on SEA are demonstrated in figures 70 through 73, which plot SEA versus γ for combinations of $\phi = 90$ and 180 degrees, and p = 60 and 180 °/sec, while the effects of α and q are shown by figures 74 through 77 for combinations of $\alpha = 90$ and -90 degrees and q = 30 and 90 °/sec. Where ϕ and p are the variables, both Systems C and D have the lowest SEA at the same condition, 50 feet at γ = zero degrees, $\phi = 180^{\circ}$ and p = 60 °/sec. The highest SEA value is for System D with 2350 feet at $\gamma = -90^{\circ}$, $\phi = 180^{\circ}$ and p = 180 °/sec. The lowest SEA with the variables of α and q is that of System C, - 350 feet at $\gamma = 10^{\circ}$, q = 30 °/sec and $\alpha = -90^{\circ}$, while the highest is of System D with 2200 feet at $\gamma = -90^{\circ}$, q = 90 °/sec and $\alpha = 90^{\circ}$.

Approved for Public Release

Contrails

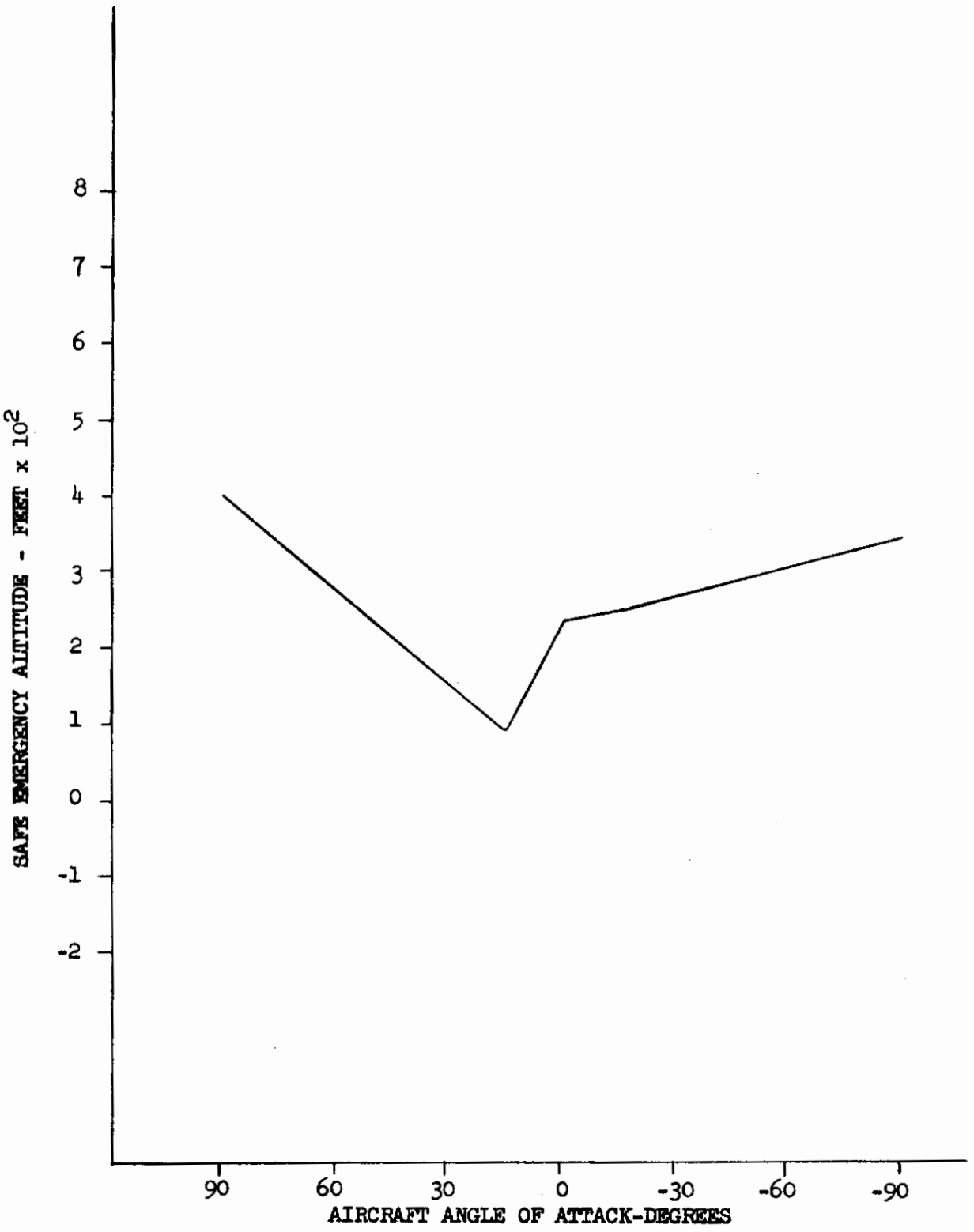

FIGURE 42-SYSTEM A SAFE EMERGENCY ALTITUDE VERSUS α
(γ = ZERO DEG; q = ZERO DEG/SEC; V = ZERO KN)

Approved for Public Release

Contrails

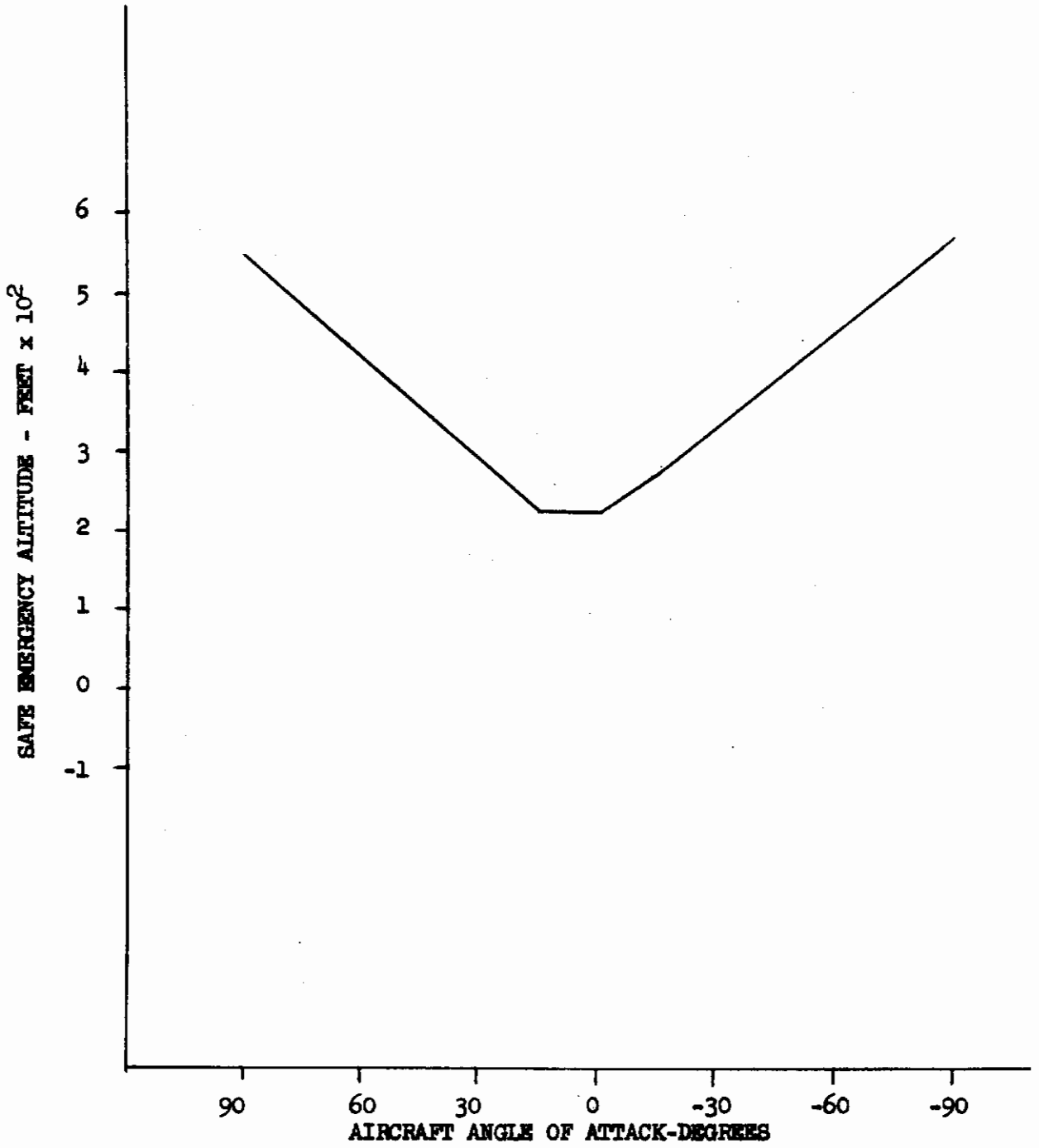

FIGURE 43-SYSTEM B SAFE EMERGENCY ALTITUDE VERSUS α
(γ = ZERO; q = ZERO DEG/SEC; V = ZERO KN)

Approved for Public Release

Contrails

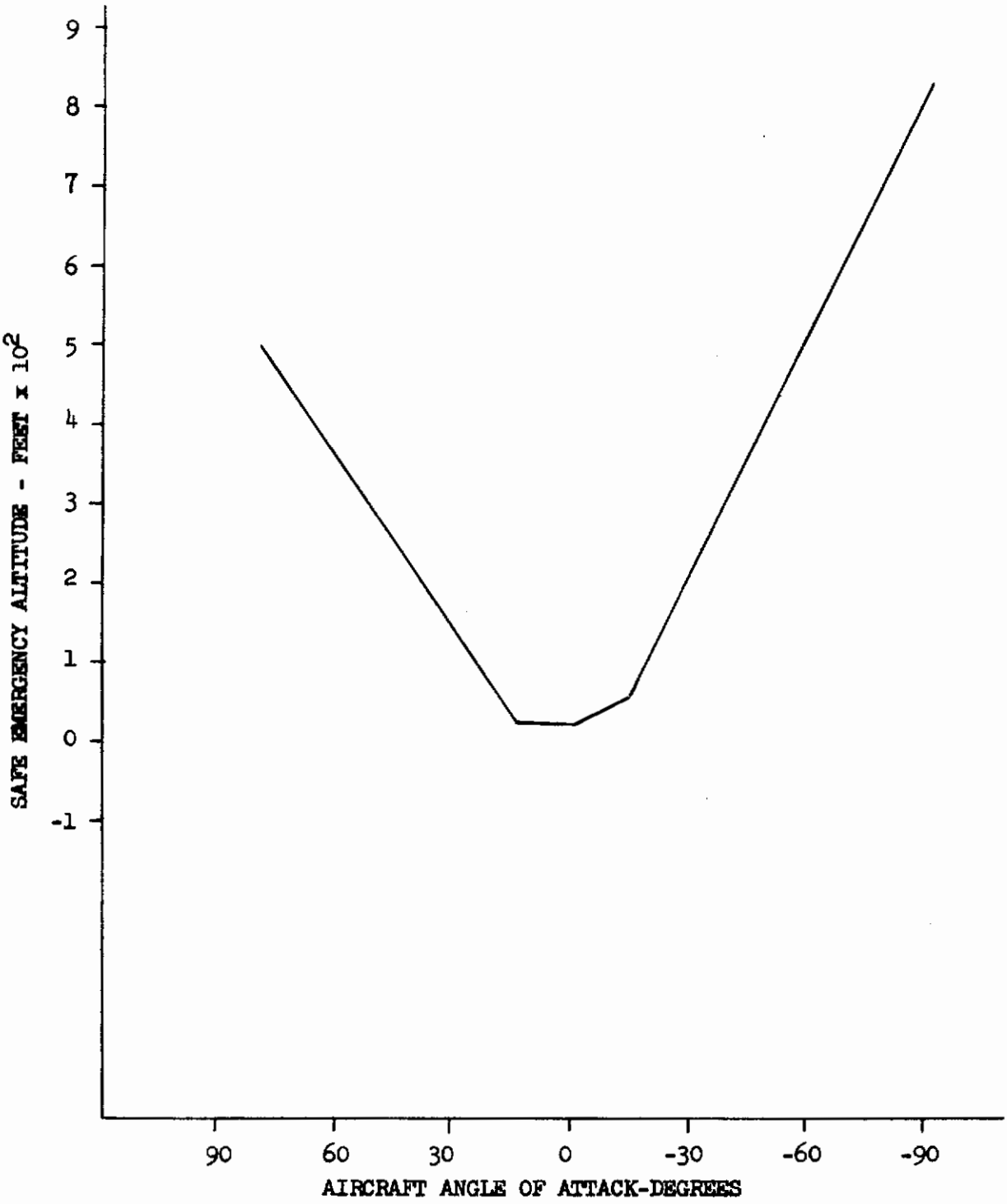

FIGURE 44-SYSTEM C SAFE EMERGENCY ALTITUDE VERSUS α
(γ = ZERO DEG; q = ZERO DEG/SEC; V = ZERO KN)

Approved for Public Release

Contrails

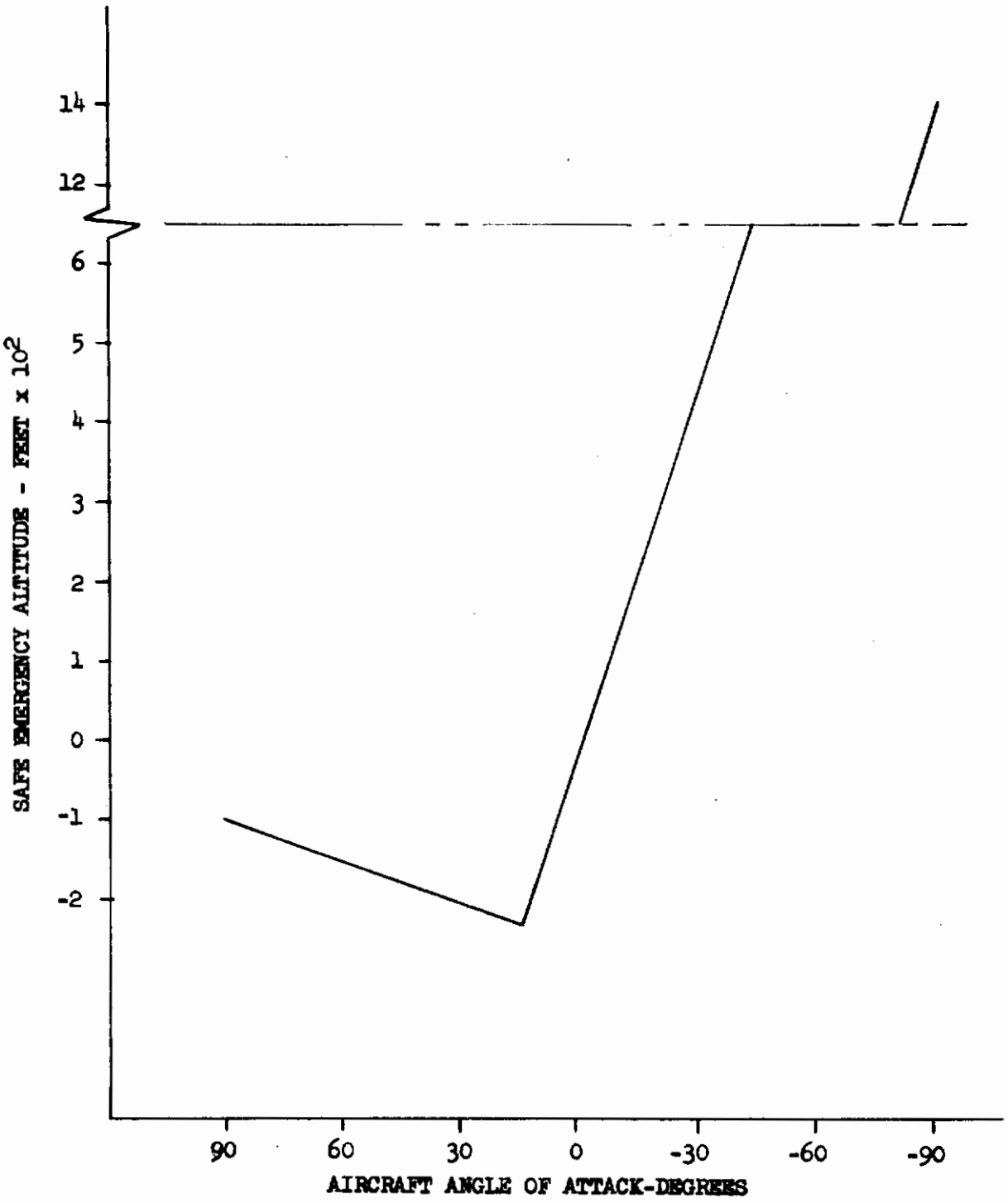

FIGURE 45 - SYSTEM D SAFE EMERGENCY ALTITUDE VERSUS α
(γ = ZERO DEG; q = ZERO DEG/SEC; V = ZERO KN)

Approved for Public Release

Contrails

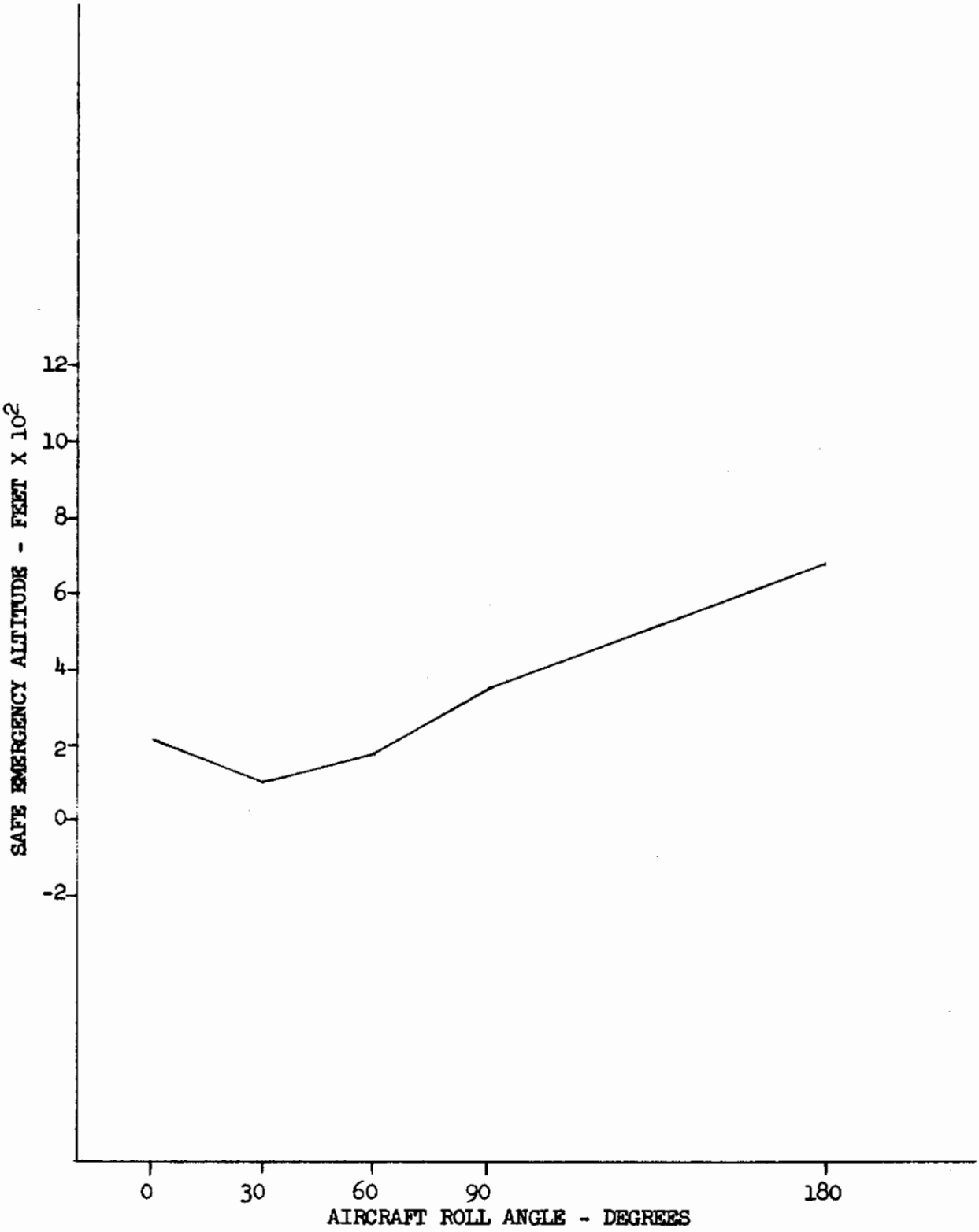

FIGURE 46 - SYSTEM A SAFE EMERGENCY ALTITUDE VERSUS ϕ
(γ = ZERO DEG; p = ZERO DEG/SEC; V = ZERO KN)

Approved for Public Release

Contrails

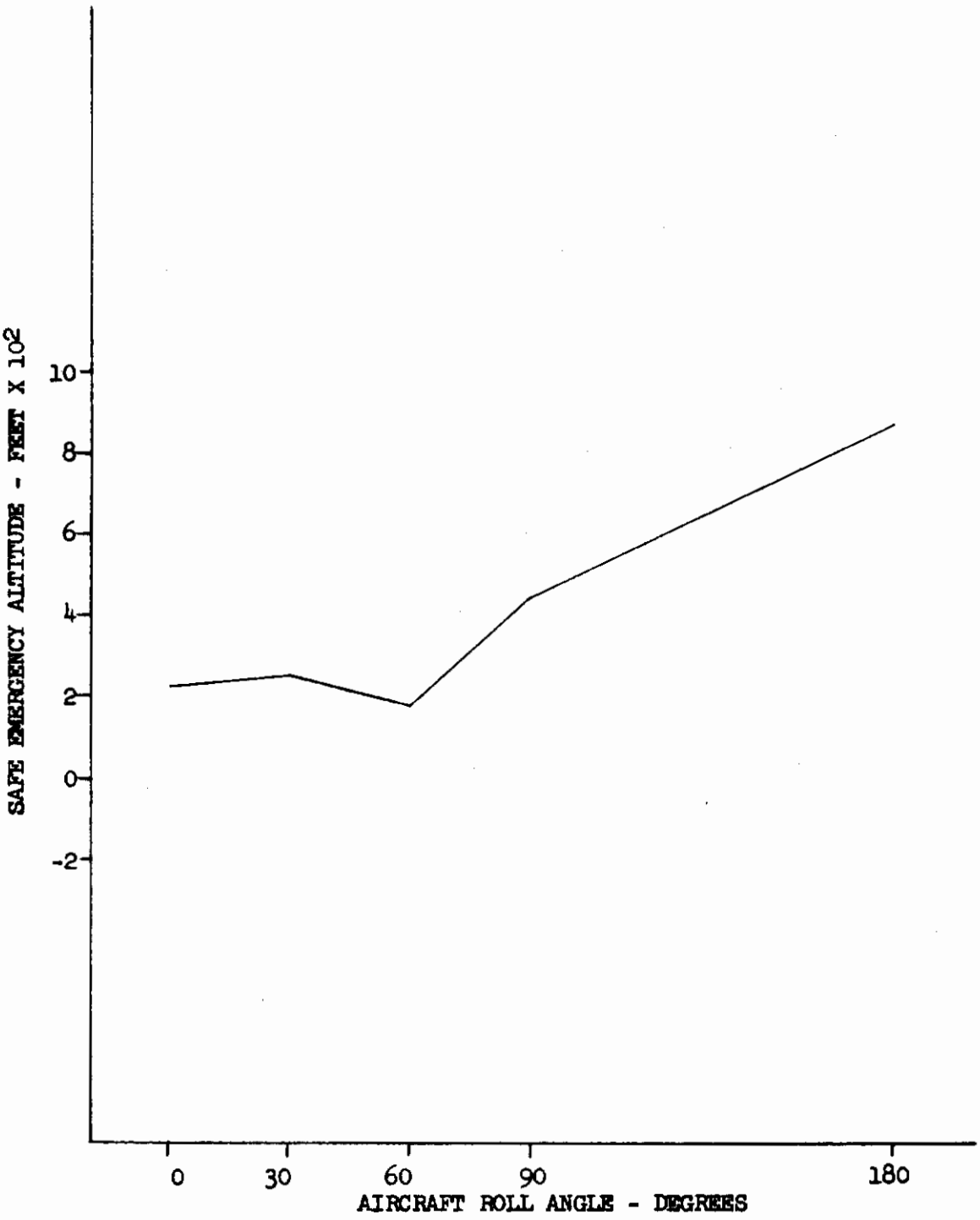

FIGURE 47 - SYSTEM B SAFE EMERGENCY ALTITUDE VERSUS ϕ
(γ = ZERO DEG; p = ZERO DEG/SEC; V = ZERO KN)

Approved for Public Release

Contrails

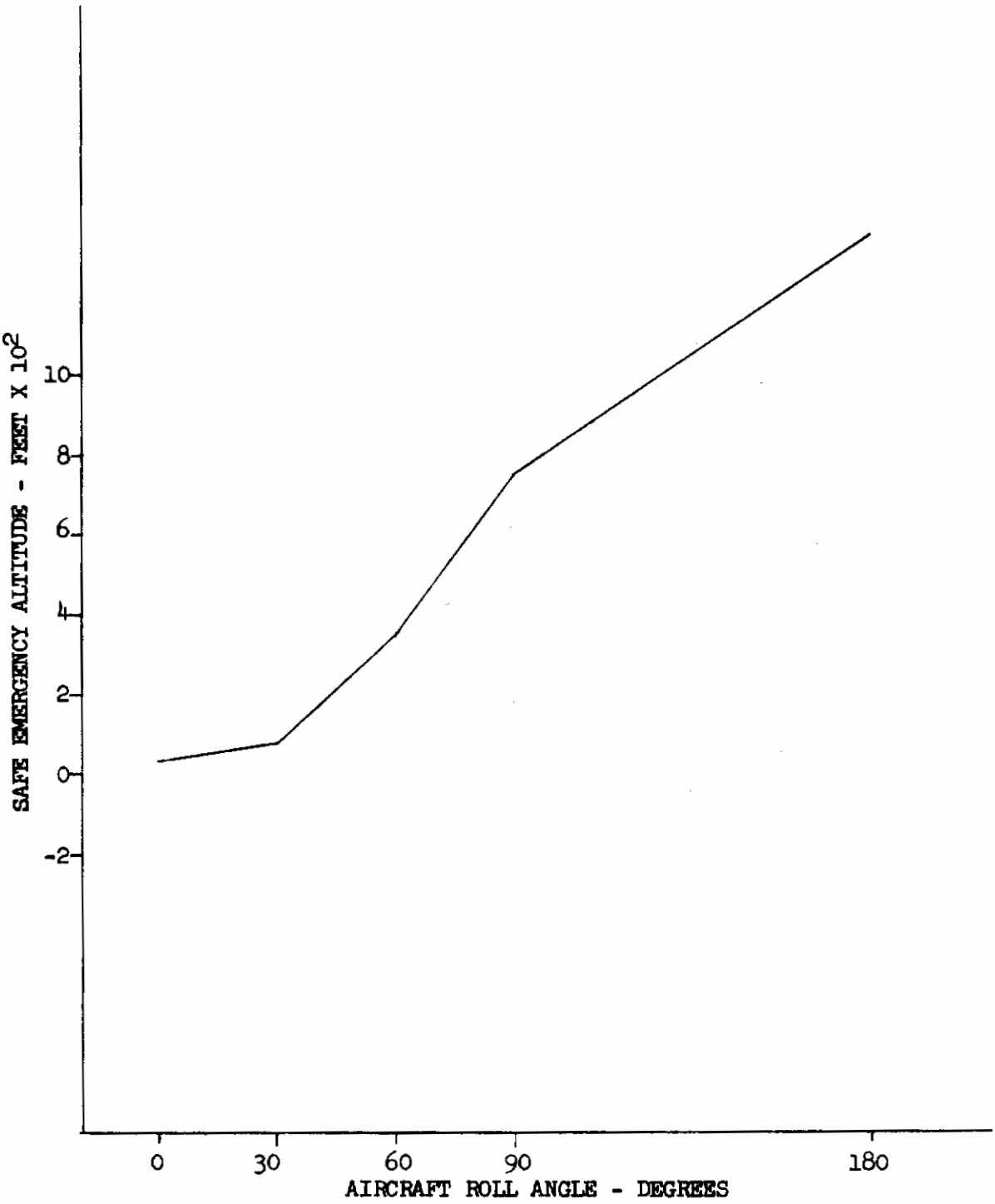

FIGURE 48 - SYSTEM C SAFE EMERGENCY ALTITUDE VERSUS ϕ
(γ = ZERO DEG; p = ZERO DEG/SEC; V = ZERO KN)

Approved for Public Release

Contrails

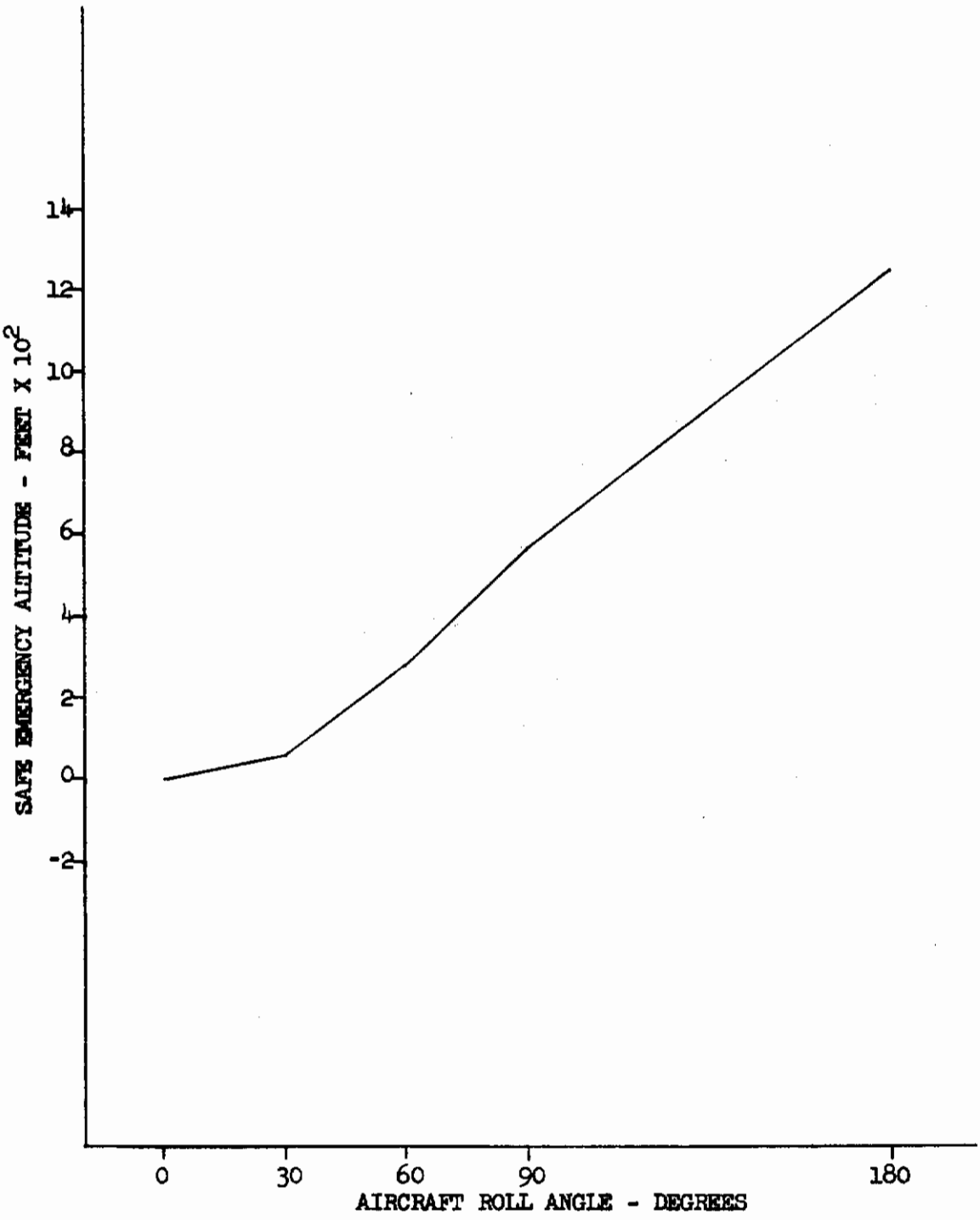

FIGURE 49 - SYSTEM D SAFE EMERGENCY ALTITUDE VERSUS ϕ
(γ = ZERO DEG; p = ZERO DEG/SEC; V = ZERO KN)

Approved for Public Release

Contrails

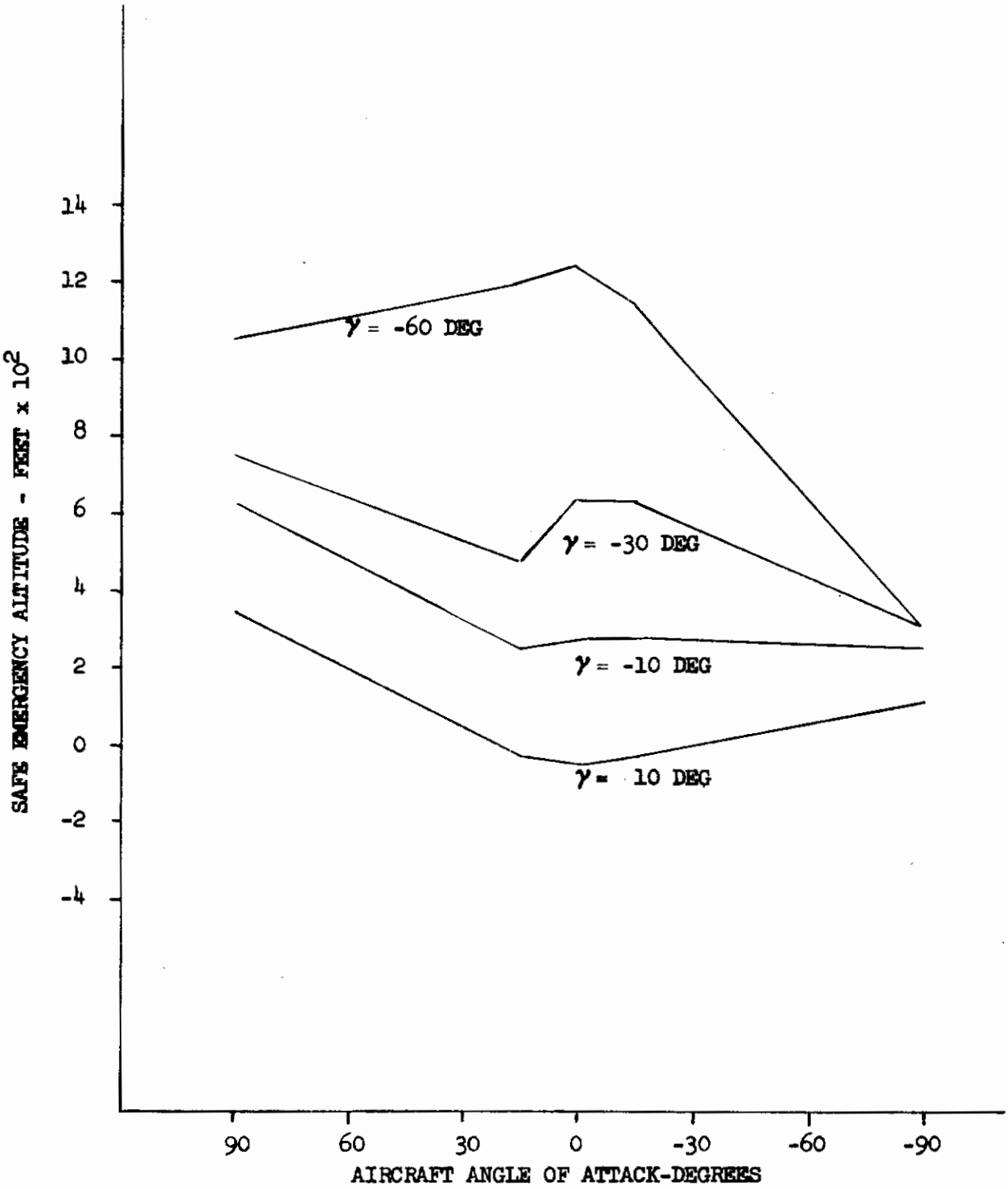

FIGURE 50 - SYSTEM A SAFE EMERGENCY ALTITUDE VERSUS α
(γ = 10, -10, -30 AND -60 DEG; q = ZERO DEG/SEC; V = 100 KN)

Approved for Public Release

Contrails

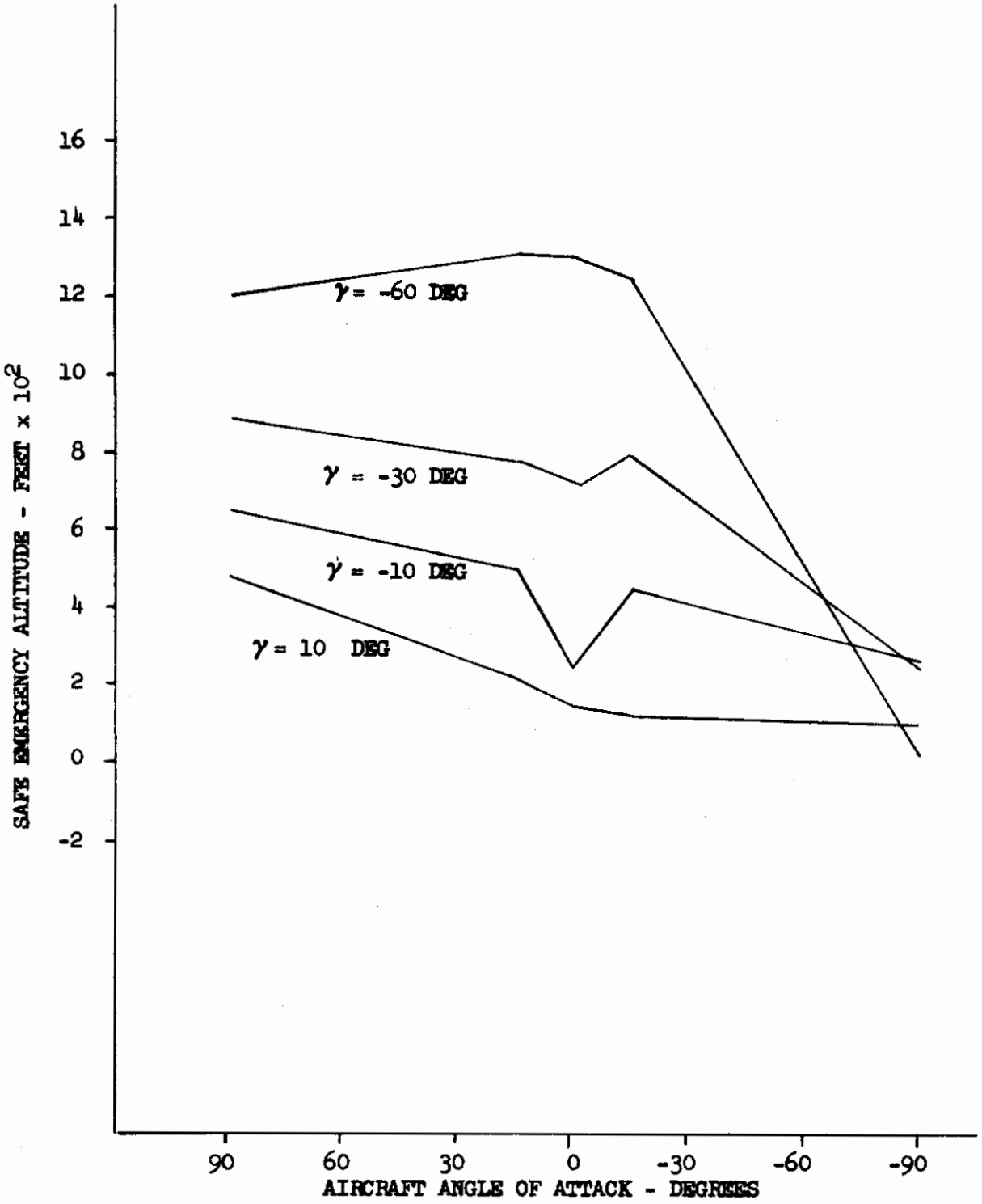

FIGURE 51 - SYSTEM B SAFE EMERGENCY ALTITUDE VERSUS α
(γ = 10, -10, -30 AND -60 DEG: q = ZERO DEG/SEC; V = 100 KN)

Approved for Public Release

Contrails

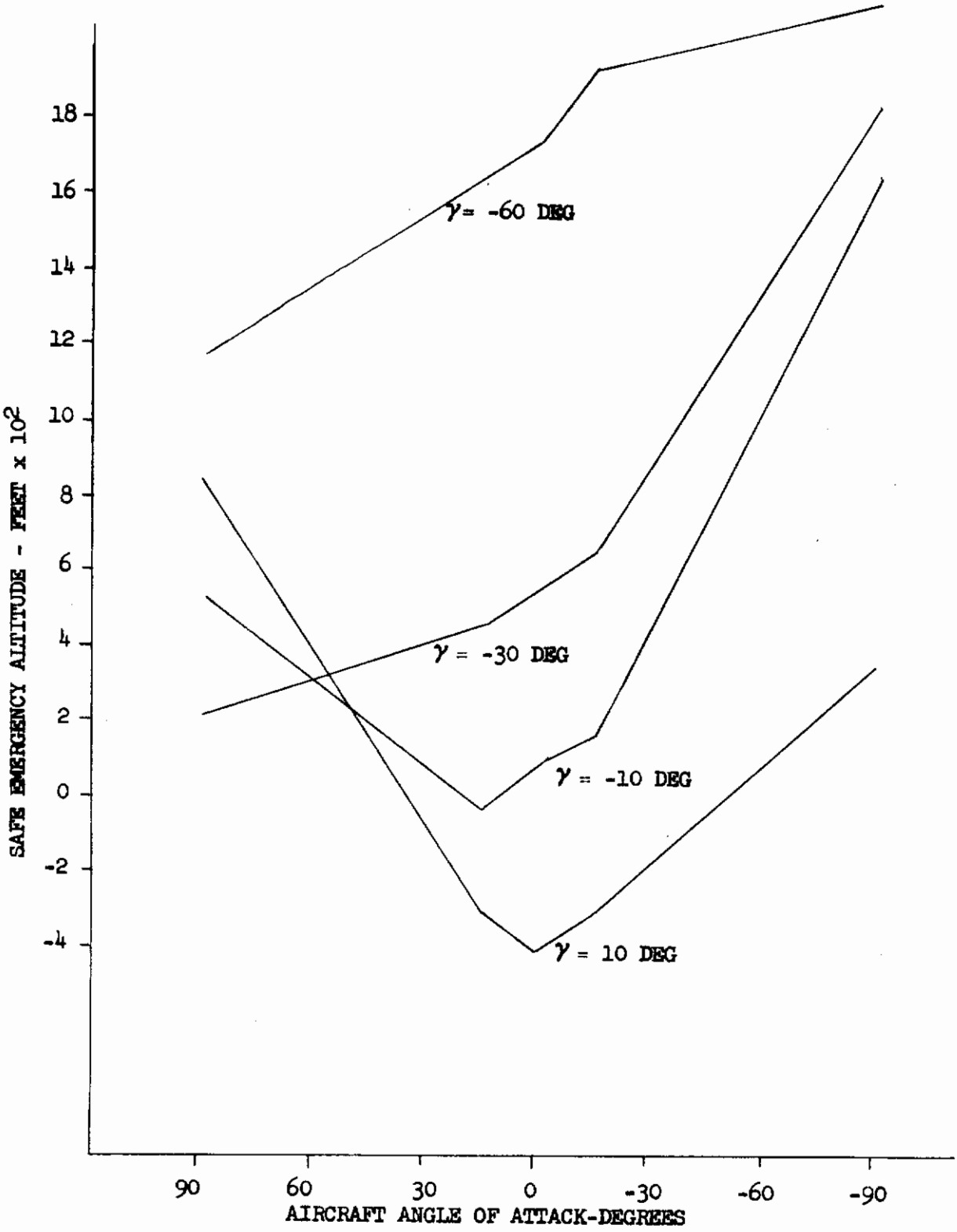

FIGURE 52- SYSTEM C SAFE EMERGENCY ALTITUDE VERSUS α
(γ = 10, -10, -30 AND -60 DEG; q = ZERO DEG/SEC; V = 100 KN)

Approved for Public Release

Contrails

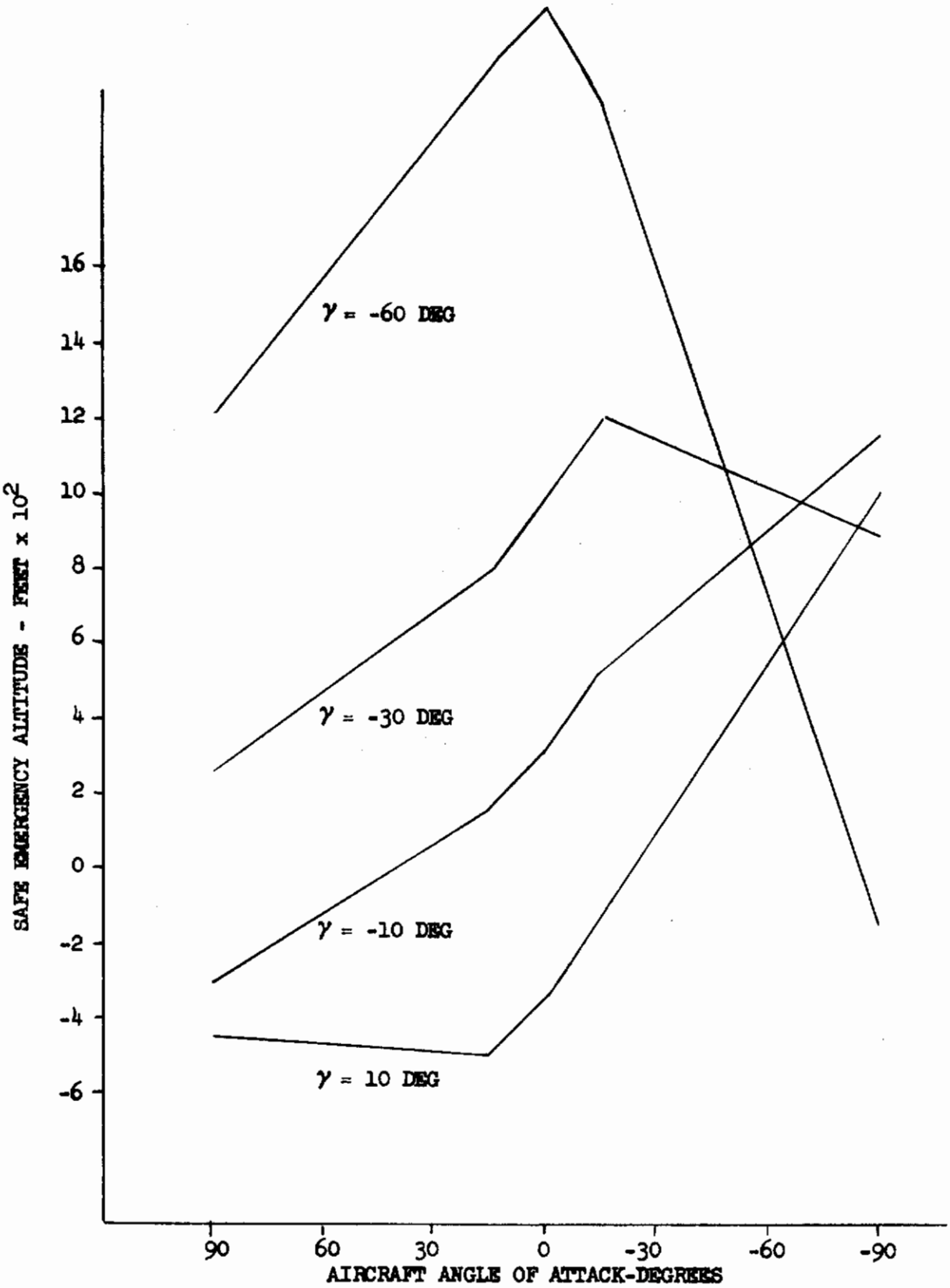

FIGURE 53 - SYSTEM D SAFE EMERGENCY ALTITUDE VERSUS α
(γ = 10, -10, -30 AND -60 DEG; q = ZERO DEG/SEC; V = 100 KN)

Approved for Public Release

Contrails

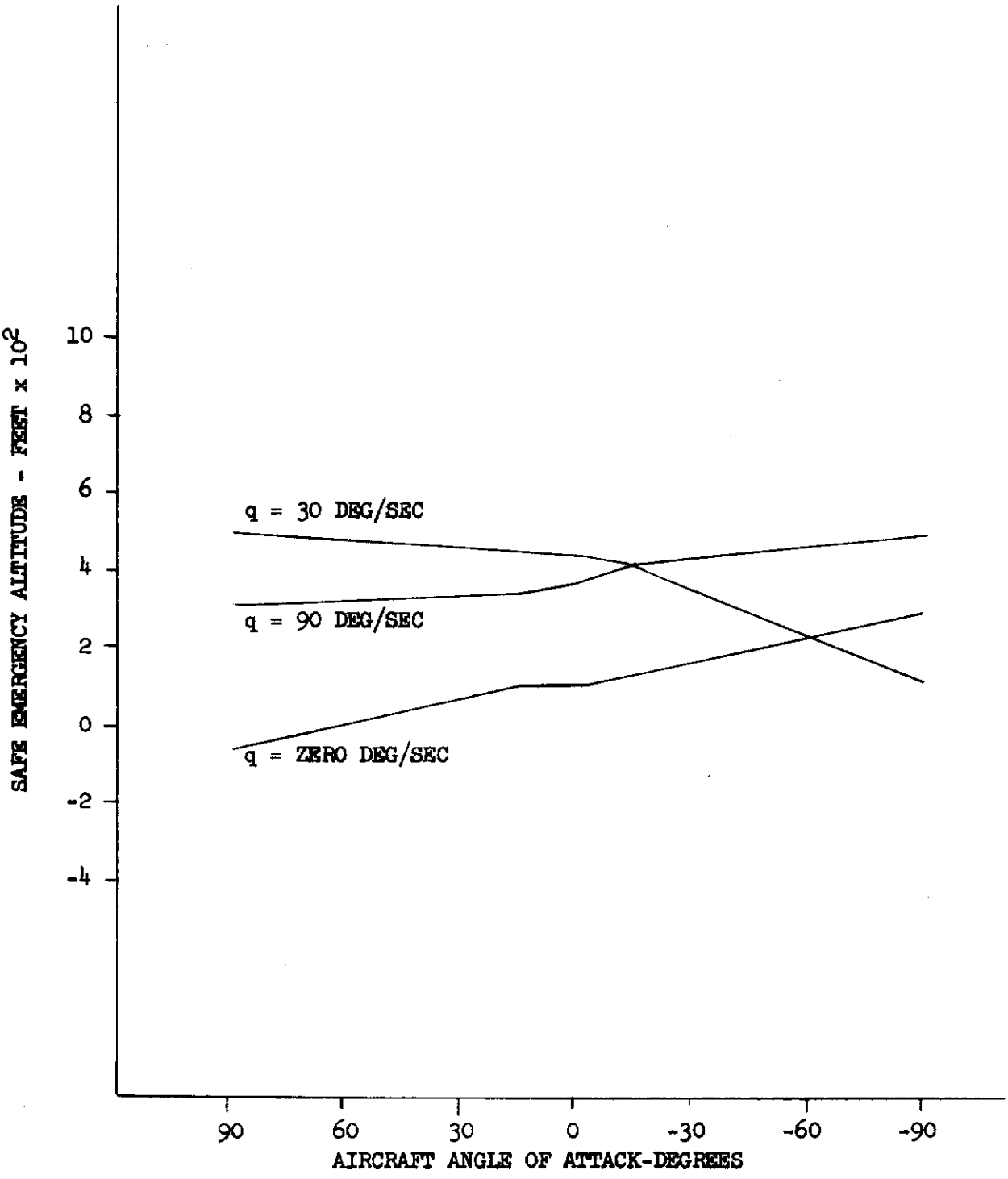

FIGURE 54-SYSTEM A SAFE EMERGENCY ALTITUDE VERSUS α
(γ = ZERO DEG; q = ZERO, 30 and 90 DEG/SEC; V = 100 KN)

Approved for Public Release

Contrails

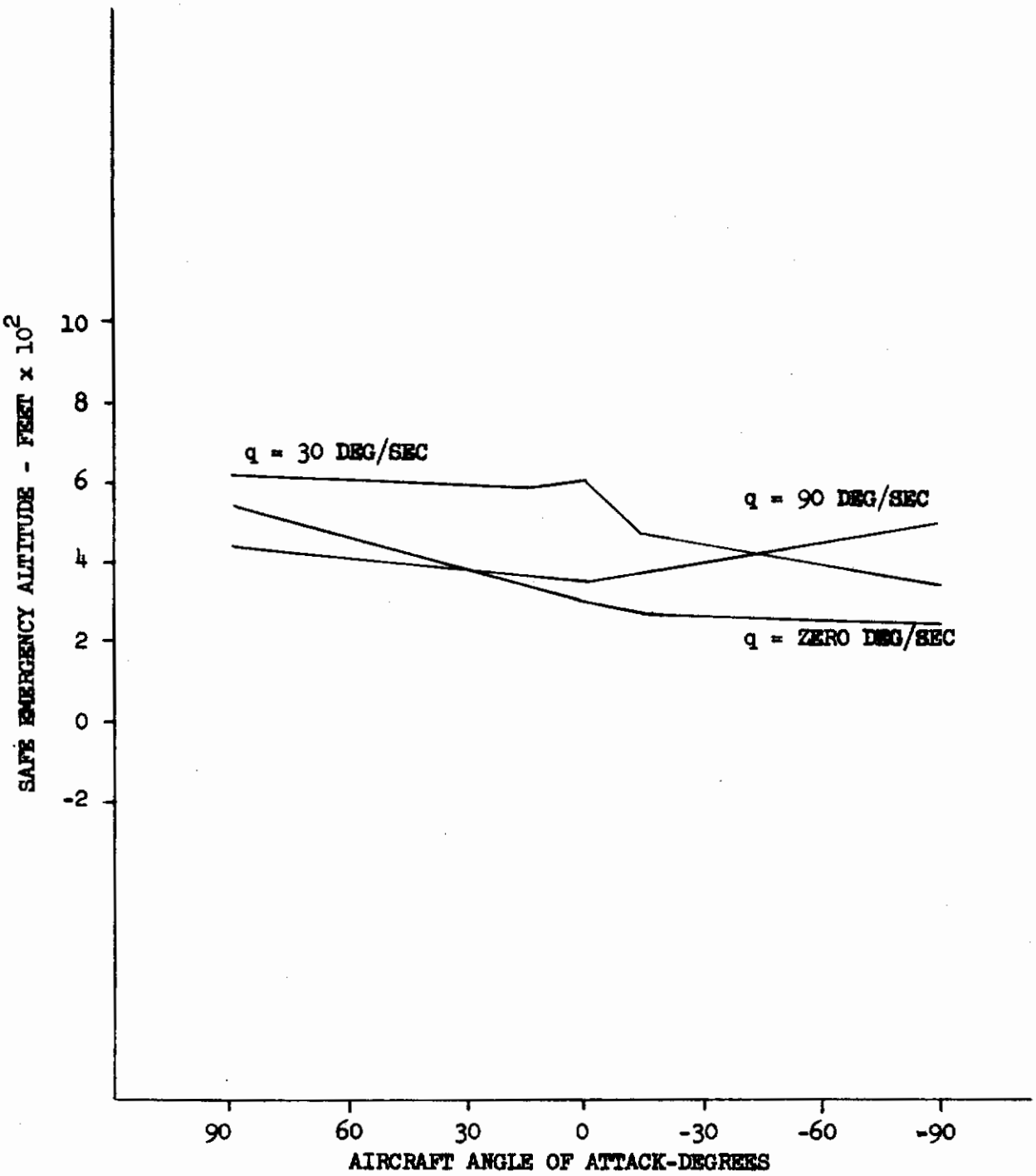

FIGURE 55 - SYSTEM B SAFE EMERGENCY ALTITUDE VERSUS α
(γ = ZERO DEG; q = ZERO, 30 AND 90 DEG/SEC; V = 100 KN)

Approved for Public Release

Contrails

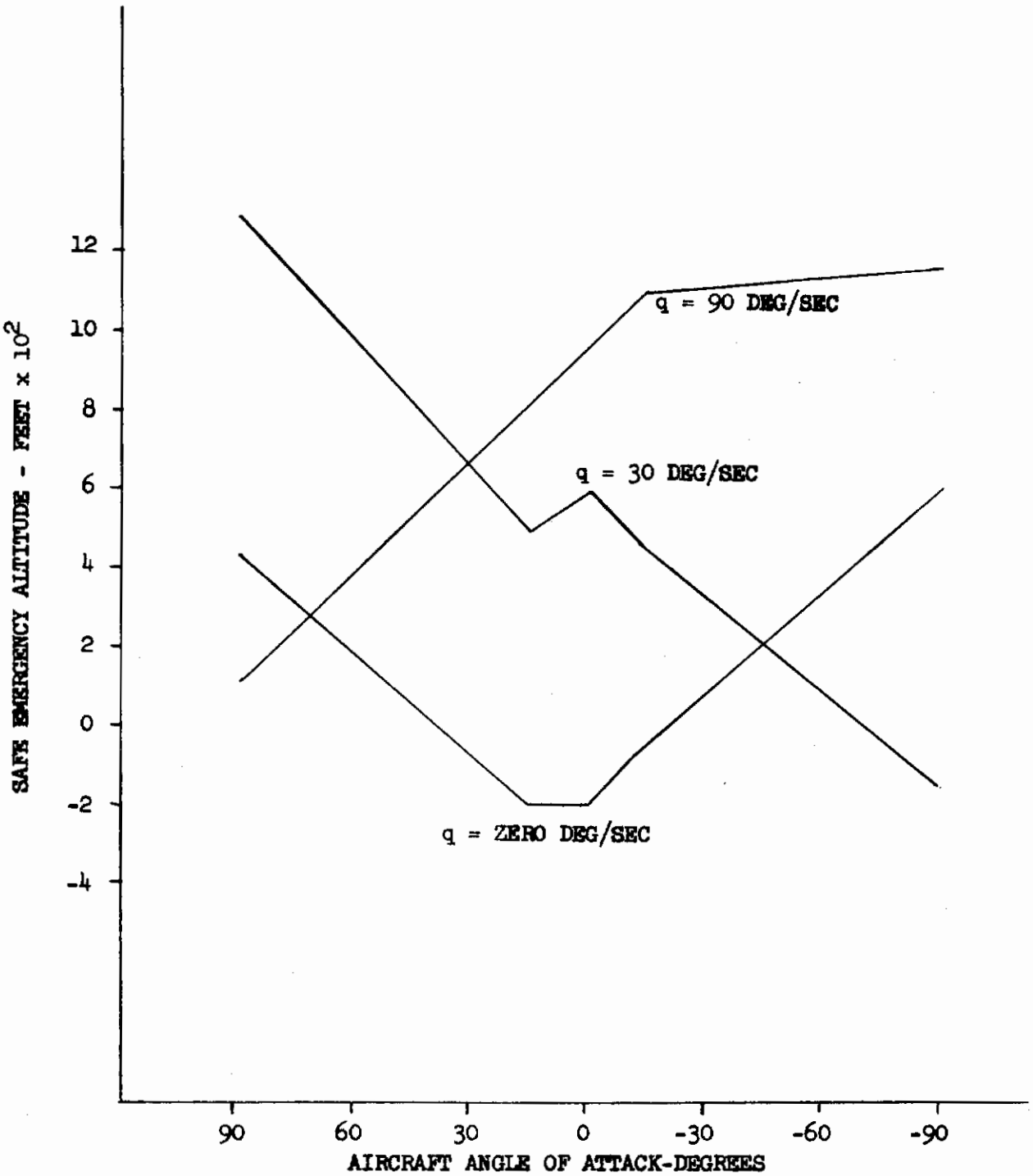

FIGURE 56 - SYSTEM C SAFE EMERGENCY ALTITUDE VERSUS α
(γ = ZERO DEG; q = ZERO, 30 AND 90 DEG/SEC; V = 100 KN)

Approved for Public Release

Contrails

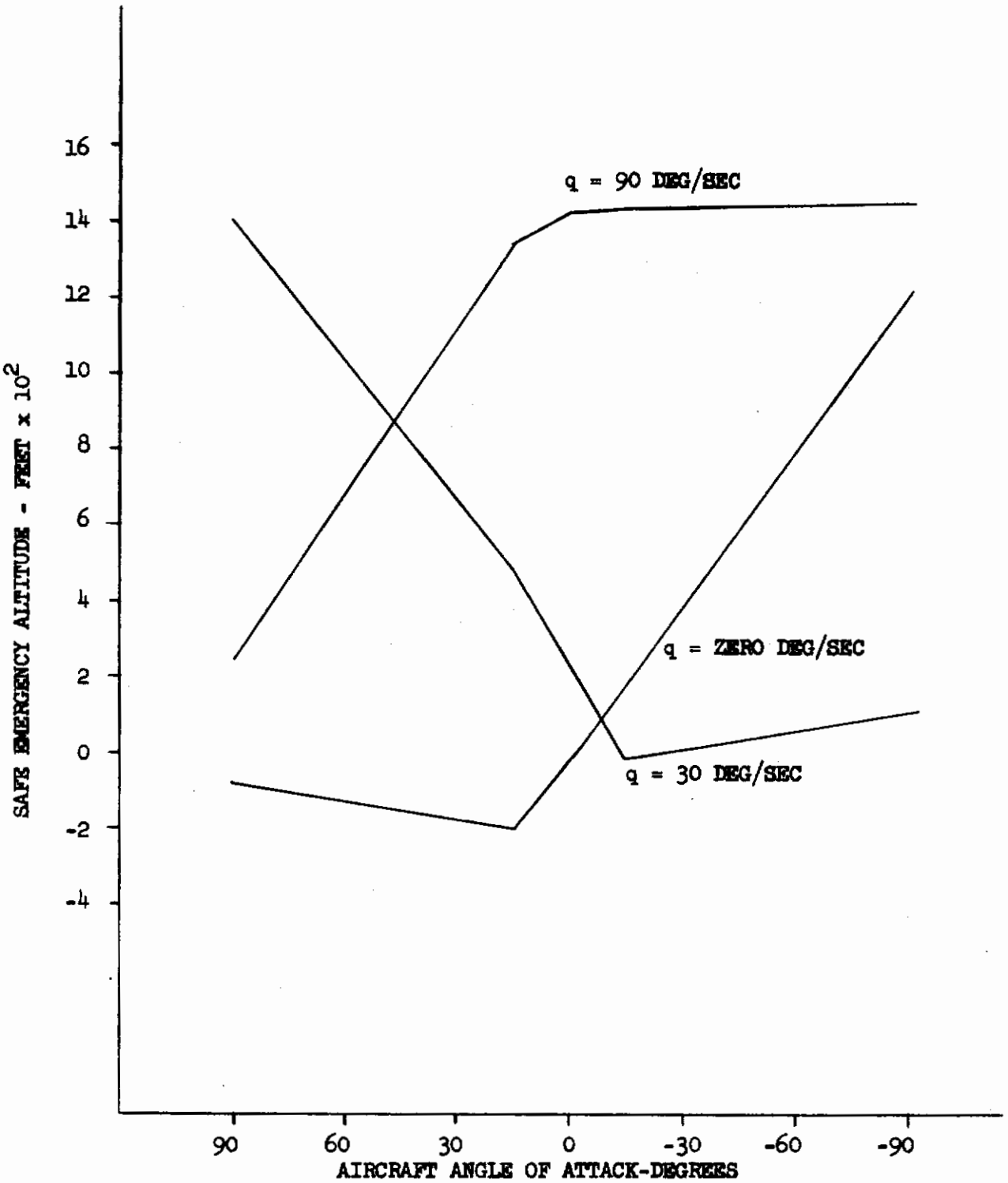

FIGURE 57 - SYSTEM D SAFE EMERGENCY ALTITUDE VERSUS α
(γ = ZERO DEG; q = ZERO, 30 AND 90 DEG/SEC; V = 100 KN)

Approved for Public Release

Contrails

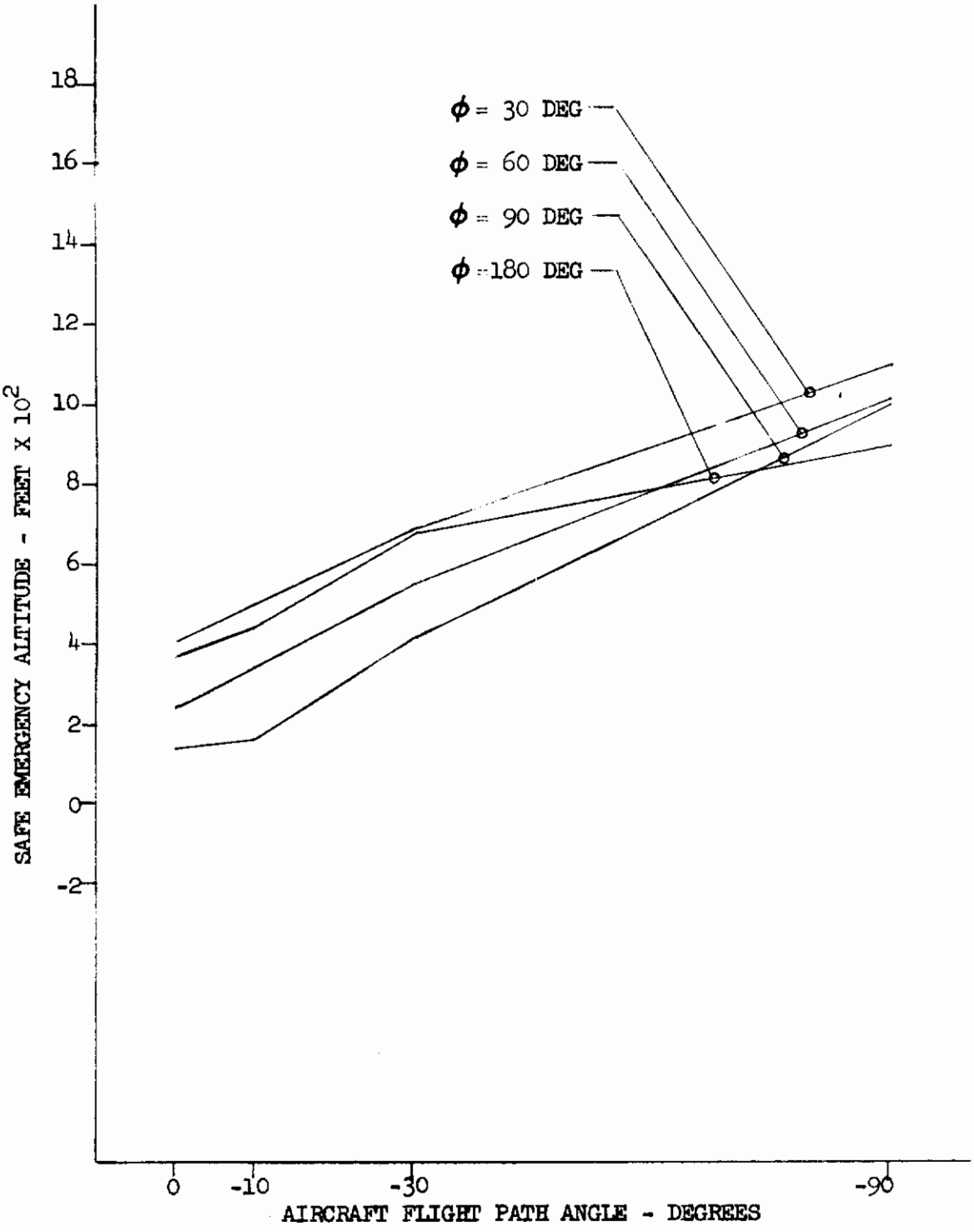

FIGURE 58 - SYSTEM A SAFE EMERGENCY ALTITUDE VERSUS γ
(α = 15 DEG, q = ZERO DEG/SEC; p = 60 DEG/SEC; V=100KN)

Approved for Public Release

Contrails

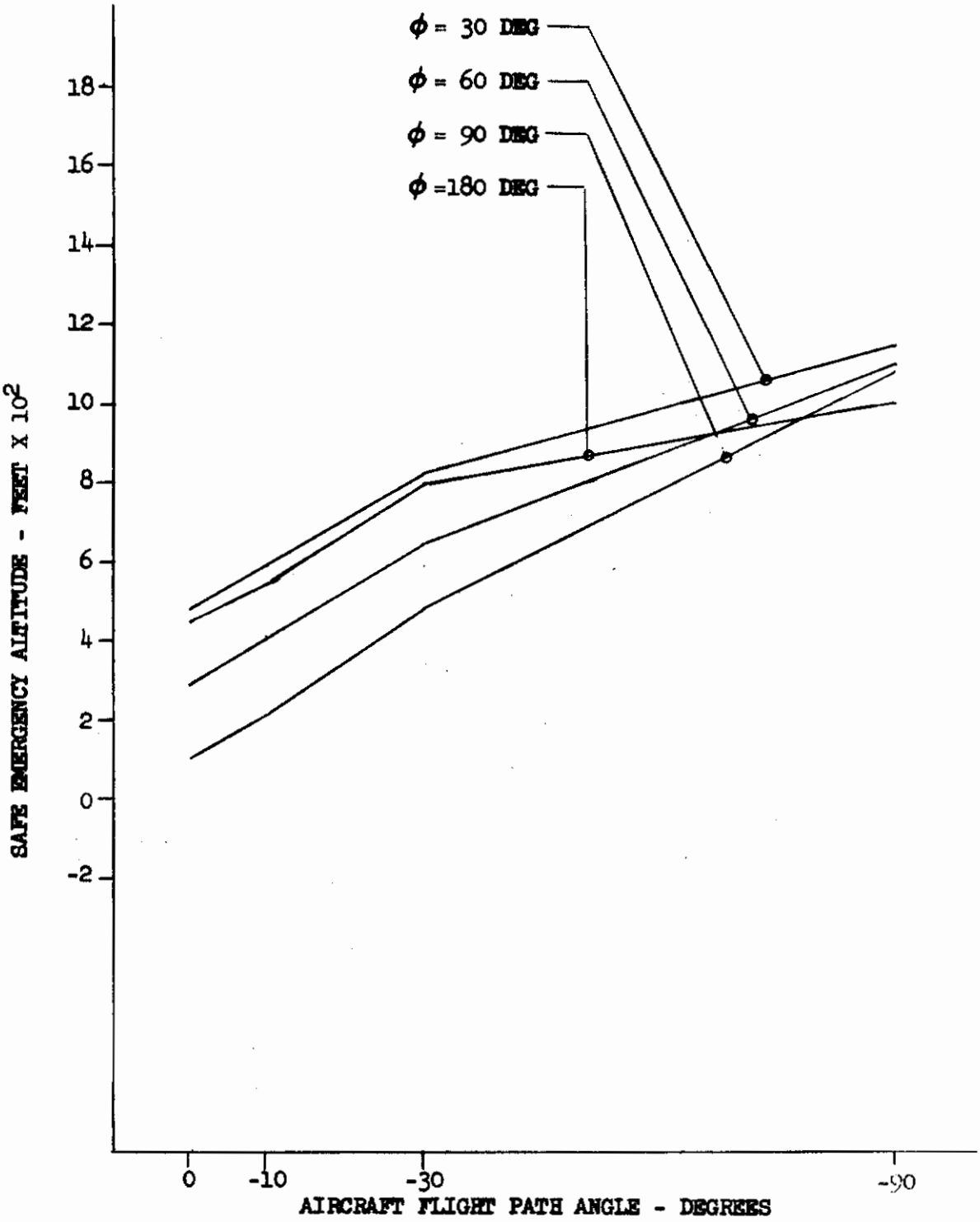

FIGURE 59 - SYSTEM B SAFE EMERGENCY ALTITUDE VERSUS γ
(α = 15 DEG, q = ZERO DEG/SEC; p = 60 DEG/SEC; V = 100 KN)

Approved for Public Release

Contrails

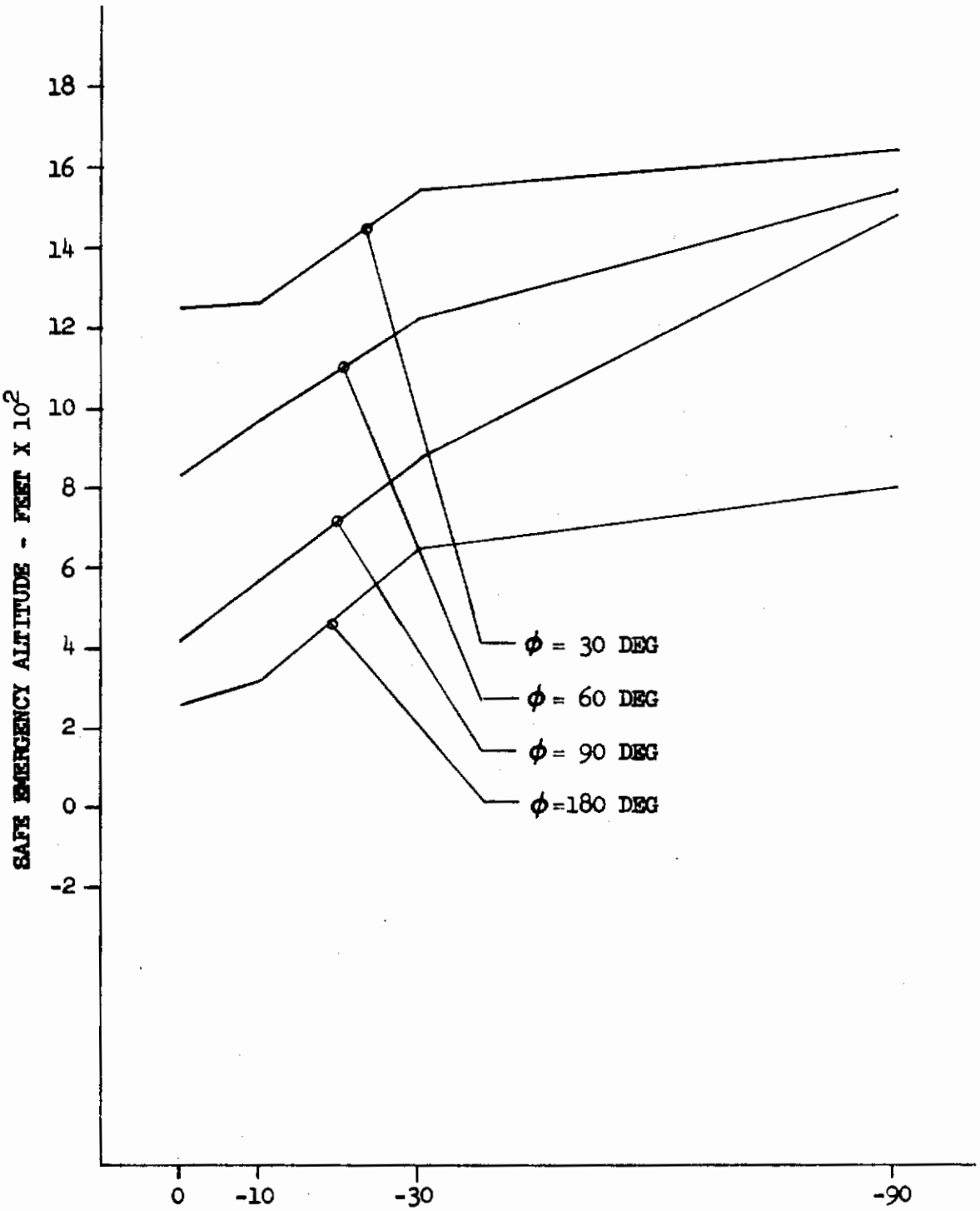

FIGURE 60 - SYSTEM C SAFE EMERGENCY ALTITUDE VERSUS γ
(α = 15 DEG, q = ZERO DEG/SEC; p = 60 DEG/SEC; V = 100 KN)

Approved for Public Release

Contrails

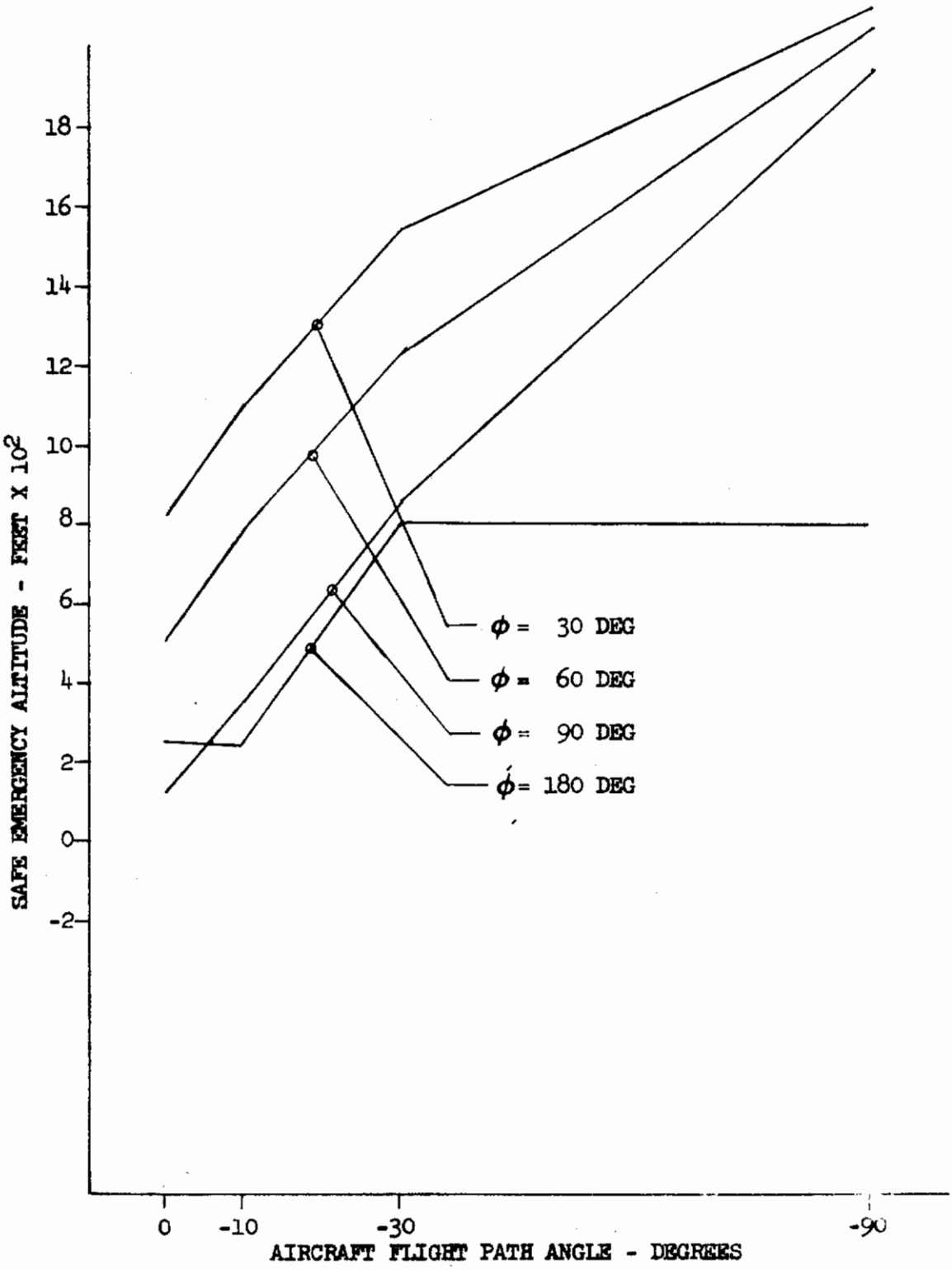

FIGURE 61 - SYSTEM D SAFE EMERGENCY ALTITUDE VERSUS γ
(α = 15 DEG, q = ZERO DEG/SEC; p = 60 DEG/SEC; V = 100 KN)

Approved for Public Release

Contrails

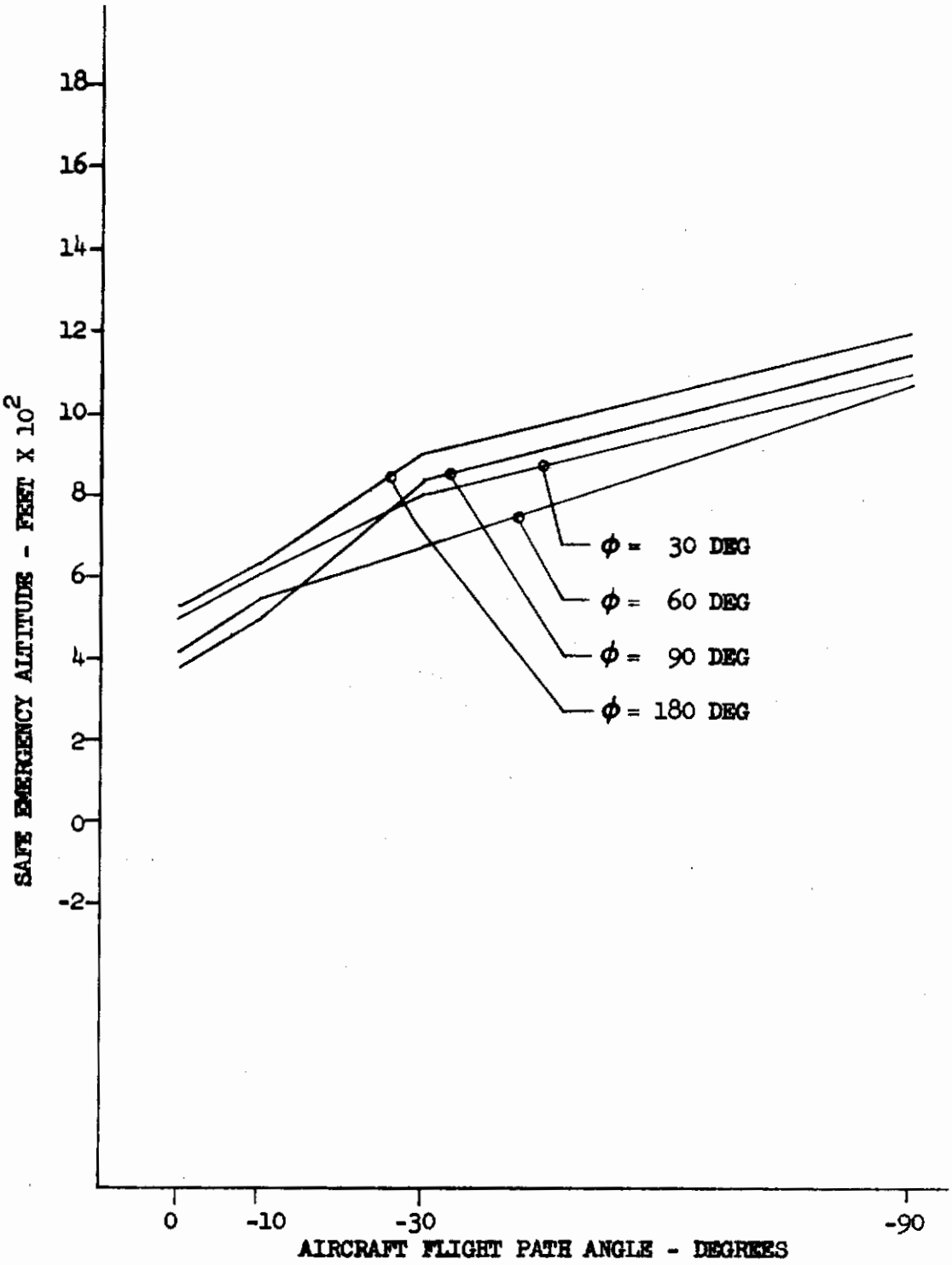

FIGURE 62 - SYSTEM A SAFE EMERGENCY ALTITUDE VERSUS γ
(α = -15 DEG; q = 30 DEG/SEC; p = 60 DEG/SEC, V = 100 KN)

Approved for Public Release

Contrails

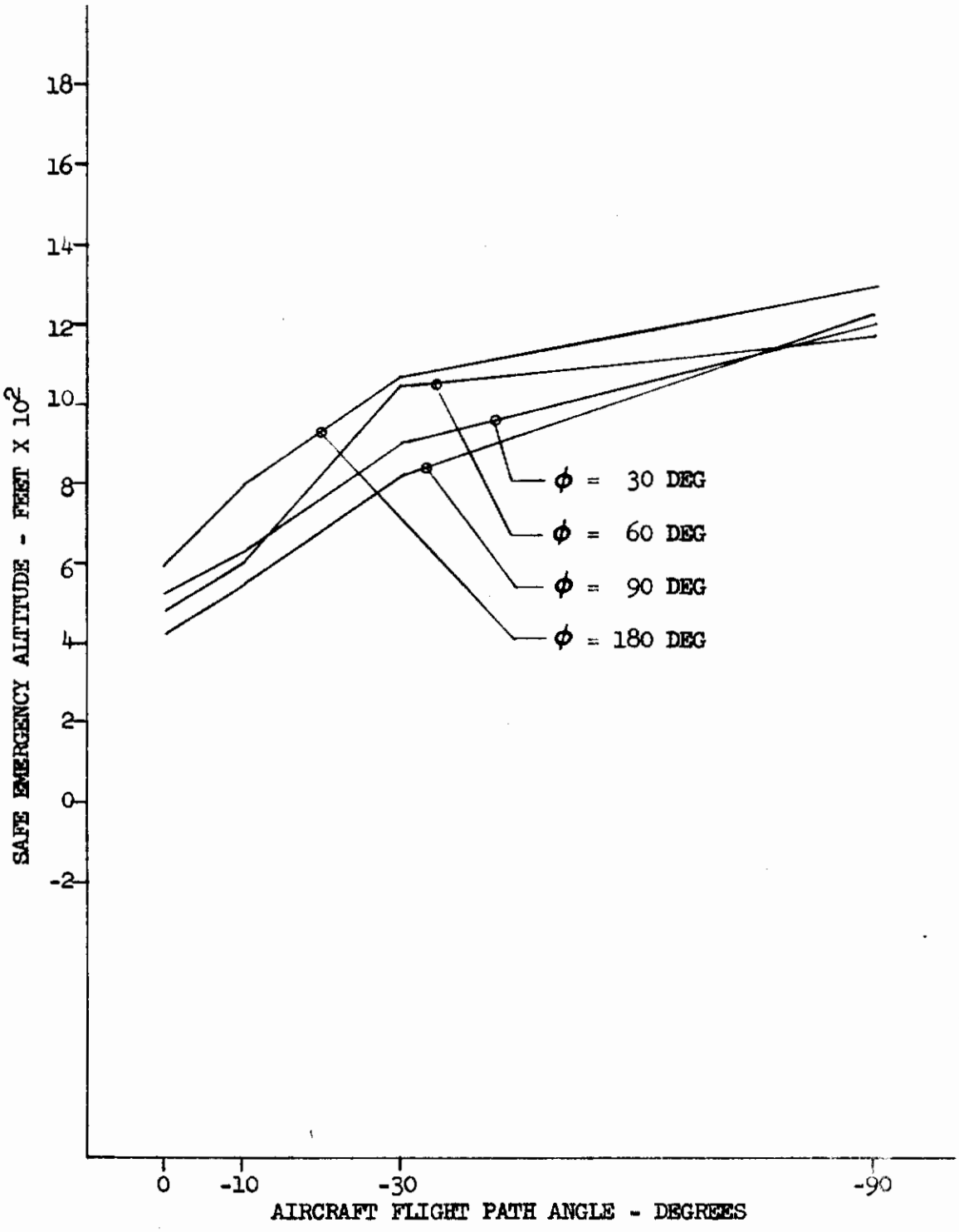

FIGURE 63 - SYSTEM B SAFE EMERGENCY ALTITUDE VERSUS γ
(α = -15 DEG; q = 30 DEG/SEC; p = 60 DEG/SEC; V = 100 KN)

Approved for Public Release

Contrails

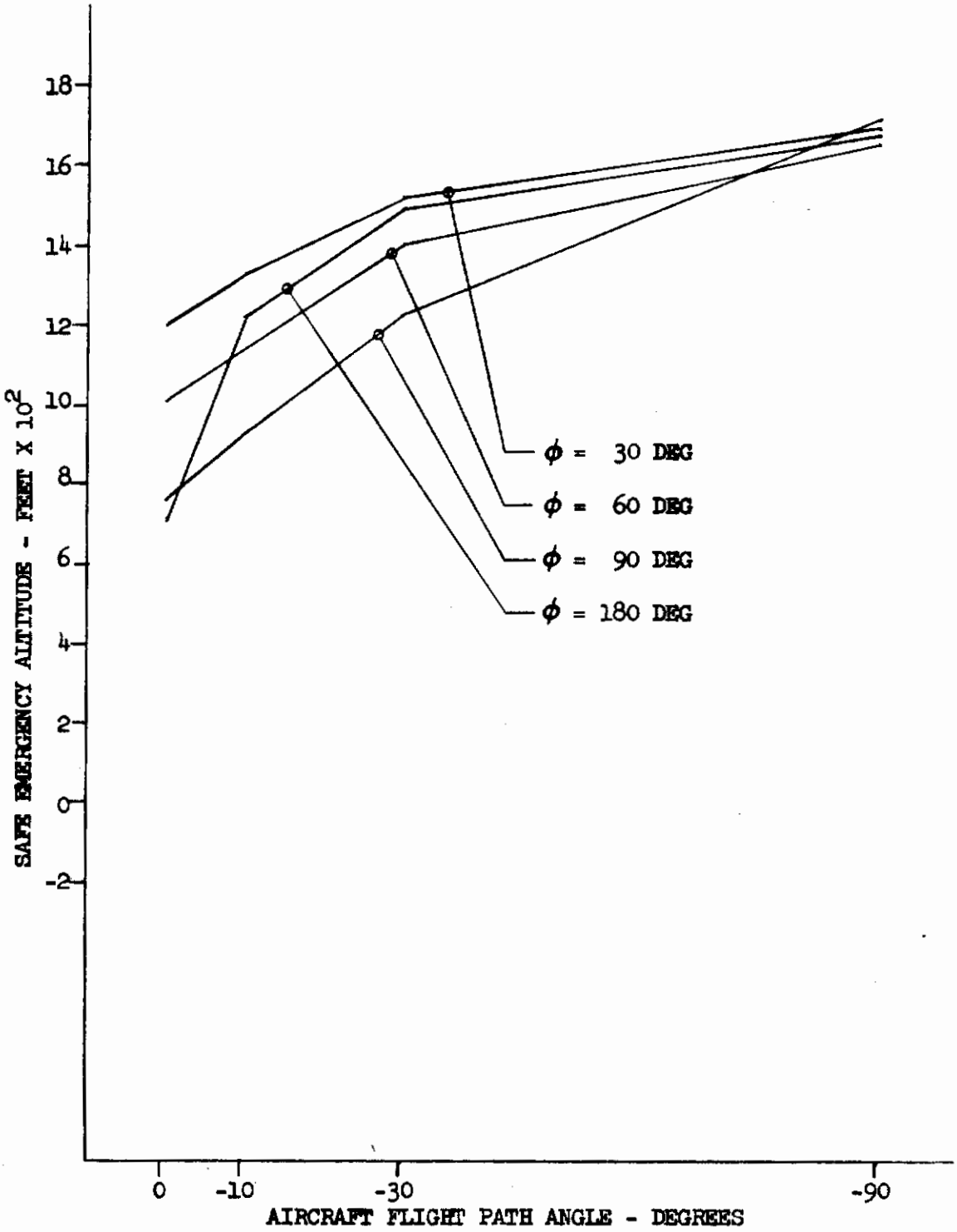

FIGURE 64 - SYSTEM C SAFE EMERGENCY ALTITUDE VERSUS γ
(α = -15 DEG; q = 30 DEG/SEC; p = 60 DEG/SEC; V = 100 KN)

Approved for Public Release

Contrails

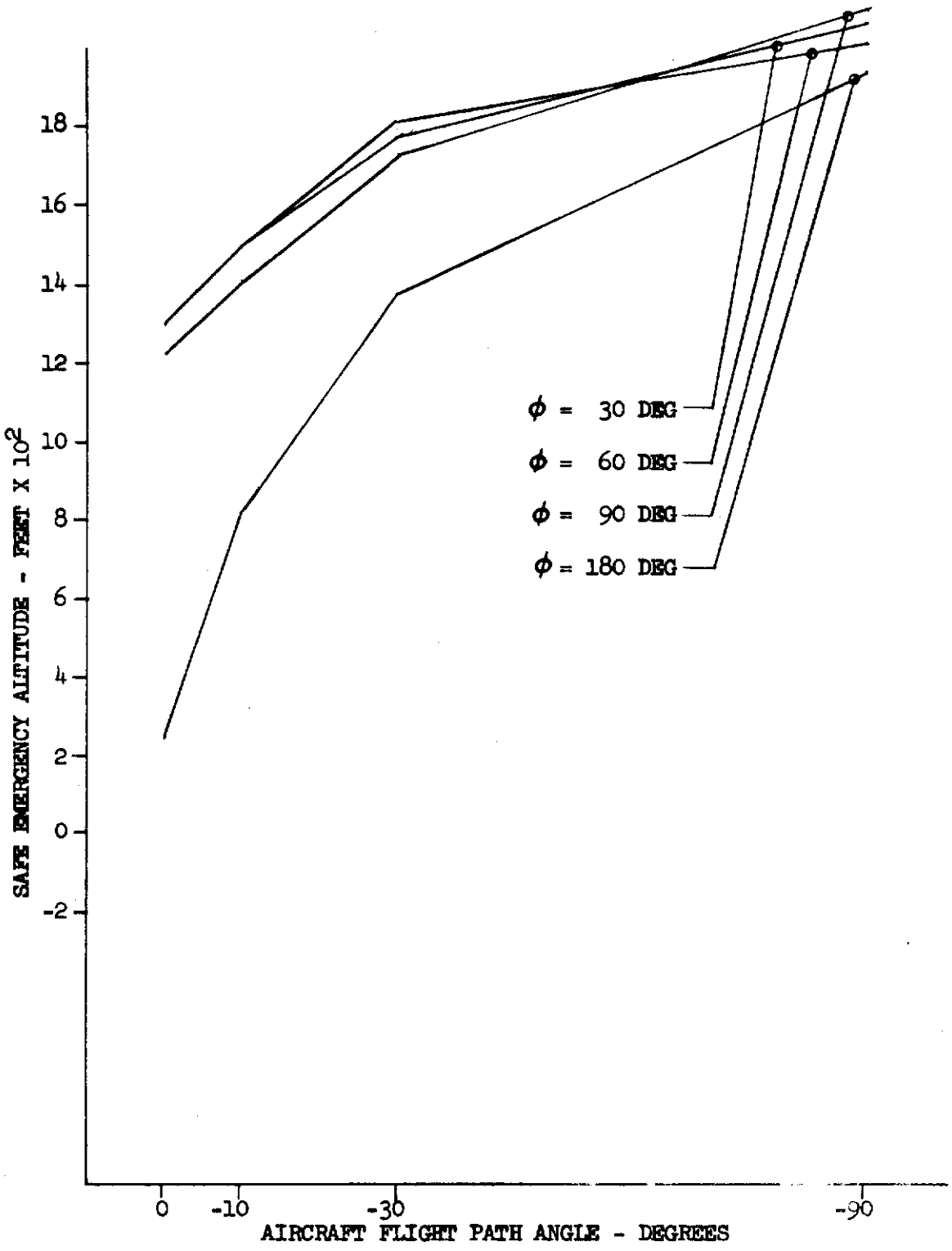

FIGURE 65- SYSTEM D SAFE EMERGENCY ALTITUDE VERSUS γ
(α = -15 DEG; q = 30 DEG/SEC; p = 60 DEG/SEC; V = 100 KN)

Approved for Public Release

Contrails

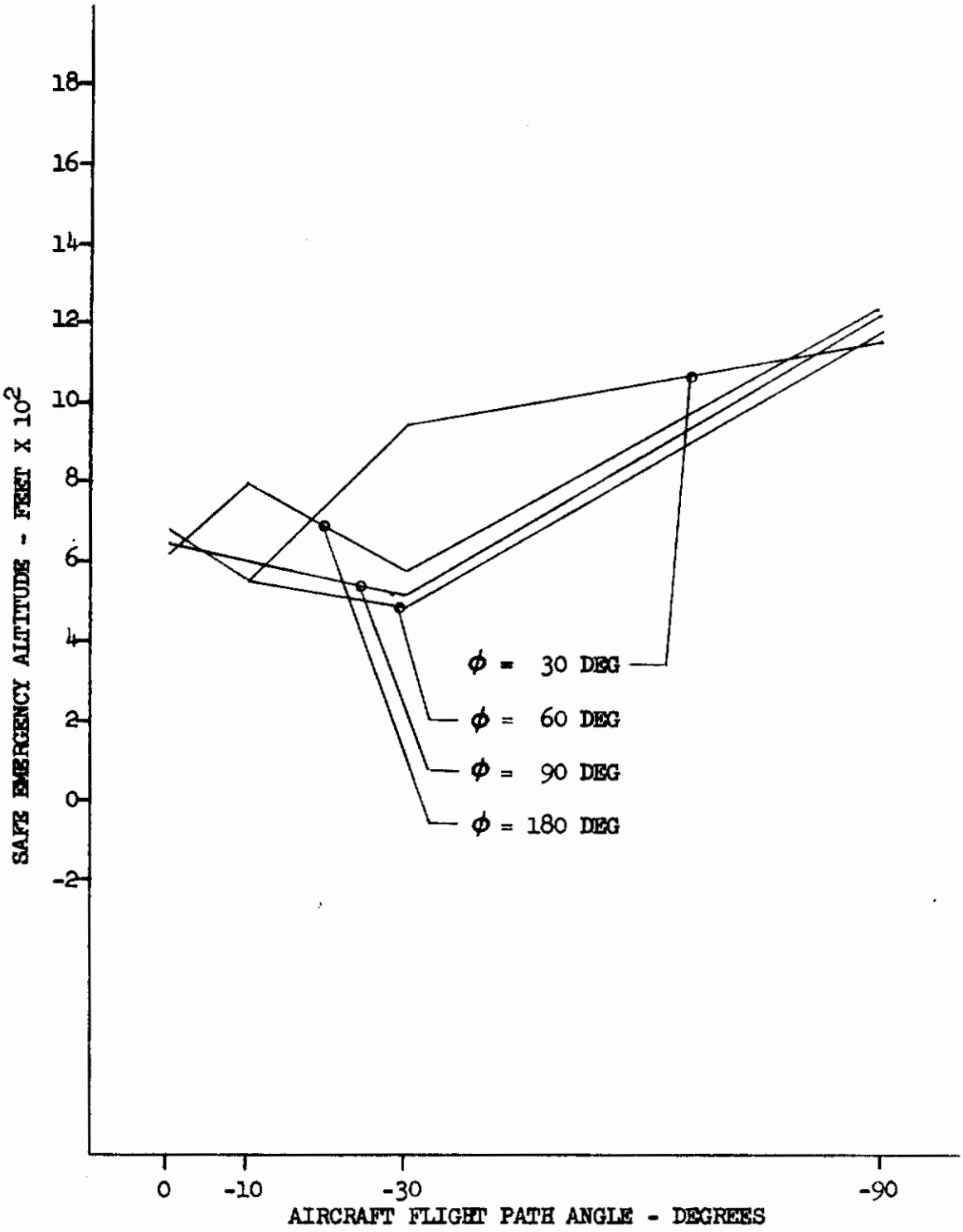

FIGURE 66. SYSTEM A SAFE EMERGENCY ALTITUDE VERSUS γ
(α = -90 DEG; q = 90 DEG/SEC; p = 180 DEG/SEC; V = 100 KN)

Approved for Public Release

Contrails

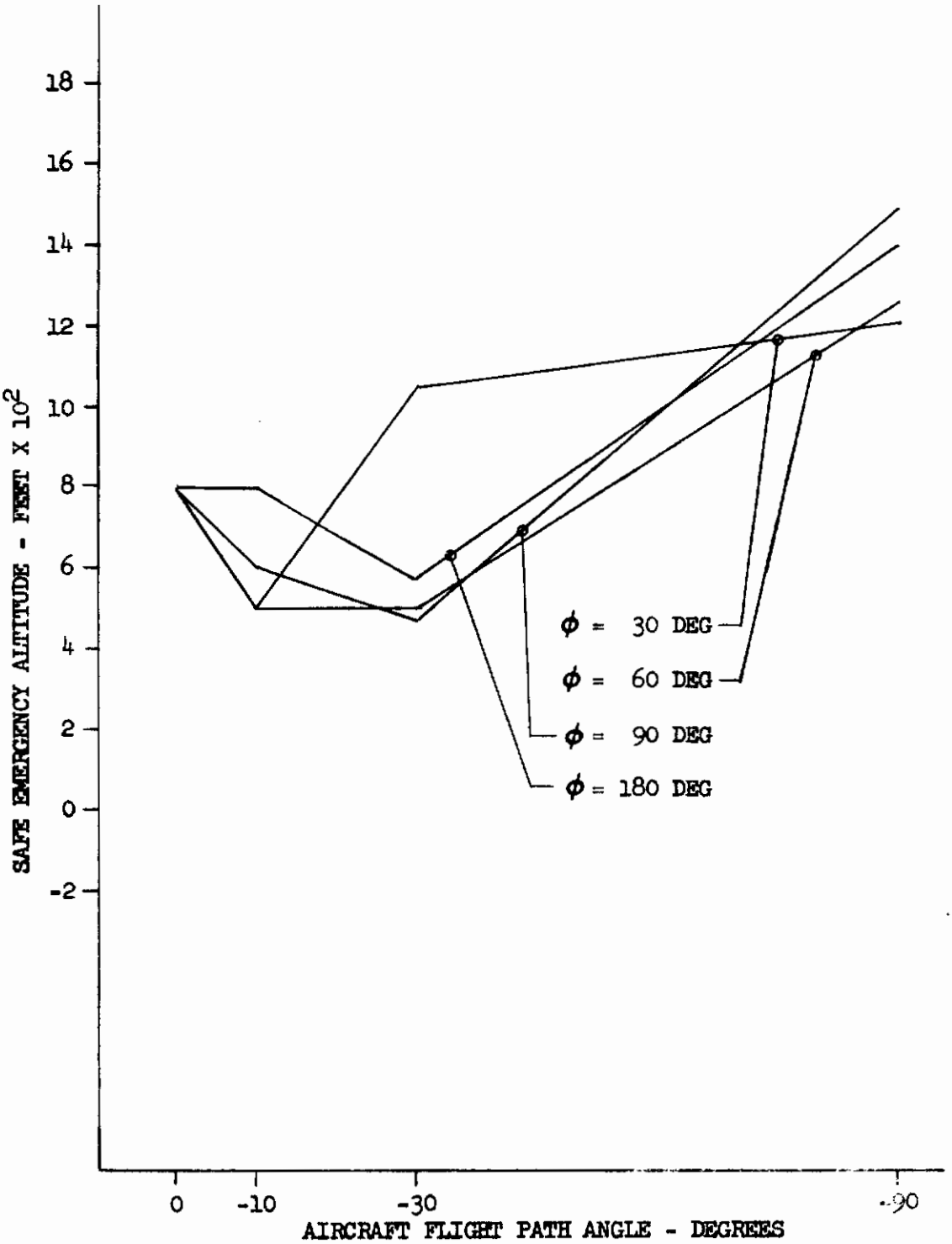

FIGURE 67 - SYSTEM B SAFE EMERGENCY ALTITUDE VERSUS γ
(α = -90 DEG; q = 90 DEG/SEC; p = 180 DEG/SEC; V = 100 KN)

Approved for Public Release

Contrails

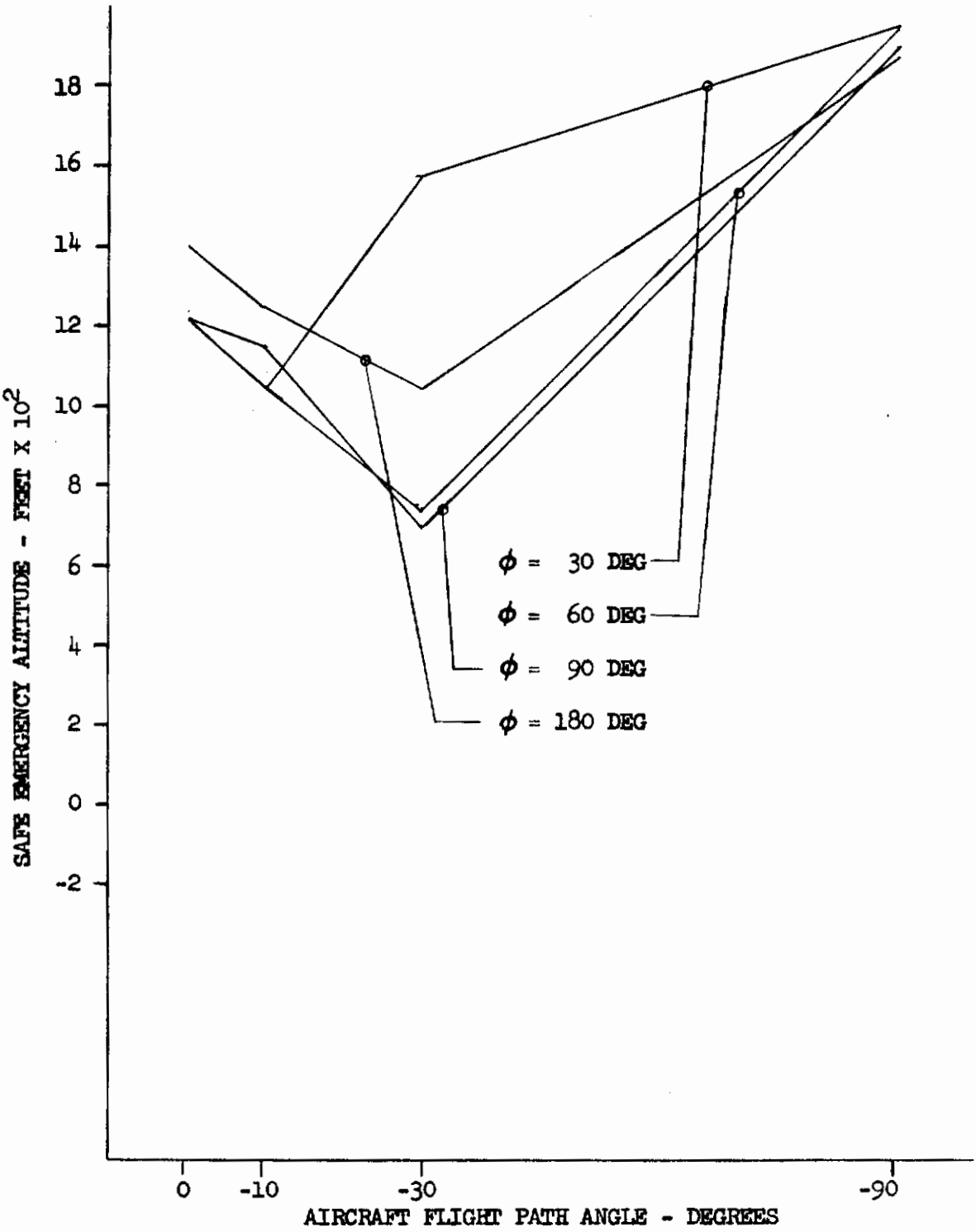

FIGURE 68 - SYSTEM C SAFE EMERGENCY ALTITUDE VERSUS γ
(α = -90 DEG; q = 90 DEG/SEC; p = 180 DEG/SEC; V = 100 KN)

Approved for Public Release

Contrails

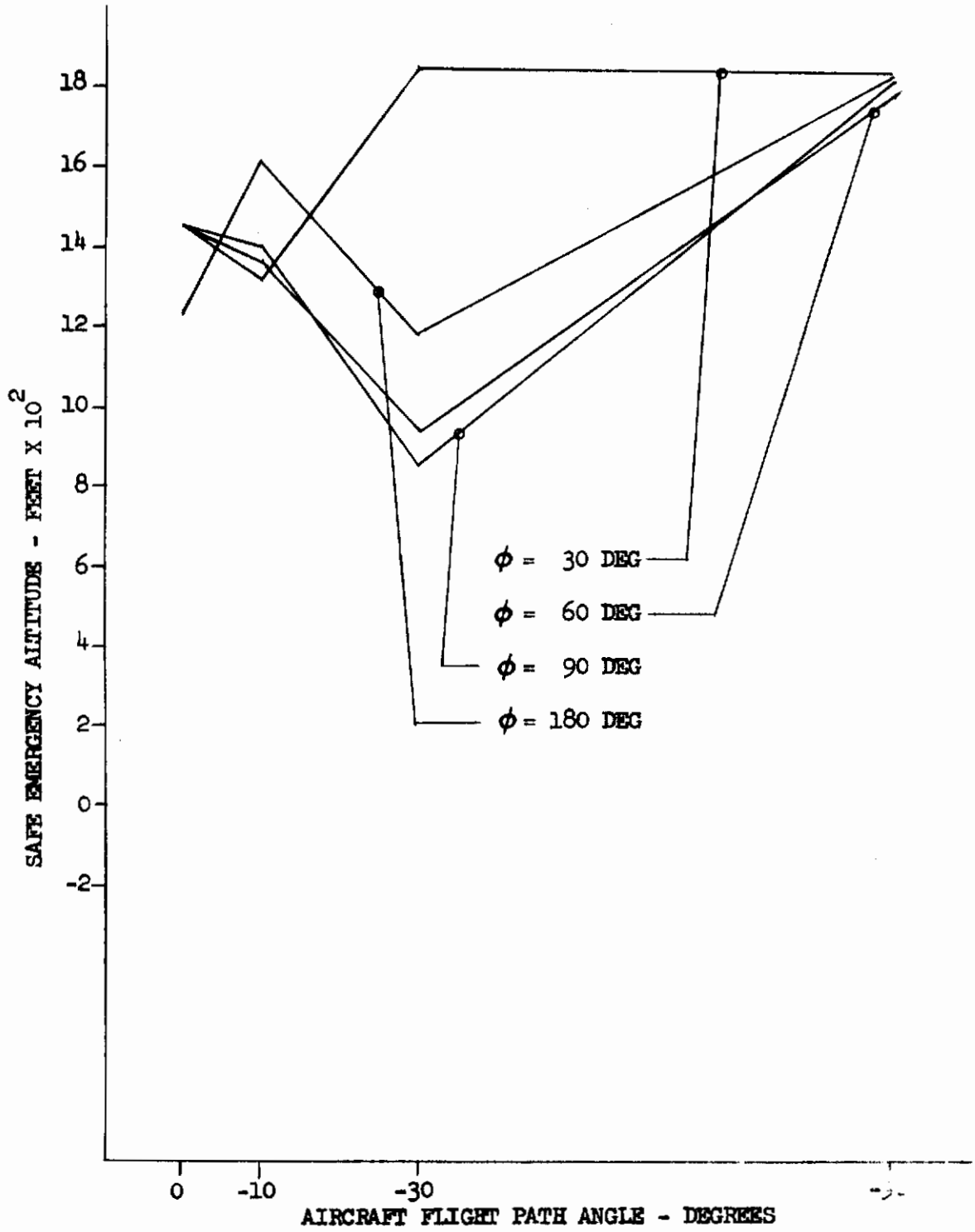

FIGURE 69 - SYSTEM D SAFE EMERGENCY ALTITUDE VERSUS γ
(α = -90 DEG; q = 90 DEG/SEC; p = 180 DEG/SEC; V = 100 KN)

Approved for Public Release

Contrails

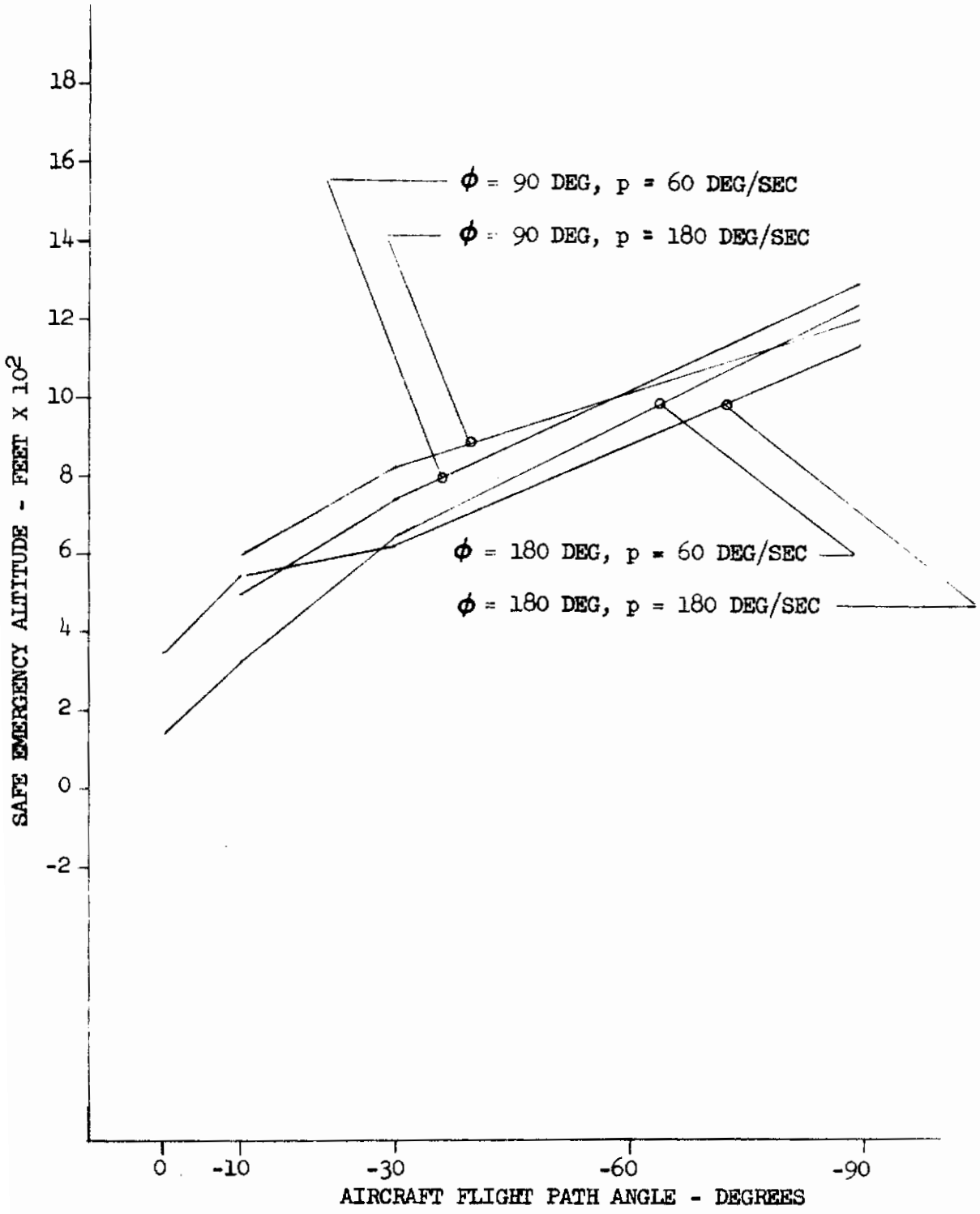

FIGURE 70 - SYSTEM A SAFE EMERGENCY ALTITUDE VERSUS γ
(ϕ = 90 and 180 DEG; p = 60 AND 180 DEG/SEC; V = 100 KN)

Approved for Public Release

Contrails

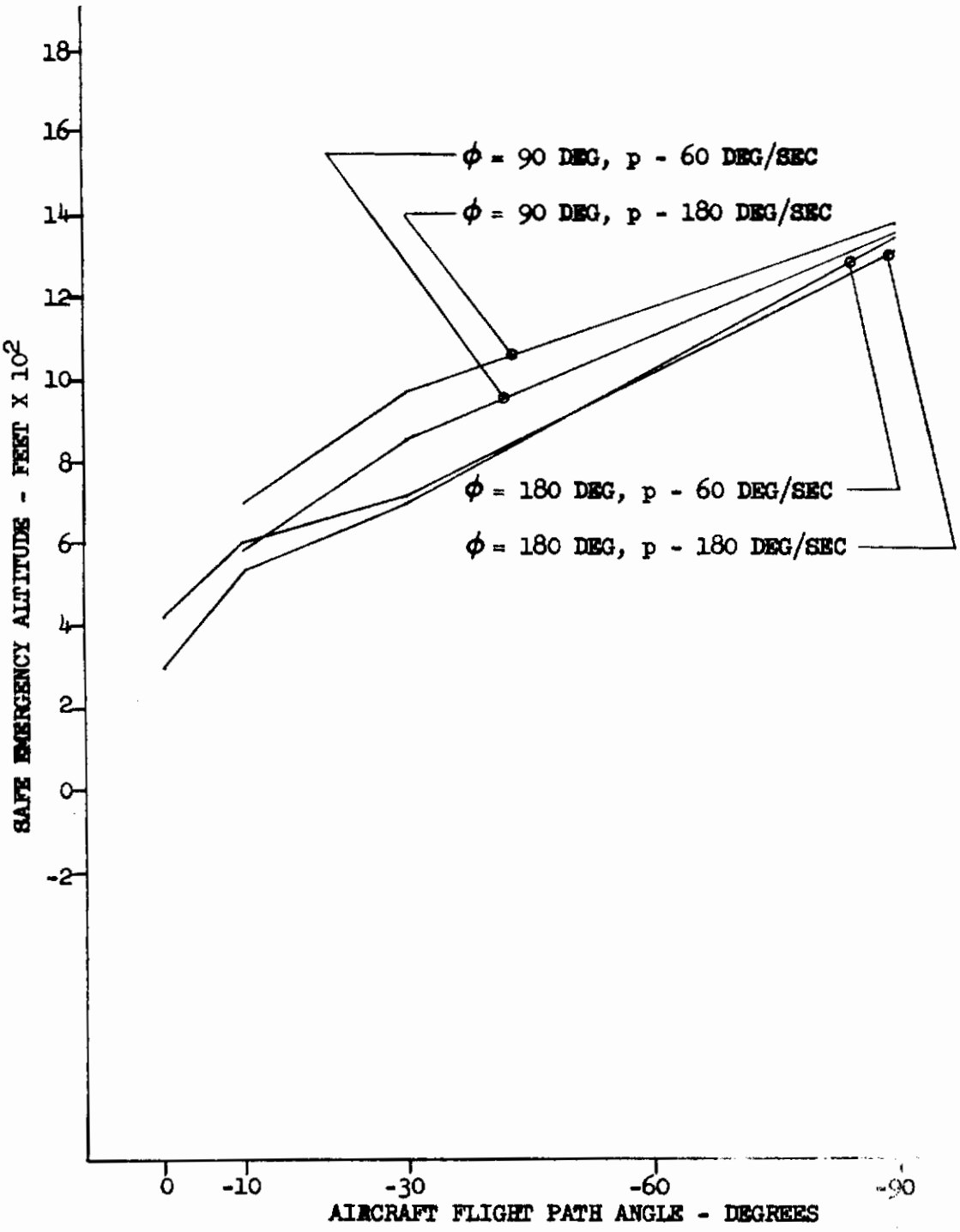

FIGURE 71 - SYSTEM B SAFE EMERGENCY ALTITUDE VERSUS γ
(ϕ = 90 AND 180 DEG; p = 60 AND 180 DEG/SEC; V = 100 KN)

Approved for Public Release

Contrails

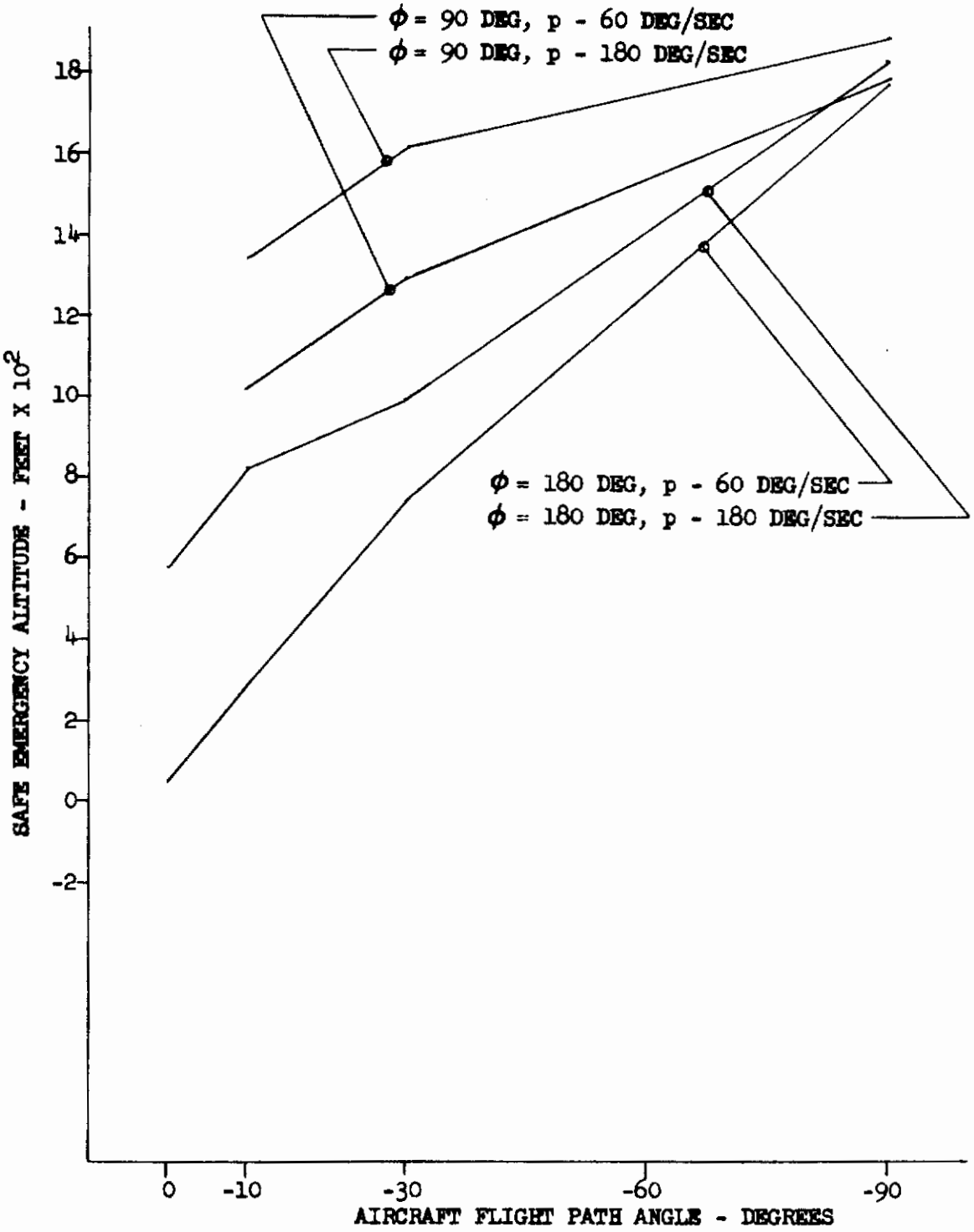

FIGURE 72 - SYSTEM C SAFE EMERGENCY ALTITUDE VERSUS γ
(ϕ = 90 AND 180 DEG; p = 60 AND 180 DEG/SEC; V = 100 KN)

Approved for Public Release

Contrails

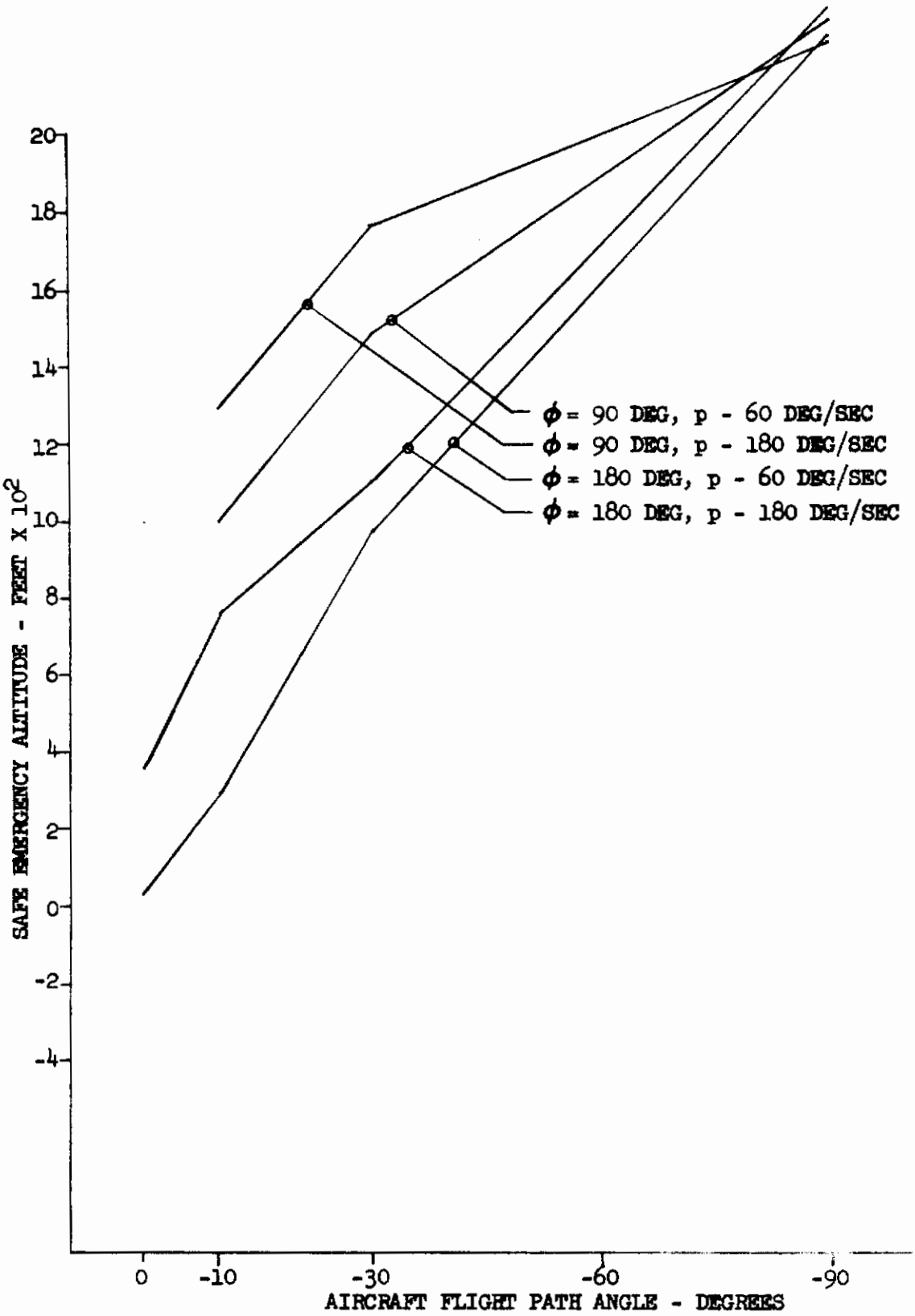

FIGURE 73 - SYSTEM D SAFE EMERGENCY ALTITUDE VERSUS γ
(ϕ = 90 AND 180 DEG; p = 60 AND 180 DEG/SEC; V = 100 KN)

Approved for Public Release

Contrails

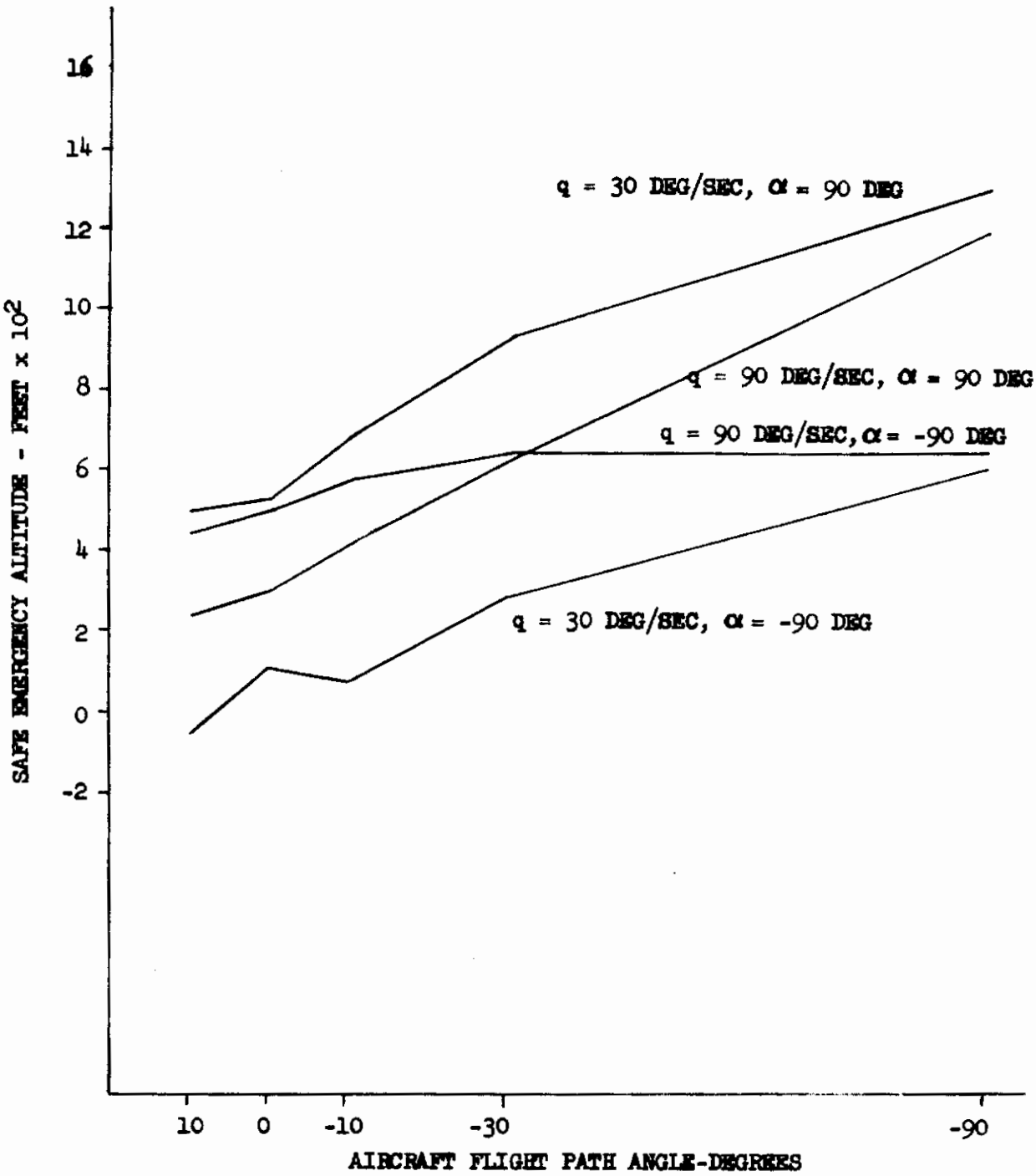

FIGURE 74 - SYSTEM A SAFE EMERGENCY ALTITUDE VERSUS γ
(q = 30 AND 90 DEG/SEC; α = 90 AND -90 DEG; v = 100 KN)

Approved for Public Release

Contrails

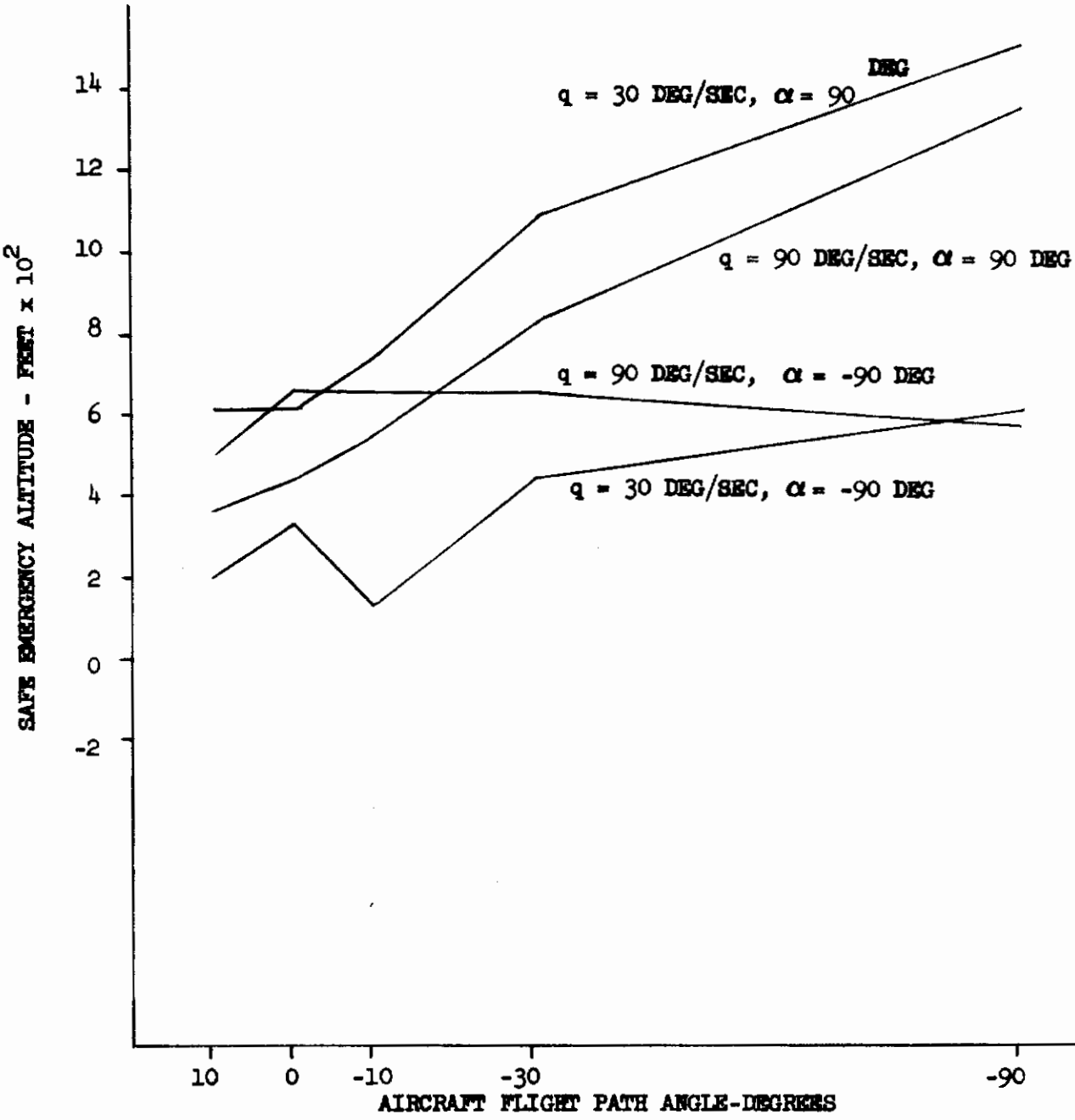

FIGURE 75 - SYSTEM B SAFE EMERGENCY ALTITUDE VERSUS γ
(q = 30 and 90 DEG/SEC; α = 90 AND -90 DEG; V = 100KN)

Approved for Public Release

Contrails

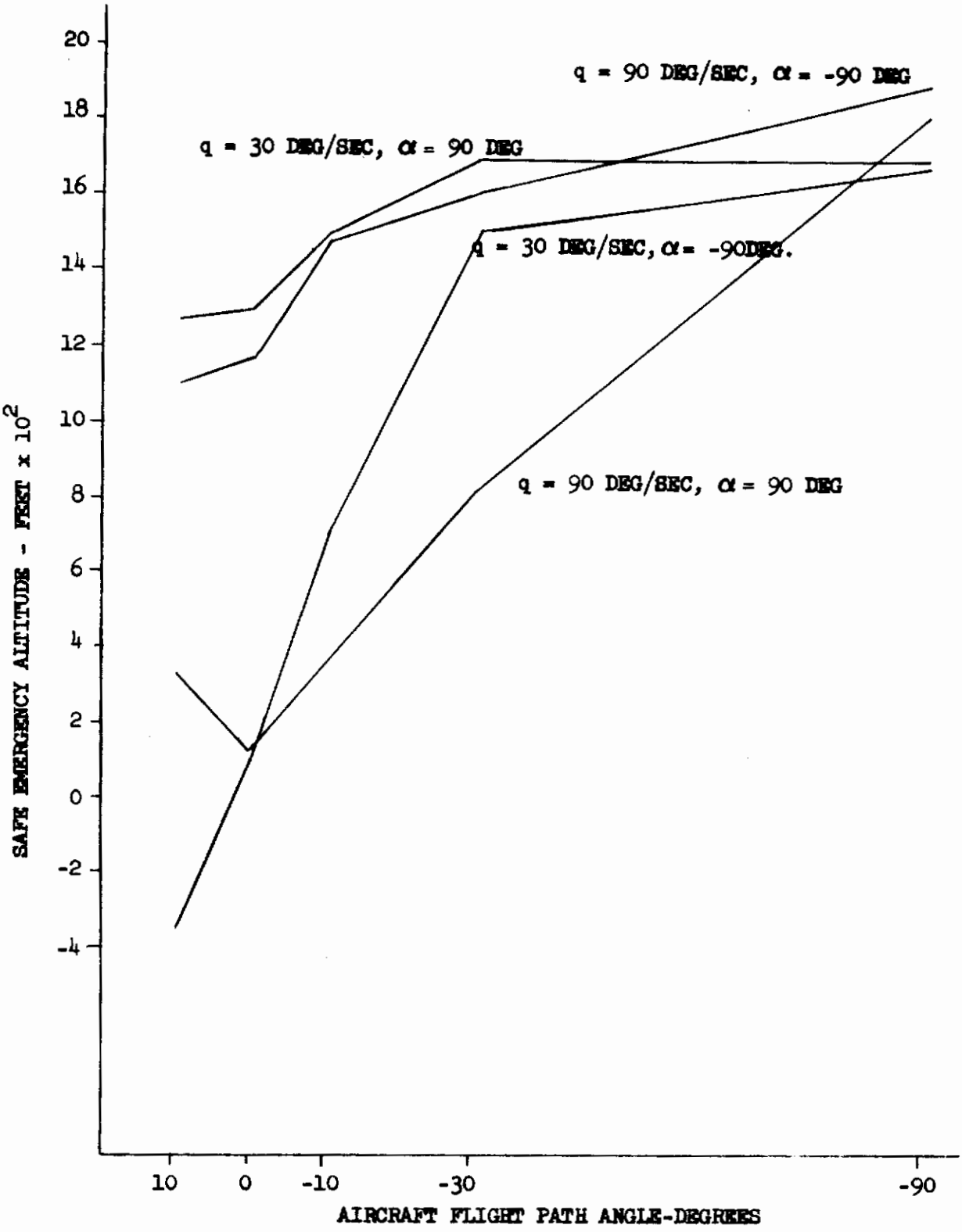

FIGURE 76-SYSTEM C SAFE EMERGENCY ALTITUDE VERSUS γ
(q = 30 AND 90 DEG/SEC; α = 90 AND -90 DEG; V = 100 KN)

Approved for Public Release

Contrails

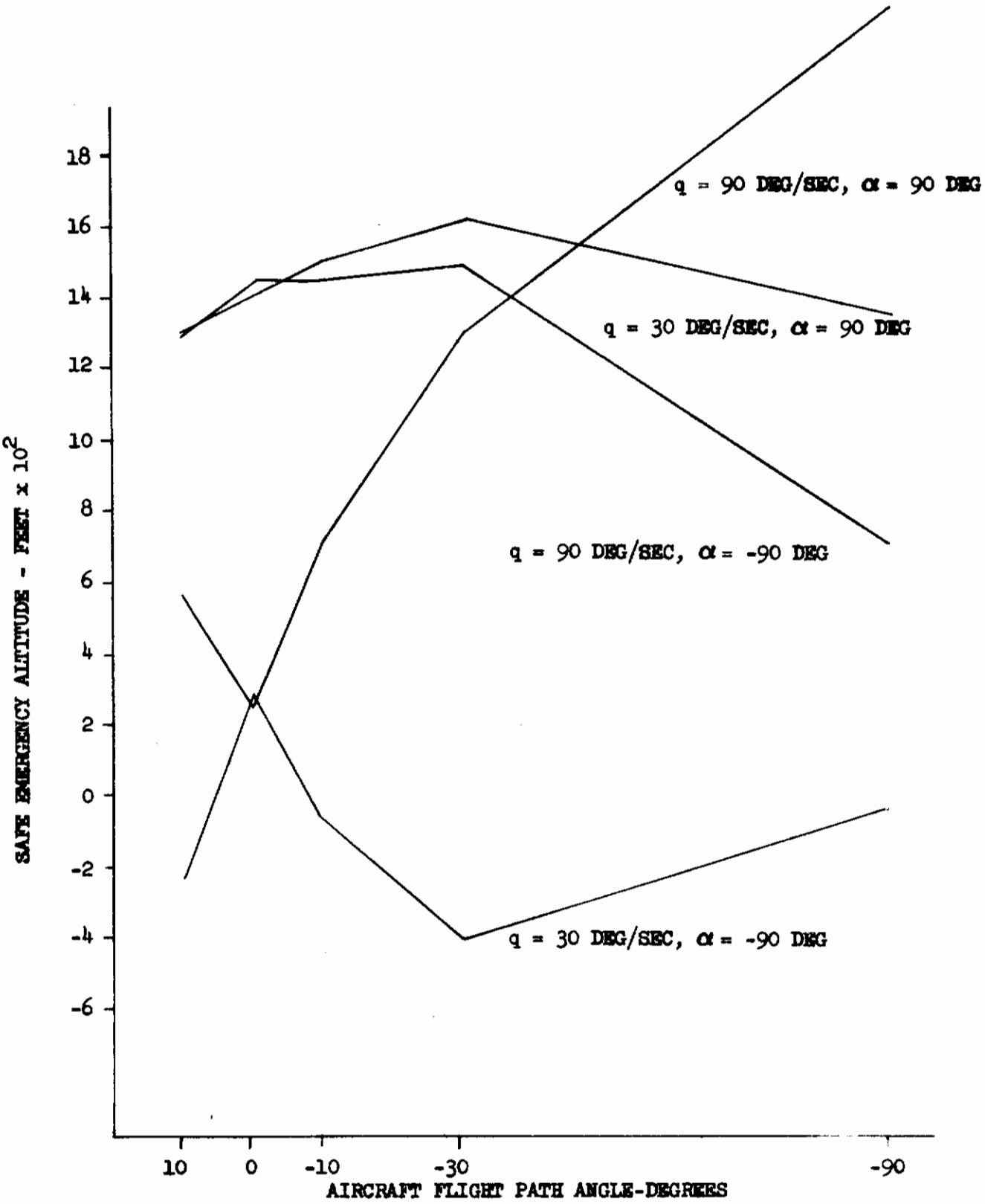

FIGURE 77 - SYSTEM D SAFE EMERGENCY ALTITUDE VERSUS γ
(q = 30 AND 90 DEG/SEC; α = 90 AND -90 DEG; V = 100 KN)

Approved for Public Release

Contrails

Figures 78 through 81 show SEA versus γ for combinations of aircraft yaw angle (ψ) of zero, 15 and 45 degrees and aircraft yawing velocity (r) = zero and 90 °/sec for the four systems. Systems C and D again show the lowest SEA value, -175 feet at conditions of γ = zero degree, ψ = 15° and r = zero °/sec for System D. The highest SEA is demanded by System D under conditions of γ = -90°, ψ = zero degree and r = zero °/sec.

Figures 82 through 85 show SEA versus γ for V = 100 knots and ψ = 15° and combinations of α and ϕ, for which System D has both the lowest and highest SEA. The lowest is -220 feet at γ = zero degree, α = 15° and ϕ = 30° and the highest at γ = -90°, α = 15° and ϕ = 90°.

Figures 86 through 89 refer to SEA versus ϕ with γ = zero, -10 and -30 degrees and V = 100 knots. System C has the lowest SEA, -200 feet at ϕ = zero degree and γ = zero degree, and System D has the highest, 1900 feet at ϕ = 180° and γ = -30°.

It can be seen from the example and a review of the figures, that Systems C and D usually form the extremes of SEA while Systems A and B normally fall between those extremes.

Figures 90 and 91 show for the various rotation rate sets, the percentage of matrix conditions for which each system produces the highest safe recovery height. For V = zero knots, System D produces the highest safe recovery height most often for pitch and System A, for roll. At V = 100 knots, System D remains highest for pitch; System C, for yaw and System A for roll, combined pitch and roll, and combined pitch, roll and yaw. At V = 800 knots, System C has the greatest percentage of highest SEA in roll, the only aircraft attitude perturbation studied at this velocity.

Figures 92, 93 and 94 show the SEA differentials due to the 0.8-second human reaction delay for γ = zero, -10 and -90°. (Escape system conditions 1 through 8 reflect a reaction time of 2.4 seconds and conditions 9 through 16, 3.2 seconds.) If it is assumed that this same 0.8 second differential is the delay between the ejection of the first crew member in a multiplace aircraft and the ejection of the last crew member, the additional height demanded may be determined so that the latter may be safely recovered. These and other data show for System A that the safe emergency altitude must be raised 68 feet at γ = -30° and 138 feet at γ = -90° to allow for the last crew member at 100 knots velocity. If the emergency should occur while the aircraft is rolling from an initial inverted attitude, the additional height necessary is of course a factor of the roll rate; if p = 60 °/sec, 43 feet are required; if p = 180 °/sec, 223 feet.

Figures 95, 96 and 97 show the influence of weight, thrust offset and impulse on SEA for Systems A through D at velocities of zero, 100 and 800 knots. The aircraft condition is in all cases upright in horizontal flight. Figure 95, weight influence on SEA, shows the additional altitude required between the minimum maximum weights. The influence of thrust offset is illustrated in figure 96, which has offset the variable as a function of weight and impulse. Impulse as a function of weight and offset is shown in figure 97. In the three figures there is a marked change in trend especially at 800 knots, due to the aerodynamic characteristics of the escape body.

Approved for Public Release

Contrails

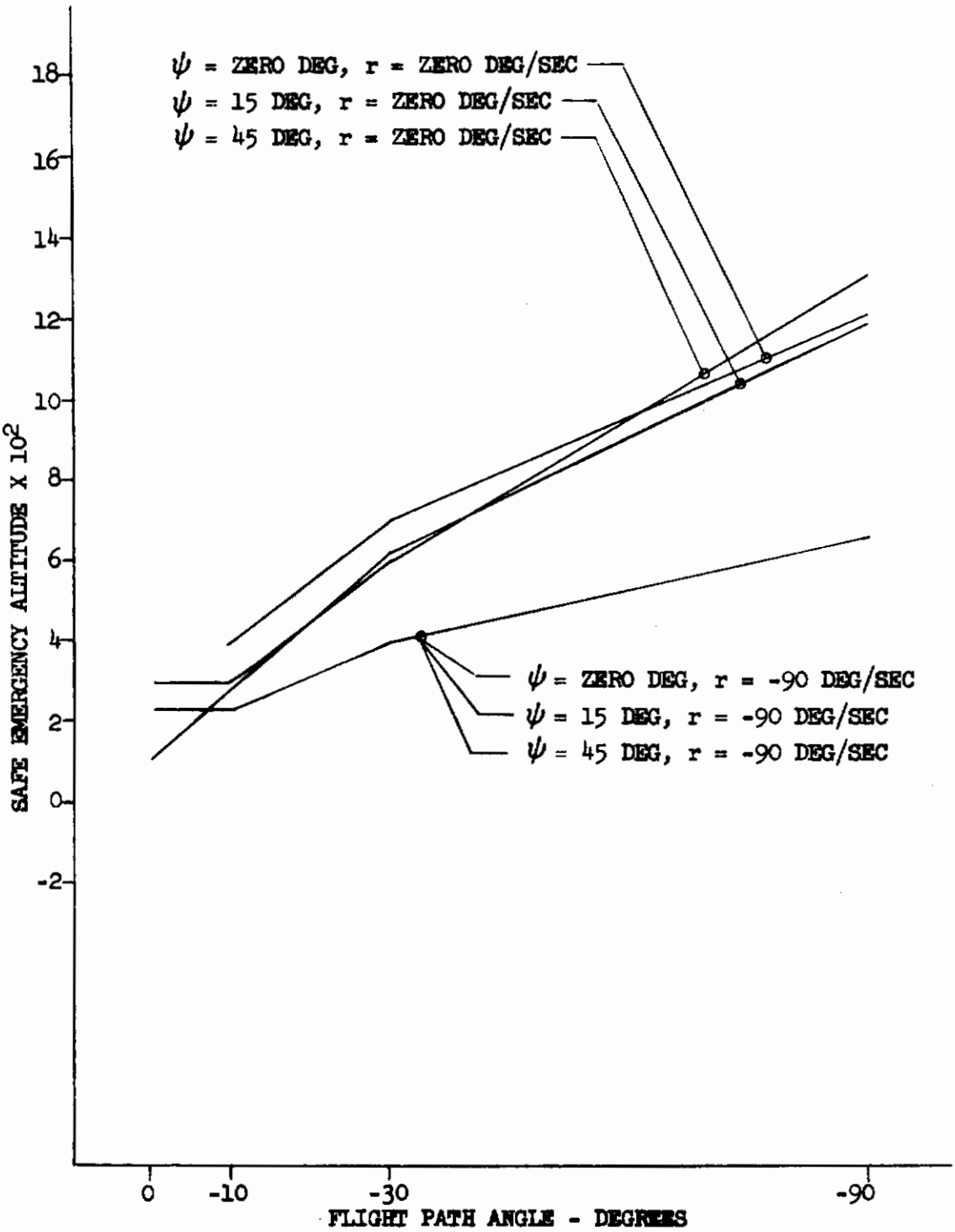

FIGURE 78 - SYSTEM A SAFE EMERGENCY ALTITUDE VERSUS γ
(ψ = ZERO, 15 AND 45 DEG; r = ZERO AND -90 DEG/SEC; V = 100 KN)

Approved for Public Release

Contrails

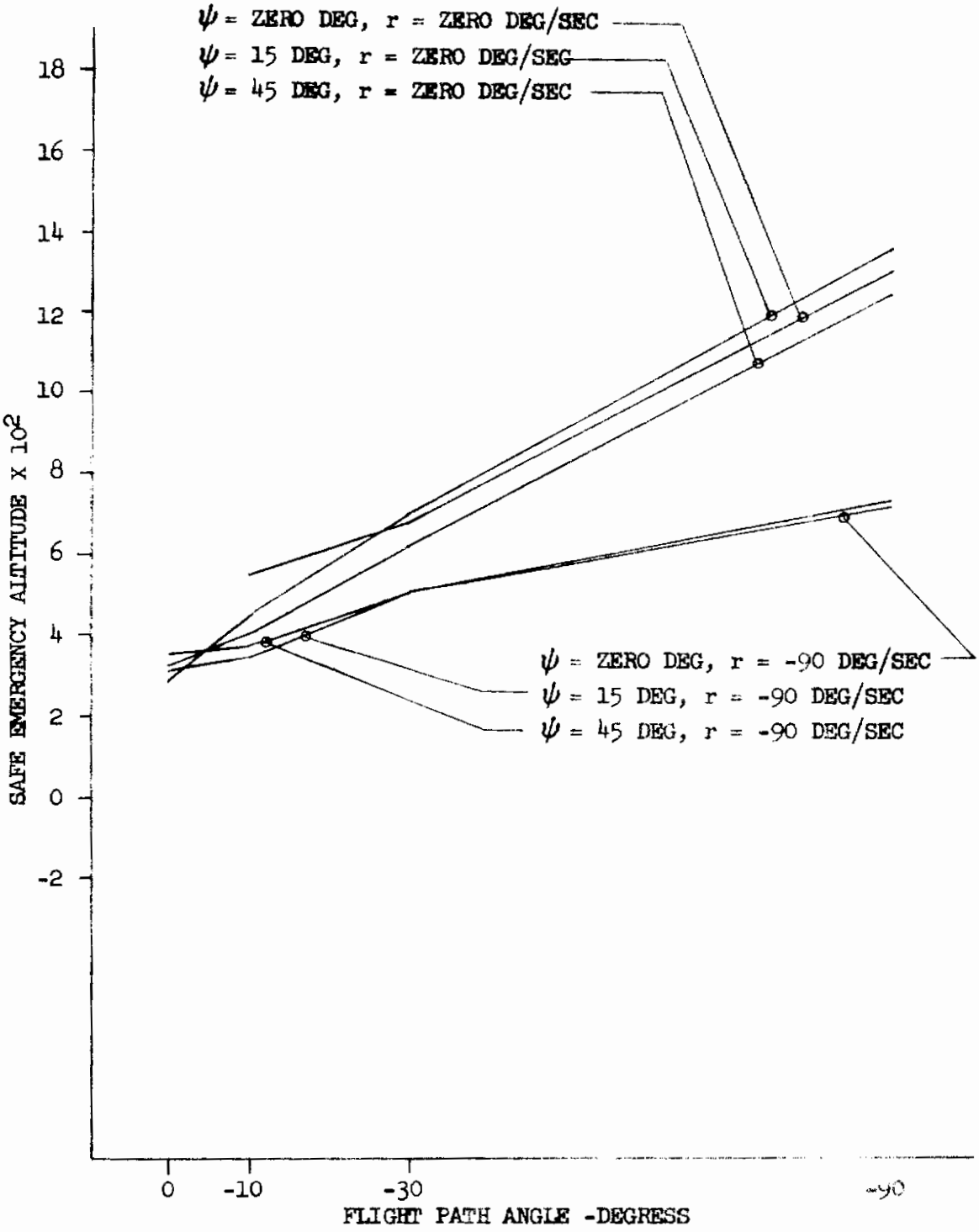

FIGURE 79- SYSTEM B SAFE EMERGENCY ALTITUDE VERSUS γ
(ψ = ZERO, 15 AND 45 DEG; r = ZERO AND -90 DEG/SEC; V = 100 KN)

Approved for Public Release

Contrails

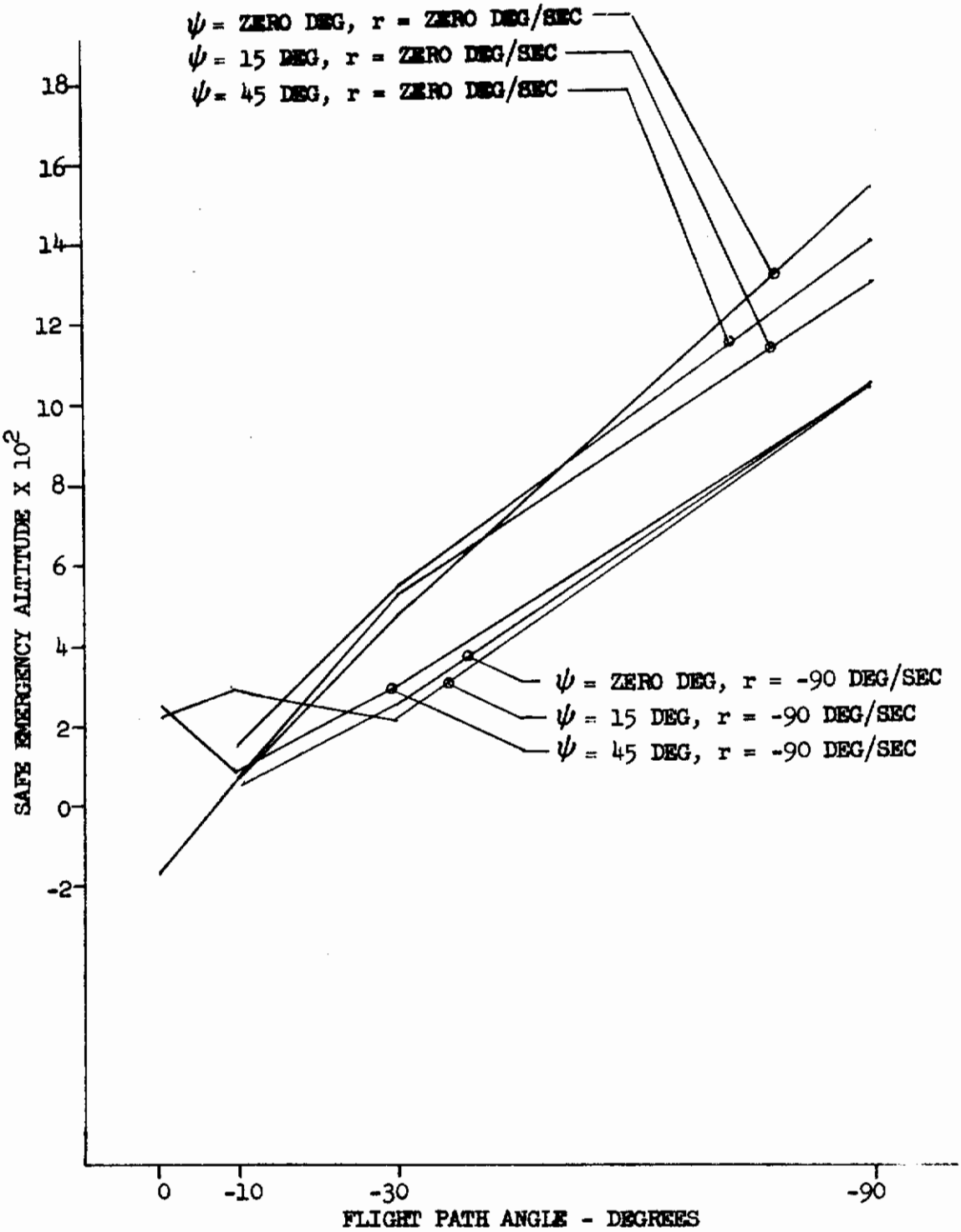

FIGURE 80 - SYSTEM C SAFE EMERGENCY ALTITUDE VERSUS γ
(ψ = ZERO, 15 AND 45 DEG; r = ZERO AND -90 DEG/SEC; V = 100 KN)

Approved for Public Release

Contrails

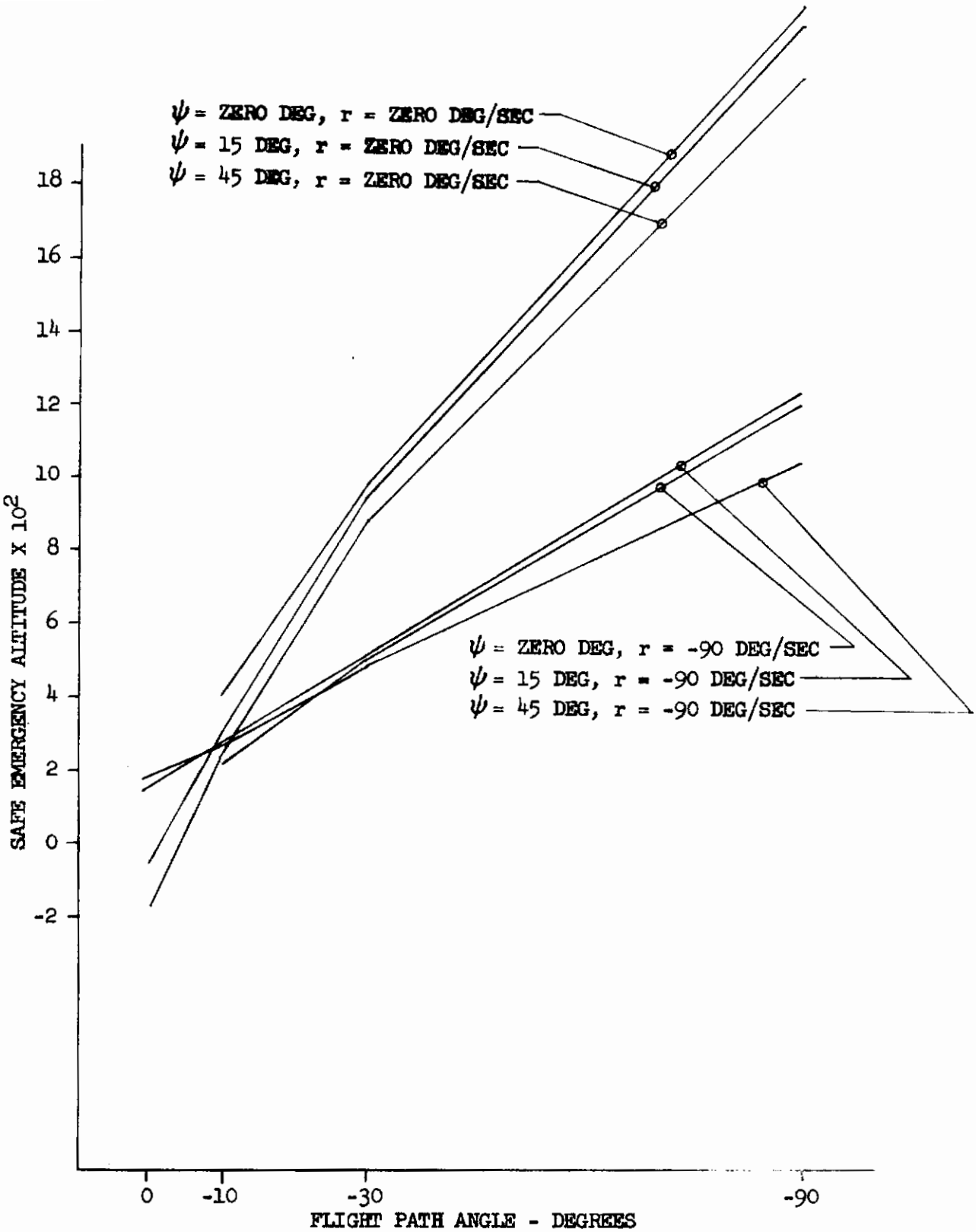

FIGURE 81 - SYSTEM D SAFE EMERGENCY ALTITUDE VERSUS γ
(ψ = ZERO, 15 AND 45 DEG; r = ZERO AND -90 DEG/SEC; V = 100 KN)

Approved for Public Release

Contrails

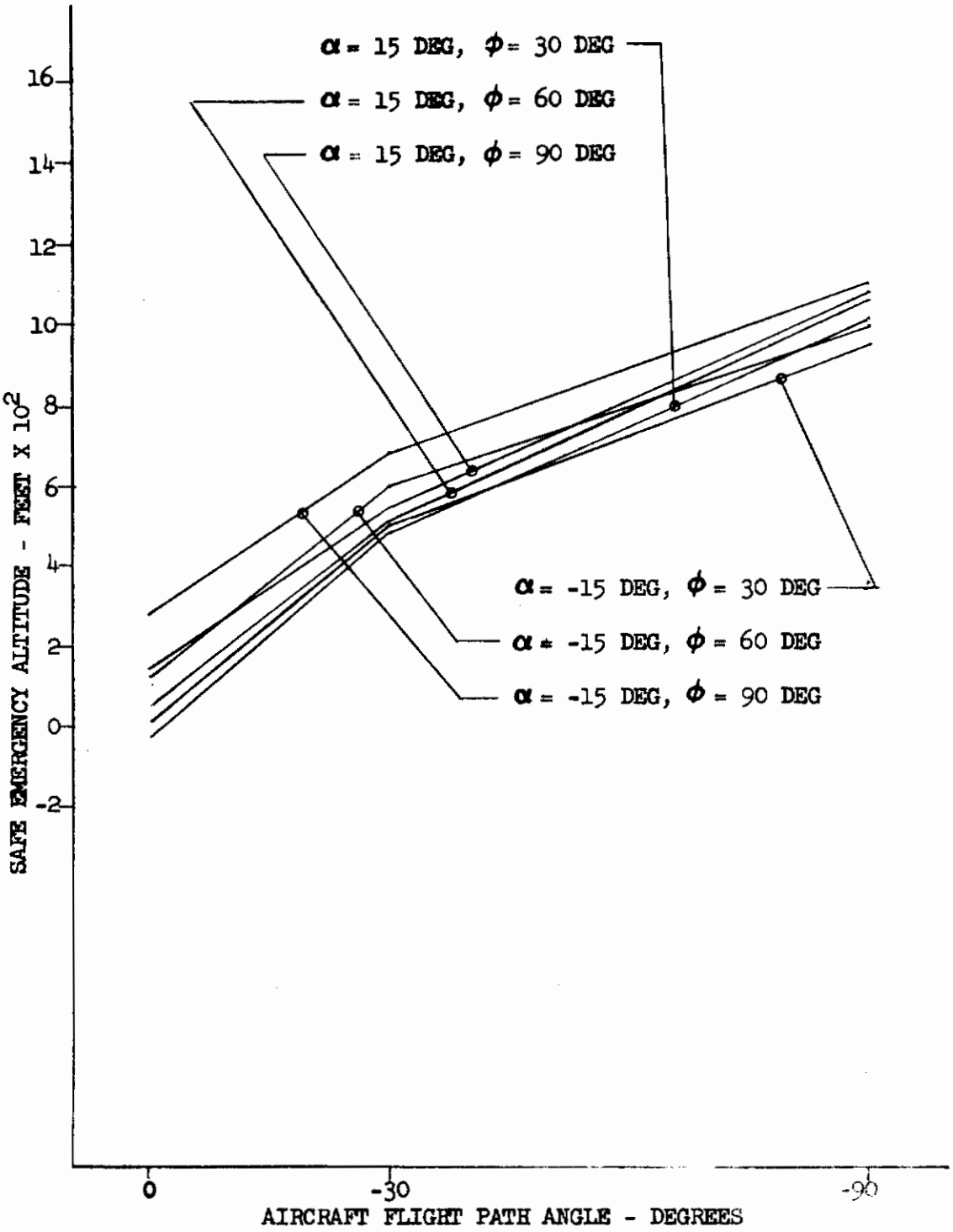

FIGURE 82 - SYSTEM A SAFE EMERGENCY ALTITUDE VERSUS γ
(ψ = 15 DEG; r = ZERO DEG/SEC; V = 100 KN)

Approved for Public Release

Contrails

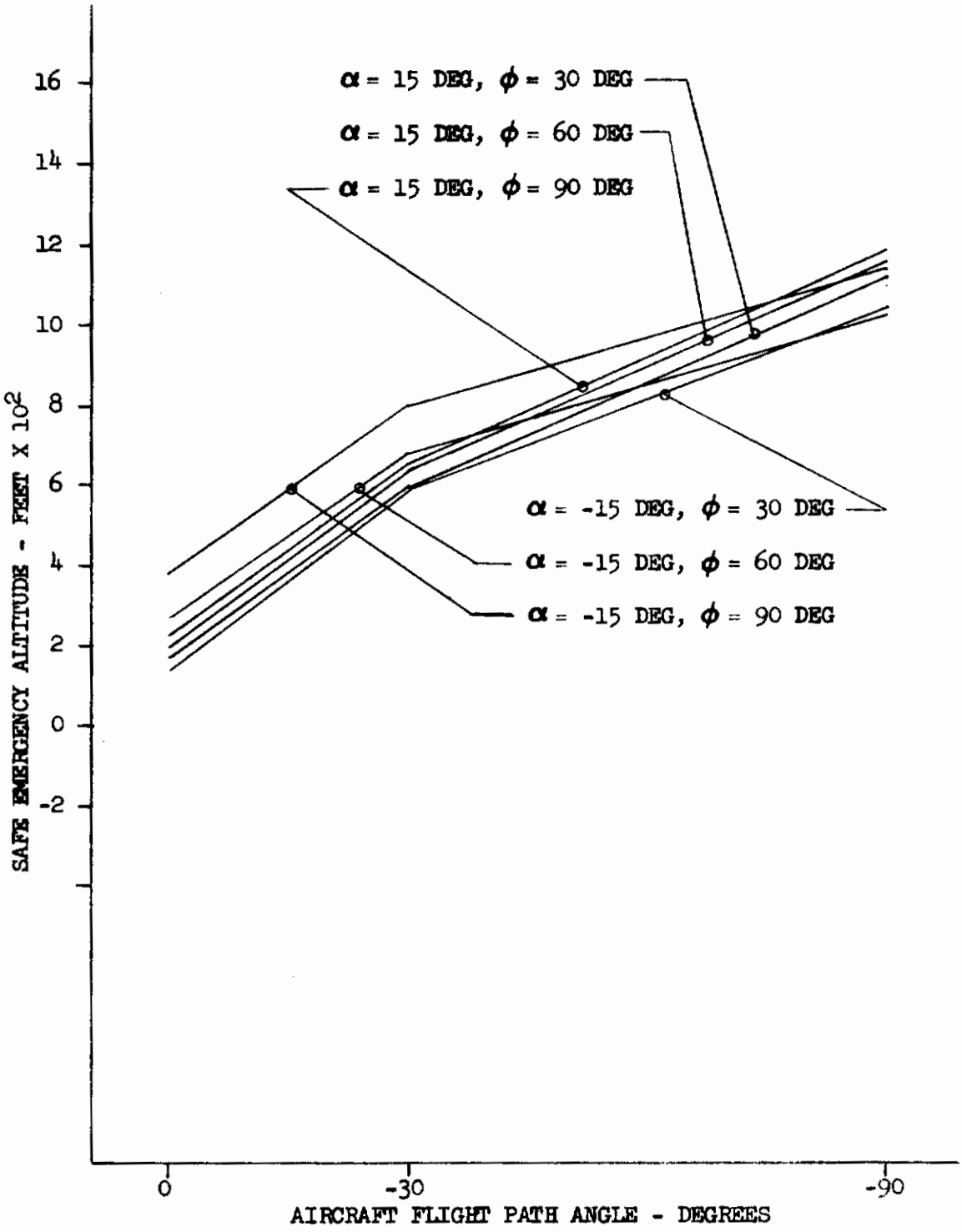

FIGURE 83 - SYSTEM B SAFE EMERGENCY ALTITUDE VERSUS γ
(ψ = 15 DEG; r = ZERO DEG/SEC; V = 100 KN)

Approved for Public Release

Contrails

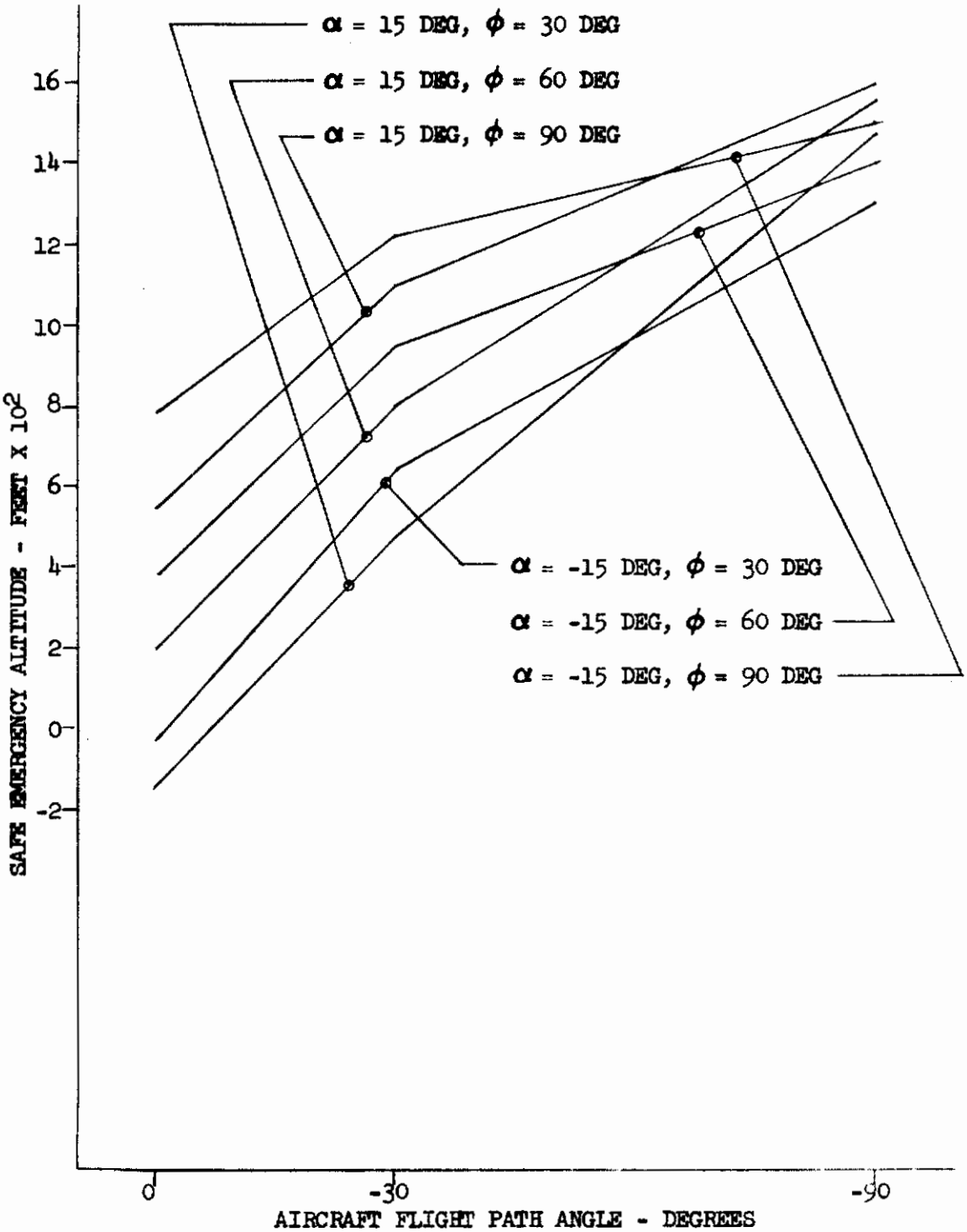

FIGURE 84 - SYSTEM C SAFE EMERGENCY ALTITUDE VERSUS γ
(ψ = 15 DEG; r = ZERO DEG/SEC; V = 100 KN)

Approved for Public Release

Contrails

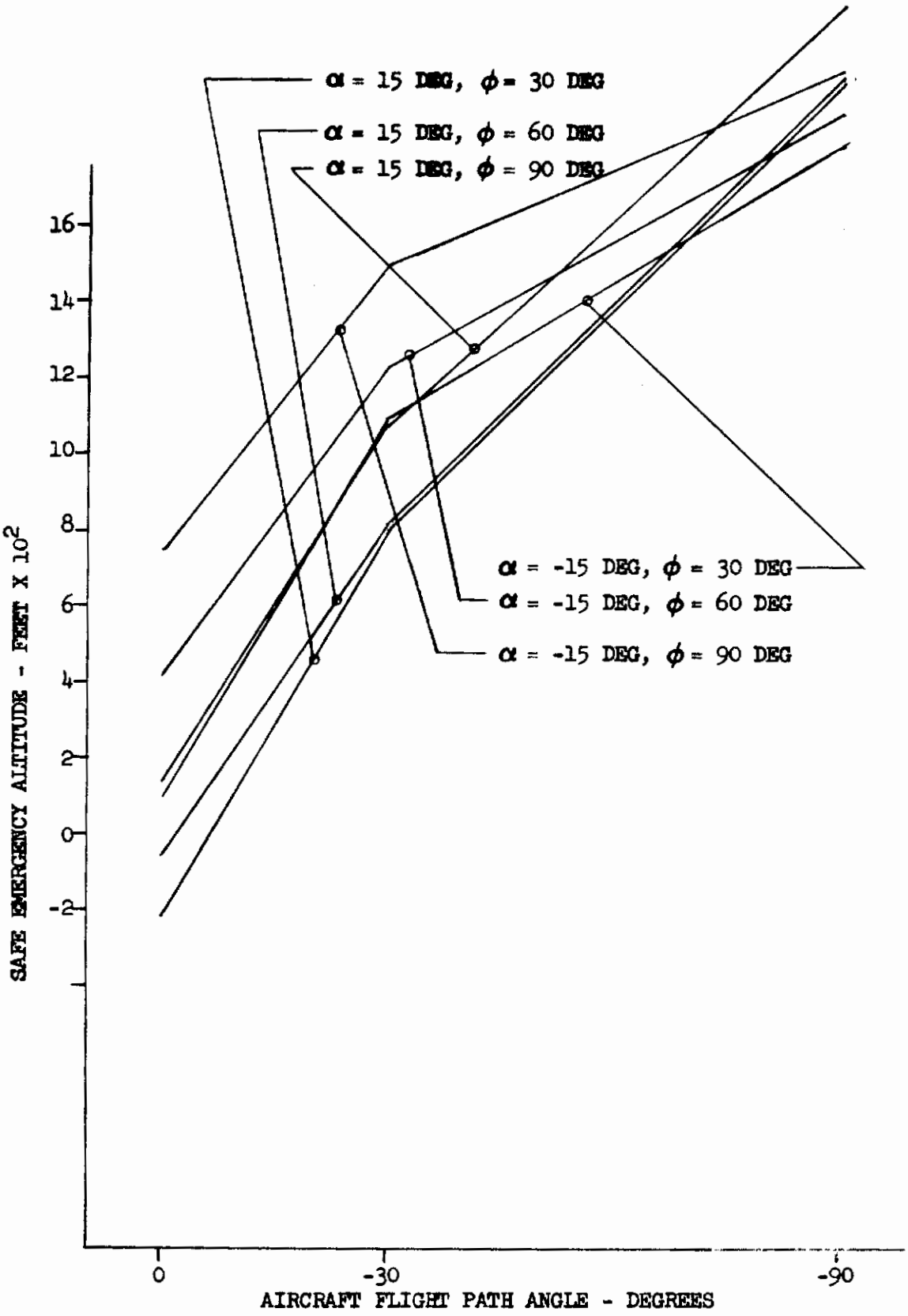

FIGURE 85 - SYSTEM D SAFE EMERGENCY ALTITUDE VERSUS γ
(ψ = 15 DEG; r = ZERO DEG/SEC; V = 100 KN)

Approved for Public Release

Contrails

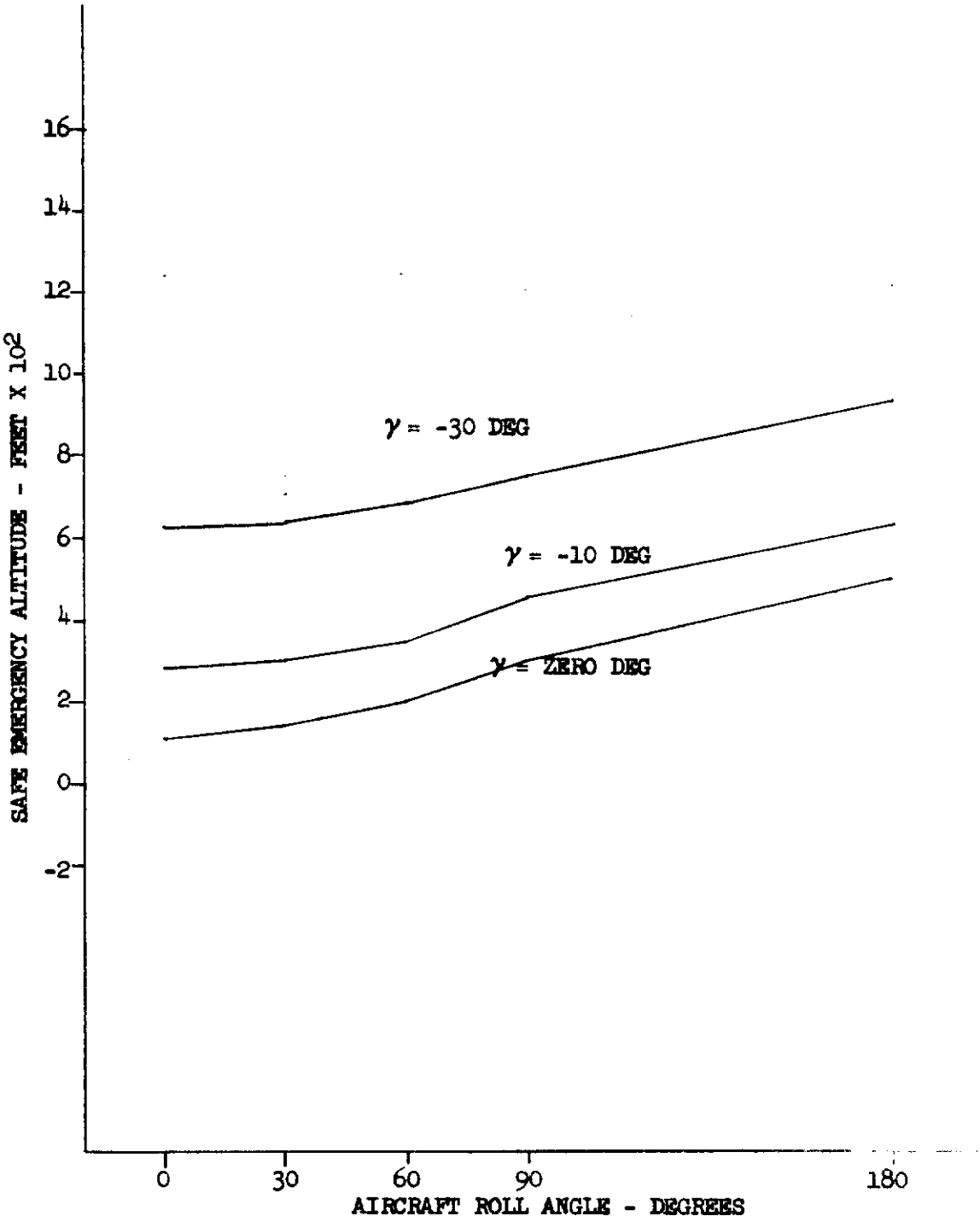

FIGURE 86 - SYSTEM A SAFE EMERGENCY ALTITUDE VERSUS ϕ
(γ = ZERO, -10 and -30 DEG; p = ZERO DEG/SEC; V= 100 KN)

Approved for Public Release

Contrails

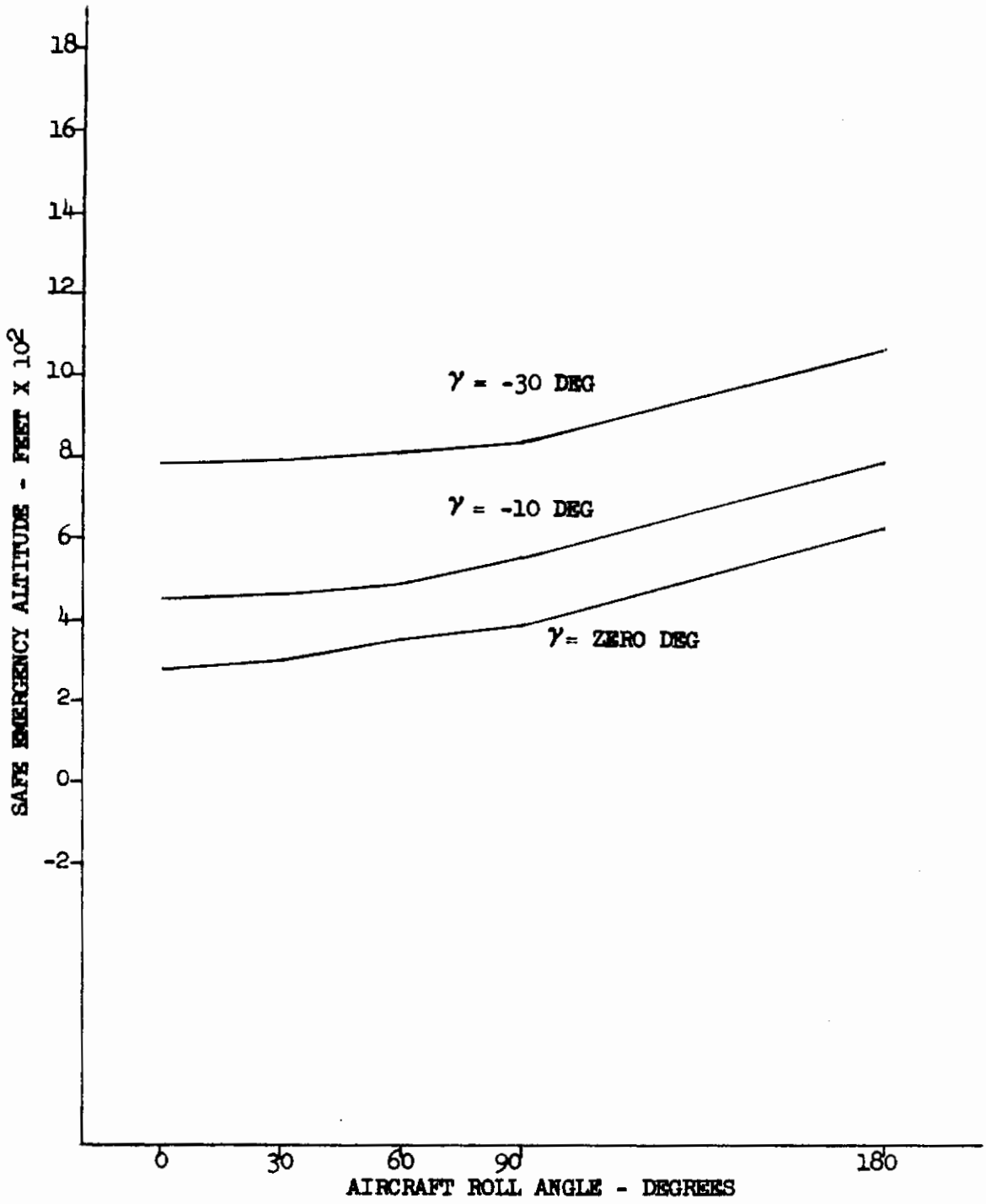

FIGURE 87 - SYSTEM B SAFE EMERGENCY ALTITUDE VERSUS ϕ
(γ = ZERO, -10 AND -30 DEG; p = ZERO DEG/SEC; V = 100 KN)

Approved for Public Release

Contrails

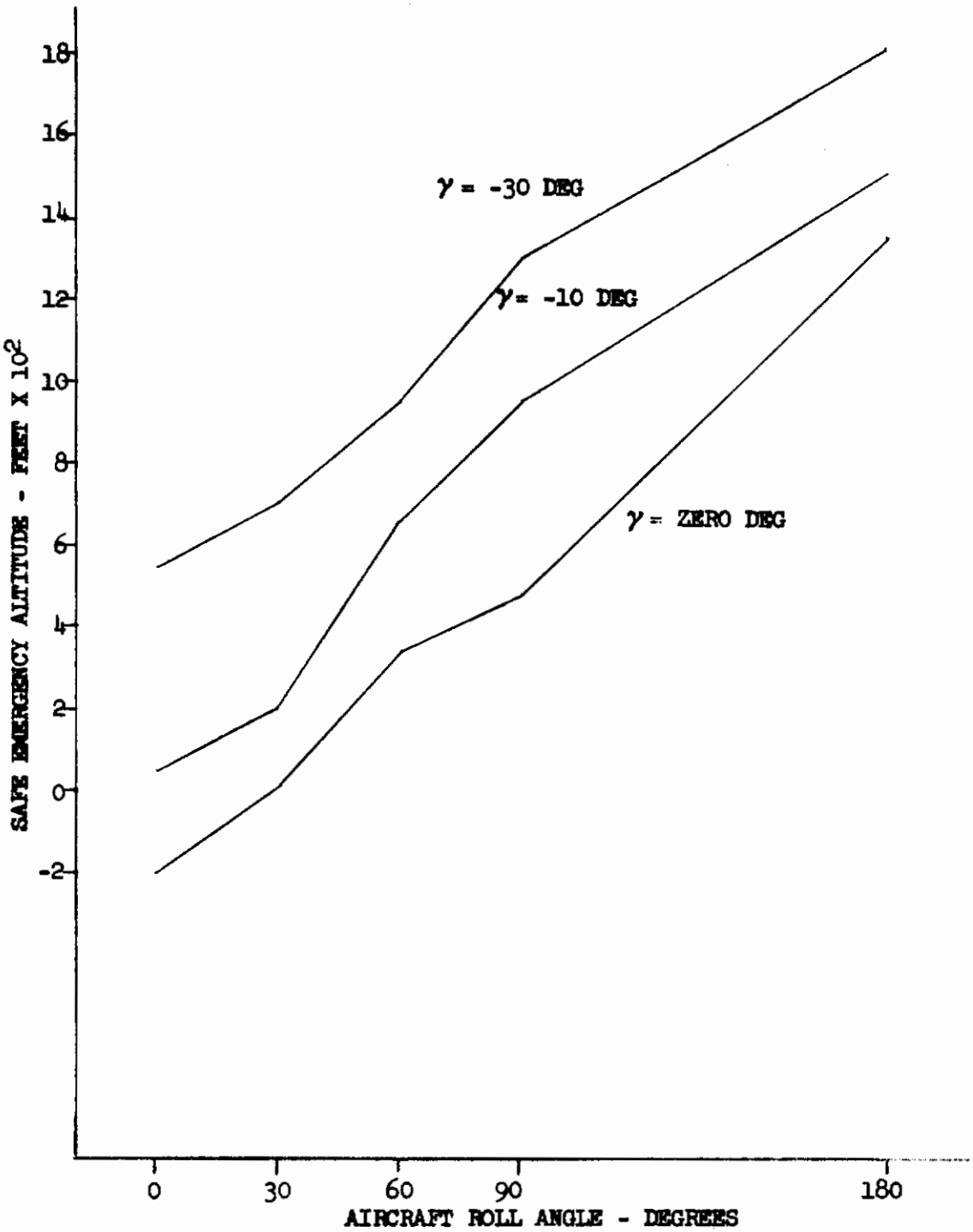

FIGURE 88 - SYSTEM C SAFE EMERGENCY ALTITUDE VERSUS ϕ
(γ = ZERO, -10 AND -30 DEG; p = ZERO DEG/SEC; V = 100 KN)

Approved for Public Release

Contrails

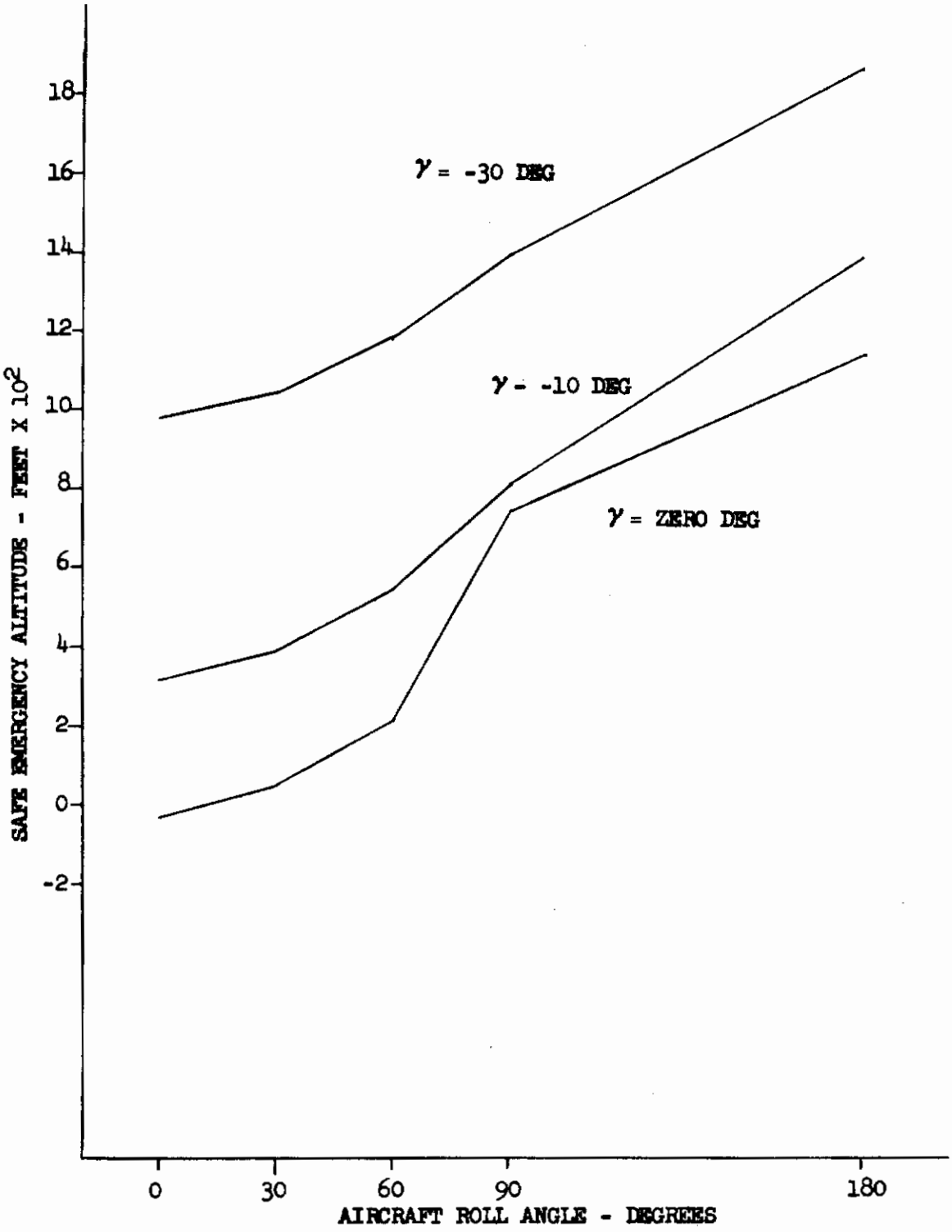

FIGURE 89 - SYSTEM D SAFE EMERGENCY ALTITUDE VERSUS ϕ
(γ = ZERO, -10 AND -30 DEG; p = ZERO DEG/SEC; V = 100 KN)

Approved for Public Release

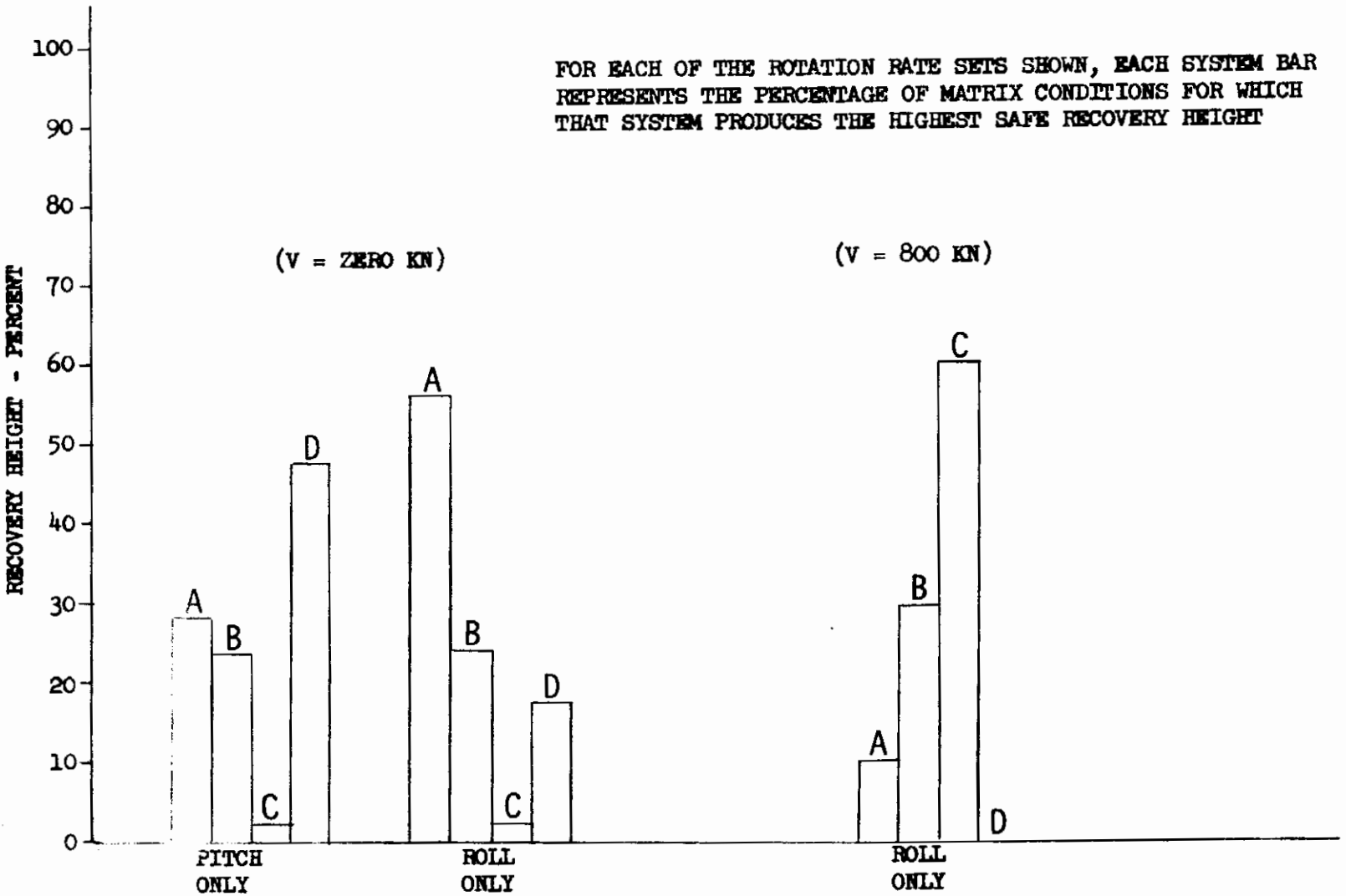

FIGURE 90 - BEST RECOVERY HEIGHT VS AIRCRAFT CONDITION FOR TOTAL MATRIX

Approved for Public Release

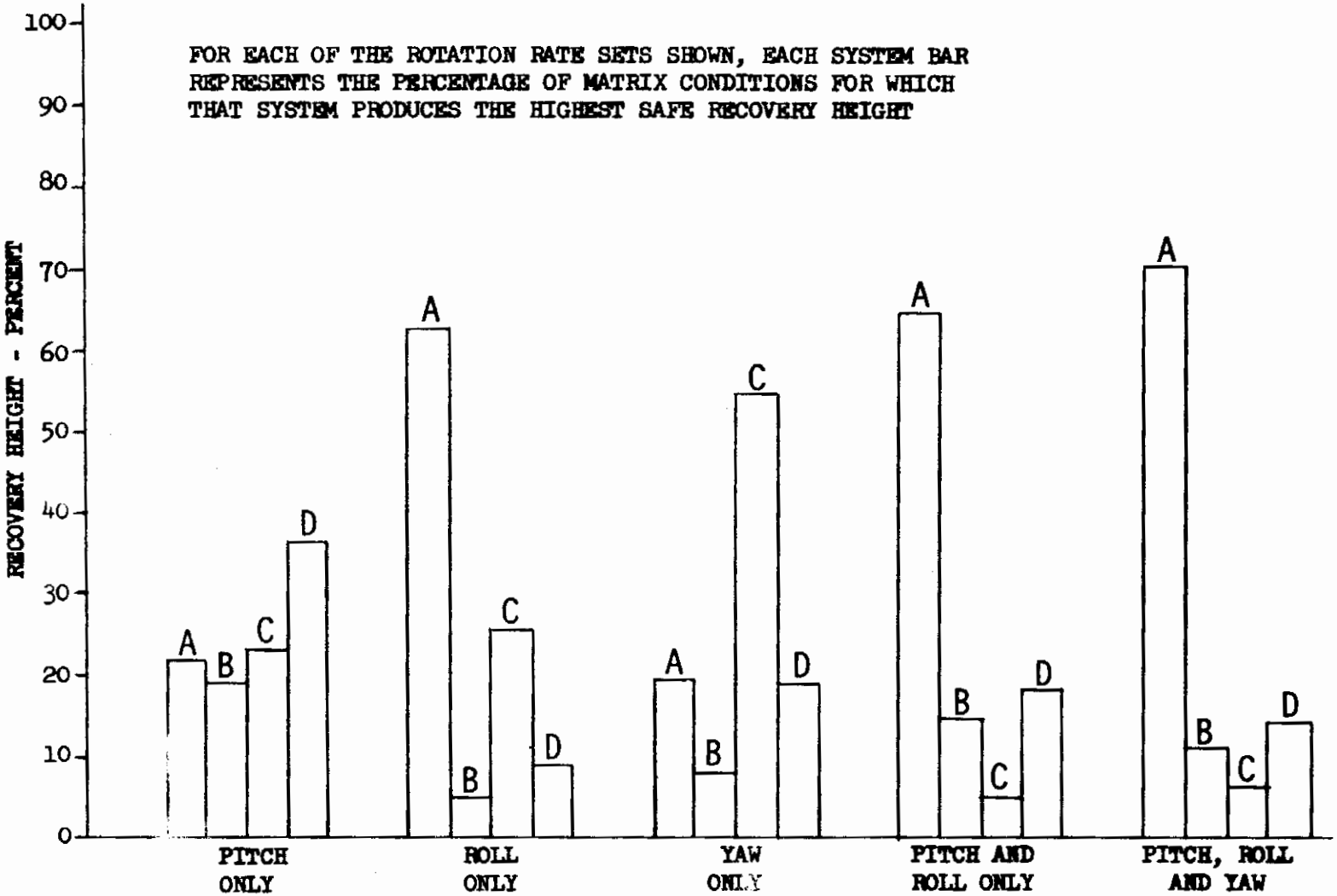

FIGURE 91 - BEST RECOVERY HEIGHT VS AIRCRAFT CONDITION FOR TOTAL MATRIX (V = 100 KN)

Approved for Public Release

Contrails

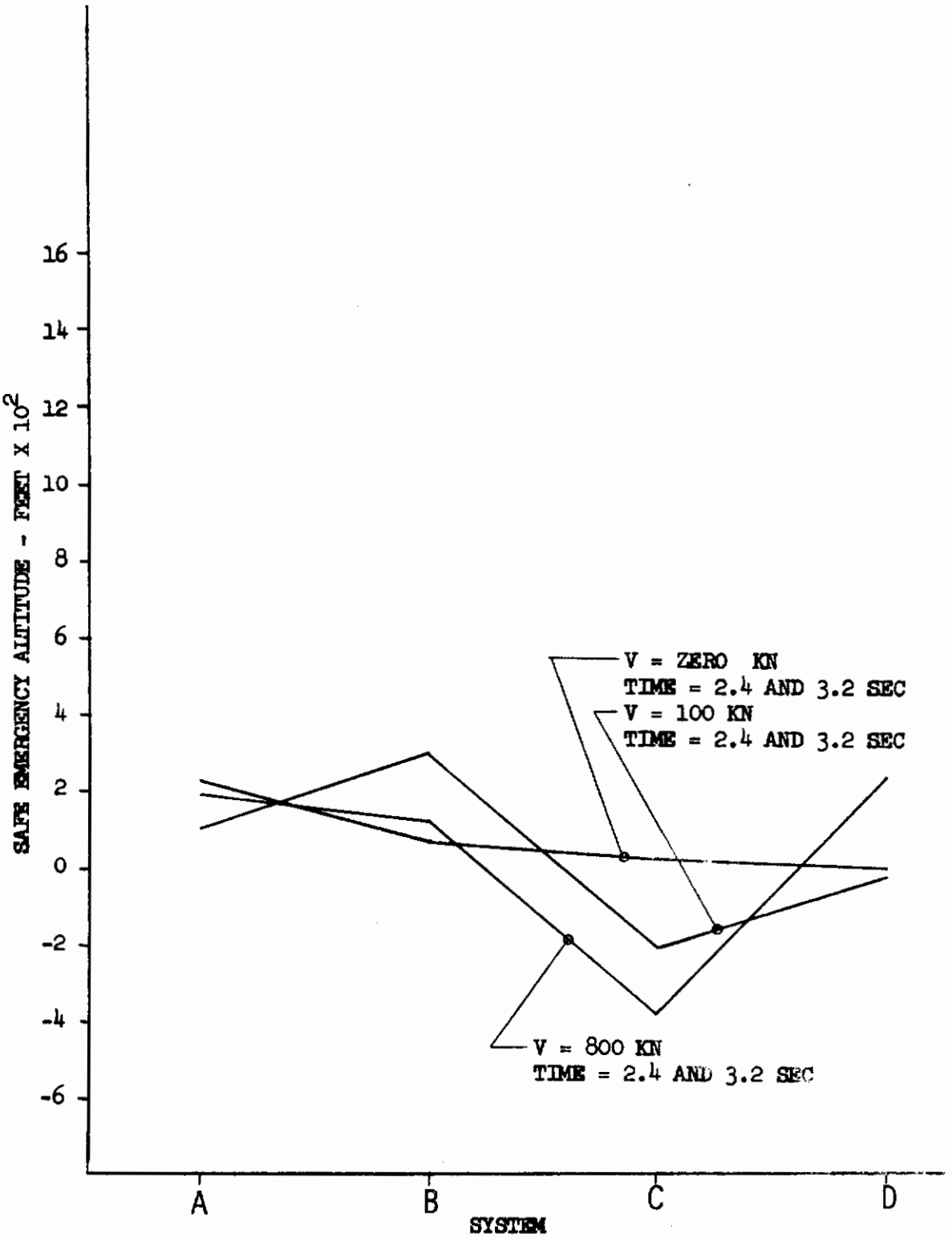

FIGURE 92 - SAFE EMERGENCY ALTITUDE VERSUS SYSTEM
(γ = ZERO DEG; V = ZERO, 100 AND 800 KN, TIME = 2.4 AND 3.2 SECONDS)

Approved for Public Release

Contrails

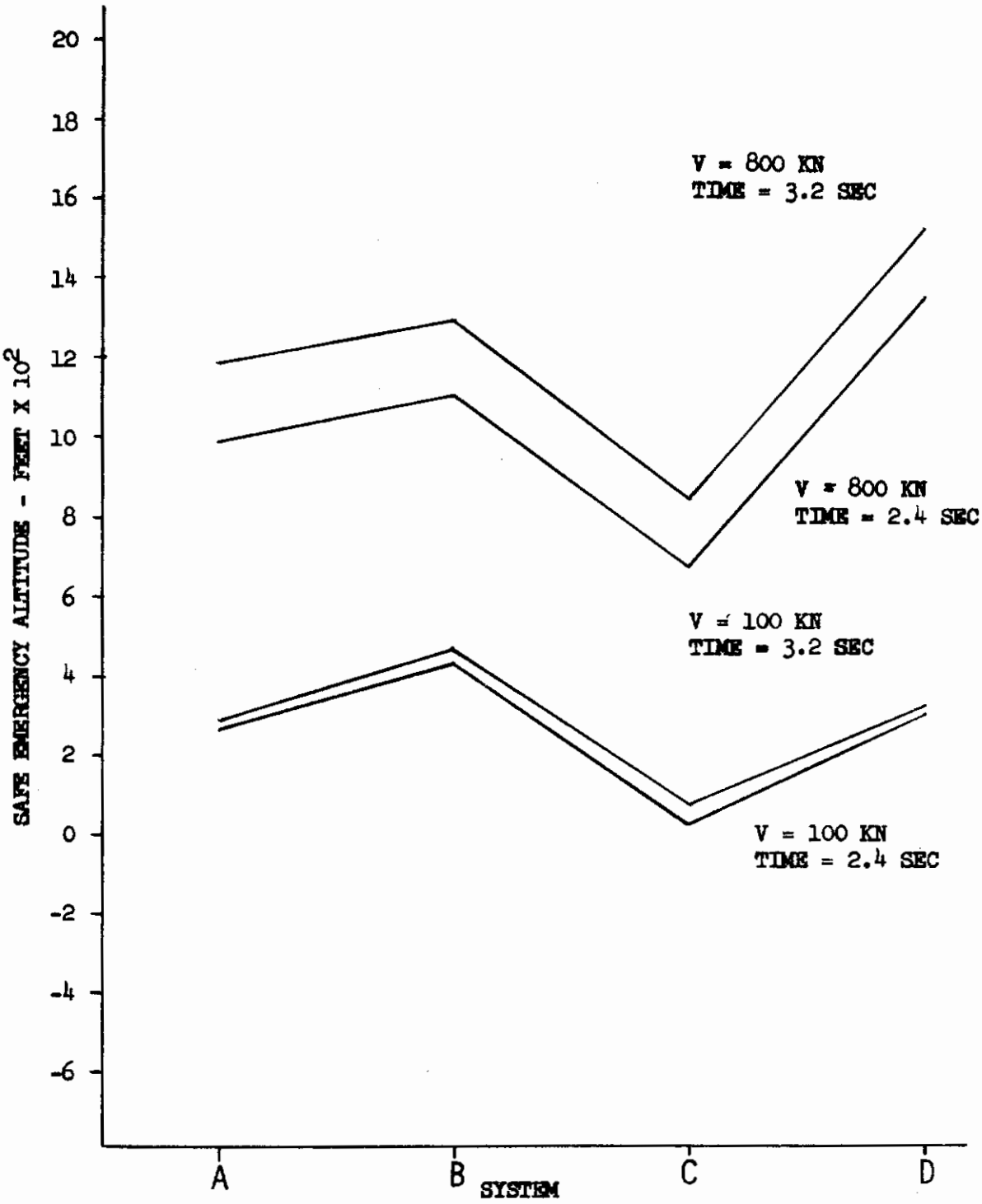

FIGURE 93 - SAFE EMERGENCY ALTITUDE VERSUS SYSTEM
(γ = -10 DEG; V = 100 AND 800 KN; TIME = 2.4 AND 3.2 SECONDS)

Approved for Public Release

Contrails

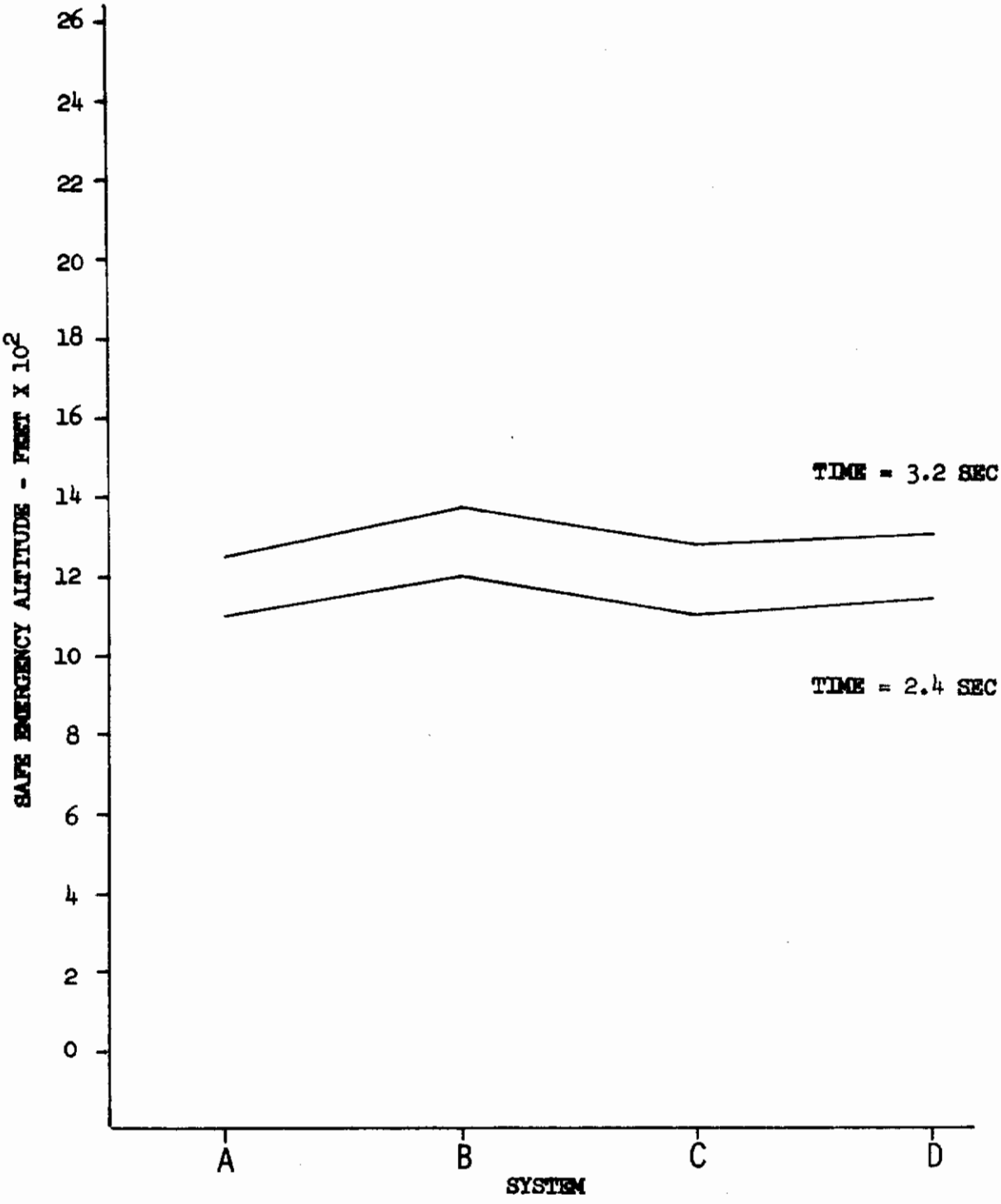

FIGURE 94 - SAFE EMERGENCY ALTITUDE VERSUS SYSTEM
(γ = -90 DEG; V = 100 KN; TIME = 2.4 AND 3.2 SECONDS)

Approved for Public Release

Contrails

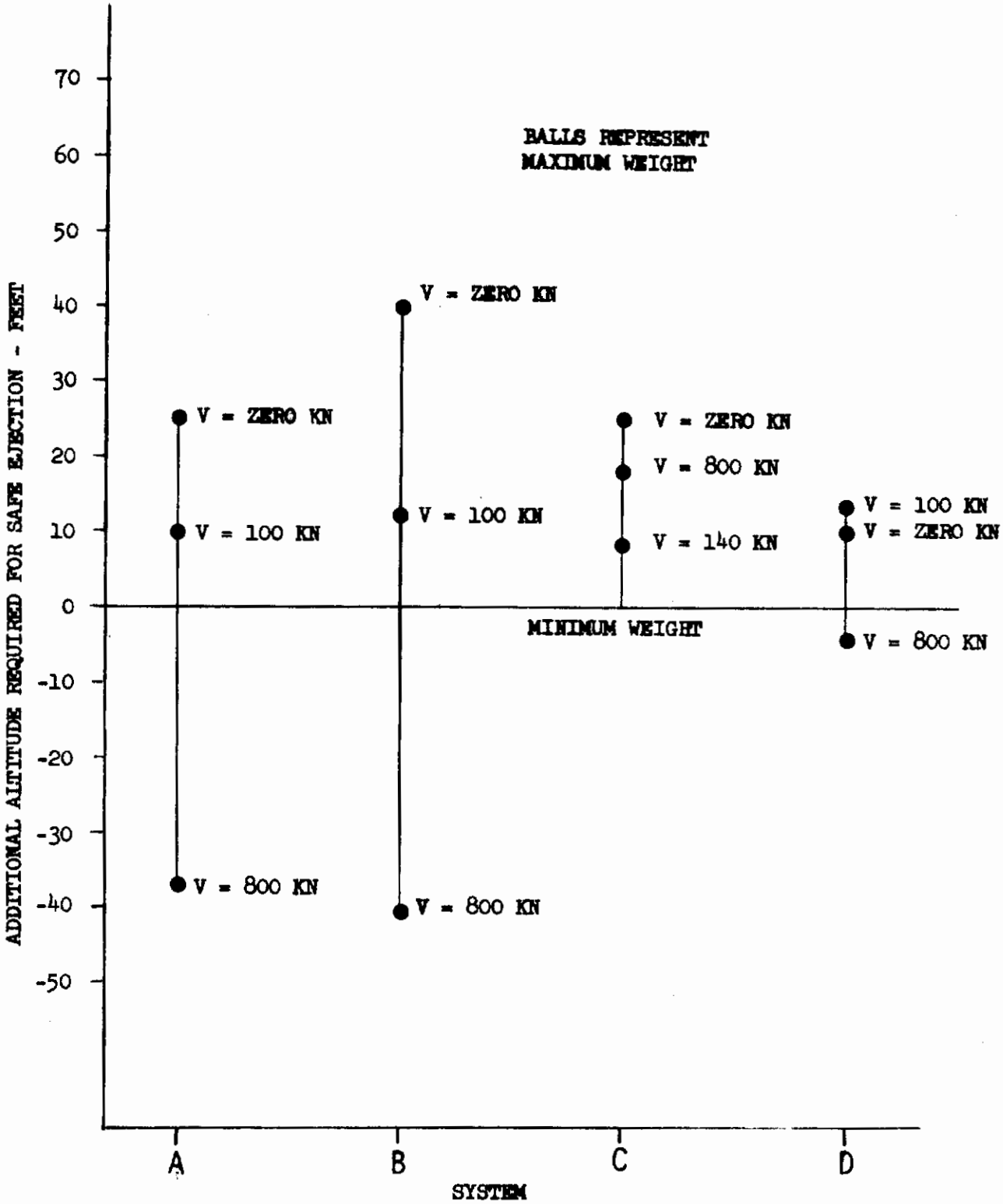

FIGURE 95 - WEIGHT INFLUENCE ON SEA

Approved for Public Release

Contrails

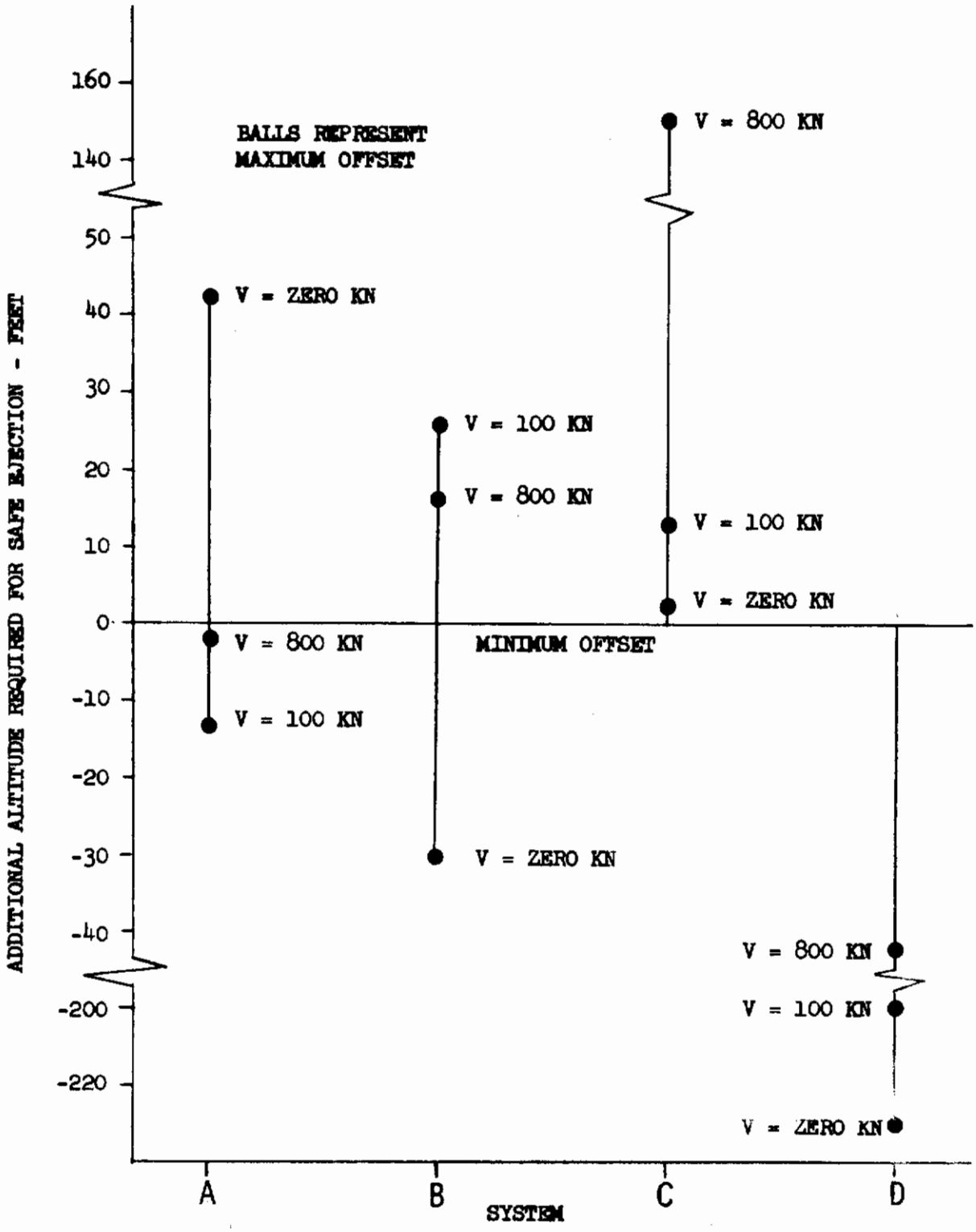

FIGURE 96 - THRUST LINE OFFSET INFLUENCE ON SEA

Approved for Public Release

Contrails

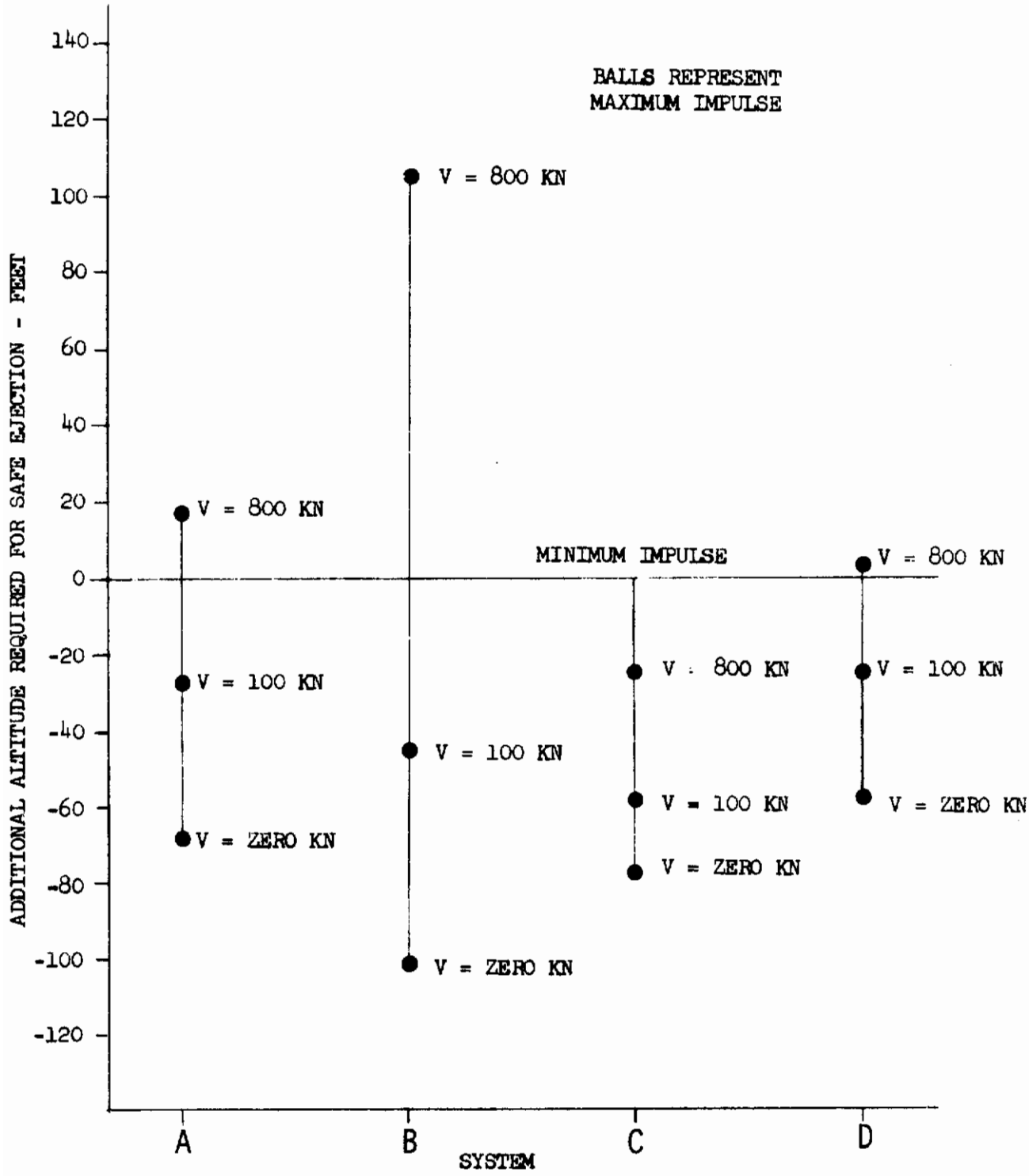

FIGURE 97 – IMPULSE INFLUENCE ON SEA

Approved for Public Release

Contrails

4. ACCELERATION ANALYSIS

The crew member's tolerance to acceleration is keyed to Point (A) which is chosen as described under heading V.2. For the four system concepts, figures 98 through 101 provide correlation of Point (A) total acceleration magnitudes with increasing velocities, with defined influences of rolling and pitching rates.

a. Acceleration Magnitude Limitations

The small effect of adding rolling velocity as high as 180°/sec to an initially rotationless aircraft is shown by comparison of figure 101, with rolling, to figure 99 which lacks rotation about any axis. Conversely, with the exception of System D, above 300 knots velocity the imposition of 180°/sec roll upon the escape body pitching positively at 90°/sec produces a salutary acceleration-reducing influence, referring to figures 98 and 100. System D demonstrates a small increase in "G" as rolling is added to the pitching body.

As indicated by figures 98 and 99, the introduction of positive pitching onto the previously rotationless aircraft markedly augments acceleration above a velocity of 300 knots for systems excepting D for which the increase occurs above 450 knots.

Aircraft true speeds (knots, 10,000 feet altitude) above which total acceleration at Point (A) appreciably exceeds human tolerance are shown below for each system:

p°/sec	q°/sec	A	B	C	D
0	0	550	700	700	800
180	0	550	700	700	800
0	90	350	375	400	600
180	90	450	600	600	650

Since yawing produces acceleration patterns similar to those of pitching, but lateral acceleration is generally less tolerable than vertical or longitudinal, allowable airspeed must be reduced for cases which generate sufficient aircraft yaw to impose dominant side loads on the escape body at high dynamic pressure. Nevertheless, it may be deduced that all four systems are adequate, from an acceleration standpoint, below 300 knots aircraft velocity throughout the matrix.

Point (A) maximum total acceleration relationships to propulsion impulse and thrust offset in ejection phases I and III are presented in figures 102 through 106. Weight changes within the matrix limits are roughly equivalent to the inverse of impulse variations. Phase I maximum accelerations for Systems A and B, as may be expected, vary almost directly with impulse (in this circumstance, thrust), as demonstrated by figure 102. The effects of impulse variations on all systems in Phase III are illustrated in figures 103 and 104 which indicate expected trends.

Approved for Public Release

Contrails

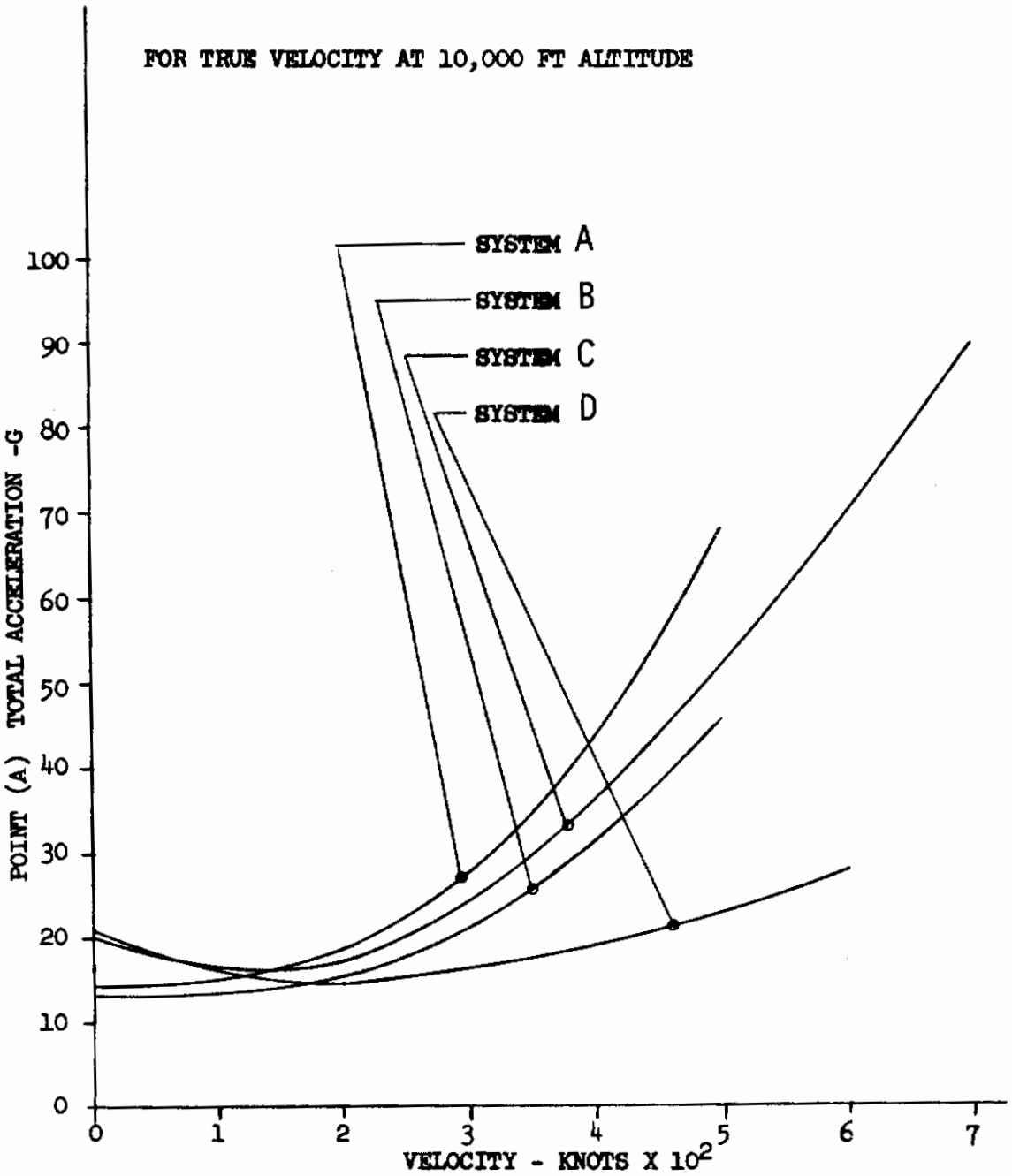

FIGURE 98 - SYSTEM COMPARISON OF TOTAL ACCELERATION VERSUS VELOCITY
(p = ZERO DEG/SEC; q = 90 DEG/SEC)

Approved for Public Release

Contrails

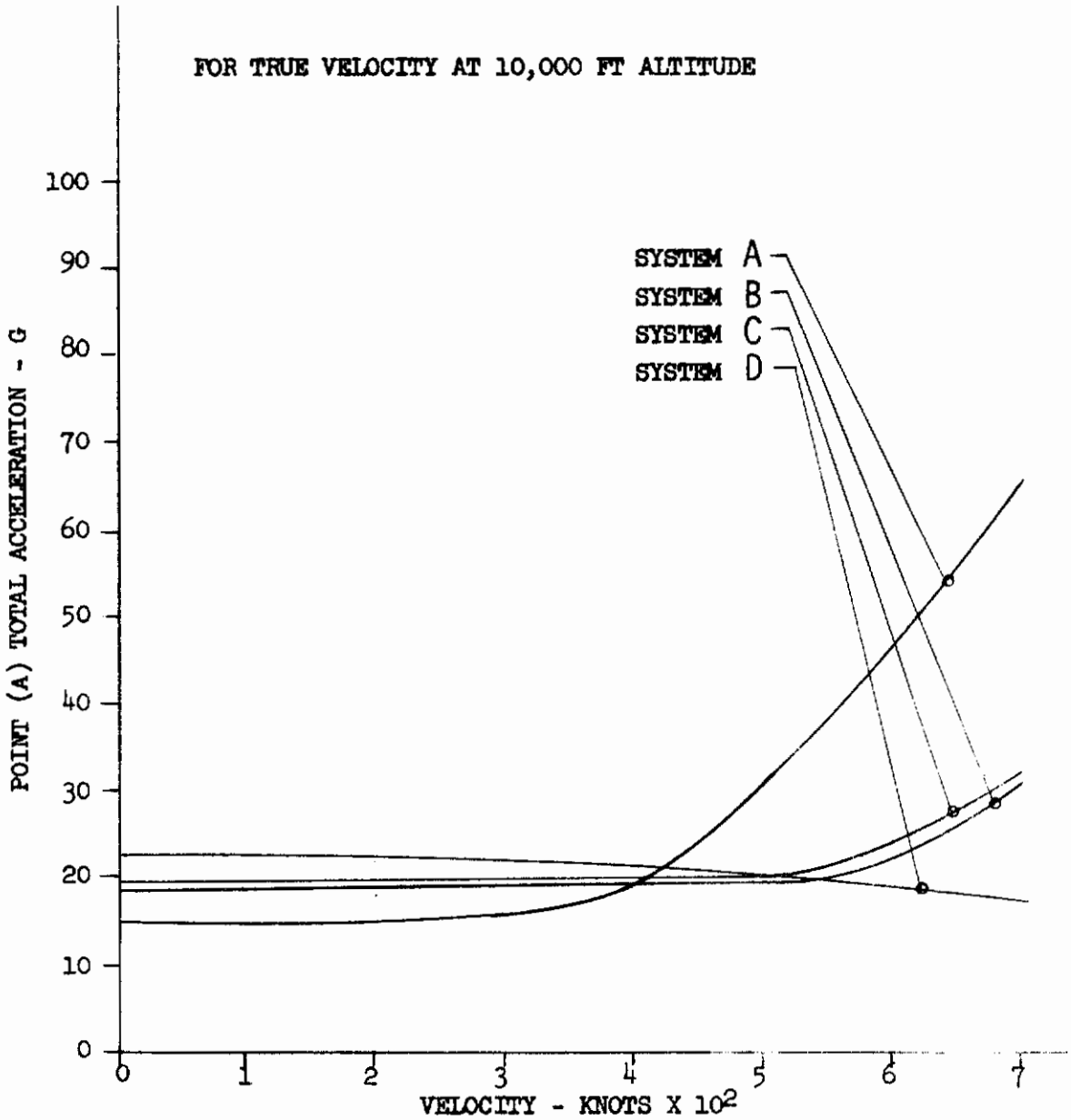

FIGURE 99 - SYSTEM COMPARISON OF TOTAL ACCELERATION VERSUS VELOCITY
(p = ZERO DEG/SEC; q = ZERO DEG/SEC)

Approved for Public Release

Contrails

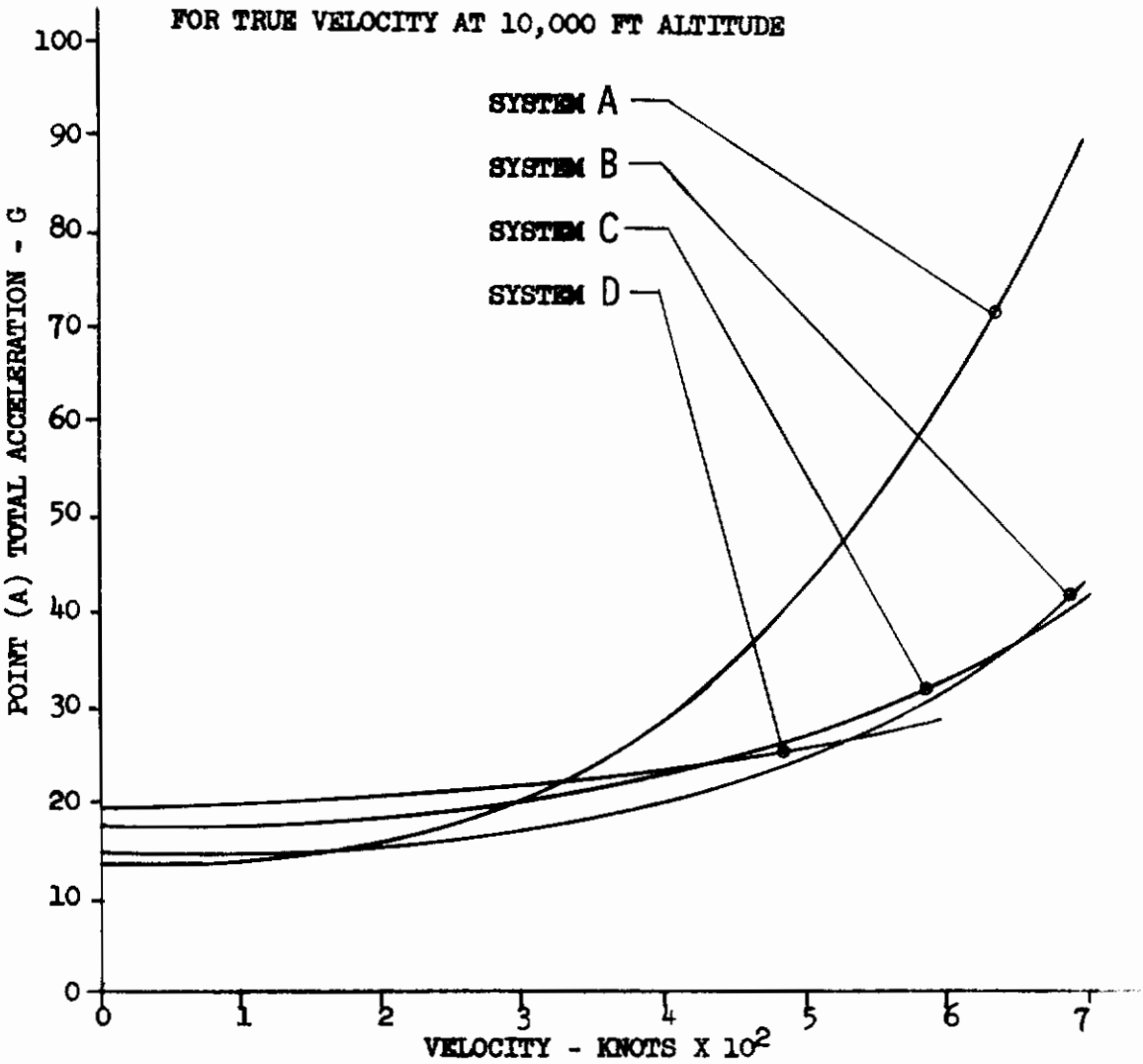

FIGURE 100 - SYSTEM COMPARISON OF TOTAL ACCELERATION VERSUS VELOCITY
(p = 180 DEG/SEC; q = 90 DEG/SEC)

Approved for Public Release

Contrails

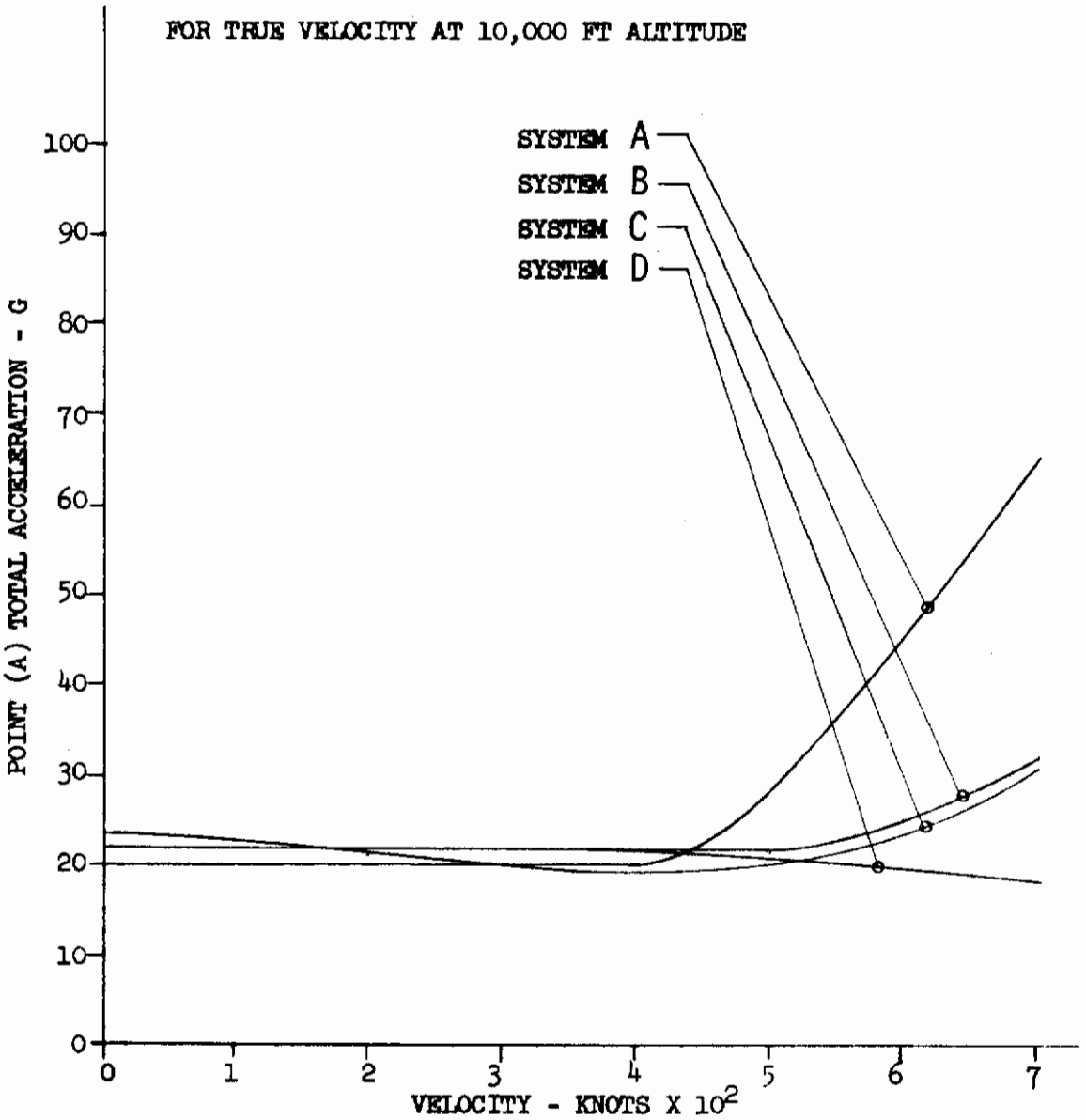

FIGURE 101- SYSTEM COMPARISON OF TOTAL ACCELERATION VERSUS VELOCITY
(p = 180 DEG/SEC; q = ZERO DEG/SEC)

Approved for Public Release

Contrails

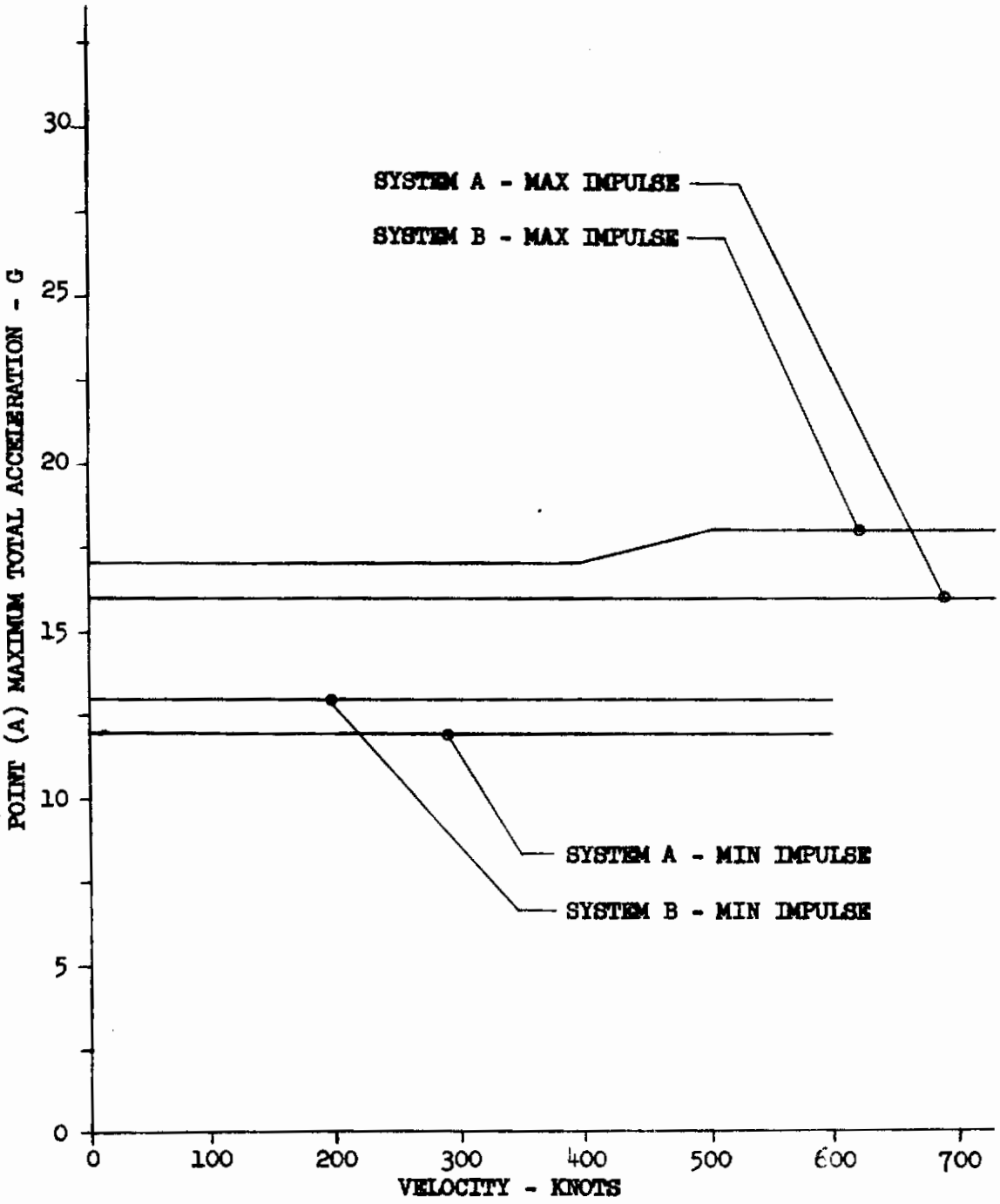

FIGURE 102 - SYSTEM A AND B TOTAL PHASE I ACCELERATION VERSUS VELOCITY (MIN OFFSET, MIN AND MAX IMPULSE, 10,000 FT)

Approved for Public Release

Contrails

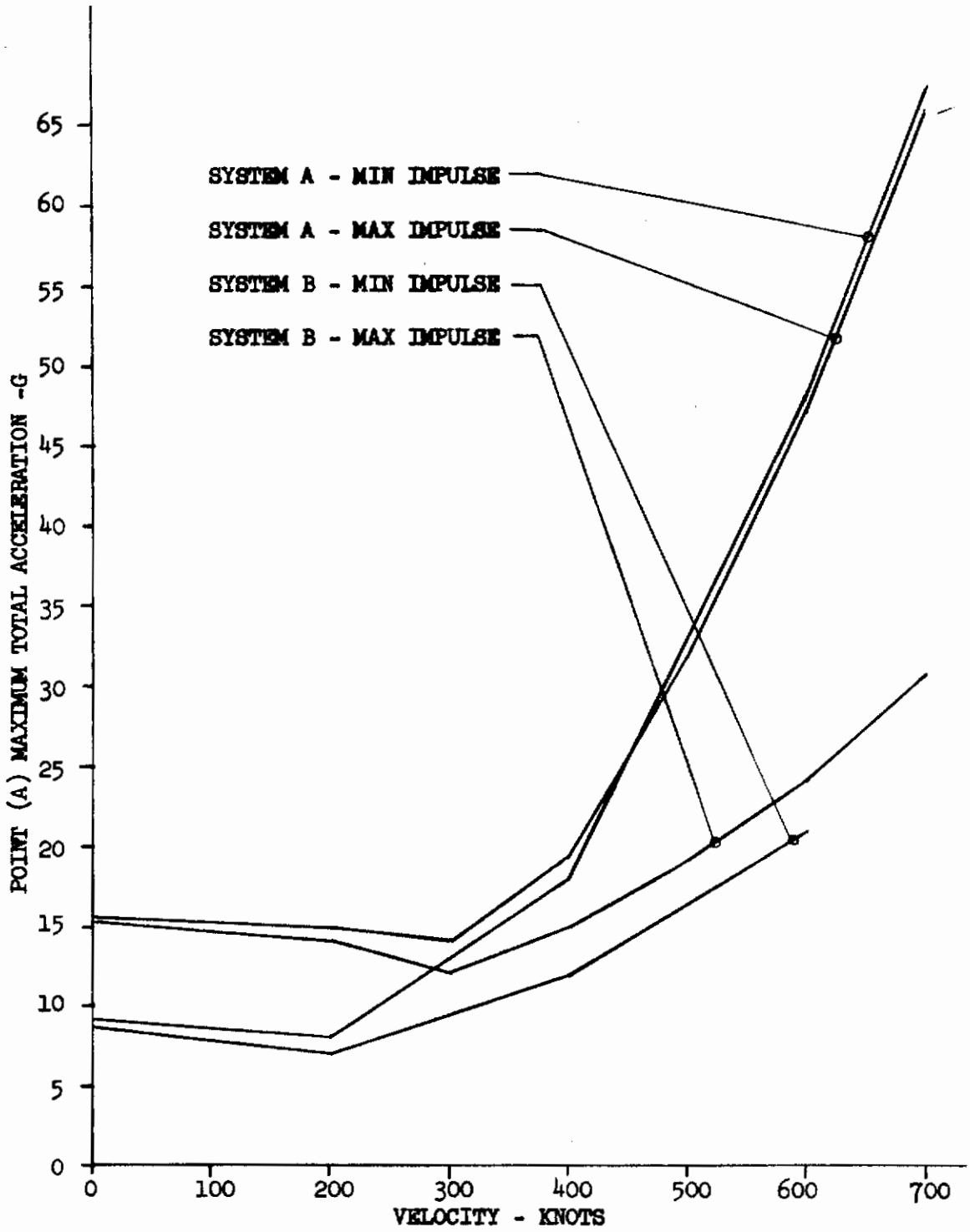

FIGURE 103- SYSTEM A AND B TOTAL PHASE III ACCELERATION VERSUS VELOCITY (MIN OFFSET, MIN AND MAX IMPULSE, 10,000 FT)

Approved for Public Release

Contrails

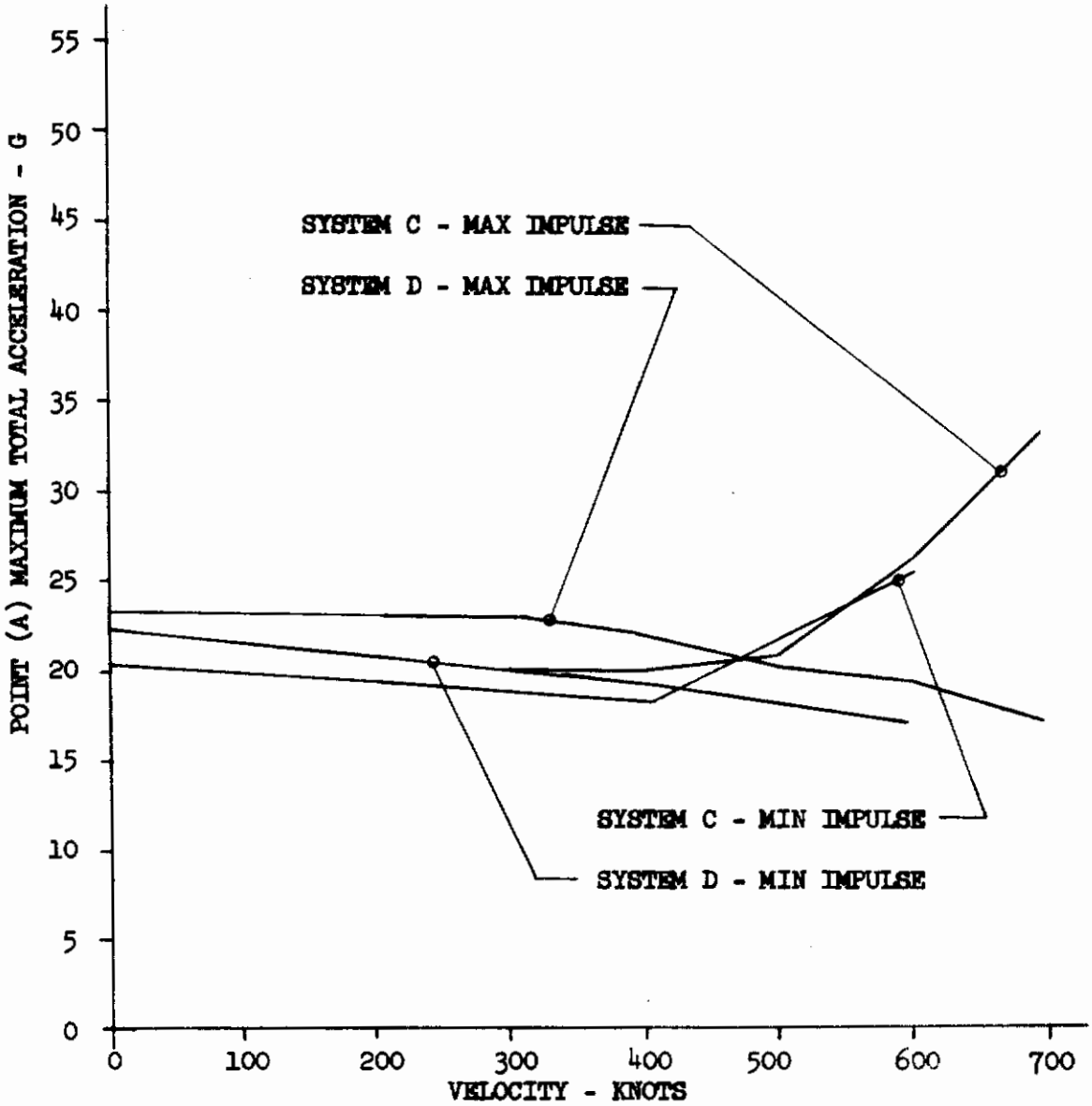

FIGURE 104 - SYSTEM C AND D TOTAL PHASE III ACCELERATION VERSUS VELOCITY (MIN OFFSET, MIN AND MAX IMPULSE, 10,000 FT)

Approved for Public Release

Contrails

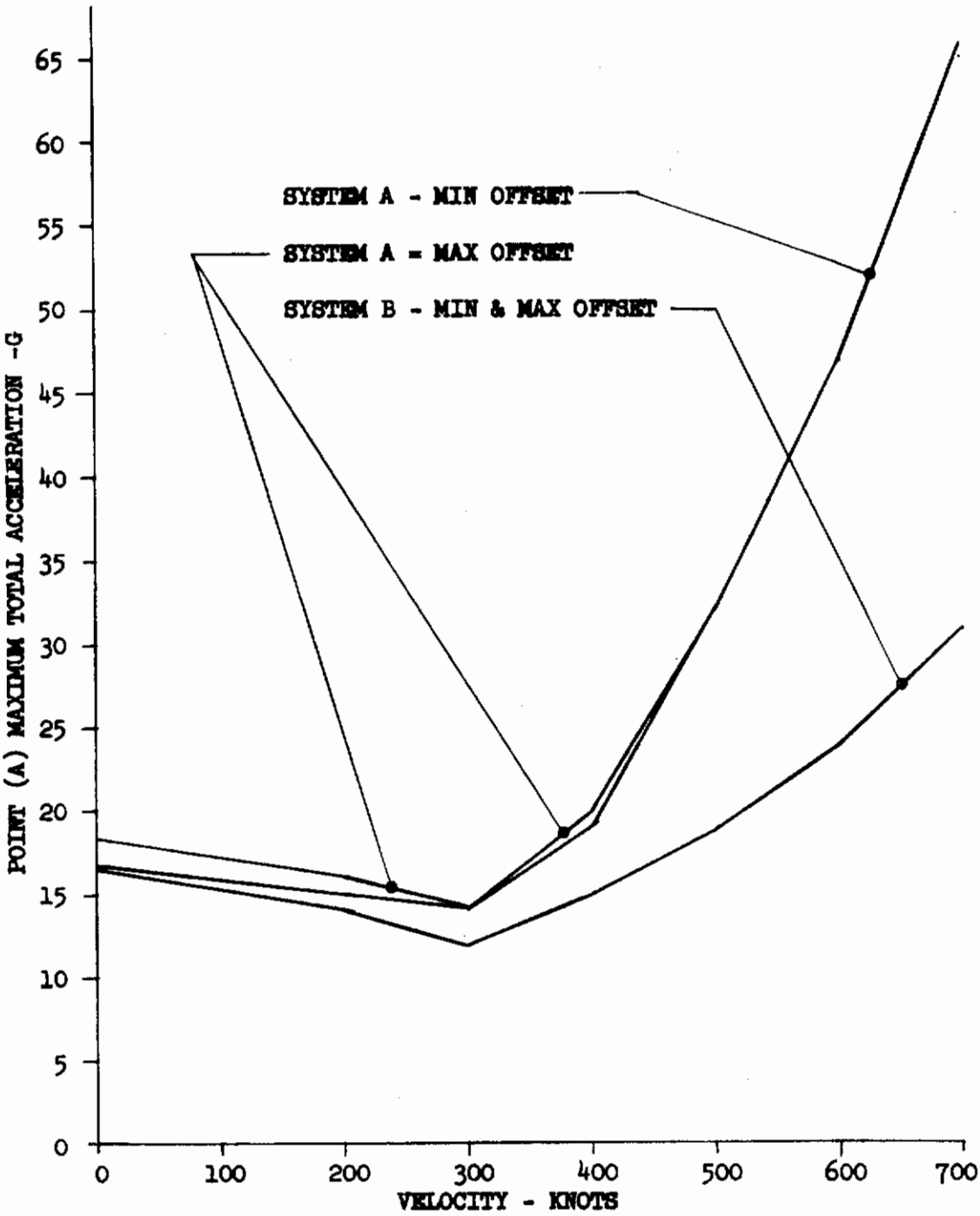

FIGURE 105 - SYSTEM A AND B TOTAL PHASE III ACCELERATION VERSUS VELOCITY (MAX IMPULSE, MIN AND MAX OFFSET, 10,000 FT)

Approved for Public Release

Contrails

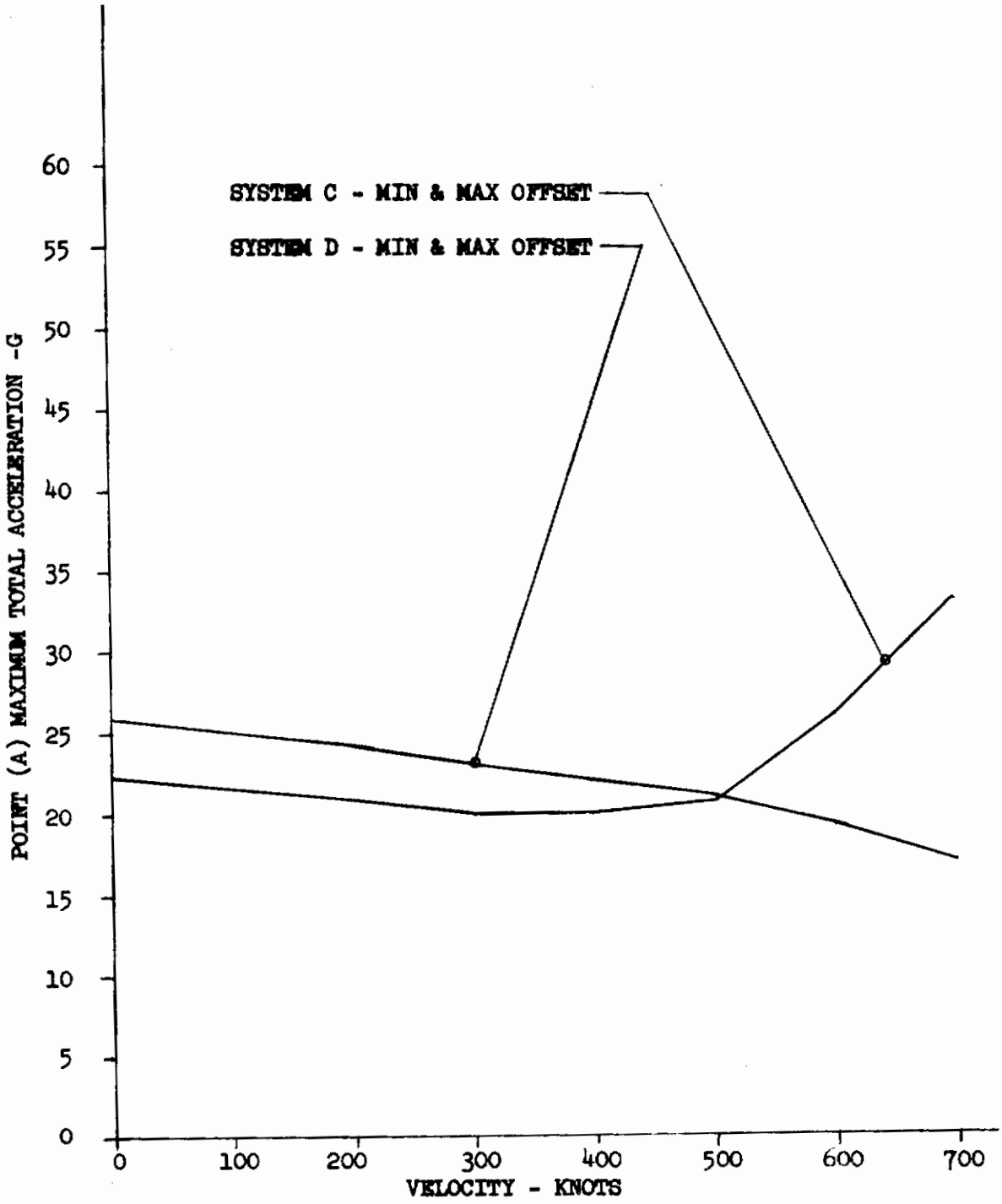

FIGURE 106 - SYSTEM C AND D TOTAL PHASE III ACCELERATION VERSUS VELOCITY (MAX IMPULSE, MIN AND MAX OFFSET, 10,000 FT)

Approved for Public Release

Contrails

The influence of propulsion rocket thrust offset on maximum acceleration magnitude is discernable solely in System A, and then only at airspeeds below 500 knots. Rotations imposed by matrix thrust offsets are insufficient to generate significant total acceleration increments, as shown in figures 105 and 106.

b. Acceleration Rates of Onset

Within the investigated matrix representing the likely range of maneuvers of VTOL and conventional aircraft at low altitude, the following generalizations emerge:

1. Systems A and B can be expected to exceed acceleration onset limits in Phase II (tip-off as escape body rotates about lower roller moving pivot) during ejection at airspeeds above 200 KEAS, and sometimes to exceed onset limits in Phase III at 700 KEAS and above.

2. Systems C and D, if aerodynamically stable, remain within onset limits at airspeeds up to 800 KEAS.

3. Equivalent airspeed, manifested by dynamic pressure, is the dominant factor in onset values.

Approved for Public Release

Contrails

5. DISCUSSION

The two previous sections described the analyses of the computer program output data for definition of safe emergency altitudes and acceleration limits of the four crew escape concepts. These analyses yielded data useful in discussion of several aspects of escape under adverse flight conditions. (Refer to figure 21.)

It should be borne in mind that the objective of this analysis is not the comparing of four escape concepts, but rather the defining of capabilities and limitations of four representative systems to each of which are arbitrarily attributed certain features with equally arbitrary performances thereby granting, or withholding, an advantage during low-altitude escape. The single common denominator is equality of the safe emergency altitude for each escape concept at zero altitude, zero airspeed, aircraft upright and static. Significantly, all systems are improvable within the current art.

Further, no attempt has been made to integrate matrix cases into aircraft mission profiles by assigning relative frequencies of expected occurrence. Each aircraft maneuver case, however exotic or commonplace, carries equal weight.

A very minor limitation in the computer analysis should be noted. Even though the frequency of calculation, resulting in computation intervals as small as 0.002 second, is programmed to increase as rates of change increase, some lag in generation of end values is inherent but of no real consequence.

a. Escape Concept Capabilities and Limitations

In determining the limitations and capabilities of the four escape concepts, stringent combinations of escape system configuration parameters are considered in order to arrive at conservative conclusions. Sixteen combinations of escape system minimum and maximum initiation time, propulsion impulse, thrust misalignment and escape body weight are included in the investigation matrix. The conservative establishment of operational boundaries for each system concept is performed by selection of the maximum safe emergency altitude (SEA) from each set of 16 system conditions for the 208 adverse flight cases.

The Appendix contains cross plots of SEA versus system conditions for all of the 208 flight cases. The immediate discussion is restricted to the zero-to-100-knot, level and descending flight velocity range most important to crew escape in VTOL and conventional takeoff and landing situations.

Limitations for System A, the open ejection seat, vary from an SEA of -160 feet under VTOL emergency flight condition of zero knots and angle of attack of 0° to an SEA of 1450 feet at an aircraft performance point of 100 knots at -90° angle of attack and -90° dive. This defines the total range of minimal altitudes at which the zero and 100 knot, level and diving flight matrix of aircraft maneuvers, both favorable and unfavorable, may be accompanied by emergencies requiring and resulting in System A safe escape despite the most adverse combination of variable initiation time, impulse, offset and weight.

Approved for Public Release

Contrails

System B, the encapsulated seat, has a minimal SEA of -229 feet at 100 knots at 90° roll, 15° angle of attack and 60°/sec roll rate, and the upper SEA is 1630 feet at the aircraft case of 100 knots, angle of attack of -90° and -90° dive.

System C, the inset cabin capsule concept, encounters a great spread in SEA extremes in that the lower SEA is -502 feet at aircraft velocity of 100 knots at 15° angle of attack and +10° dive, and 2103 feet altitude is required at flight conditions of 100 knots, angle of attack of -90° and -90° dive.

The nose capsule, System D, exceeds the SEA limits of the other concepts studied. This system has a minimal SEA of -875 feet at 30°/sec pitch rate, and an upper SEA of 2287 feet in the case of 100 knots and -90° dive.

b. Improvement Potentials for Escape Concepts

The capabilities of the limited escape system concepts subjected to the computerized analysis may be improved by several feasible methods without exceeding human acceleration tolerances. Methodology may include utilization of forced parachute deployment, aneroid timers for parachute mode selection, variable propulsion burn times, and attitude and position control.

Forced parachute deployment by mortar and forced opening by radially fired slugs are current methods which have the advantage of projecting the parachute to full stretch of the shroud lines and quickly developing the canopy skirt, thus shortening the required time and distance to fully open. Forced deployment is especially advantageous during a low speed, low altitude, high-sink-rate ejection where the trajectory is short and the distance required to open the unaided parachute exceeds that available.

Employment of an aircraft speed sensor and aneroid timer increases the low-altitude capability of all of the escape concepts by automatically selecting a parachute deployment mode to match the altitude and velocity encountered at the time of ejection. This device assures that the parachute subsystem structural capacity is not compromised by high dynamic pressure, yet deploys the parachute as rapidly as possible to promote satisfactory operation under low altitude conditions.

Propulsion rocket burn time of course may be augmented without reducing the present thrust level, by increasing the specific impulse or amount of propellant. Application of a longer burntime is advantageous only if the escape body retains an upward thrust vector.

The low altitude escape performance from an aircraft in adverse attitude or experiencing rapid attitude changes may be increased through control which assures proper orientation of the escape body thrust vector. The rate, hence the acceleration, with which this orientation can be imposed upon the body governs what useful thrust remains for prolongation of the escape trajectory. An inverted aircraft attitude combined with low altitude imposes severe penalties upon the escape system since under these circumstances the height

Approved for Public Release

Contrails

must be sufficient to allow for the propelled descent, the distance required for full deployment of the recovery parachute, and reduction of the descent velocity to safe touch-down values. In the inverted case, it is desirable to limit the expenditure of propellant to that necessary only for separation from the aircraft, because any additional thrust consumes valuable altitude. A gyro-controlled rocket mode selector could accomplish this improvement.

To further increase capabilities in the inverted flight envelope, it is possible to apply a maximal amount of escape rocket impulse in extending the trajectory. As long as the rocket vector is orientated toward the upper hemisphere, the thrust augments the low altitude performance; the rocket thrust may be interrupted, after adequate separation from the aircraft, in coordination with an automatically induced roll to maximize impulse utilization. Addition of a gyro-governed roll rocket is useful to produce the most advantageous rate of change in the roll attitude.

c. Further Exploration of Low Altitude Escape

The analyzed escape concepts are deliberately limited in sophistication so that basically characteristic data may be developed for each. The application of various methods of stability control, forceable parachute deployment and thrust vector orientation should be further considered. Investigation of attitude sensors and vernier rockets under adverse attitude conditions would yield valuable data on the desirability of these devices. Additional types of escape systems, such as those incorporating a tractor rocket, selectable-direction ejection and high glide ratios, should be analyzed in an attempt to improve low-altitude escape.

d. Critical Problem Areas of the Attitude Profile

Those combinations of aircraft conditions which result in the initiation of ejection when the propulsion thrust vector is directed below the horizon present a great barrier to the successful culmination of the escape.

Variables which generate attitudes detrimental to escape are unlimited; however of particular concern is the rate with which aircraft attitudes can change. An otherwise compatible aircraft attitude at the instant of separation may be compromised by the application of forces and moments due to aircraft rotational velocities and accelerations. A nose down pitch rate inevitably increases the rate of sink of the escape body located forward of the aircraft CG.

Analysis of aircraft cases of identical velocity and flight path angle but of upright versus inverted roll attitude demonstrates differences in altitude required for safe ejection. System A requires 650 feet of additional altitude for ejection from an inverted rotationless aircraft at 100 knots velocity, System B needs 700 additional feet, System C 1400 feet and System D 1300 feet.

Approved for Public Release

Contrails

e. Important Parameters Affecting Low Altitude Escape

If escape system characteristics alone are considered, the most important to low altitude escape is the distance required for recovery parachute opening. The basis for opening distance is the assumption, that the development of a parachute canopy is a function of the parachute construction geometry and diameter and of the distance traveled by the escape body following parachute initiation; that is, a parachute of given style and diameter will open in a distance governed by a specified multiple of that diameter. Test data prove this assumption to be sufficiently accurate. Since each of the four escape concepts incorporates a different style and diameter of parachute, figures 7 through 9, each escape body must travel a different distance to achieve full opening. As an example, System D with a 71.5-foot diameter ring slot parachute requires over three times the total opening distance of System A with a 28-foot flat circular parachute. This style-diameter-distance relationship is the reason for selection of multiple smaller rather than single large parachutes for heavy escape bodies. The importance of parachute performance is manifested by the usual design necessity of matching auxiliary components, such as escape propulsion and aneroid-timer-dynamic pressure selection devices, to the parachute rather than the reverse procedure.

Within the investigated ranges of propulsion impulse, thrust misalignment and escape body weights, the thrust-CG offset has the greatest influence of the three on low-altitude escape trajectories. Offset-generated attitude excursions of bodies with fixed thrust vectors can be seriously detrimental because of the loss of optimally directed thrust.

No single physical parameter of the escape environment is more significant than aircraft flight path angle, or sink rate, at the instant of ejection. For a rotationless upright aircraft at 100 knots, the all-system average safe emergency altitude for 10° climb is -230 feet, for horizontal flight is 0 feet, for 10° dive 180 feet, for 30° dive 650 feet, and for -90° dive 1500 feet.

Nevertheless, the importance of timely initiation of the escape system is paramount among factors governing the success of low-altitude escape. The decision to eject, whether accomplished by the pilot or by electro-mechanical sensor, must be implementable at the instant which yields optimal result. While this instant is usually the earliest possible, a rapidly rotating aircraft at very low altitude may demand selection of a favorable aircraft attitude at some later time to assure projection of the escape body away from, rather than toward, the ground.

f. Role of Stability in Escape System Performance

Passive or forceful stabilization of an escape body during the ejection is essential to success because of the pronounced effect upon the trajectory height and the accelerations encountered. Rotational rates and accelerations due to instability can cause excessive total accelerations to be imparted to the man beyond acceptable limits. Accelerations thus generated need not themselves directly produce fatalities since acceleration-induced incapacitation of the escaping crew member may result in the same end.

Approved for Public Release

Contrails

The four basic escape concepts of this analysis are limited systems in that all include features which provide passive but not forceful stabilization. The type and amount of stability control provided depends upon the degree of improvement in the escape system performance which is desired. Two methods of forceful stability control, DART and STAPAC, are discussed in Section IV. The DART system furnishes control of the pitch and roll attitude while the STAPAC system can be applied to attenuate pitch, roll or yaw. These controls improve escape system operation by minimizing perturbations in the orientation of the thrust vector.

Approved for Public Release

Contrails

Approved for Public Release

Contrails

APPENDIX

SAFE EMERGENCY ALTITUDE CROSS PLOTS

This Appendix consists of 208 graphs of Safe Emergency Altitude versus 16 escape system conditions for System A through D. Each of the 208 graphs pertains to a specific aircraft flight case described by figure 21.

Approved for Public Release

Contrails

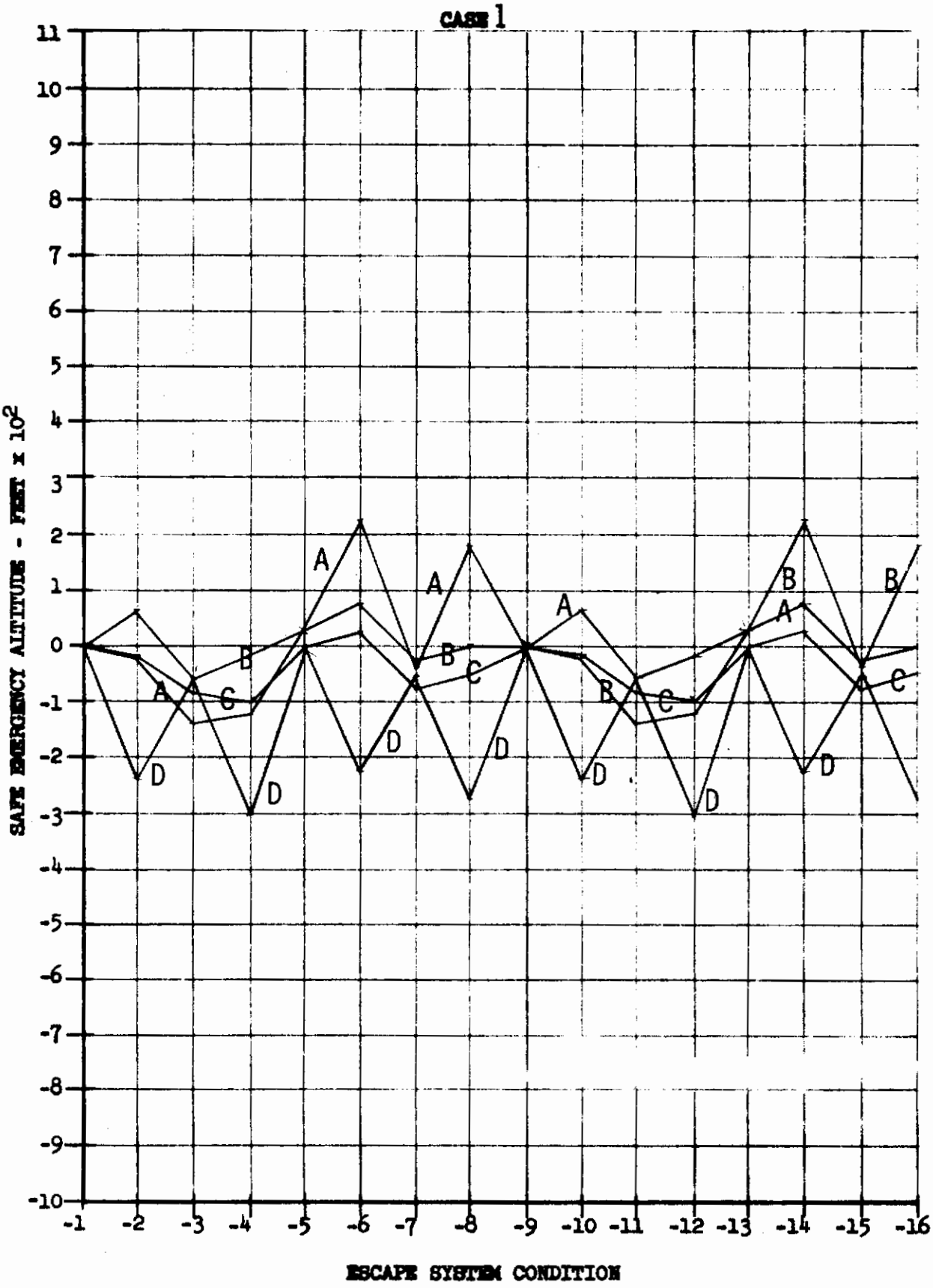

Approved for Public Release

Contrails

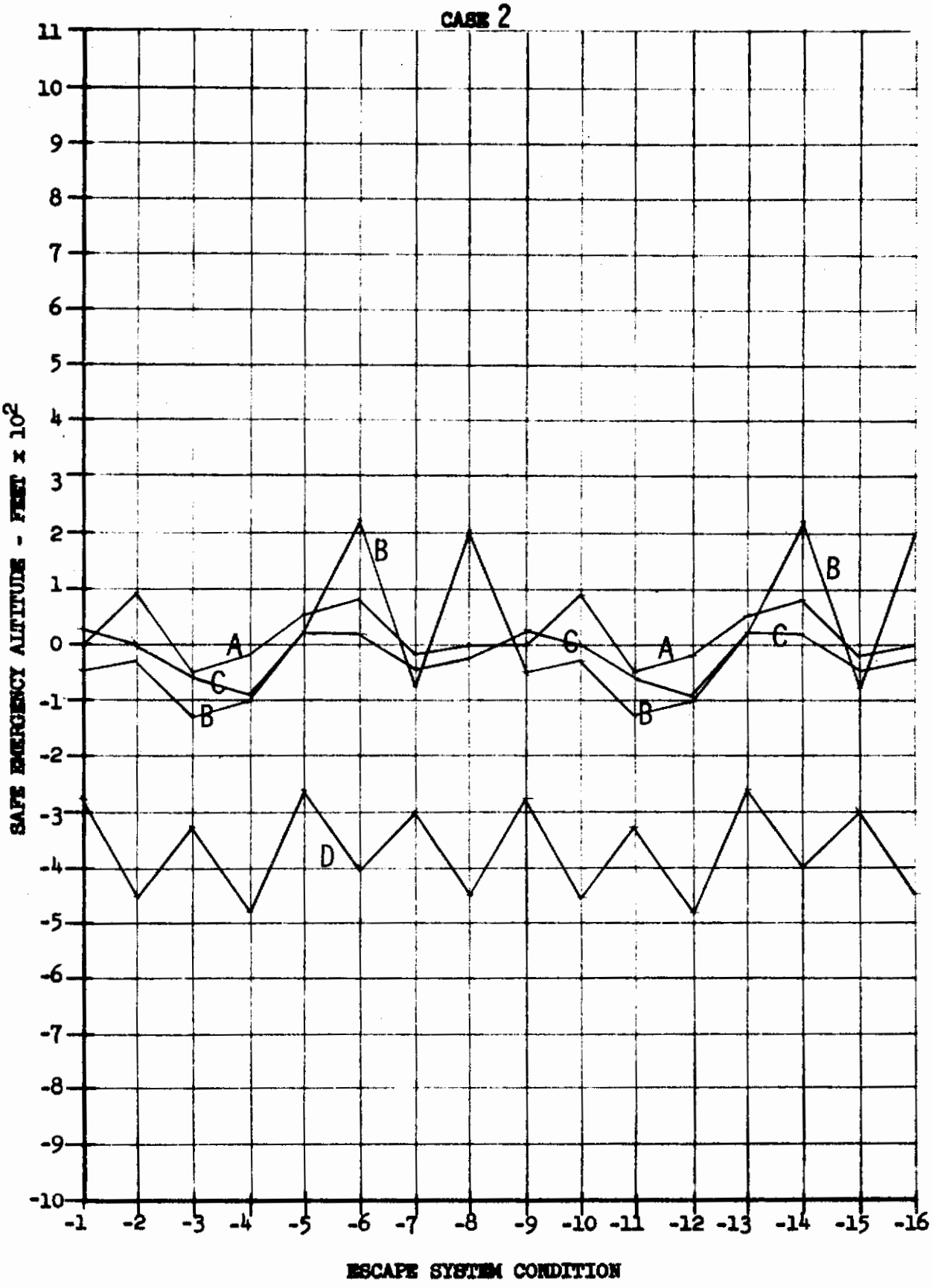

Approved for Public Release

Contrails

CASE 3

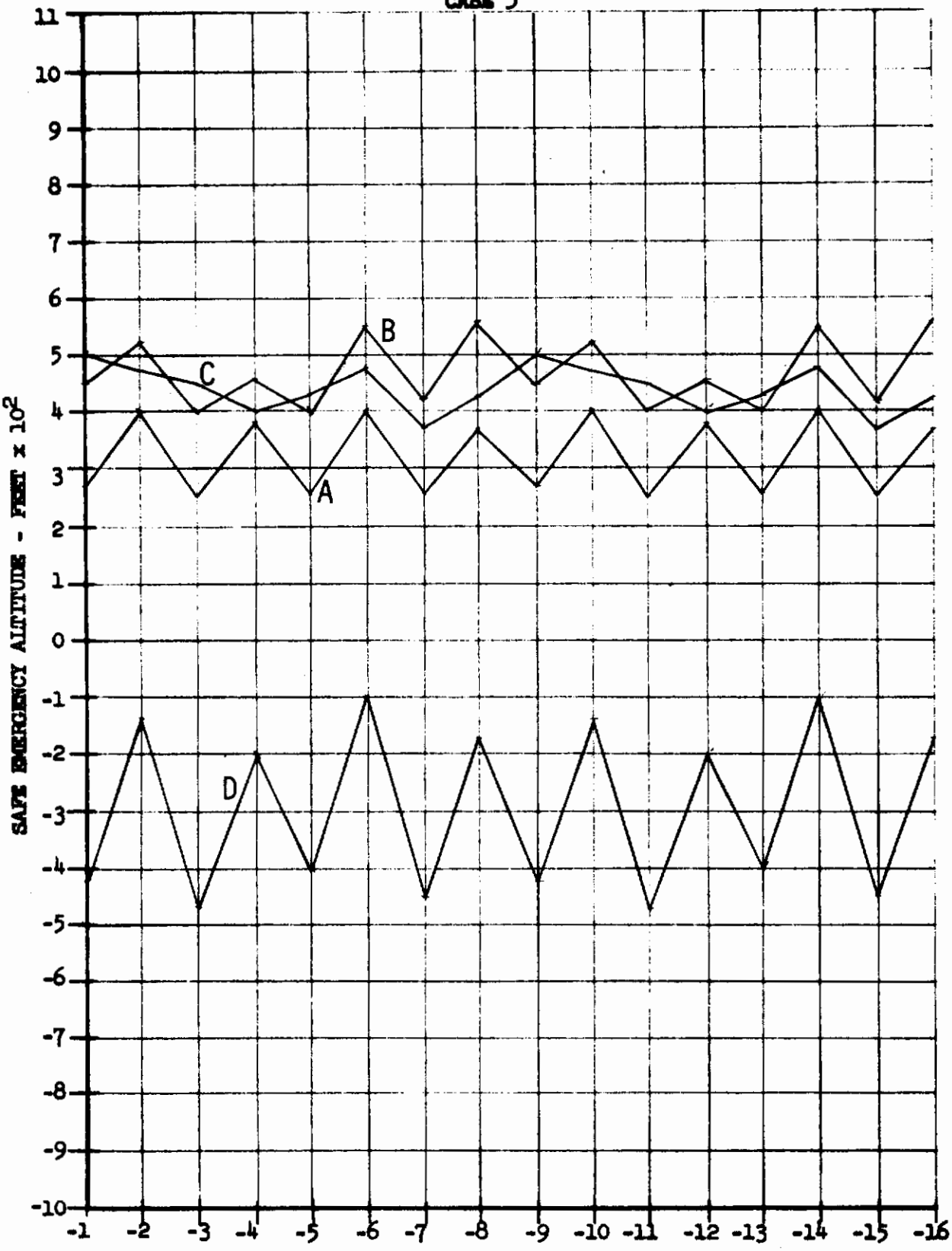

Approved for Public Release

Contrails

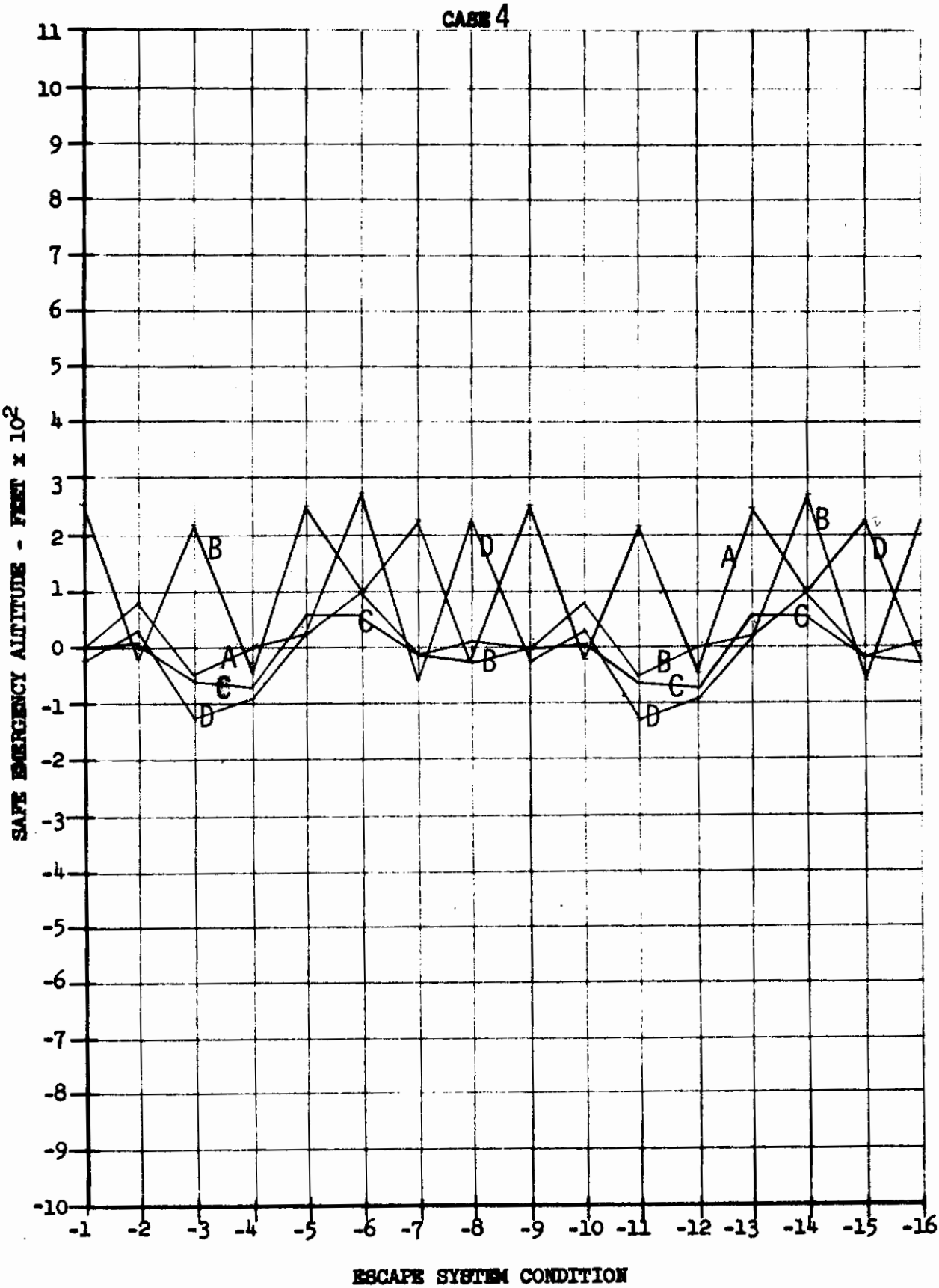

Approved for Public Release

Contrails

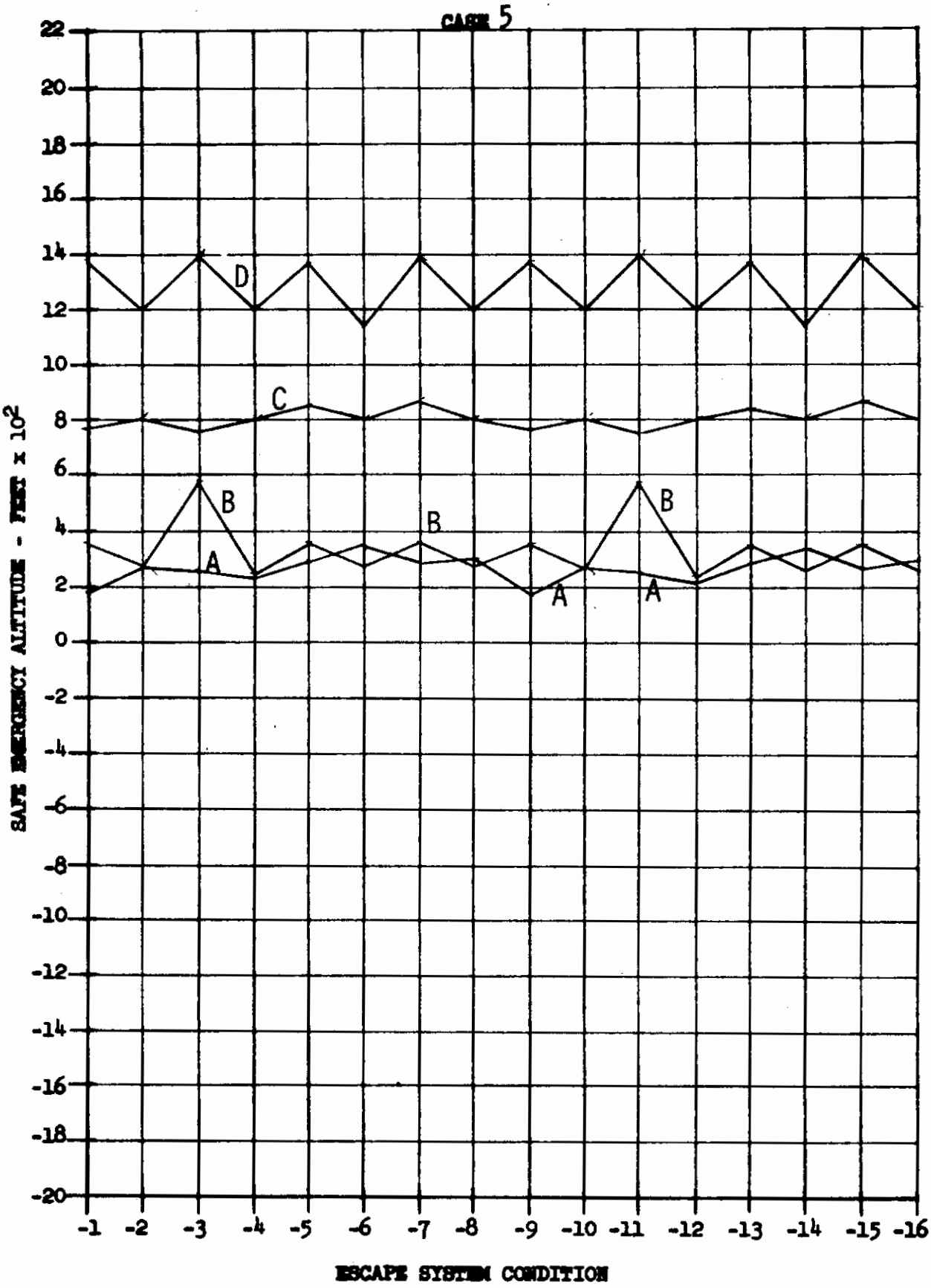

Approved for Public Release

Contrails

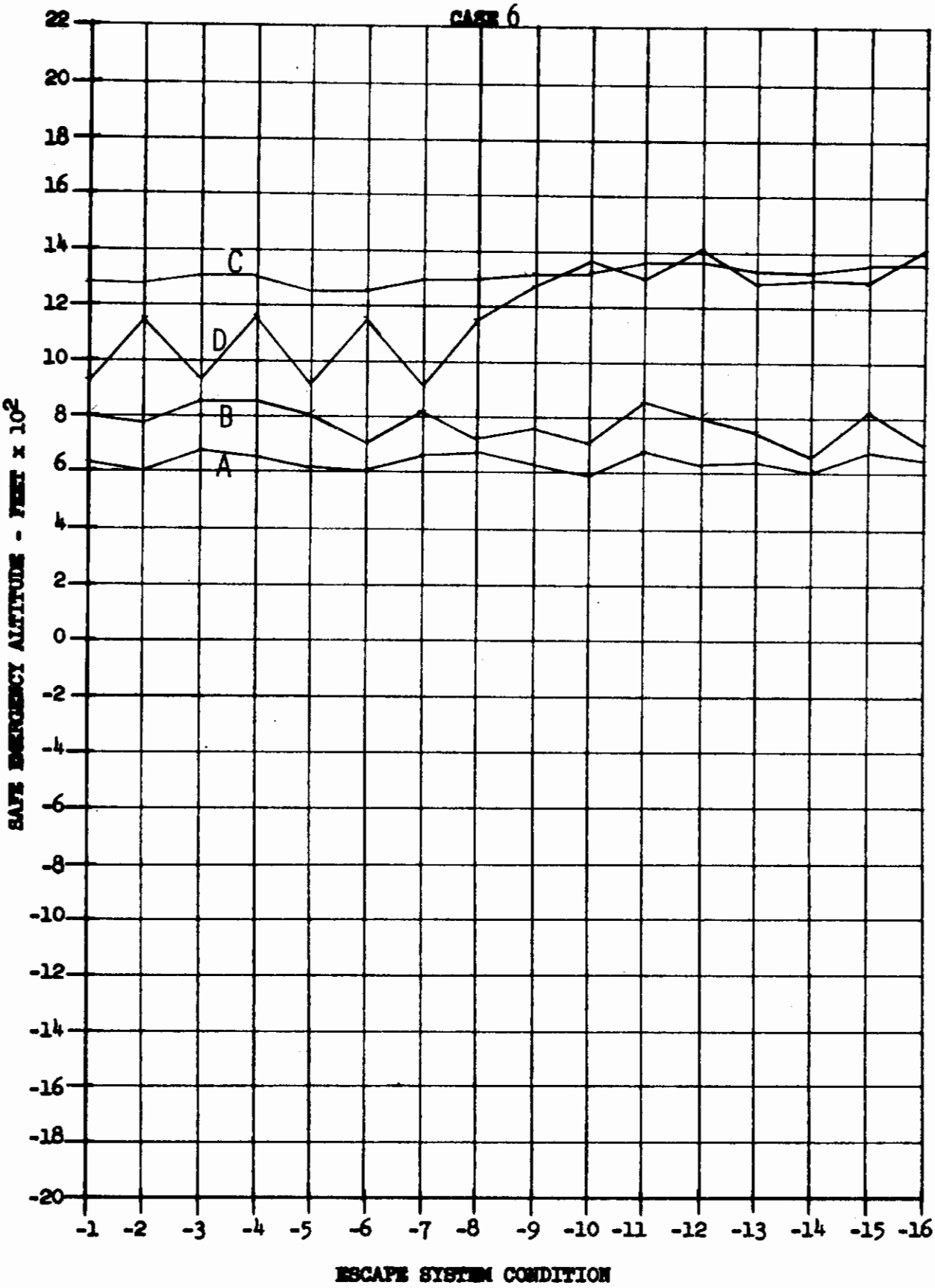

Approved for Public Release

Contrails

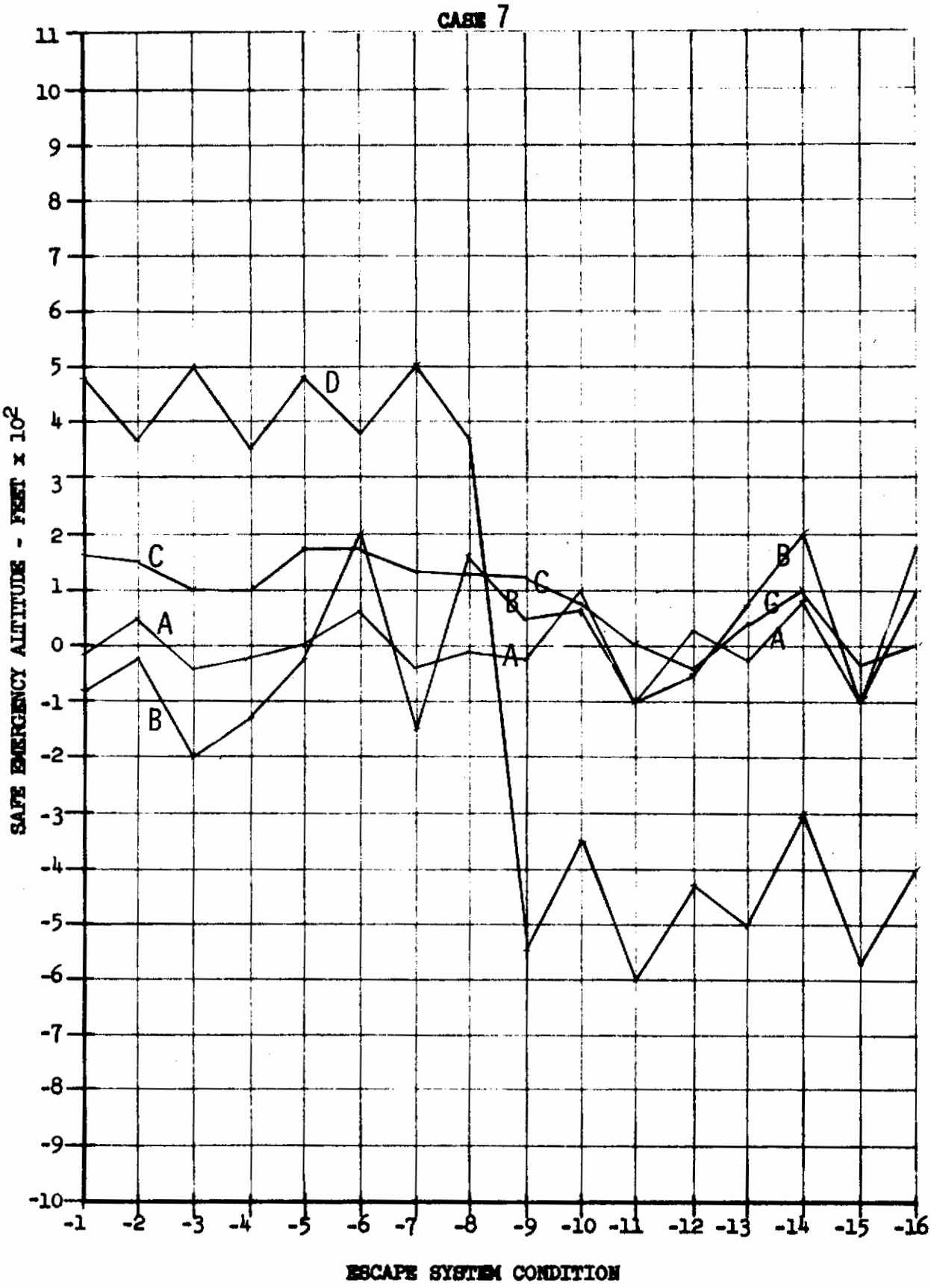

Approved for Public Release

Contrails

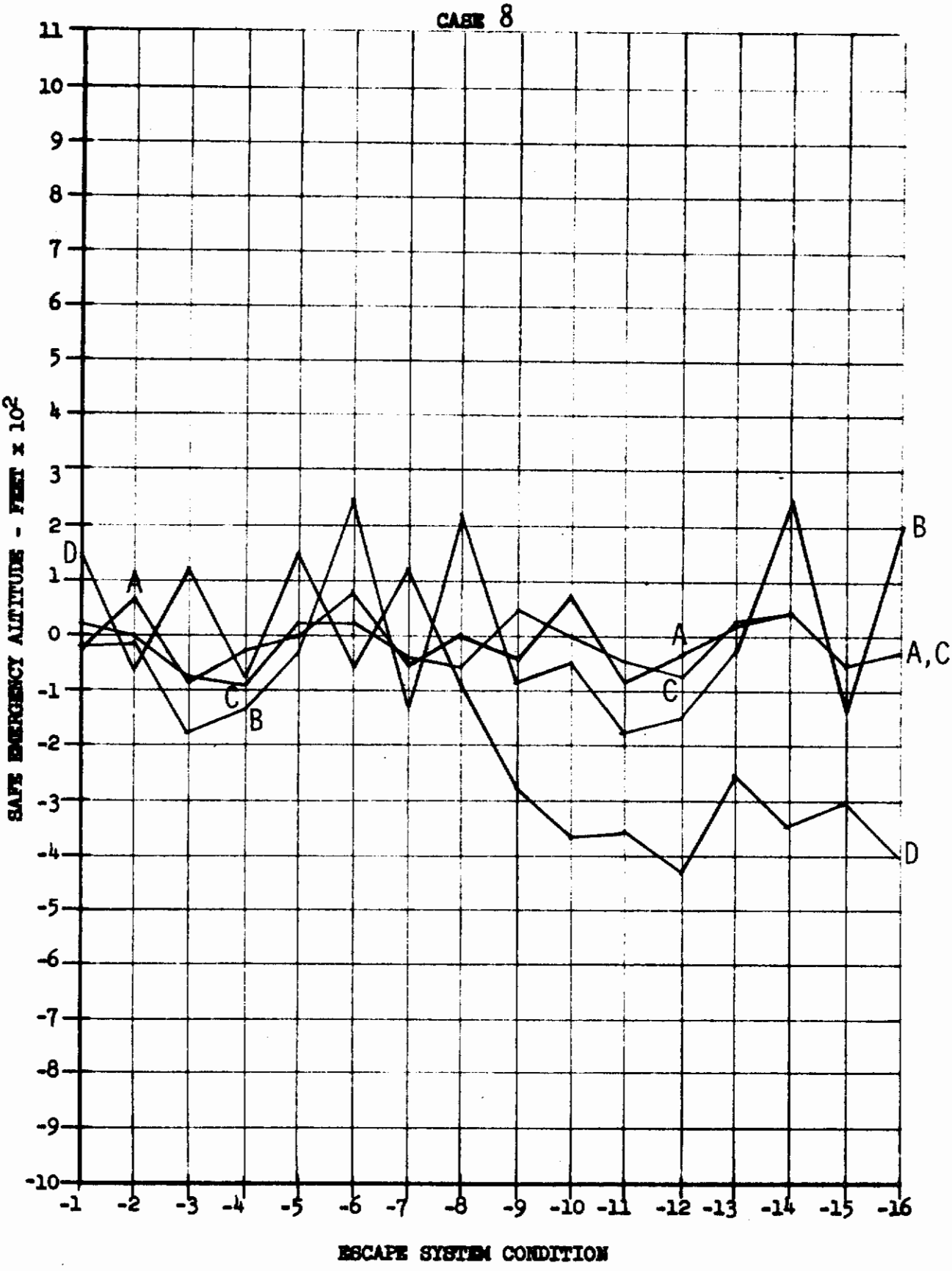

Approved for Public Release

Contrails

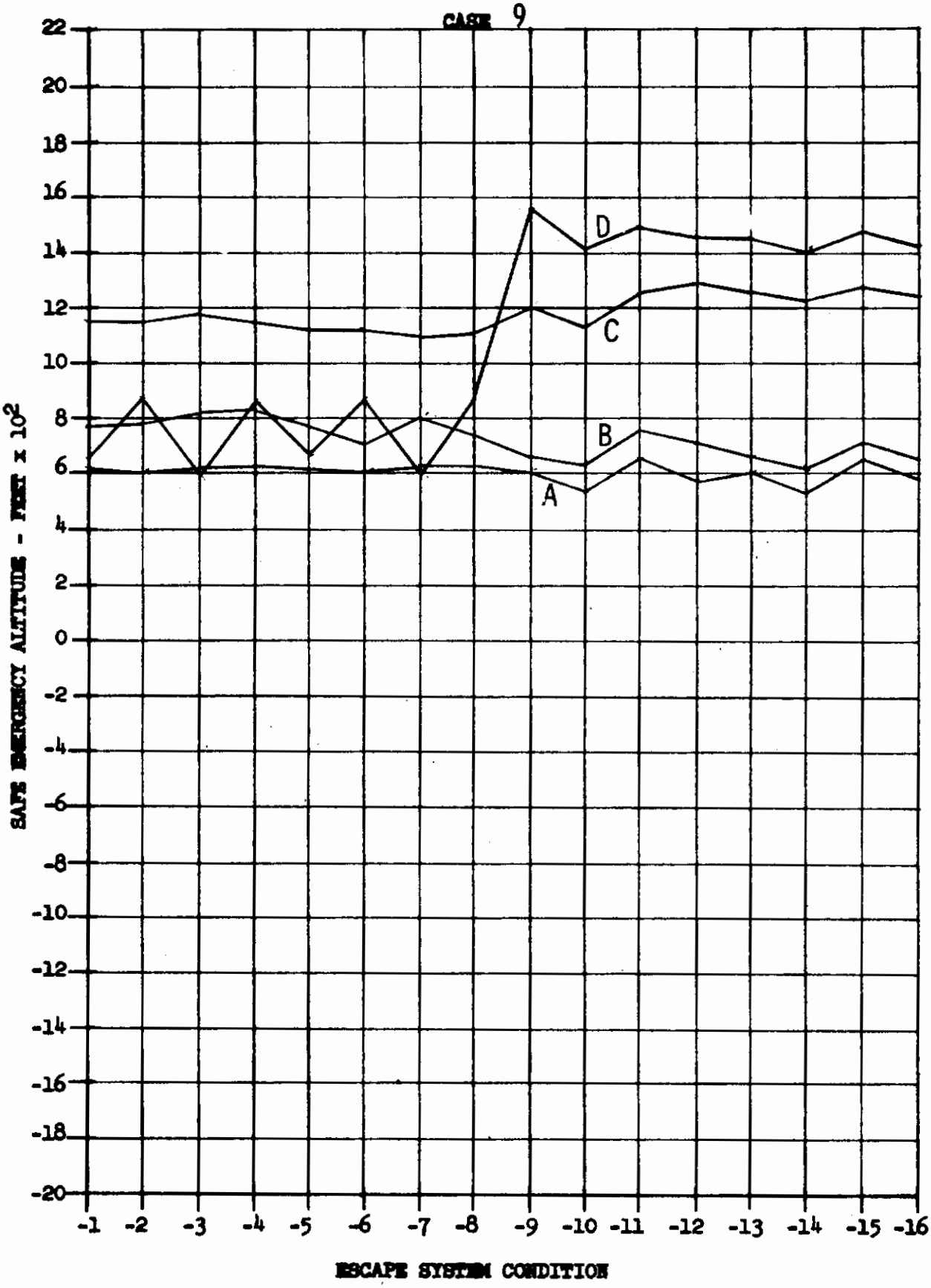

Approved for Public Release

Contrails

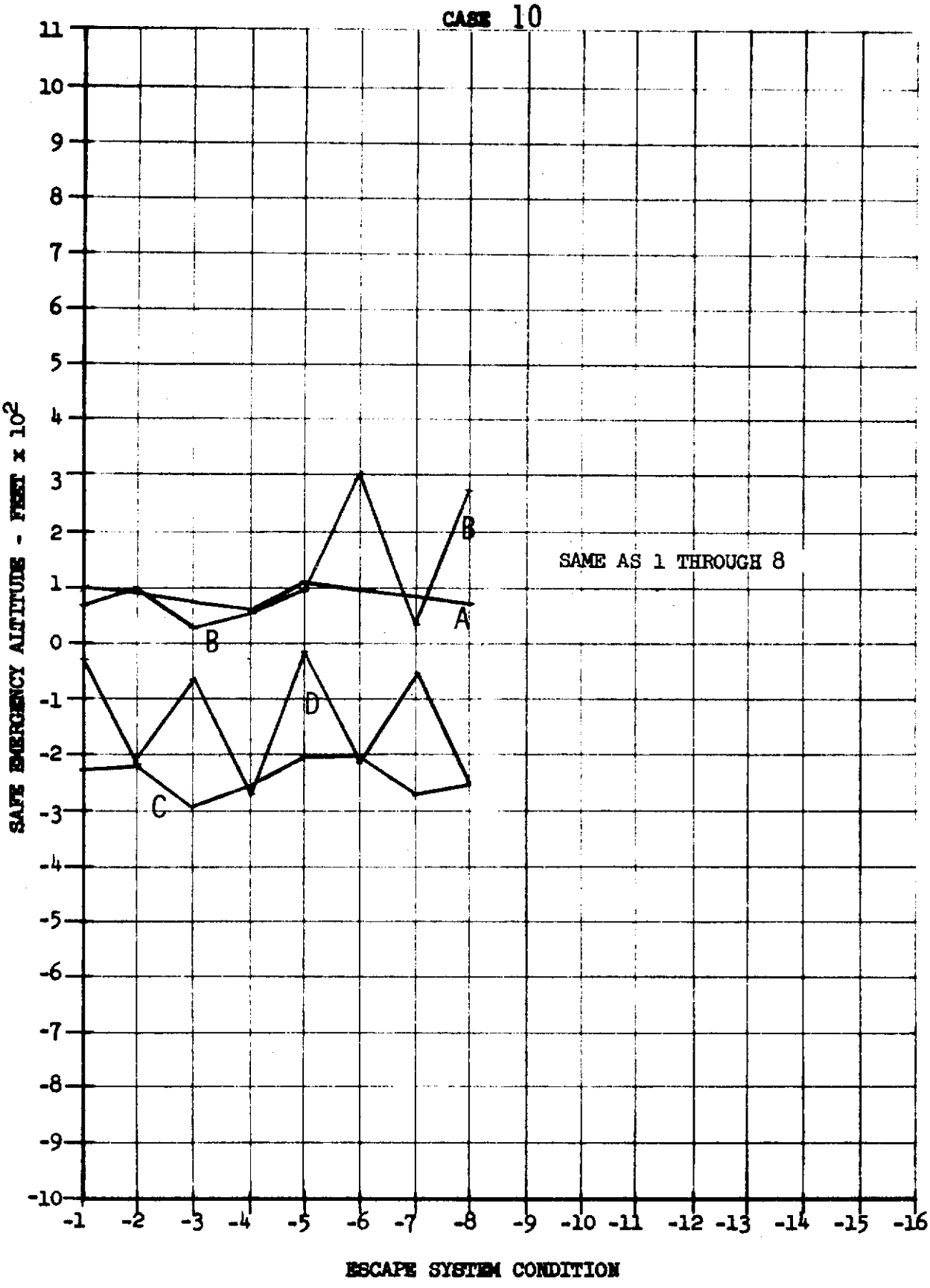

Approved for Public Release

Contrails

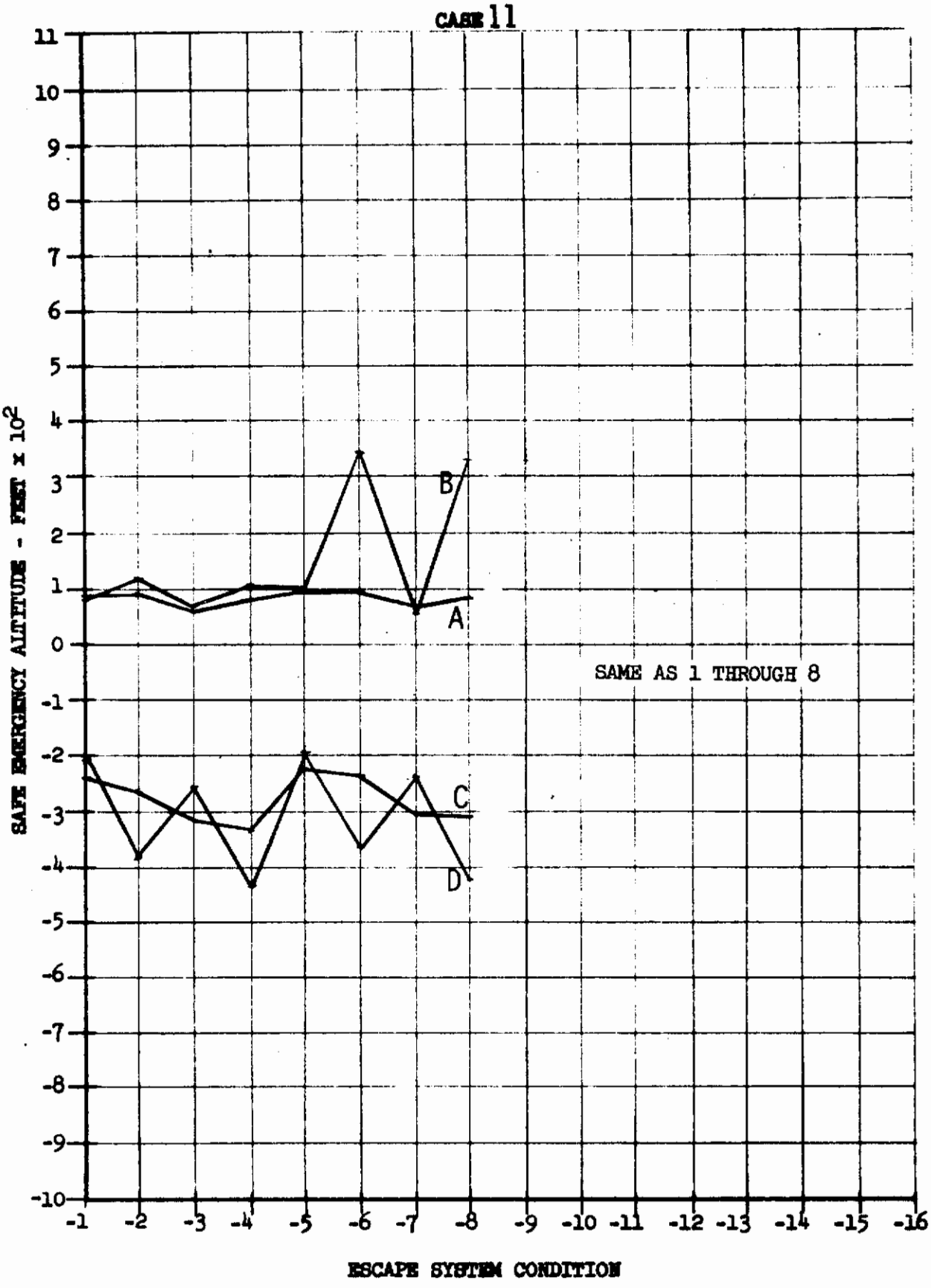

Approved for Public Release

Contrails

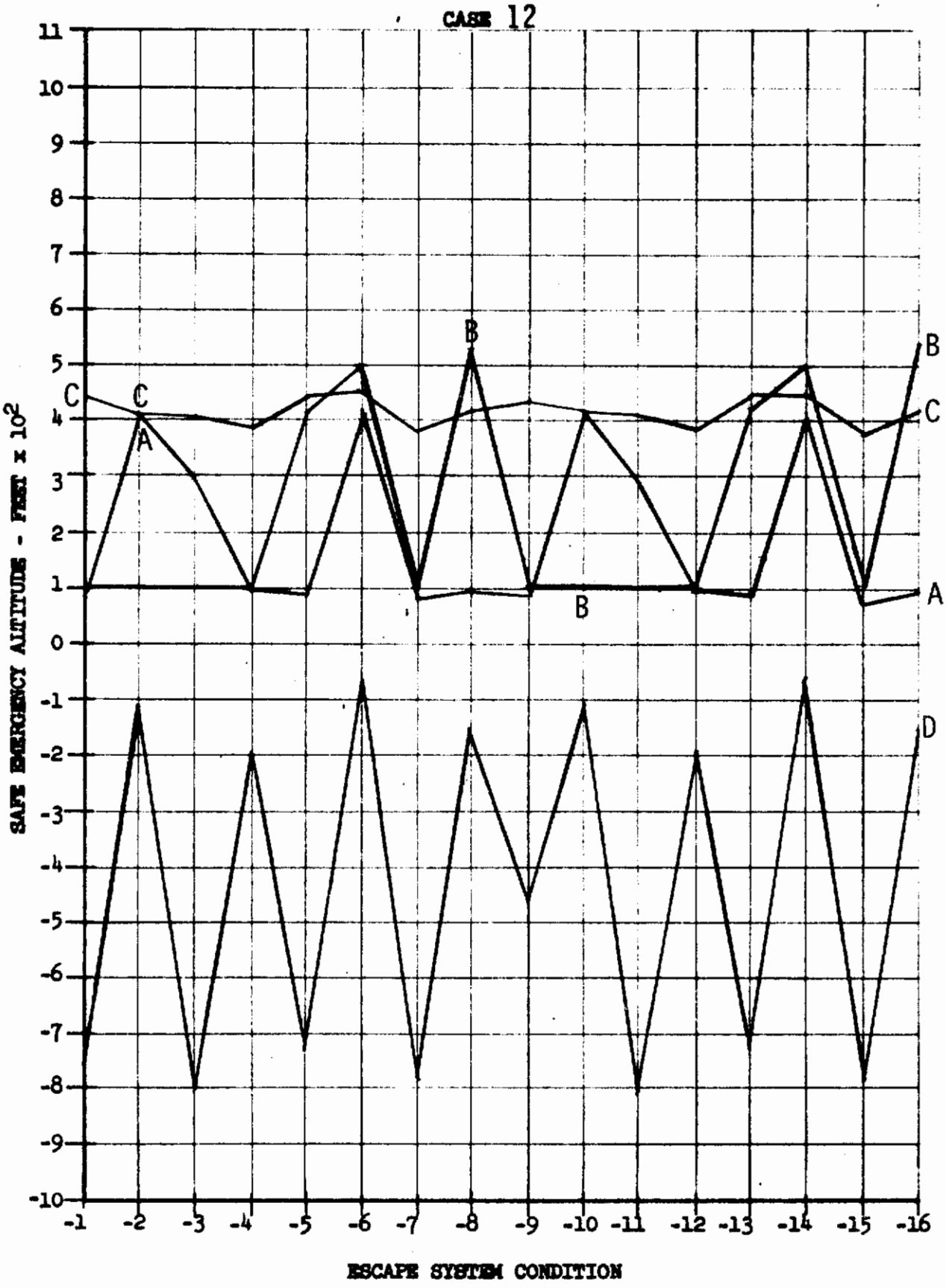

Approved for Public Release

Contrails

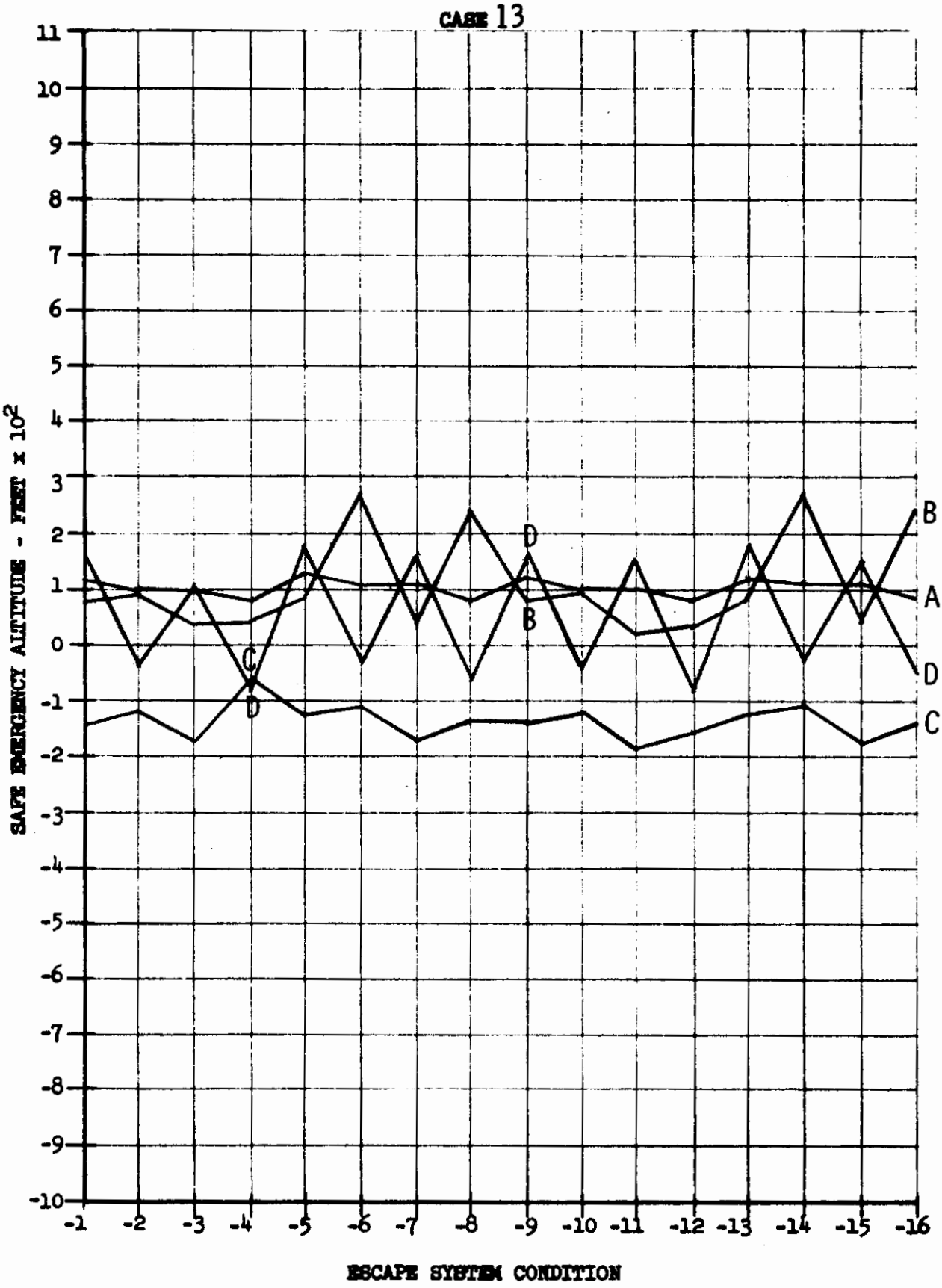

Approved for Public Release

Contrails

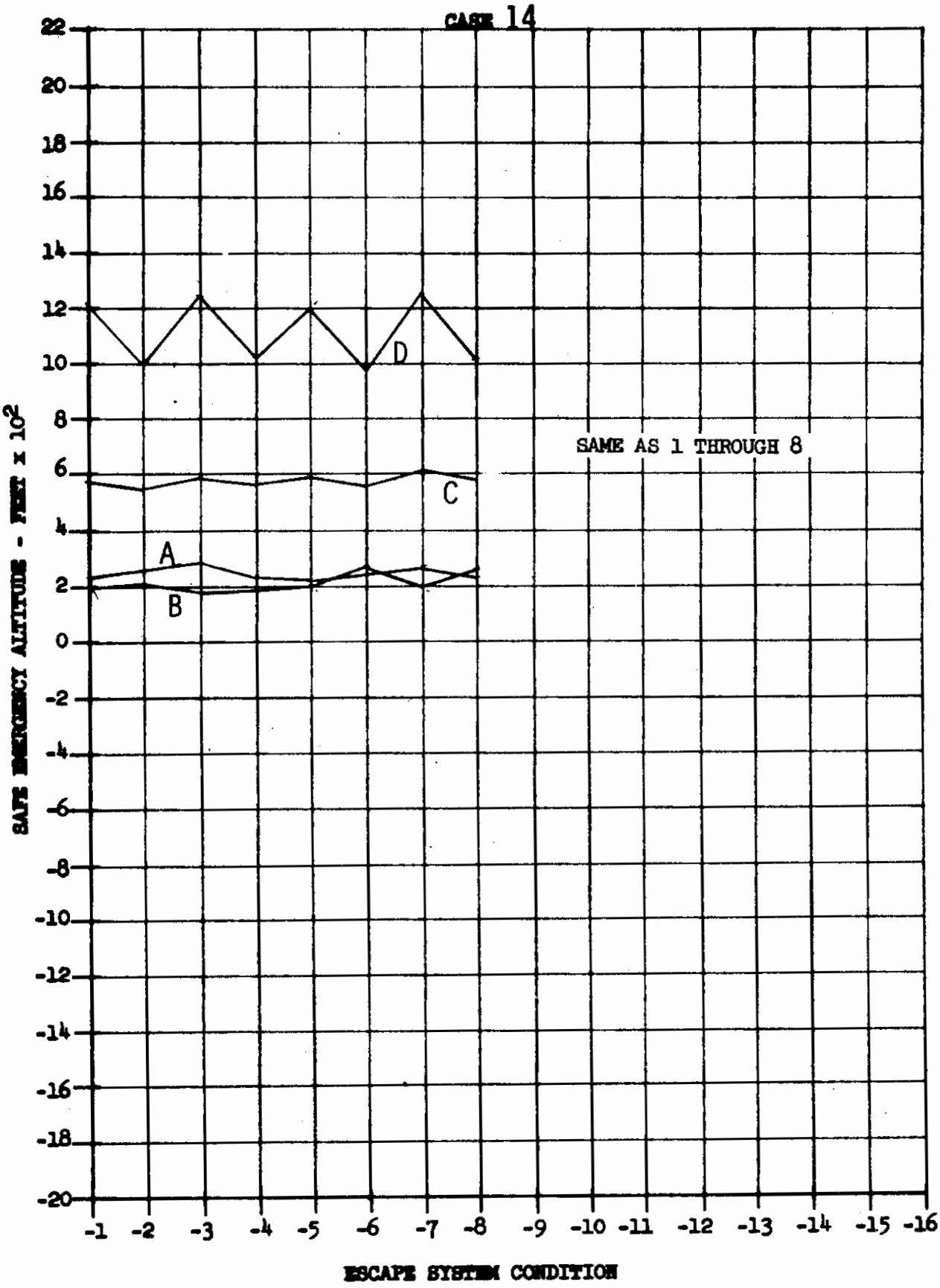

Approved for Public Release

Contrails

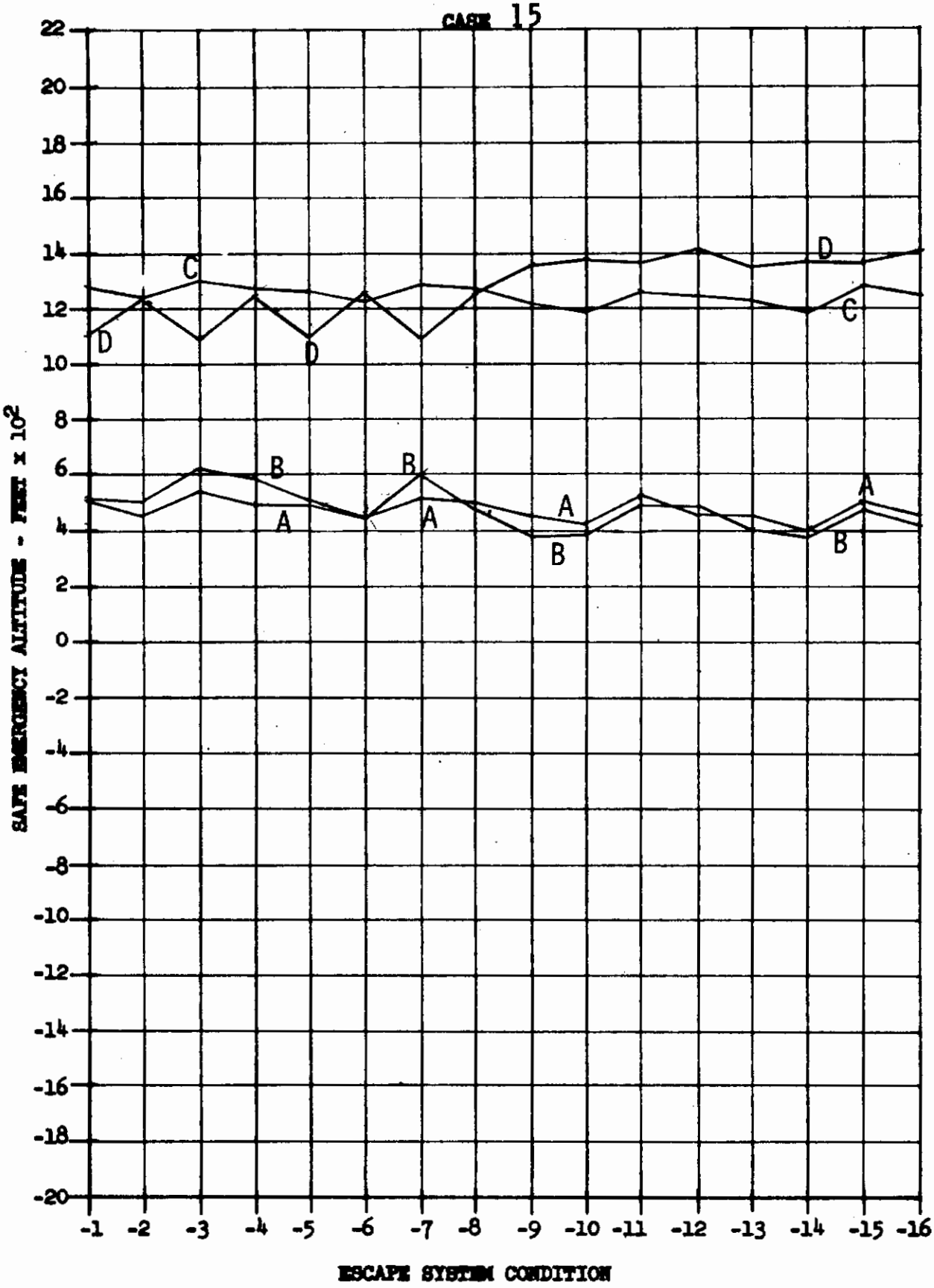

Approved for Public Release

Contrails

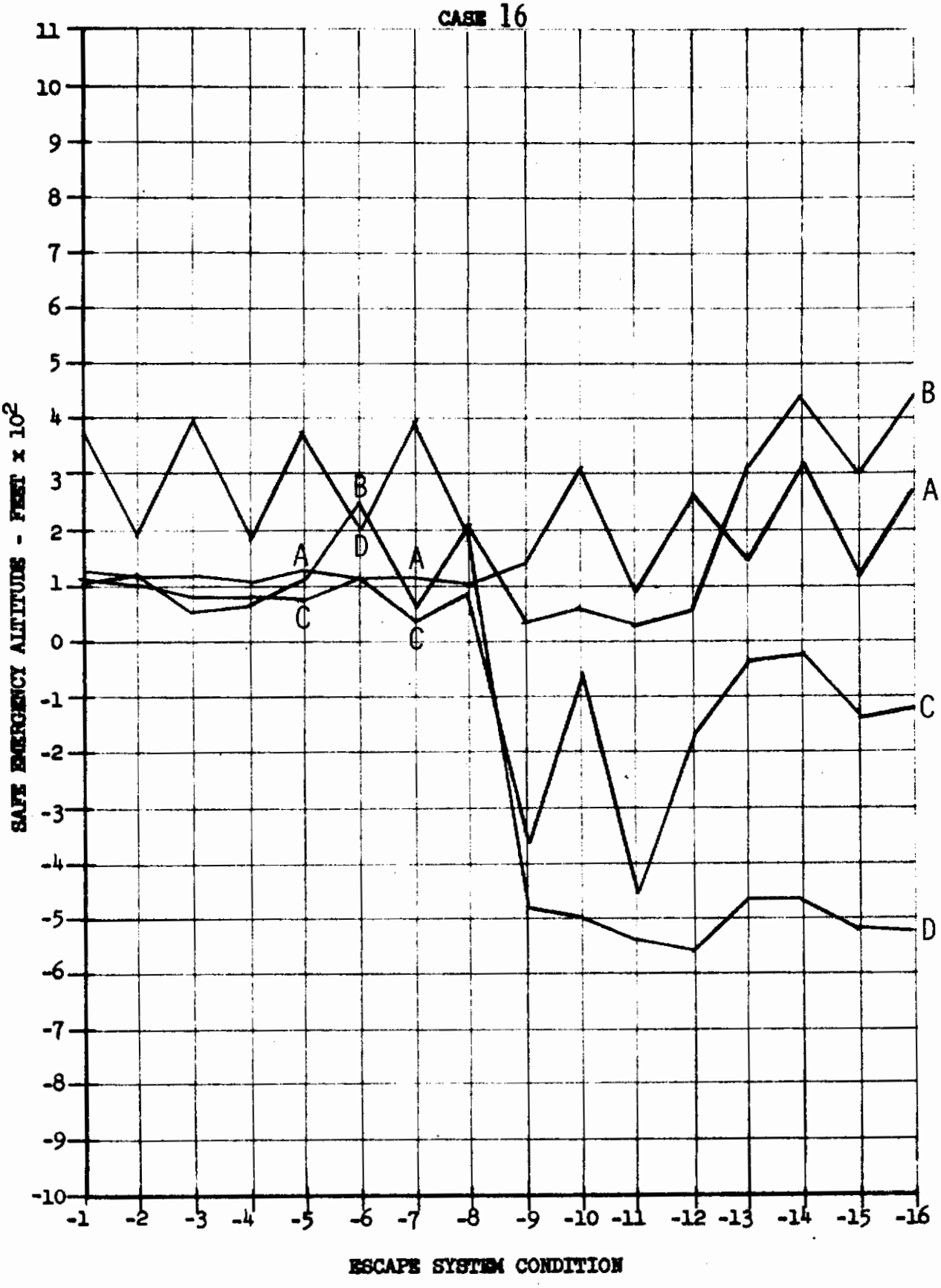

Approved for Public Release

Contrails

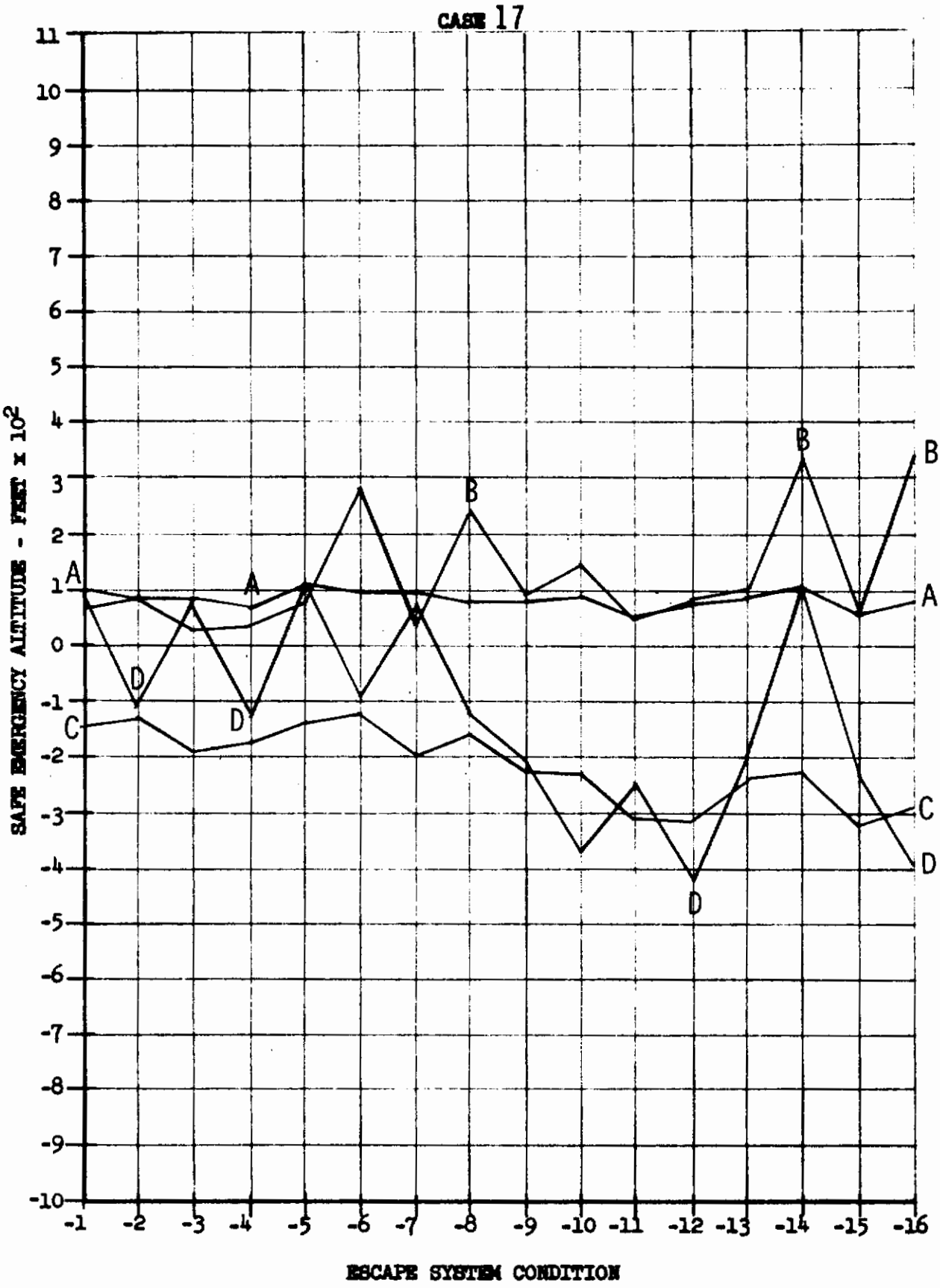

Approved for Public Release

Contrails

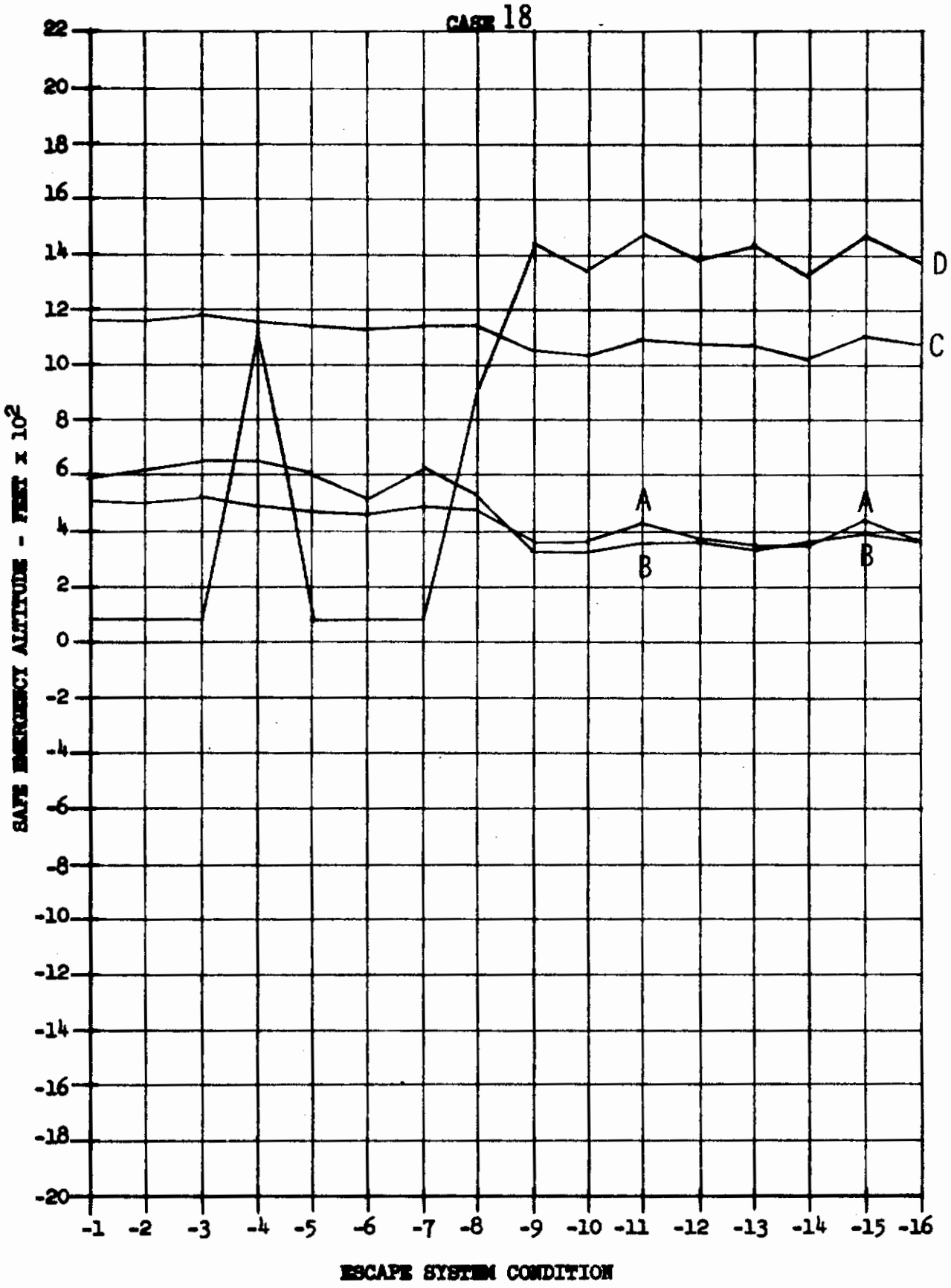

Approved for Public Release

Contrails

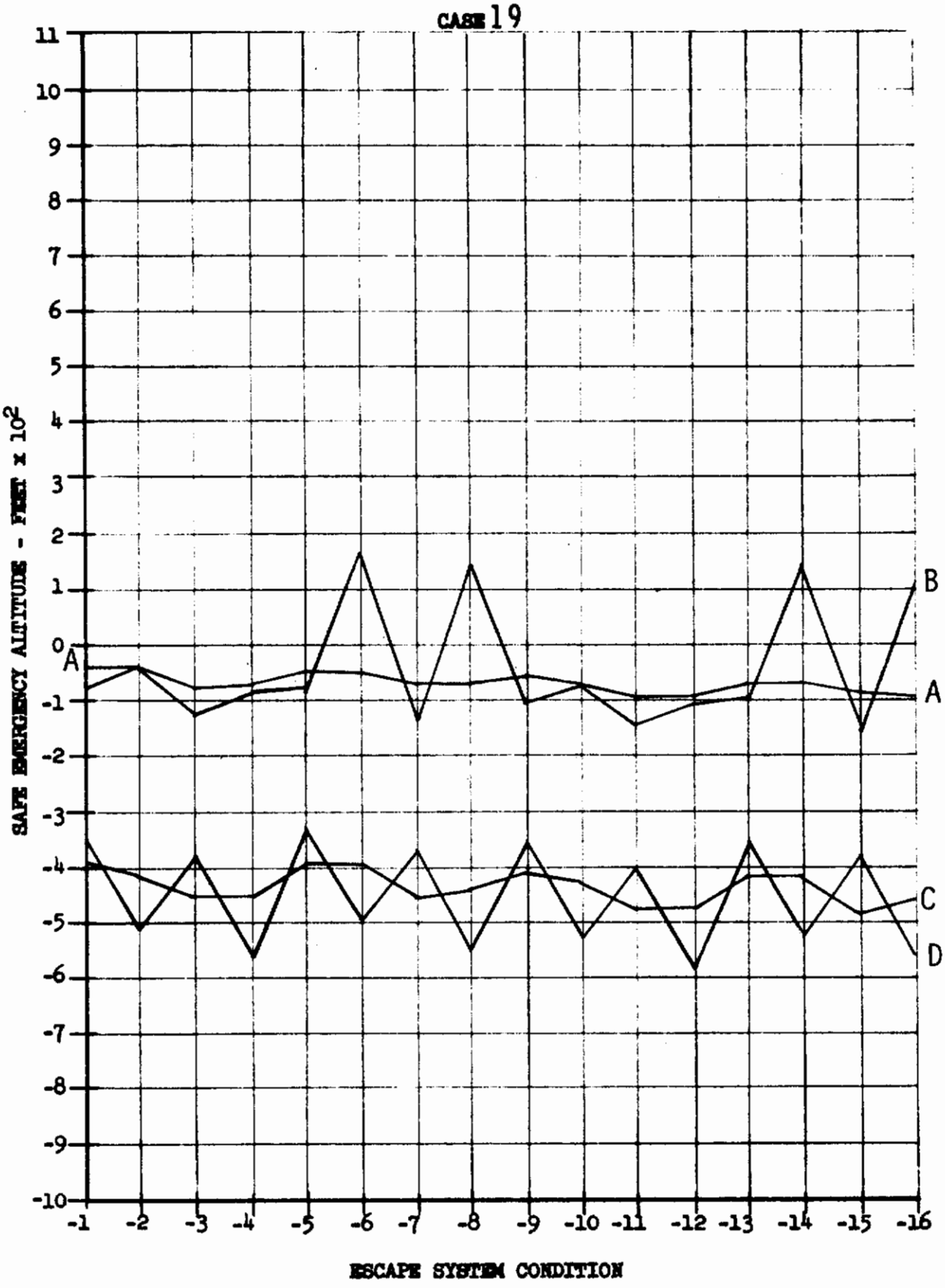

Approved for Public Release

Contrails

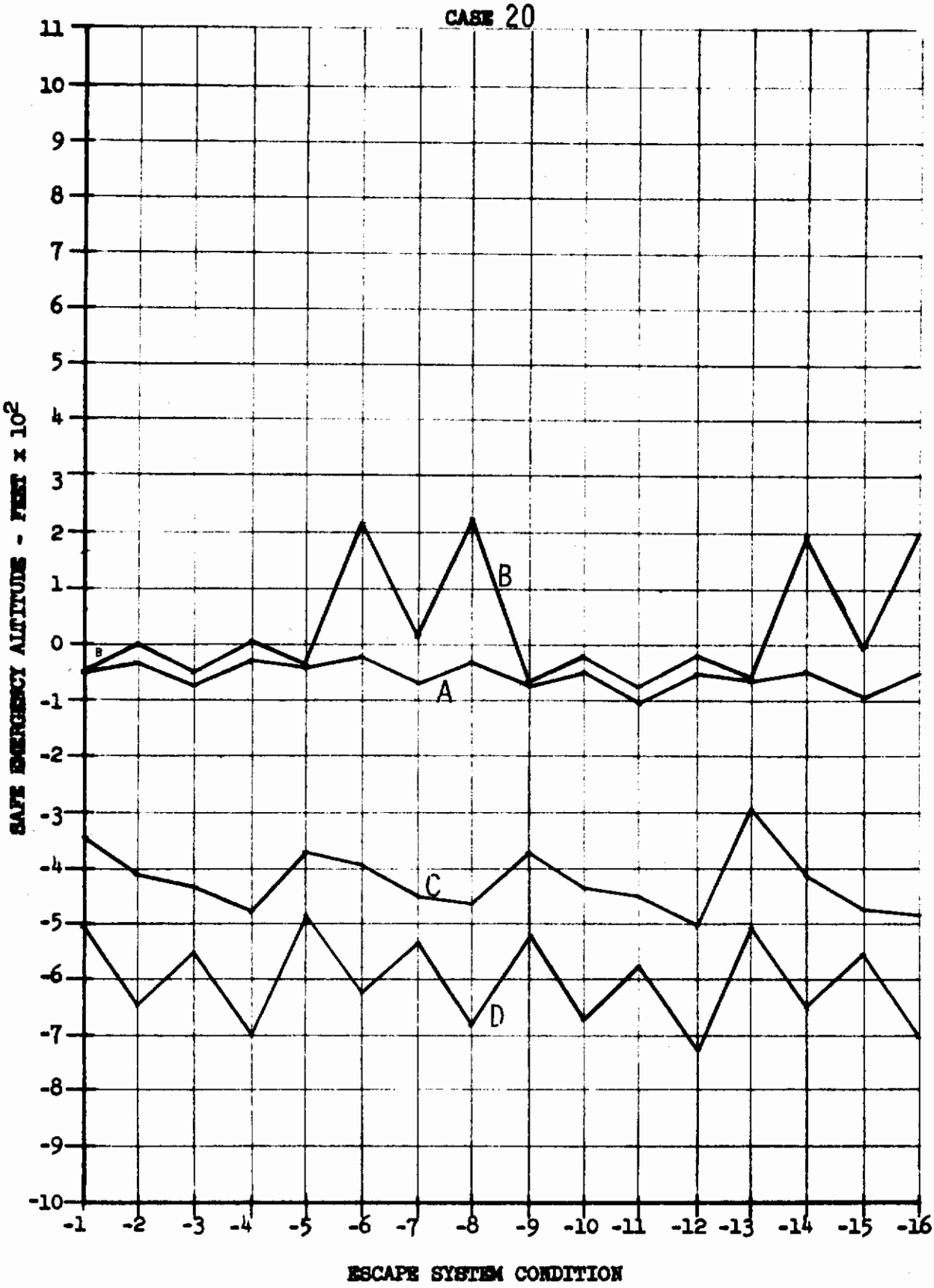

Approved for Public Release

Contrails

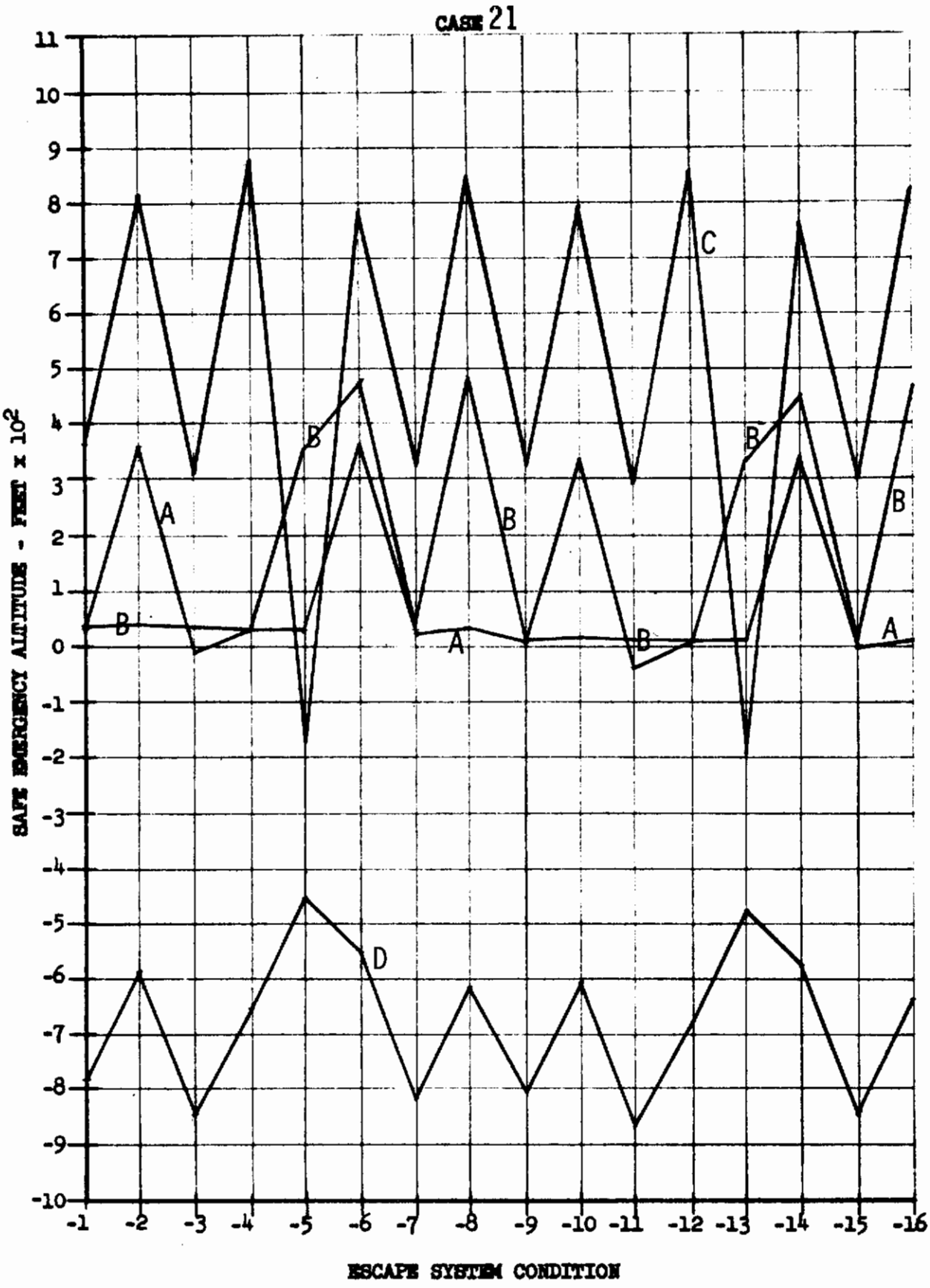

Approved for Public Release

Contrails

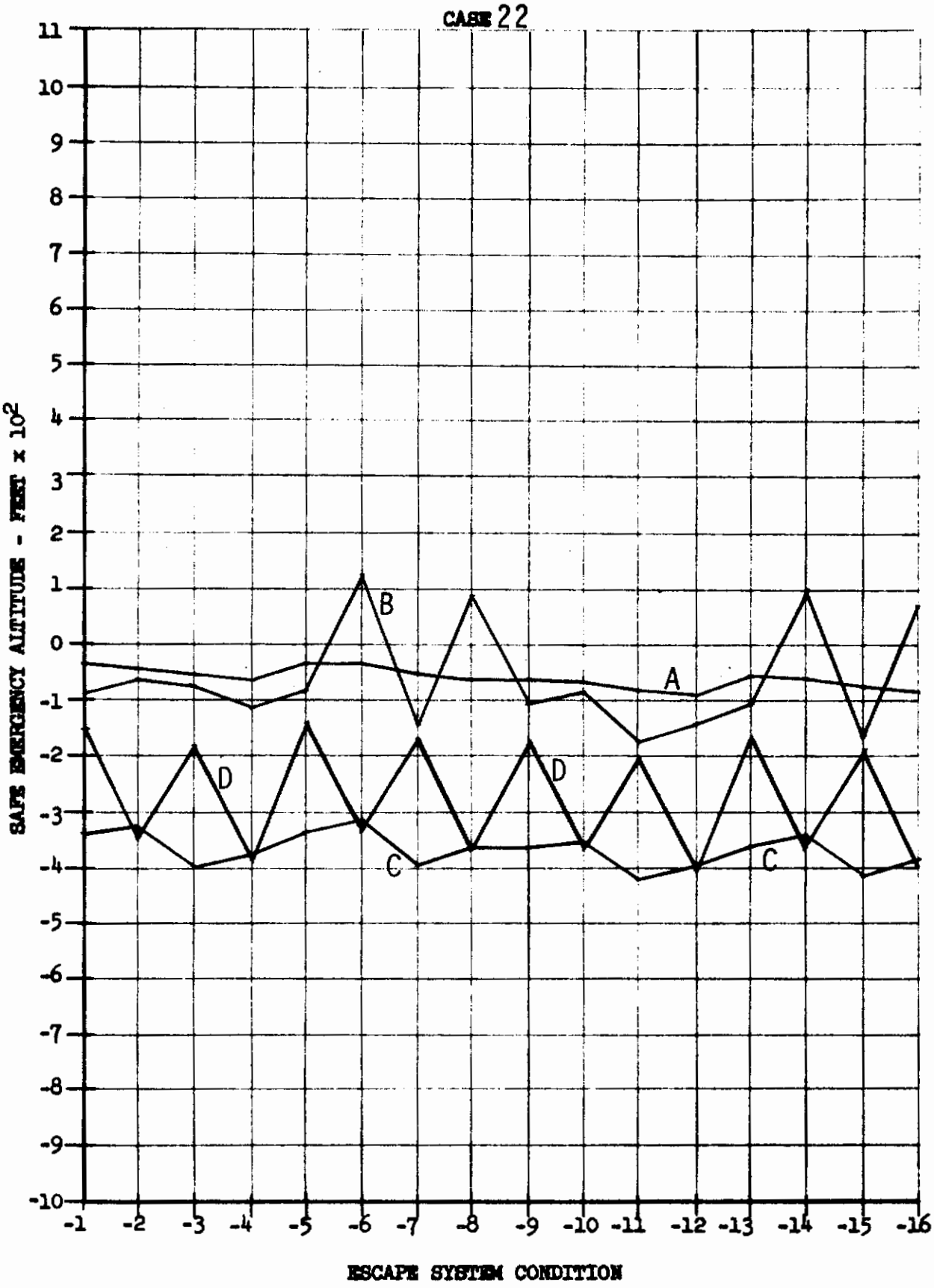

Approved for Public Release

Contrails

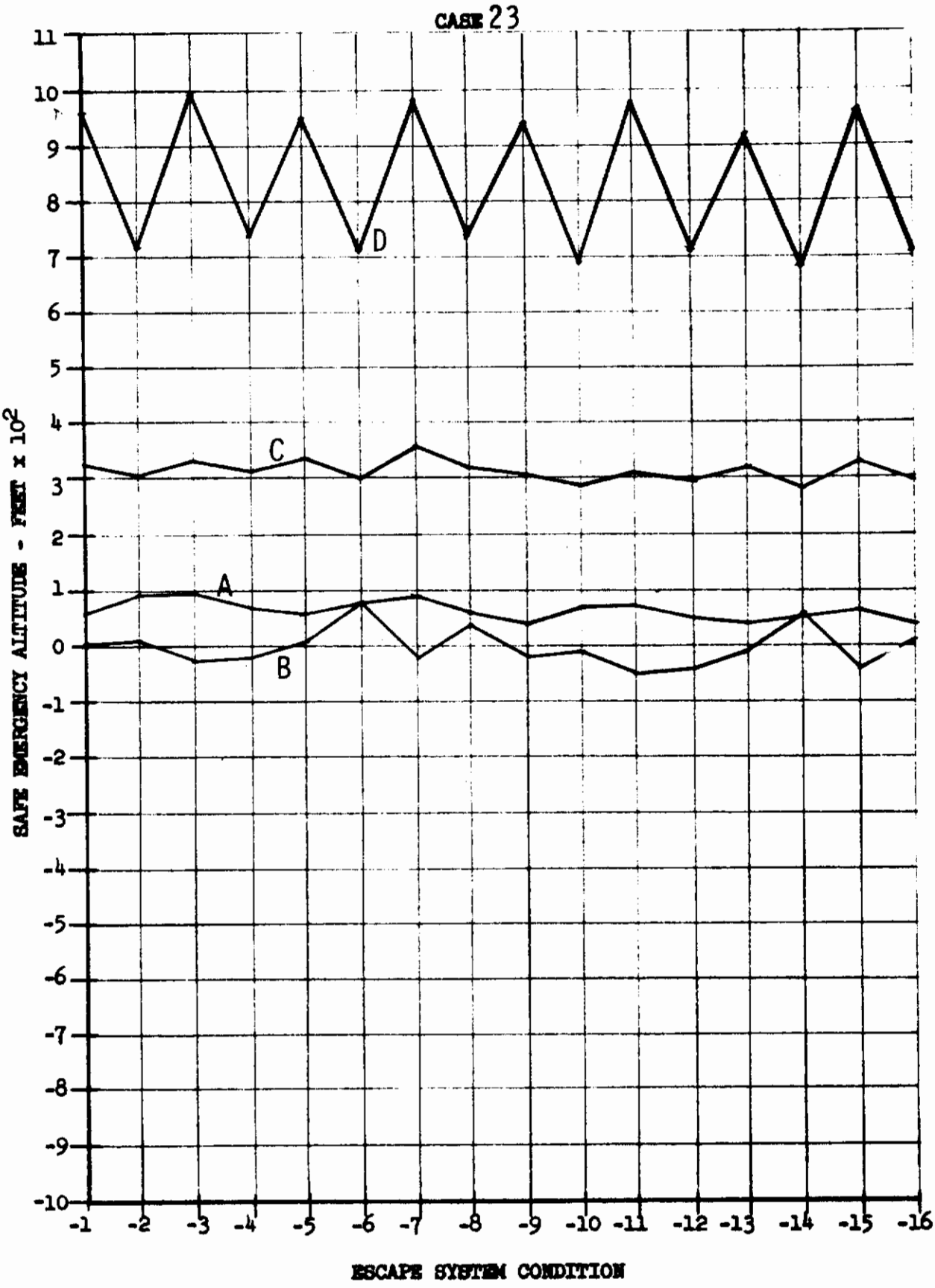

Approved for Public Release

Contrails

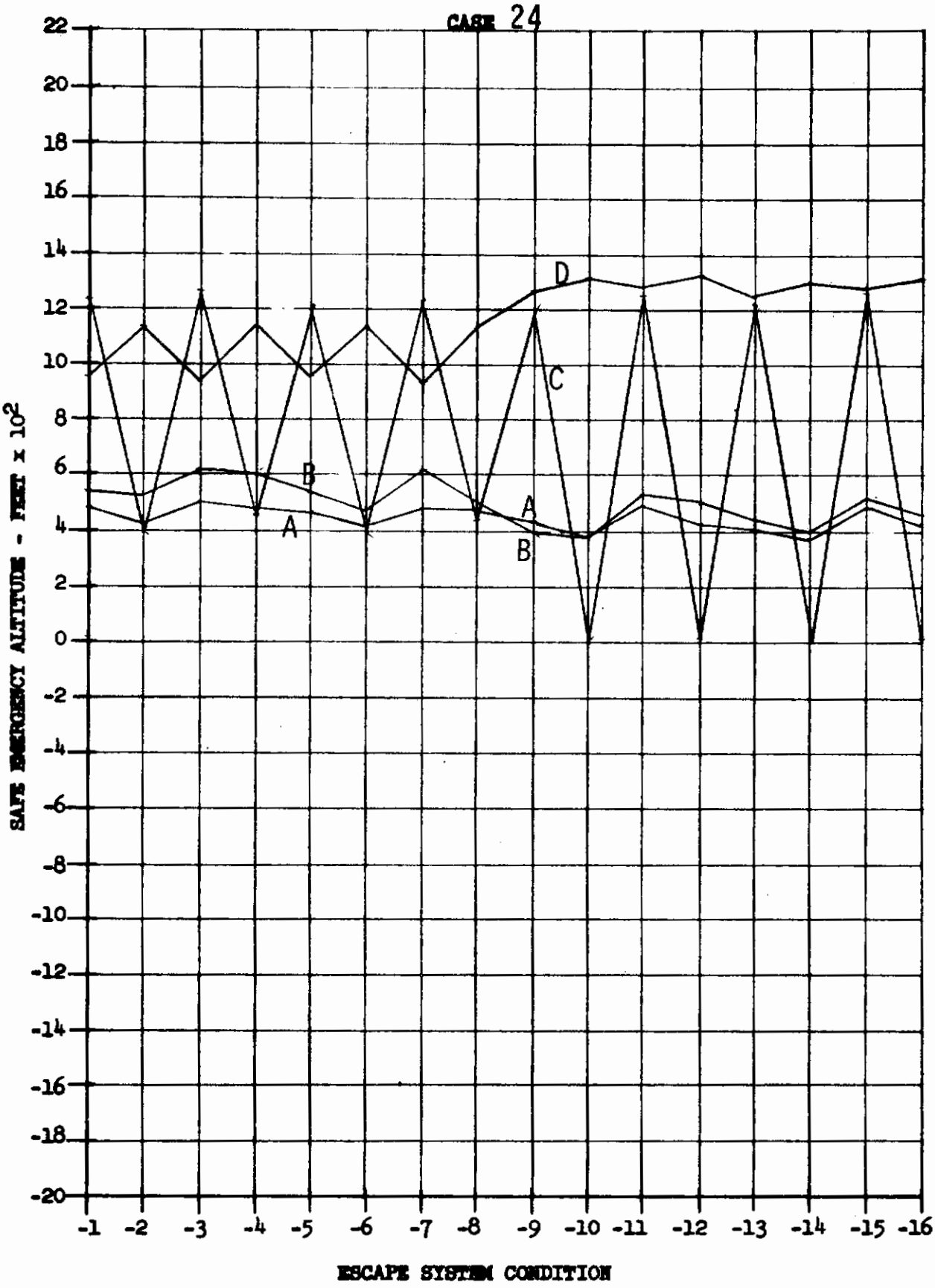

Approved for Public Release

Contrails

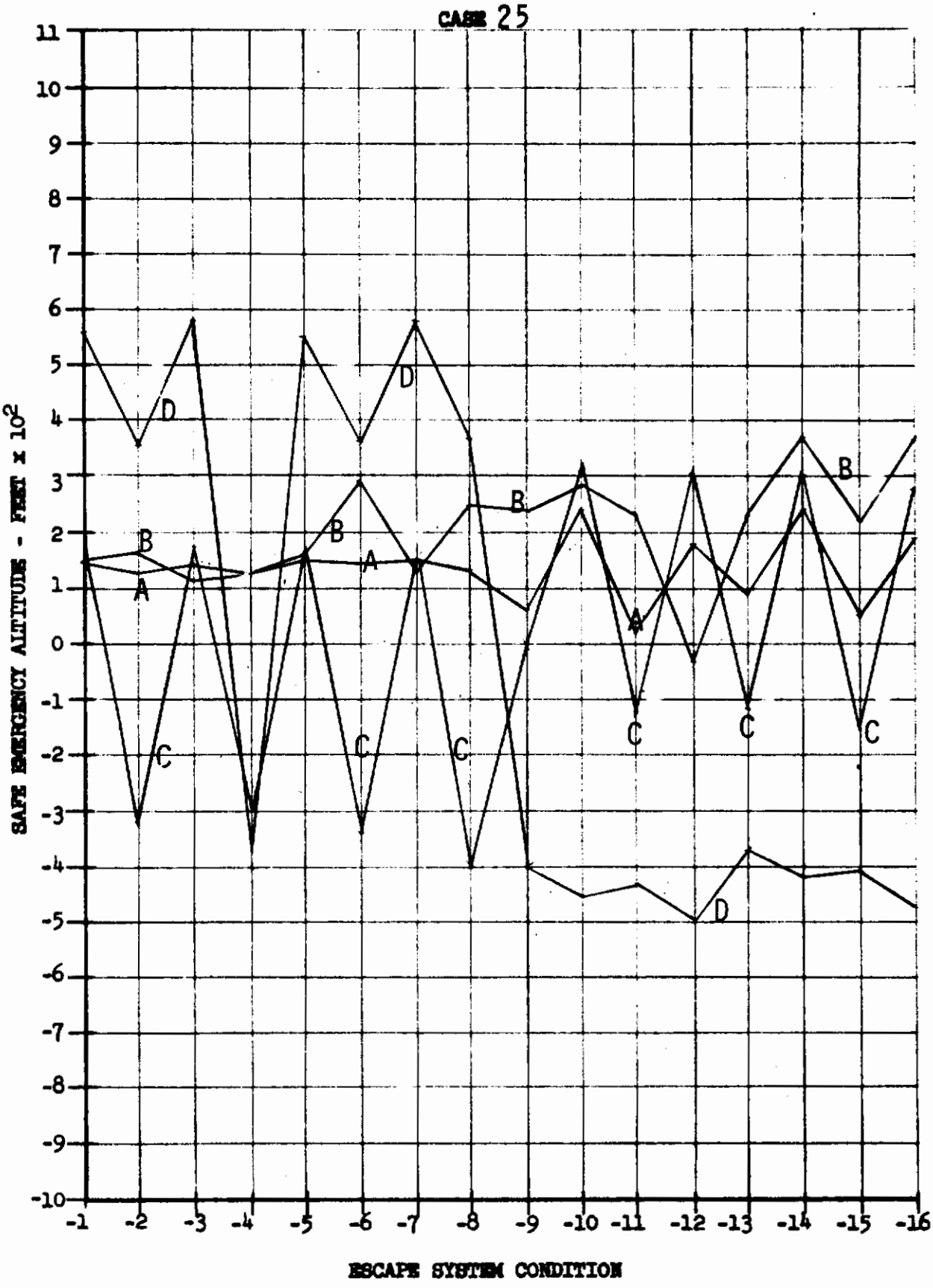

Approved for Public Release

Contrails

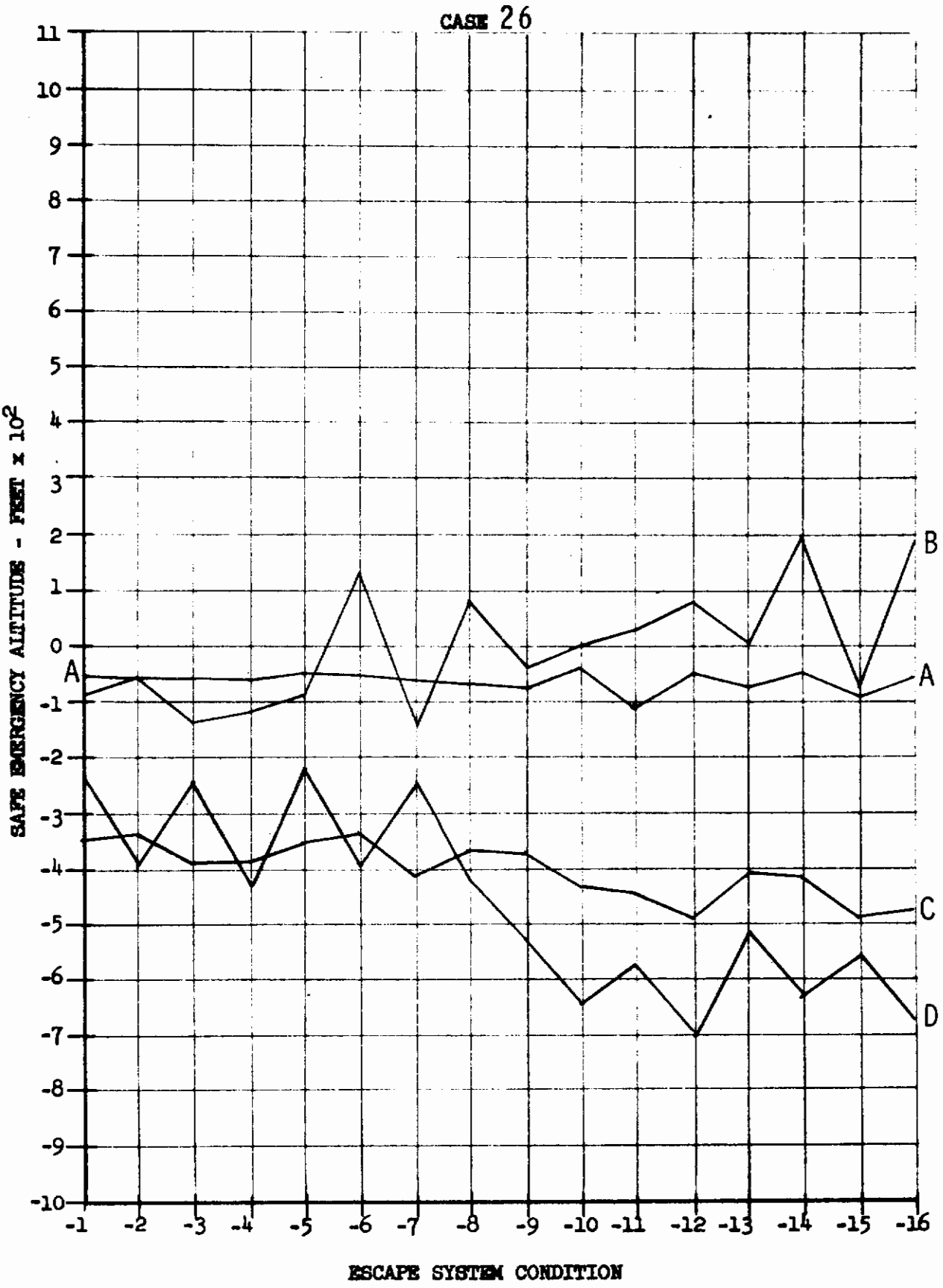

Approved for Public Release

Contrails

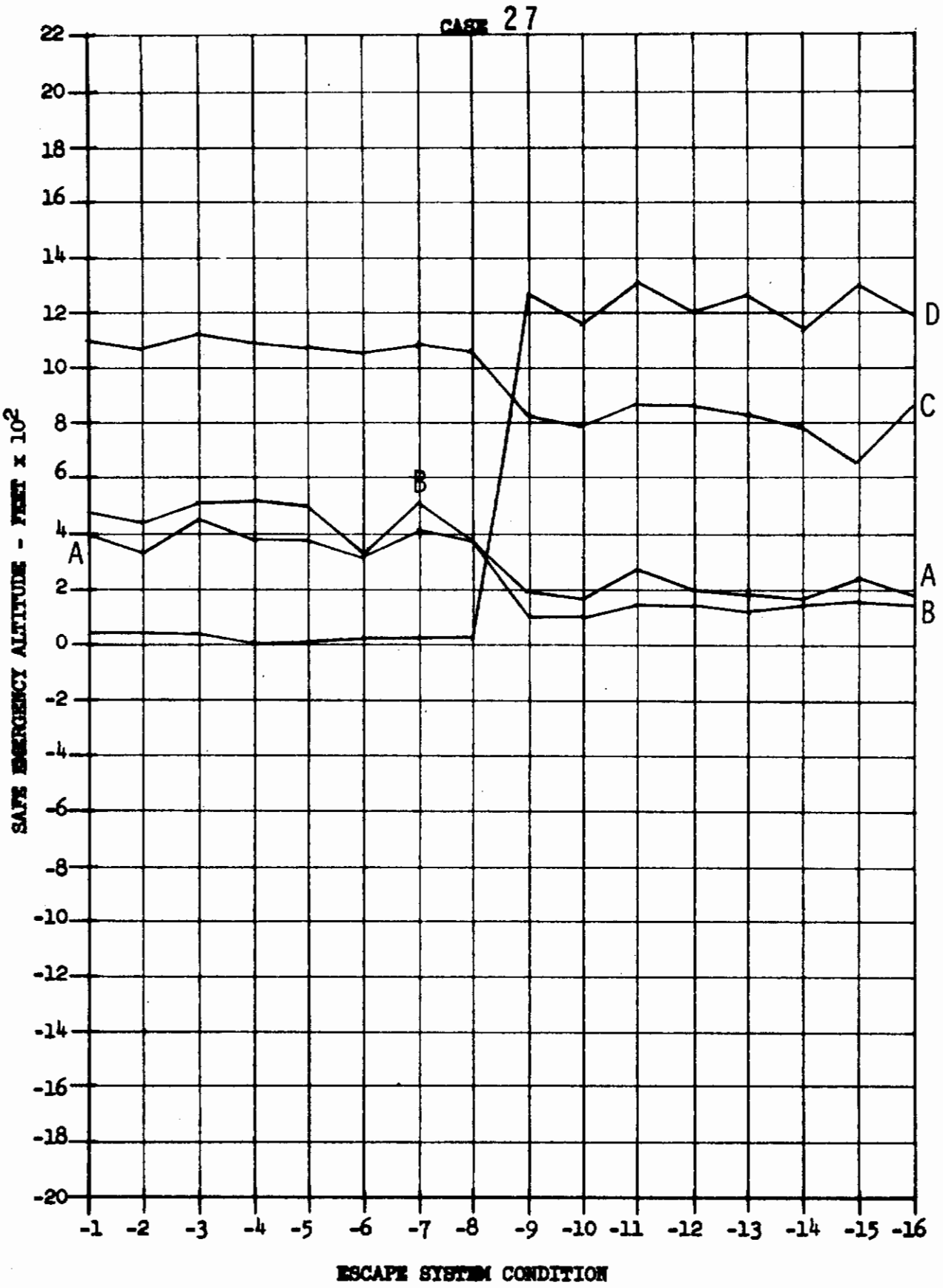

Approved for Public Release

Contrails

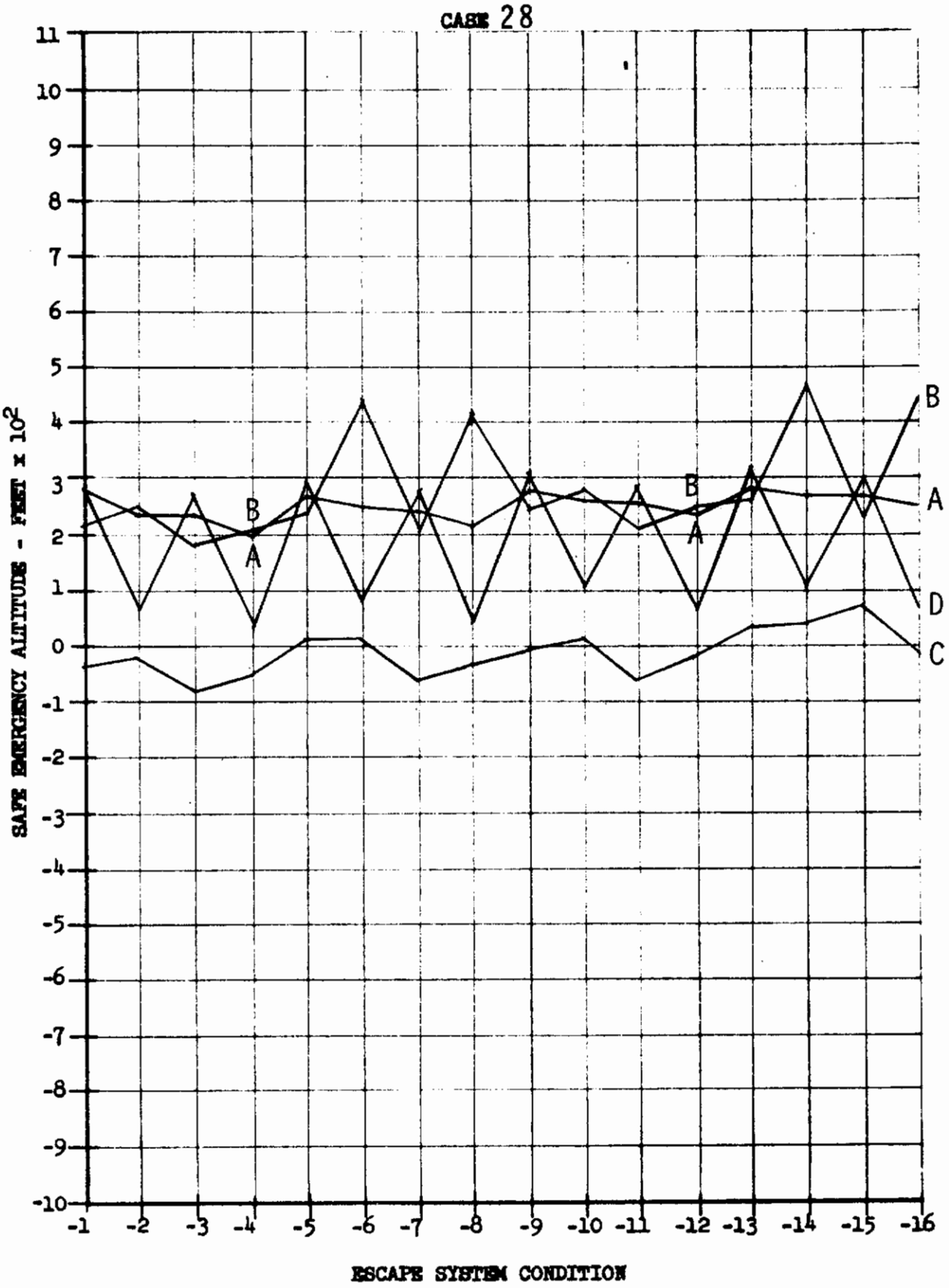

Approved for Public Release

Contrails

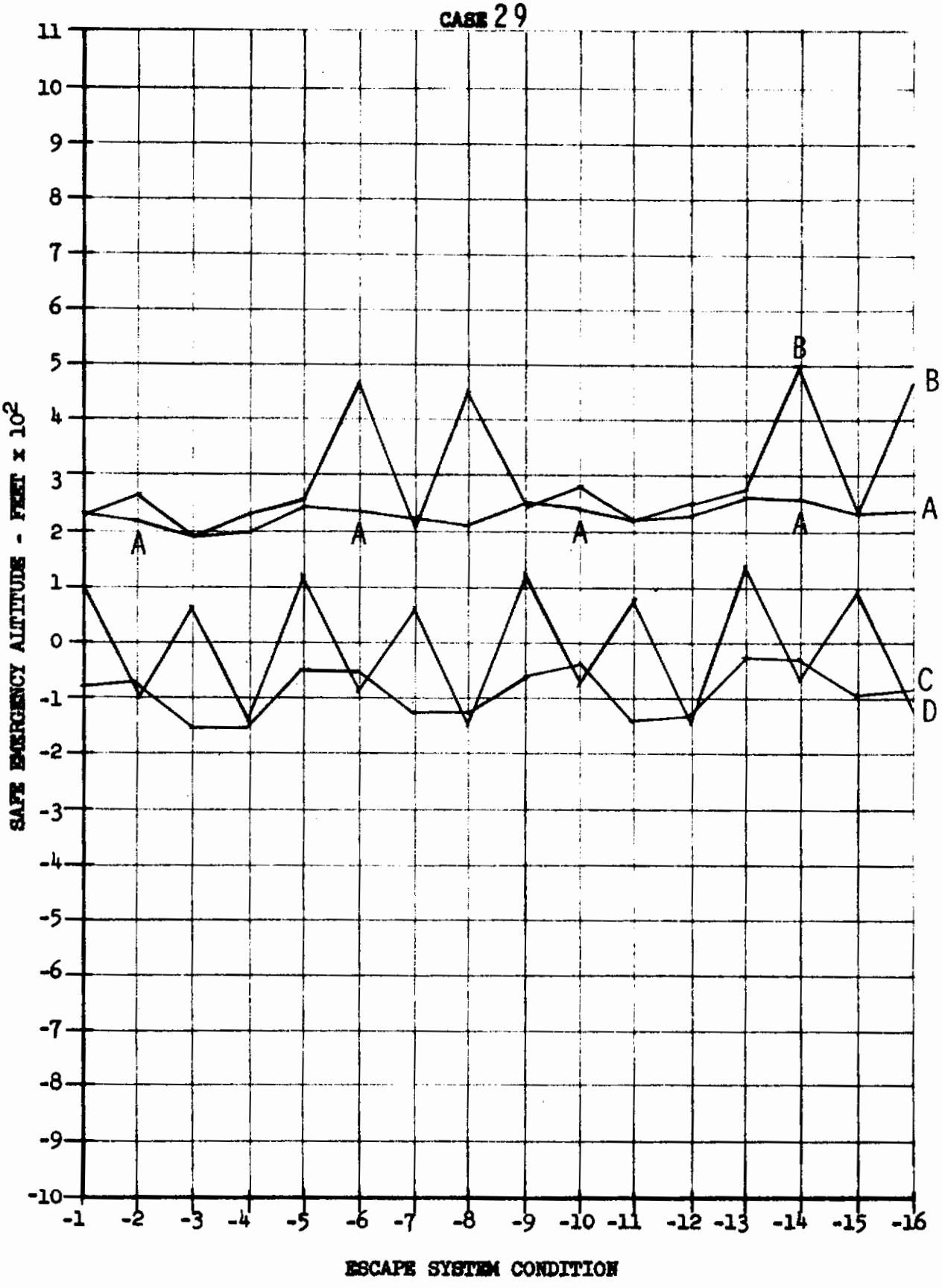

Approved for Public Release

Contrails

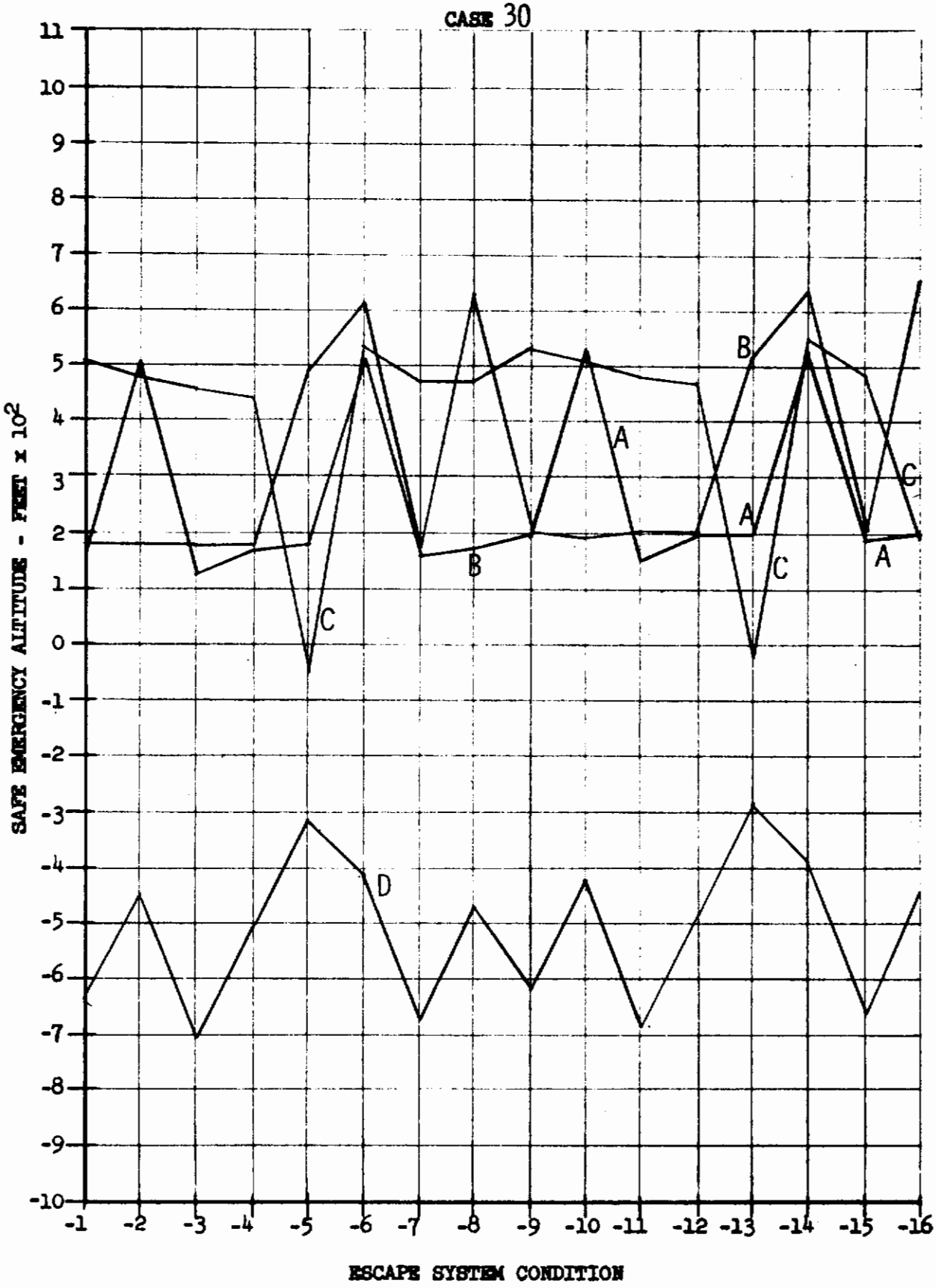

Approved for Public Release

Contrails

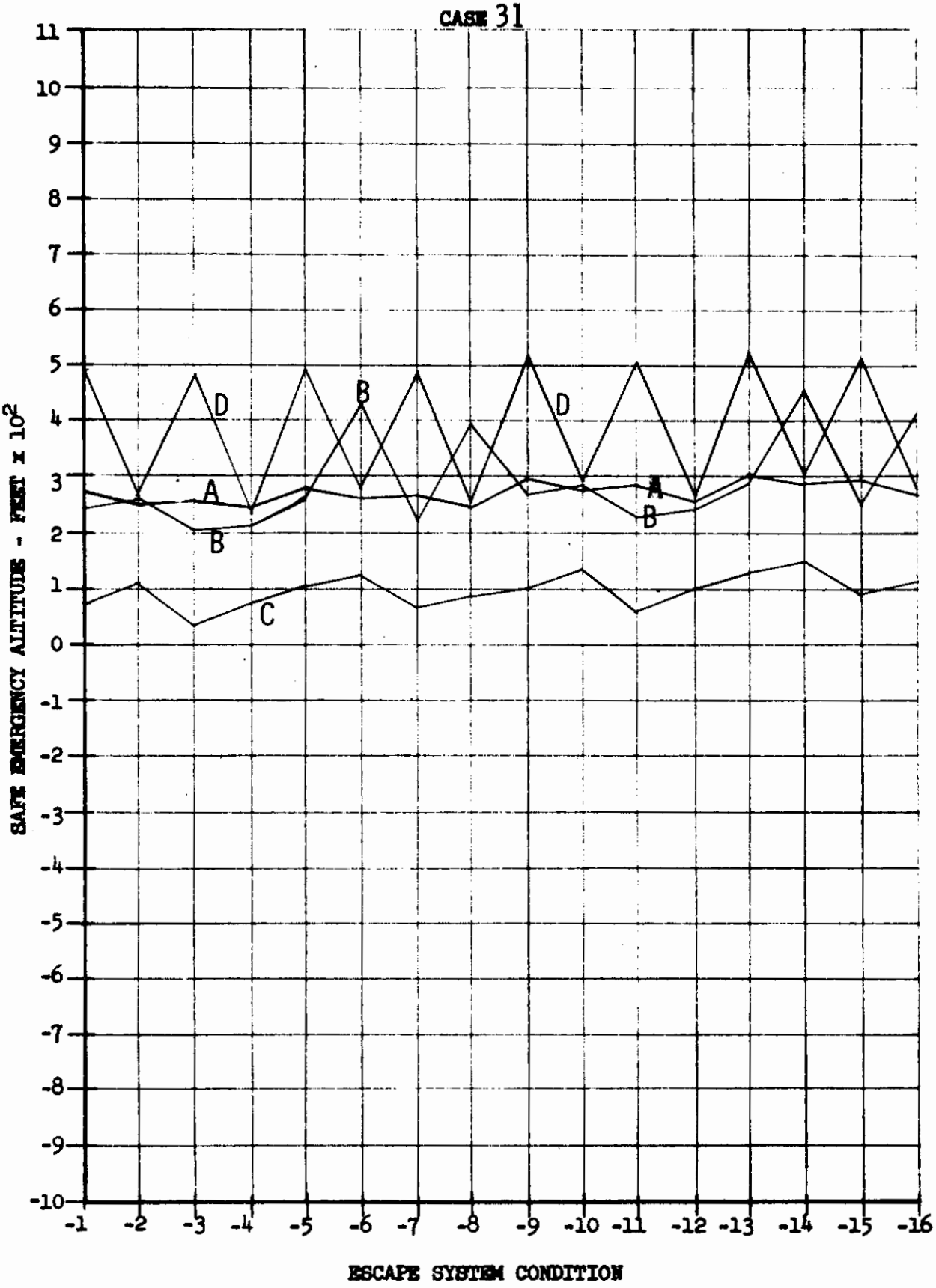

Approved for Public Release

Contrails

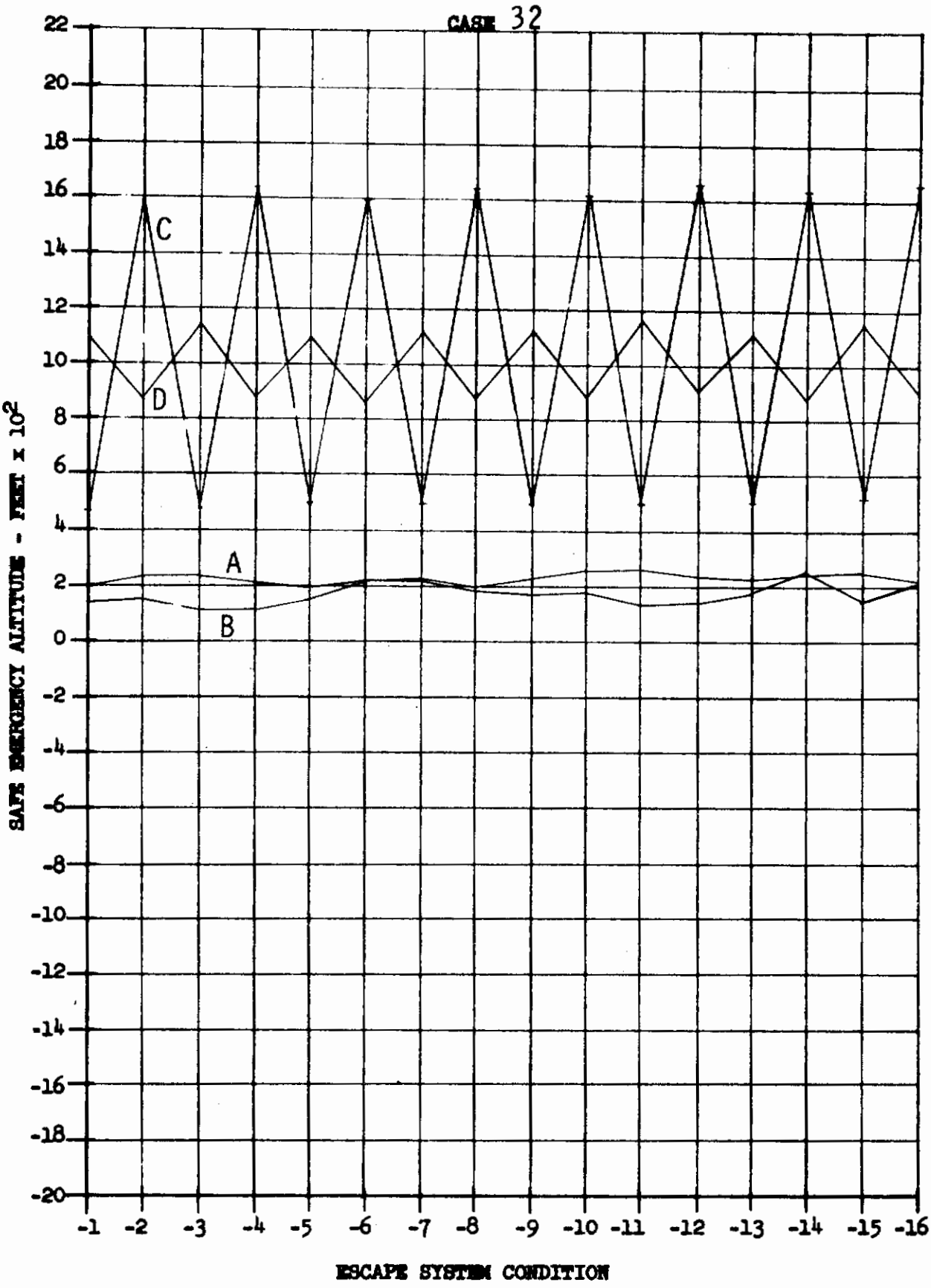

Approved for Public Release

Contrails

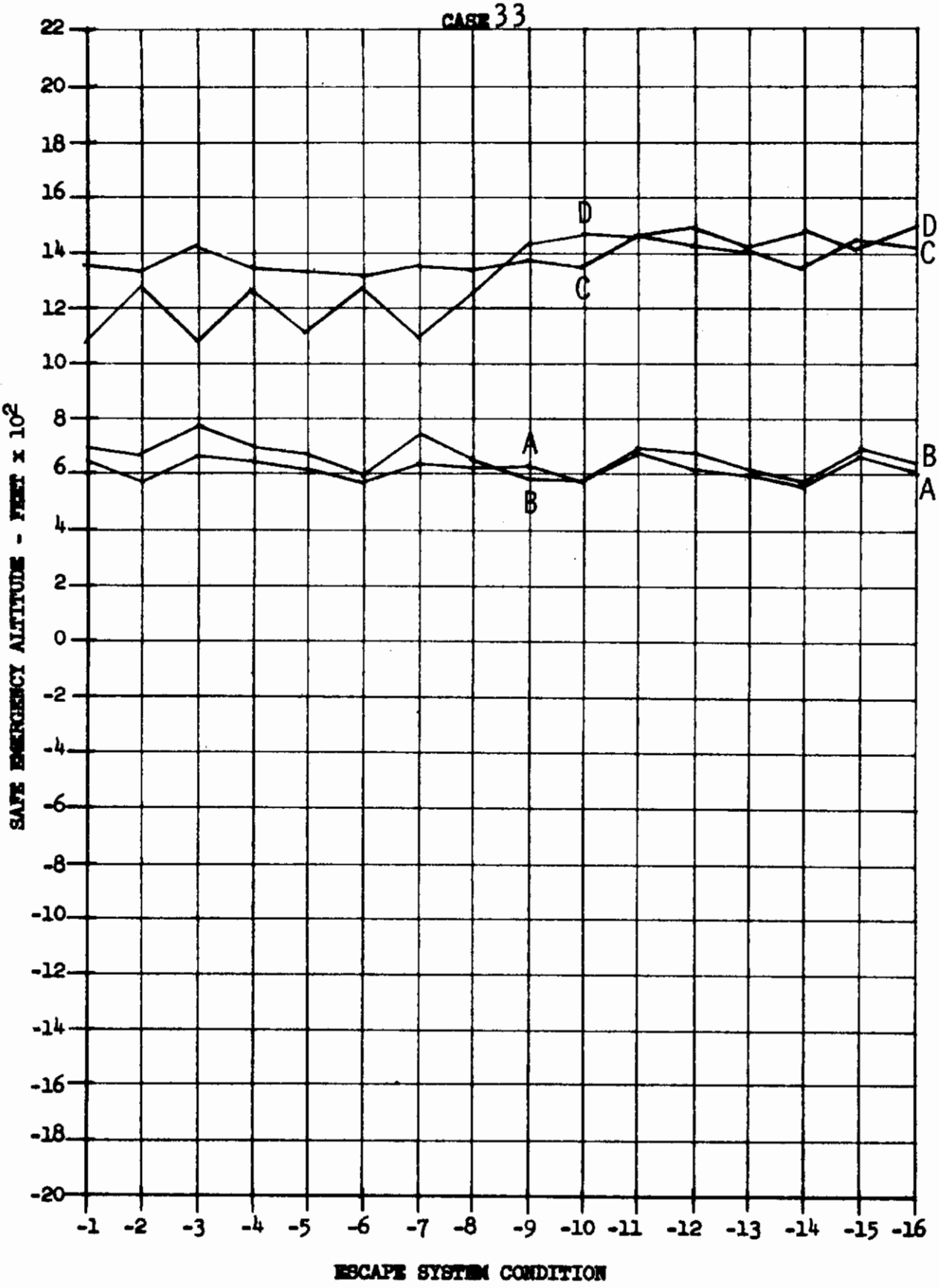

Approved for Public Release

Contrails

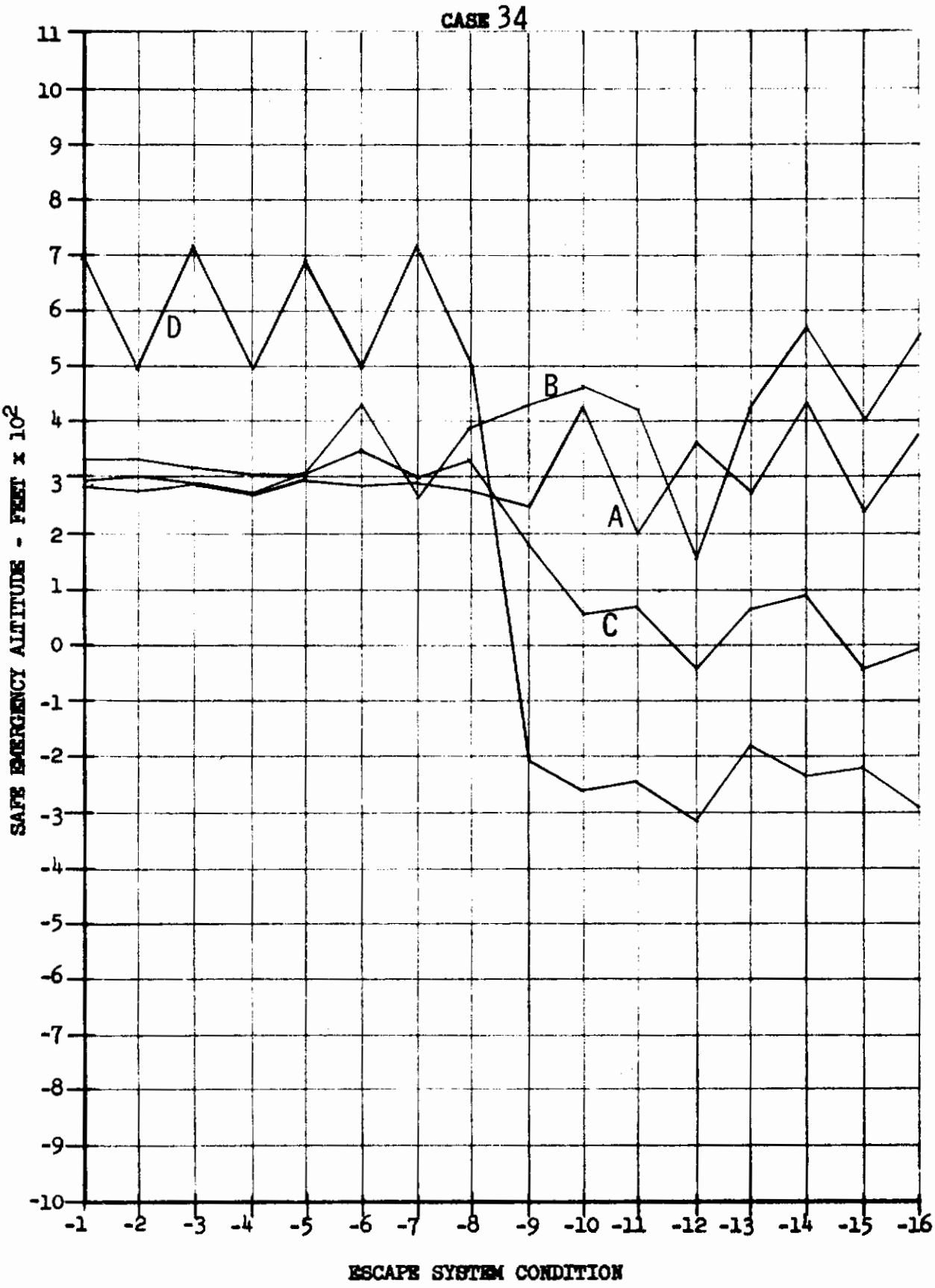

Approved for Public Release

Contrails

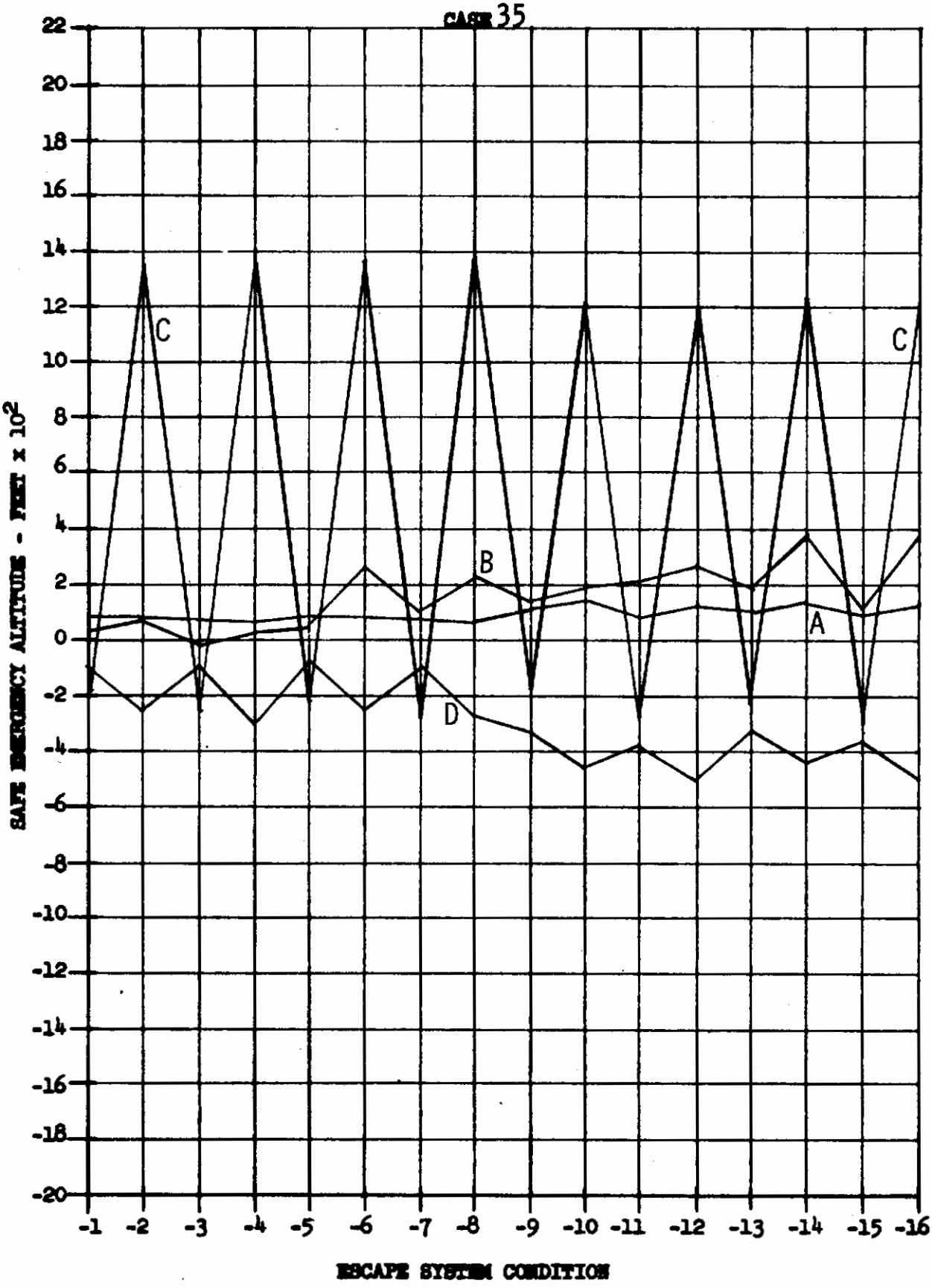

Approved for Public Release

Contrails

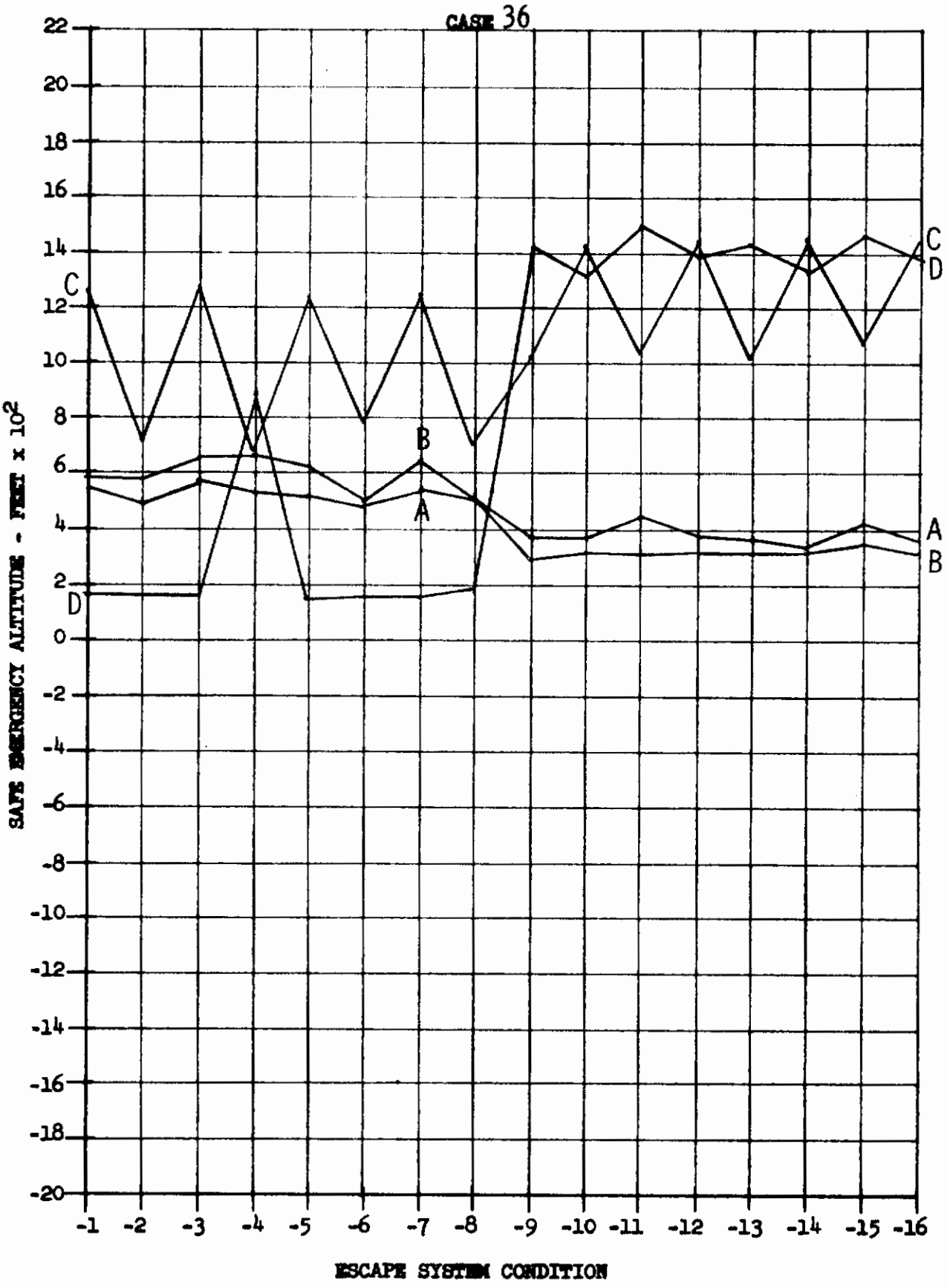

Approved for Public Release

Contrails

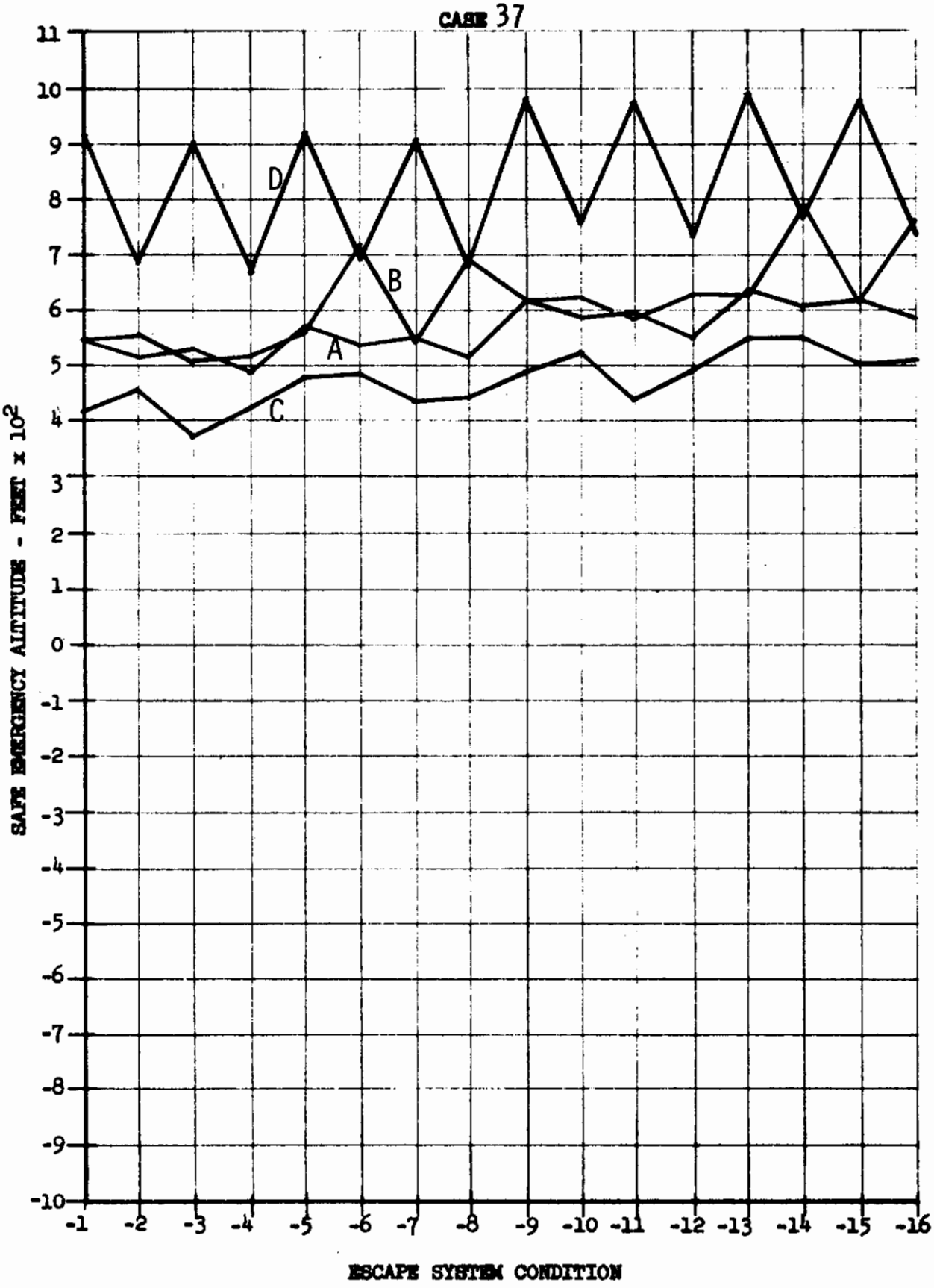

Approved for Public Release

Contrails

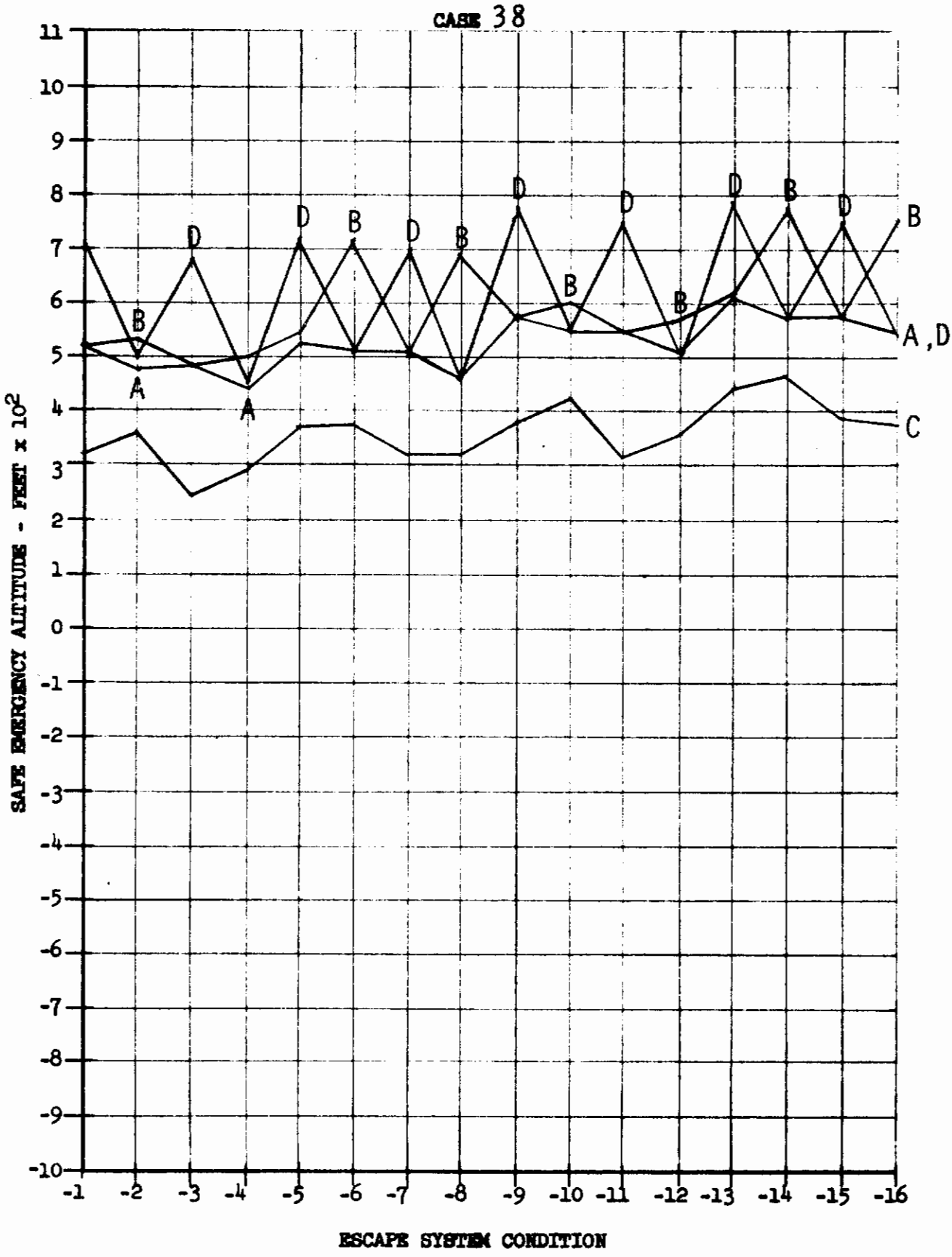

Approved for Public Release

Contrails

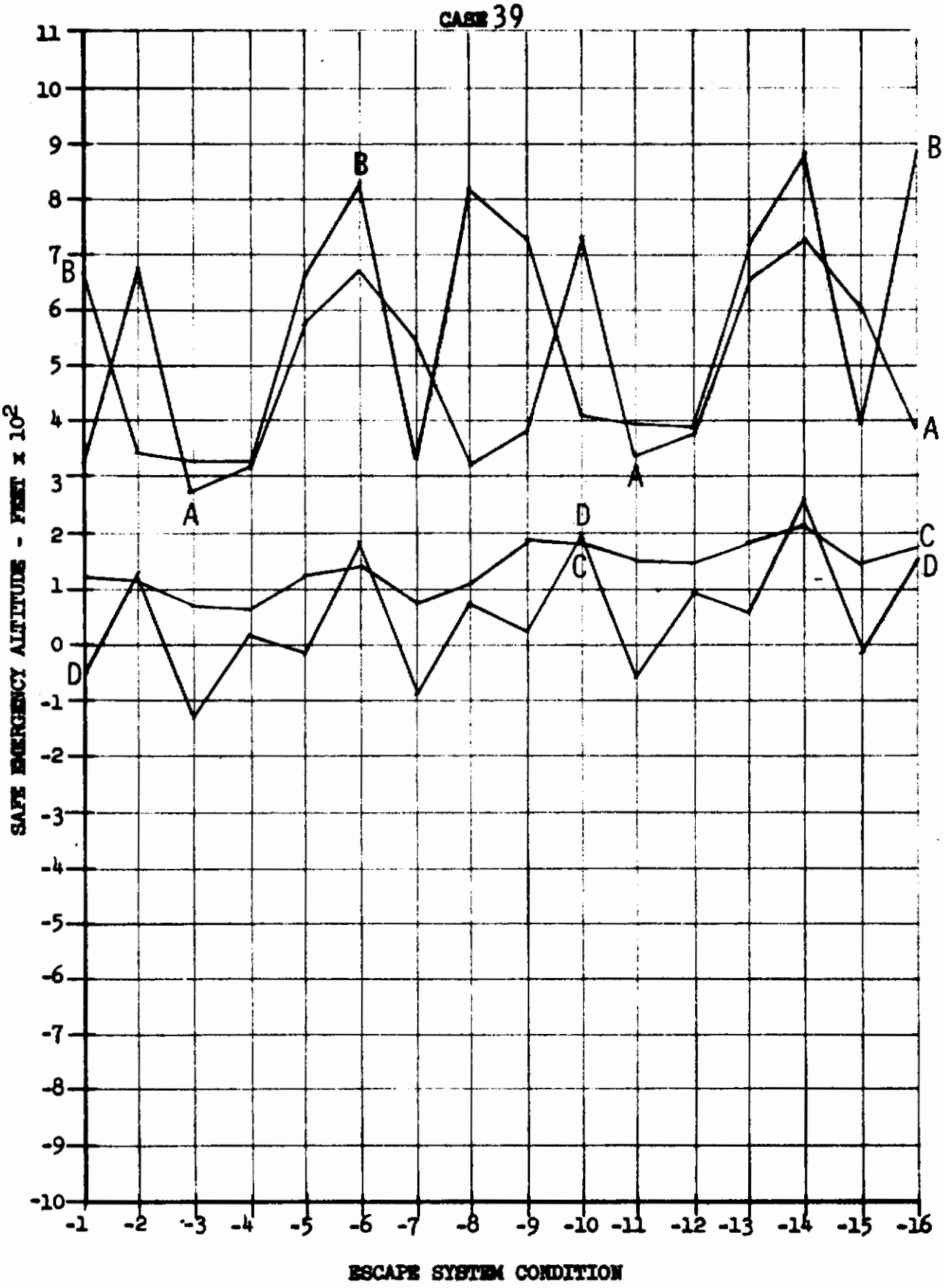

Approved for Public Release

Contrails

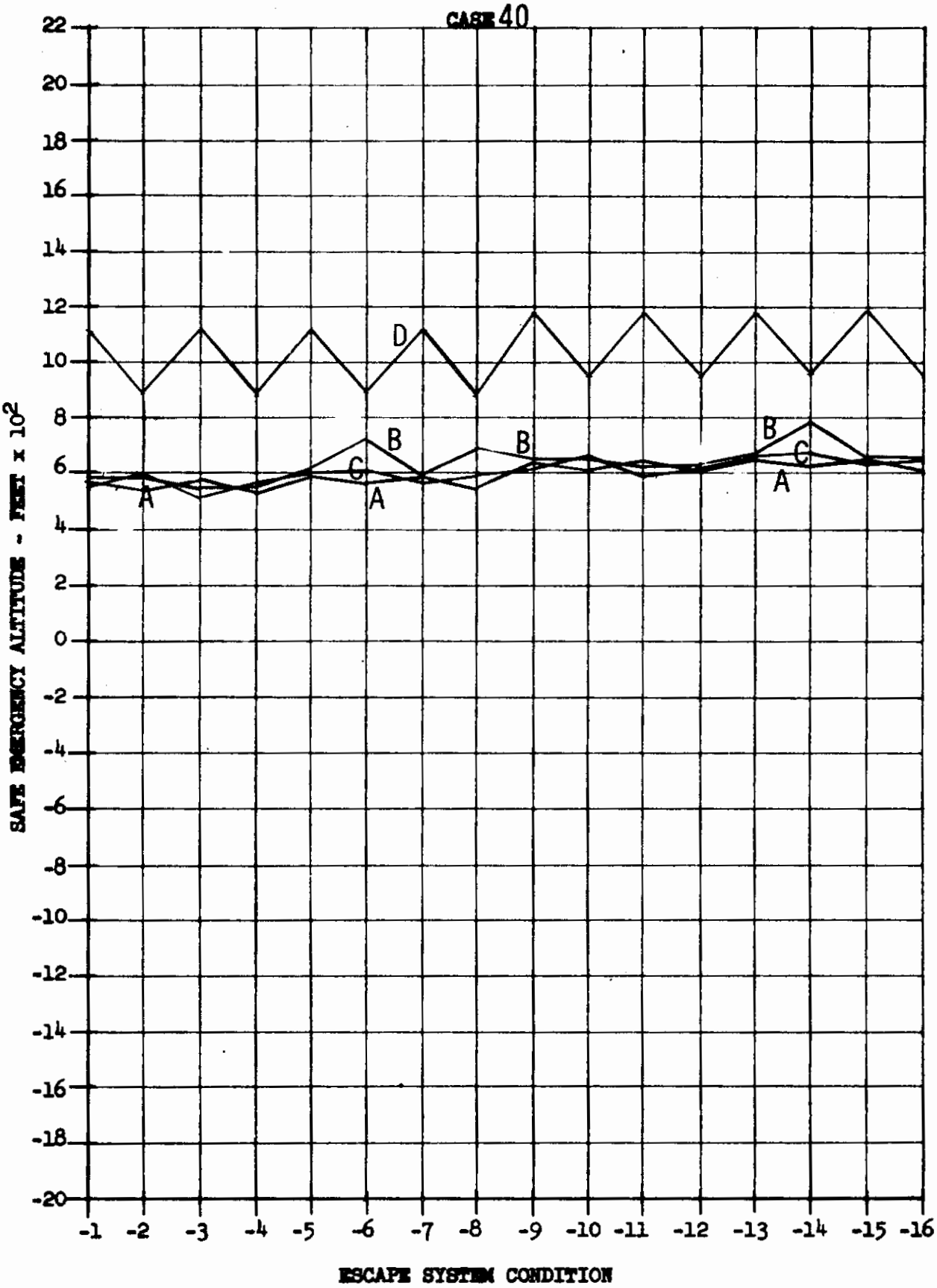

Approved for Public Release

Contrails

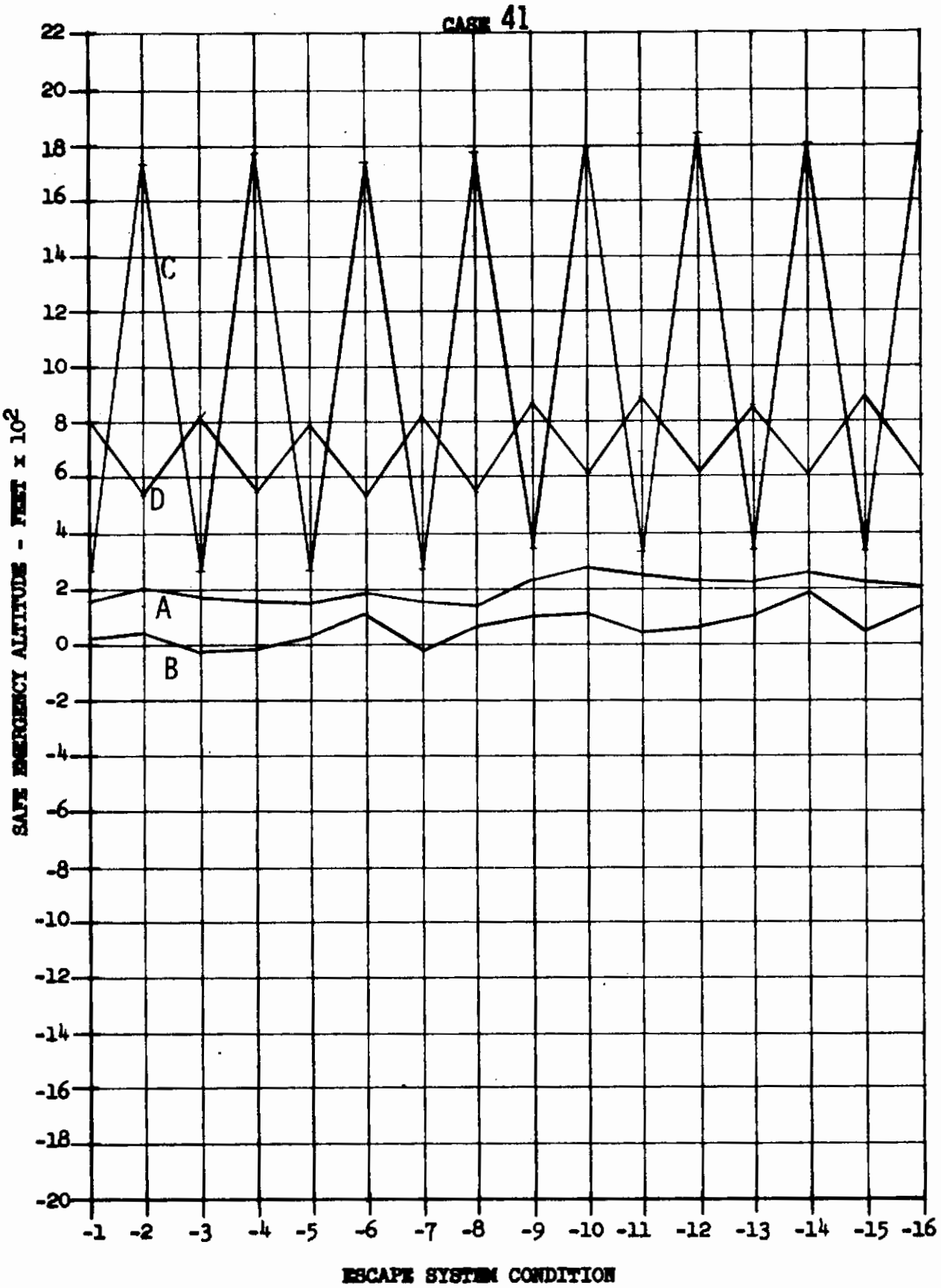

Approved for Public Release

Contrails

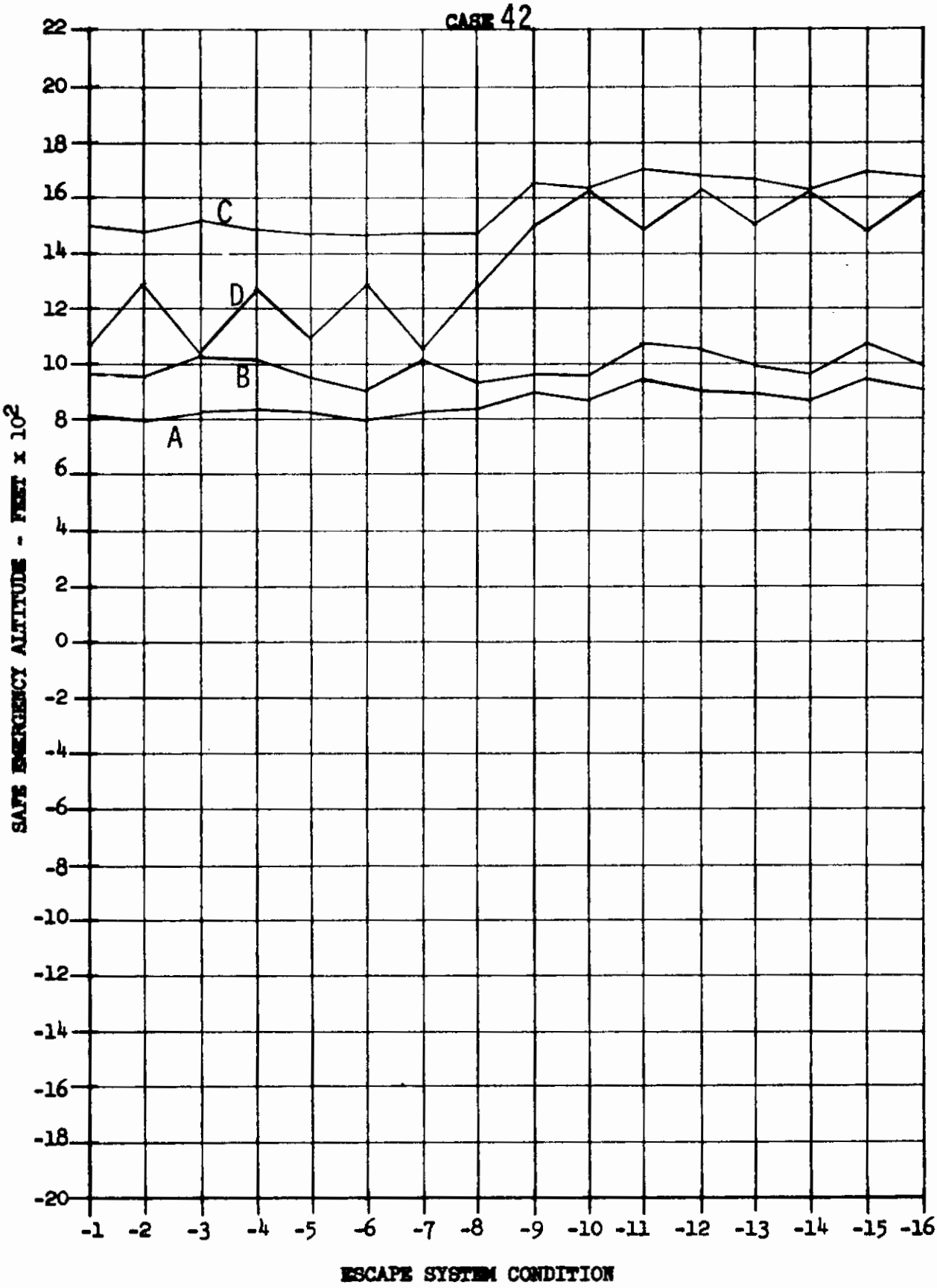

Approved for Public Release

Contrails

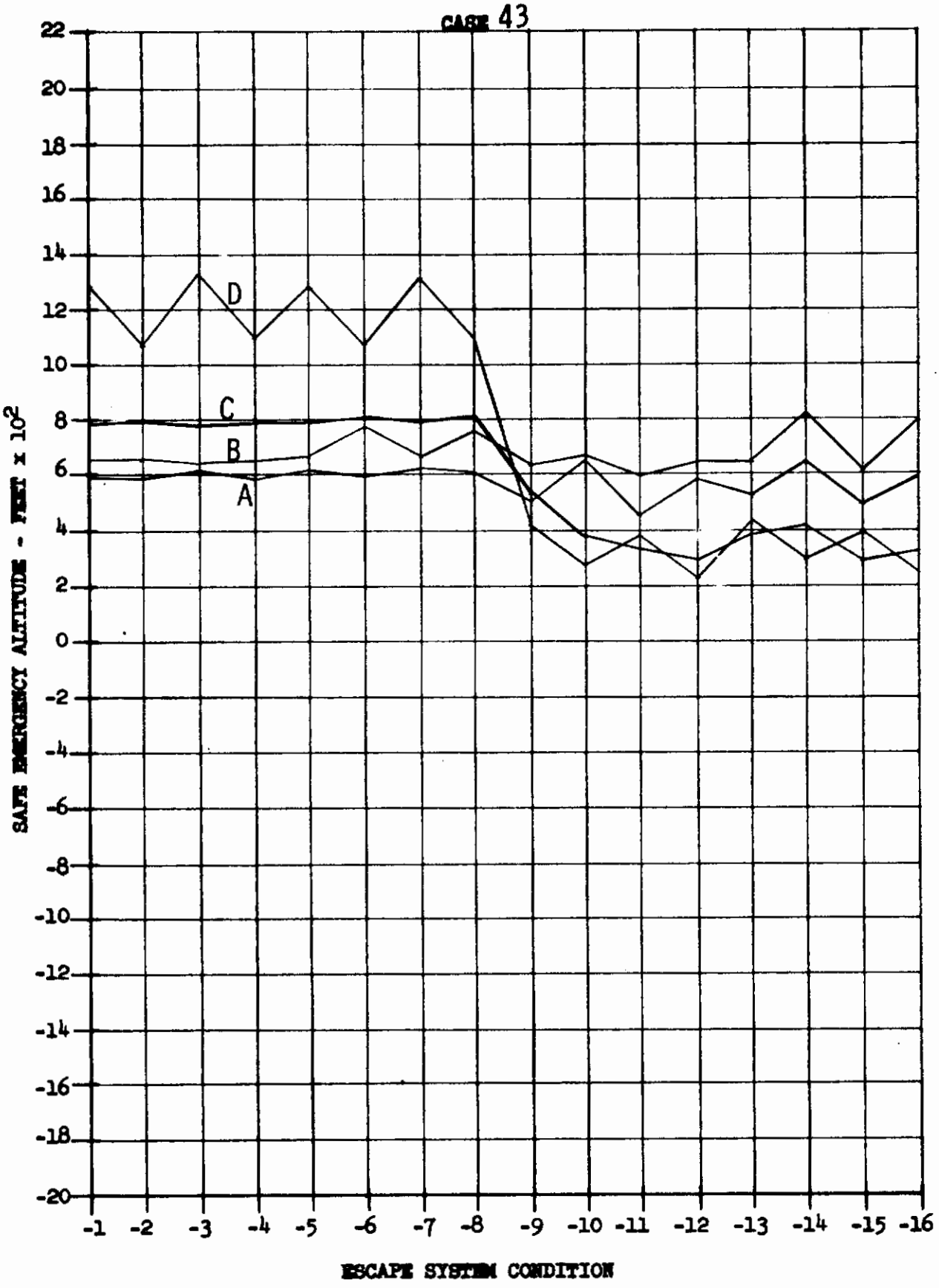

Approved for Public Release

Contrails

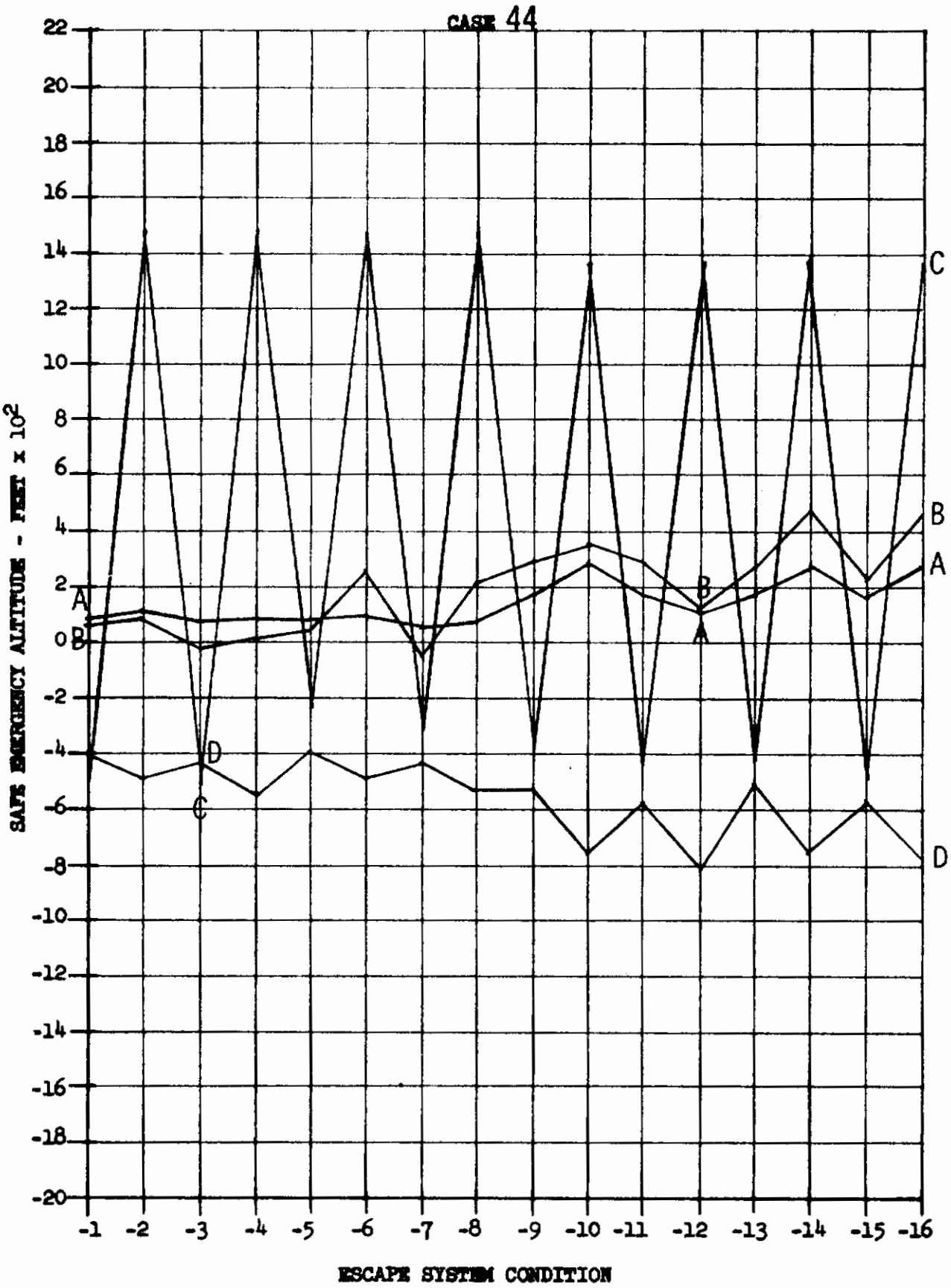

Approved for Public Release

Contrails

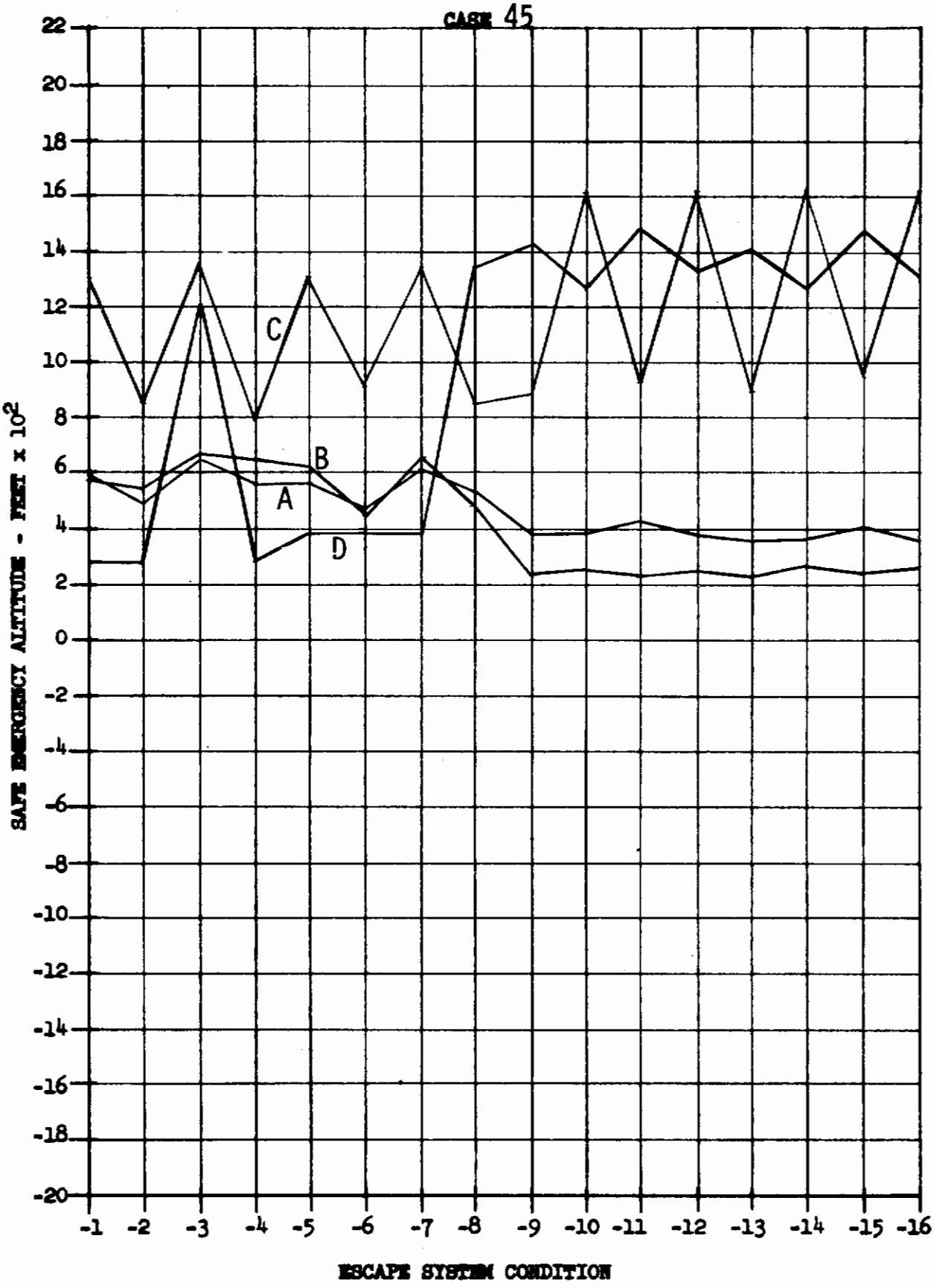

Approved for Public Release

Contrails

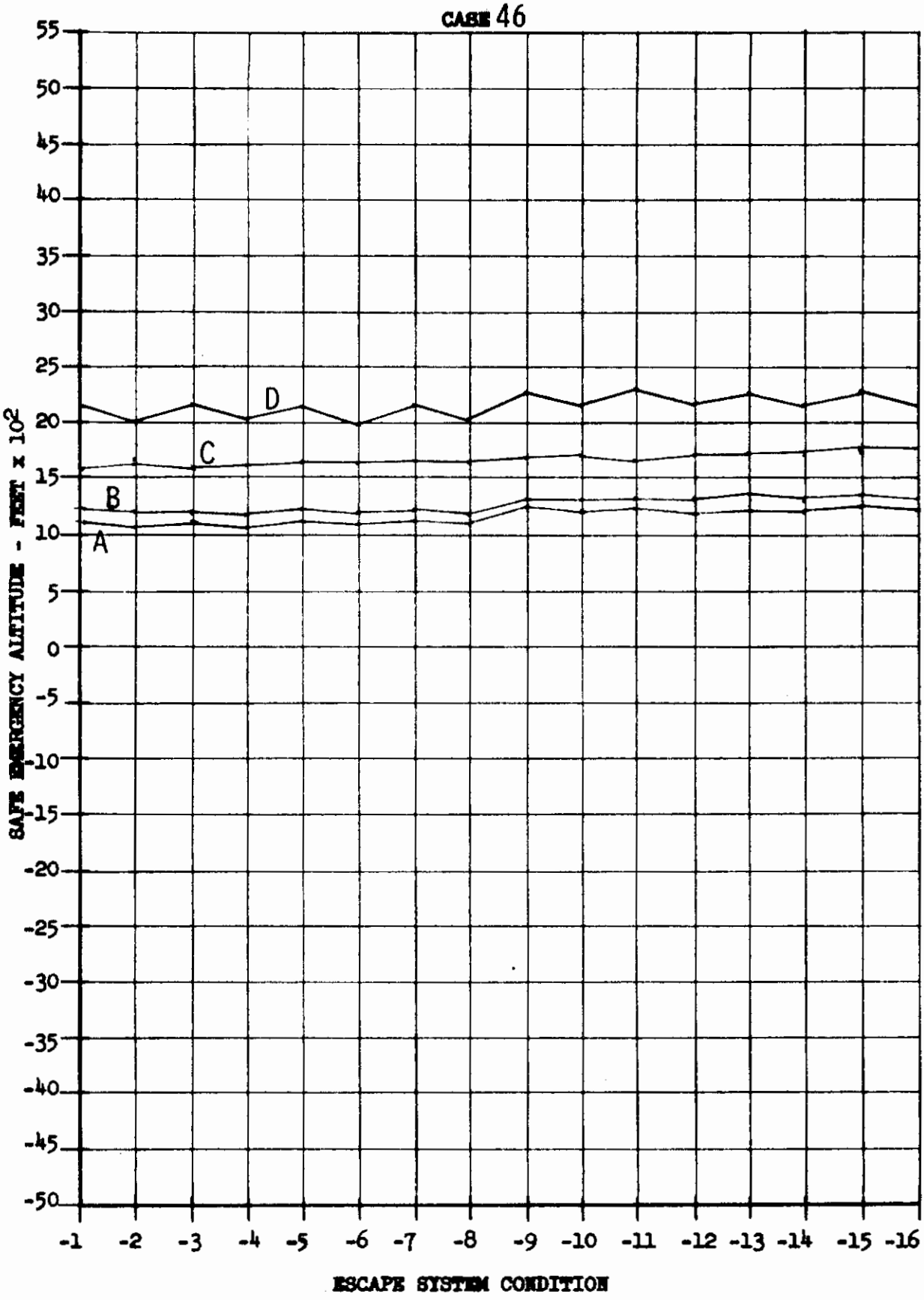

Approved for Public Release

Contrails

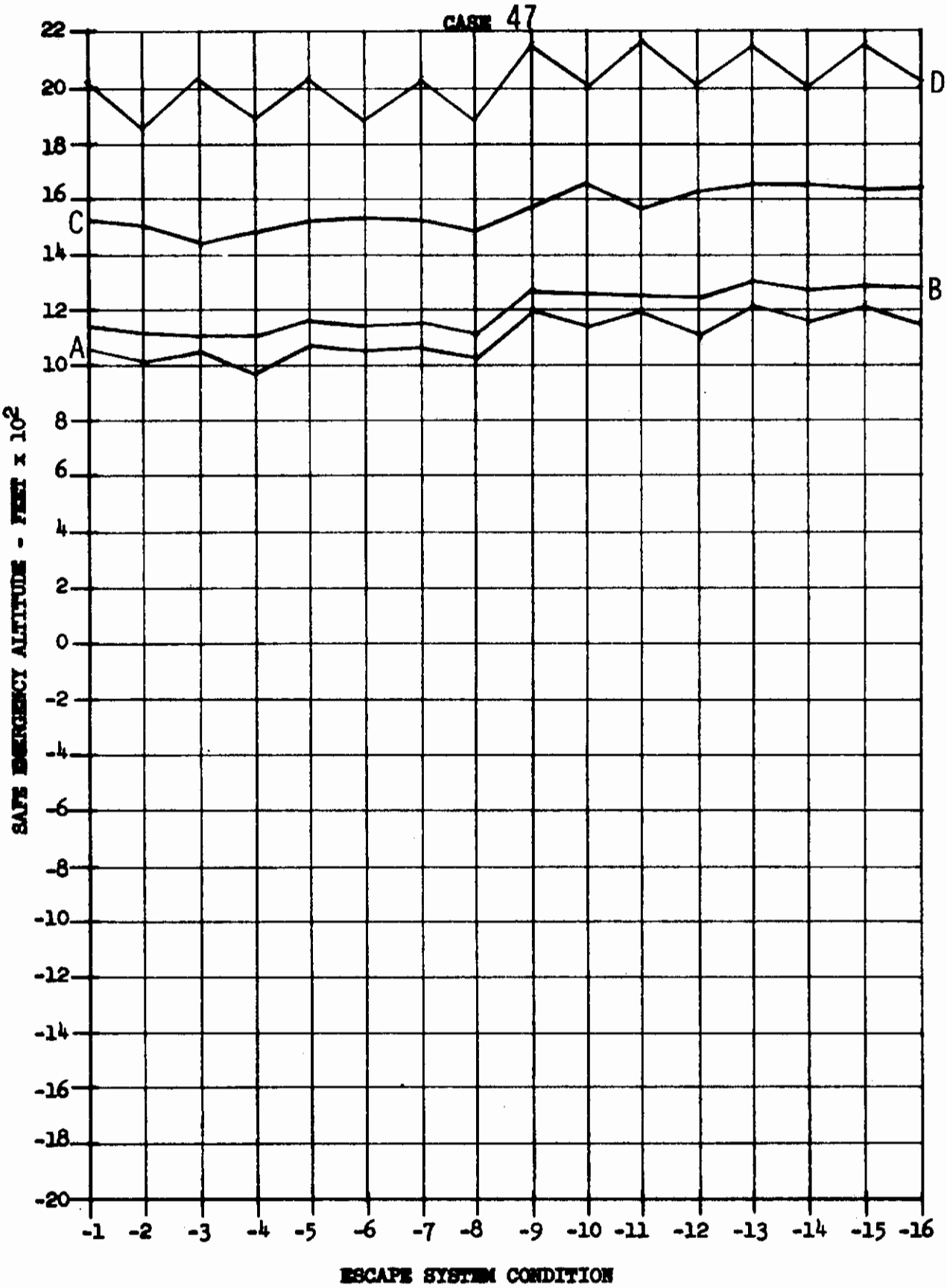

Approved for Public Release

Contrails

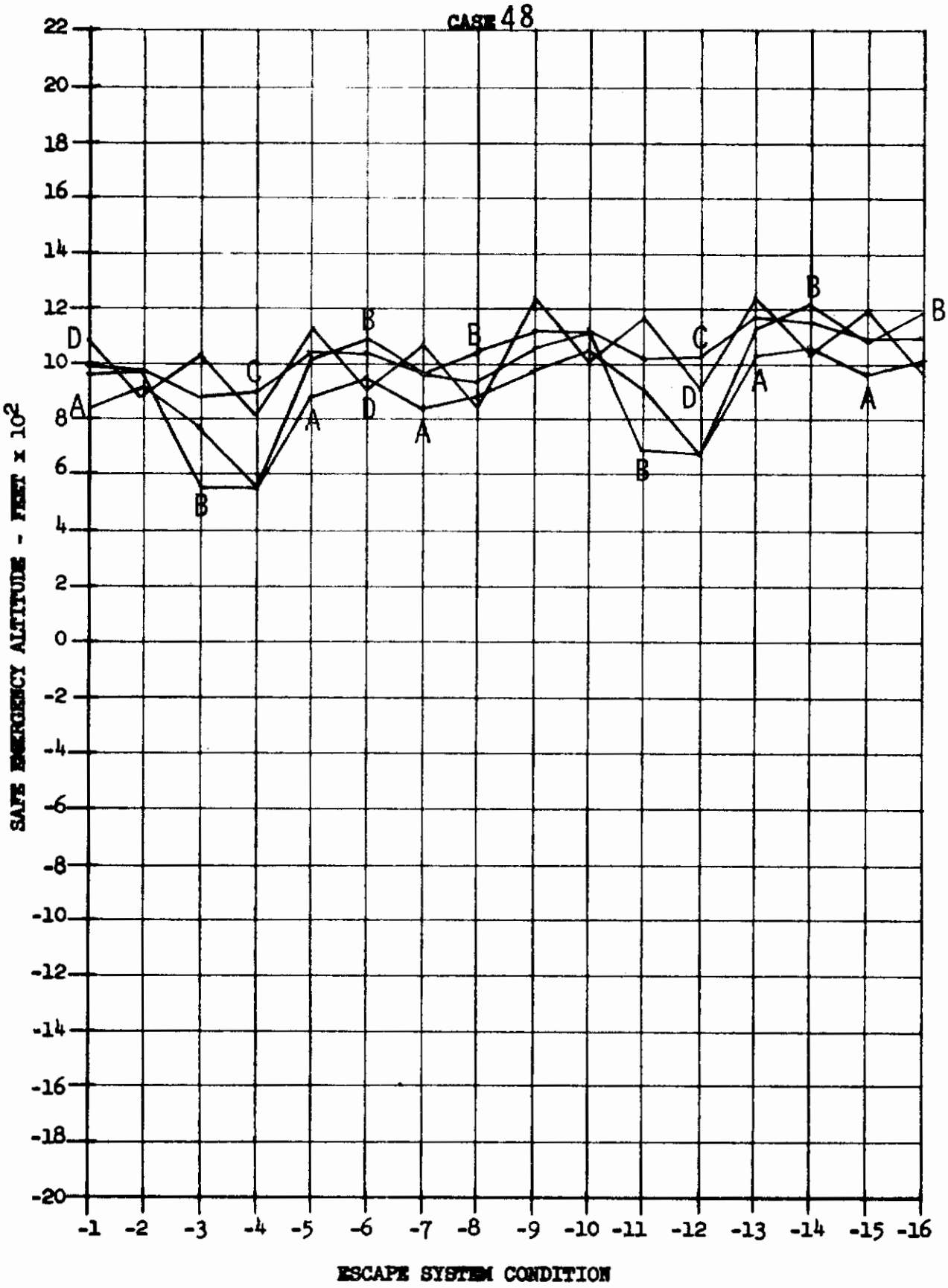

Approved for Public Release

Contrails

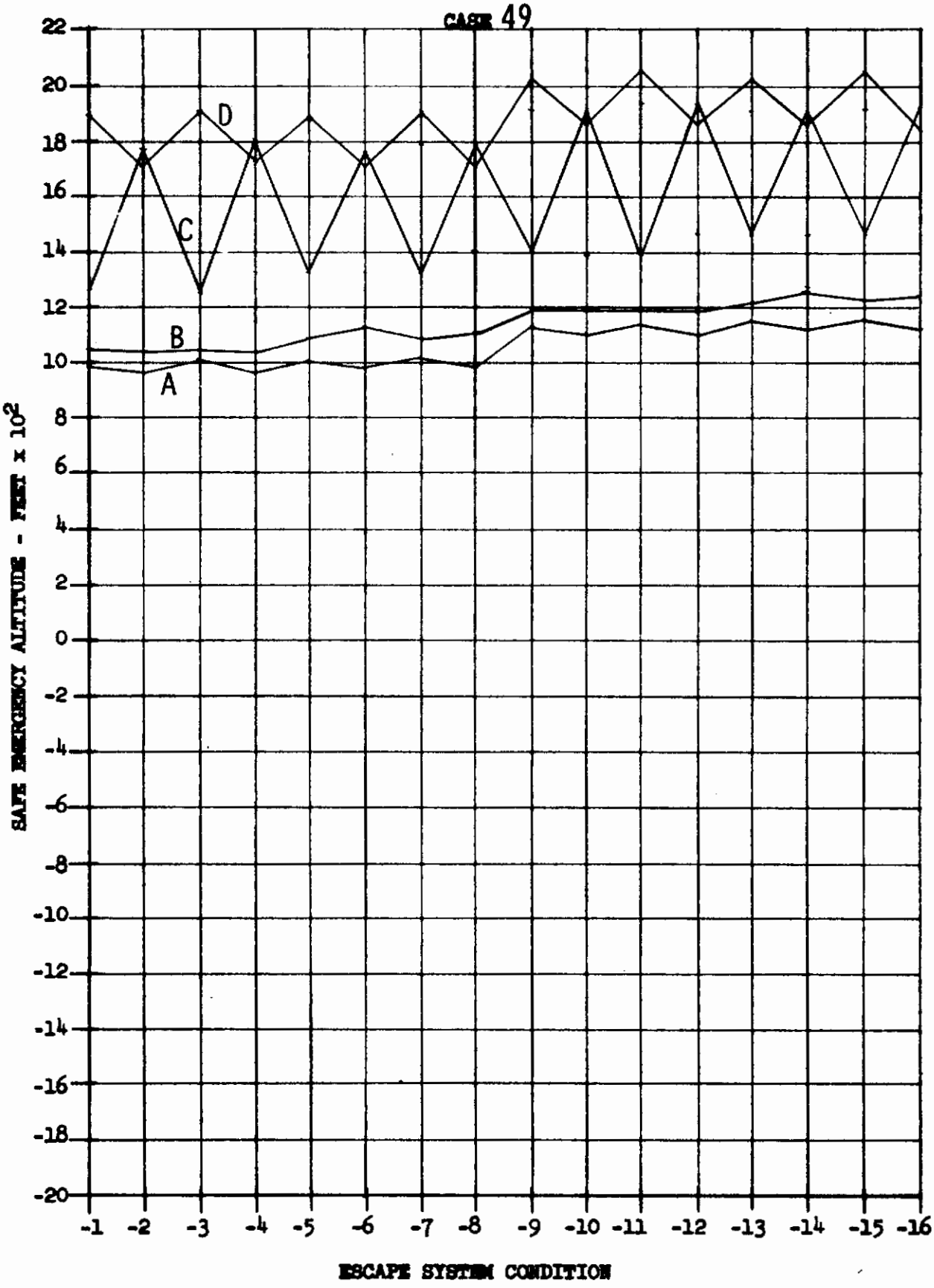

Approved for Public Release

Contrails

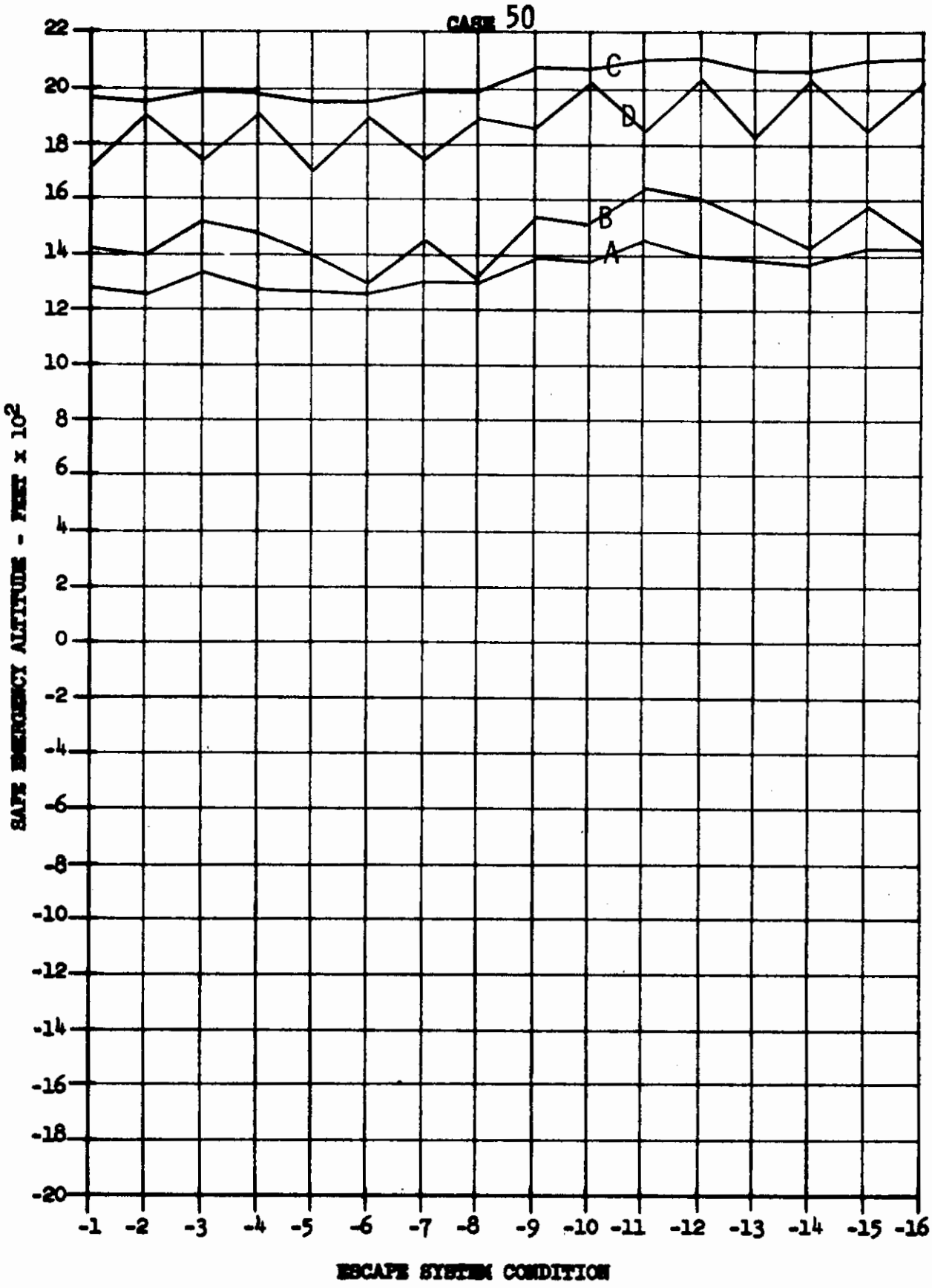

Approved for Public Release

Contrails

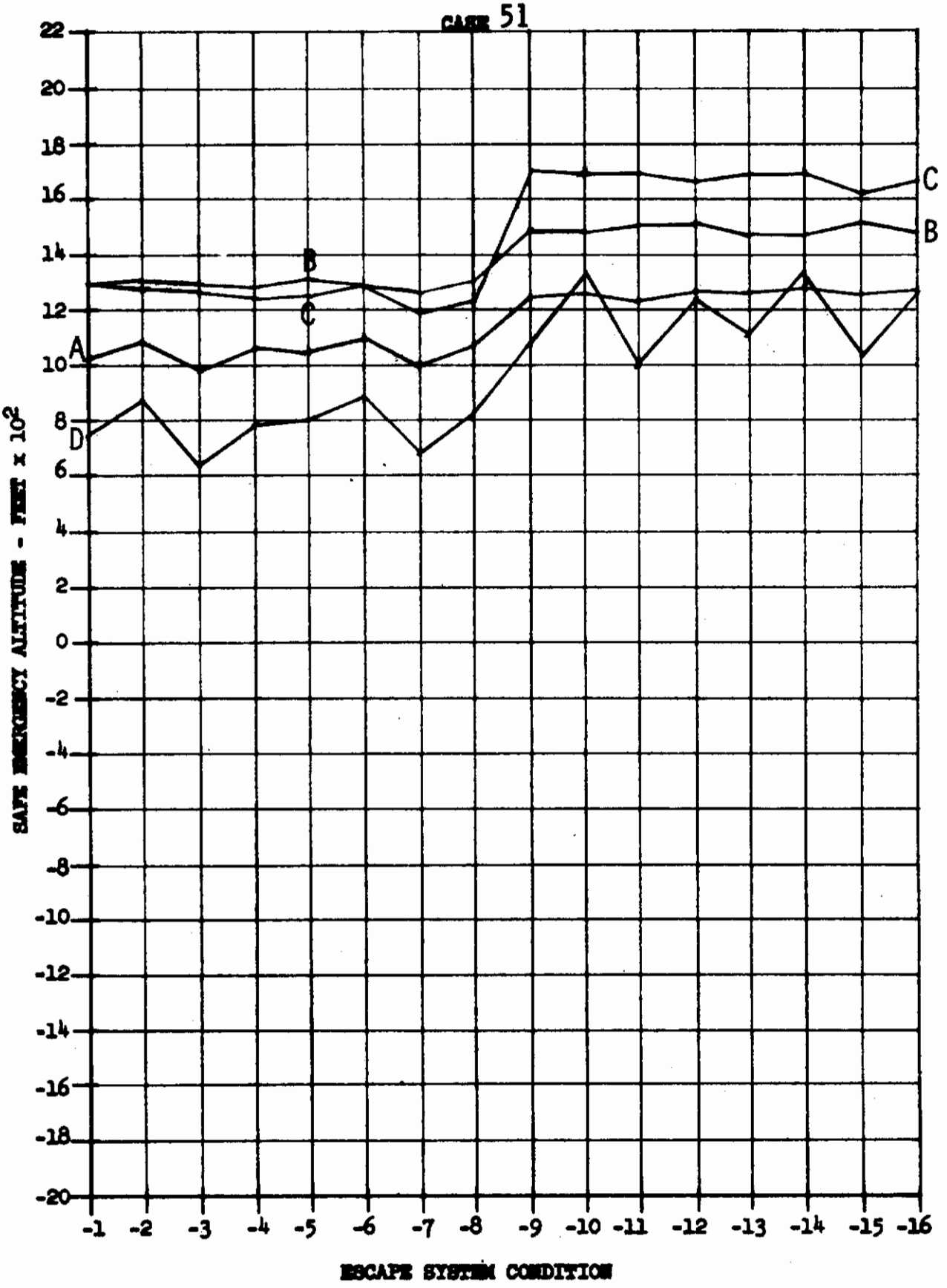

Approved for Public Release

Contrails

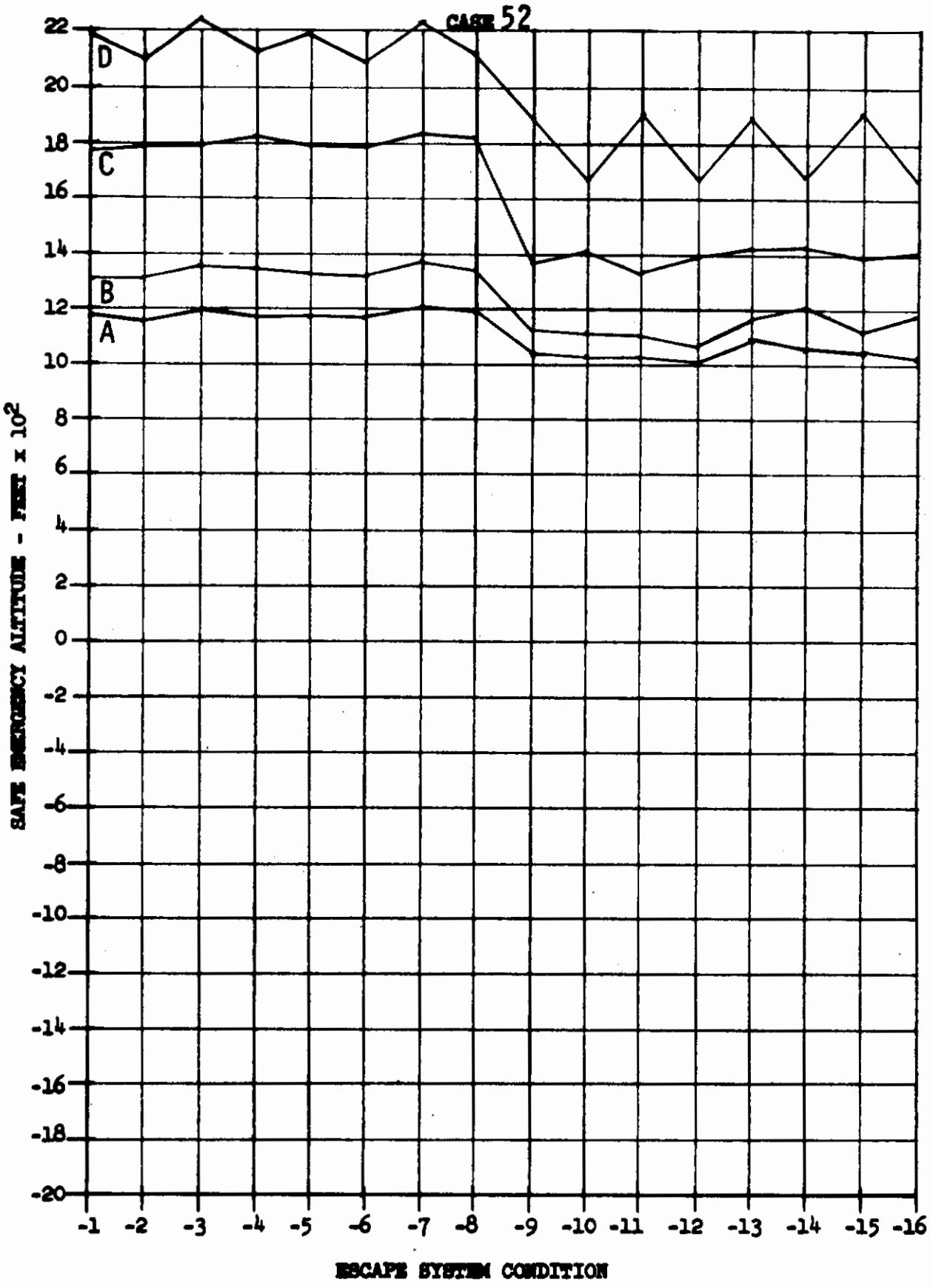

Approved for Public Release

Contrails

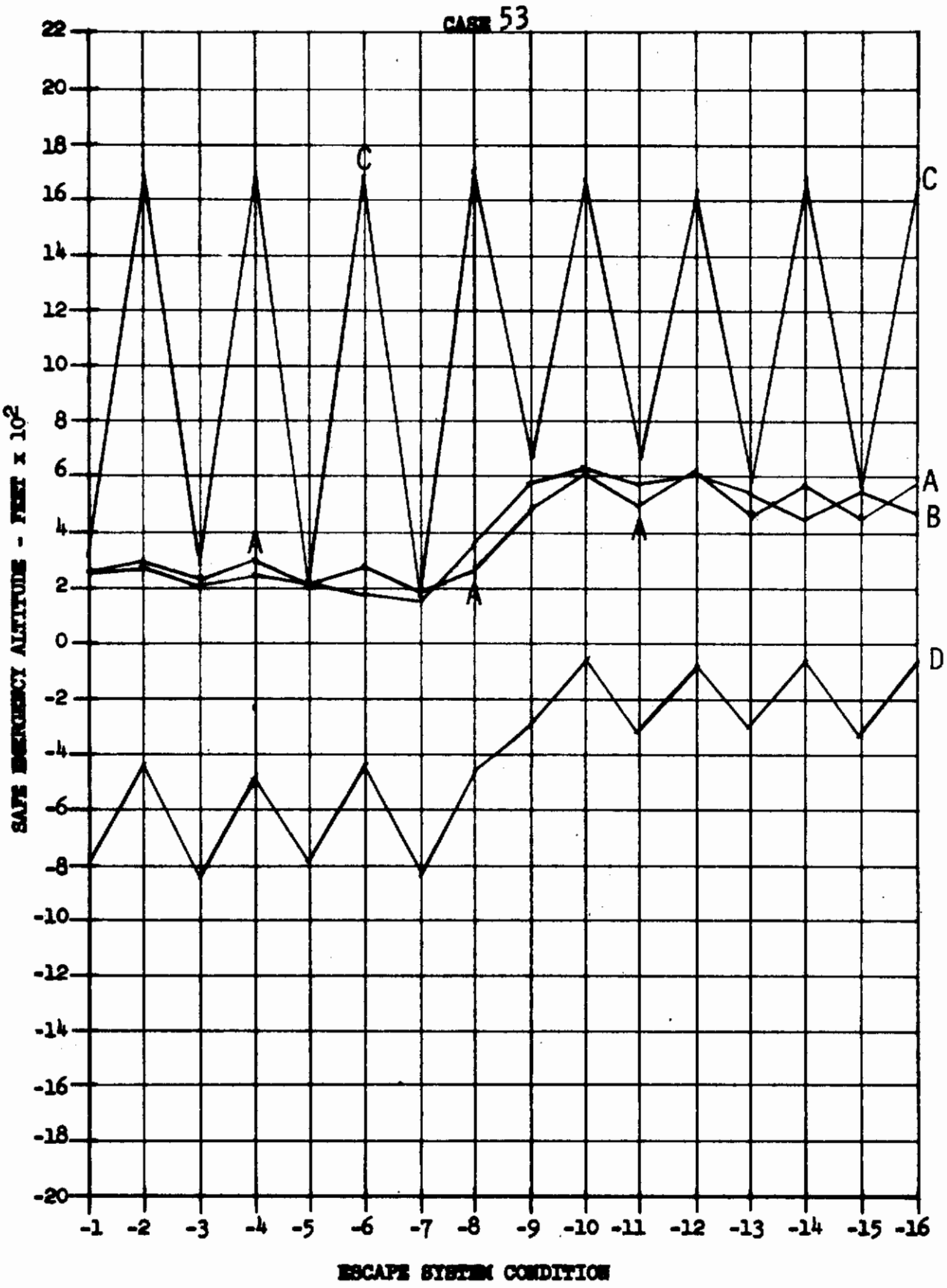

Approved for Public Release

Contrails

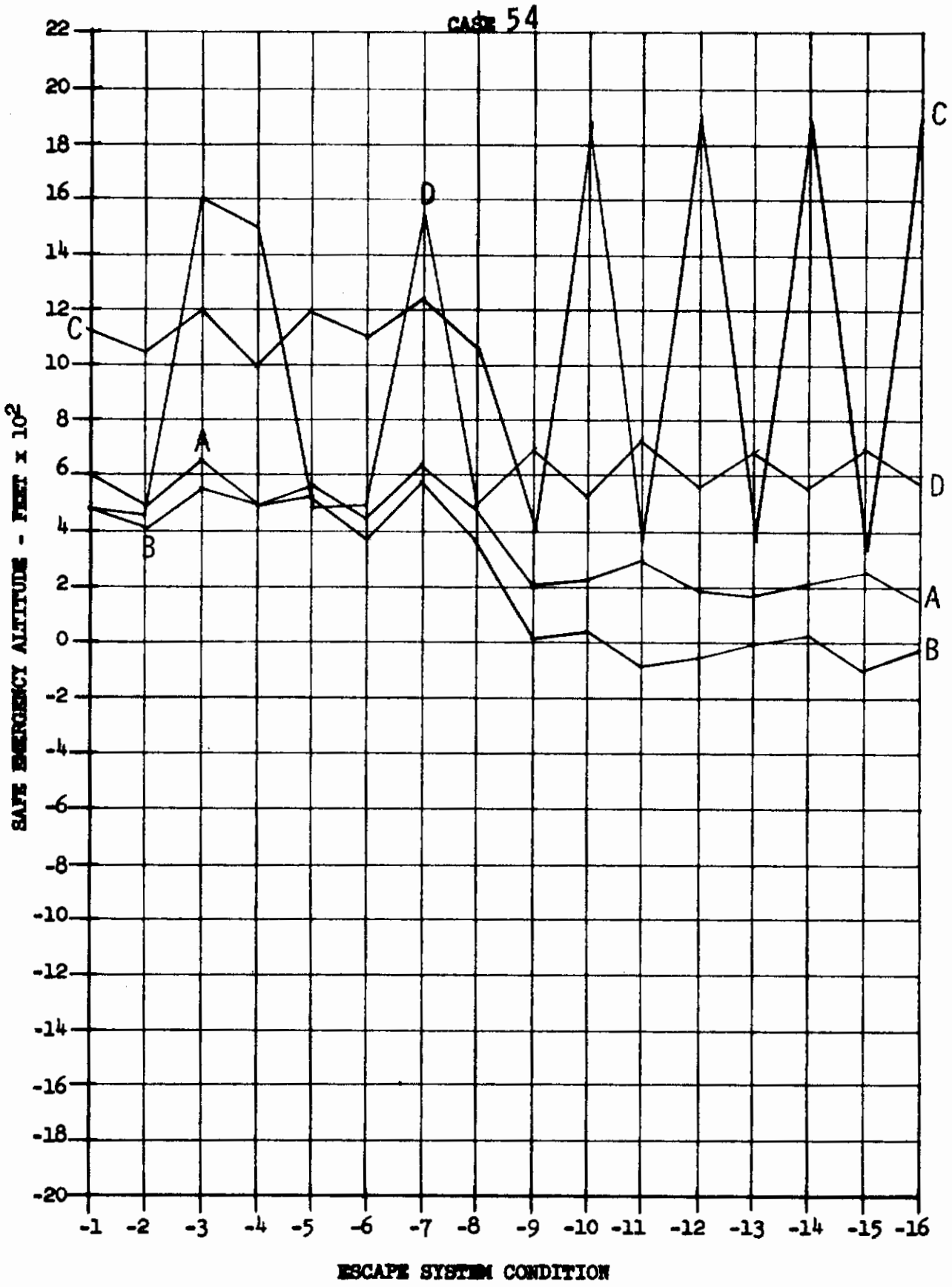

Approved for Public Release

Contrails

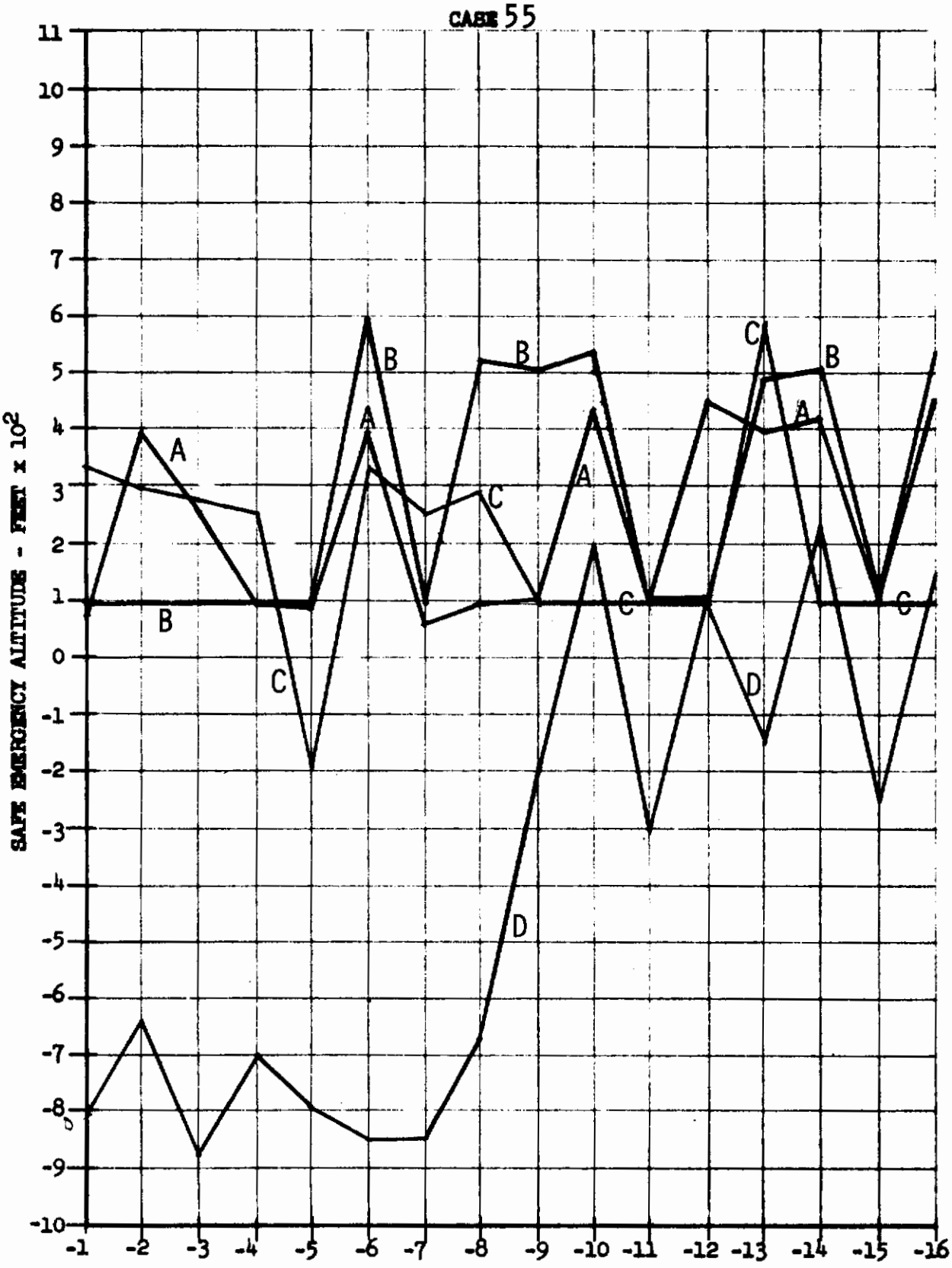

Approved for Public Release

Contrails

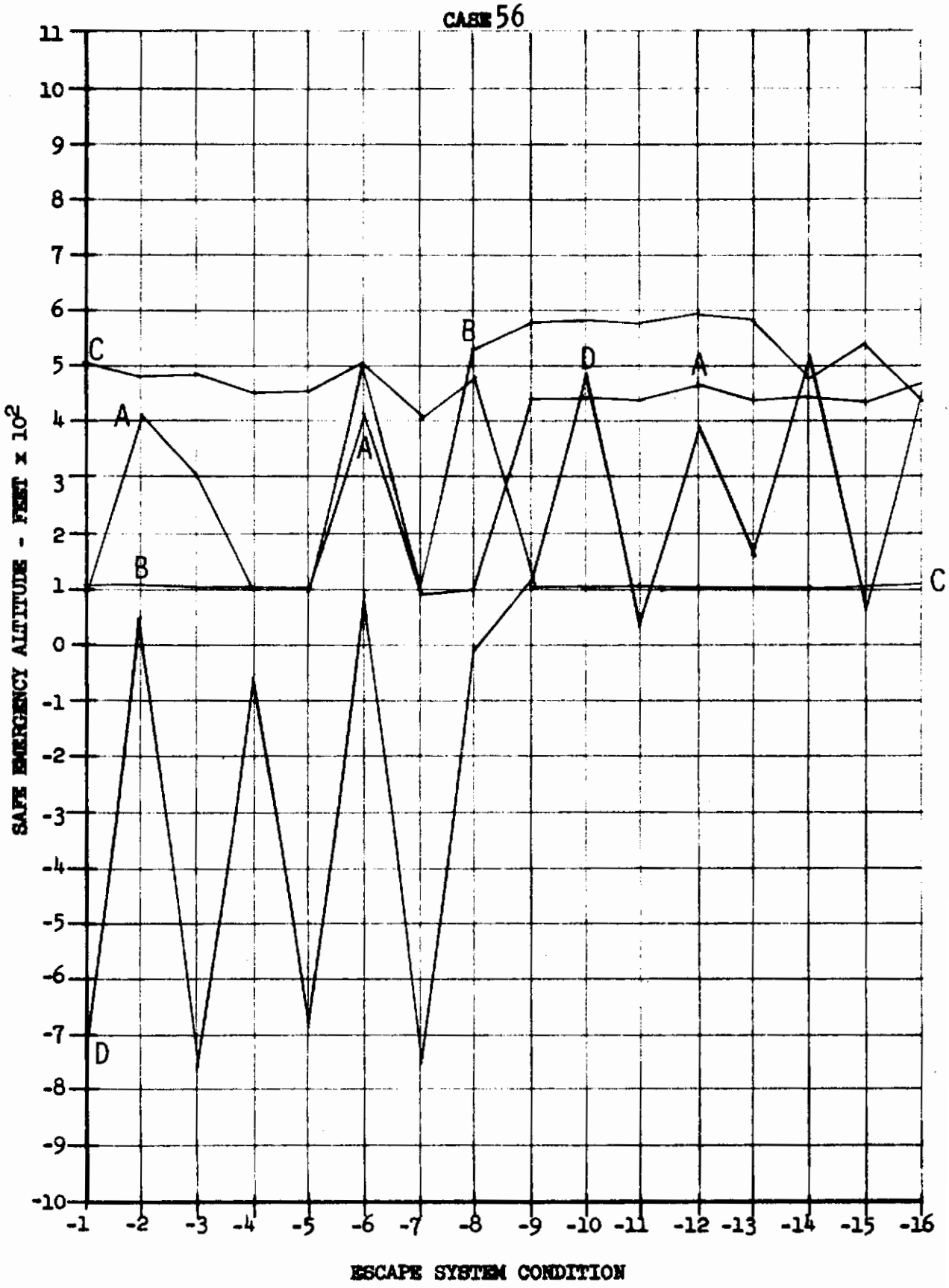

Approved for Public Release

Contrails

CASE 57

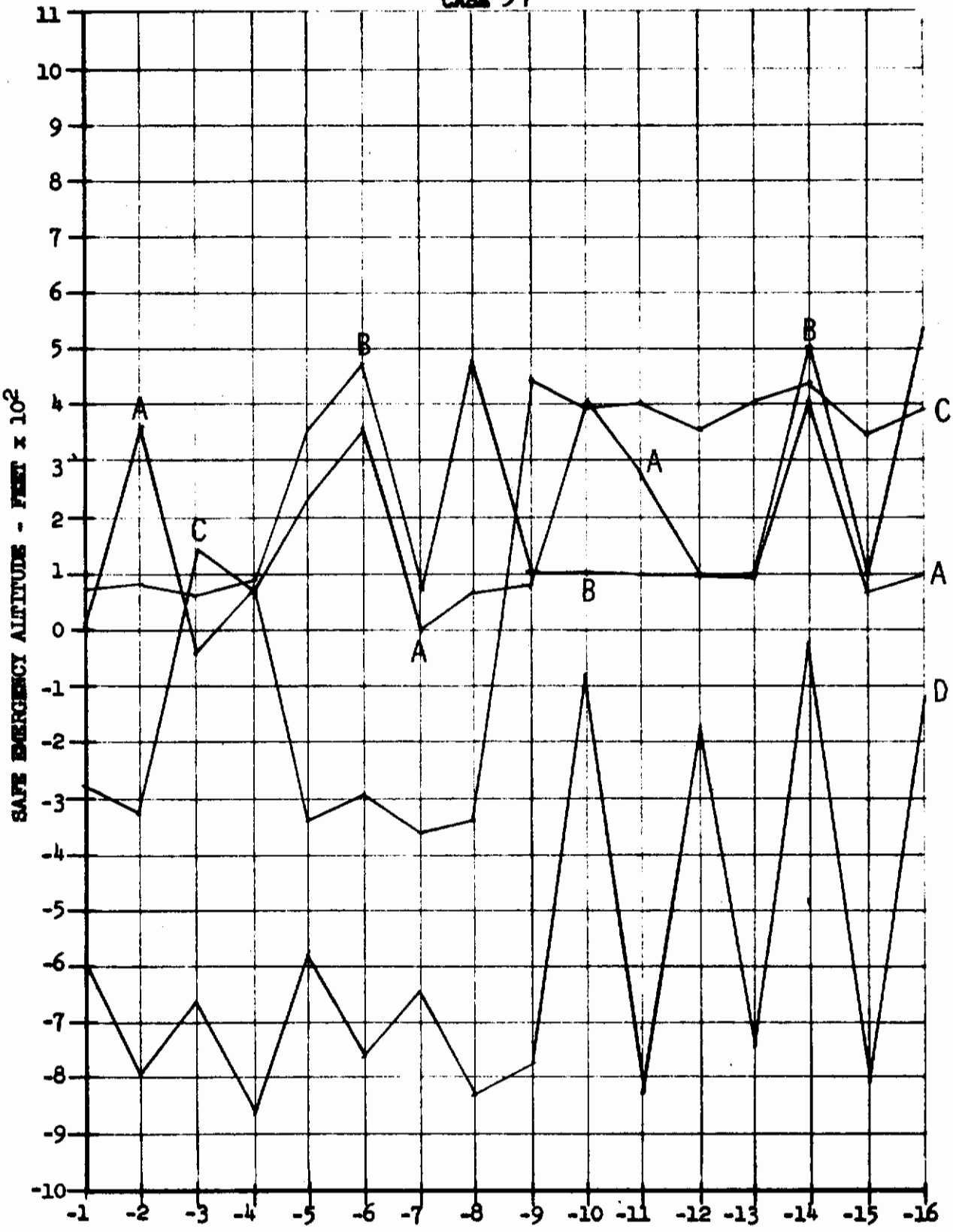

Approved for Public Release

Contrails

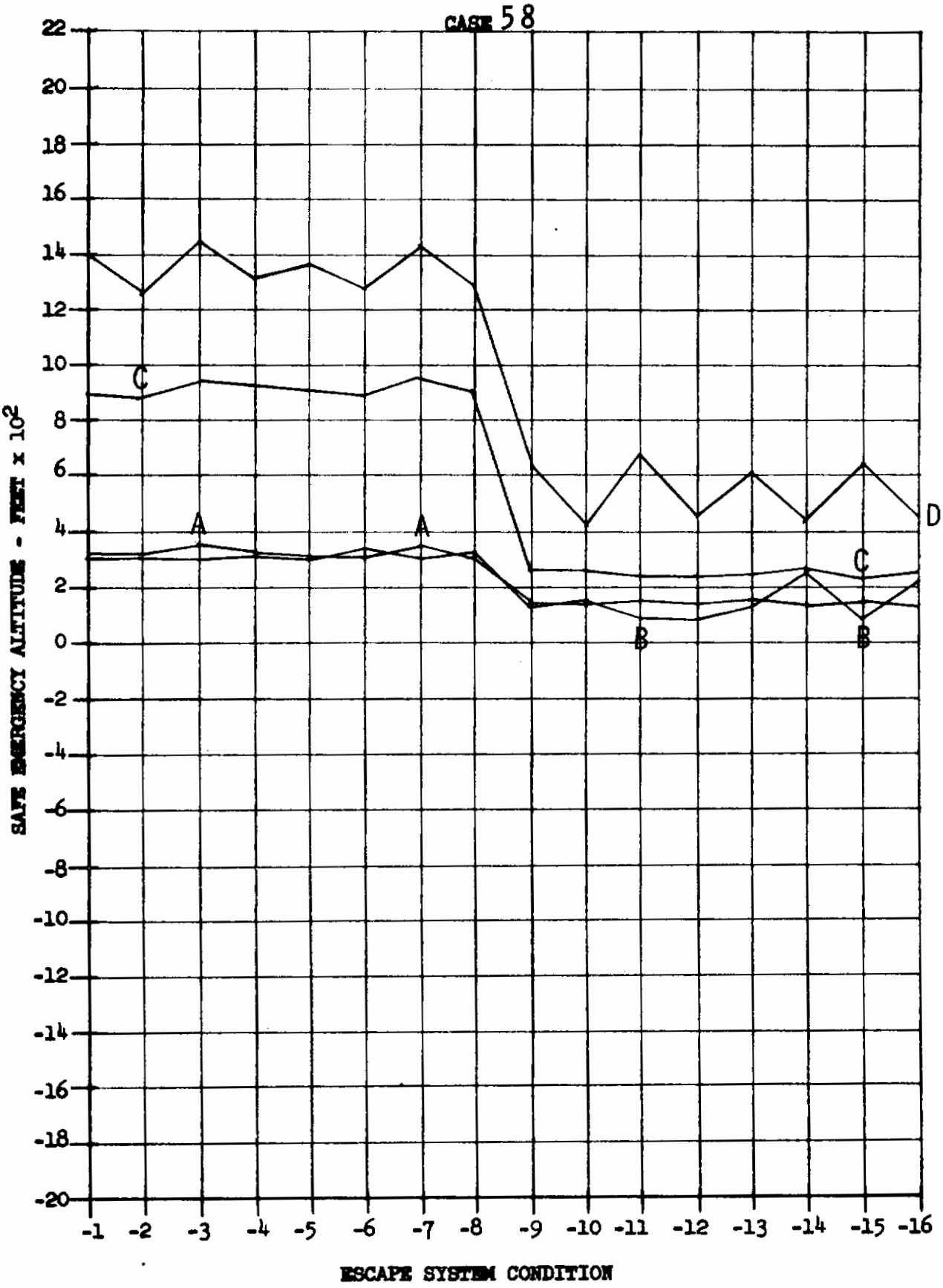

Approved for Public Release

Contrails

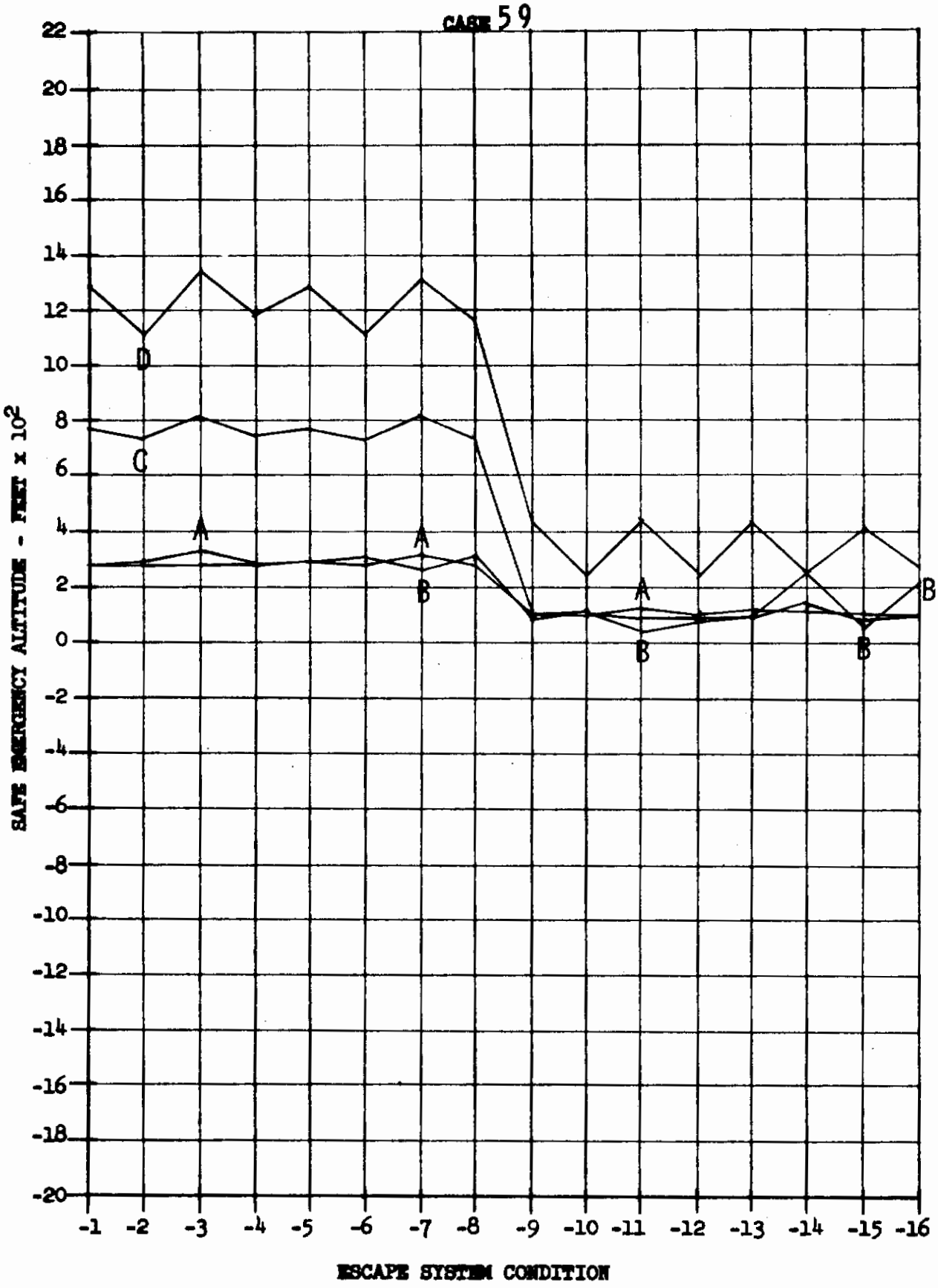

Approved for Public Release

Contrails

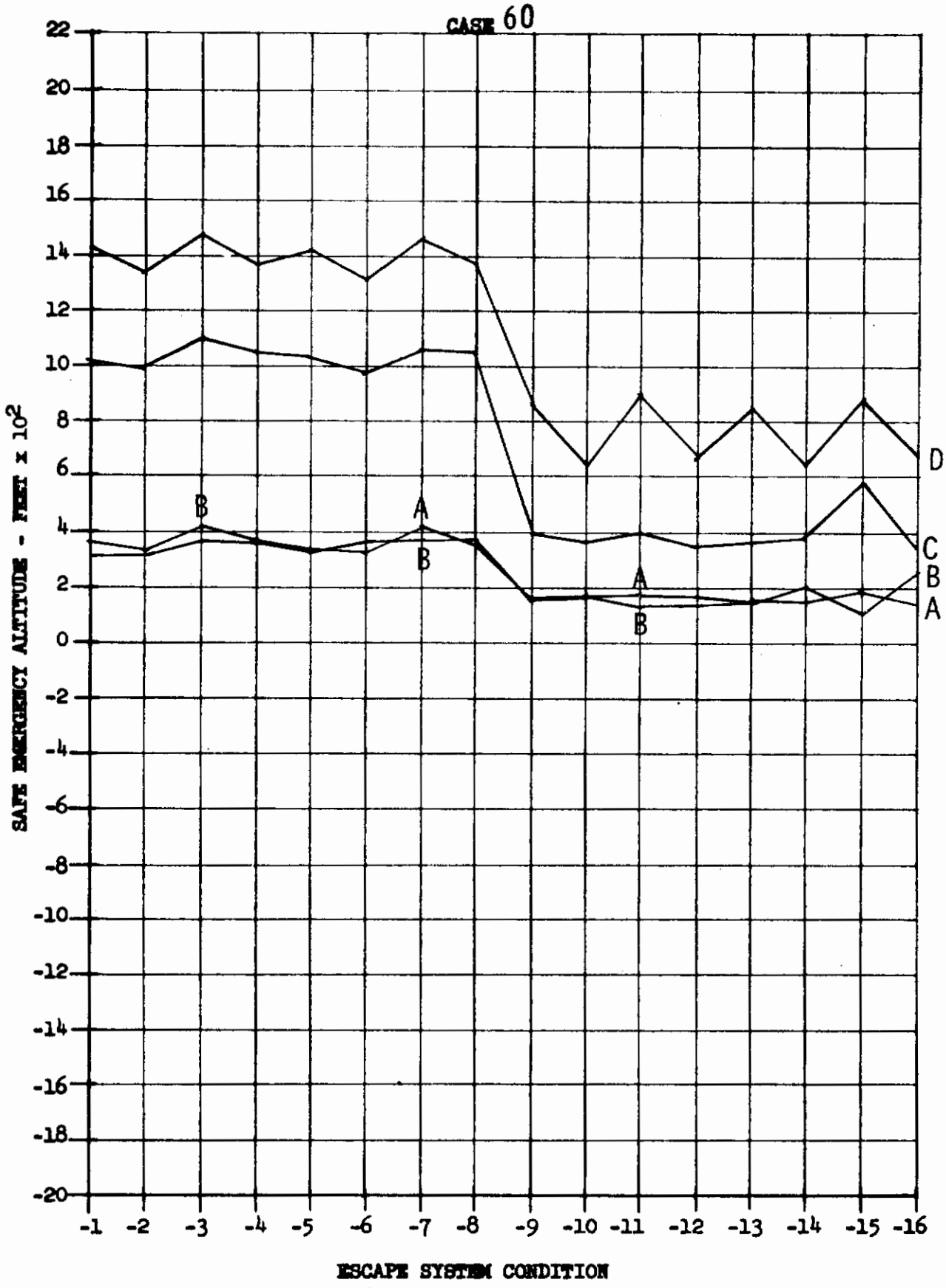

Approved for Public Release

Contrails

CASE 61

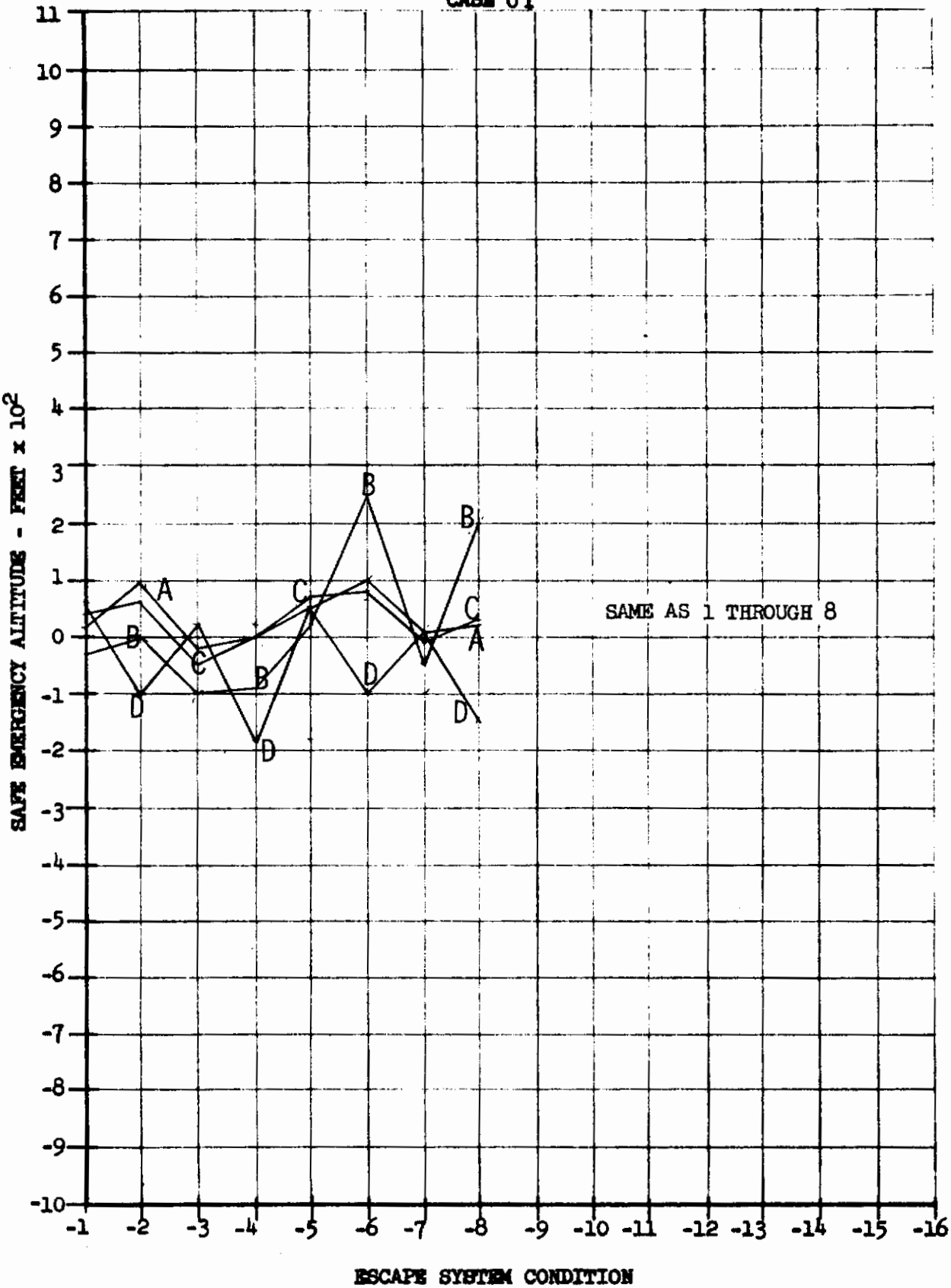

Approved for Public Release

Contrails

CASE 62

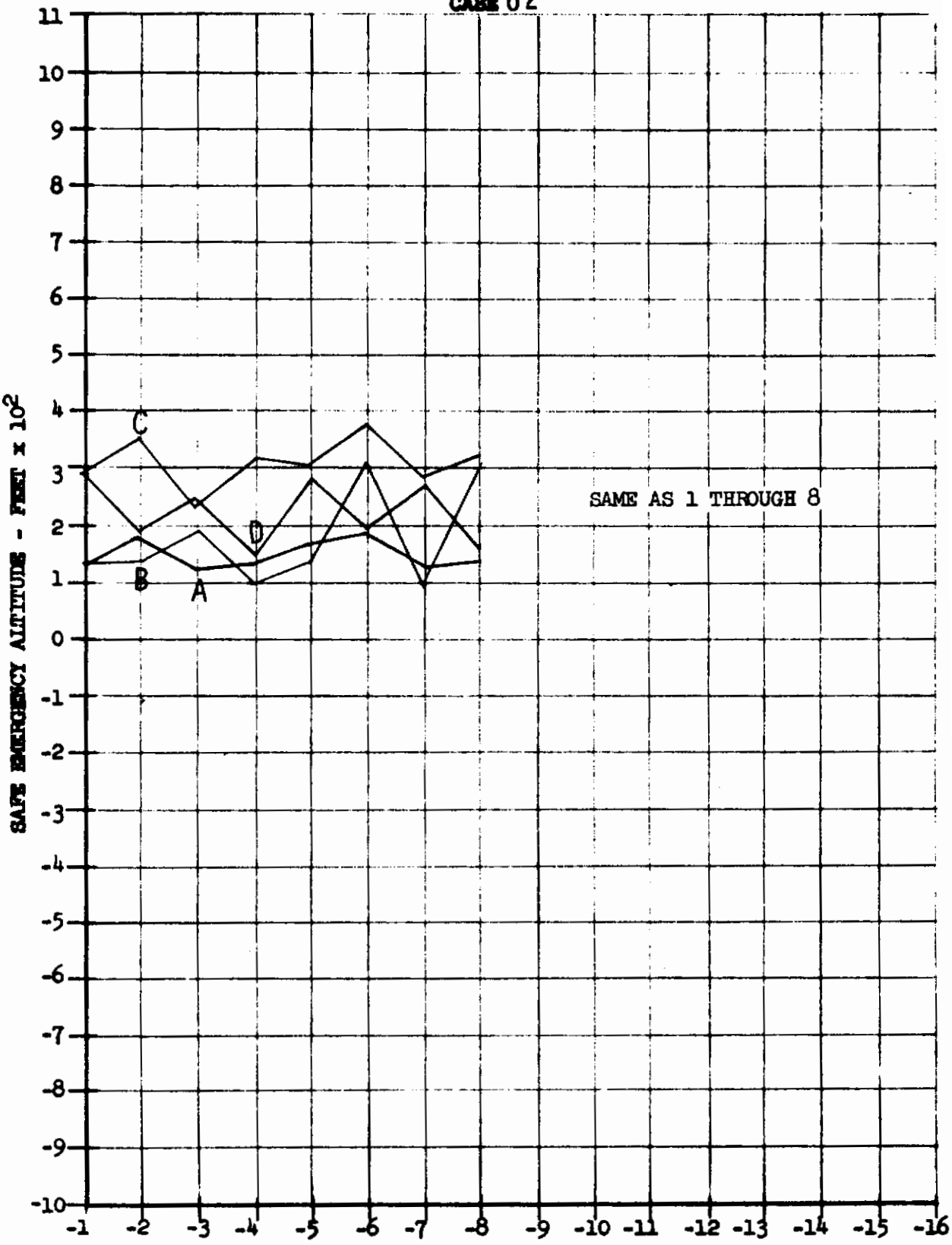

Approved for Public Release

Contrails

CASE 63

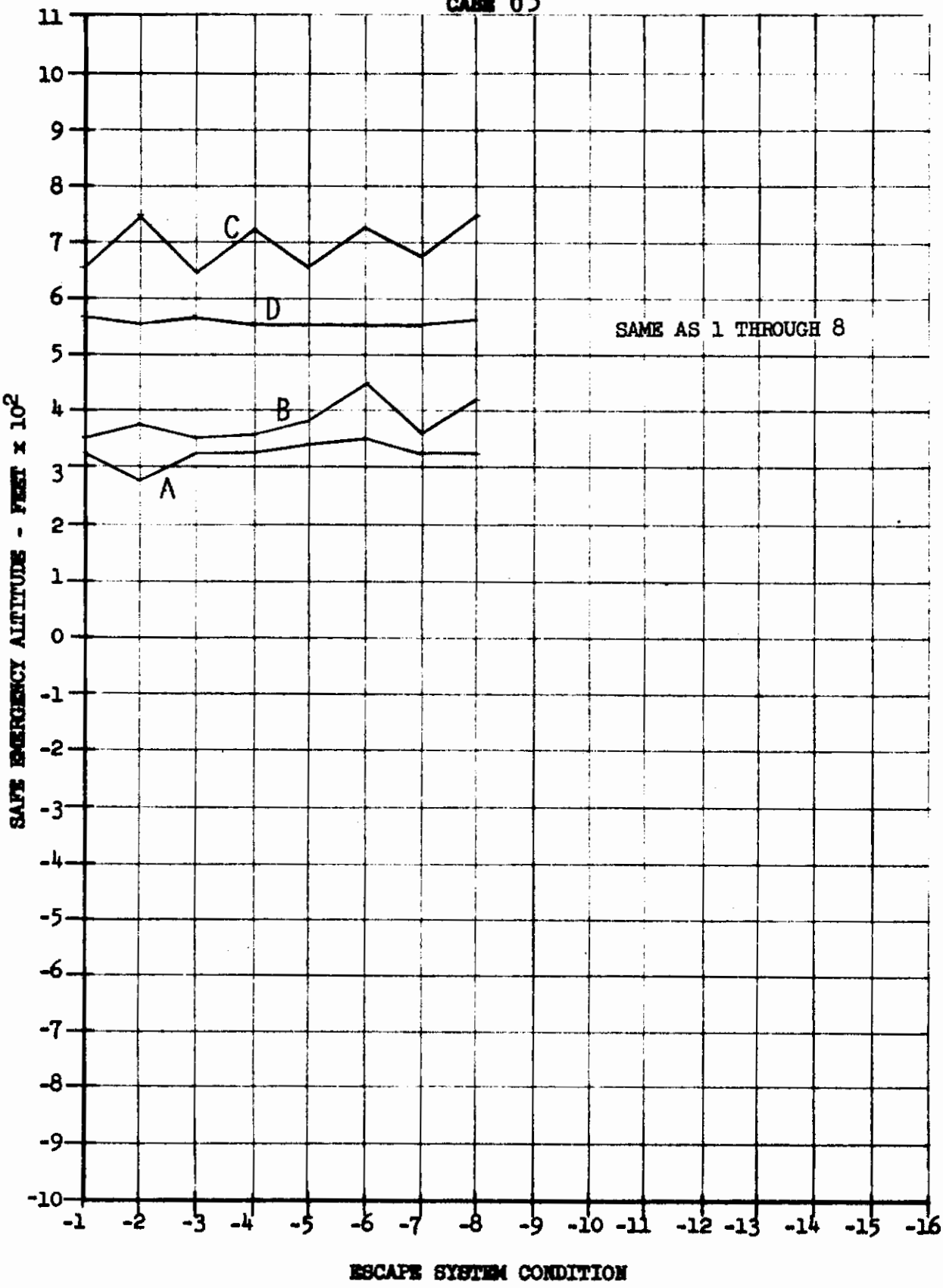

Approved for Public Release

Contrails

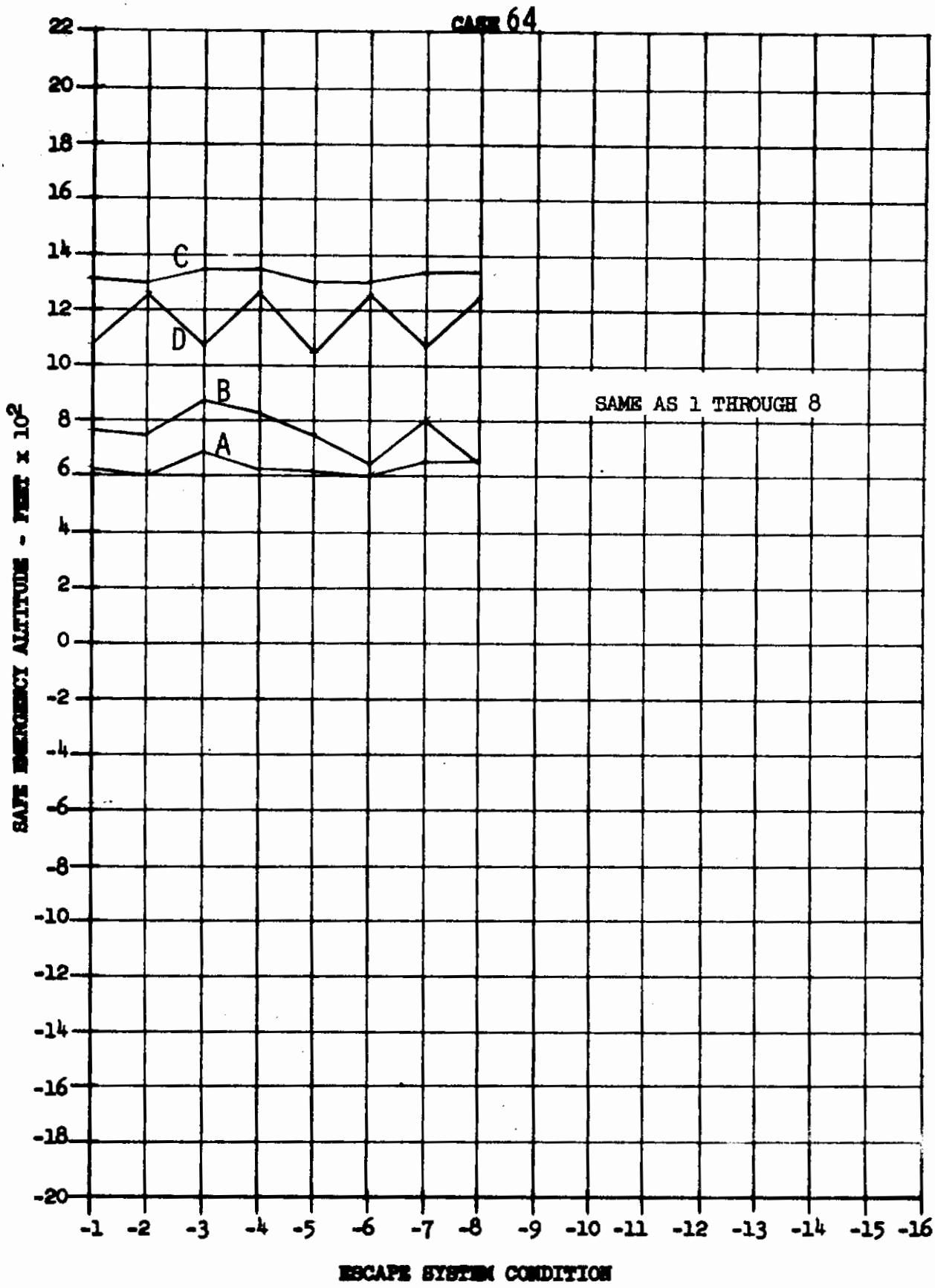

Approved for Public Release

Contrails

CASE 65

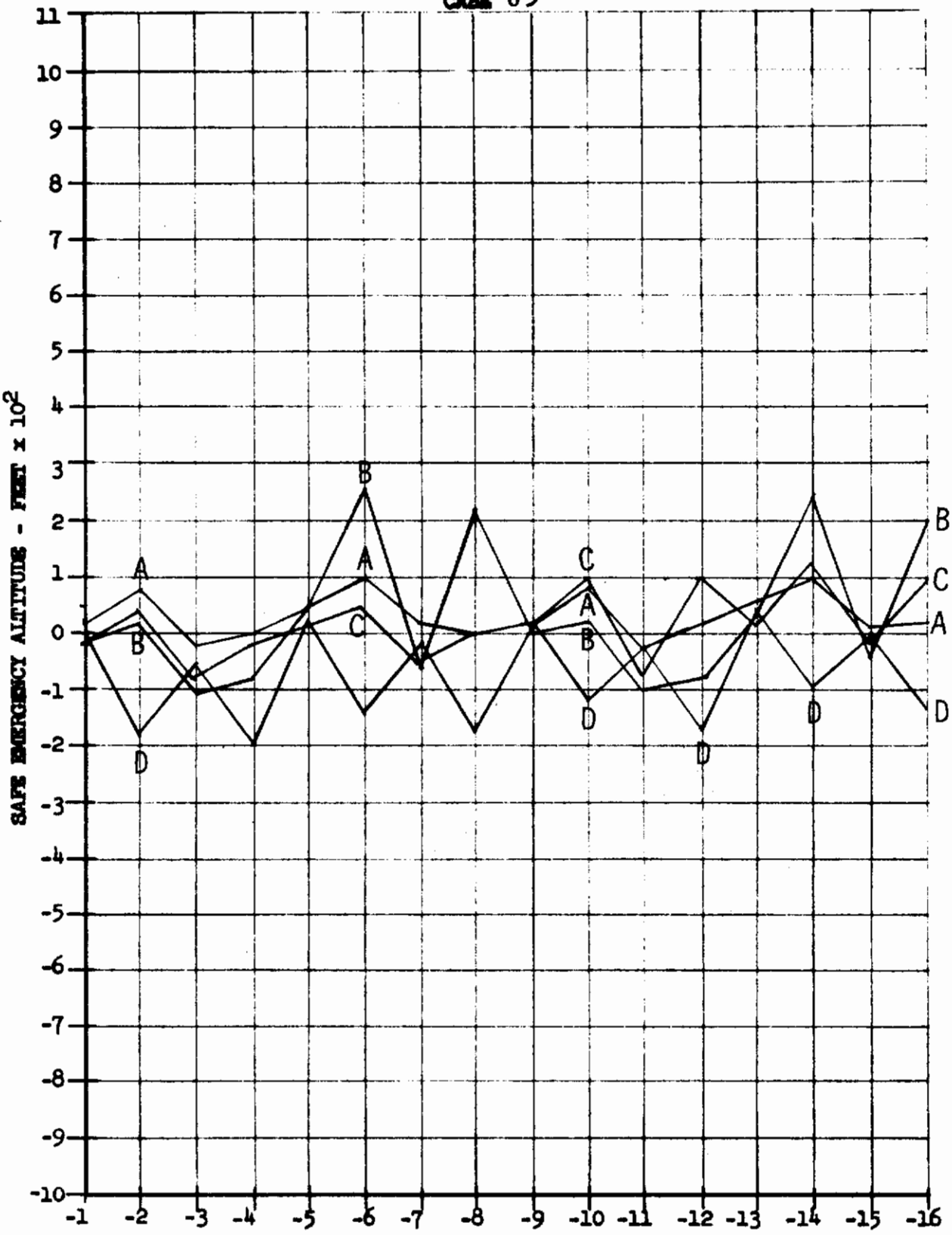

Approved for Public Release

Contrails

CASE 66

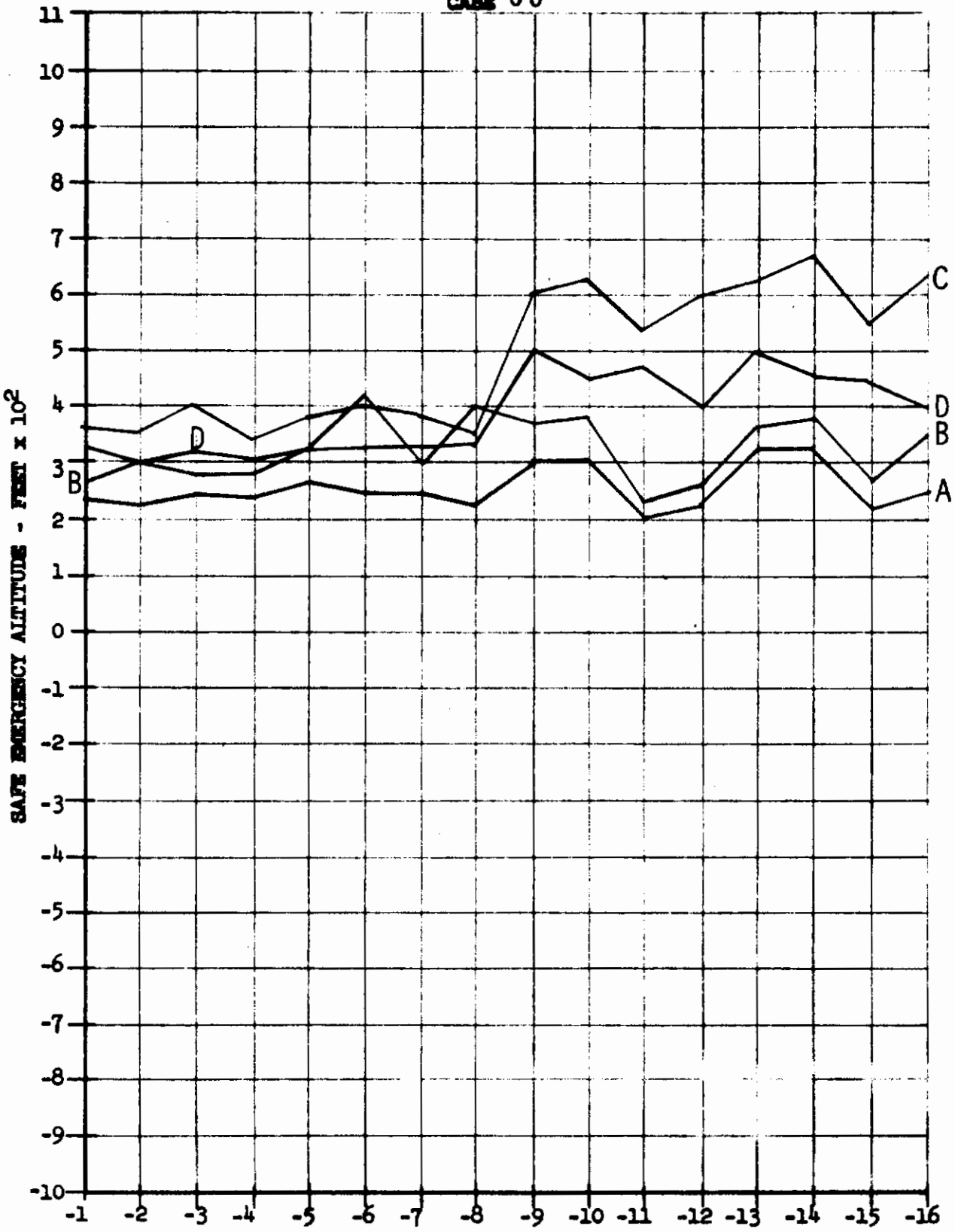

Approved for Public Release

Contrails

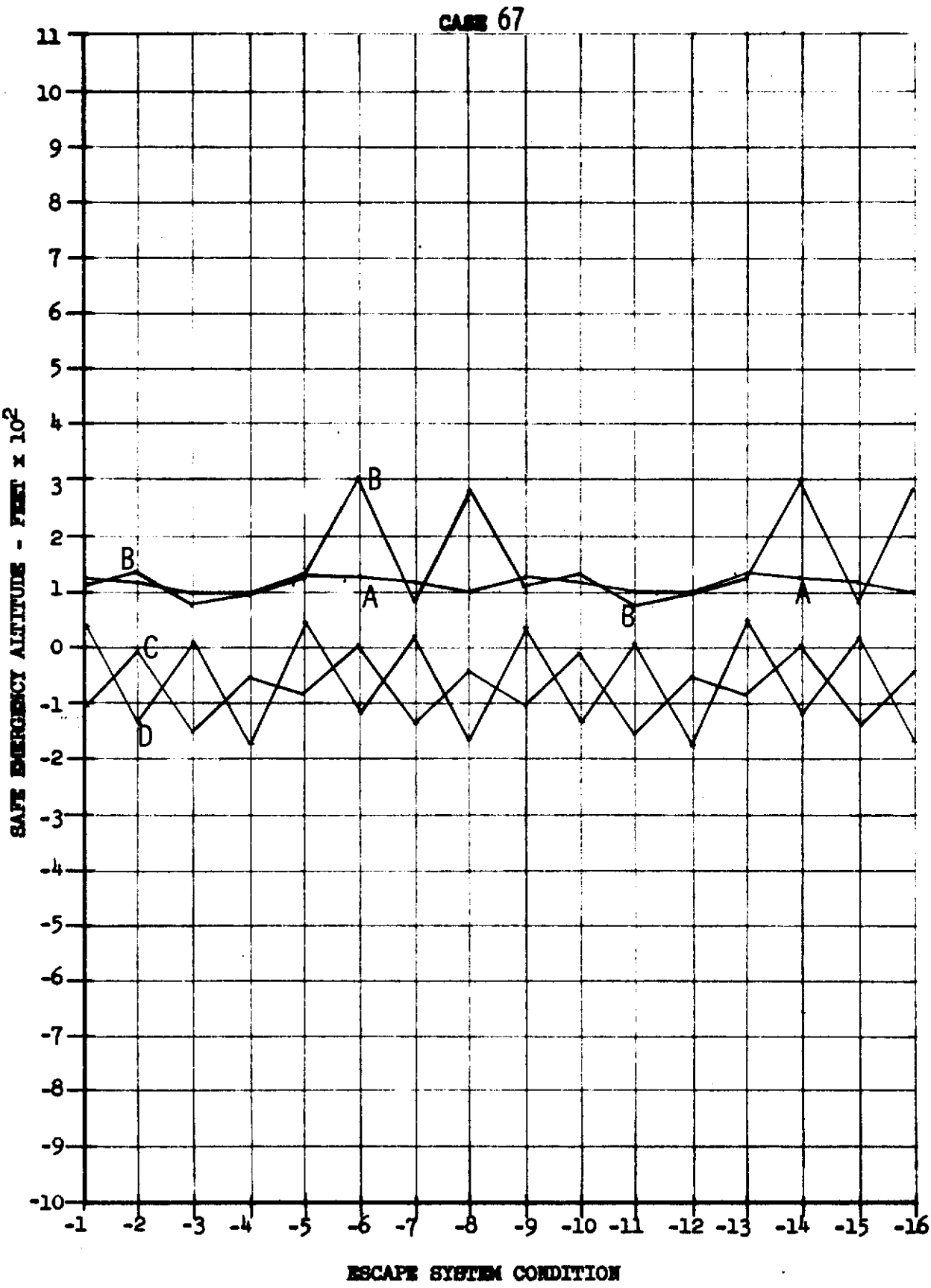

Approved for Public Release

Contrails

CASE 68

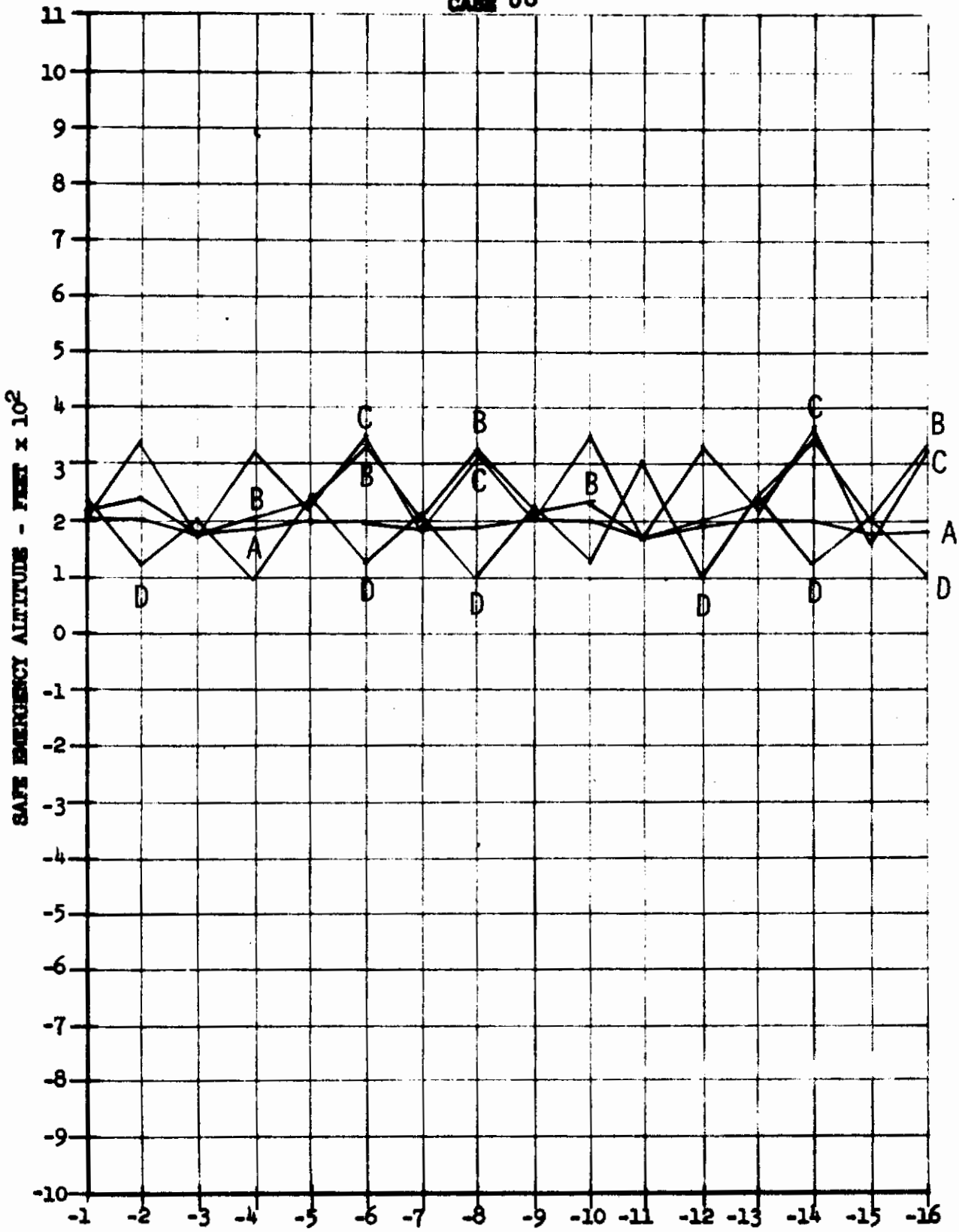

Approved for Public Release

Contrails

CASE 69

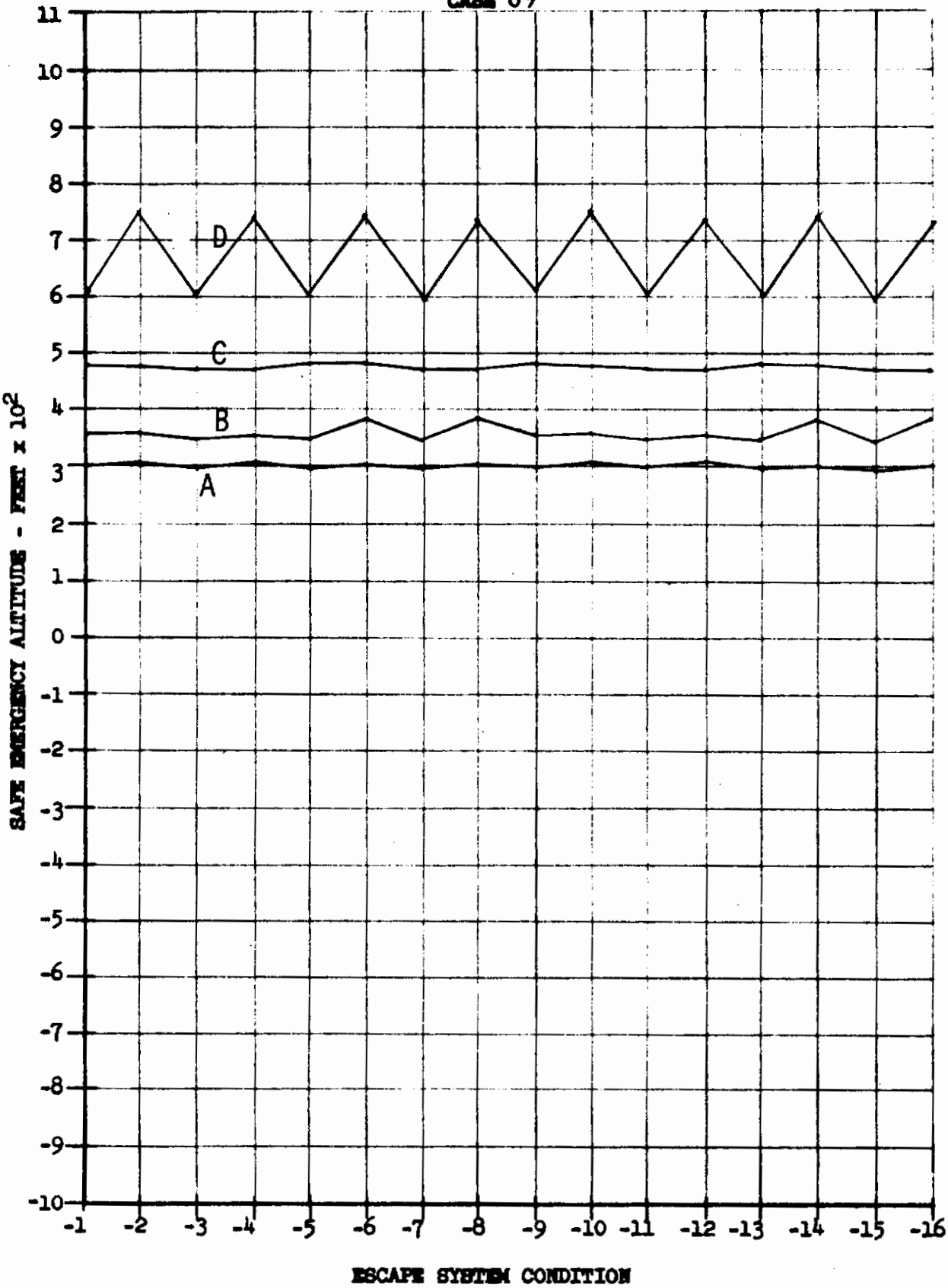

Approved for Public Release

Contrails

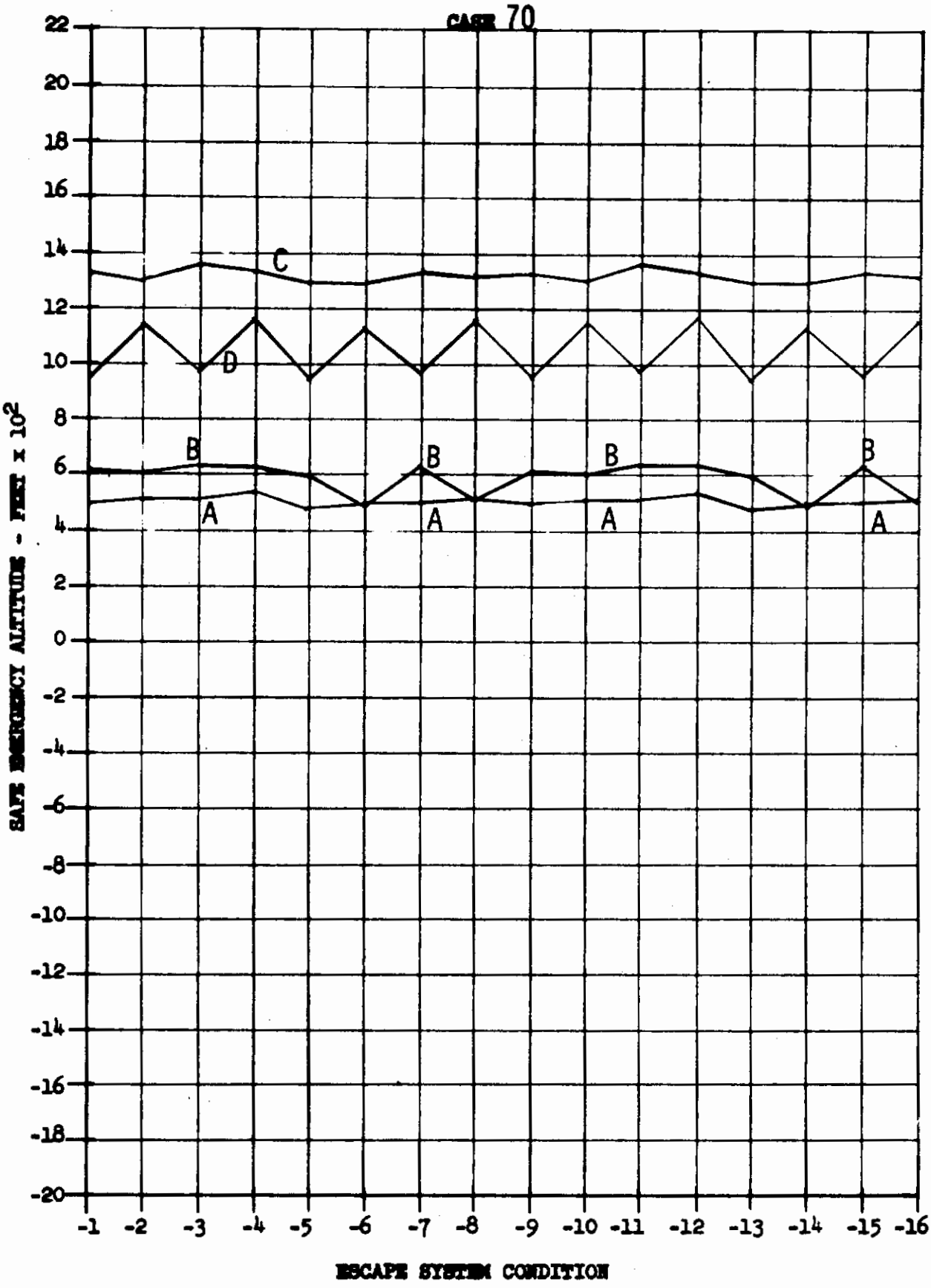

Approved for Public Release

Contrails

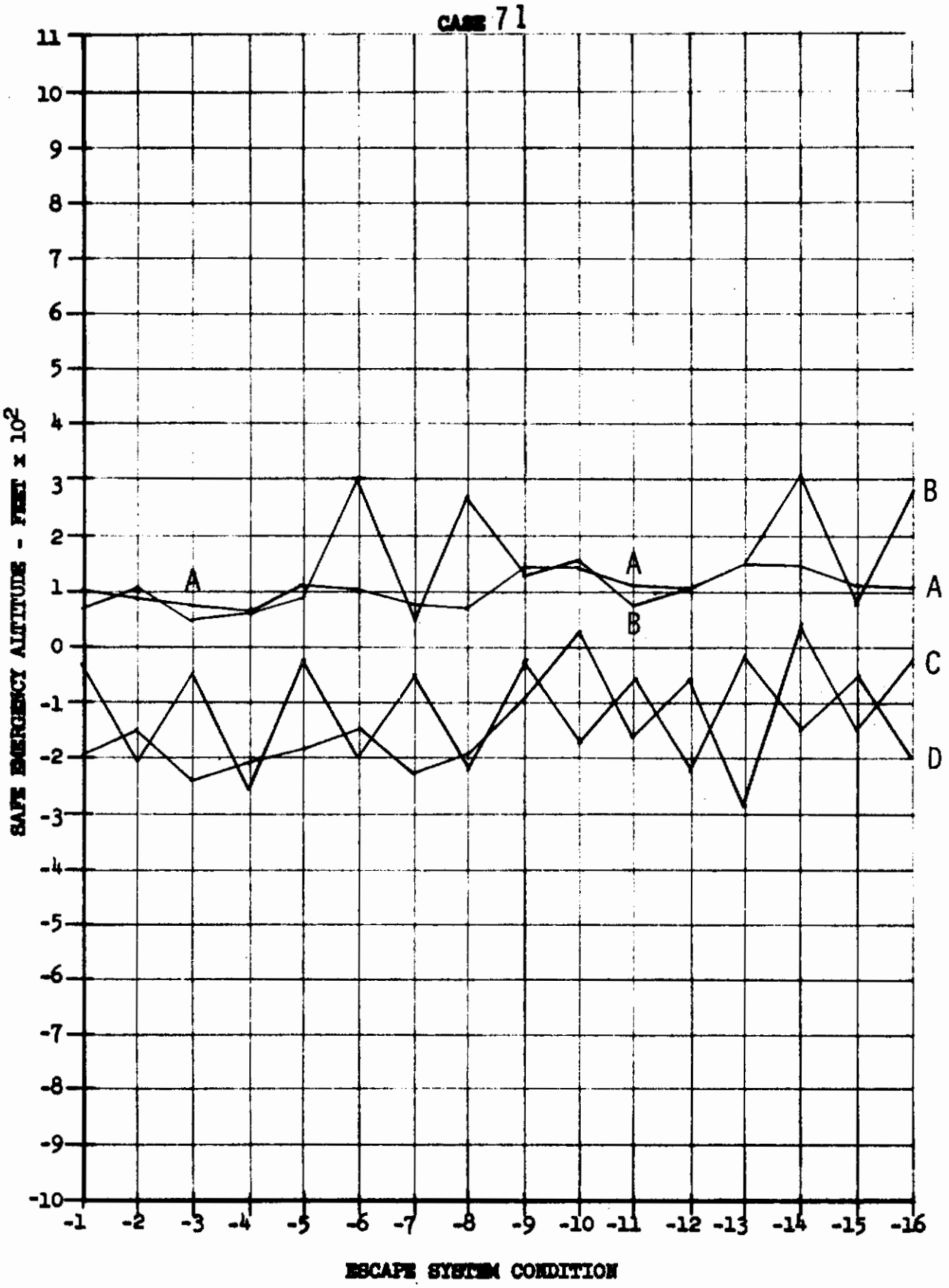

Approved for Public Release

Contrails

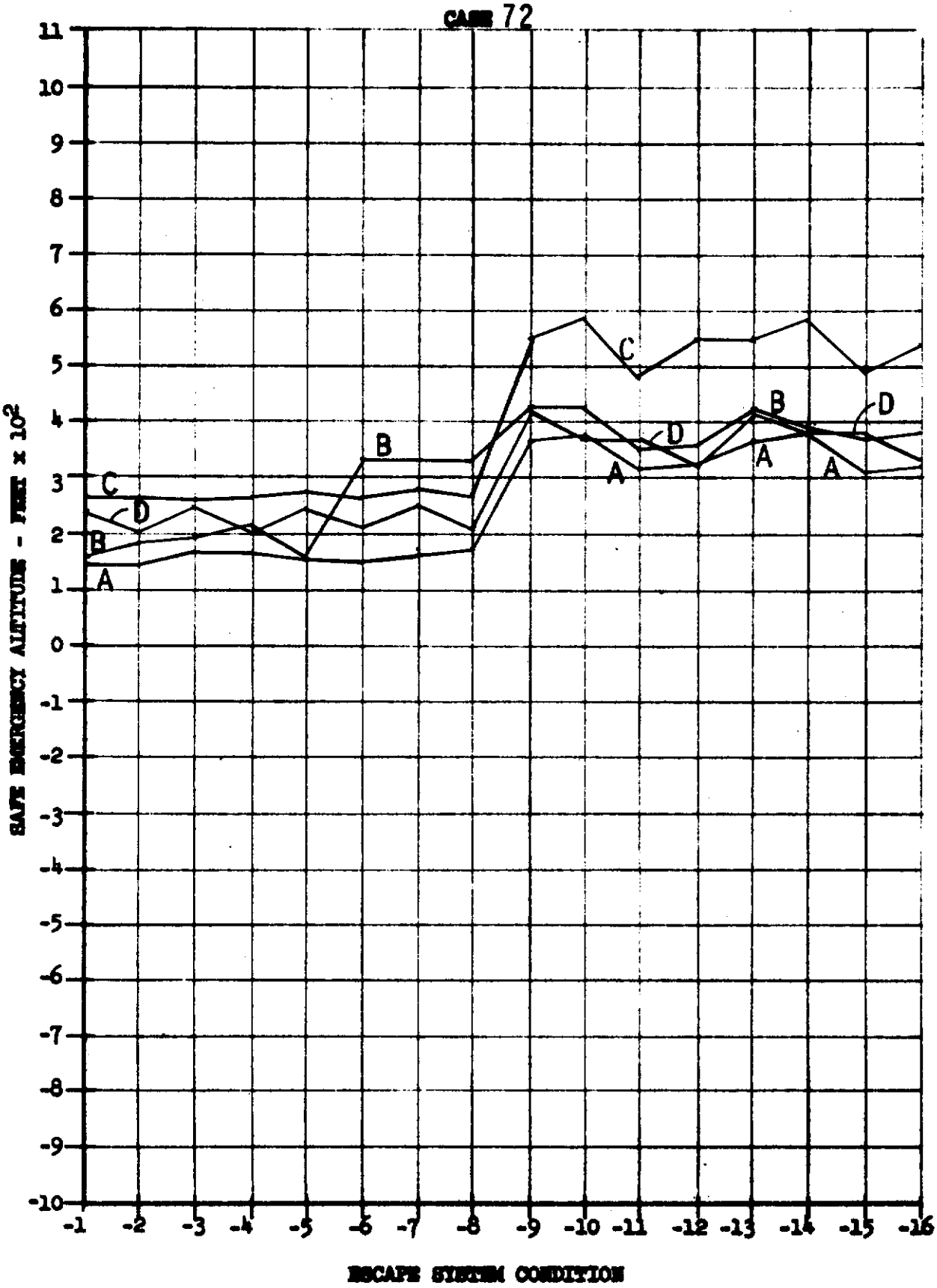

Approved for Public Release

Contrails

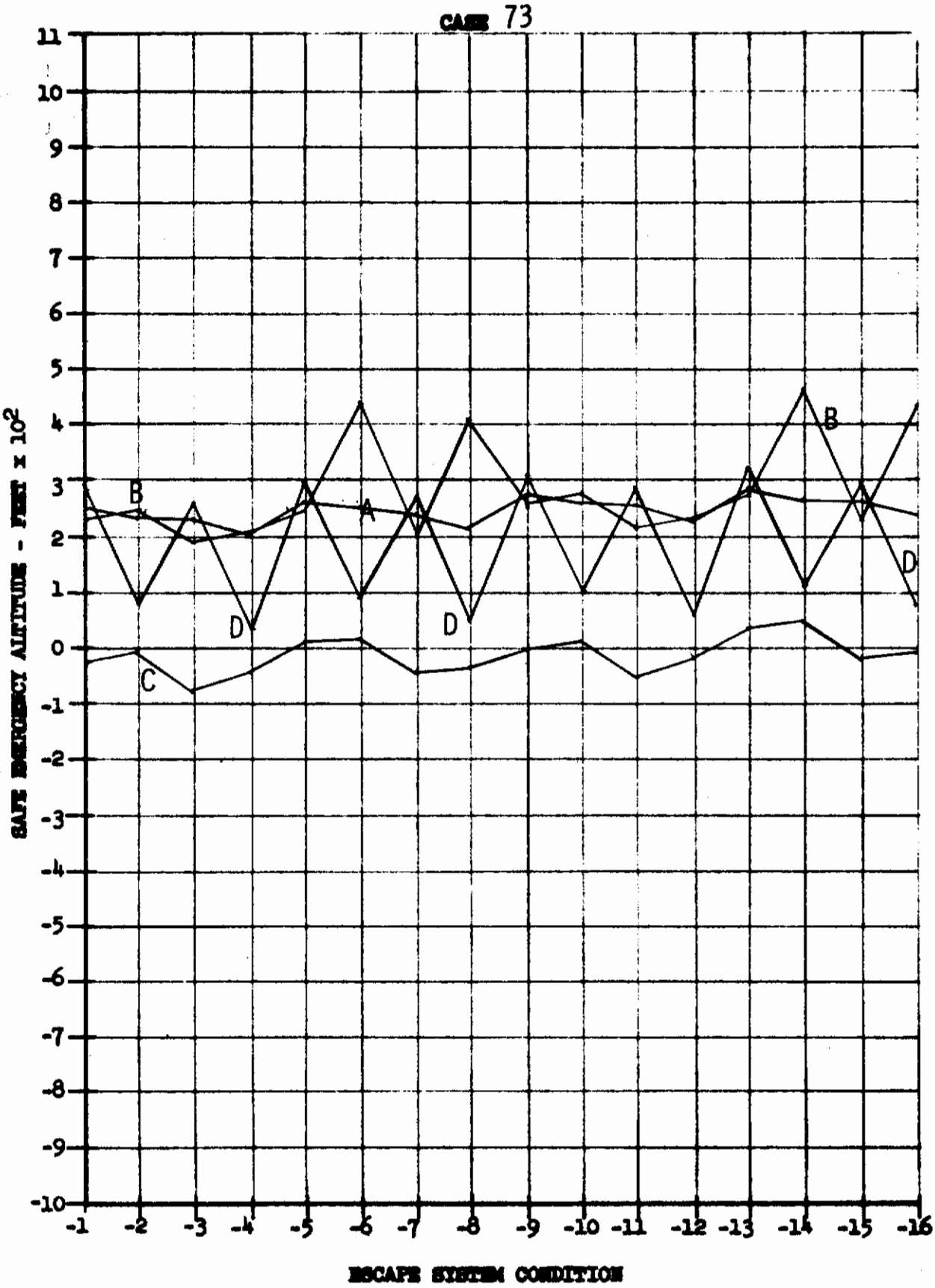

Approved for Public Release

Contrails

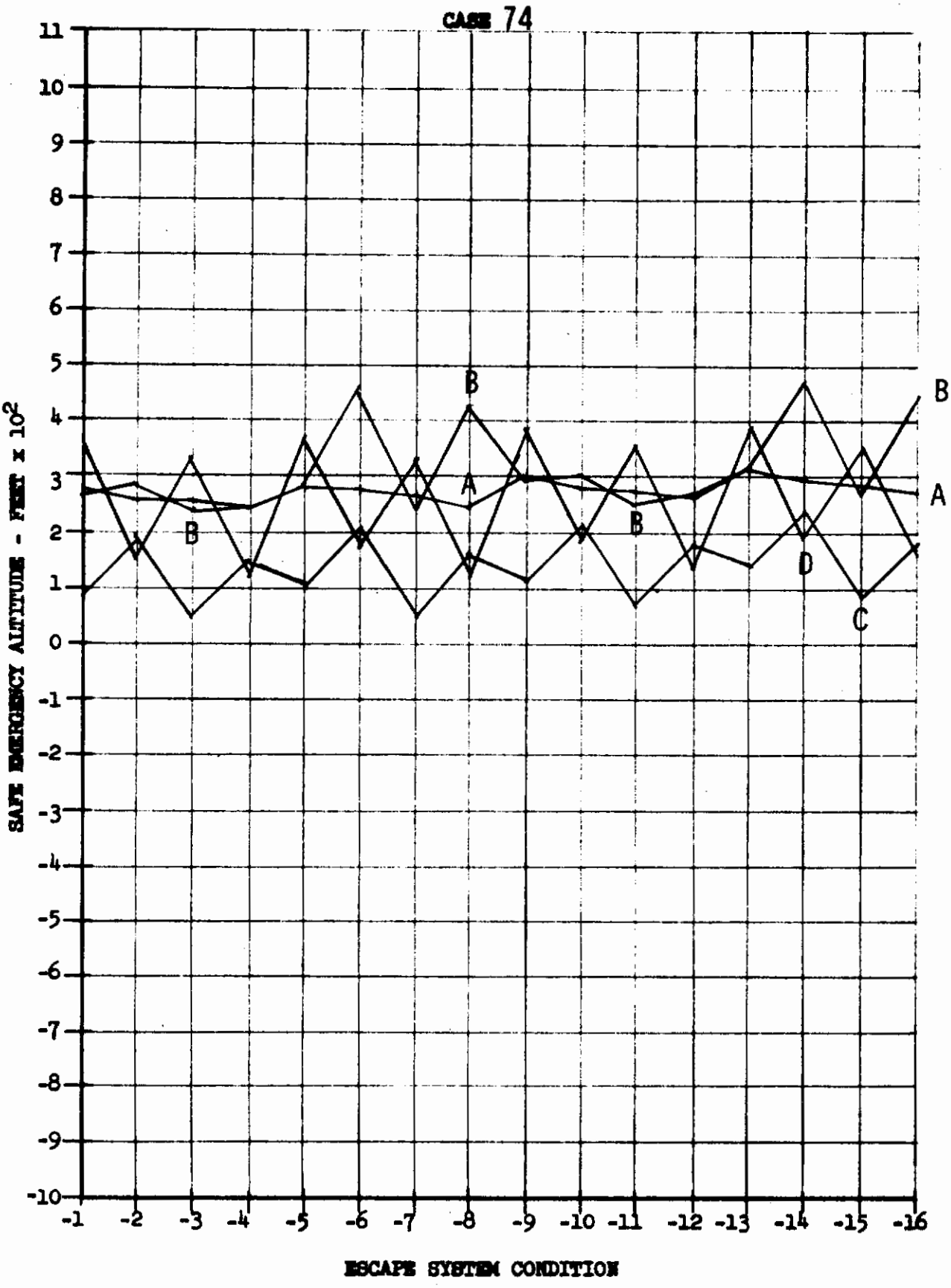

Approved for Public Release

Contrails

CASE 75

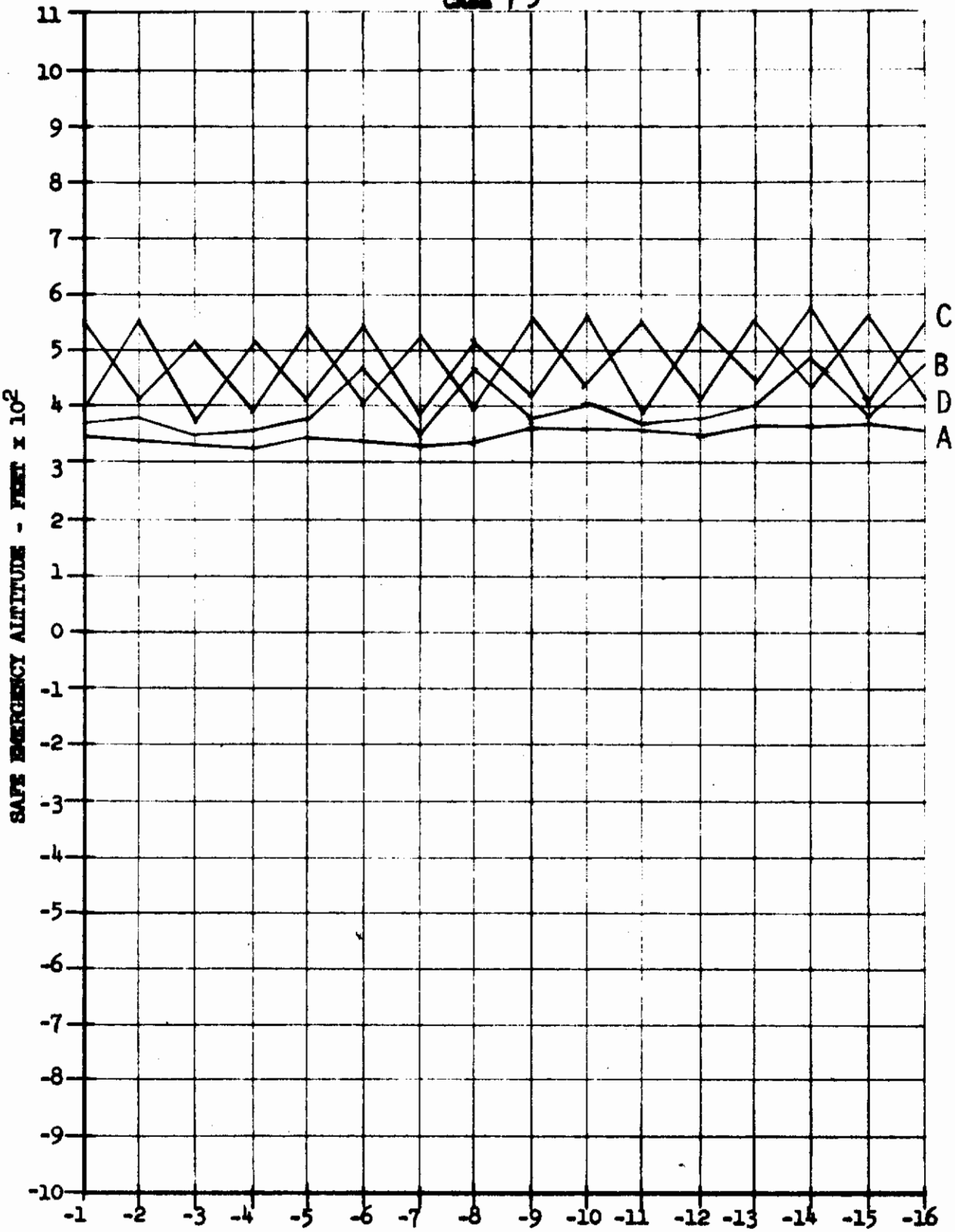

Approved for Public Release

Contrails

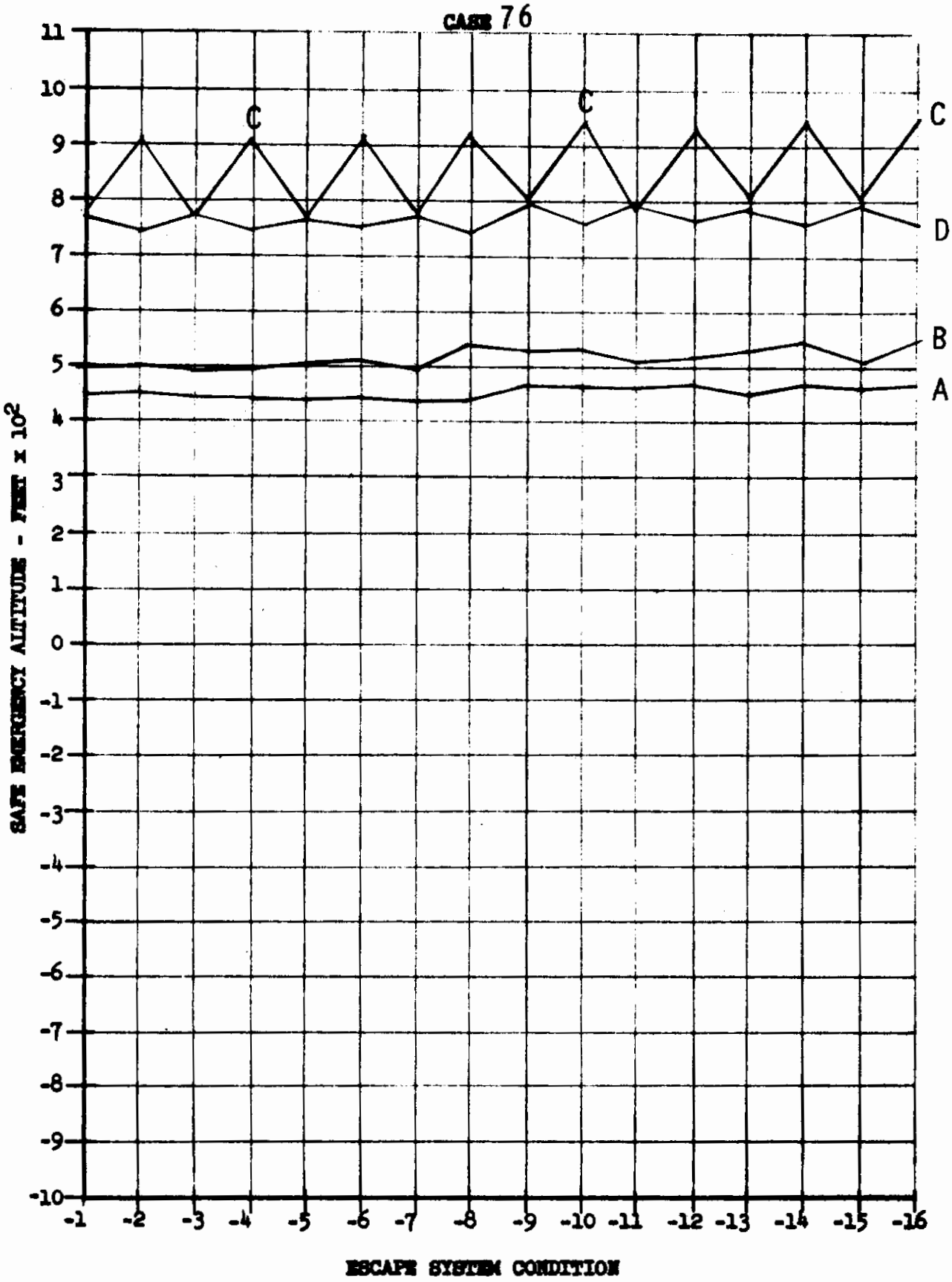

Approved for Public Release

Contrails

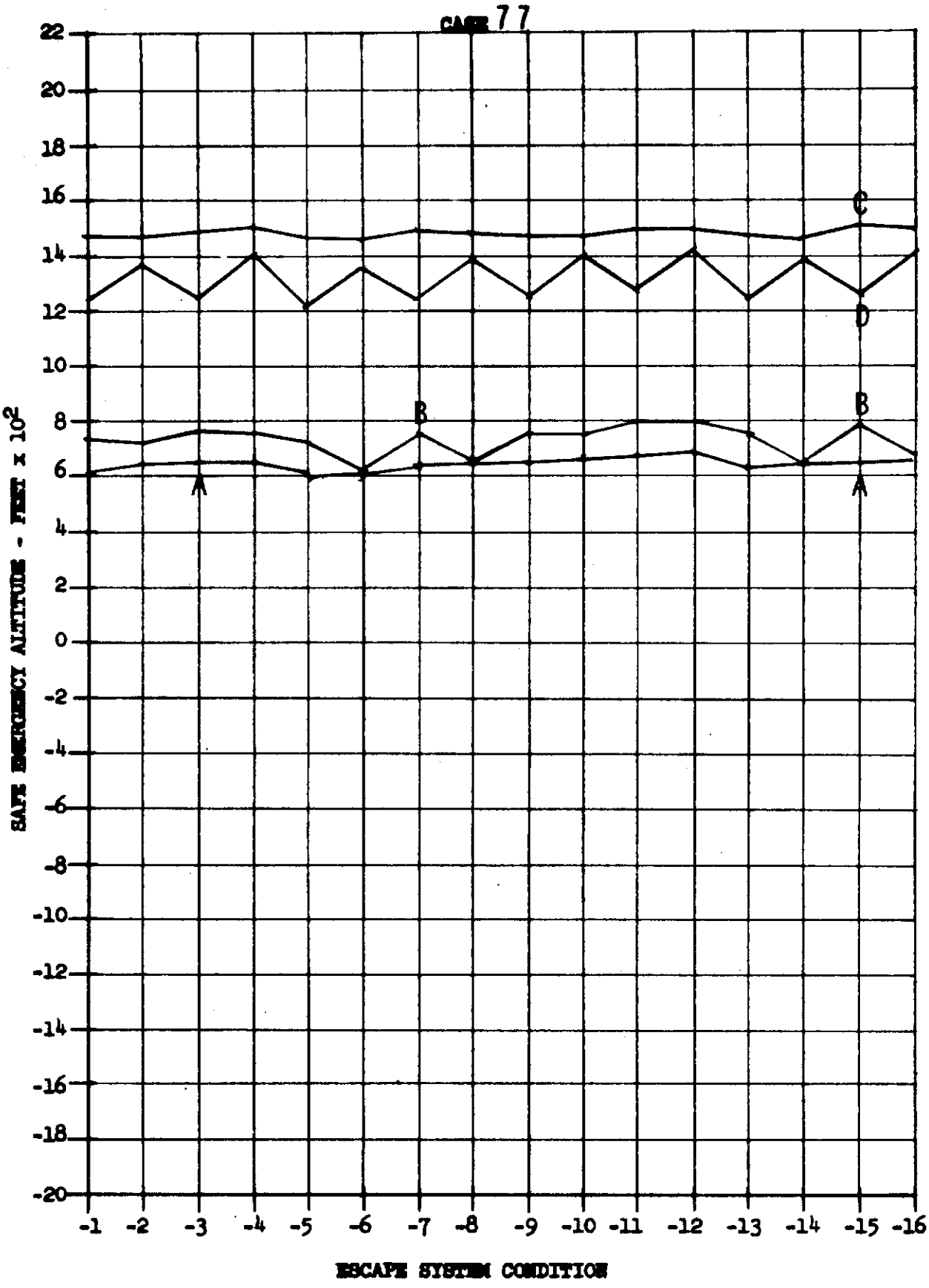

Approved for Public Release

Contrails

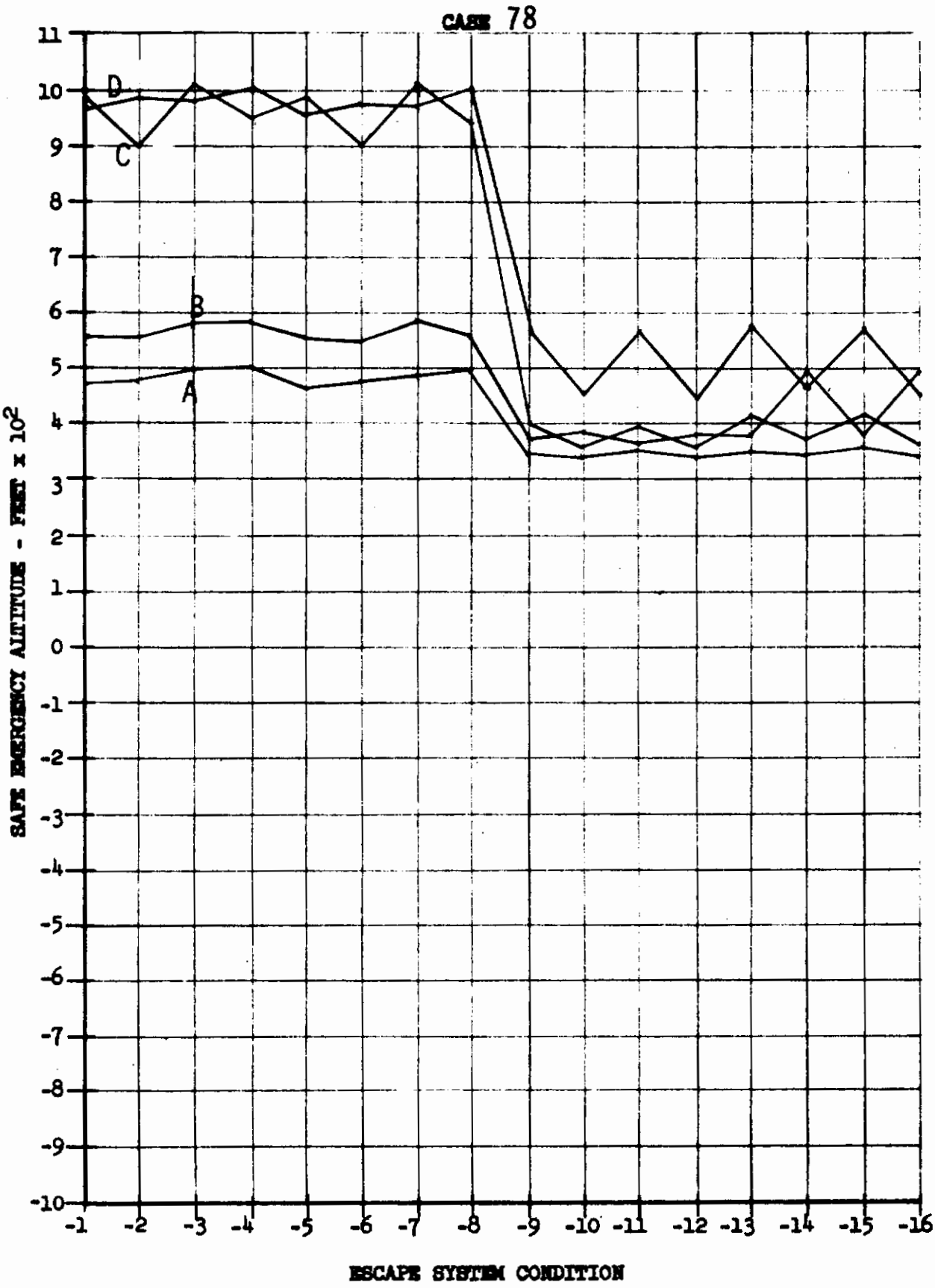

Approved for Public Release

Contrails

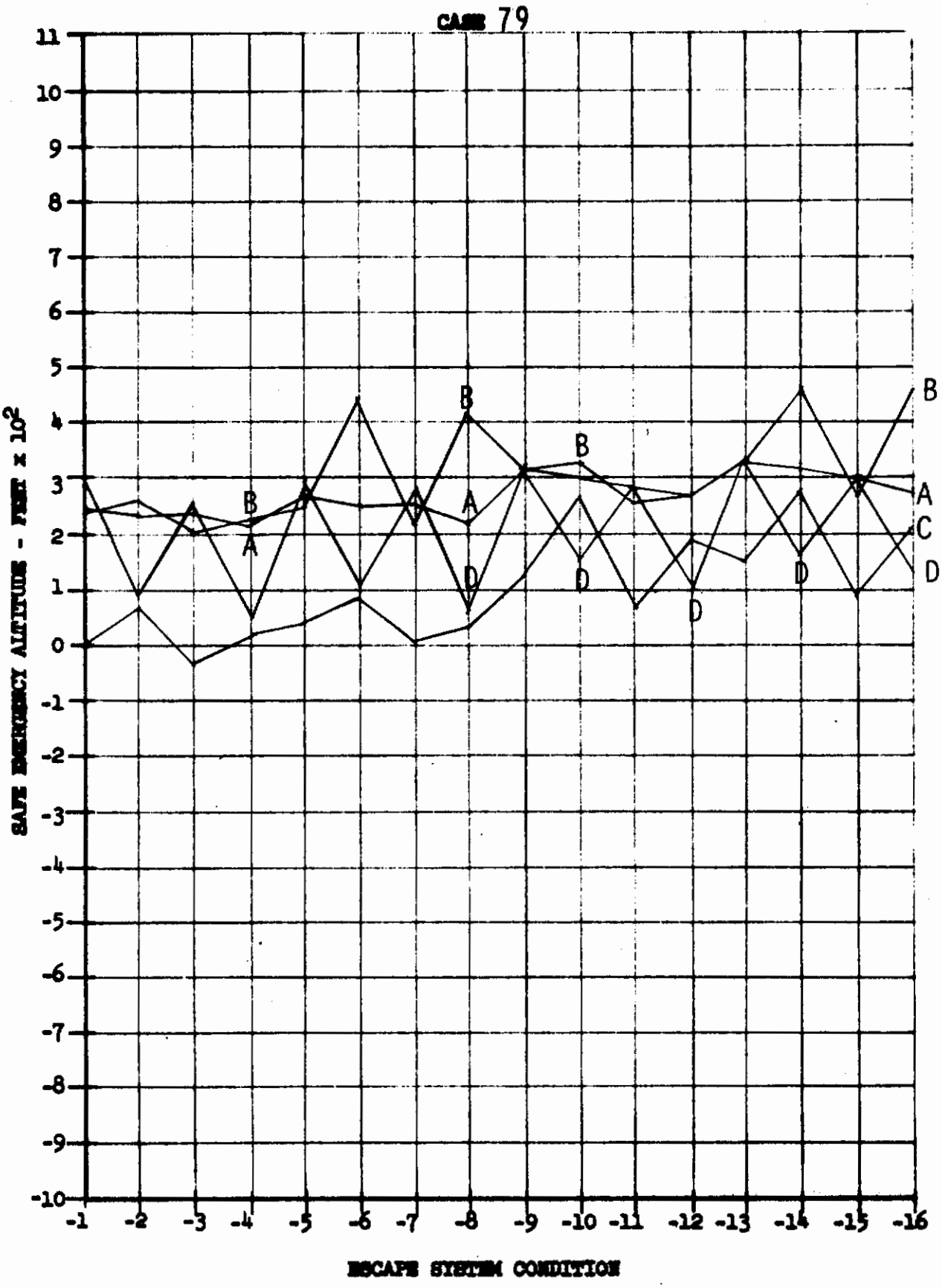

Approved for Public Release

Contrails

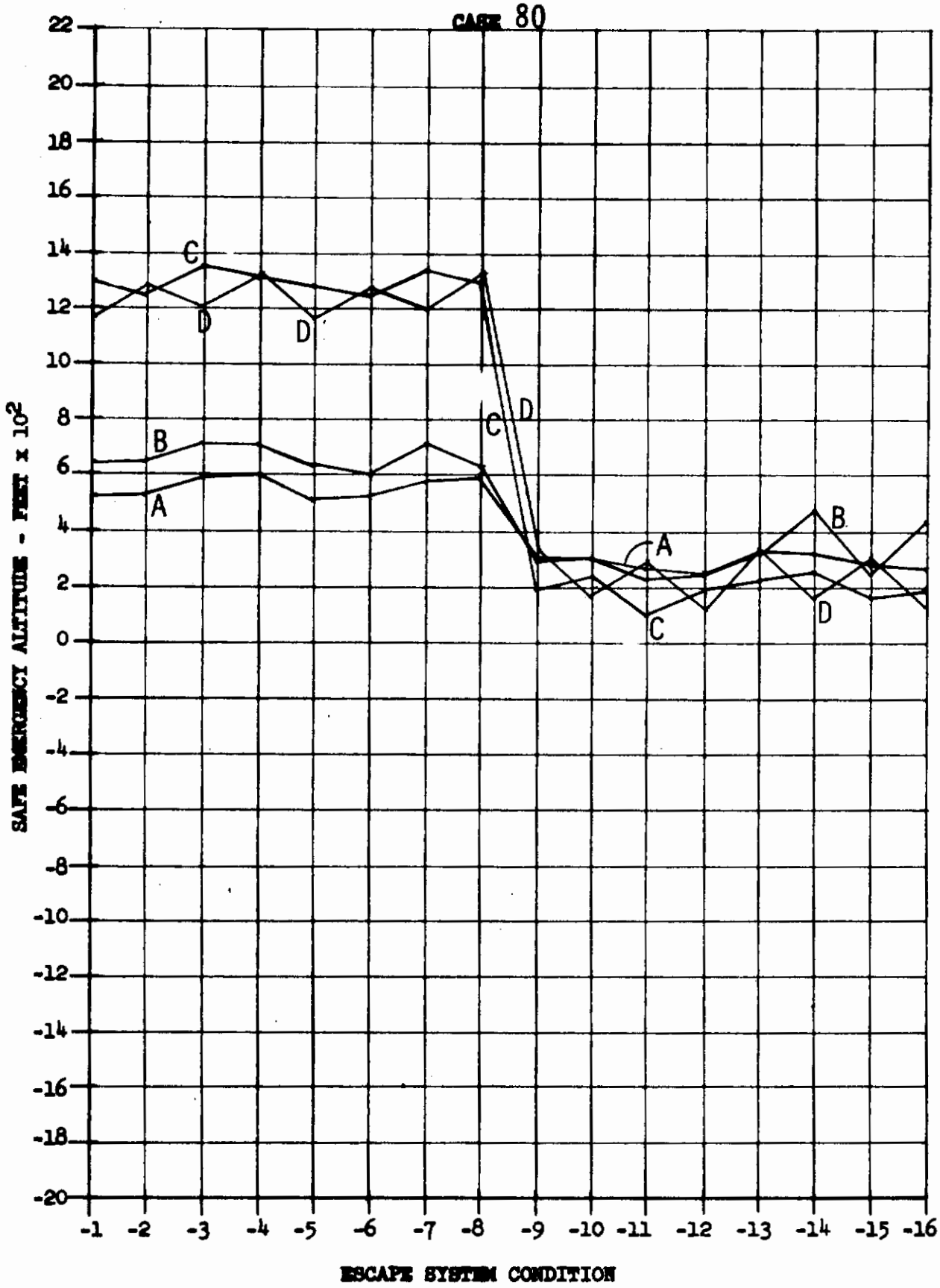

Approved for Public Release

Contrails

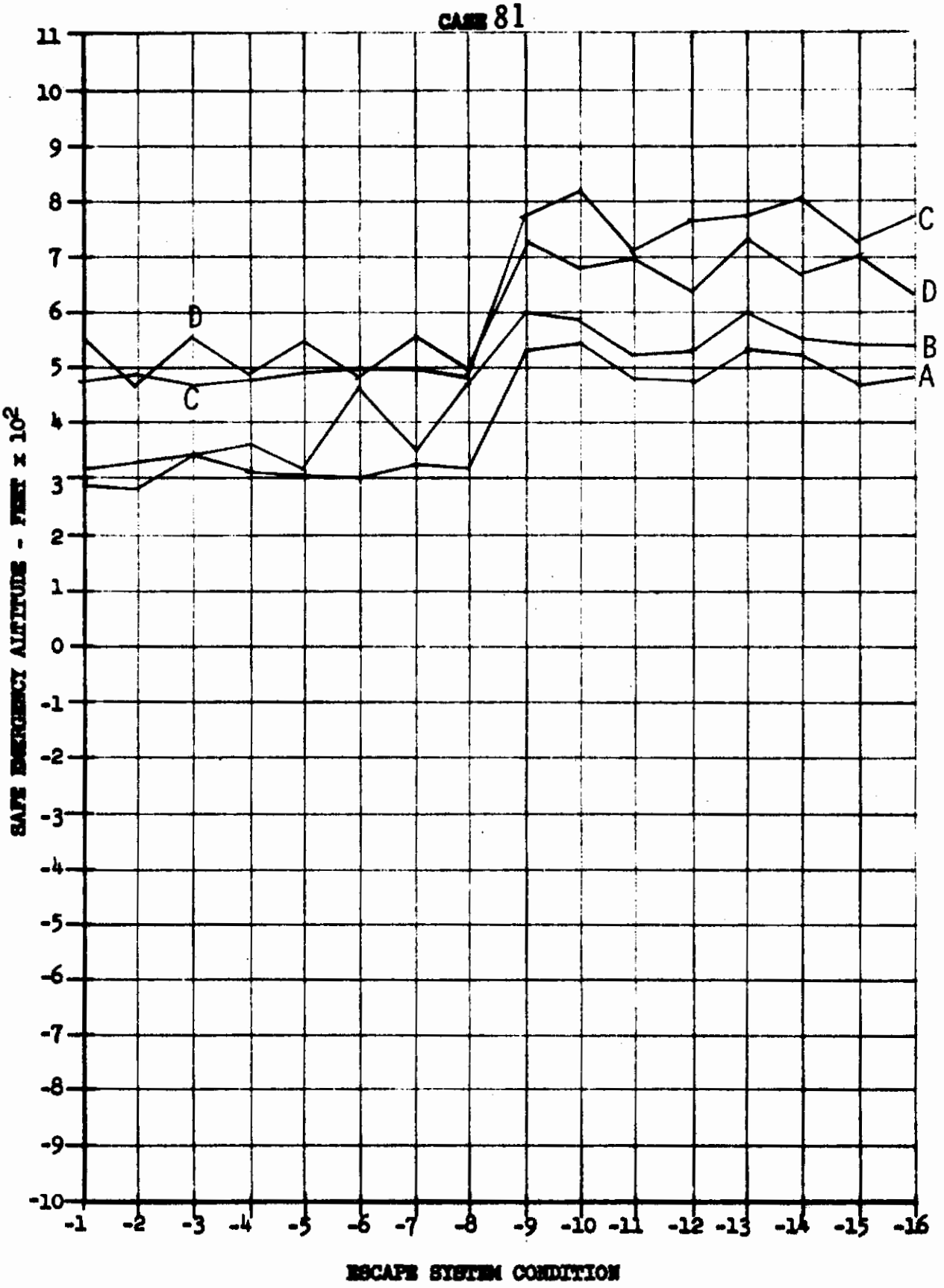

Approved for Public Release

Contrails

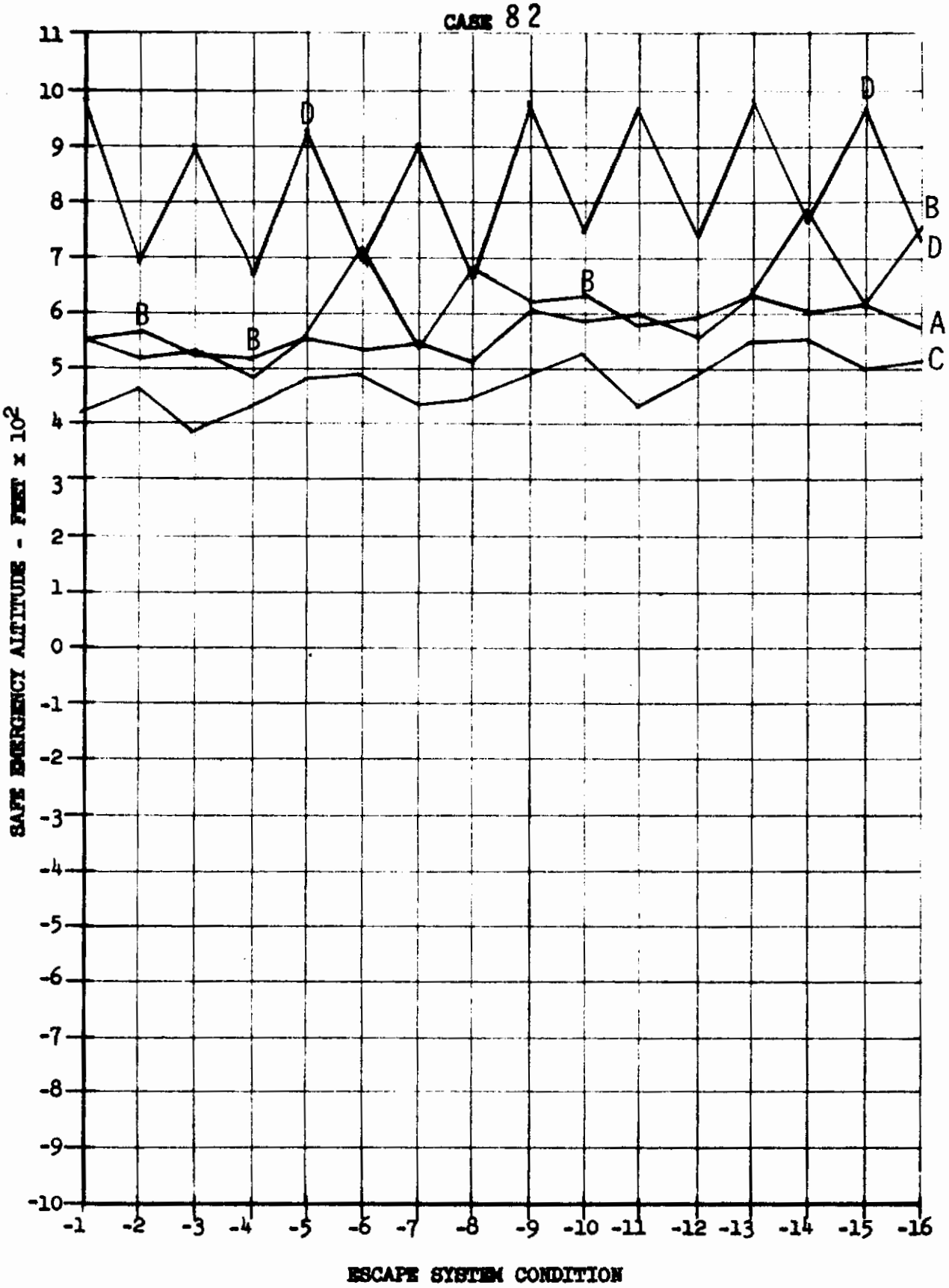

Approved for Public Release

Contrails

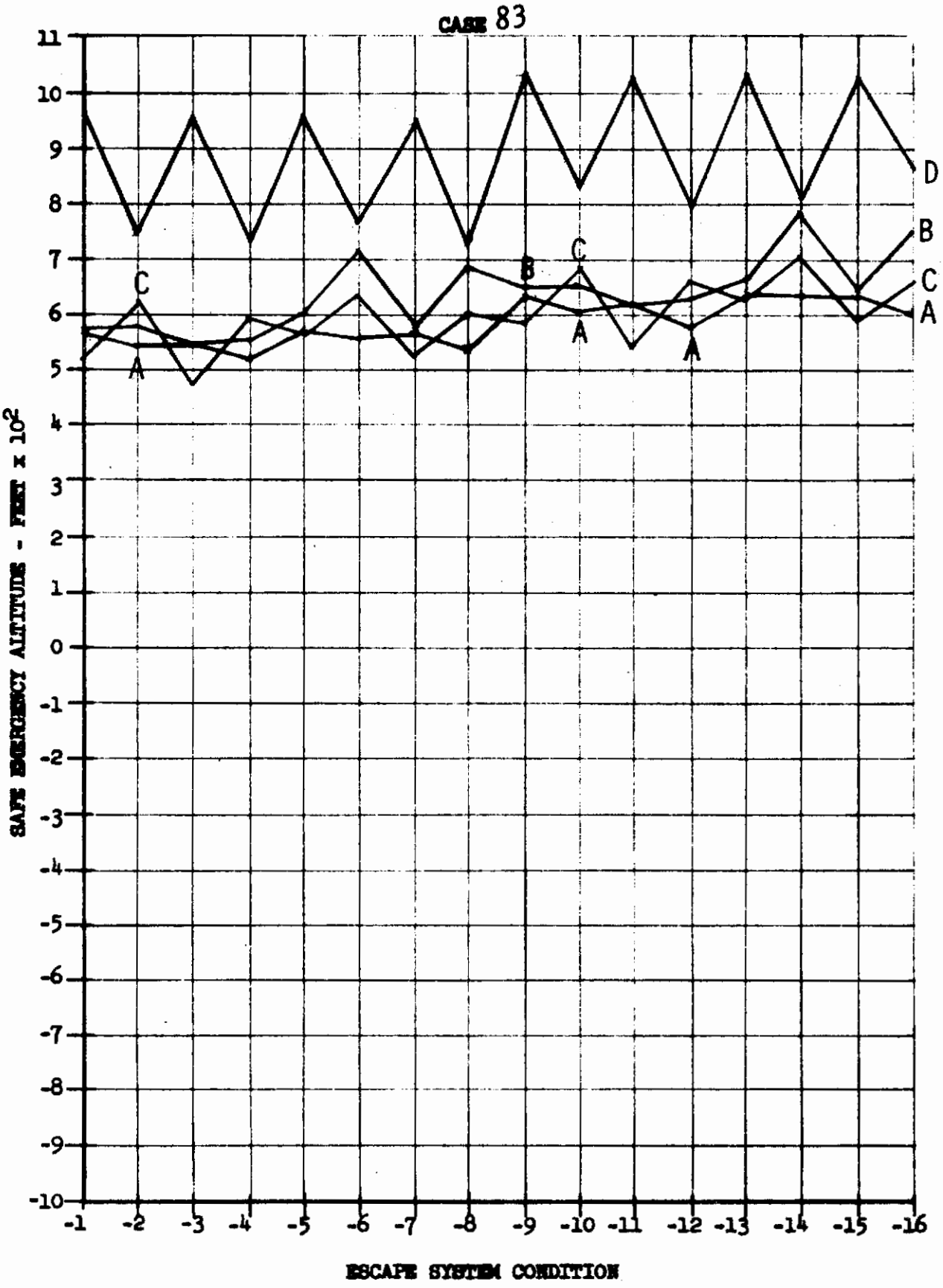

Approved for Public Release

Contrails

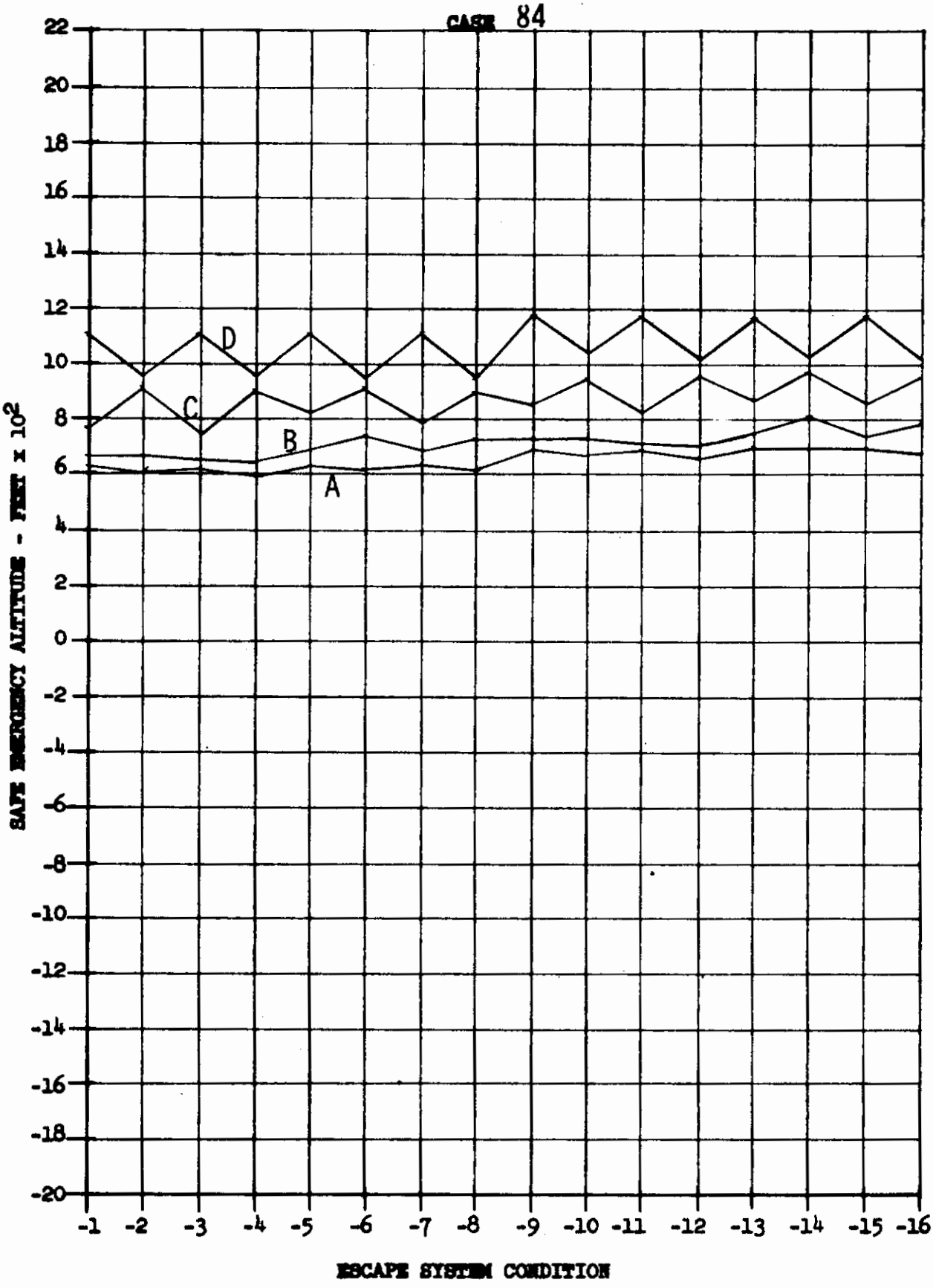

Approved for Public Release

Contrails

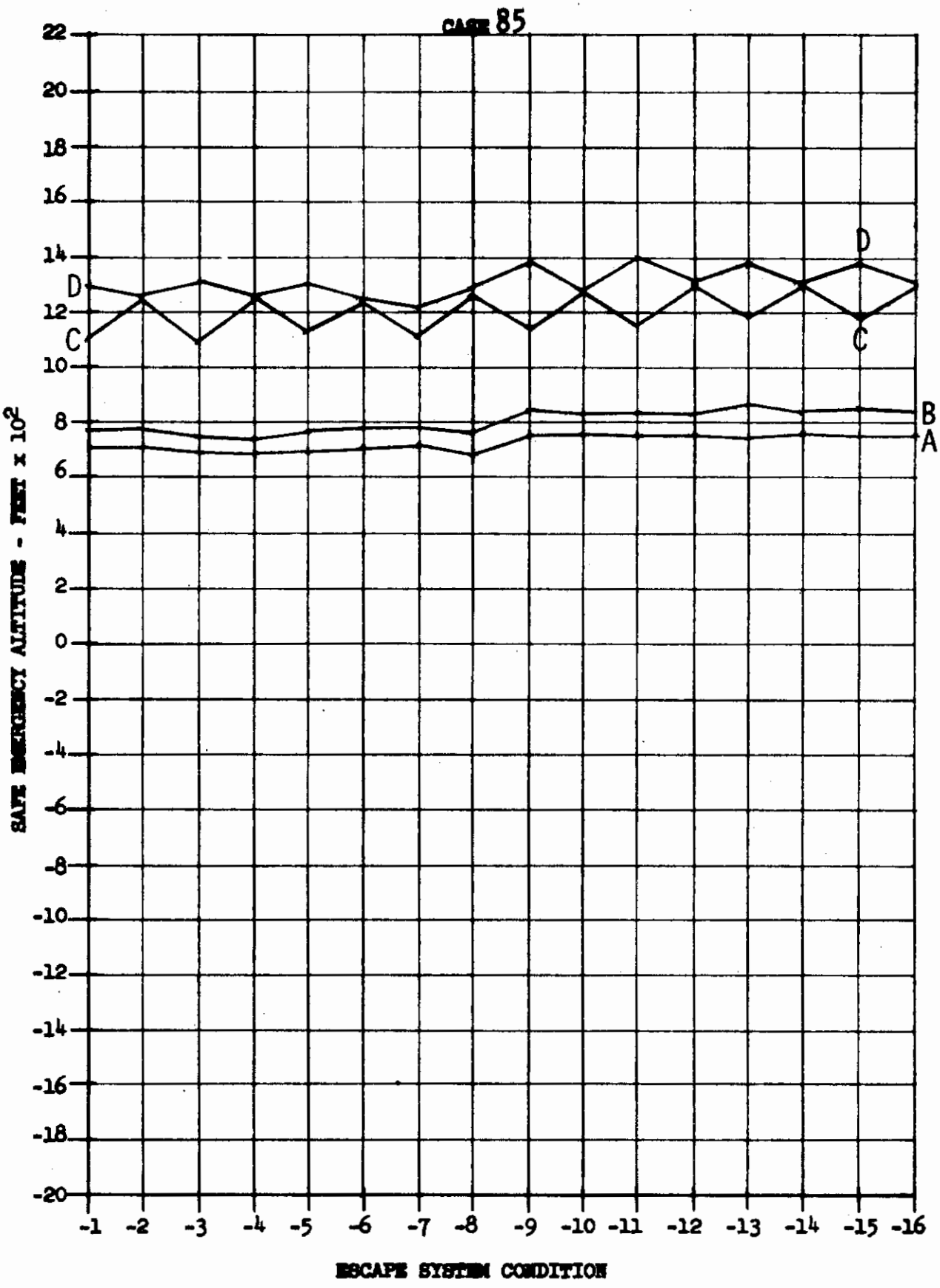

Approved for Public Release

Contrails

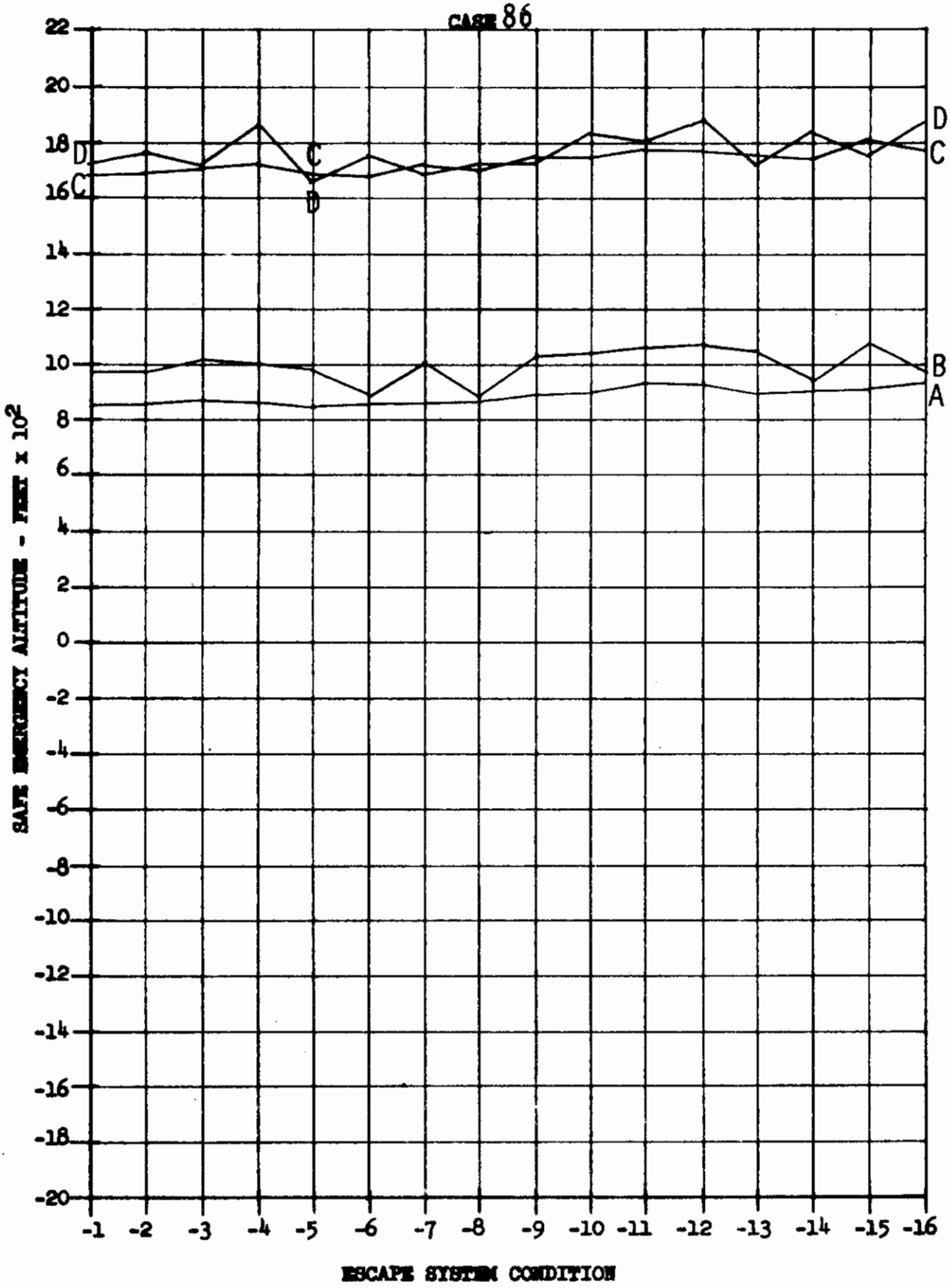

Approved for Public Release

Contrails

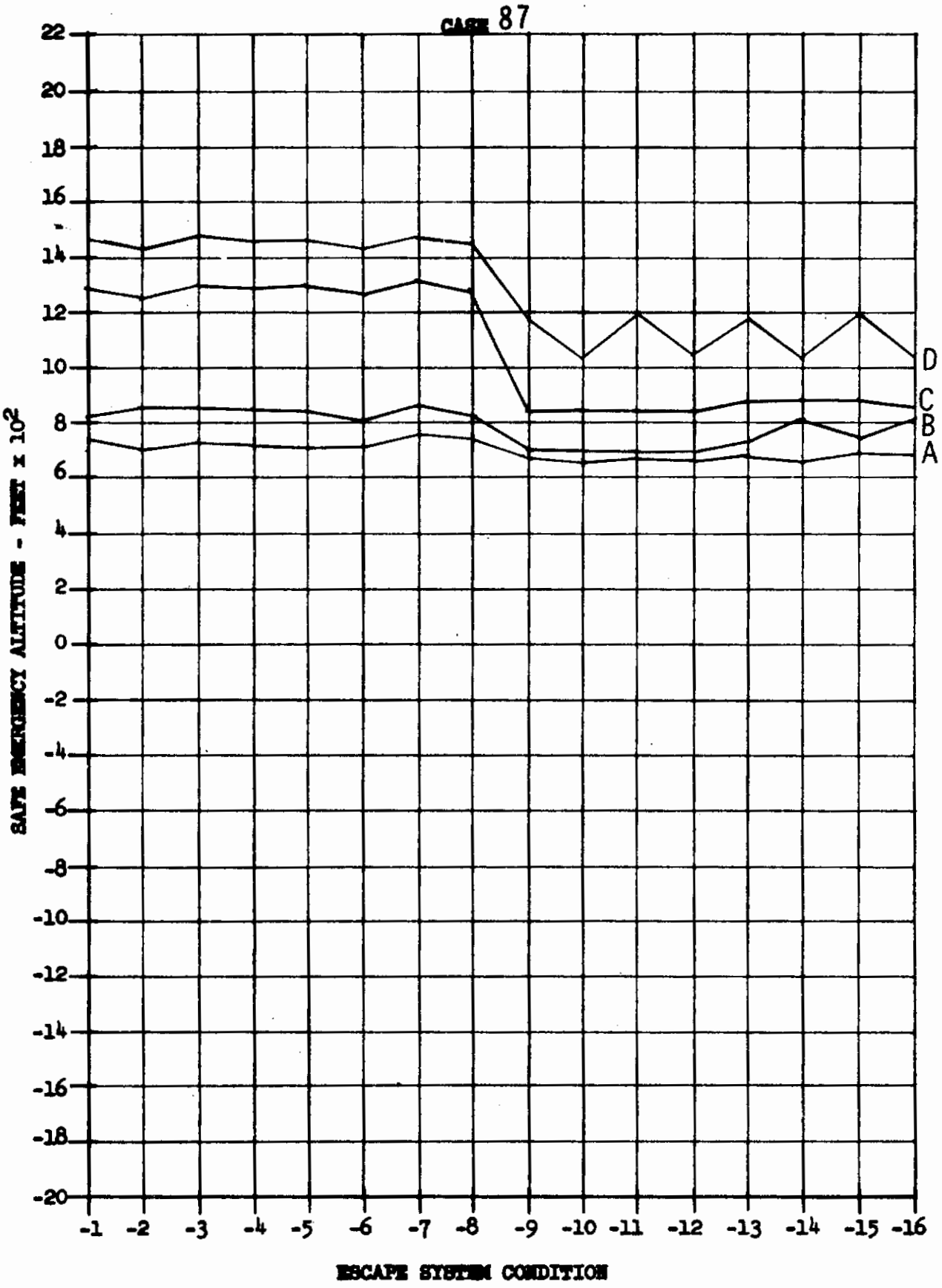

Approved for Public Release

Contrails

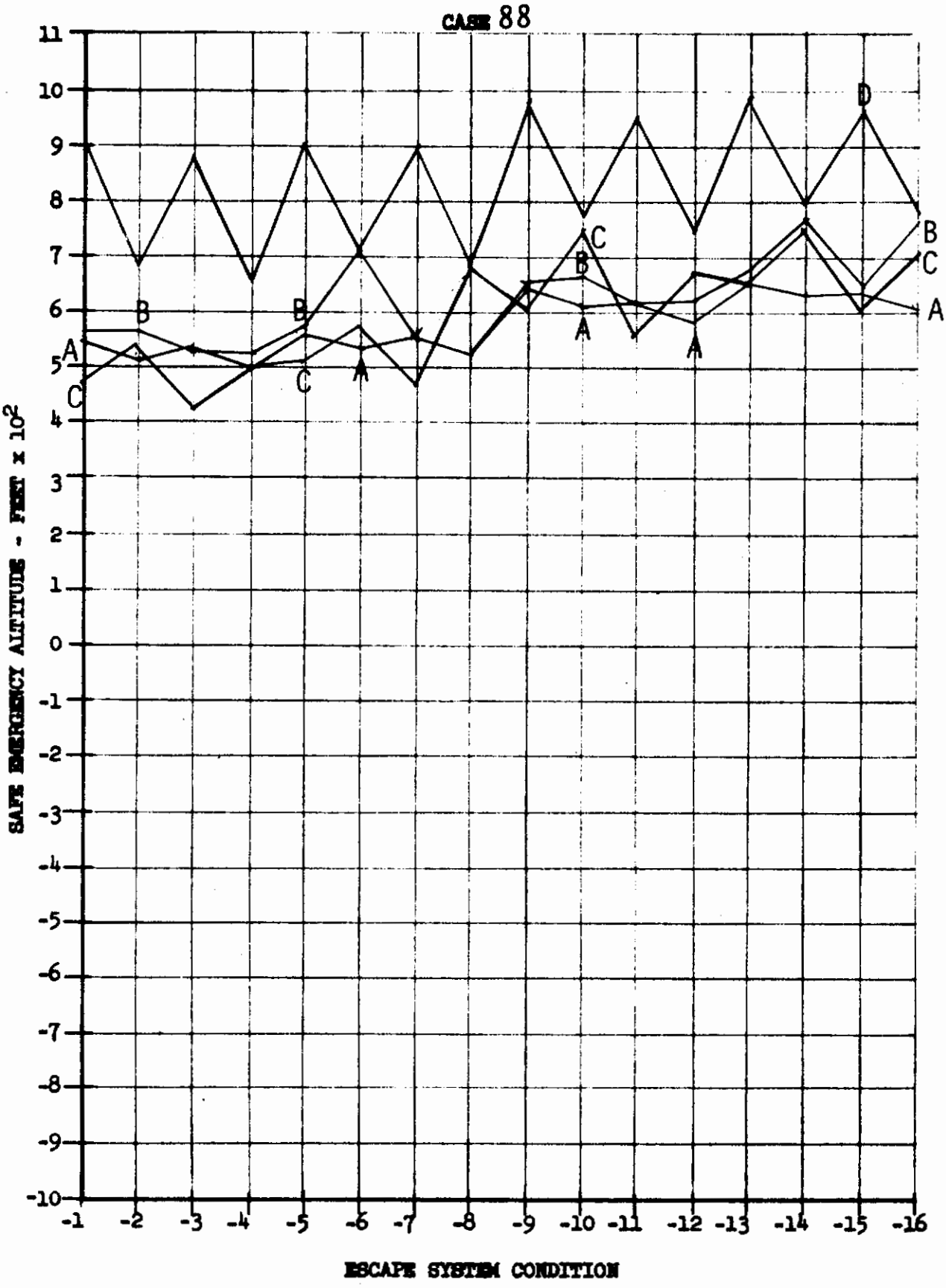

Approved for Public Release

Contrails

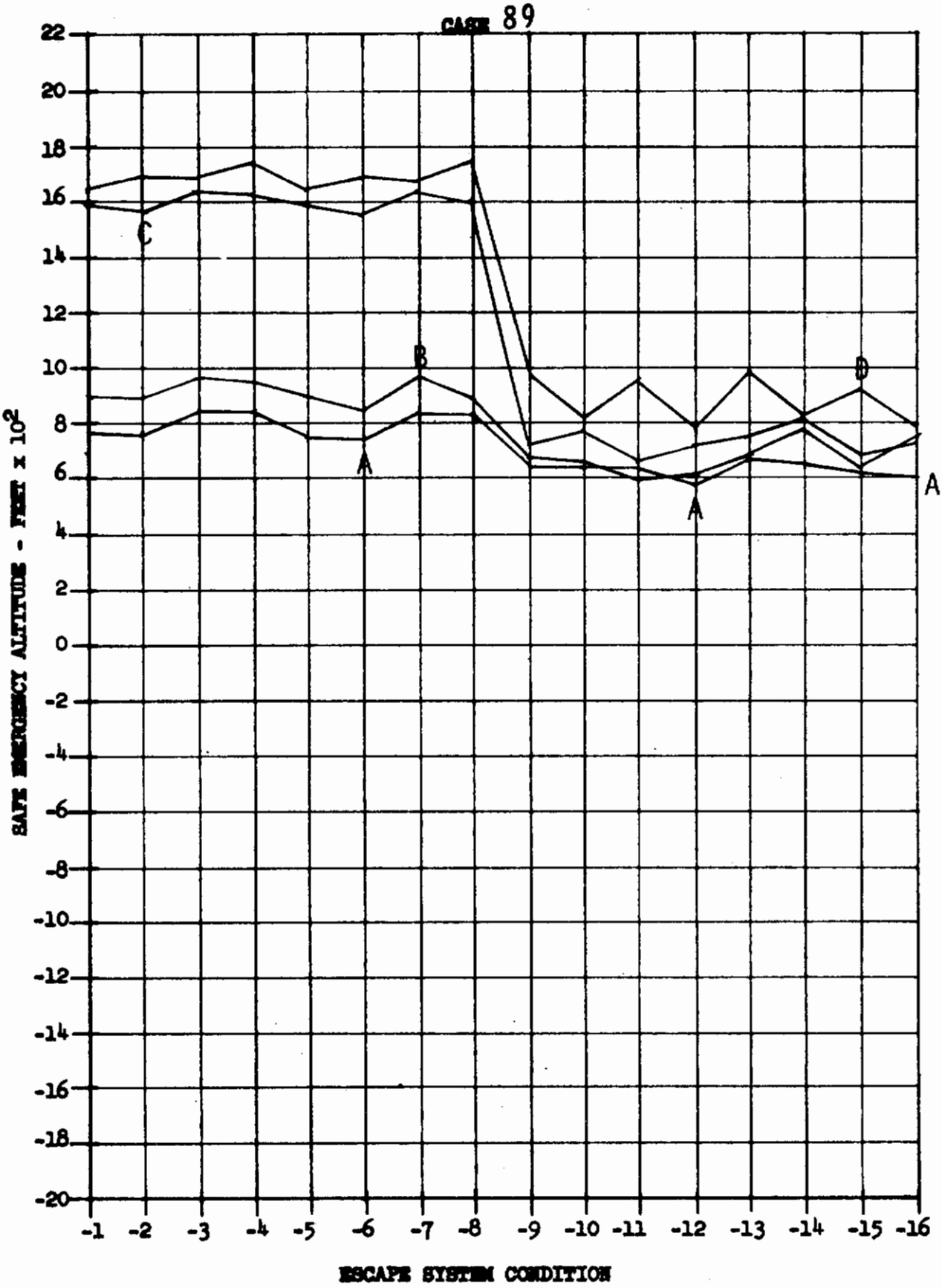

Approved for Public Release

Contrails

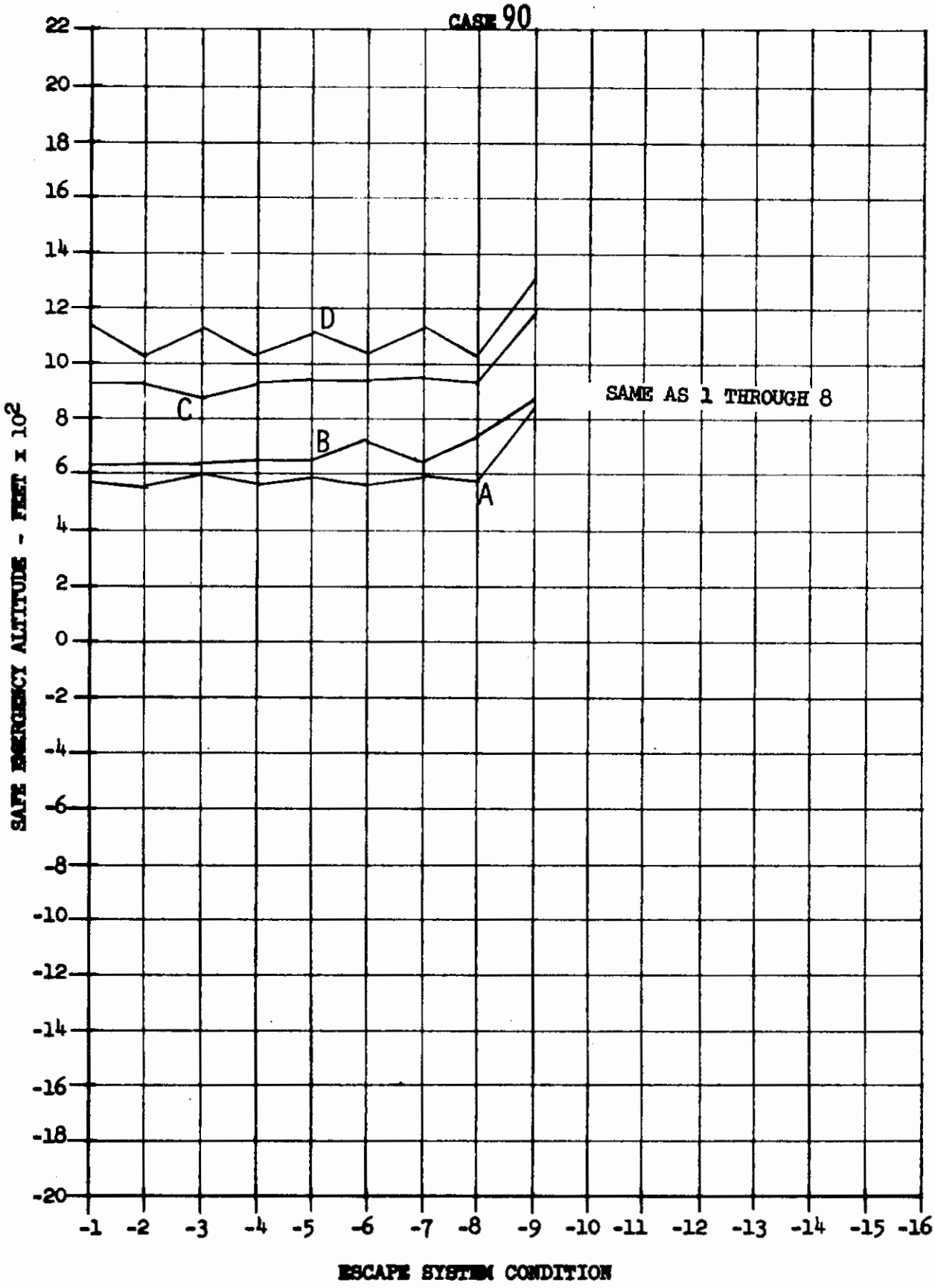

Approved for Public Release

Contrails

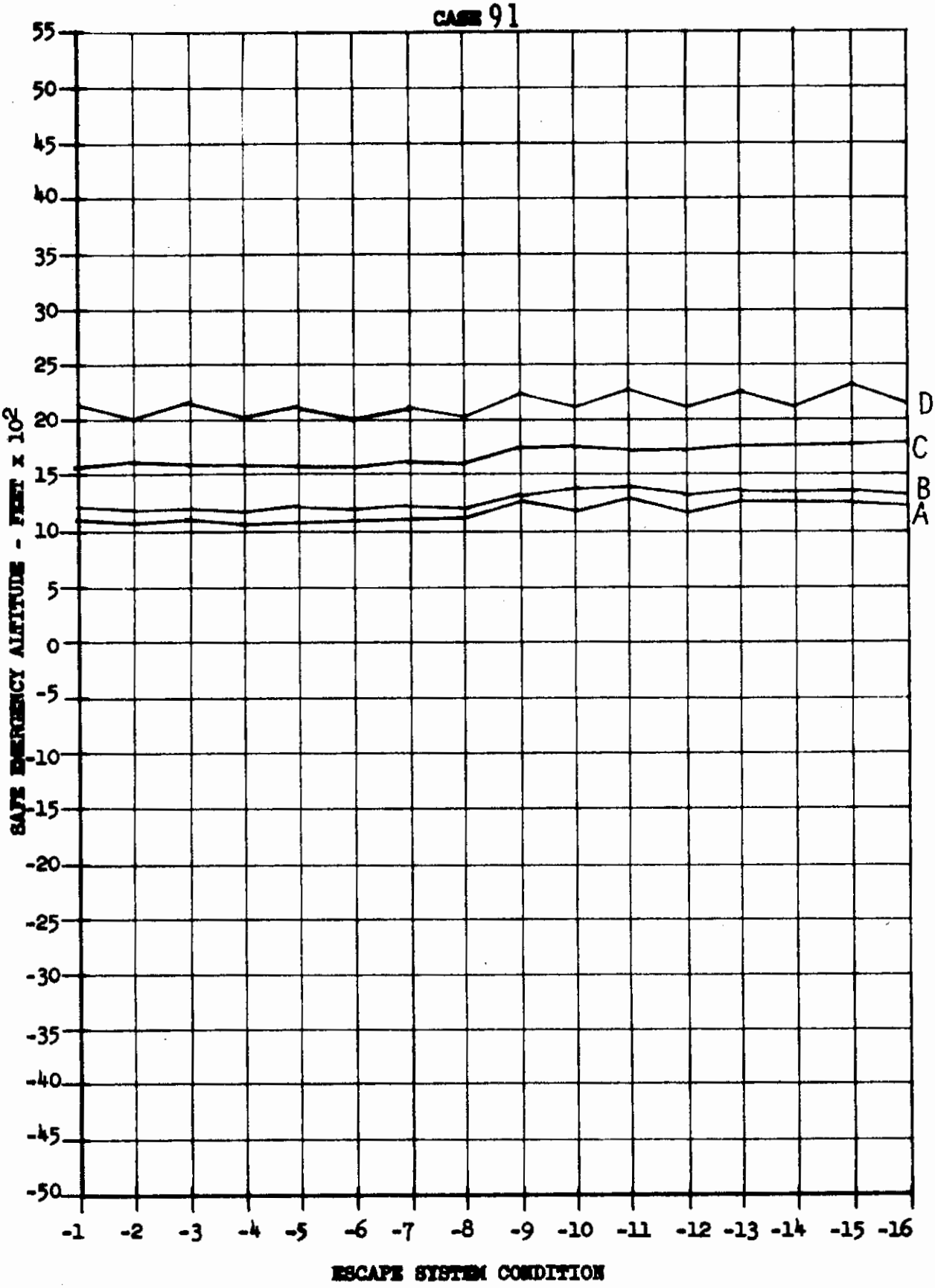

Approved for Public Release

Contrails

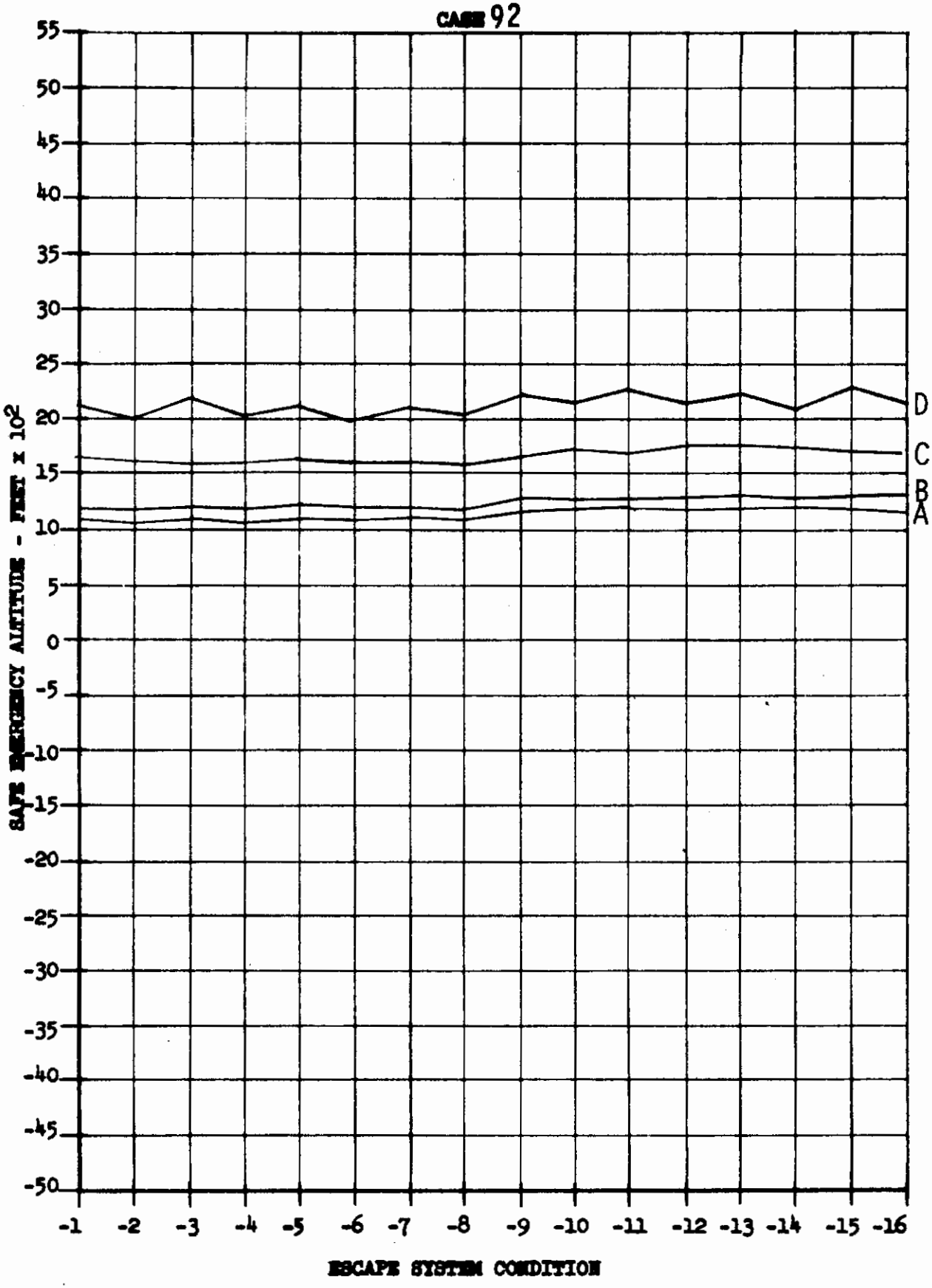

Approved for Public Release

Contrails

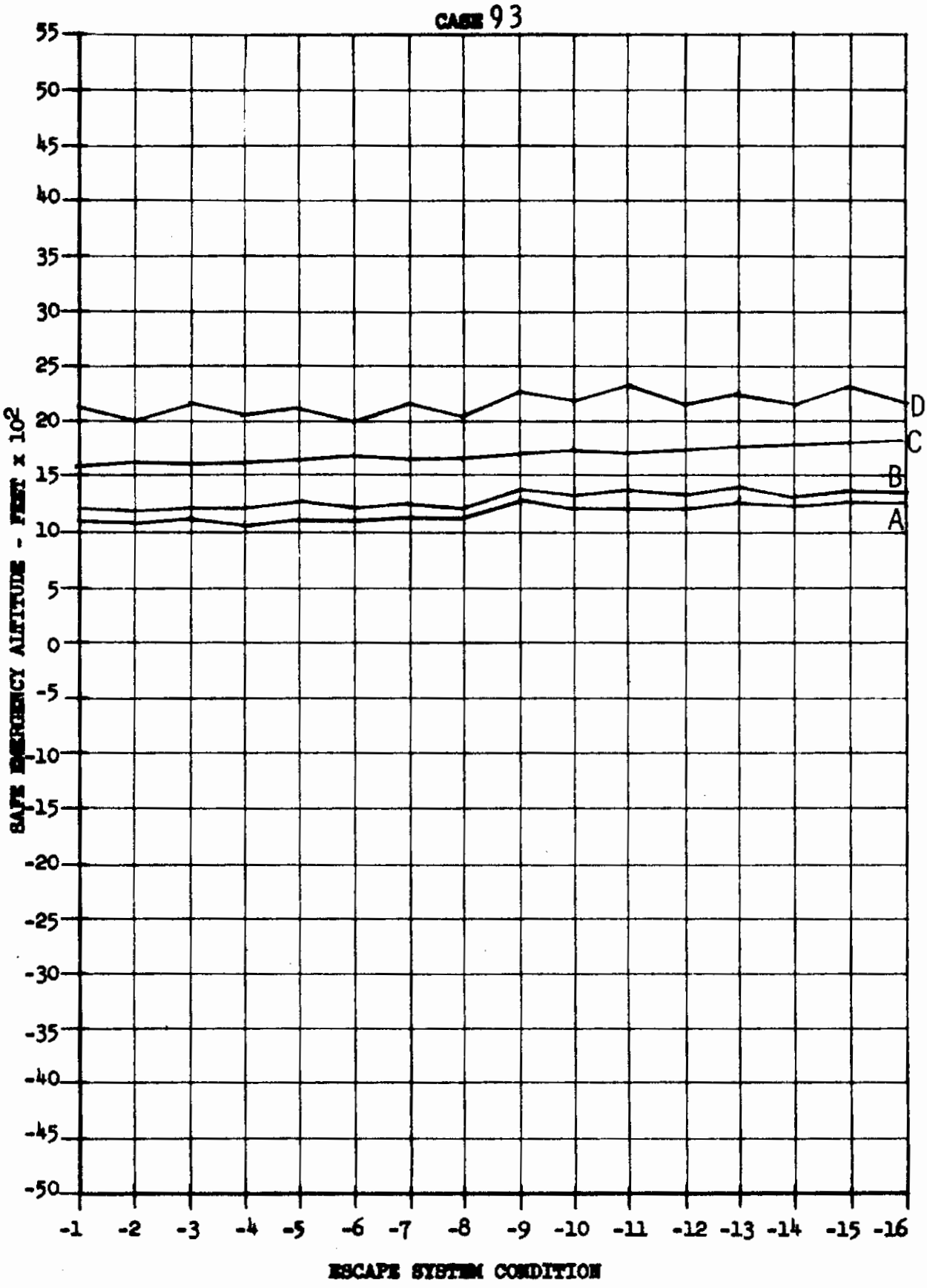

Approved for Public Release

Contrails

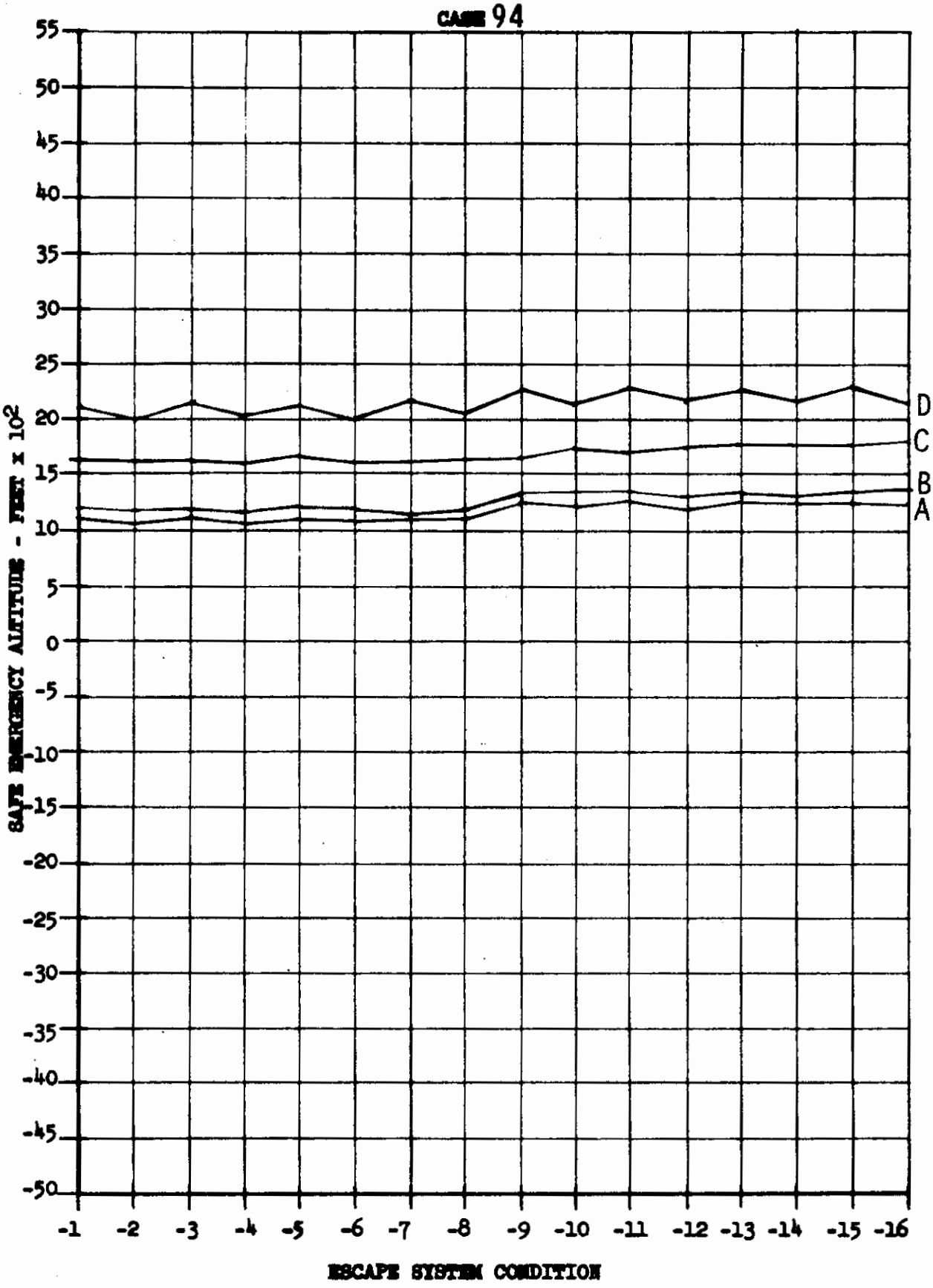

Approved for Public Release

Contrails

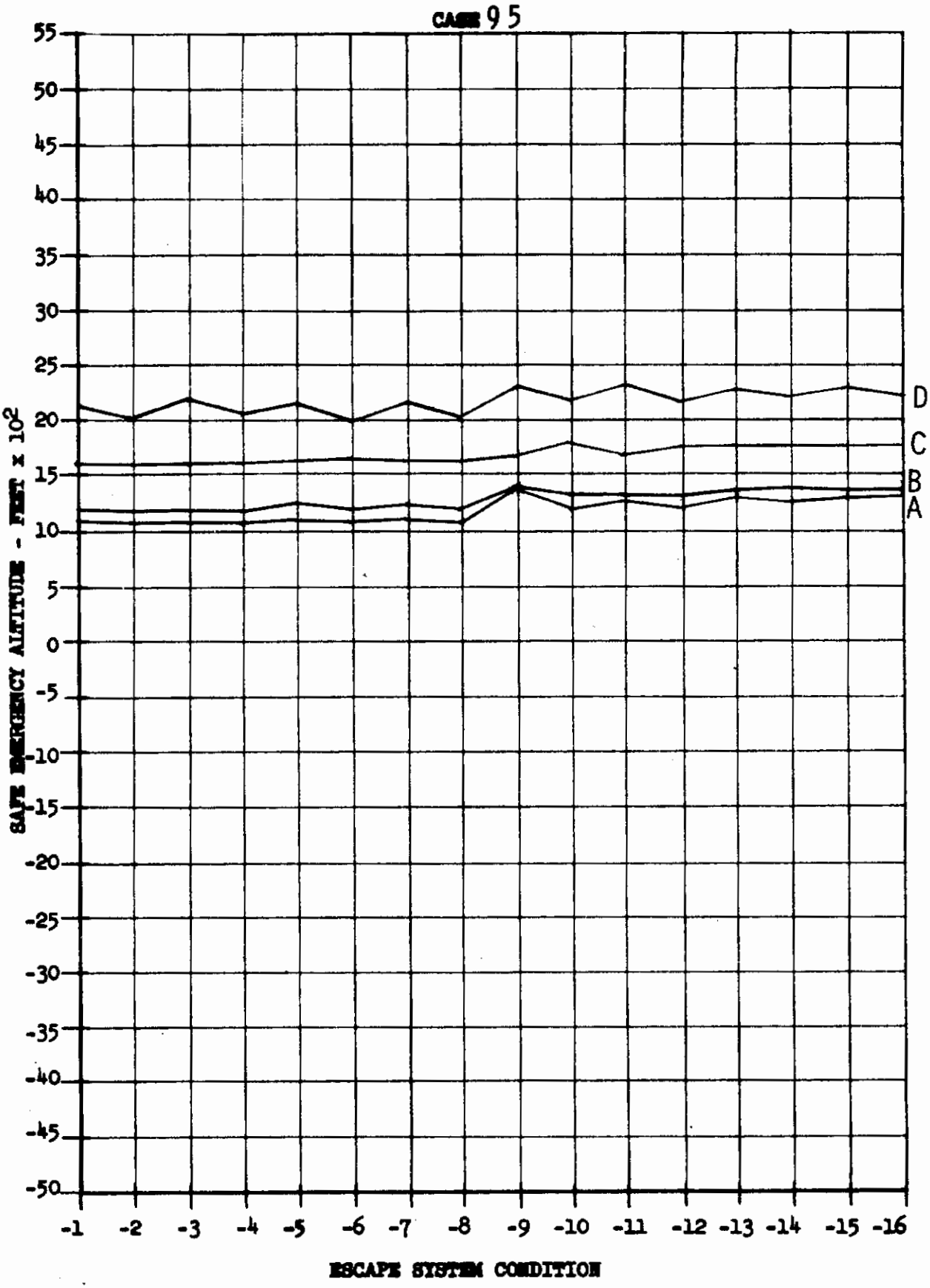

Approved for Public Release

Contrails

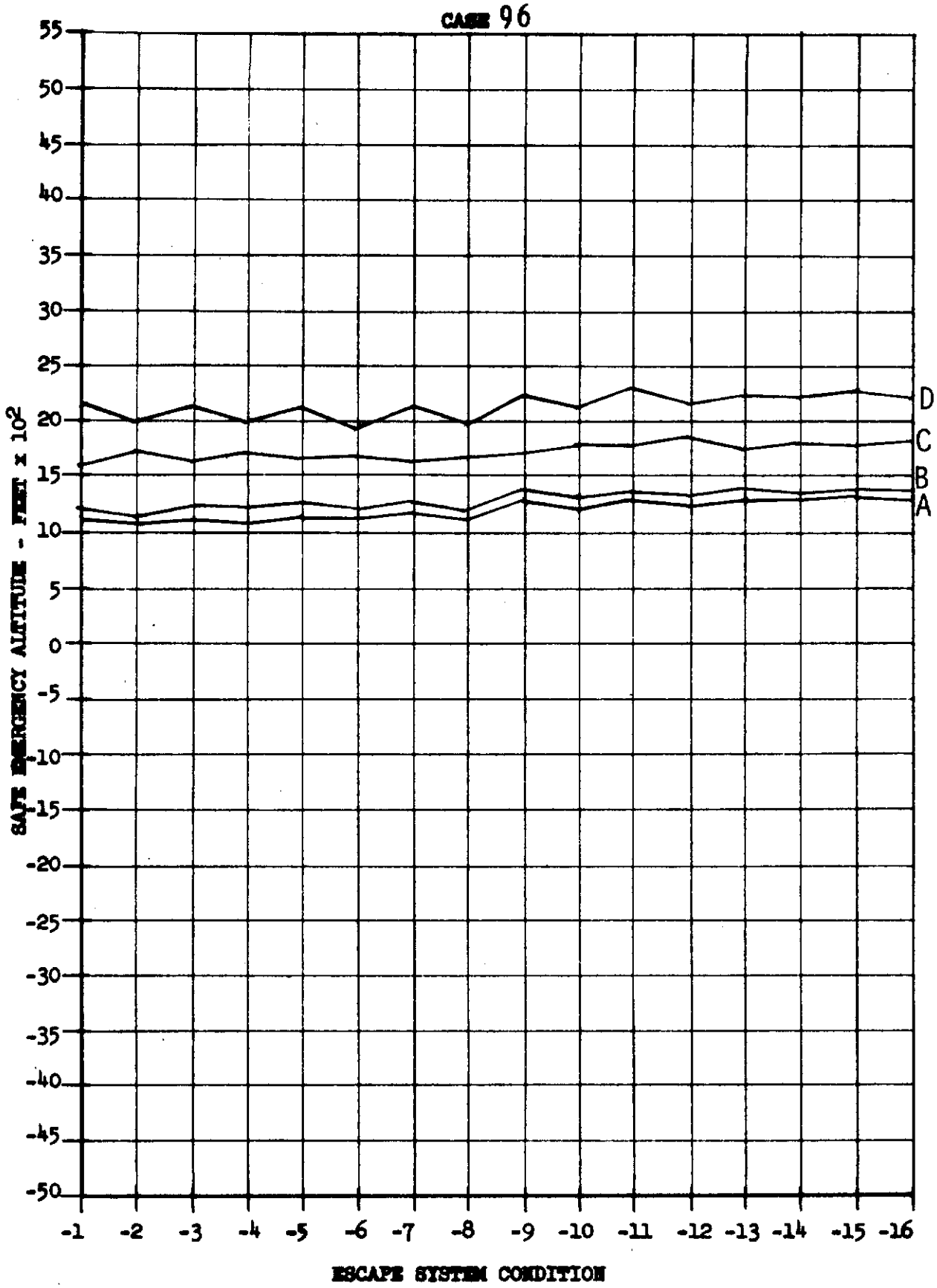

Approved for Public Release

Contrails

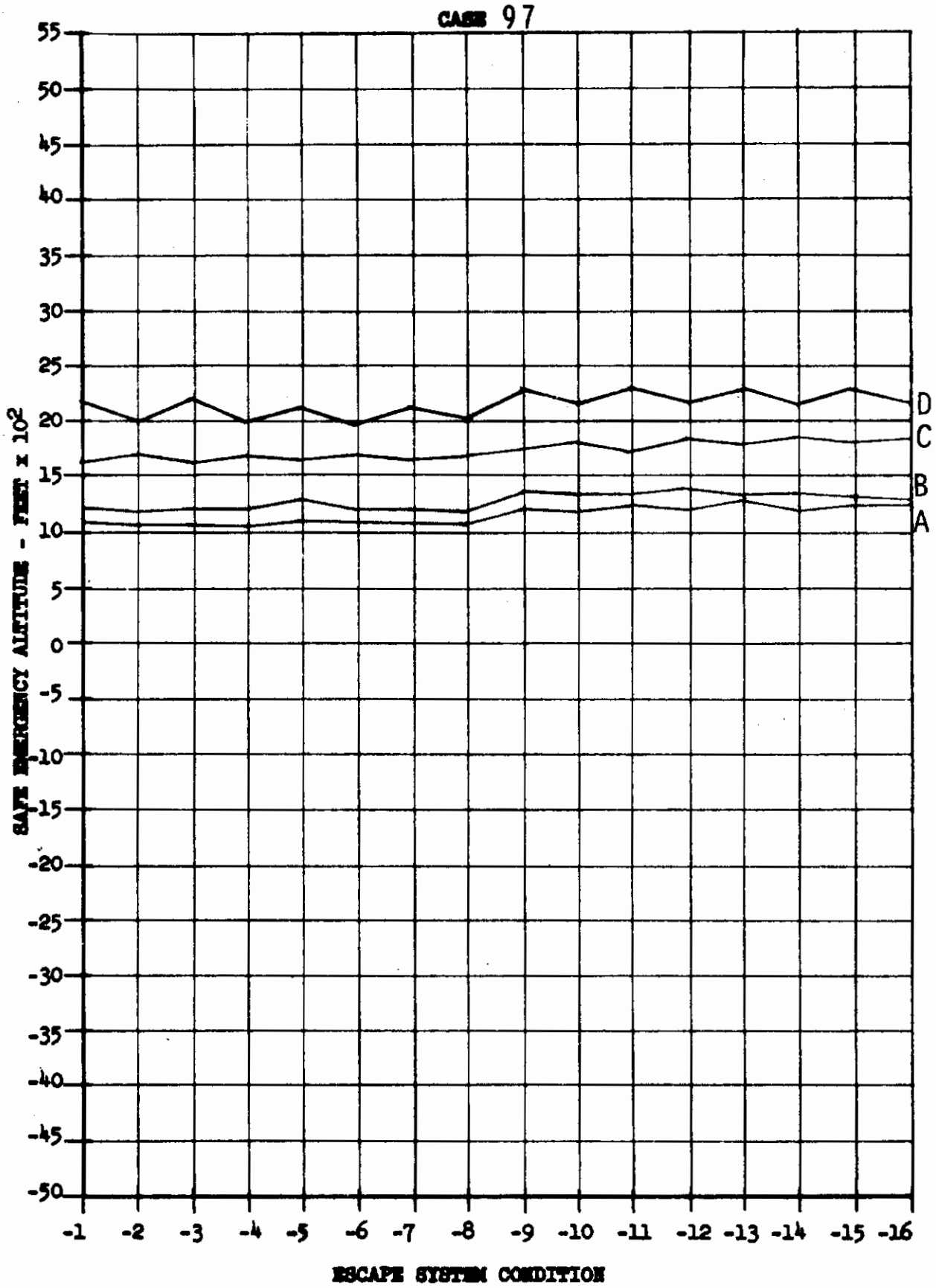

Approved for Public Release

Contrails

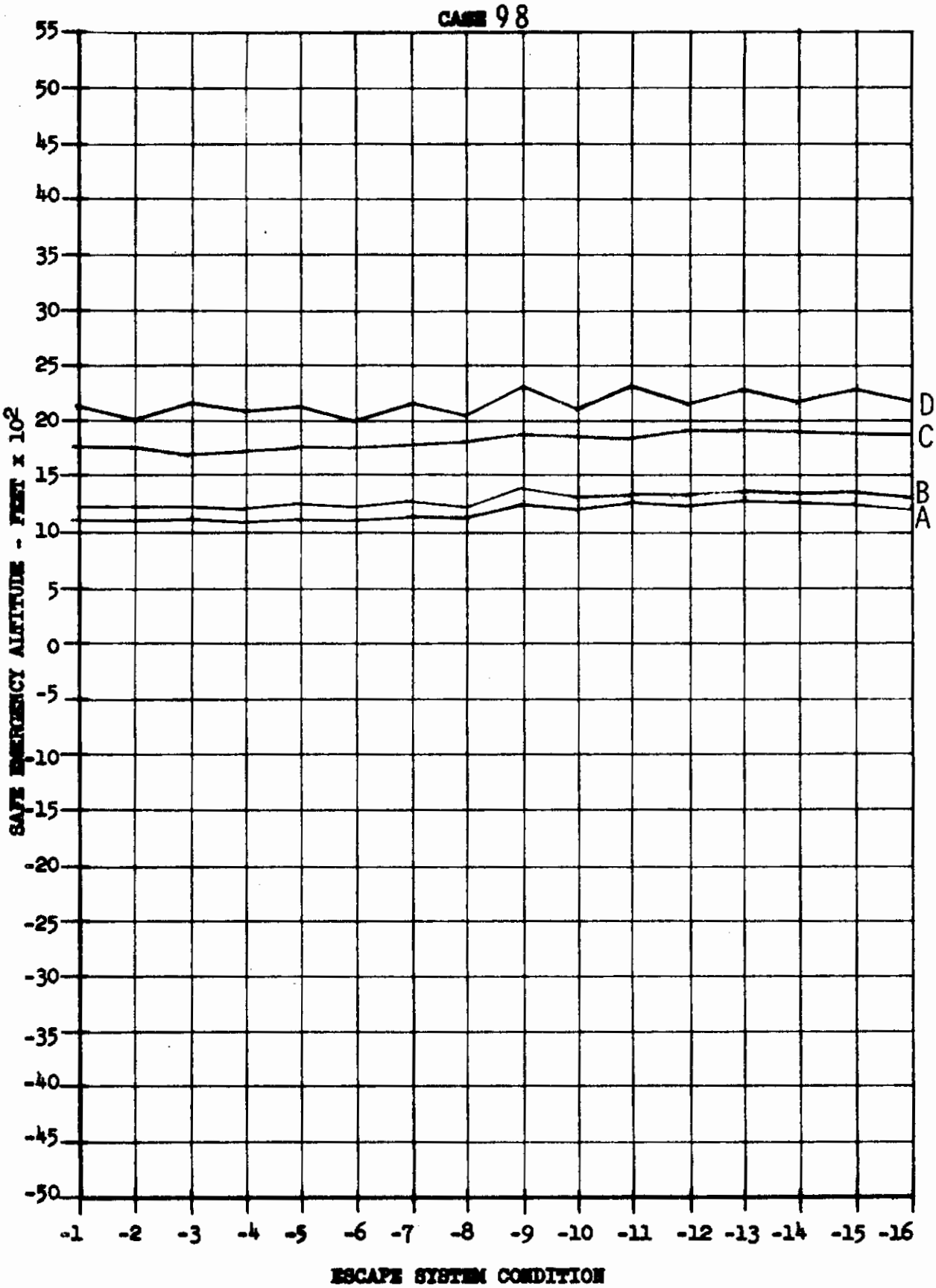

Approved for Public Release

Contrails

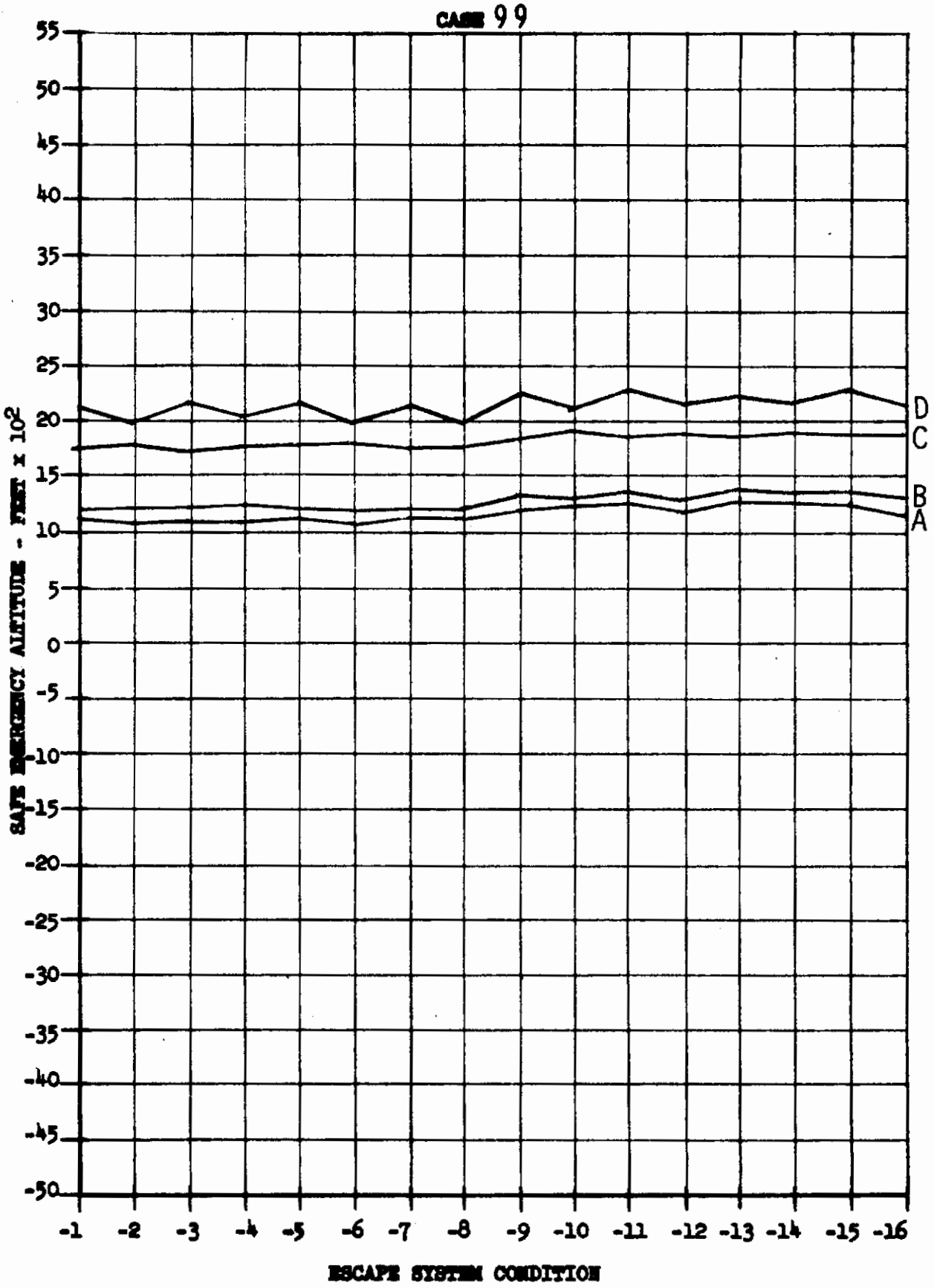

Approved for Public Release

Contrails

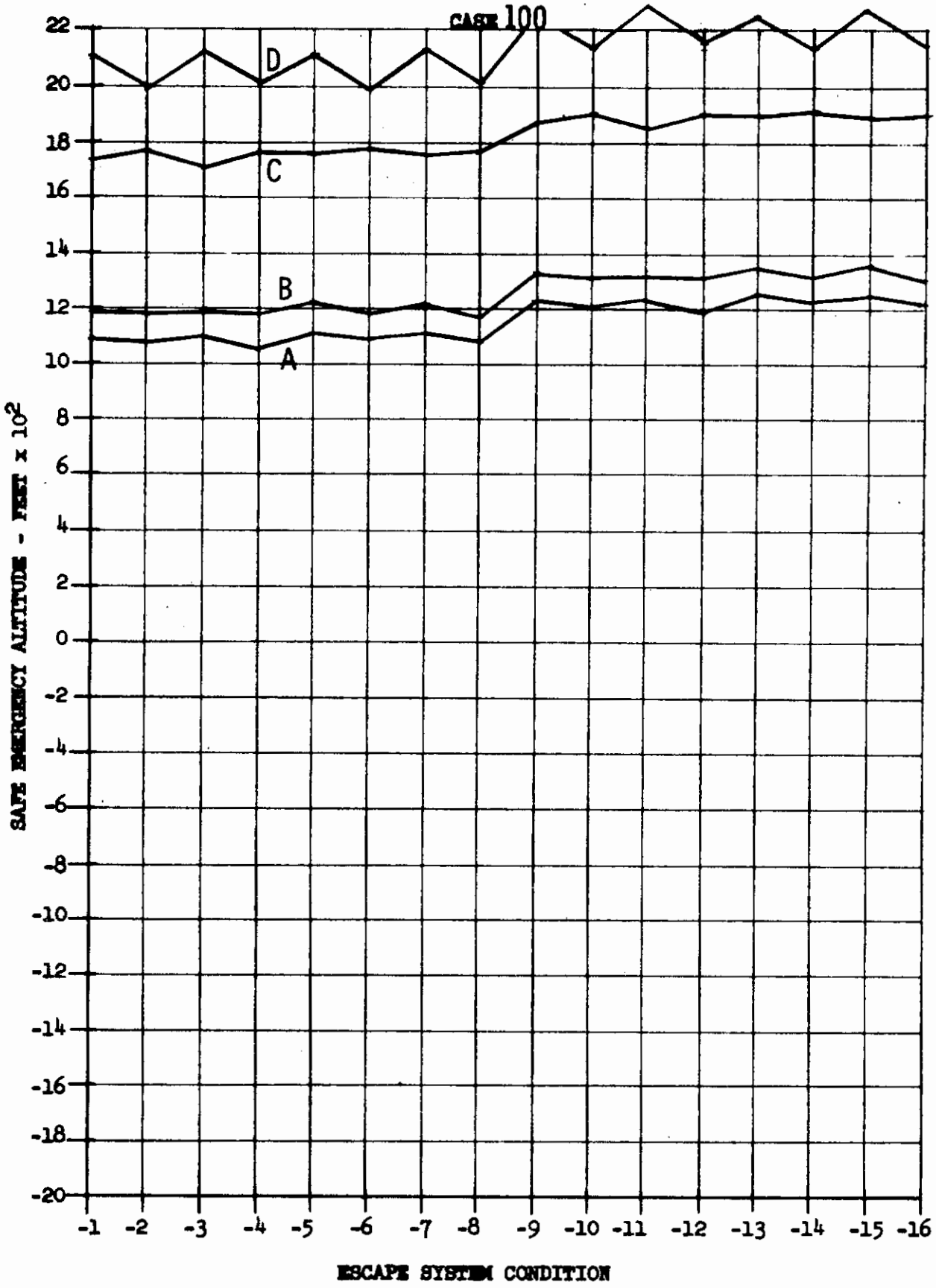

Approved for Public Release

Contrails

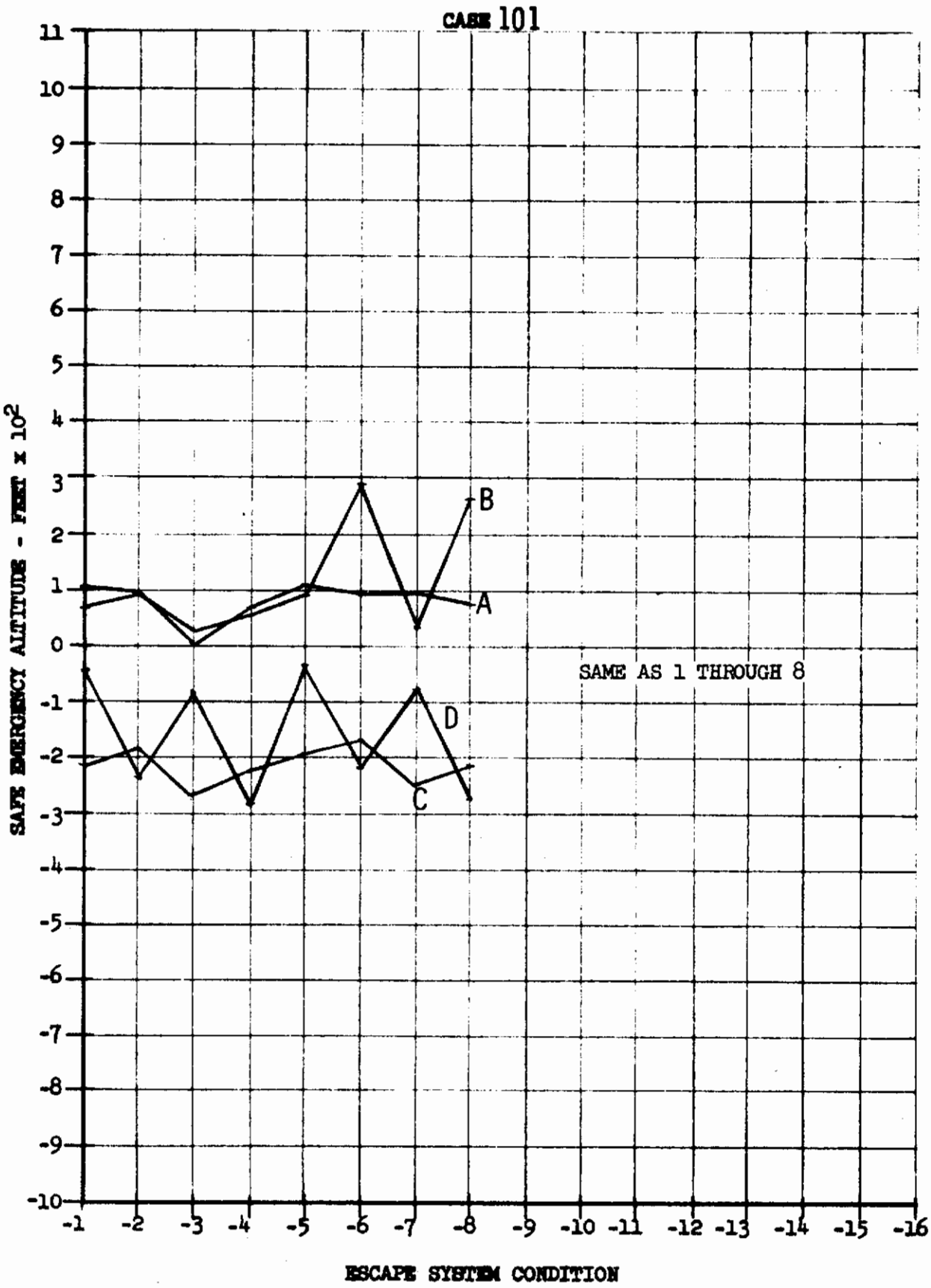

Approved for Public Release

Contrails

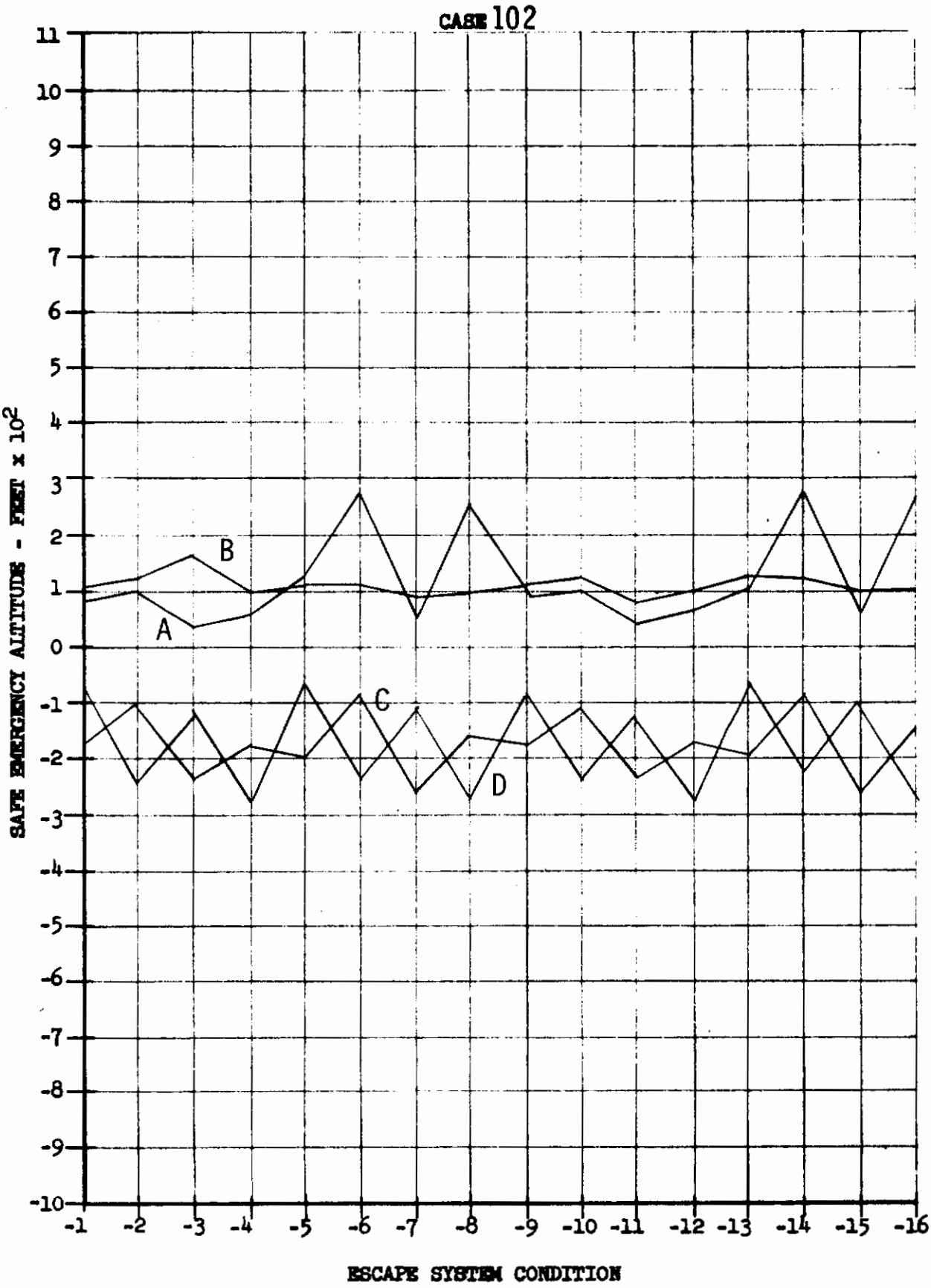

Approved for Public Release

Contrails

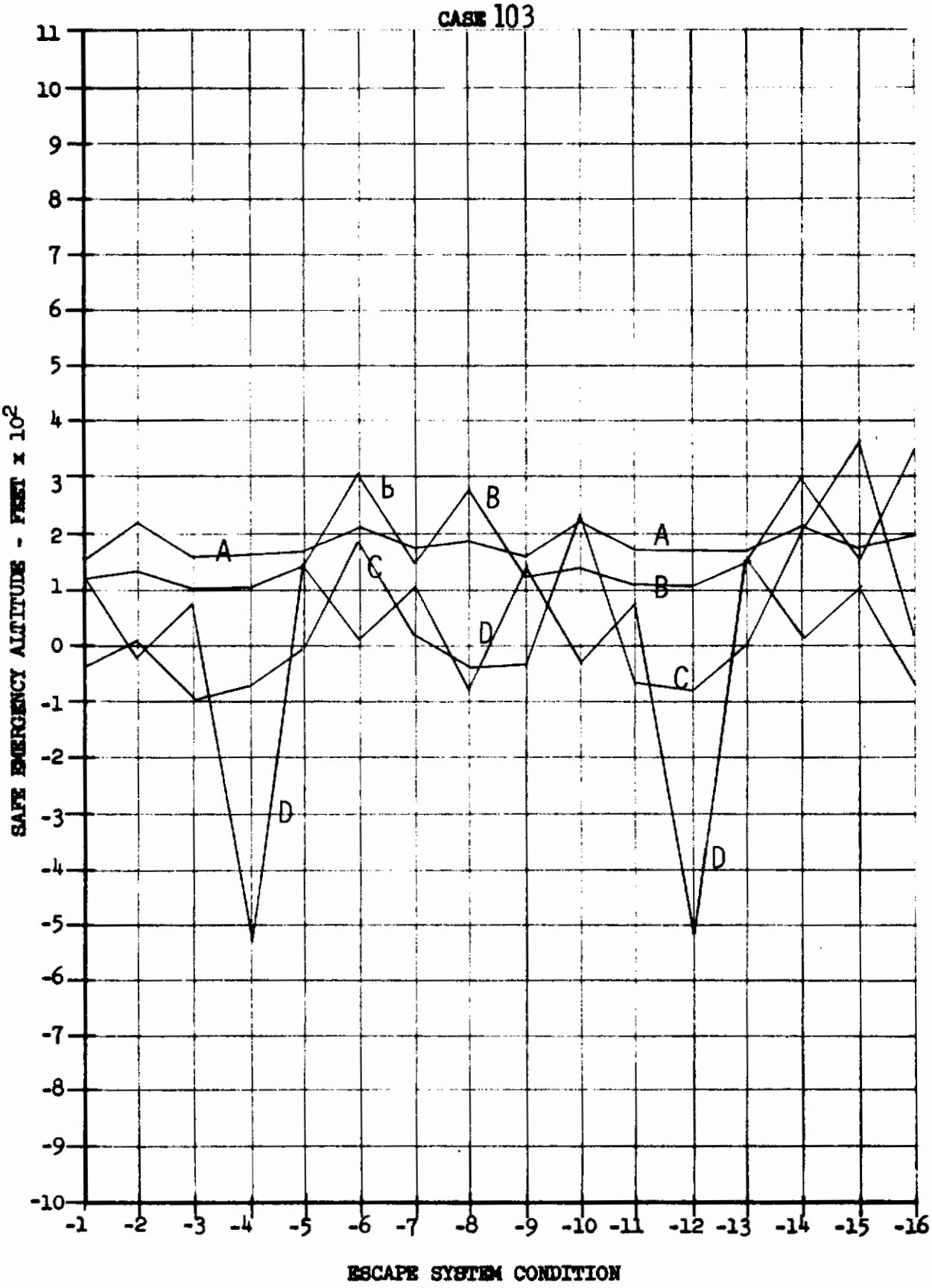

Approved for Public Release

Contrails

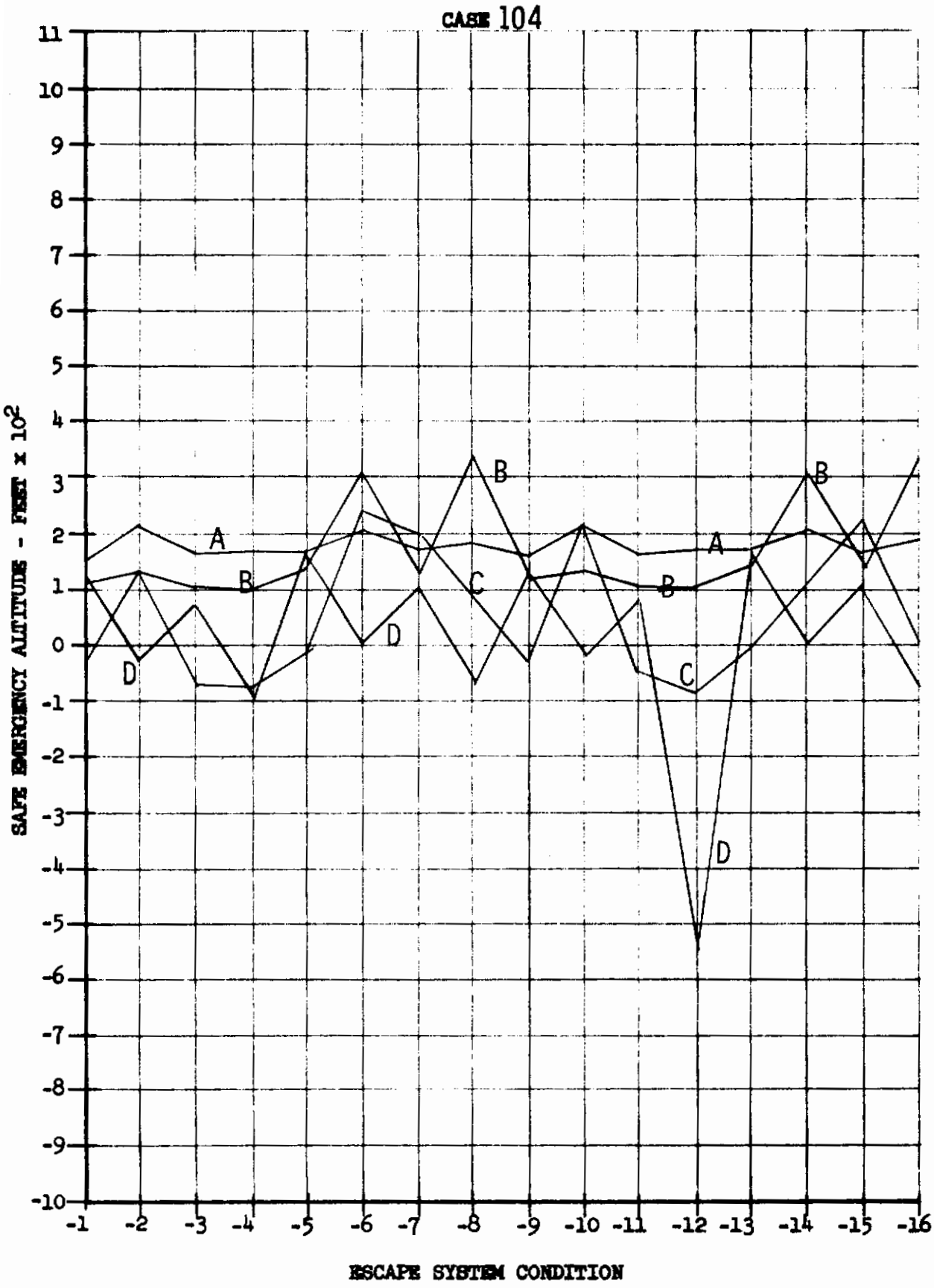

Approved for Public Release

Contrails

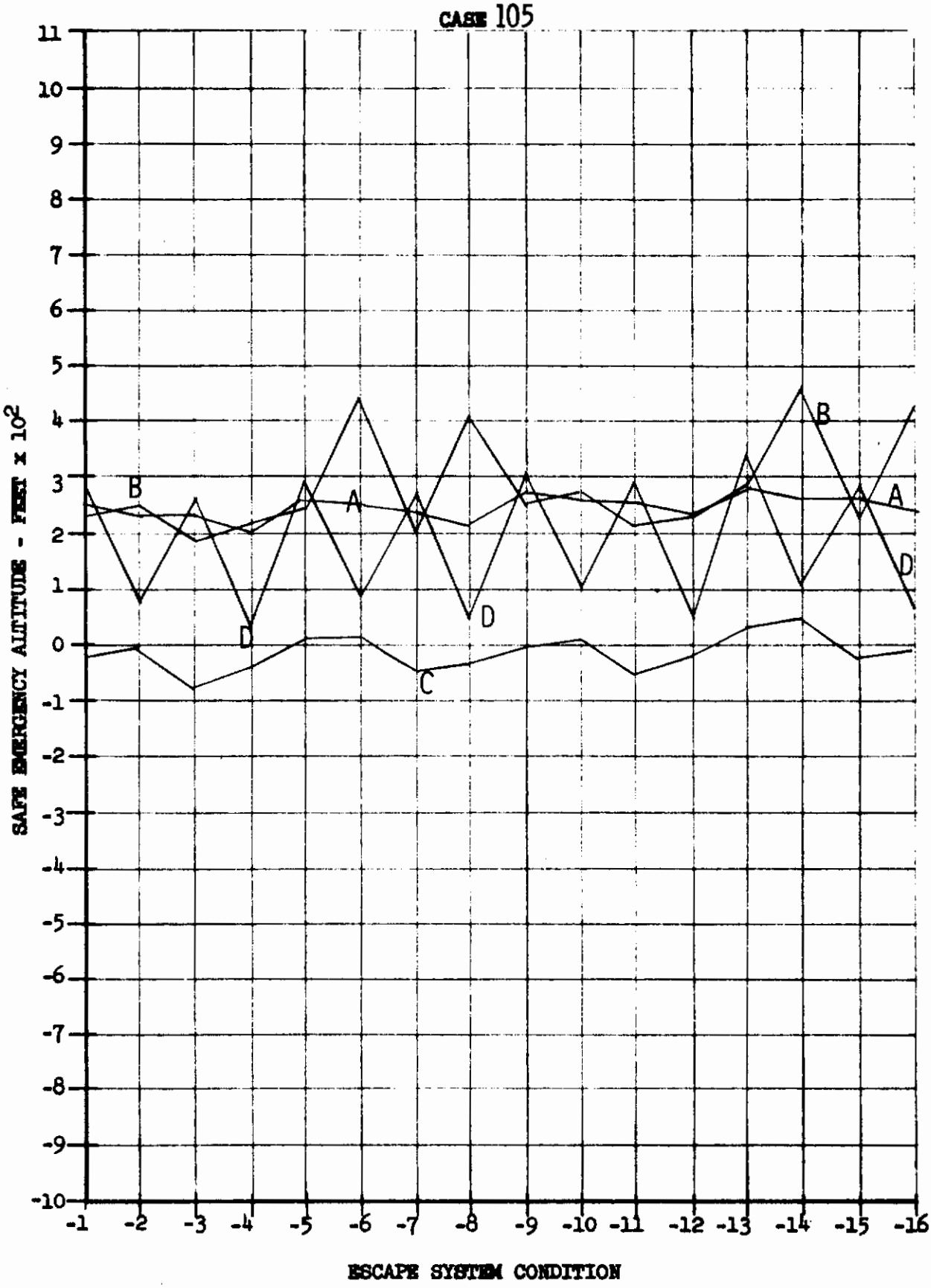

Approved for Public Release

Contrails

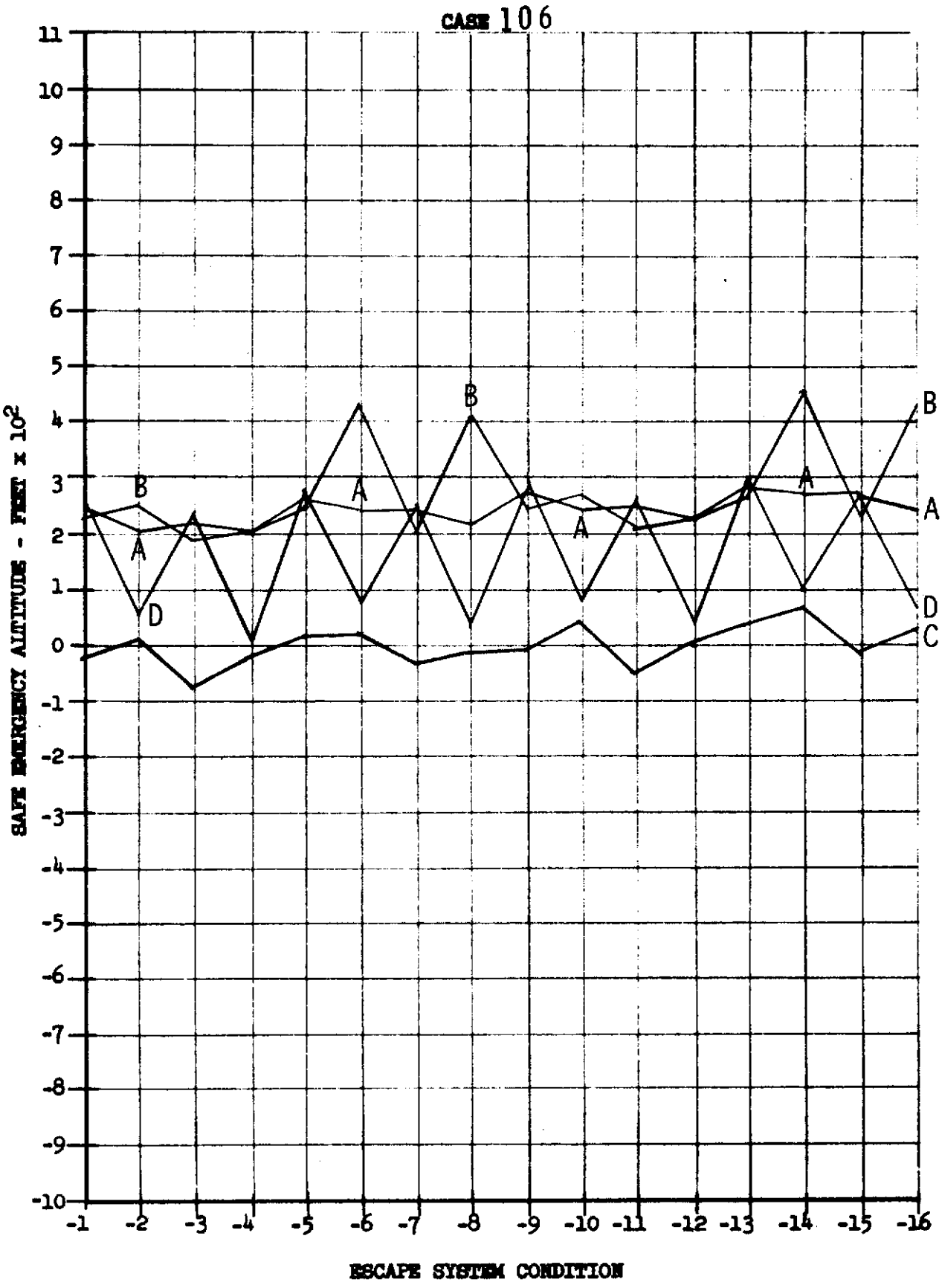

Approved for Public Release

Contrails

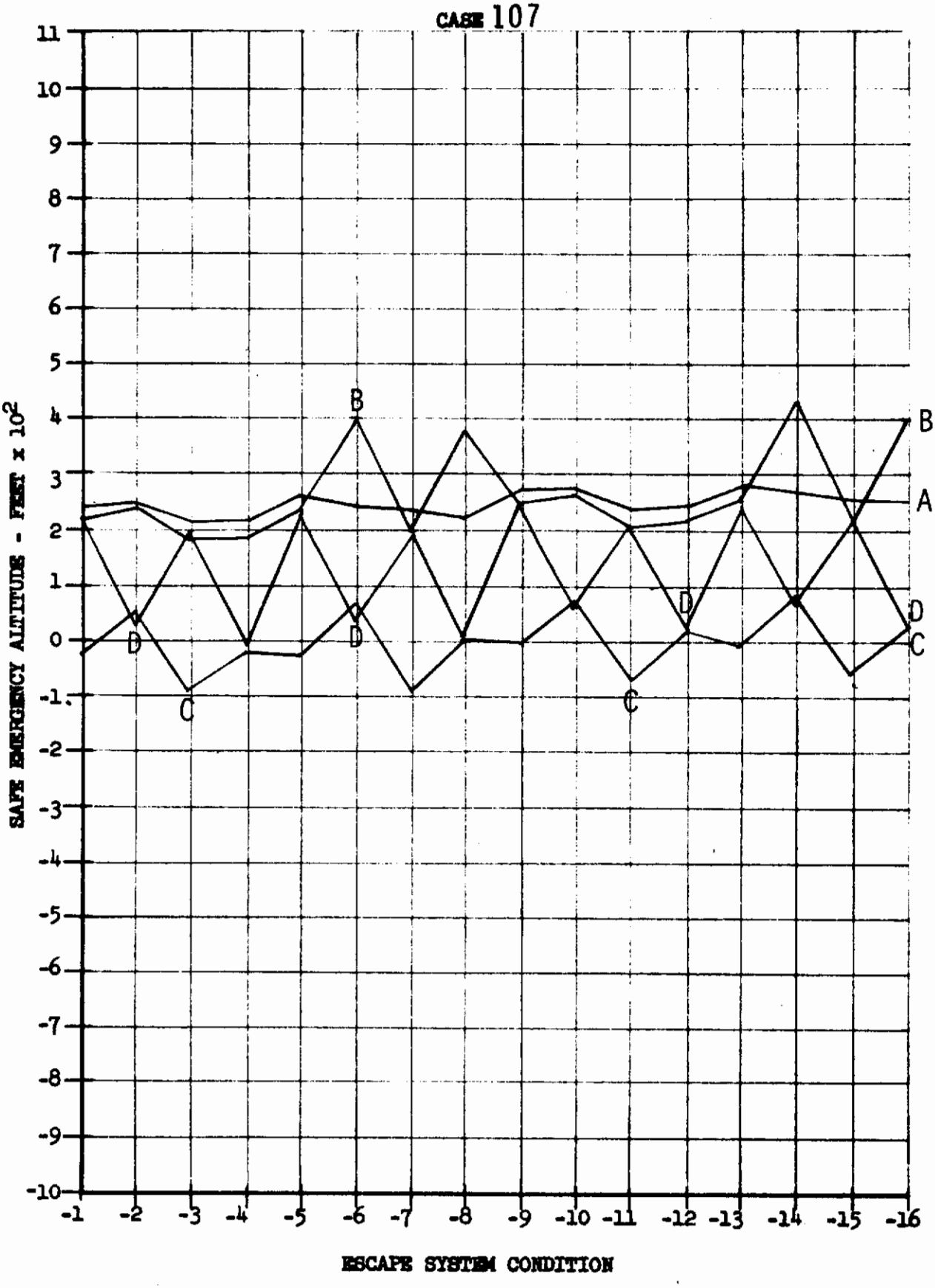

Approved for Public Release

Contrails

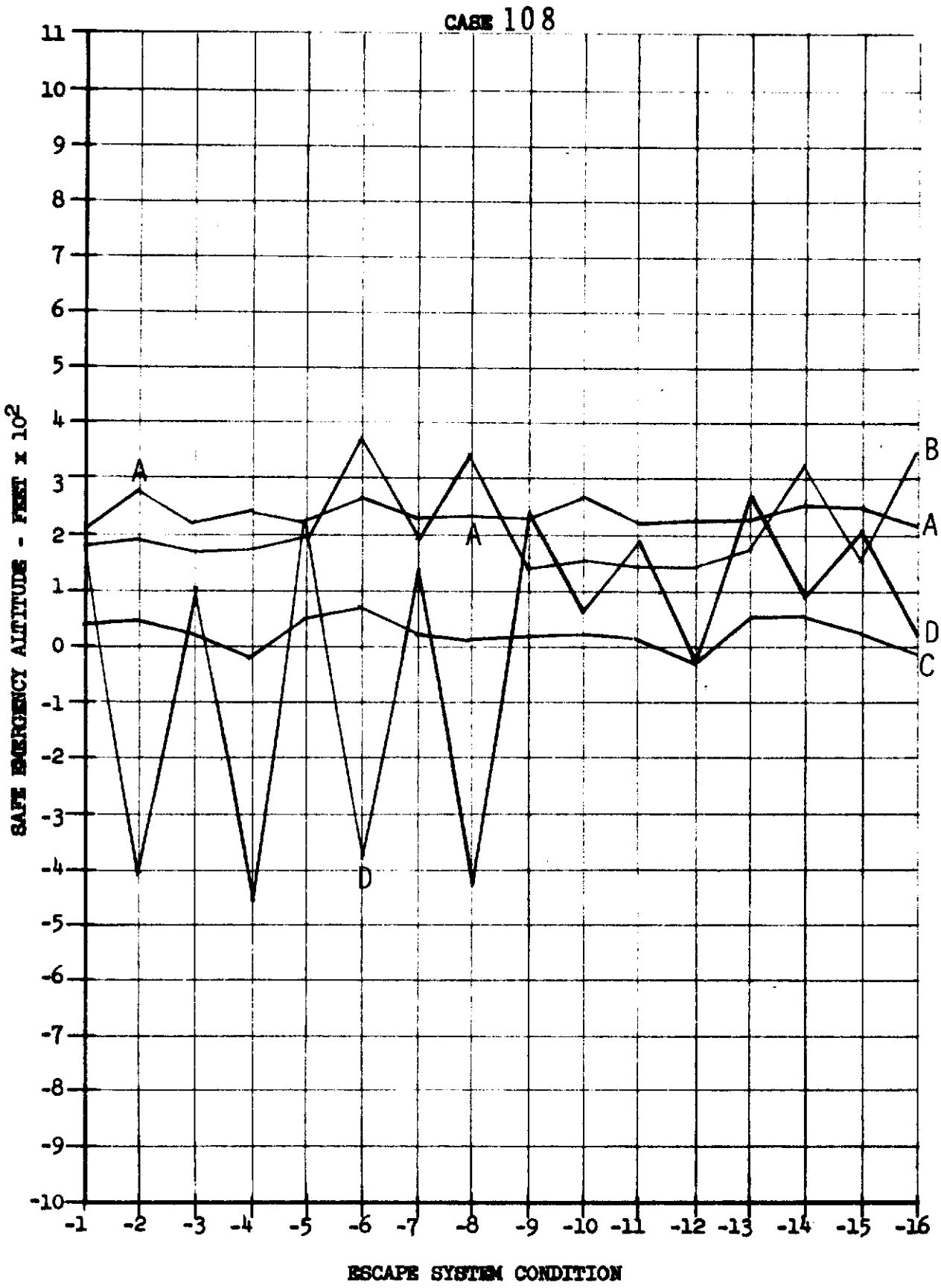

Approved for Public Release

Contrails

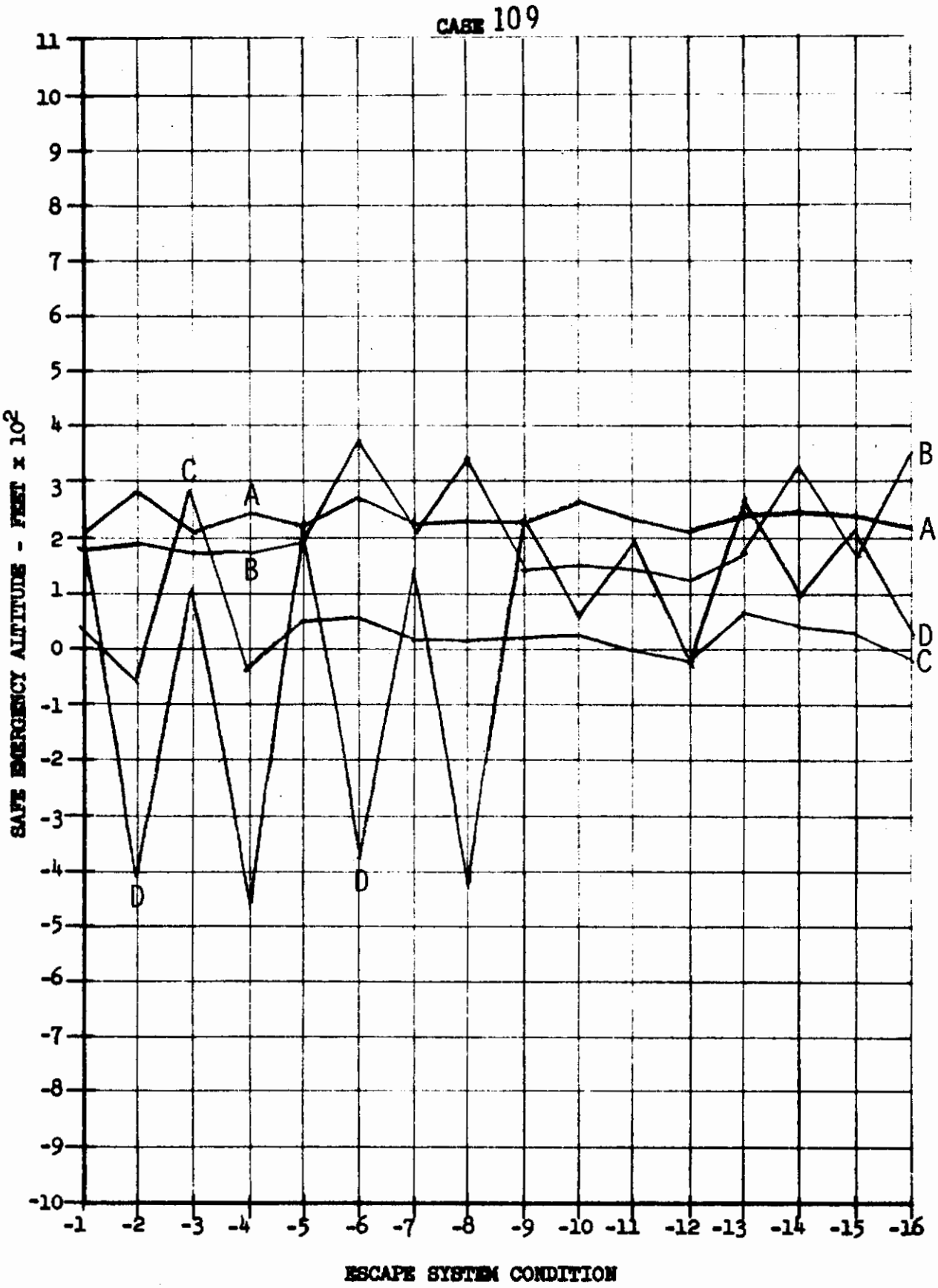

Approved for Public Release

Contrails

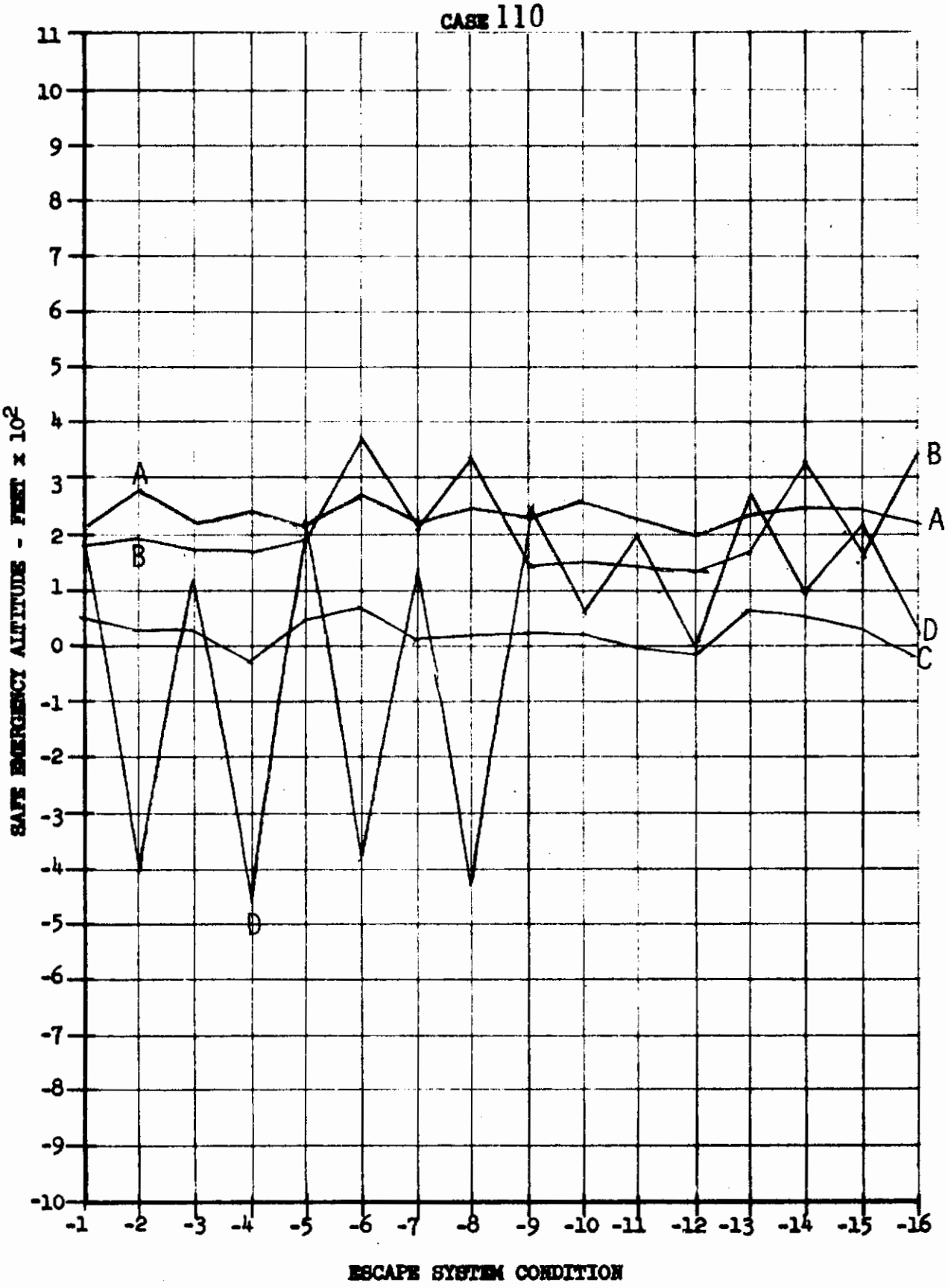

Approved for Public Release

Contrails

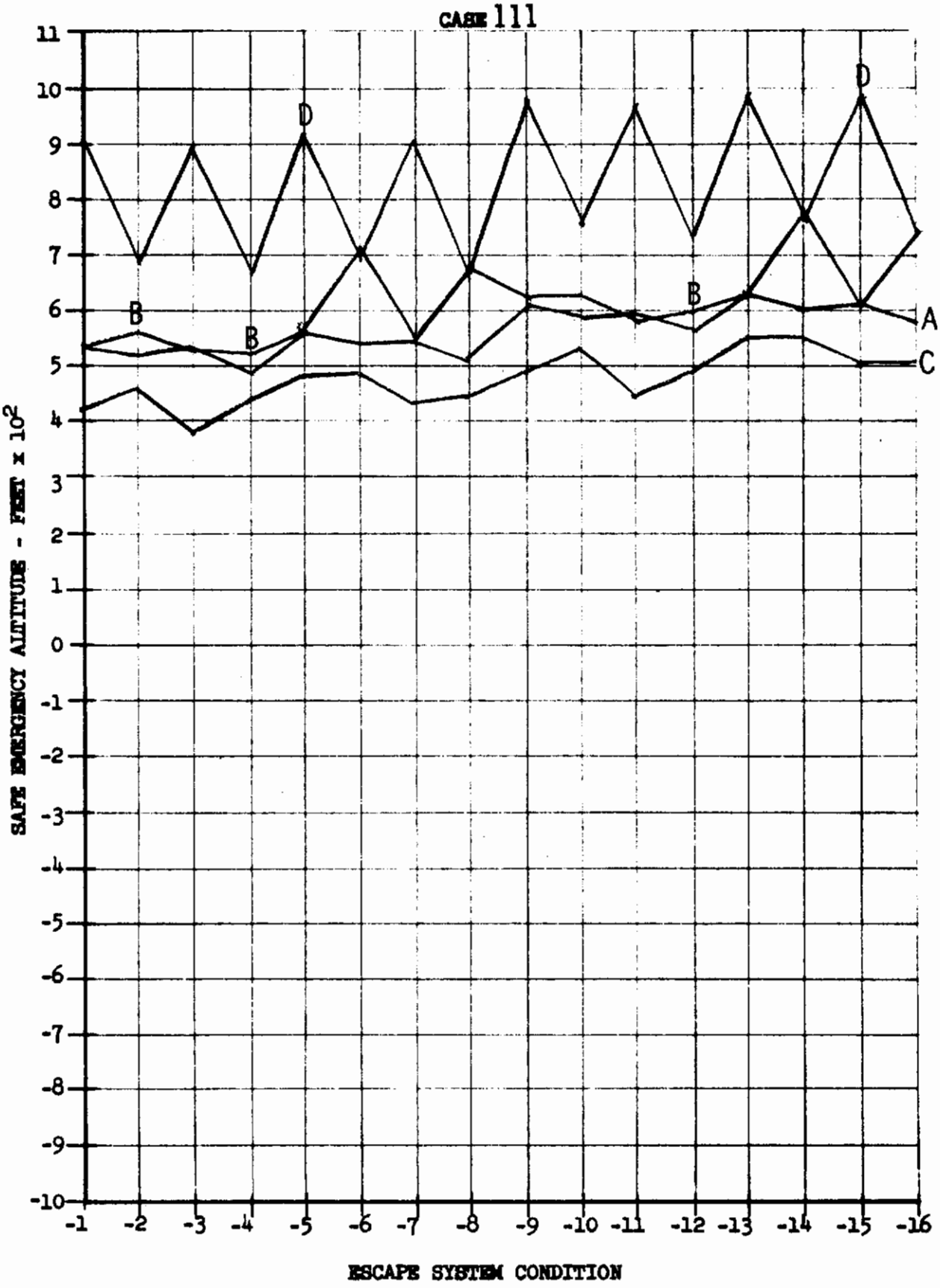

Approved for Public Release

Contrails

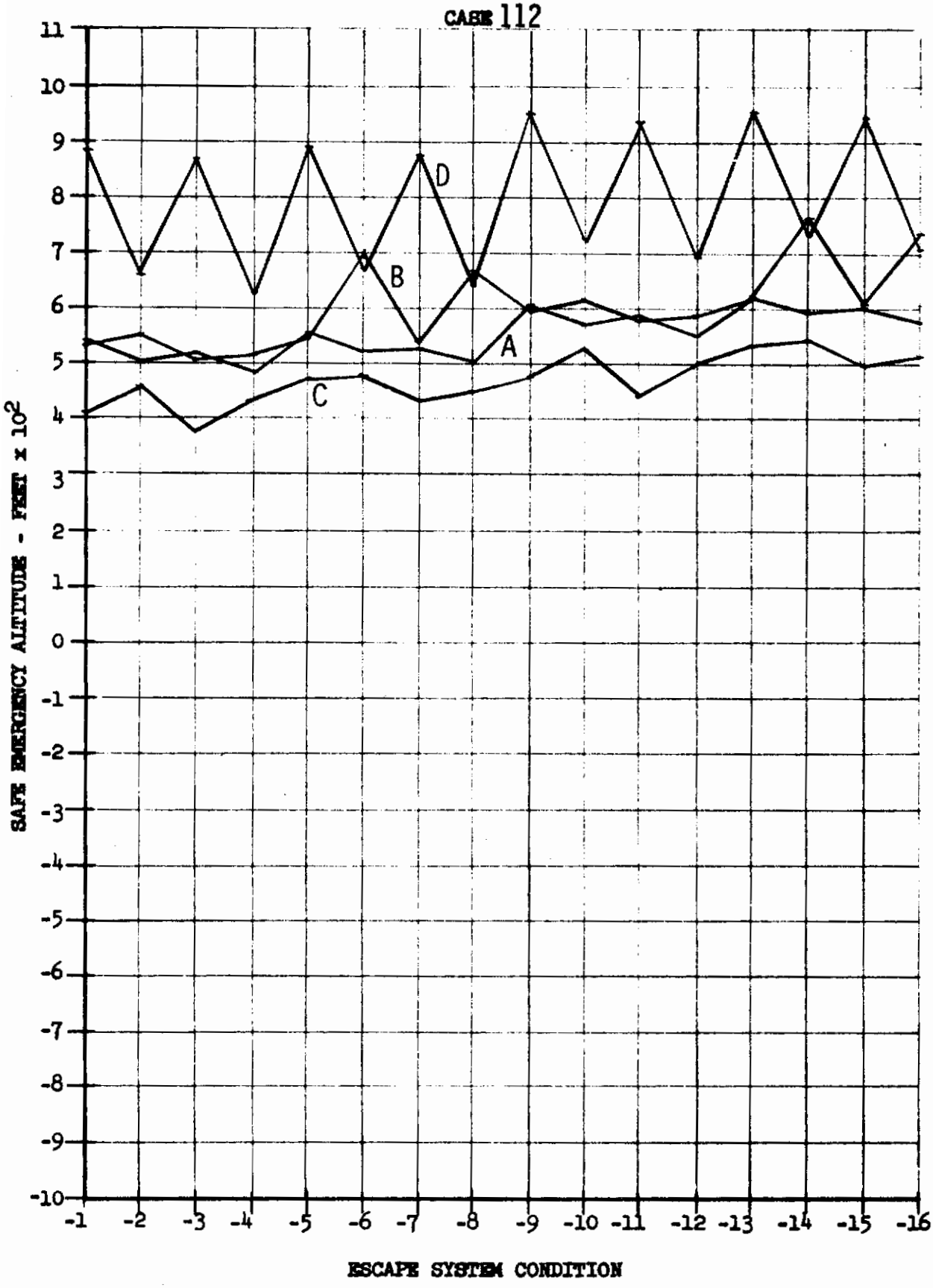

Approved for Public Release

Contrails

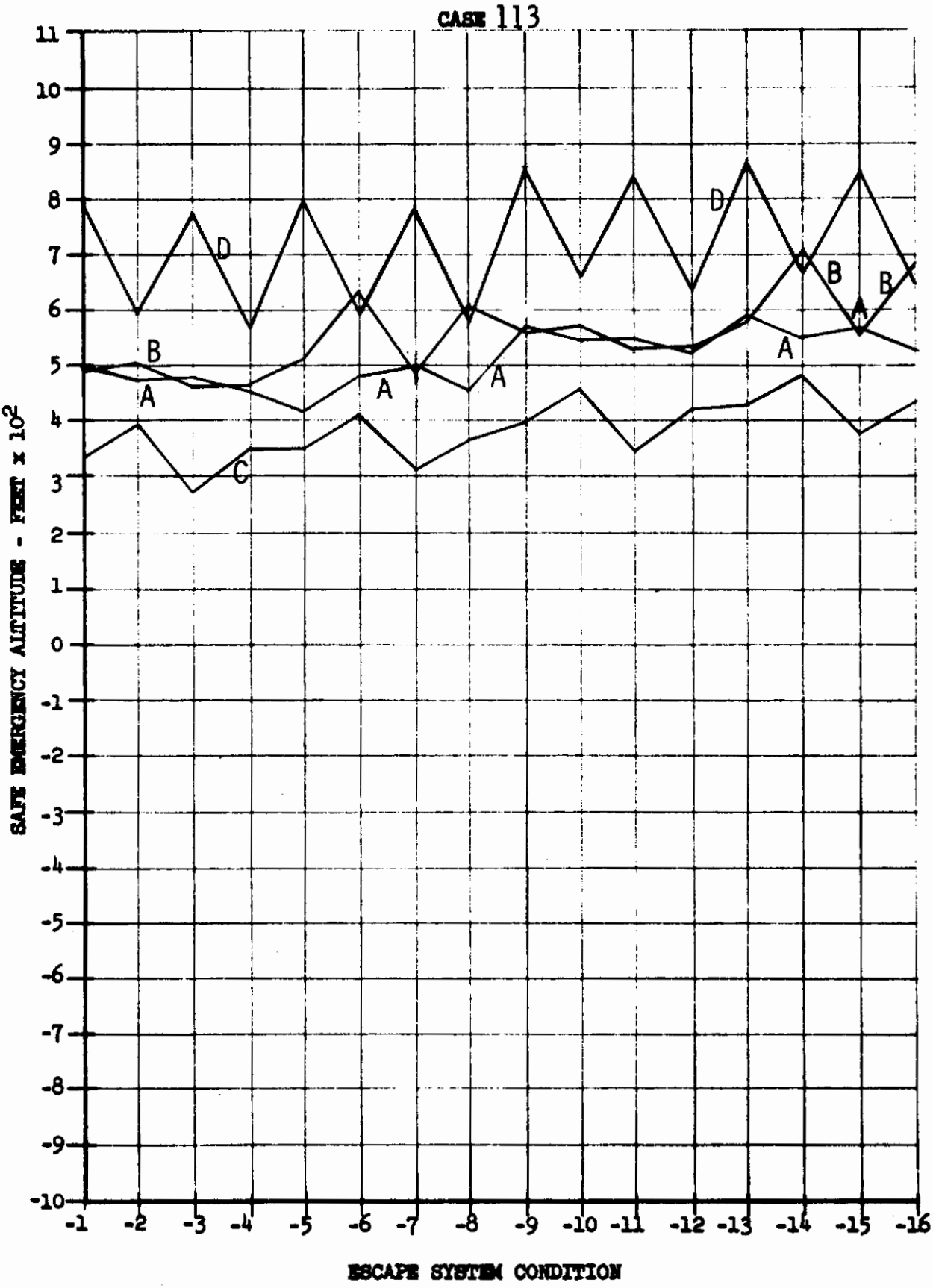

Approved for Public Release

Contrails

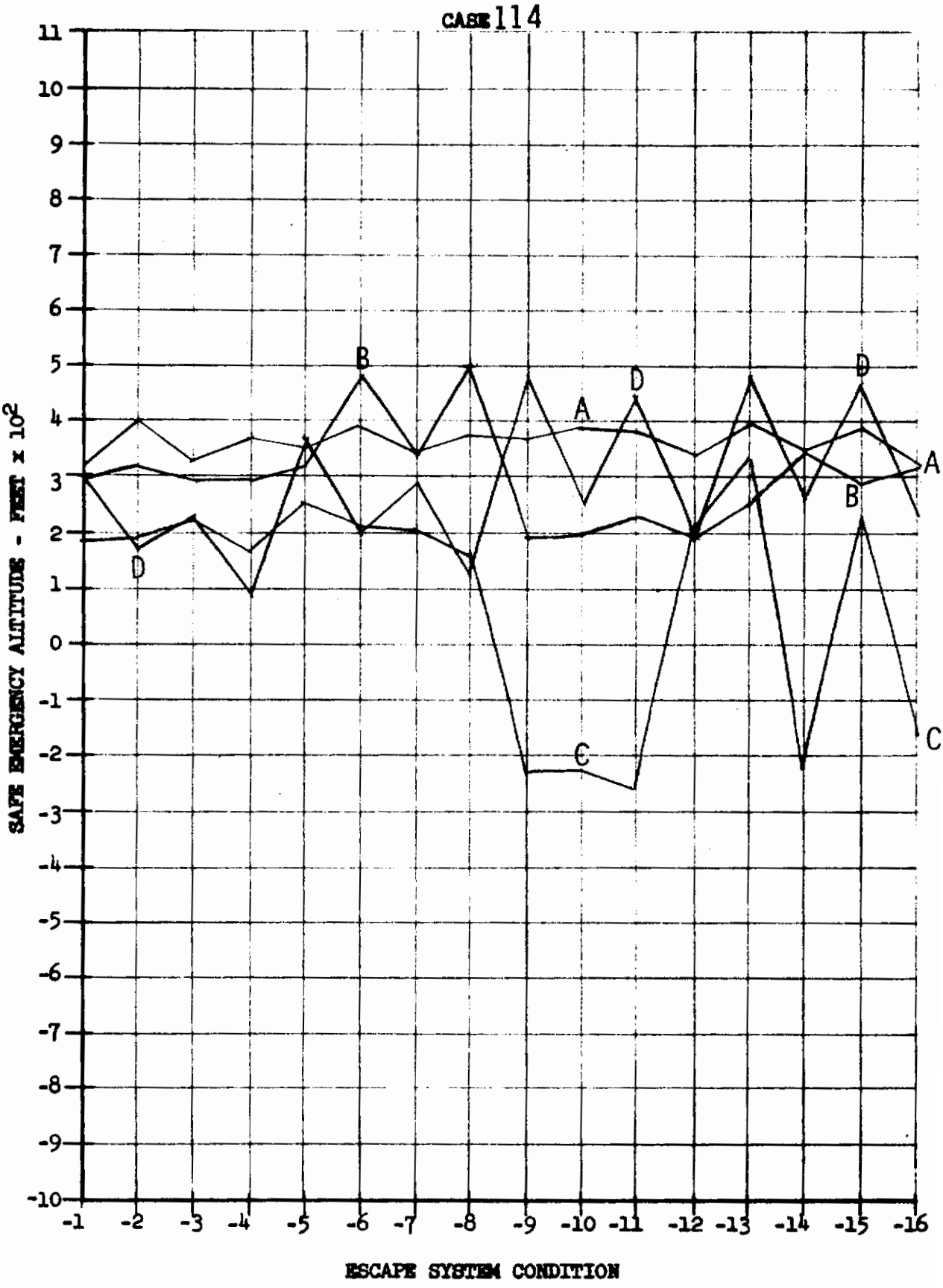

Approved for Public Release

Contrails

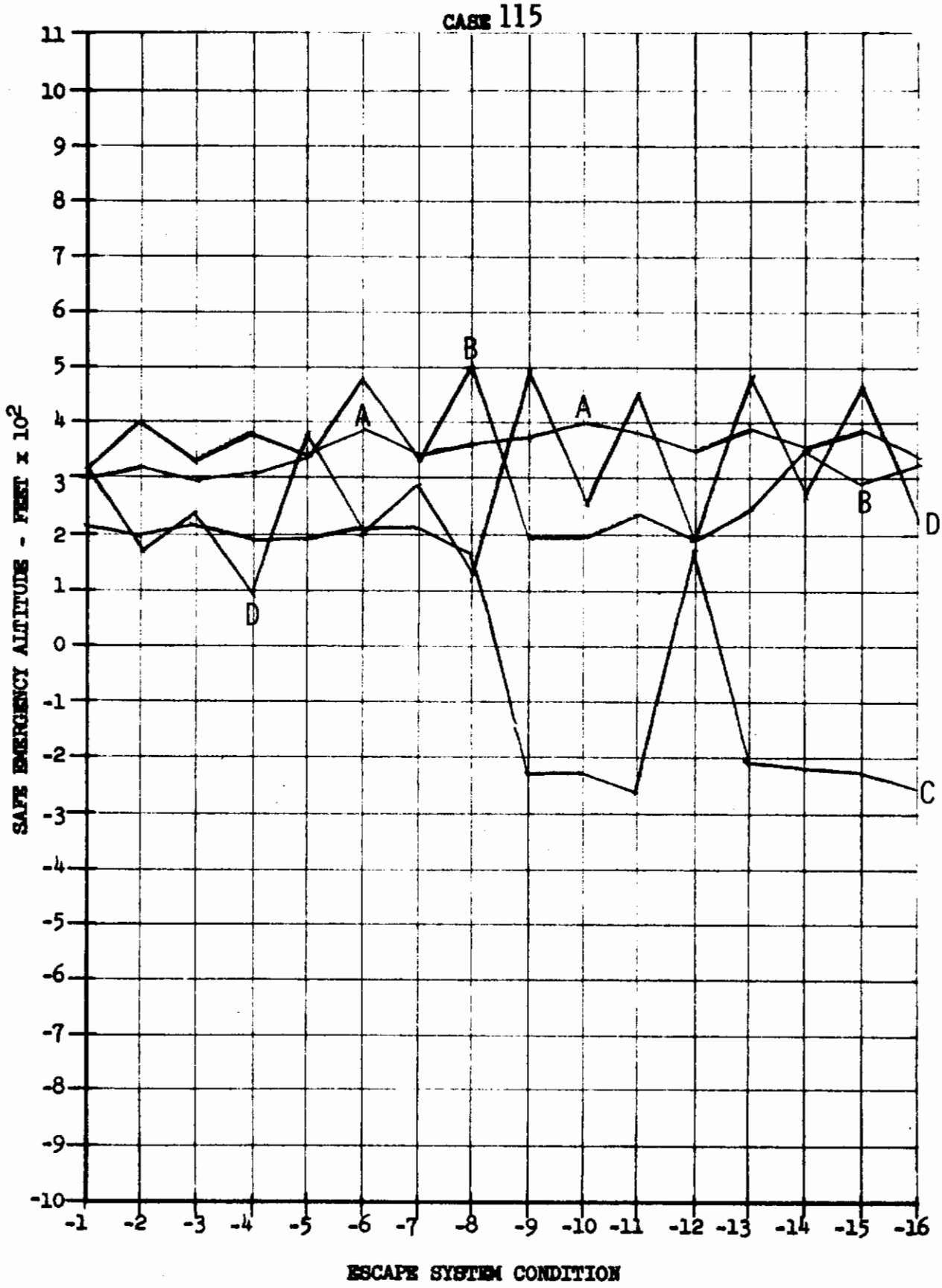

Approved for Public Release

Contrails

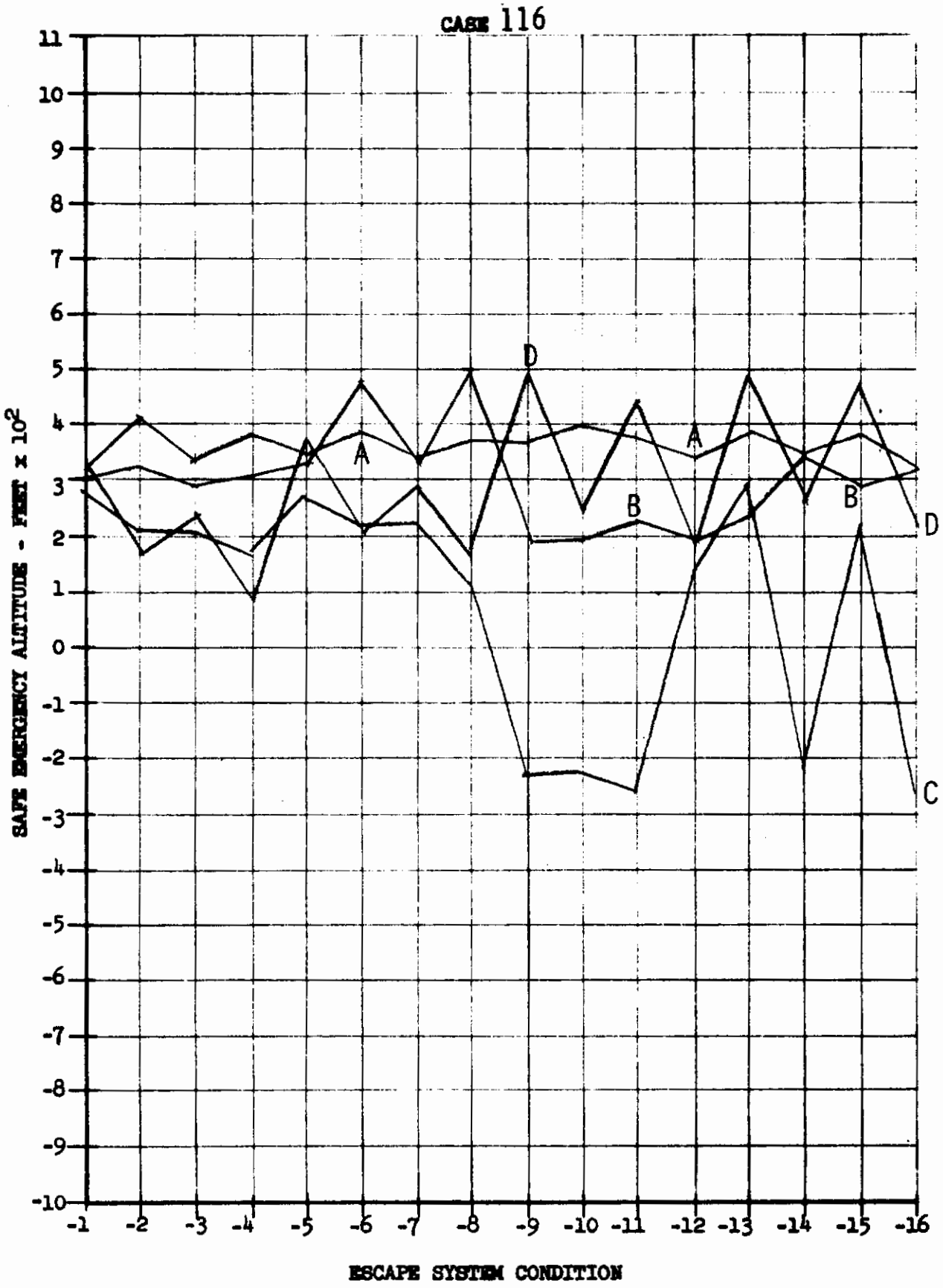

Approved for Public Release

Contrails

CASE 117

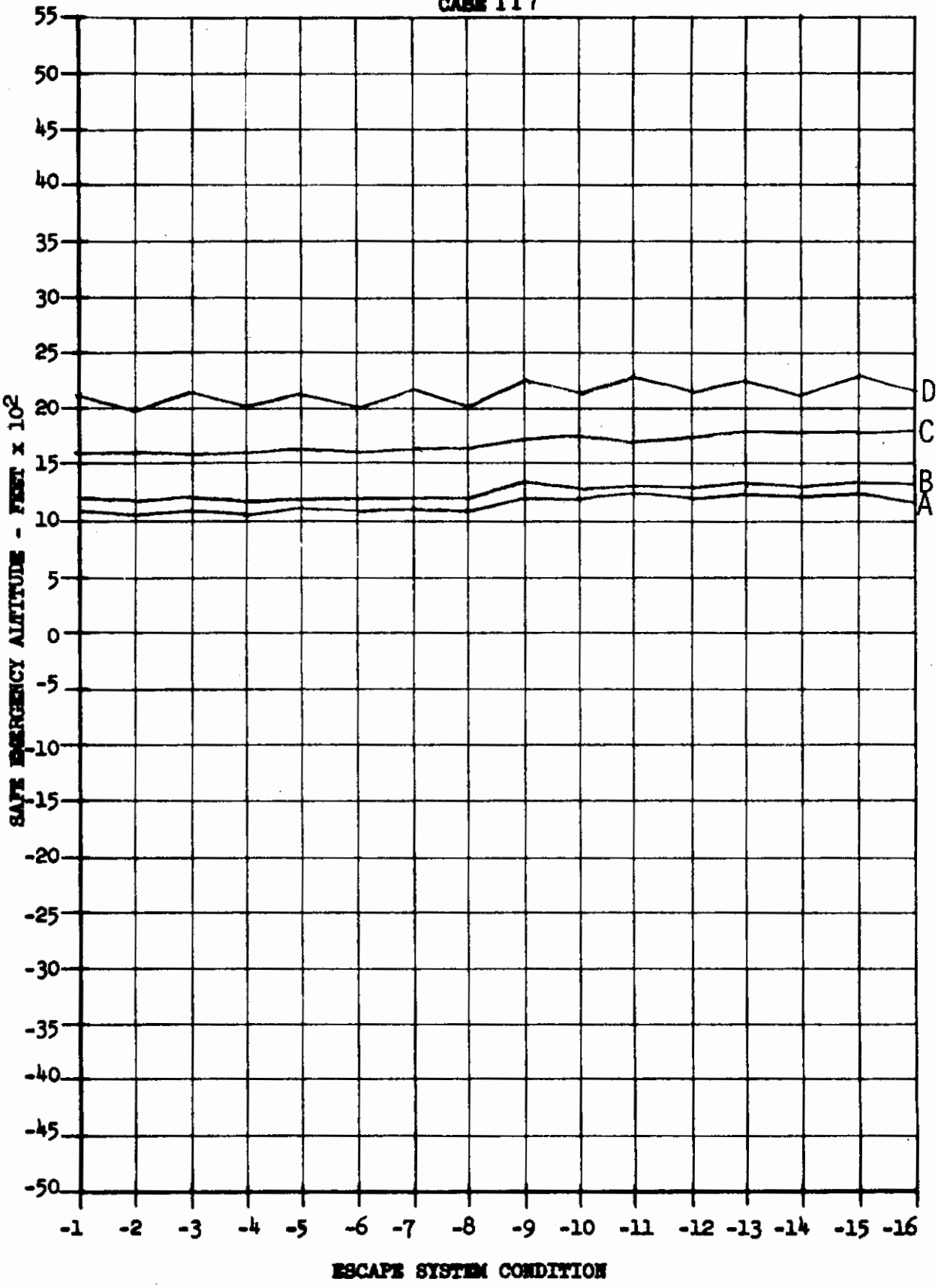

Approved for Public Release

Contrails

CASE 118

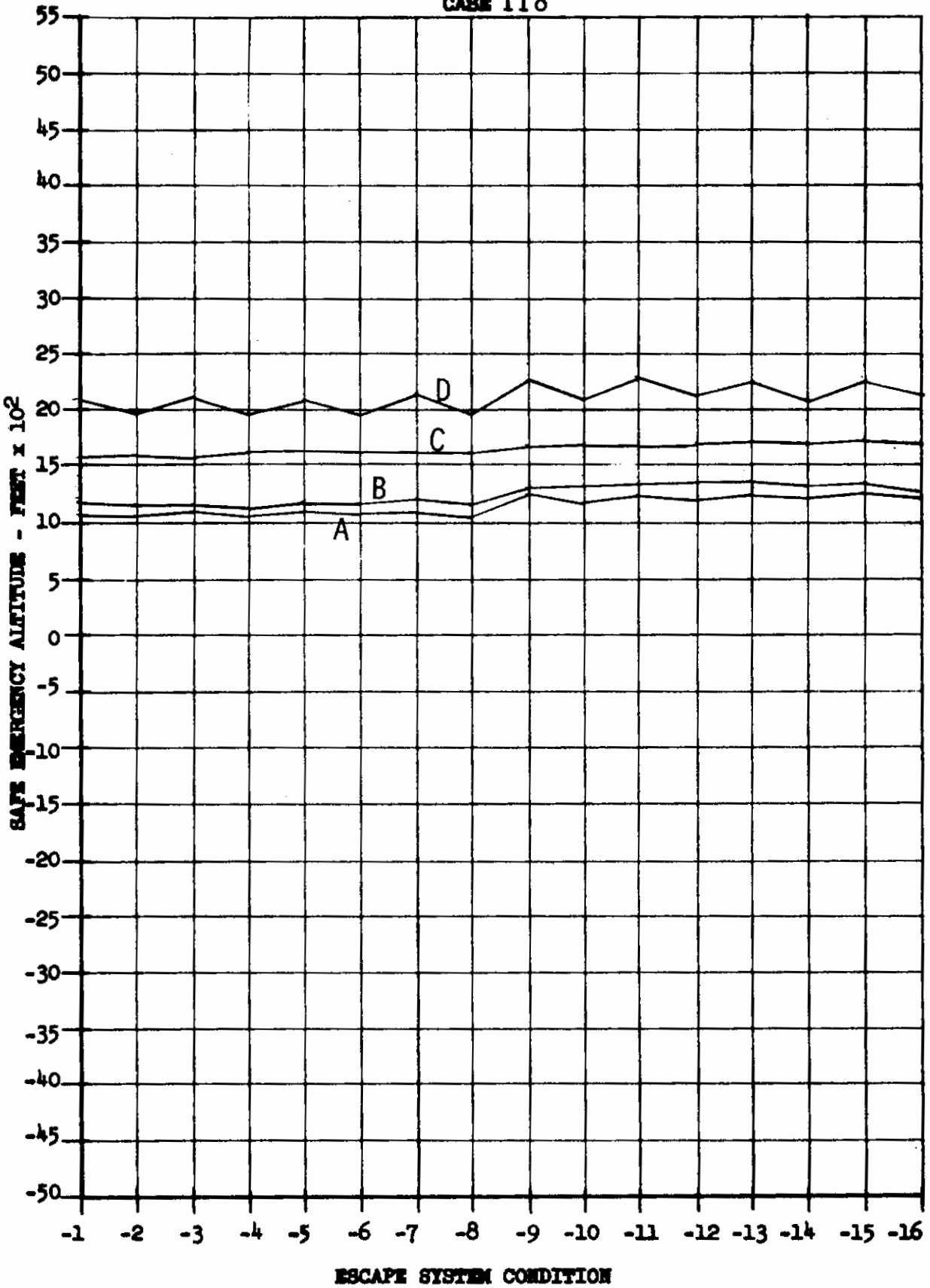

Approved for Public Release

Contrails

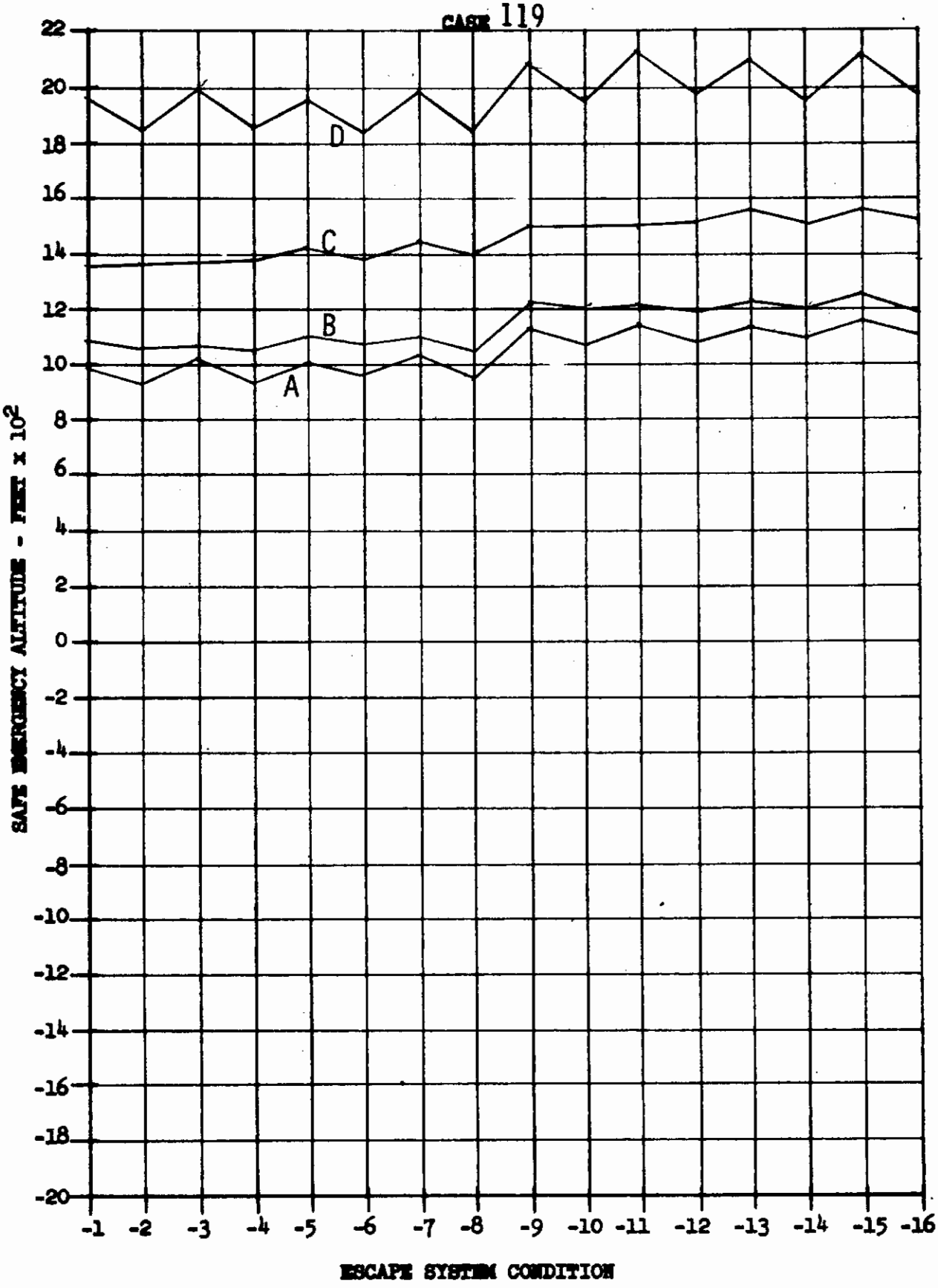

Approved for Public Release

Contrails

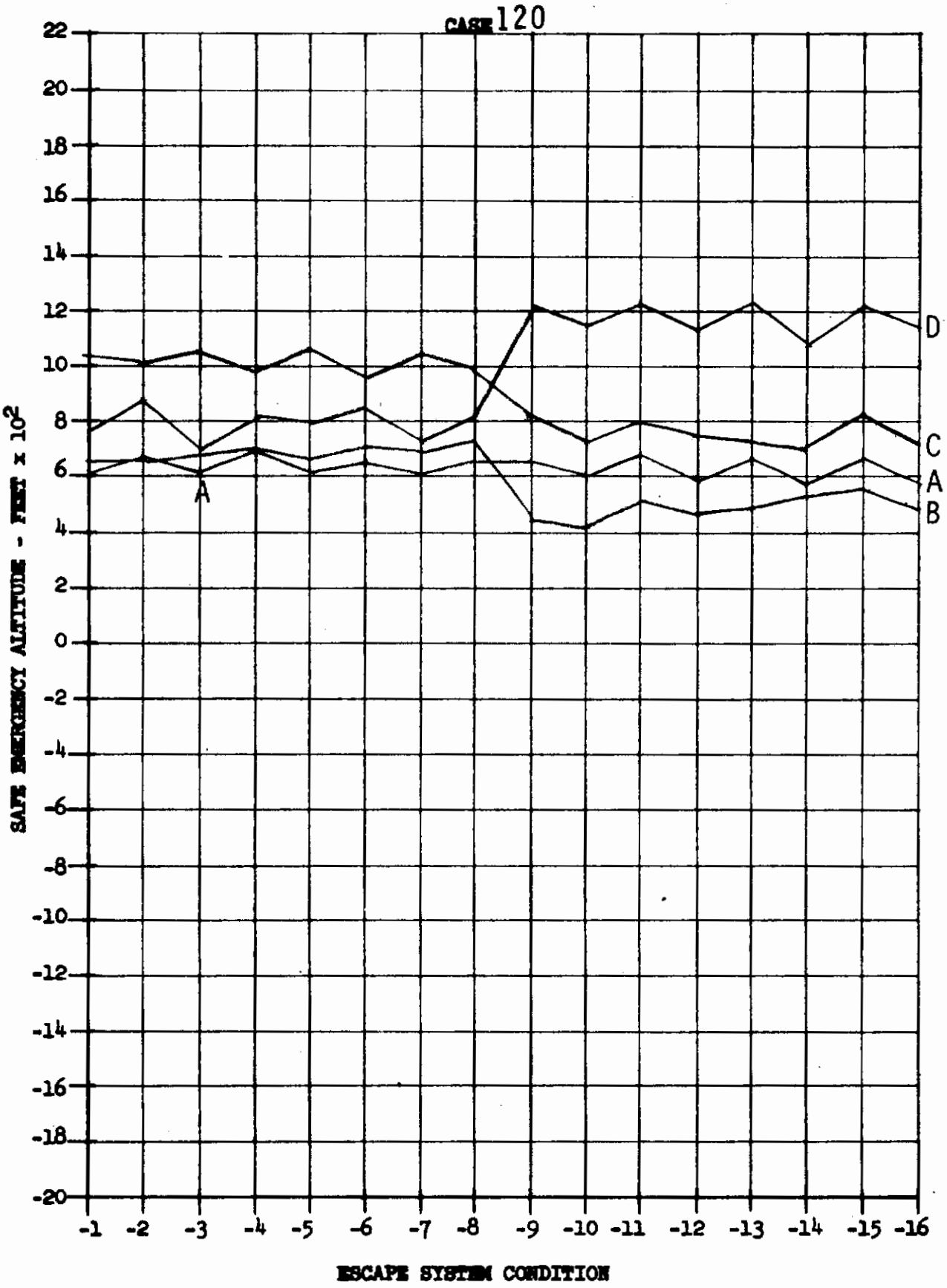

Approved for Public Release

Contrails

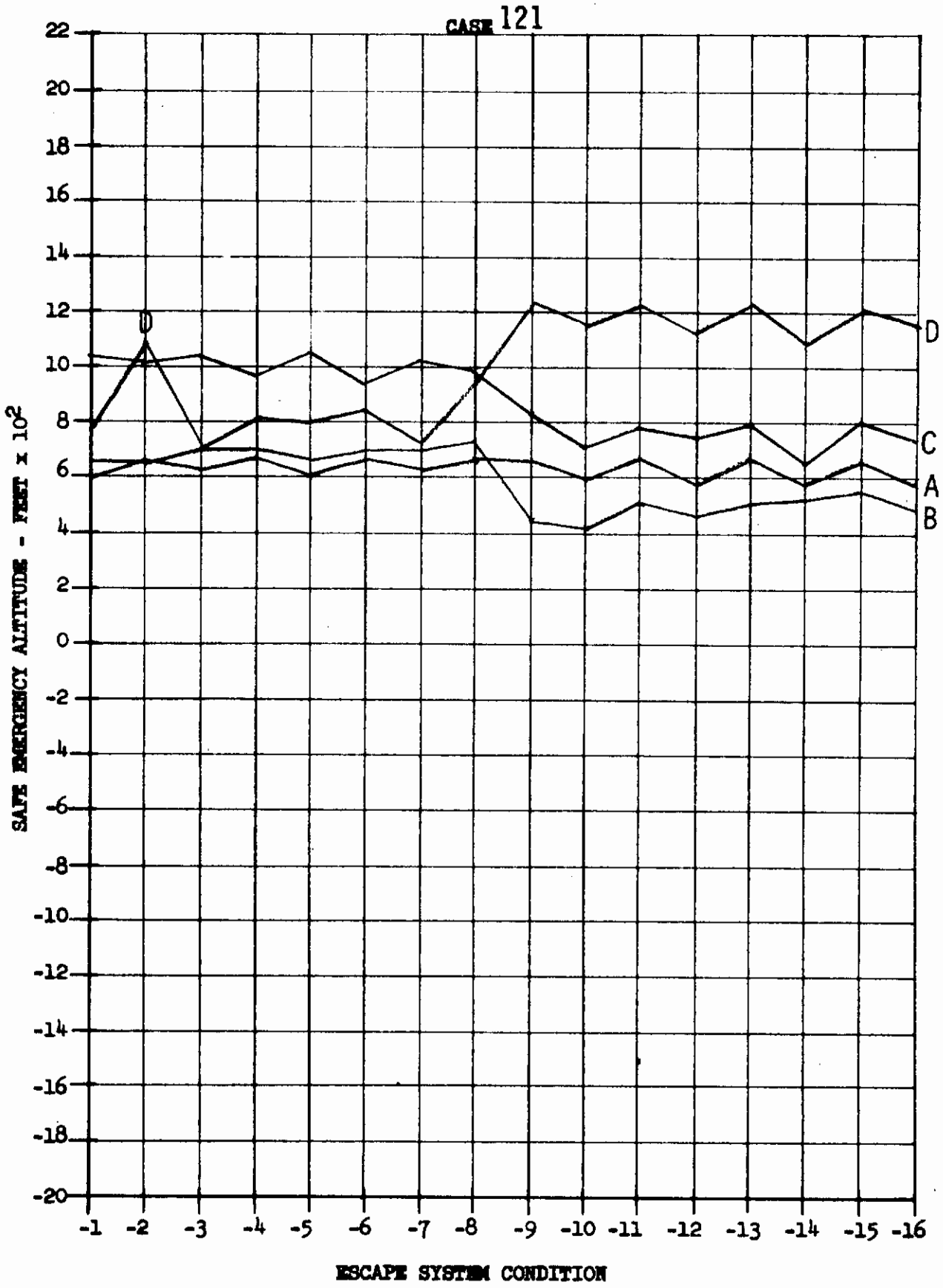

Approved for Public Release

Contrails

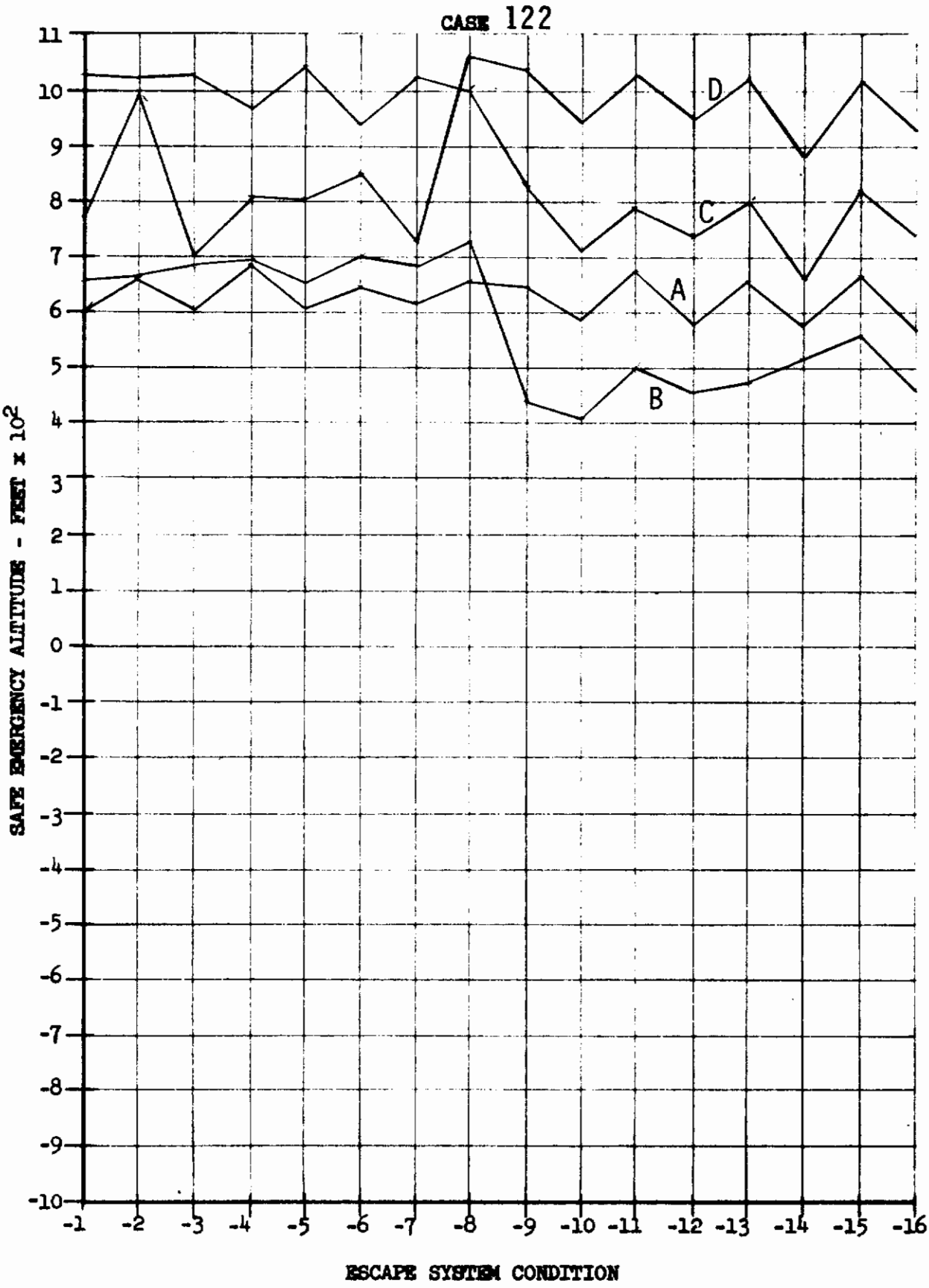

Approved for Public Release

Contrails

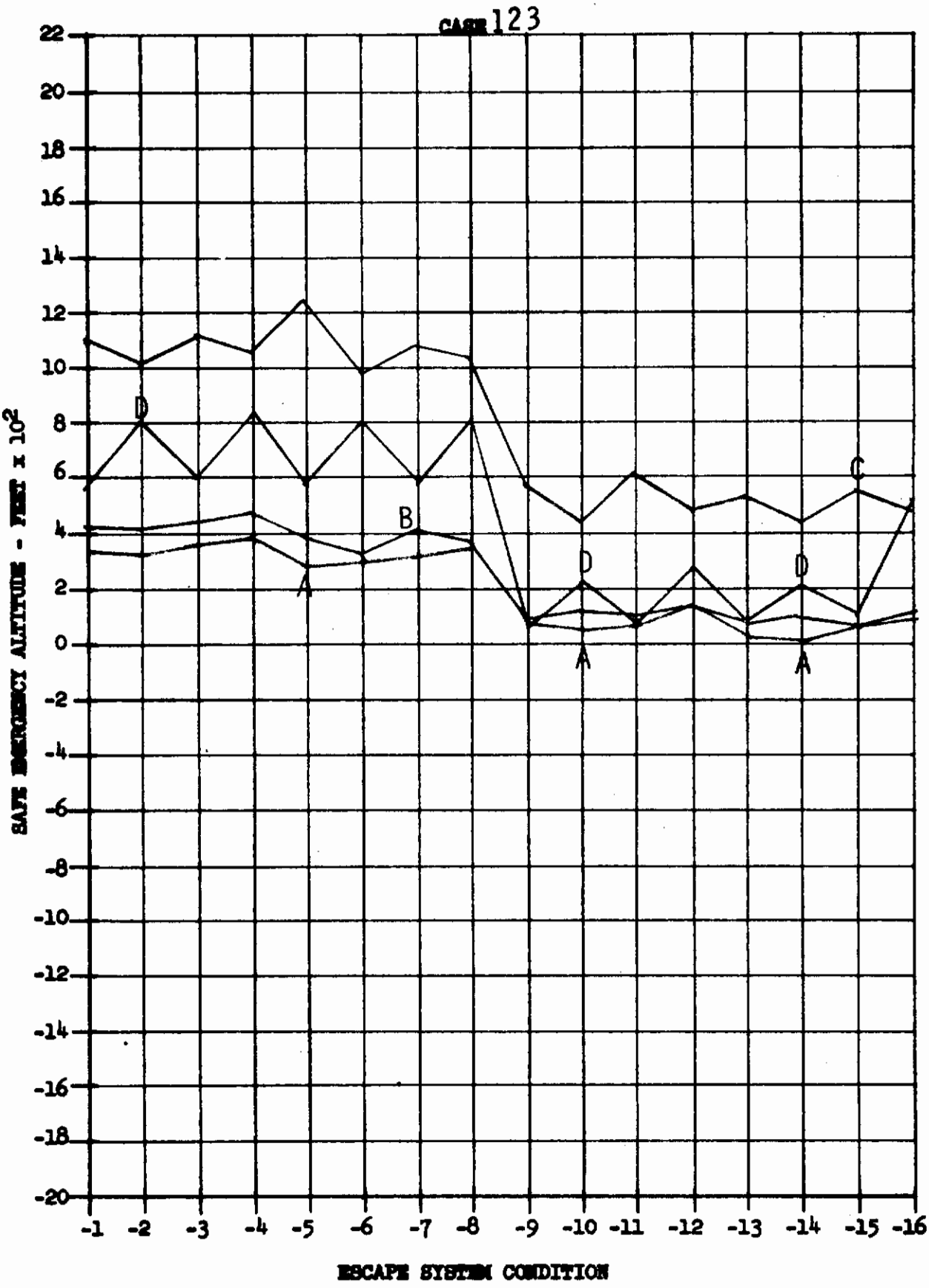

Approved for Public Release

Contrails

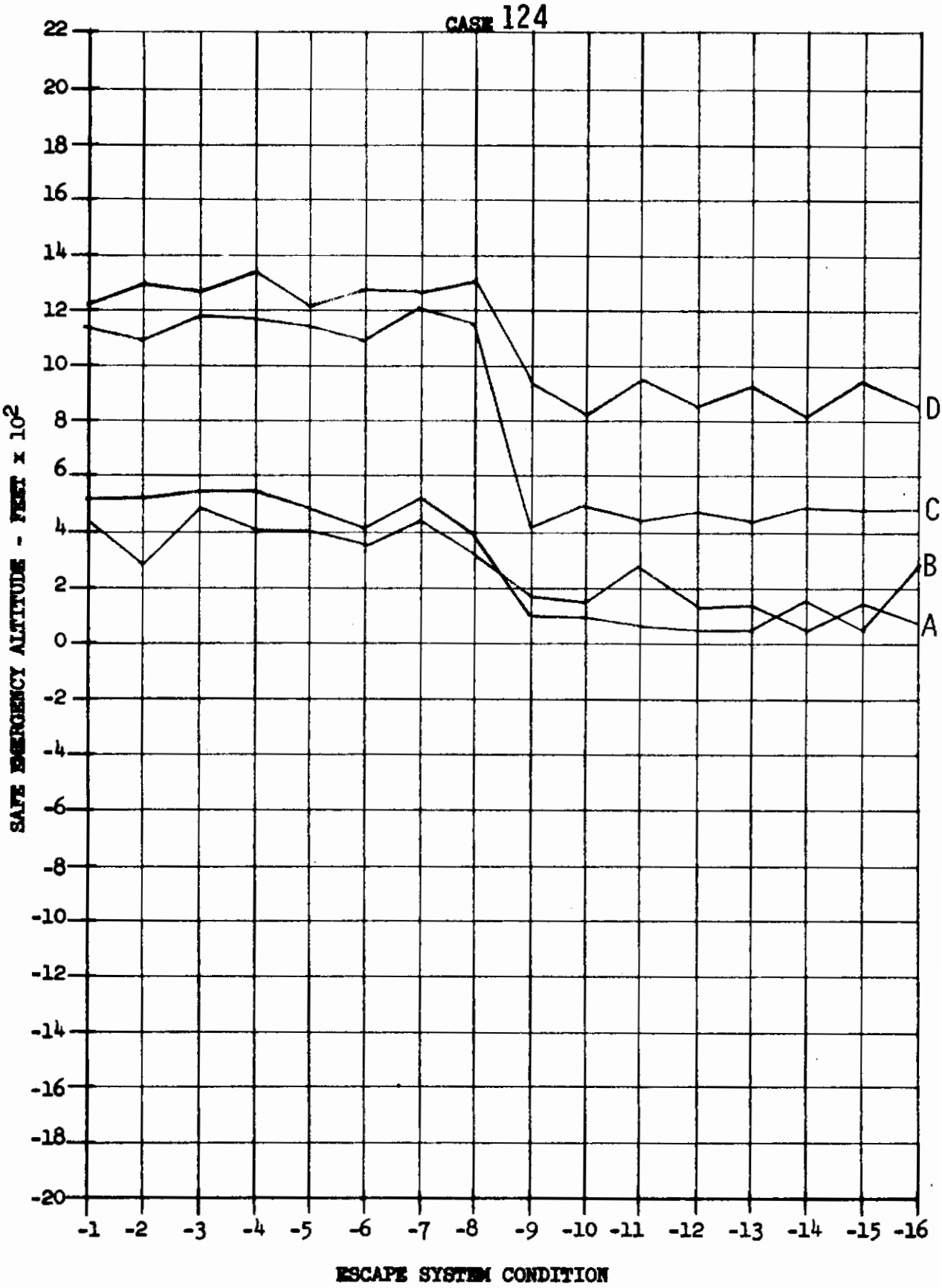

Approved for Public Release

Contrails

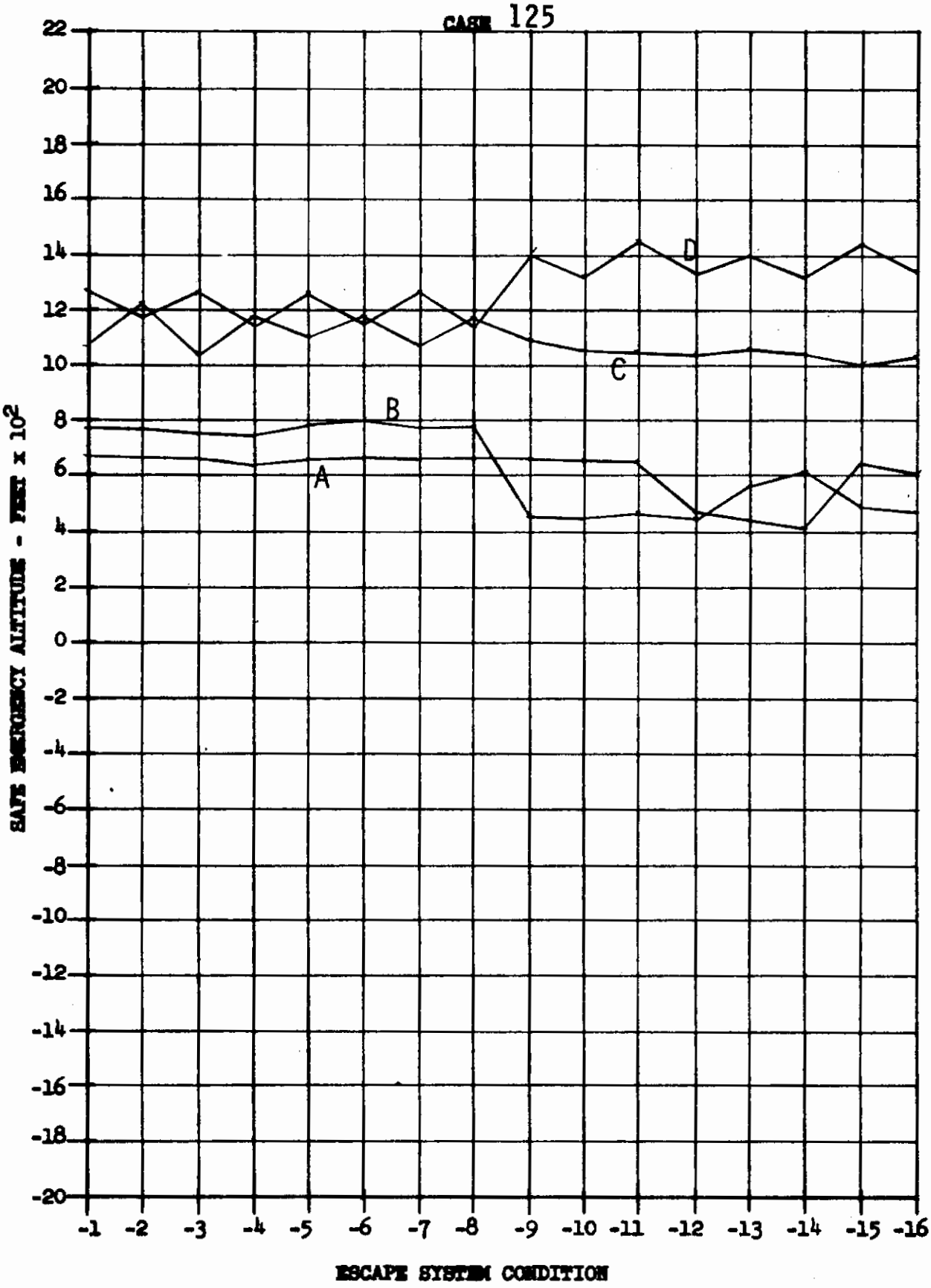

Approved for Public Release

Contrails

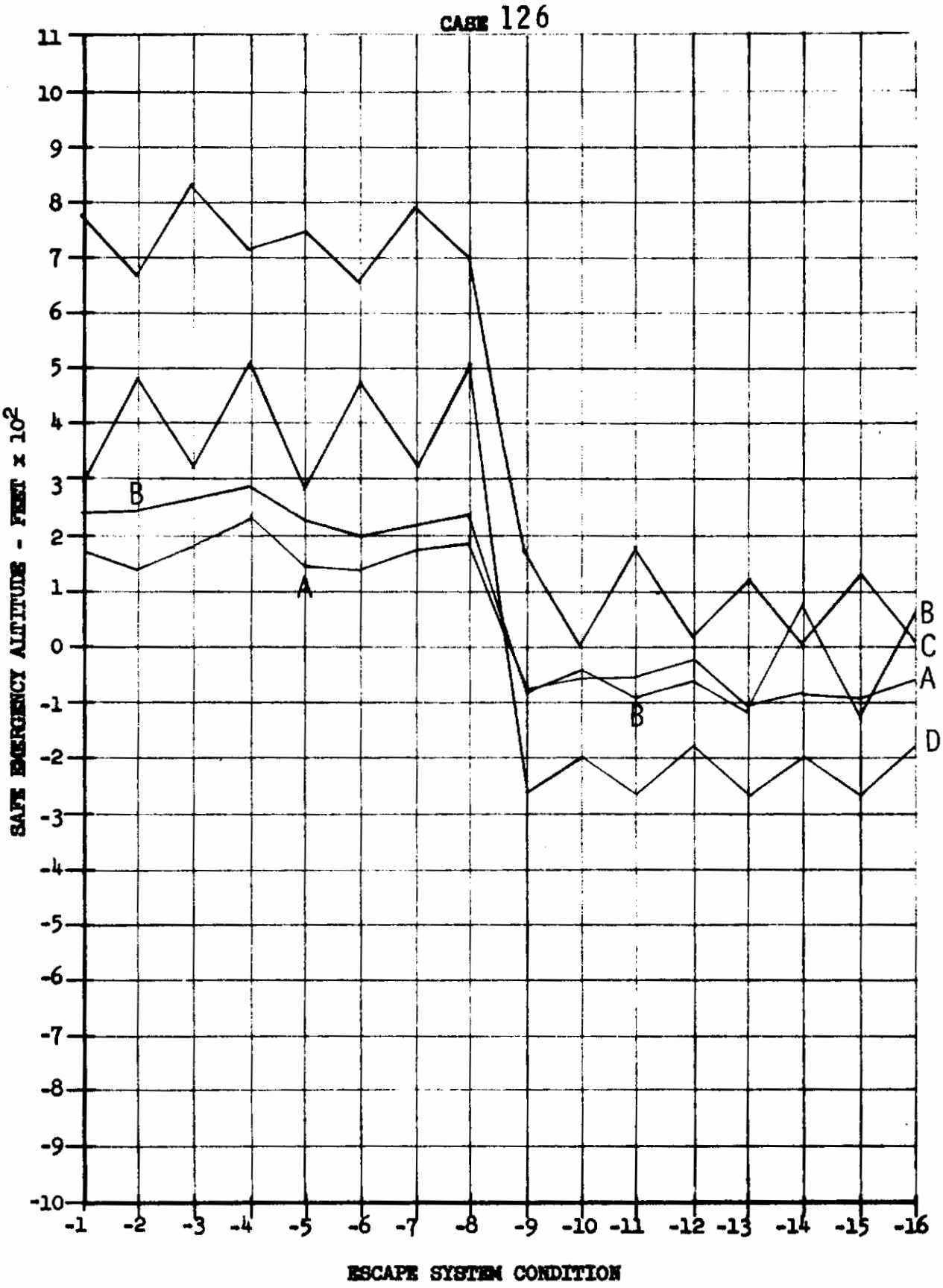

Approved for Public Release

Contrails

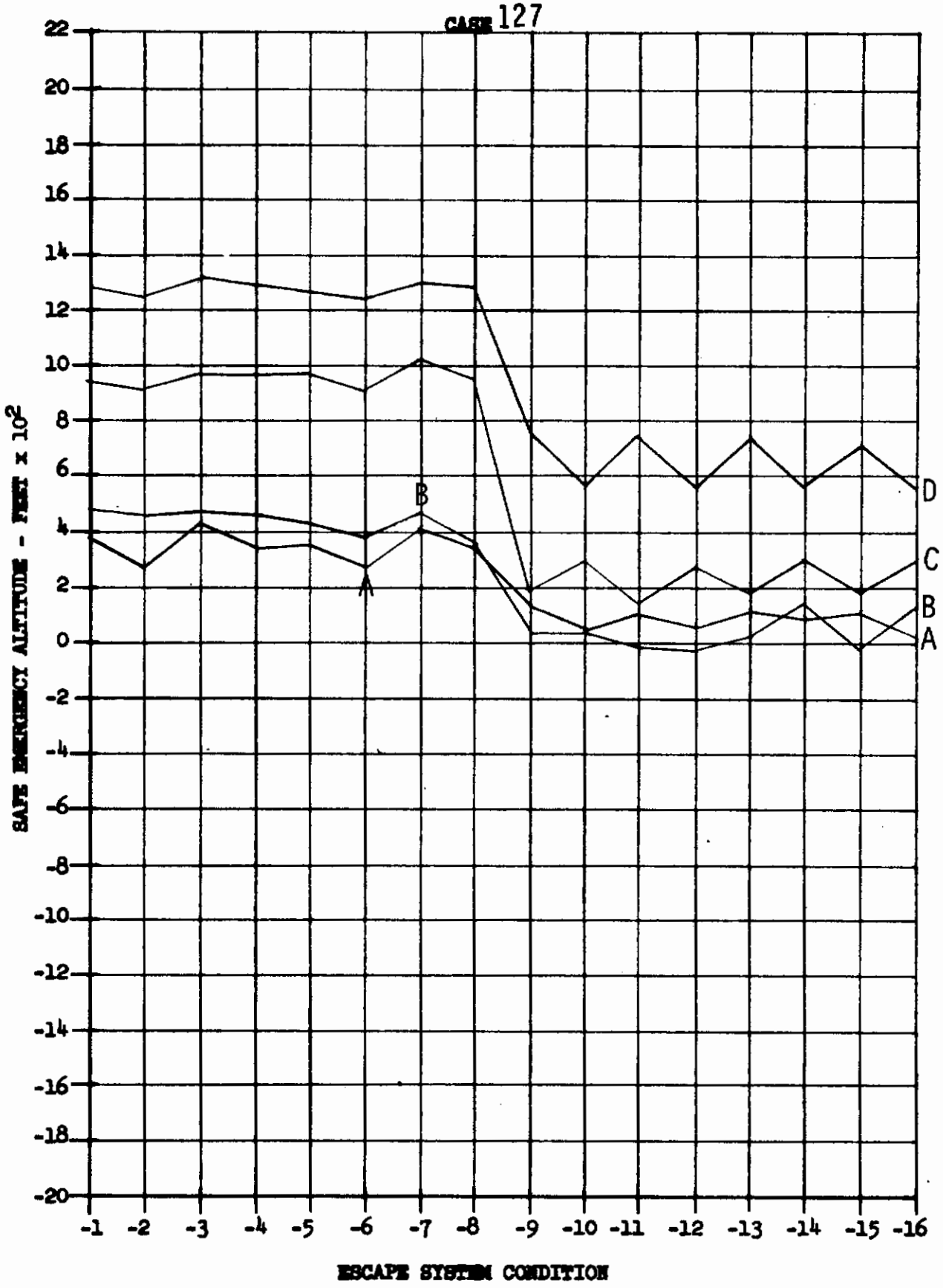

Approved for Public Release

Contrails

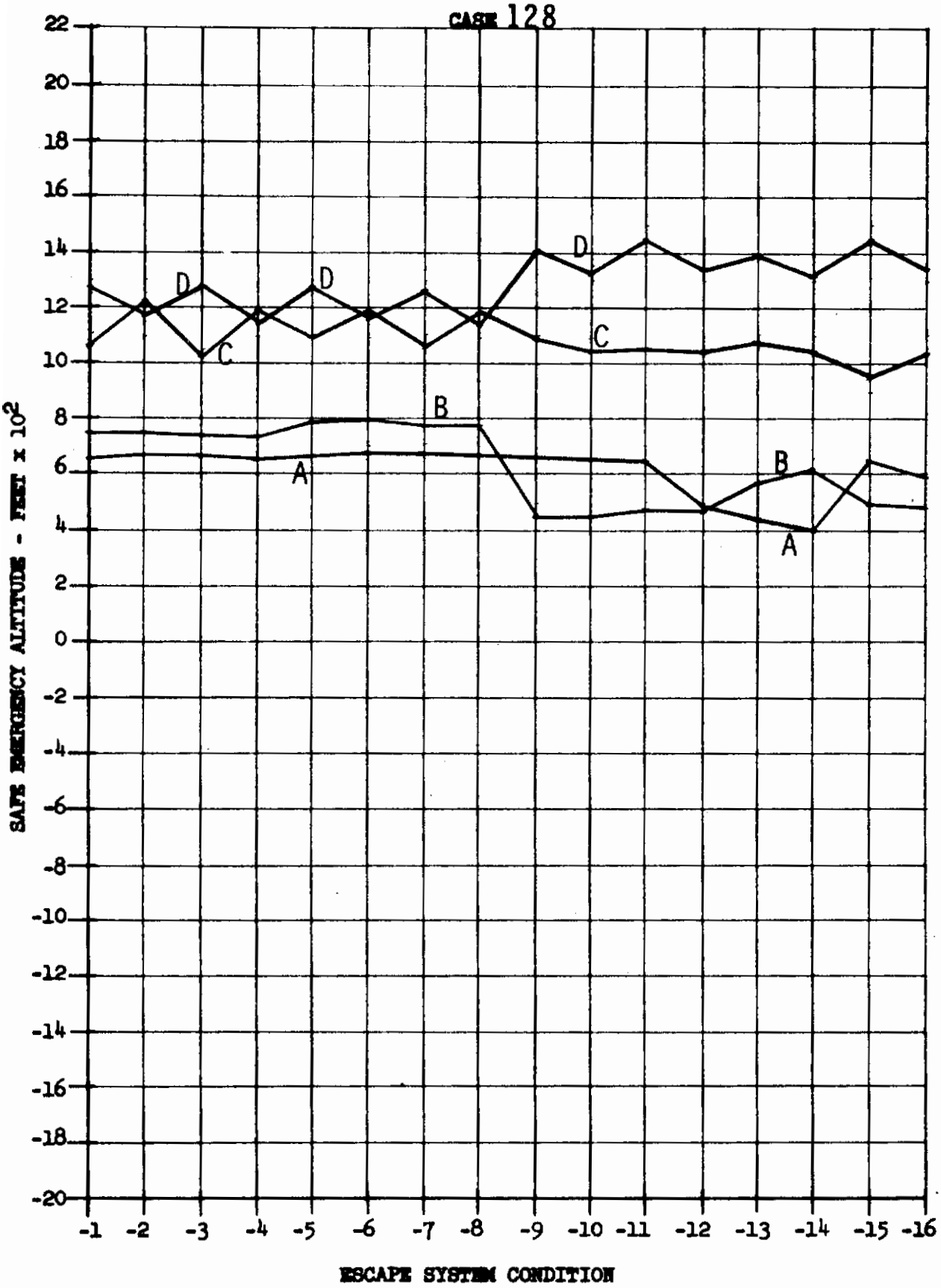

Approved for Public Release

Contrails

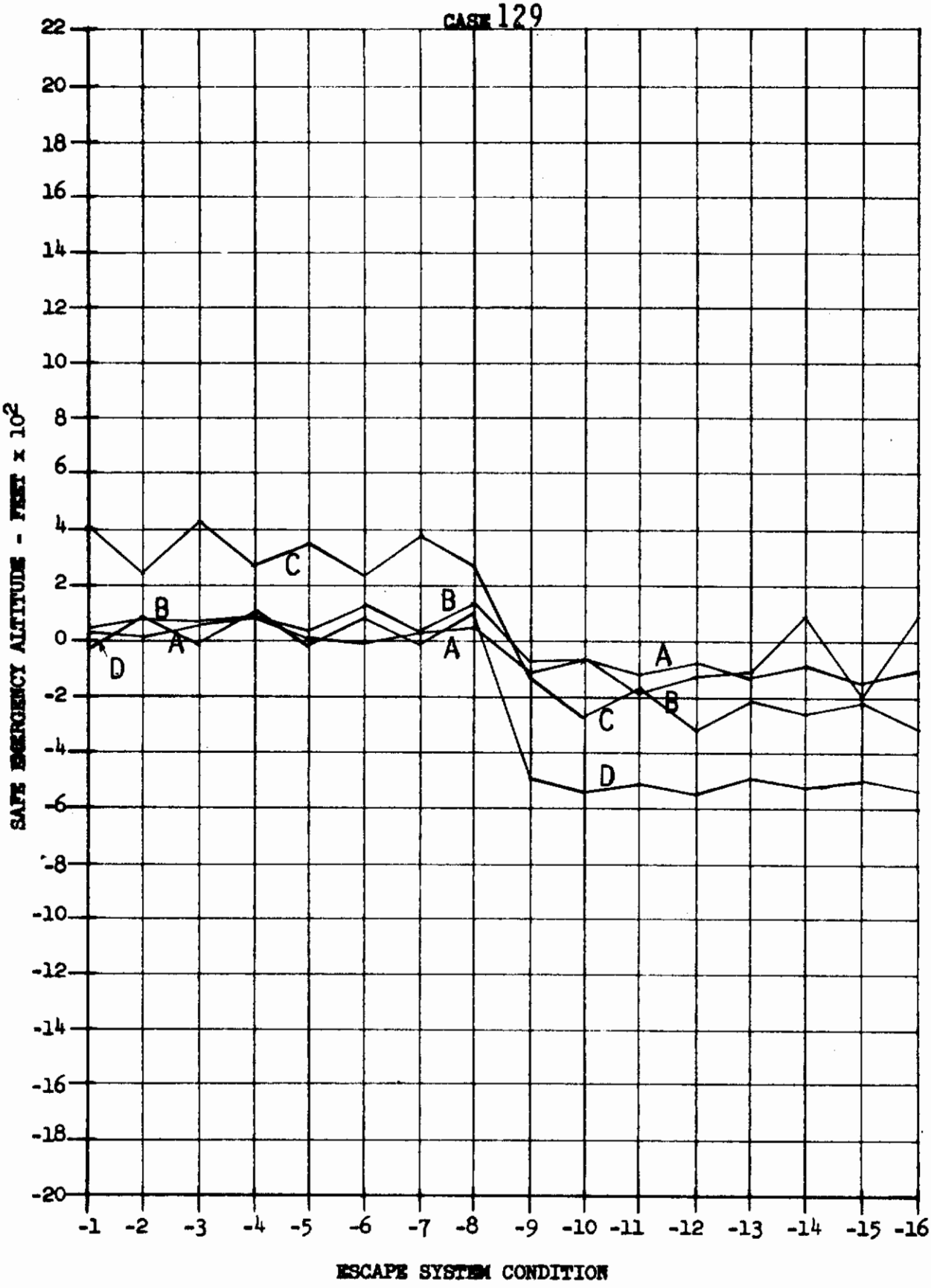

Approved for Public Release

Contrails

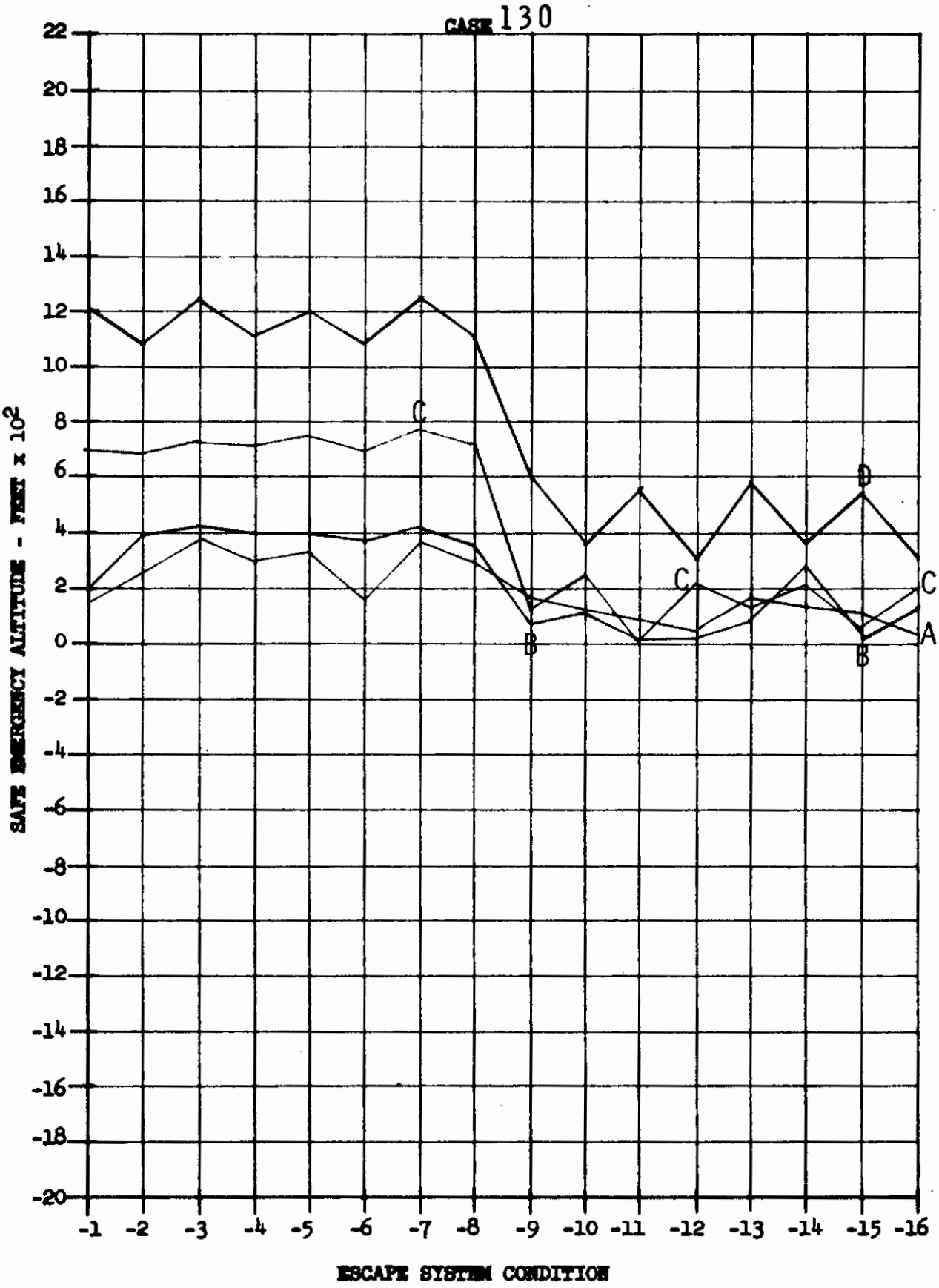

Approved for Public Release

Contrails

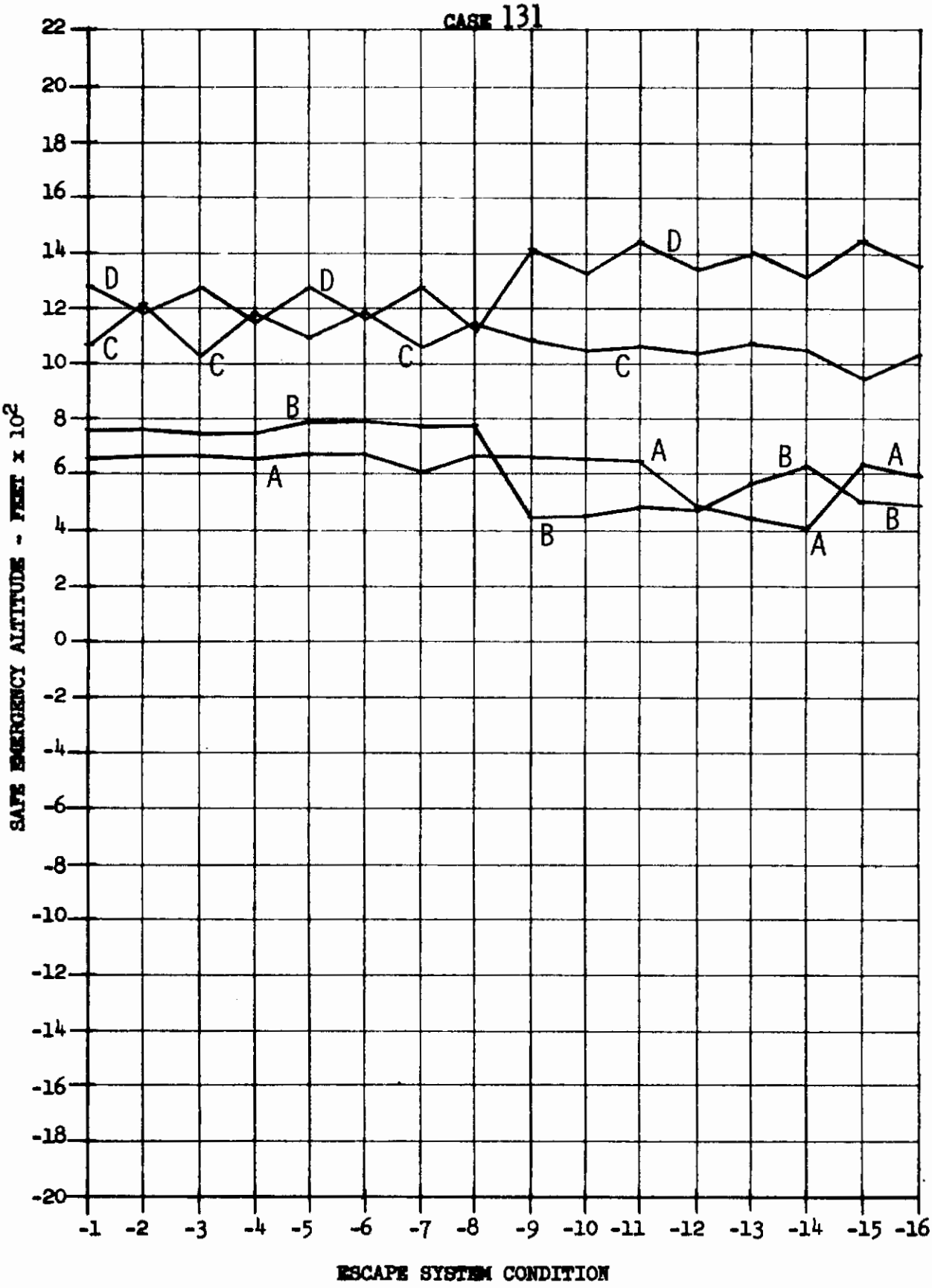

Approved for Public Release

Contrails

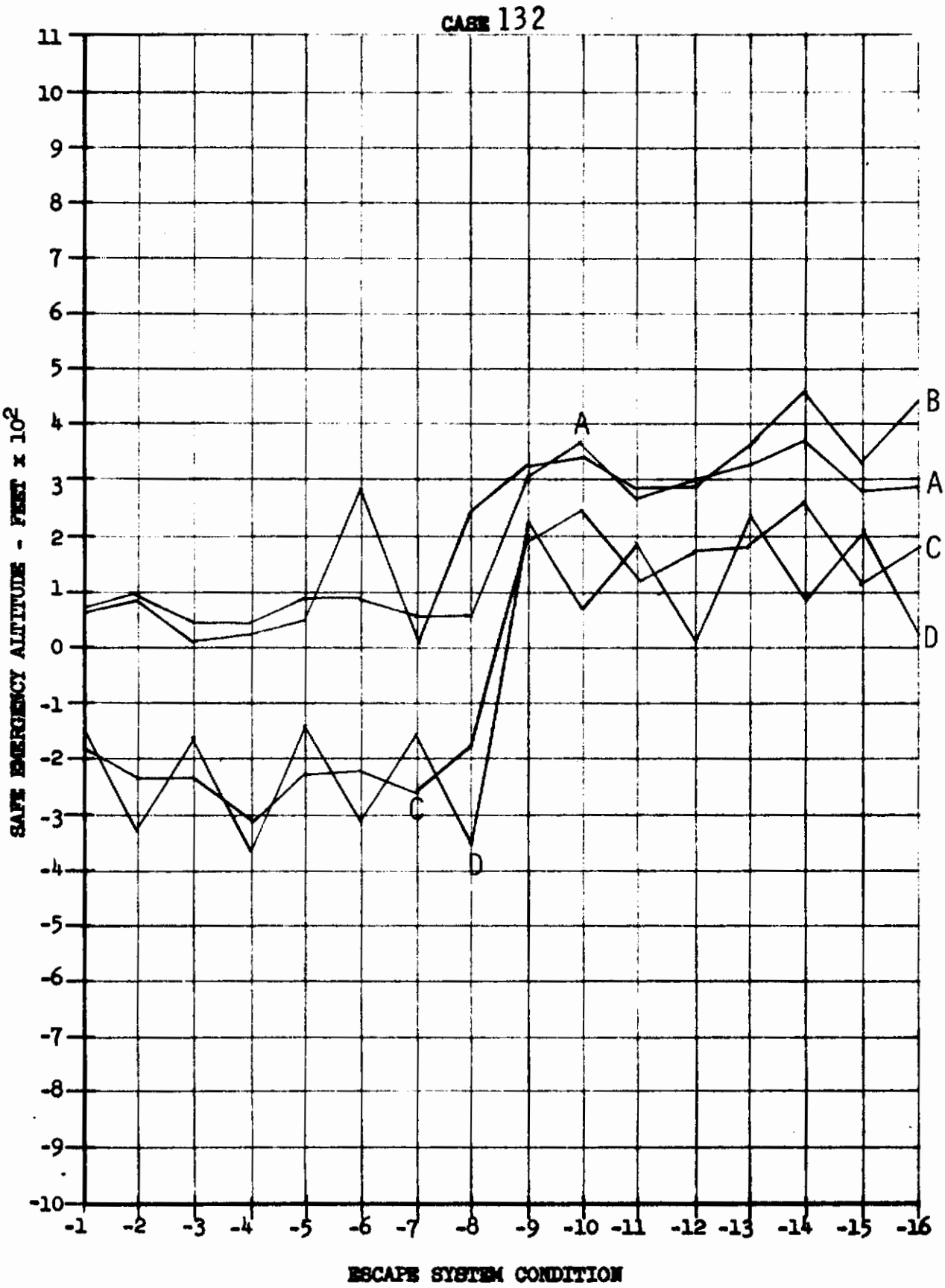

Approved for Public Release

Contrails

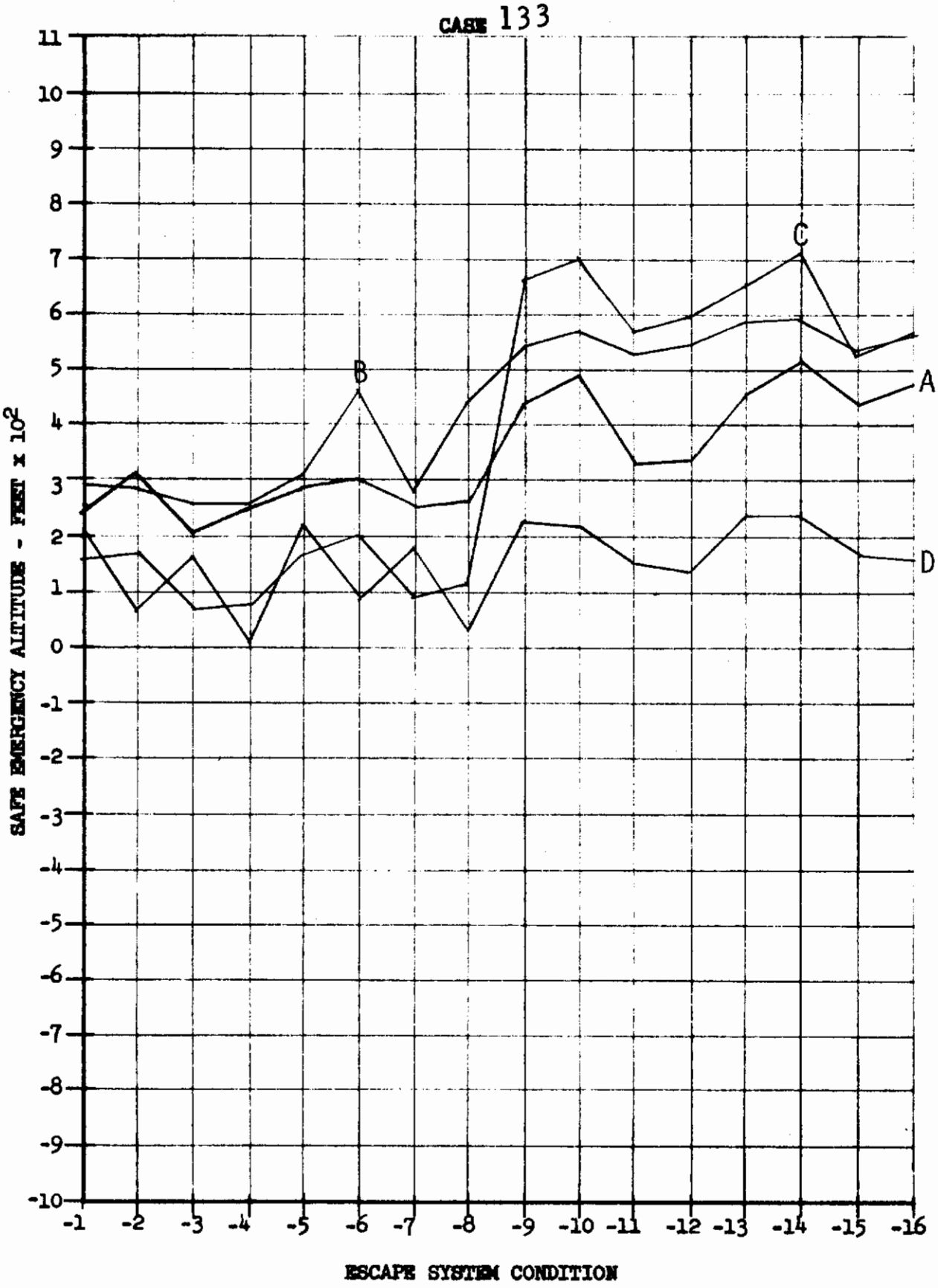

Approved for Public Release

Contrails

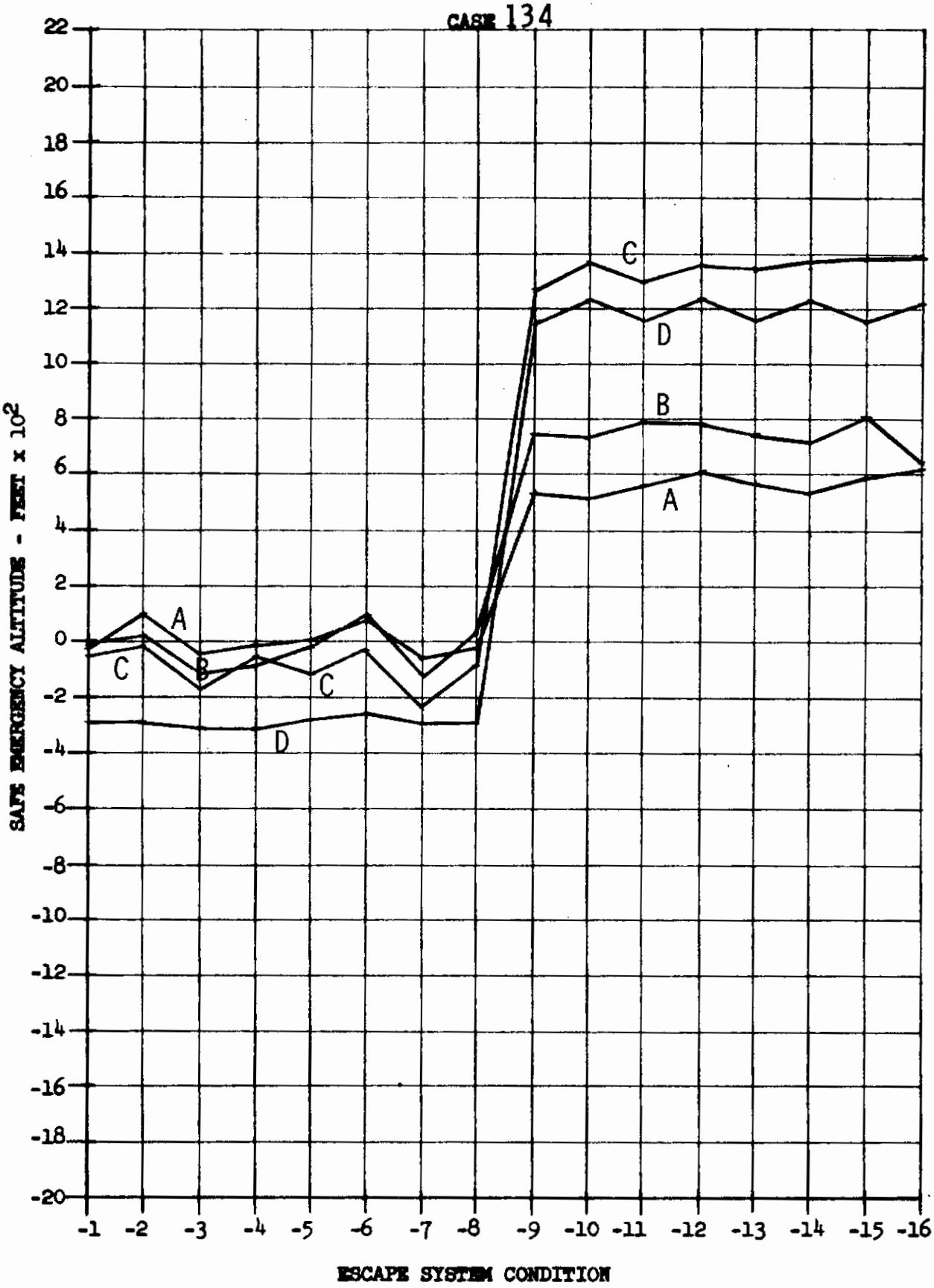

Approved for Public Release

Contrails

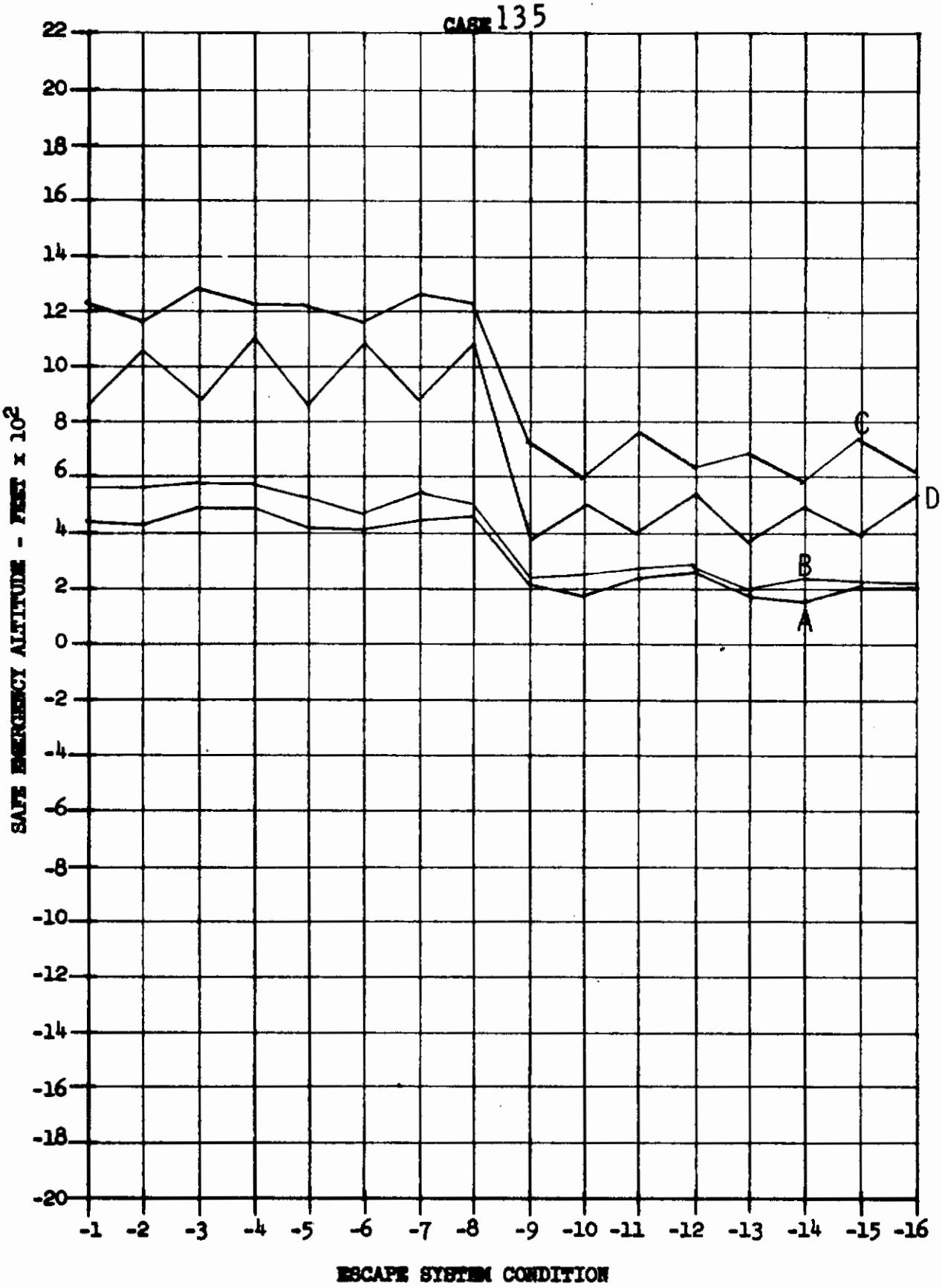

Approved for Public Release

Contrails

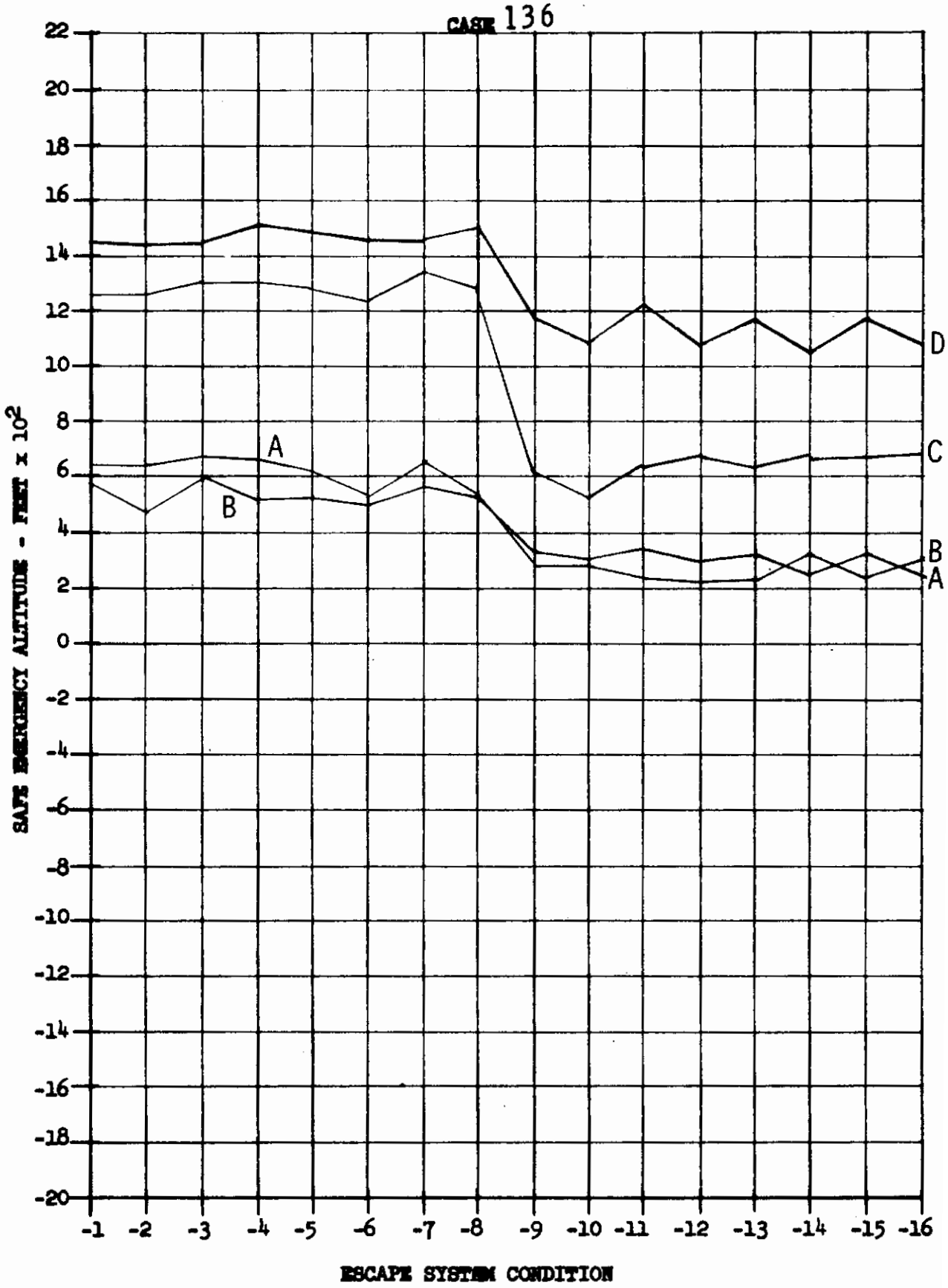

Approved for Public Release

Contrails

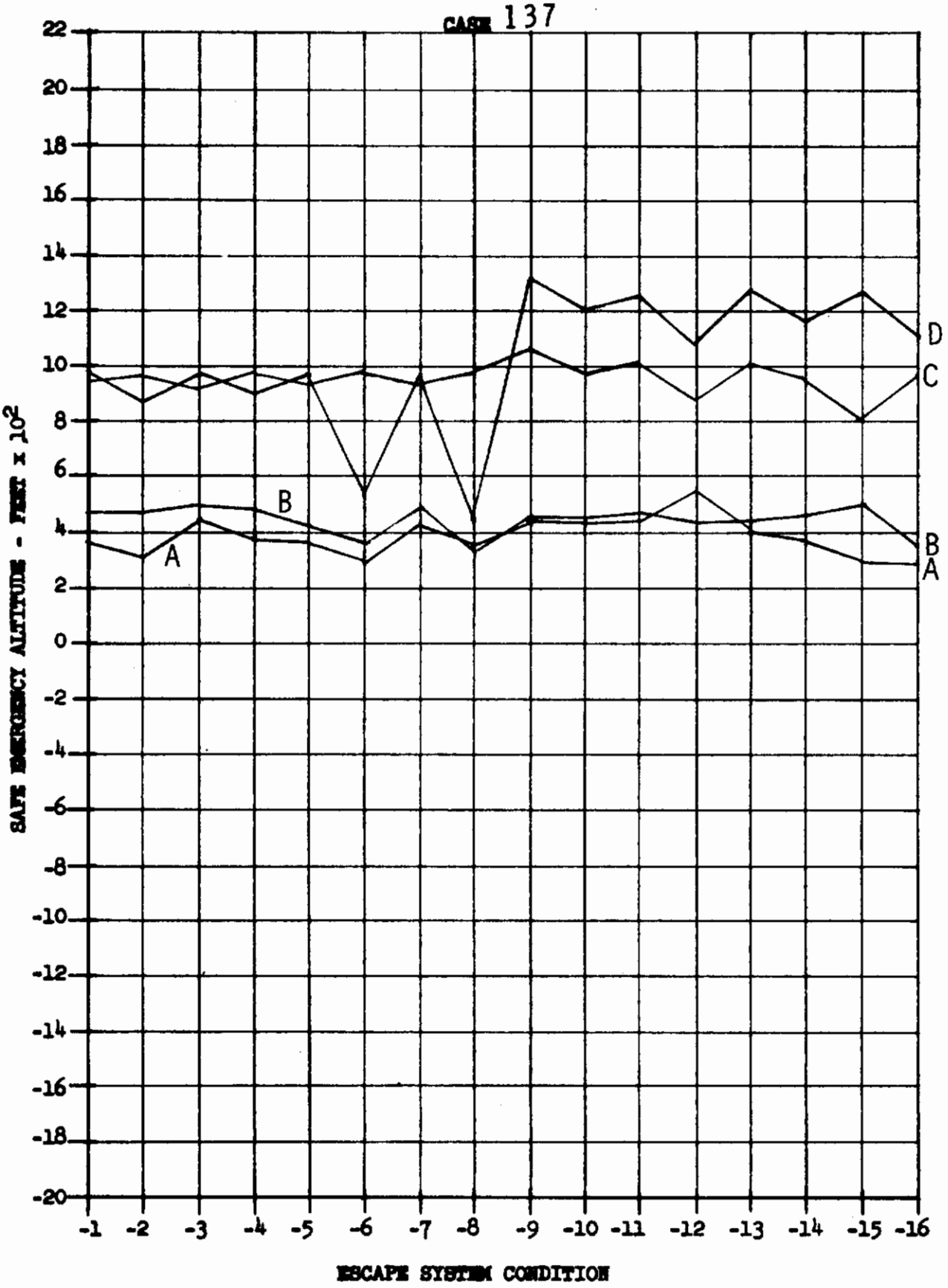

Approved for Public Release

Contrails

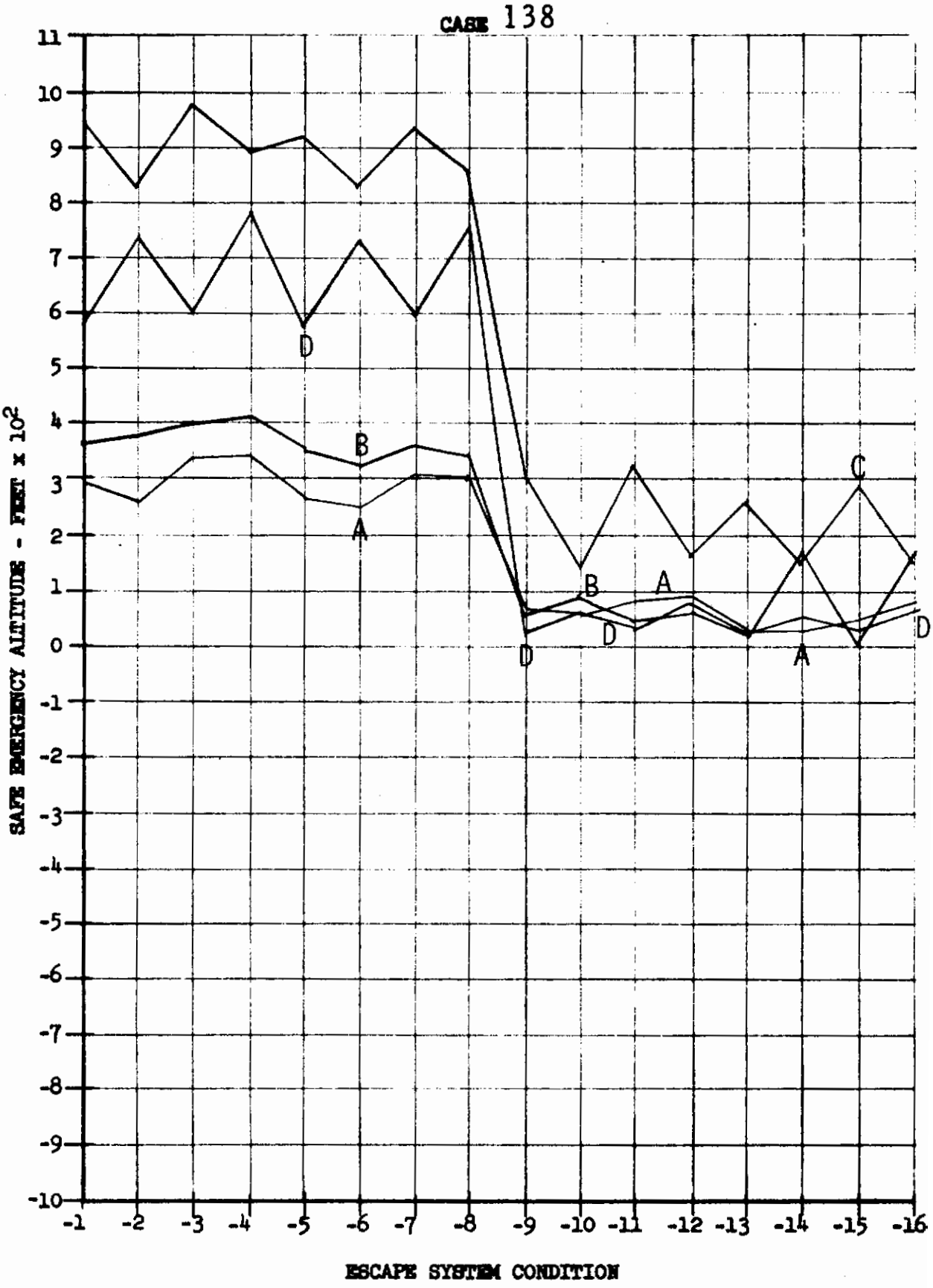

Approved for Public Release

Contrails

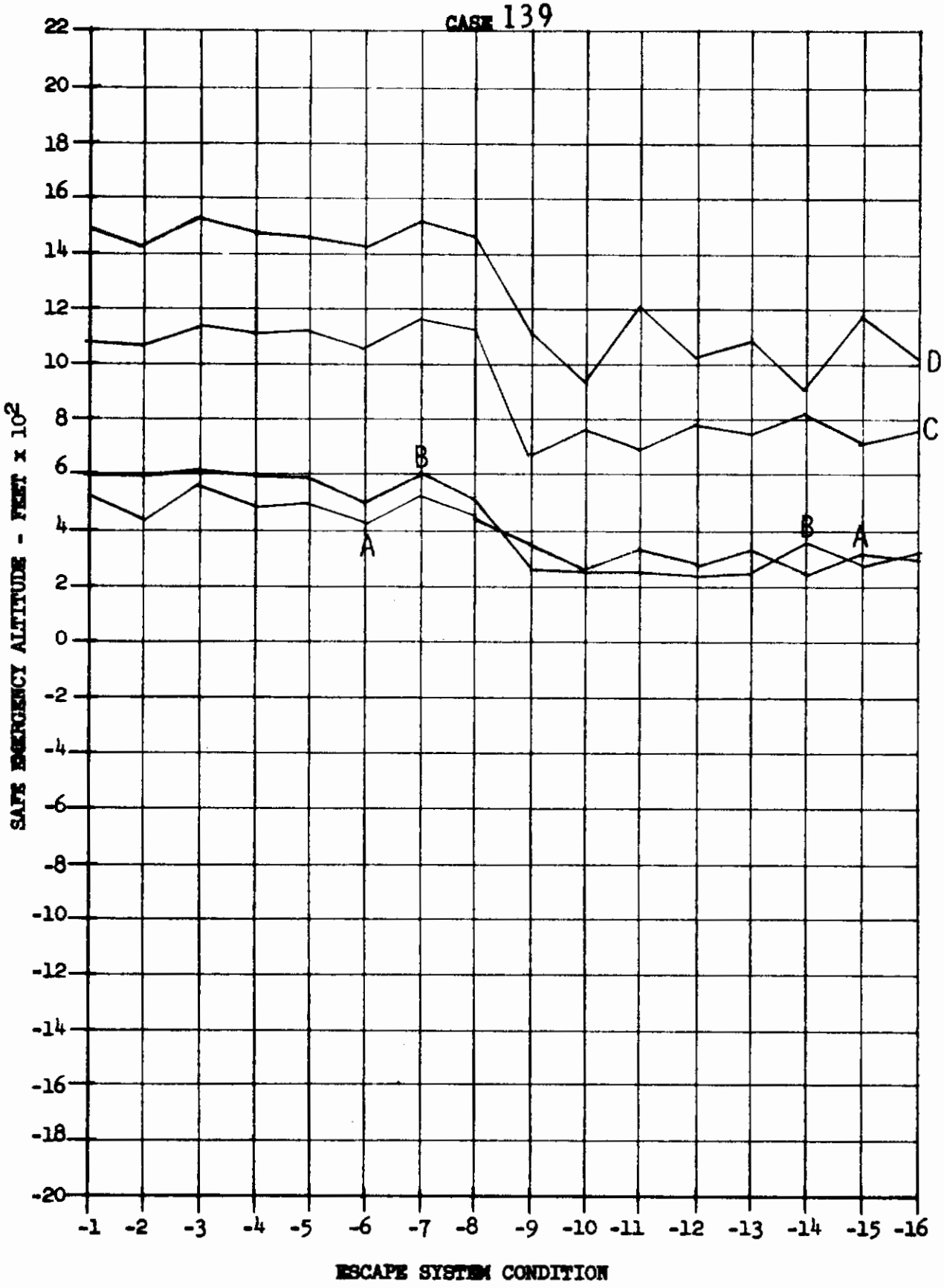

Approved for Public Release

Contrails

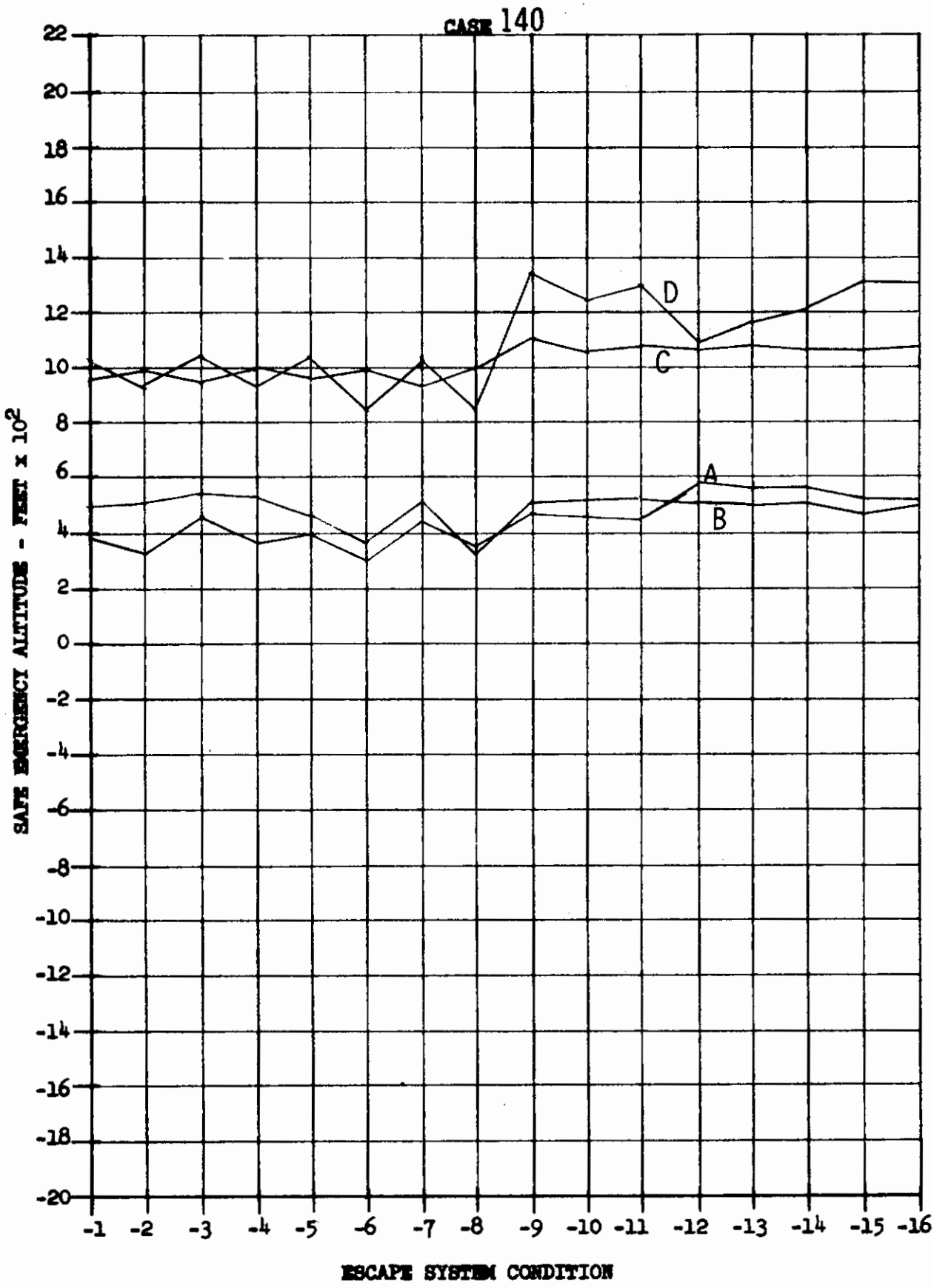

Approved for Public Release

Contrails

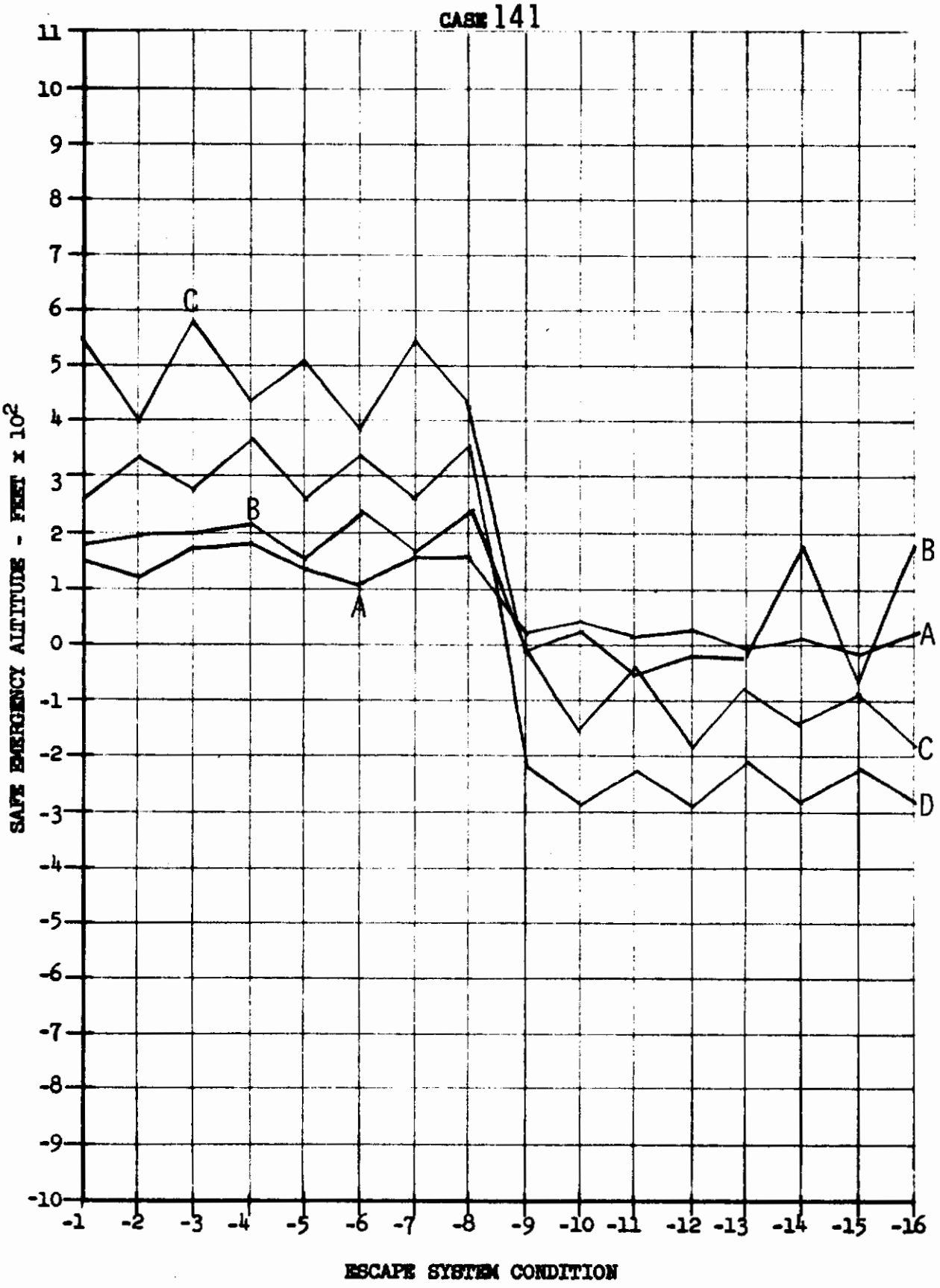

Approved for Public Release

Contrails

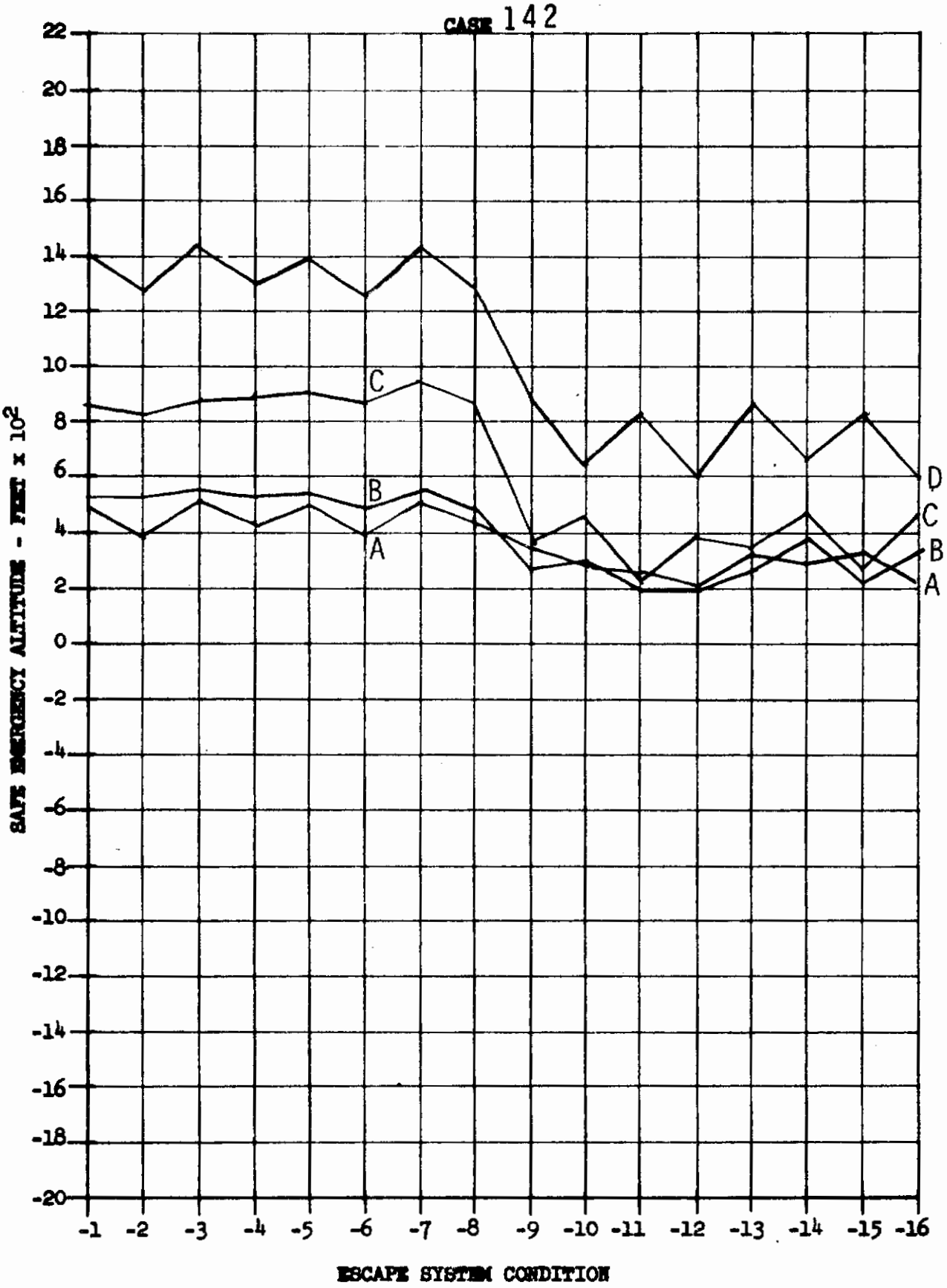

Approved for Public Release

Contrails

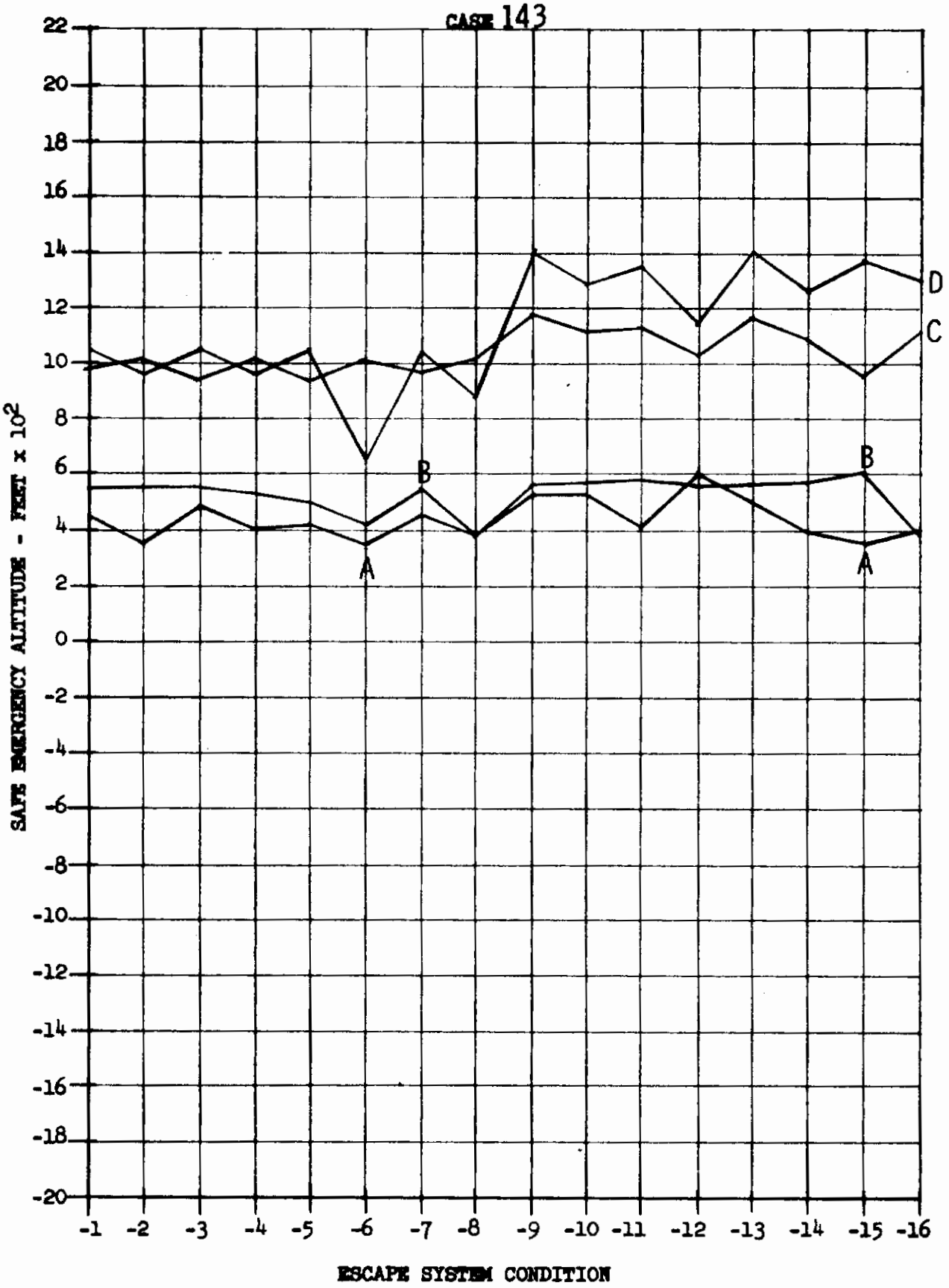

Approved for Public Release

Contrails

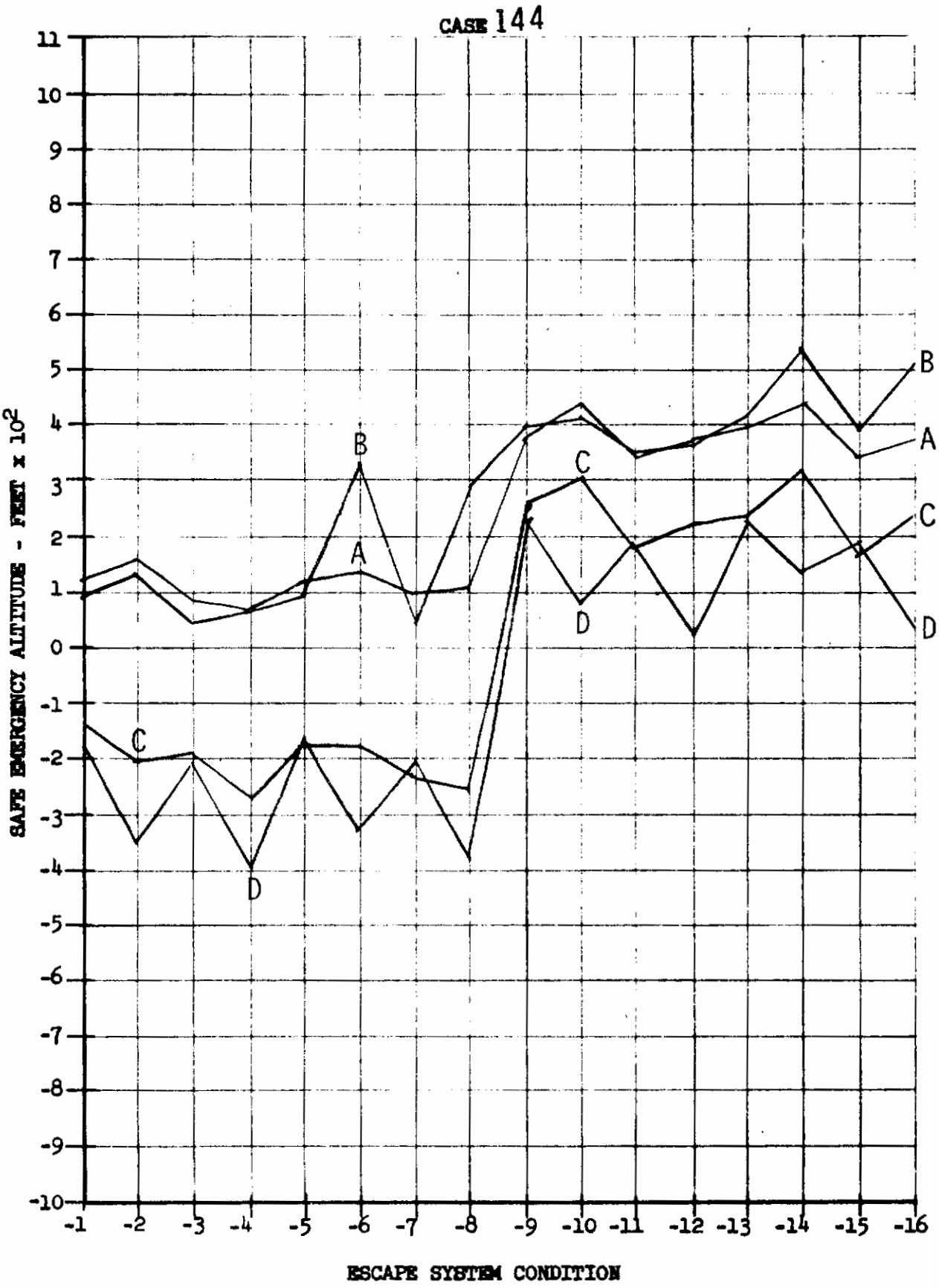

Approved for Public Release

Contrails

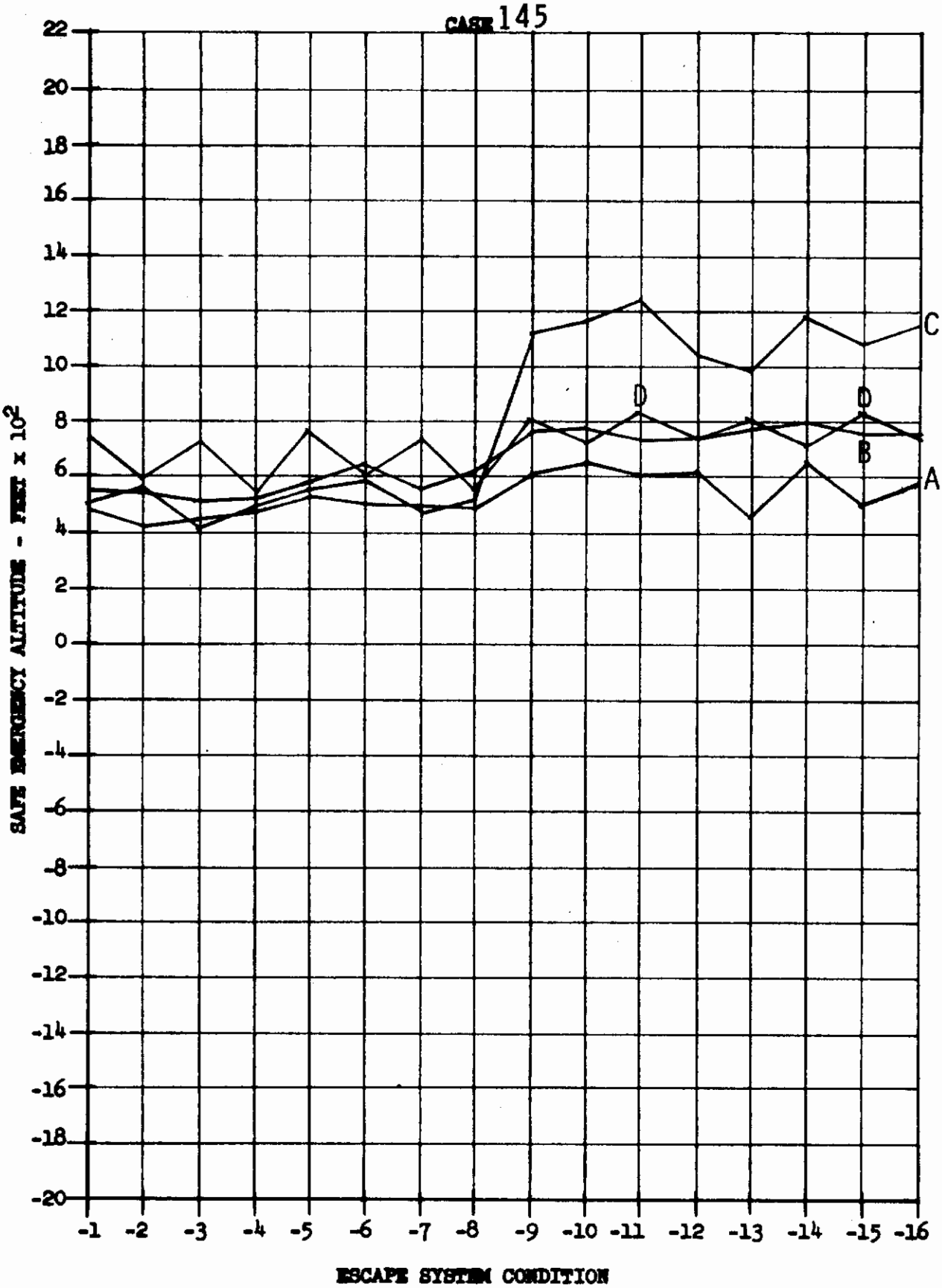

Approved for Public Release

Contrails

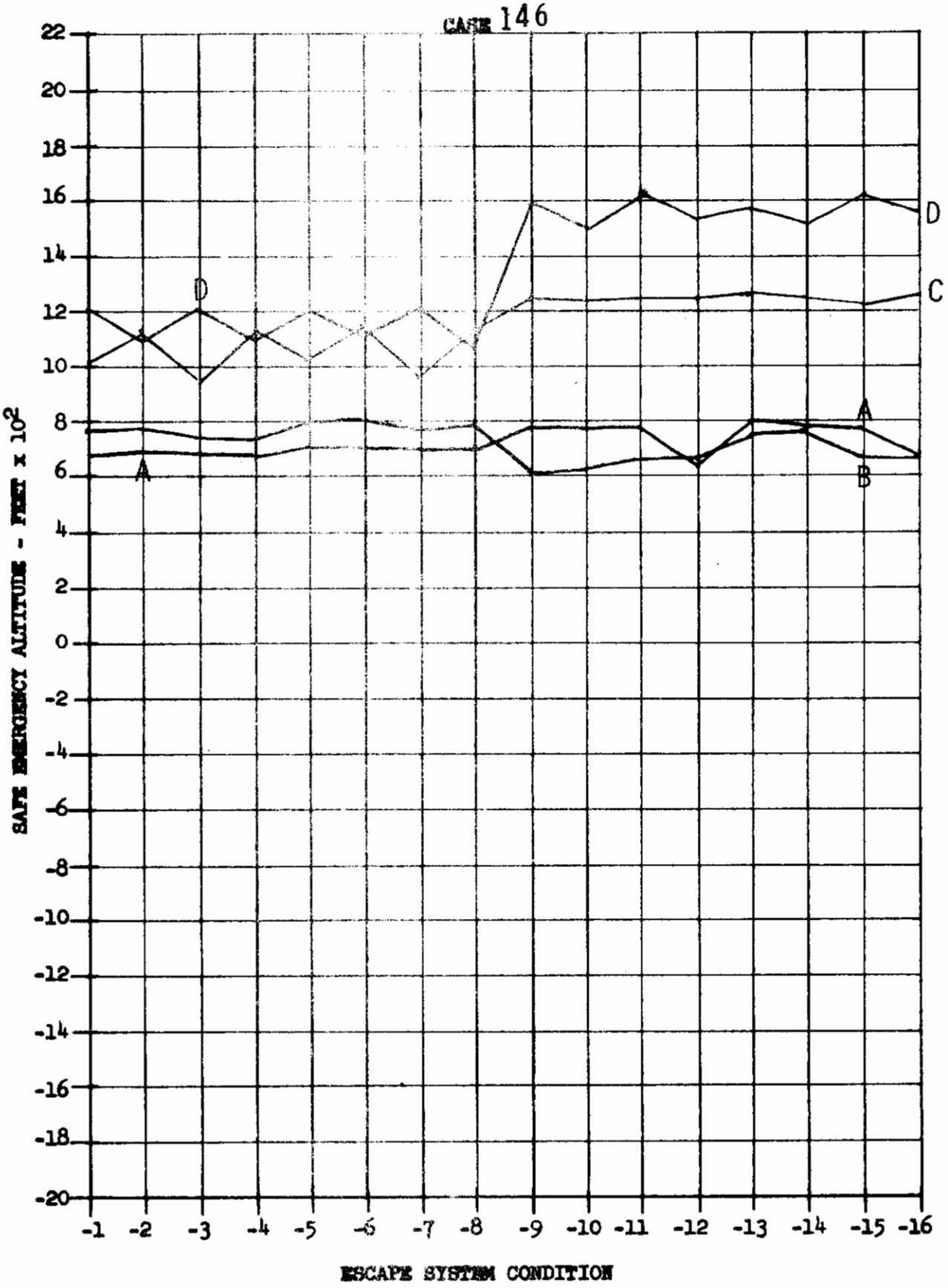

Approved for Public Release

Contrails

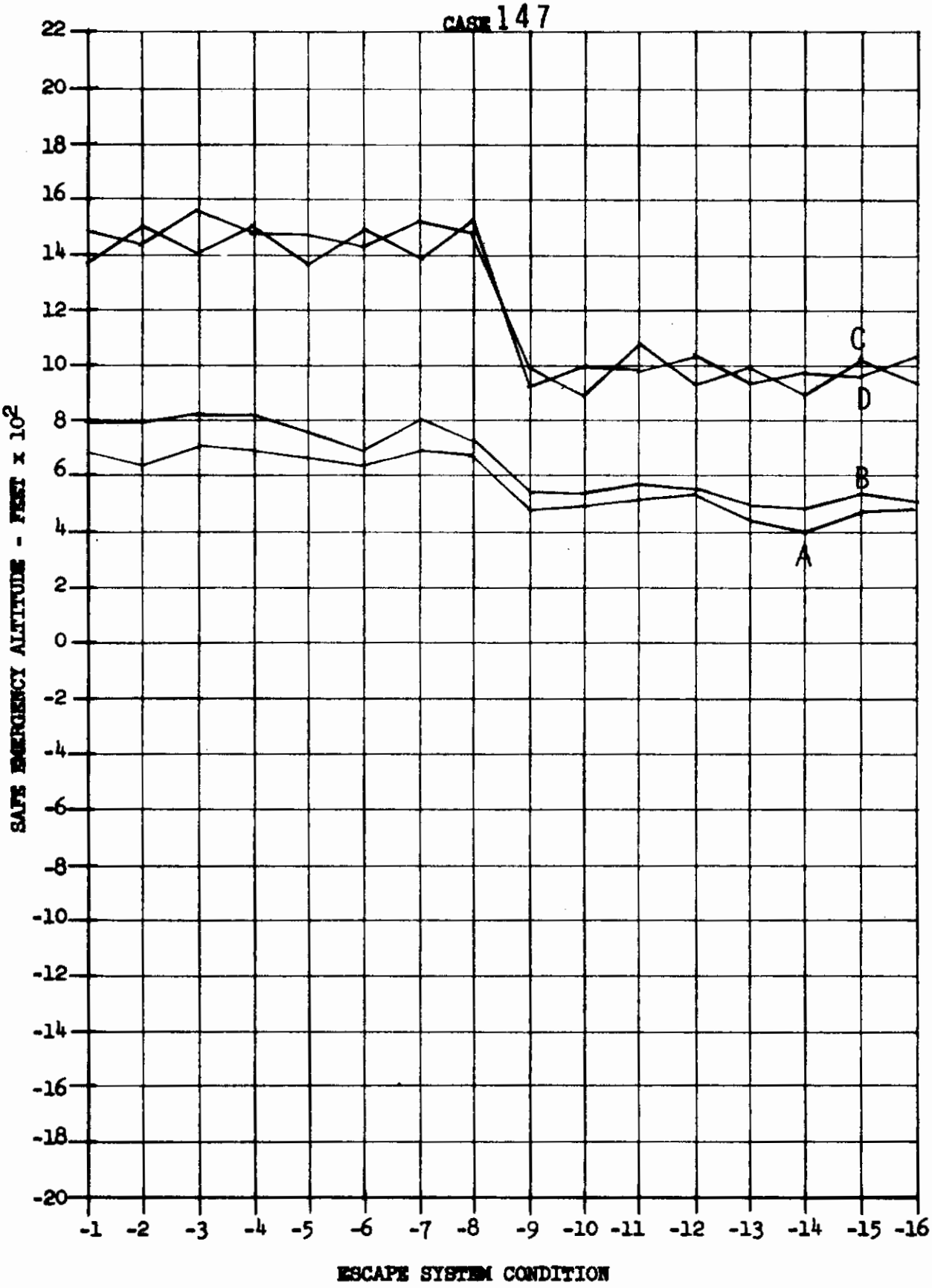

Approved for Public Release

Contrails

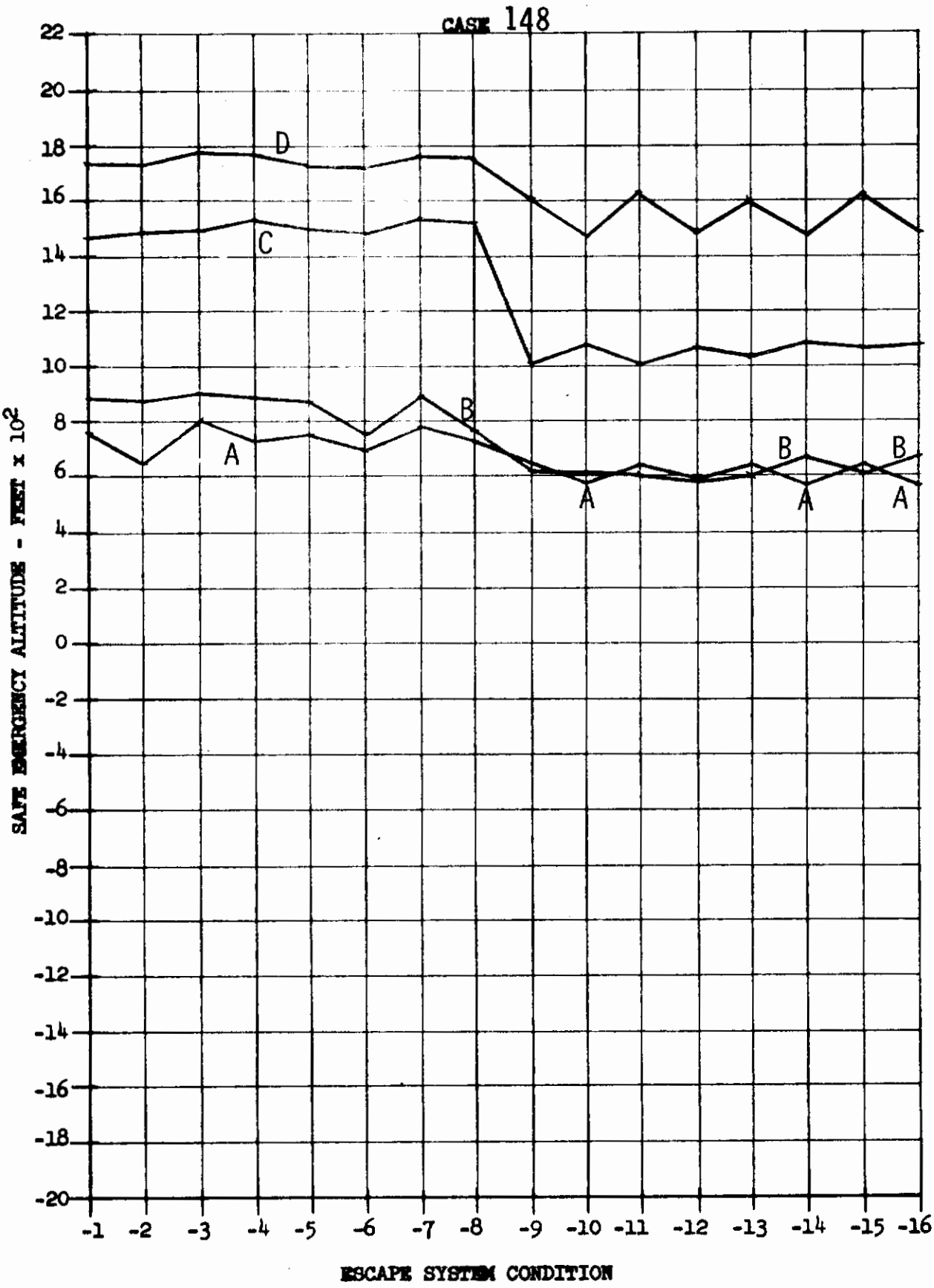

Approved for Public Release

Contrails

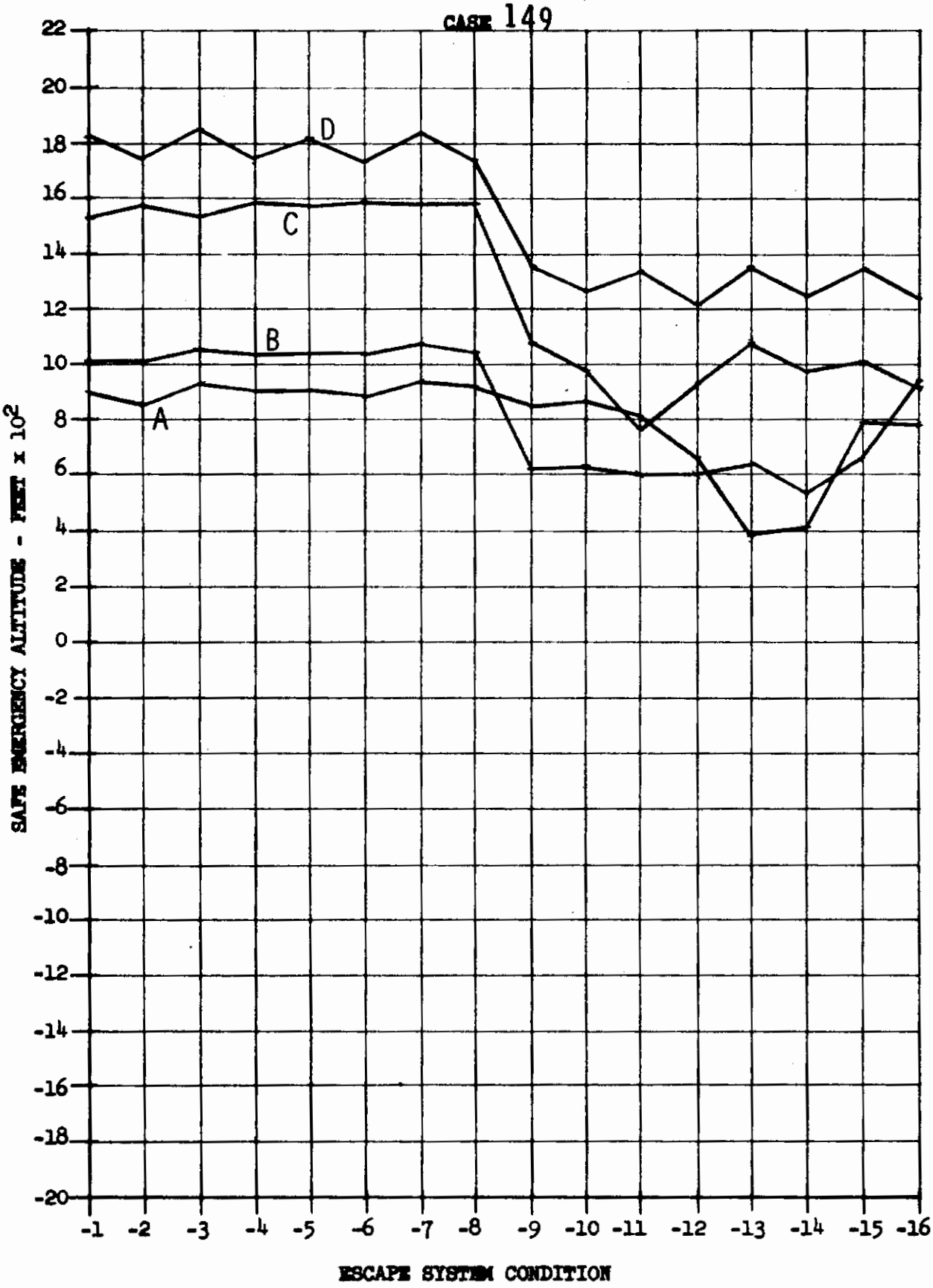

Approved for Public Release

Contrails

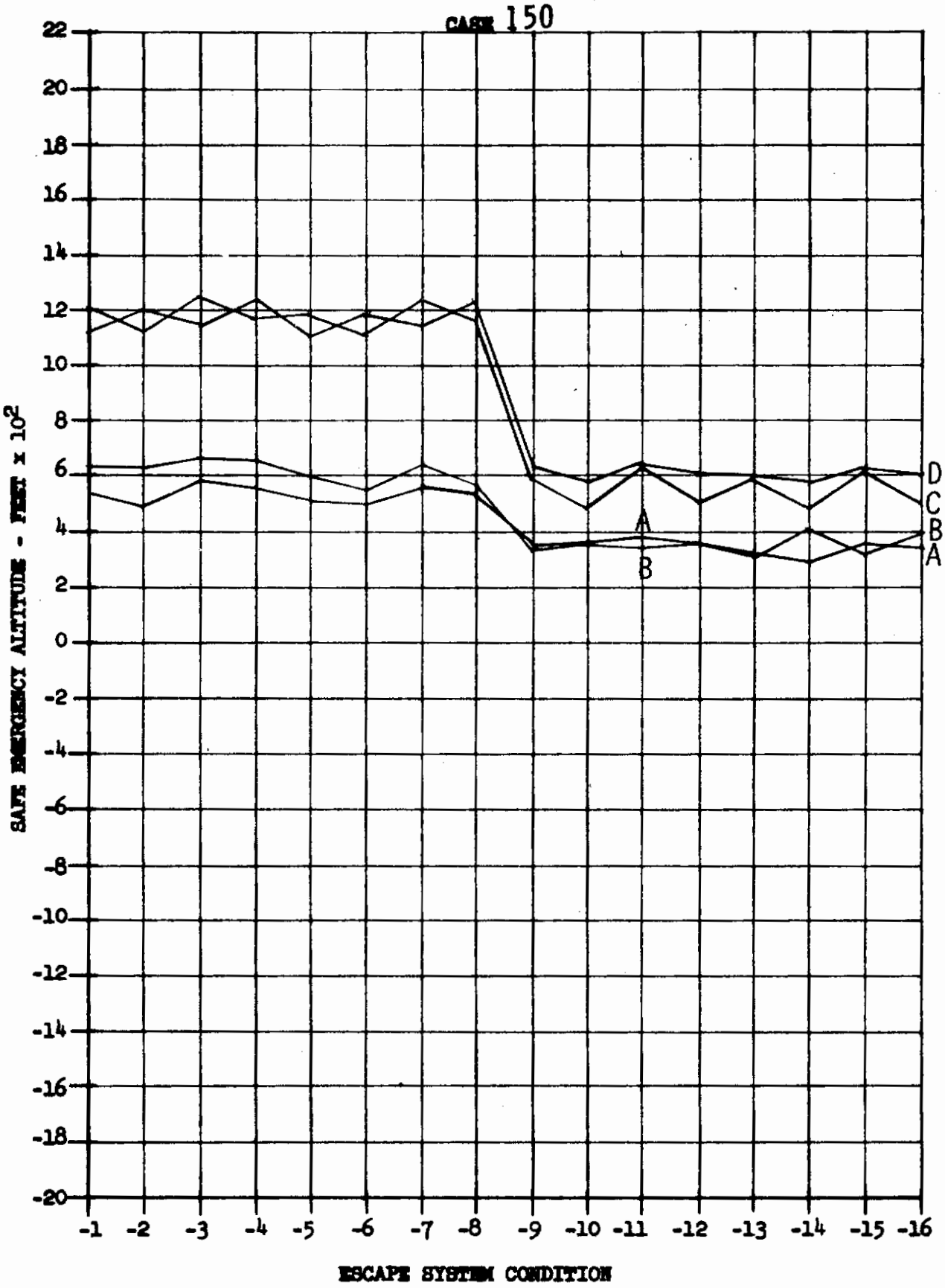

Approved for Public Release

Contrails

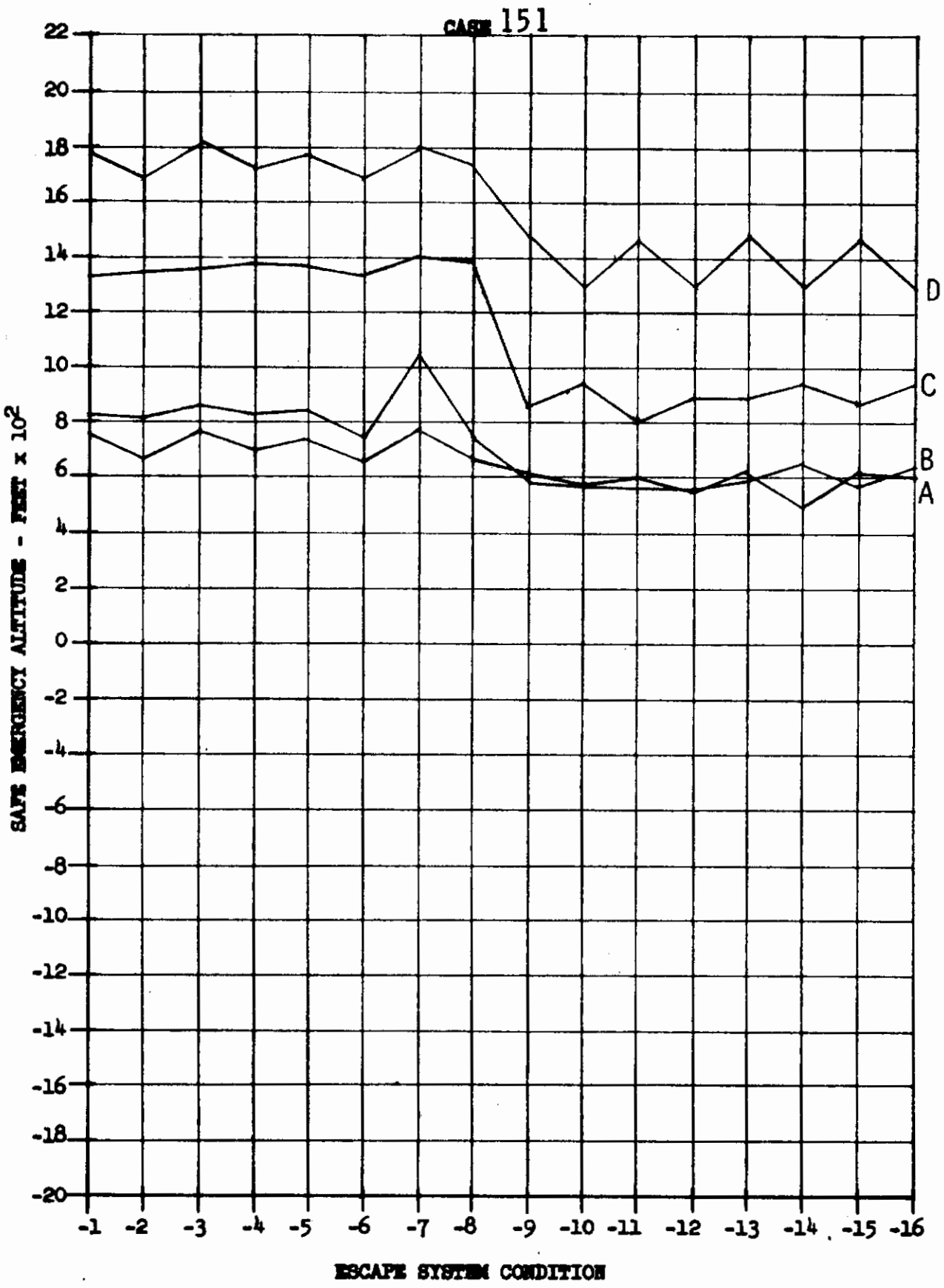

Approved for Public Release

Contrails

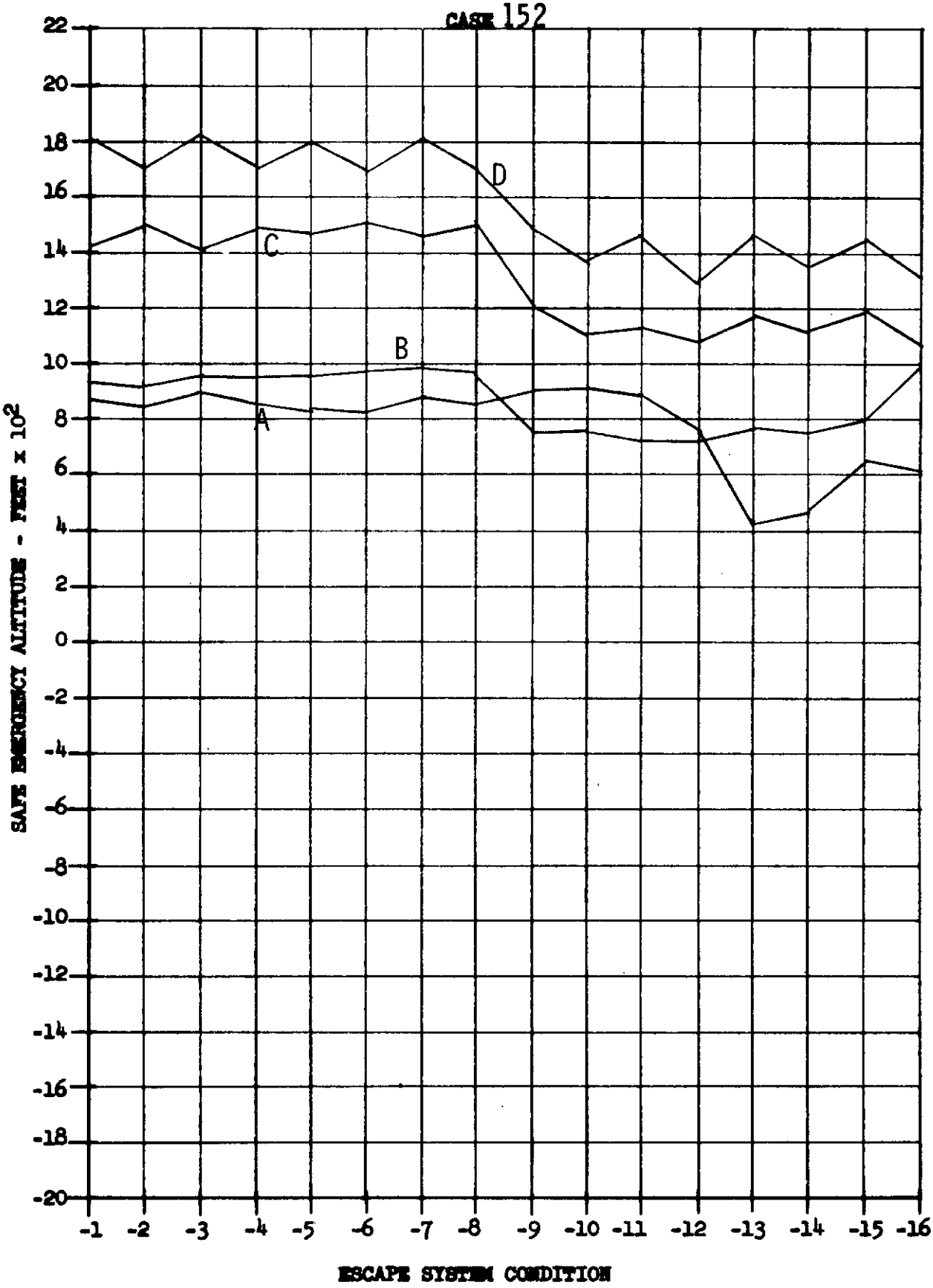

Approved for Public Release

Contrails

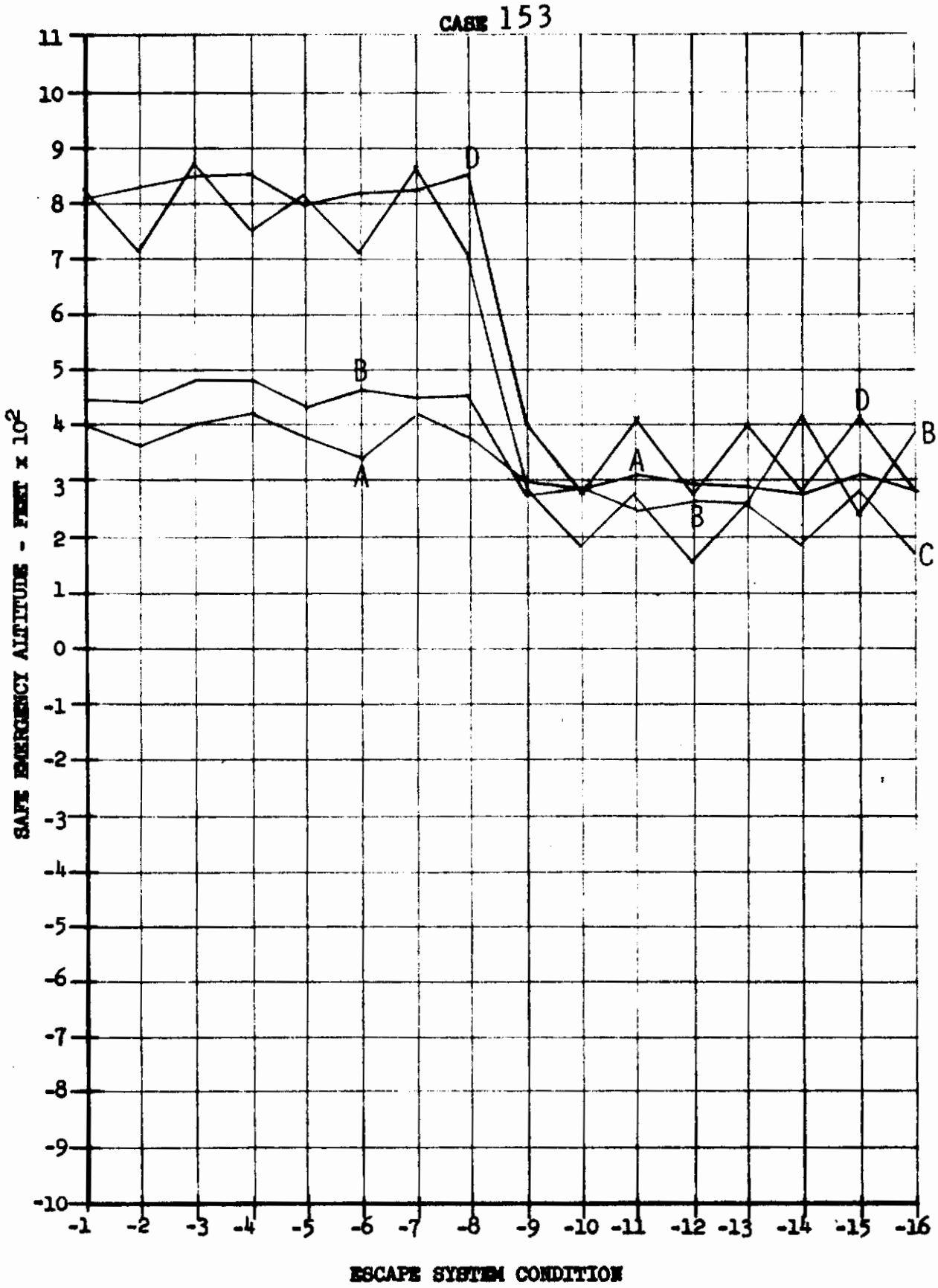

Approved for Public Release

Contrails

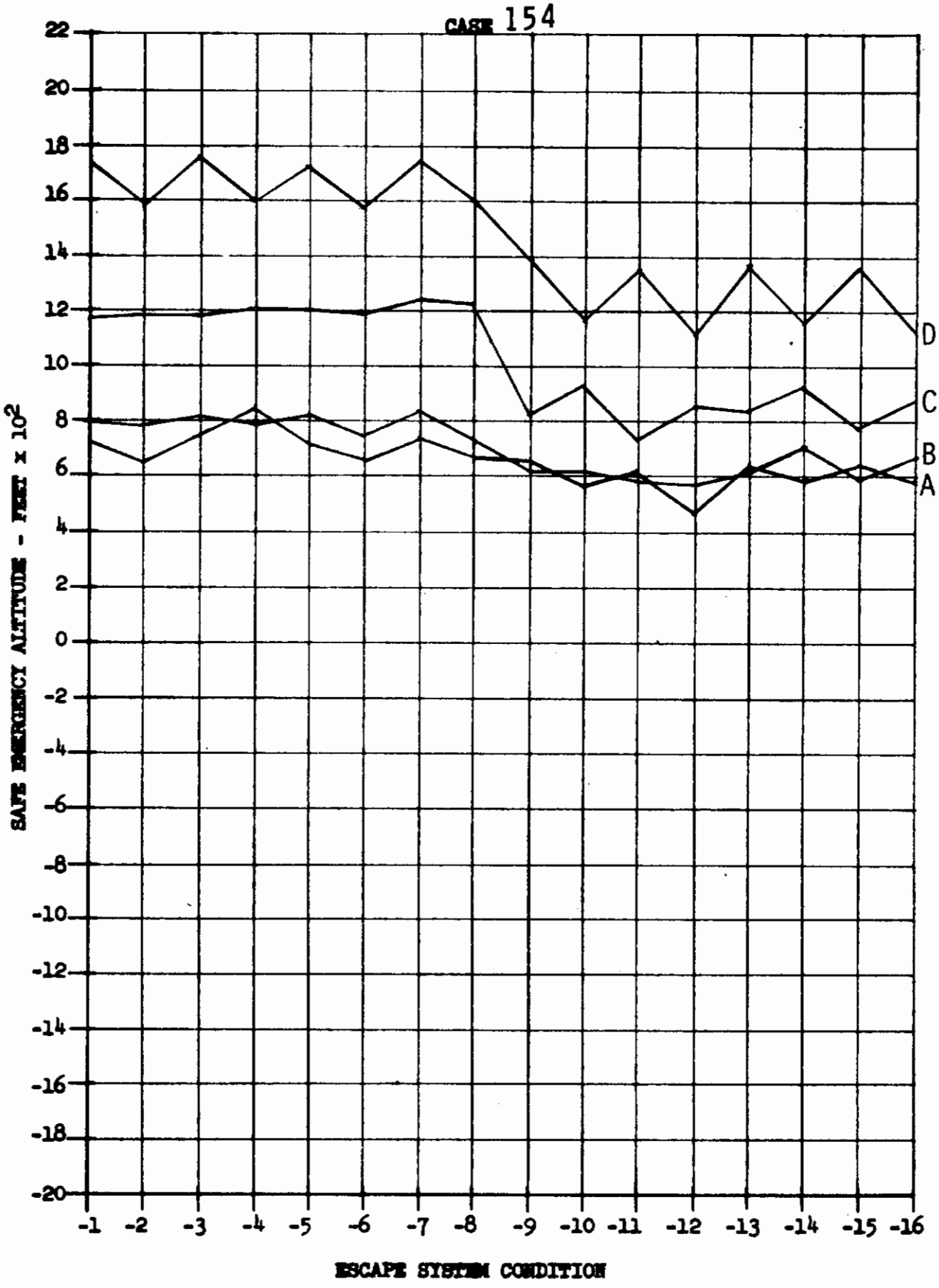

Approved for Public Release

Contrails

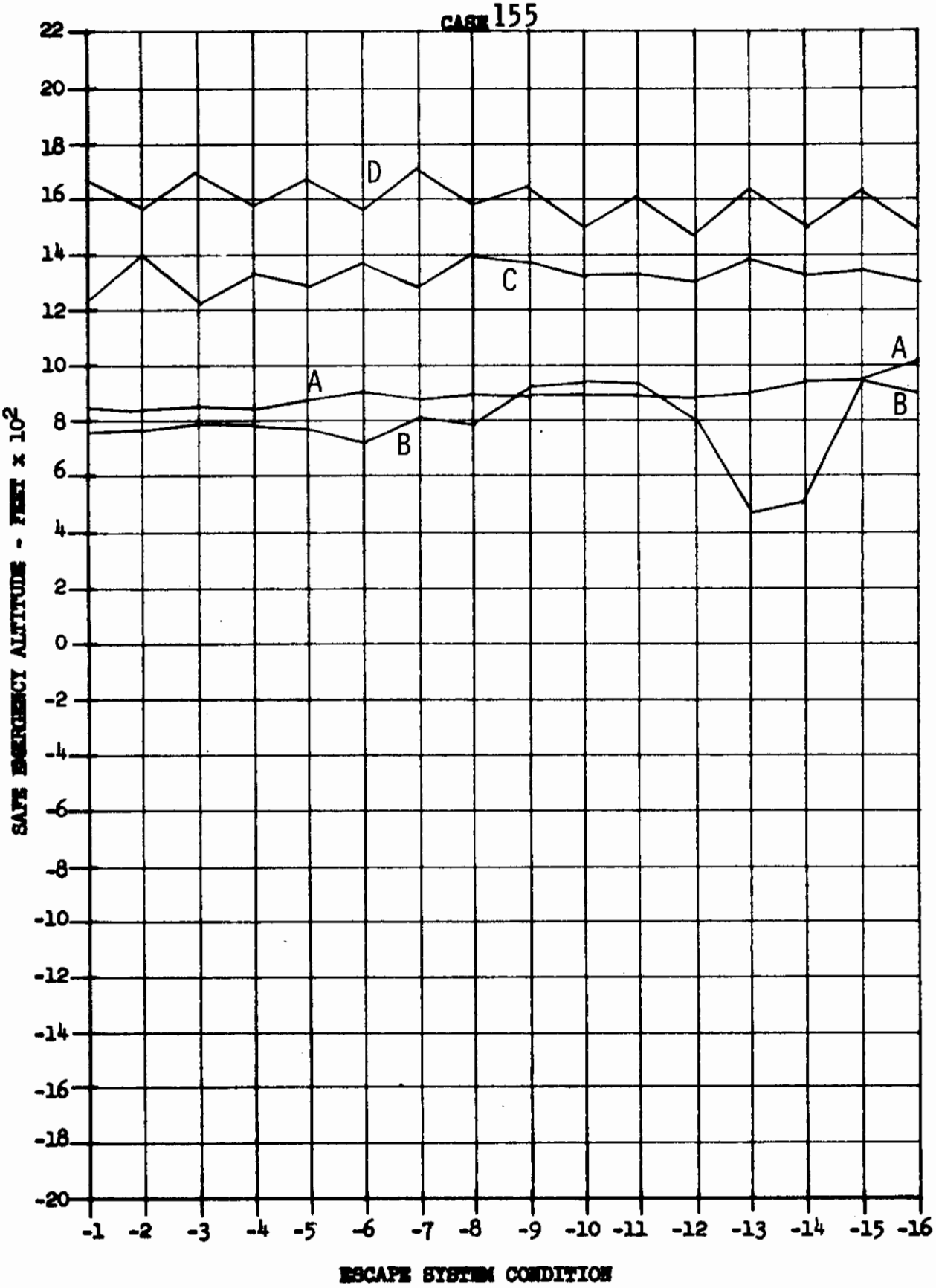

Approved for Public Release

Contrails

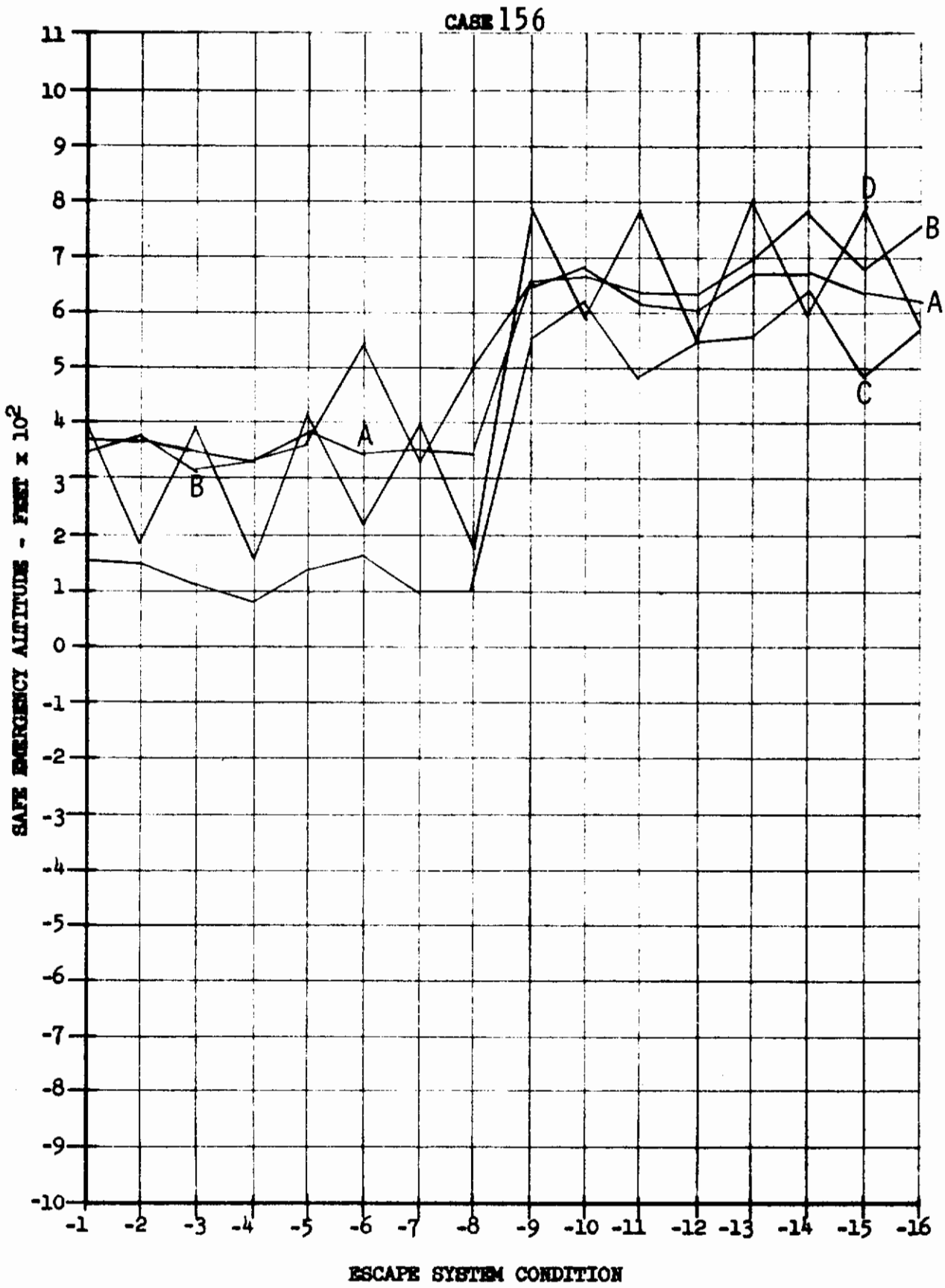

Approved for Public Release

Contrails

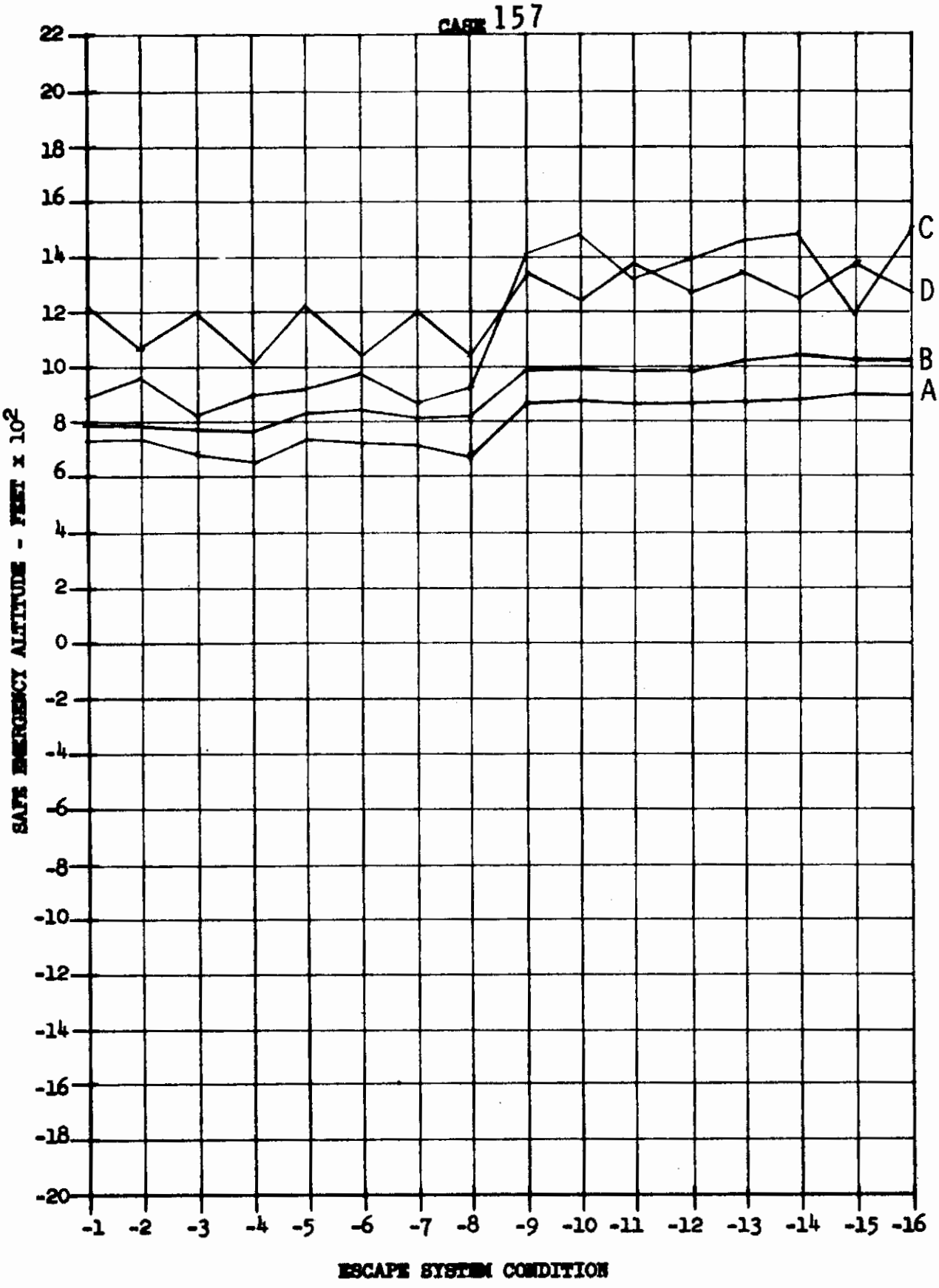

Approved for Public Release

Contrails

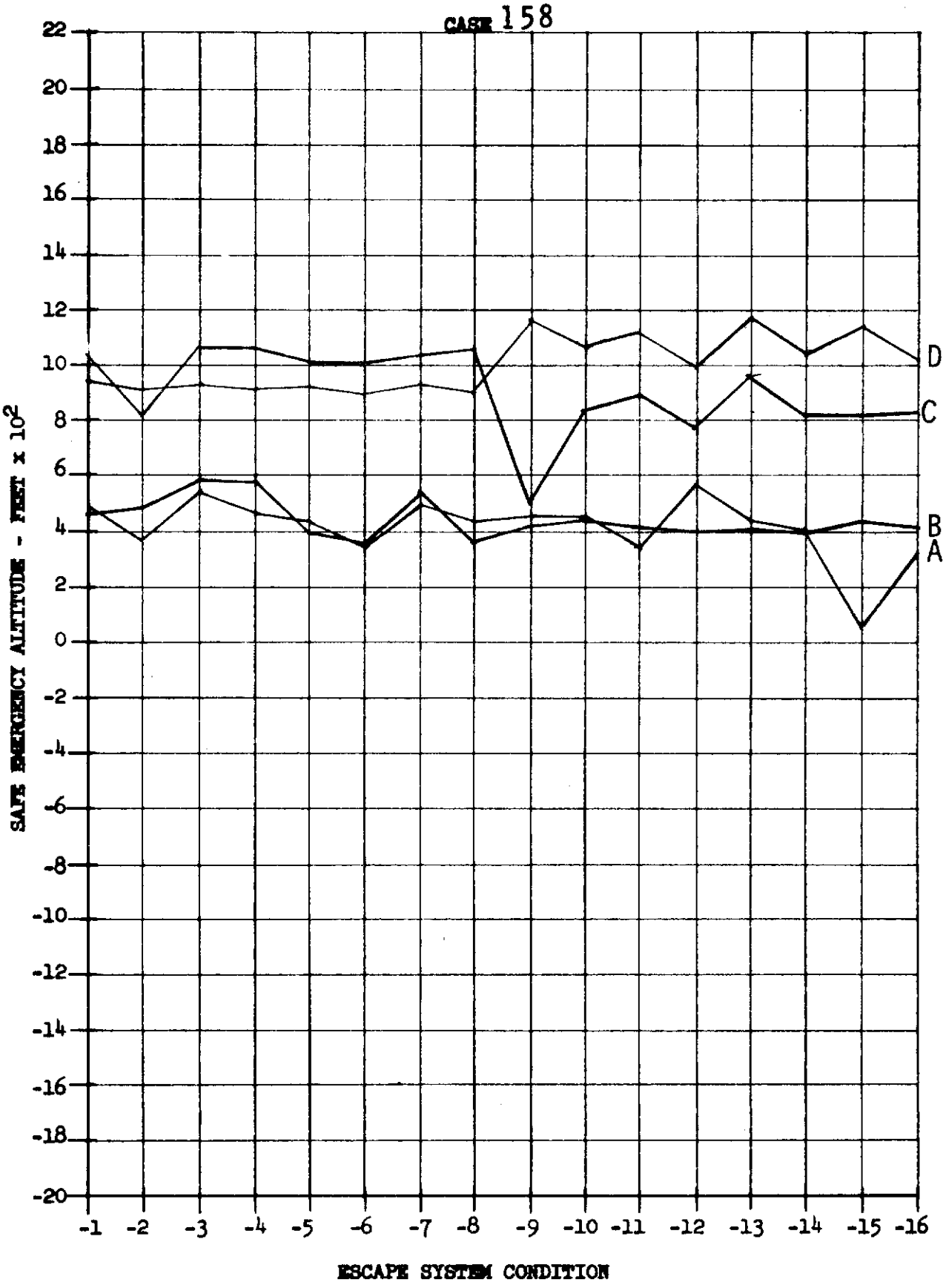

Approved for Public Release

Contrails

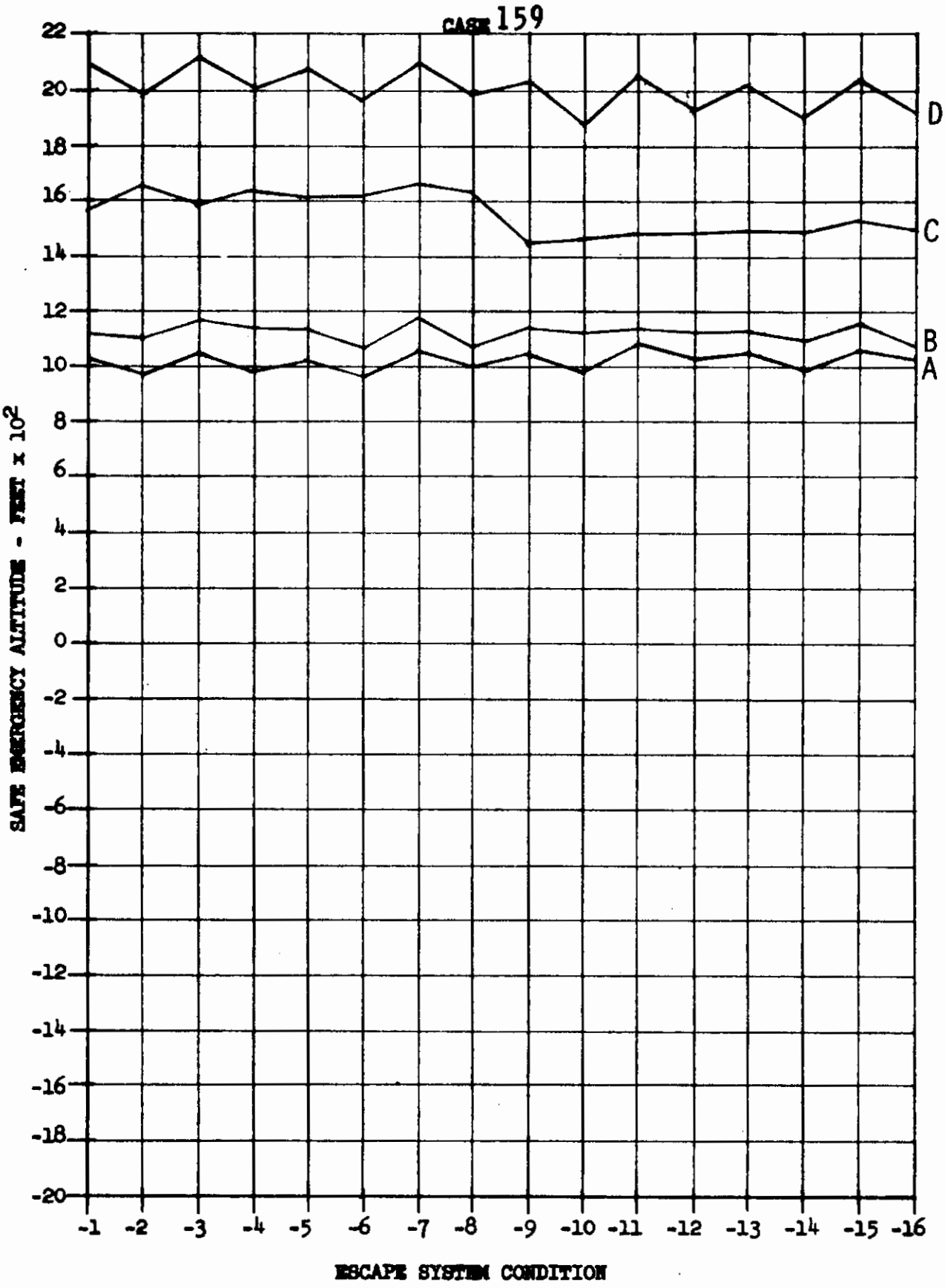

Approved for Public Release

Contrails

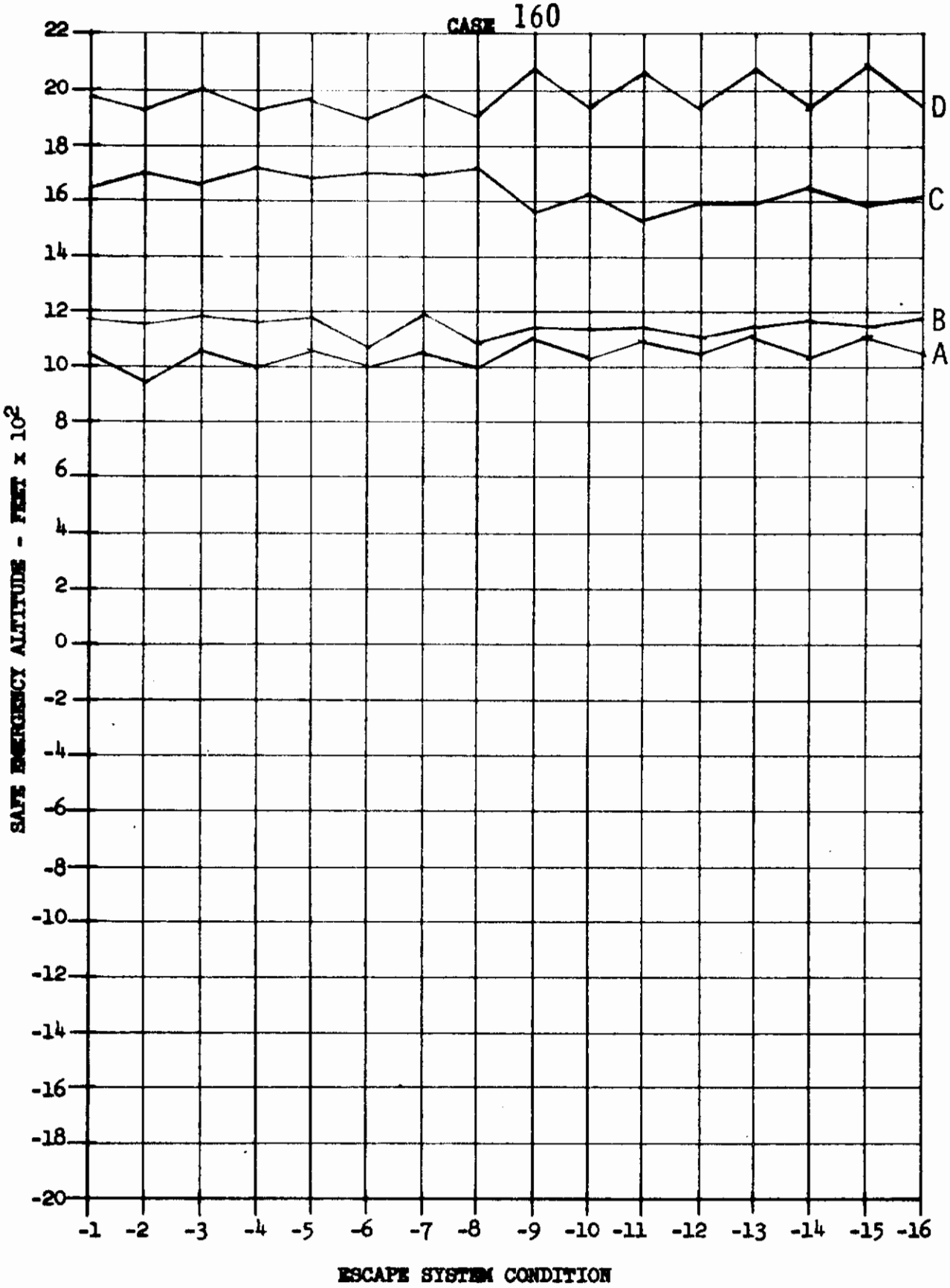

Approved for Public Release

Contrails

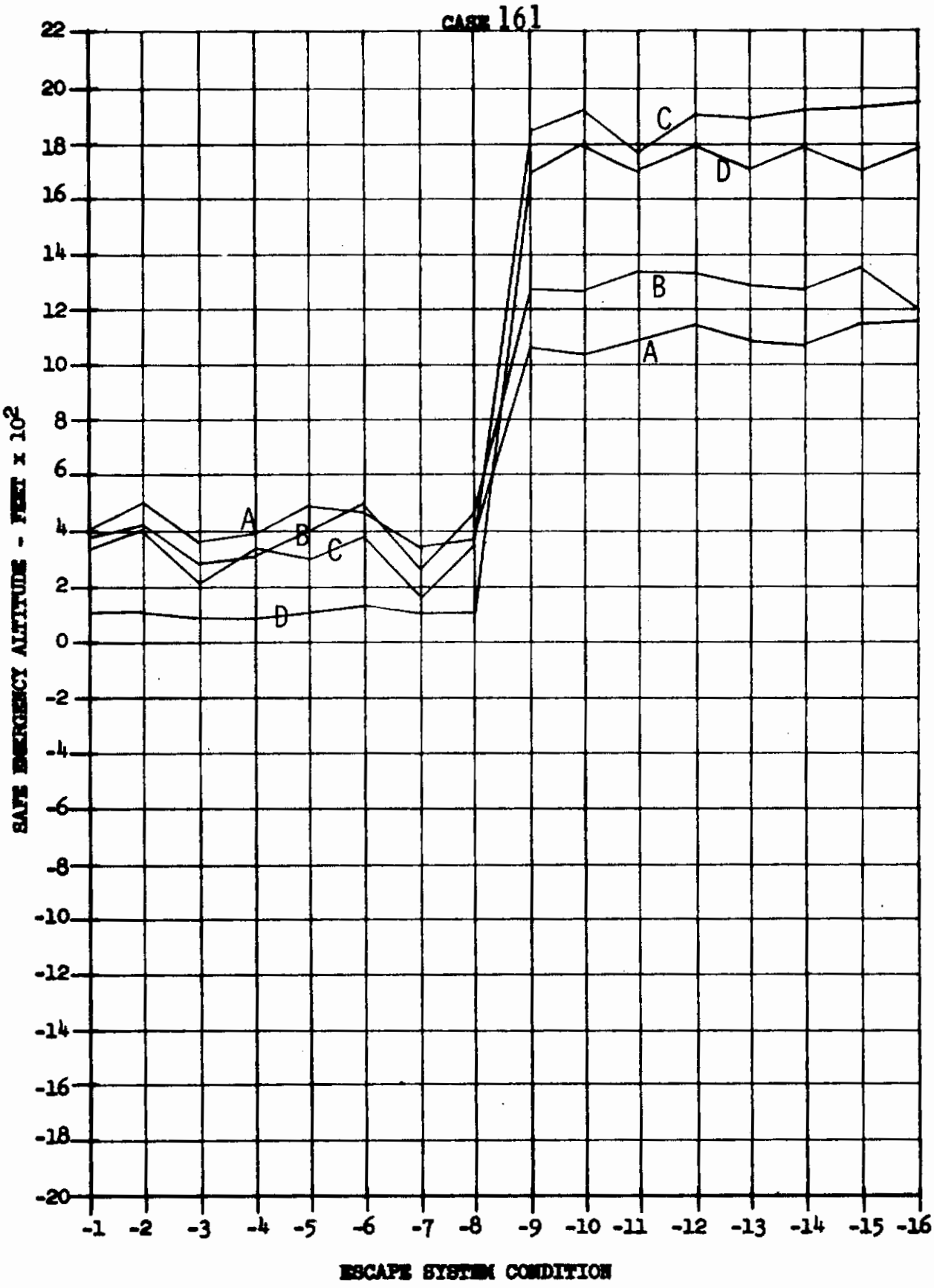

Approved for Public Release

Contrails

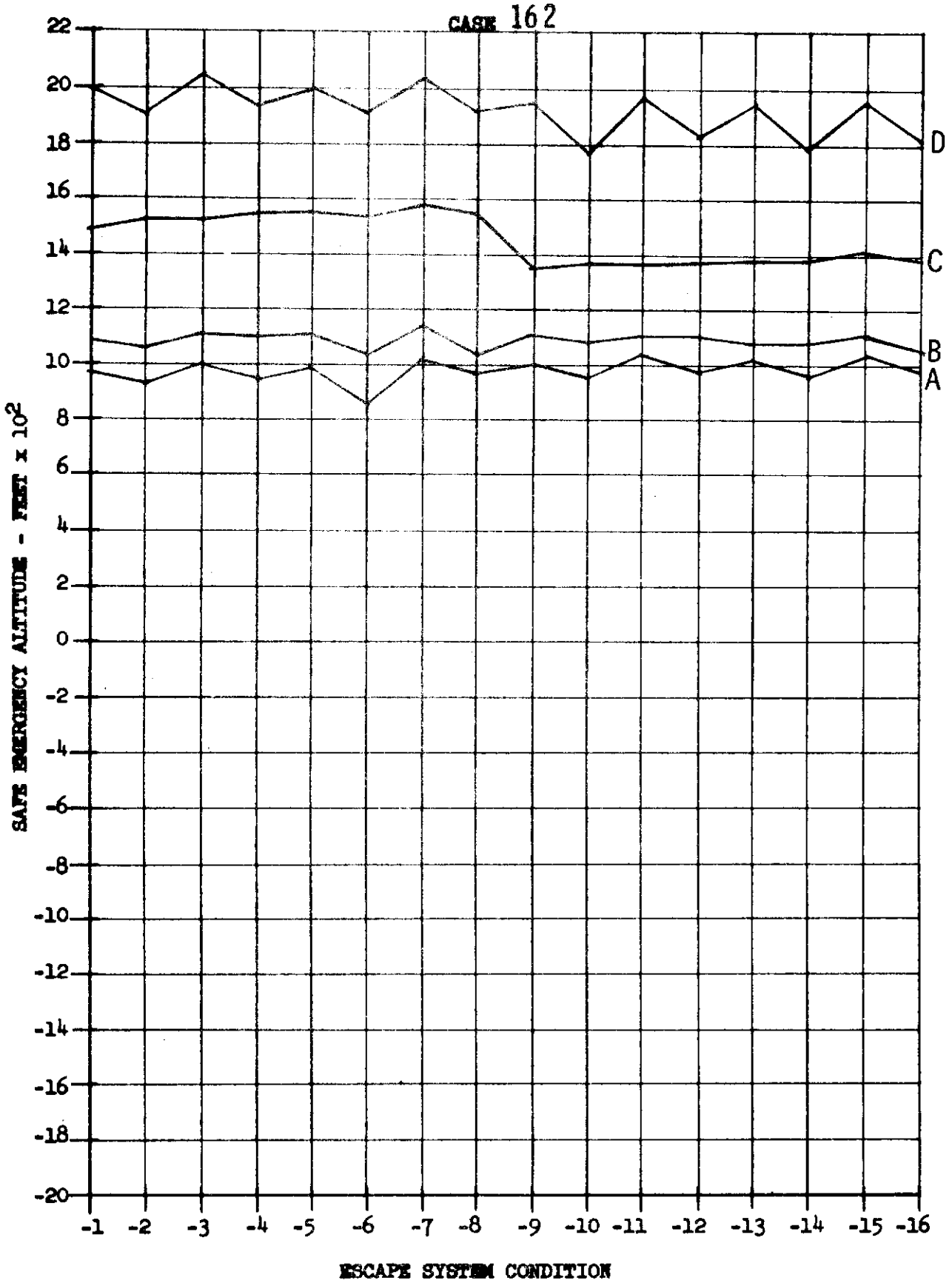

Approved for Public Release

Contrails

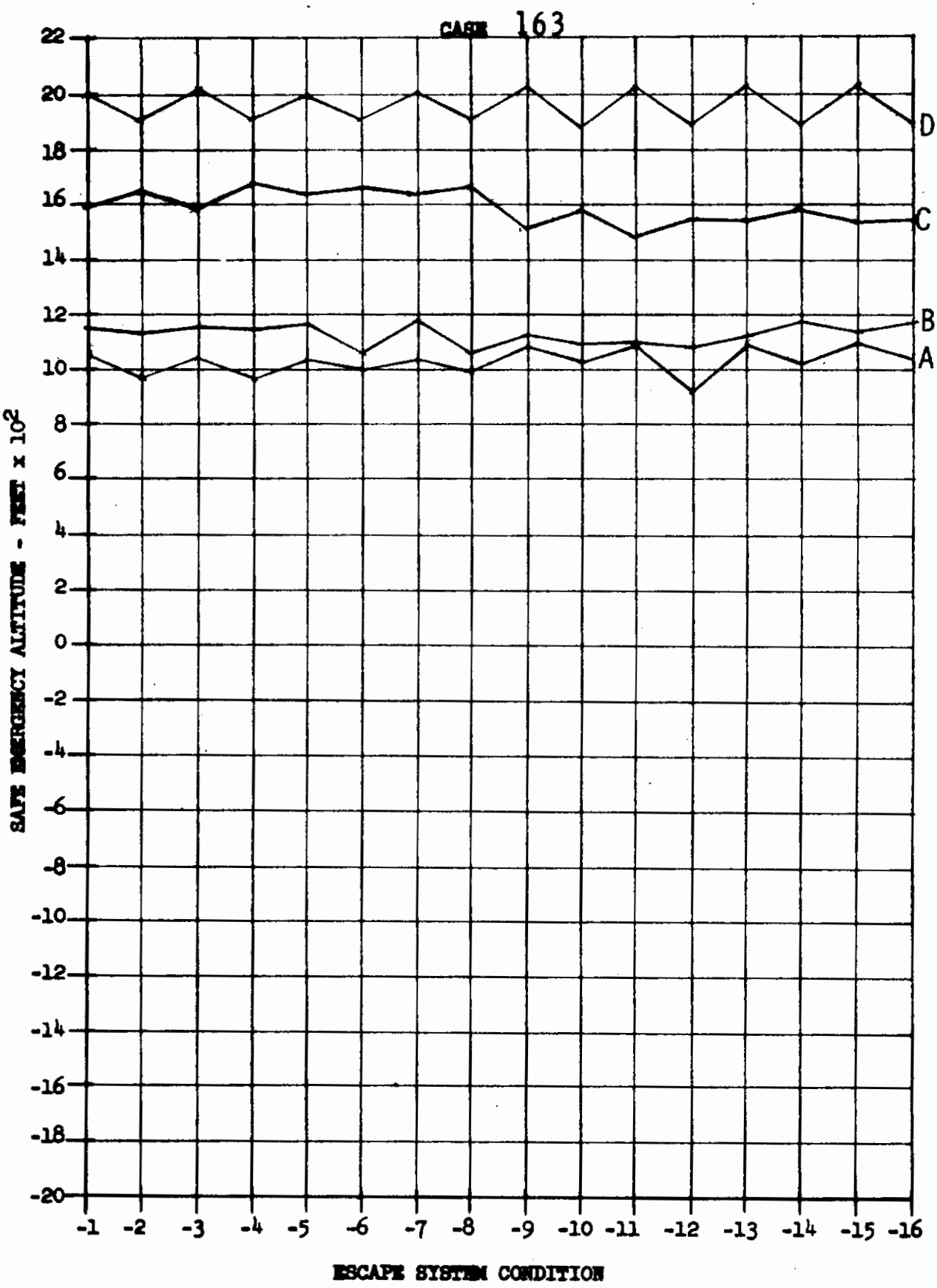

Approved for Public Release

Contrails

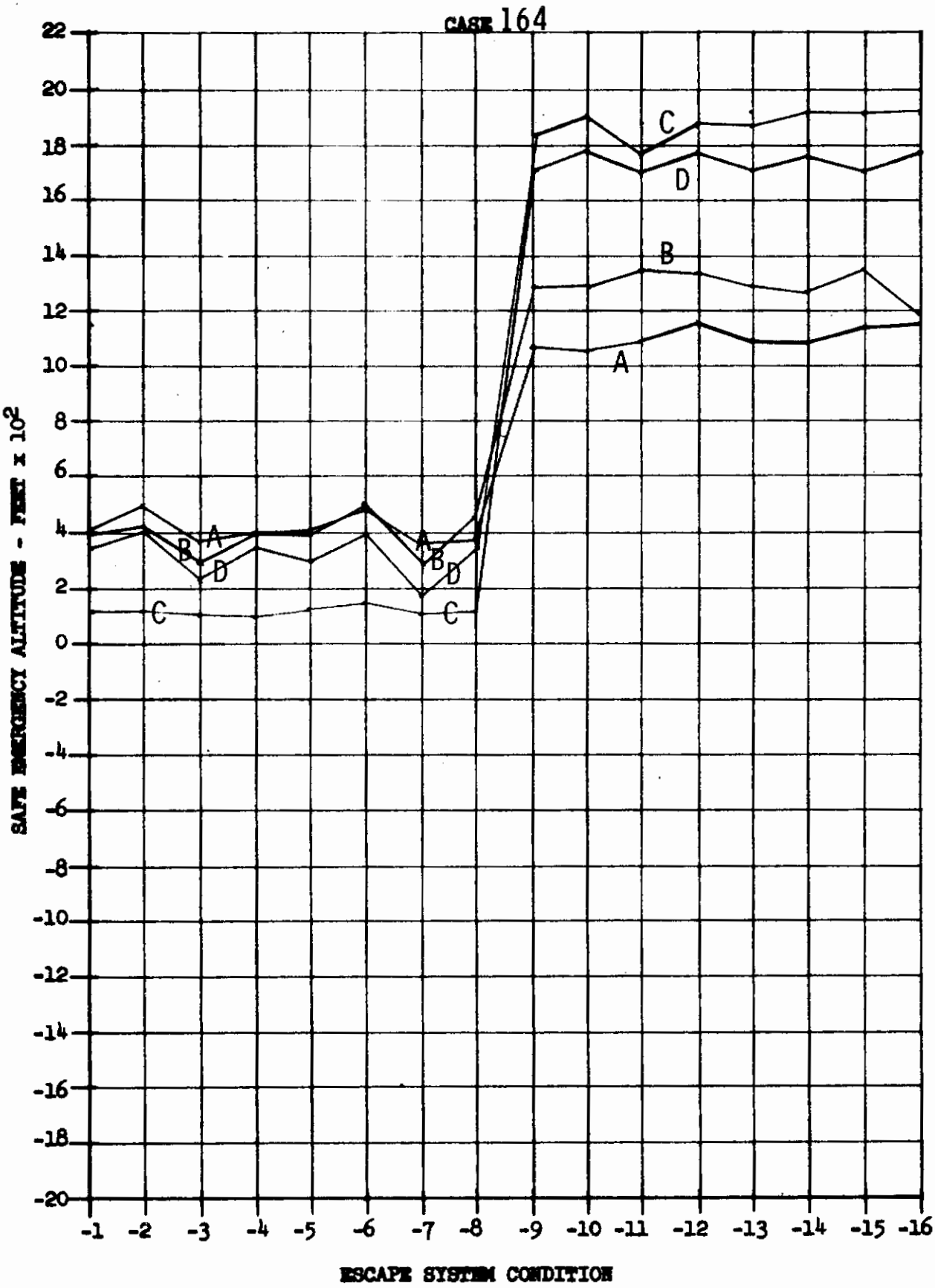

Approved for Public Release

Contrails

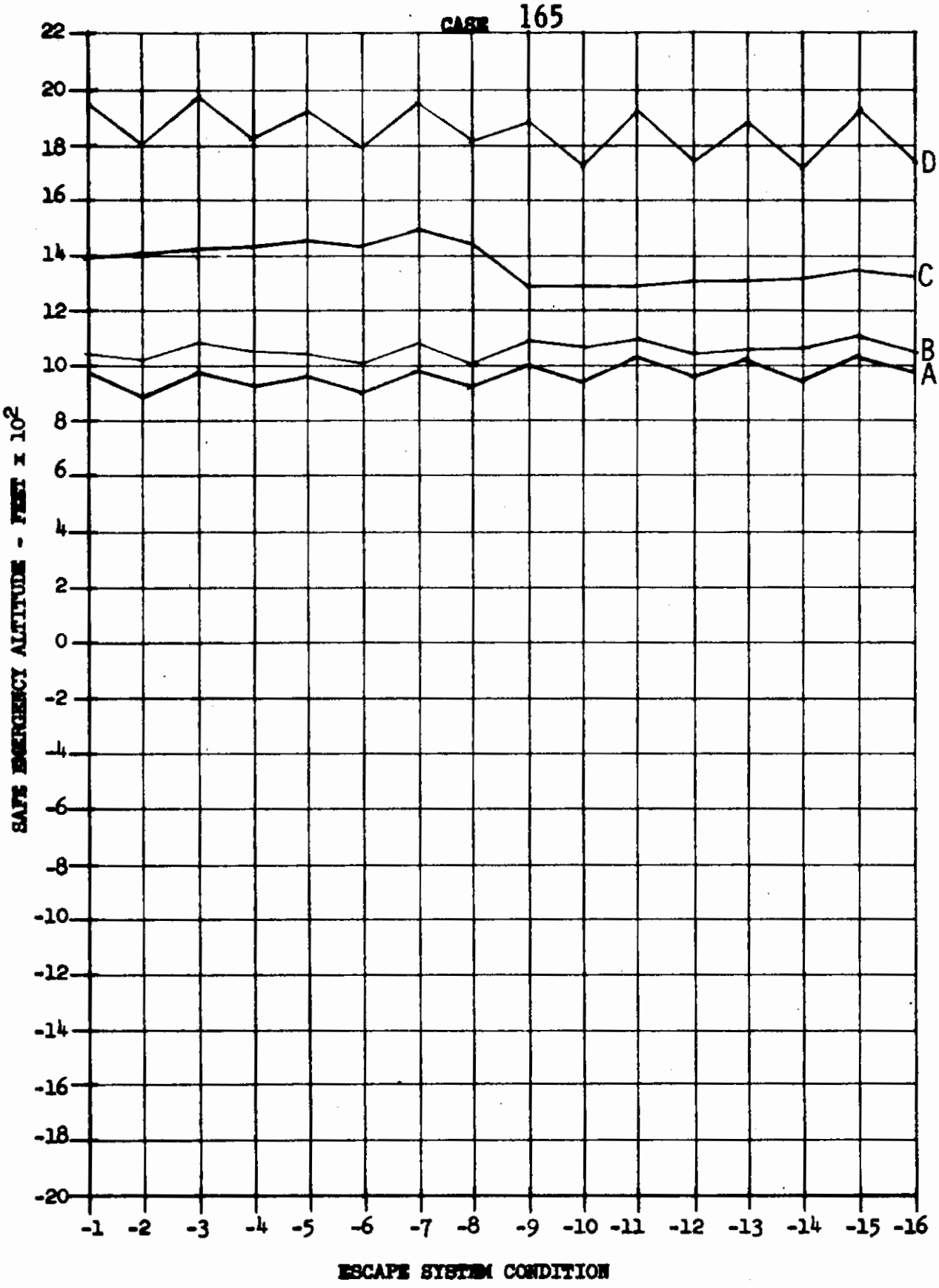

Approved for Public Release

Contrails

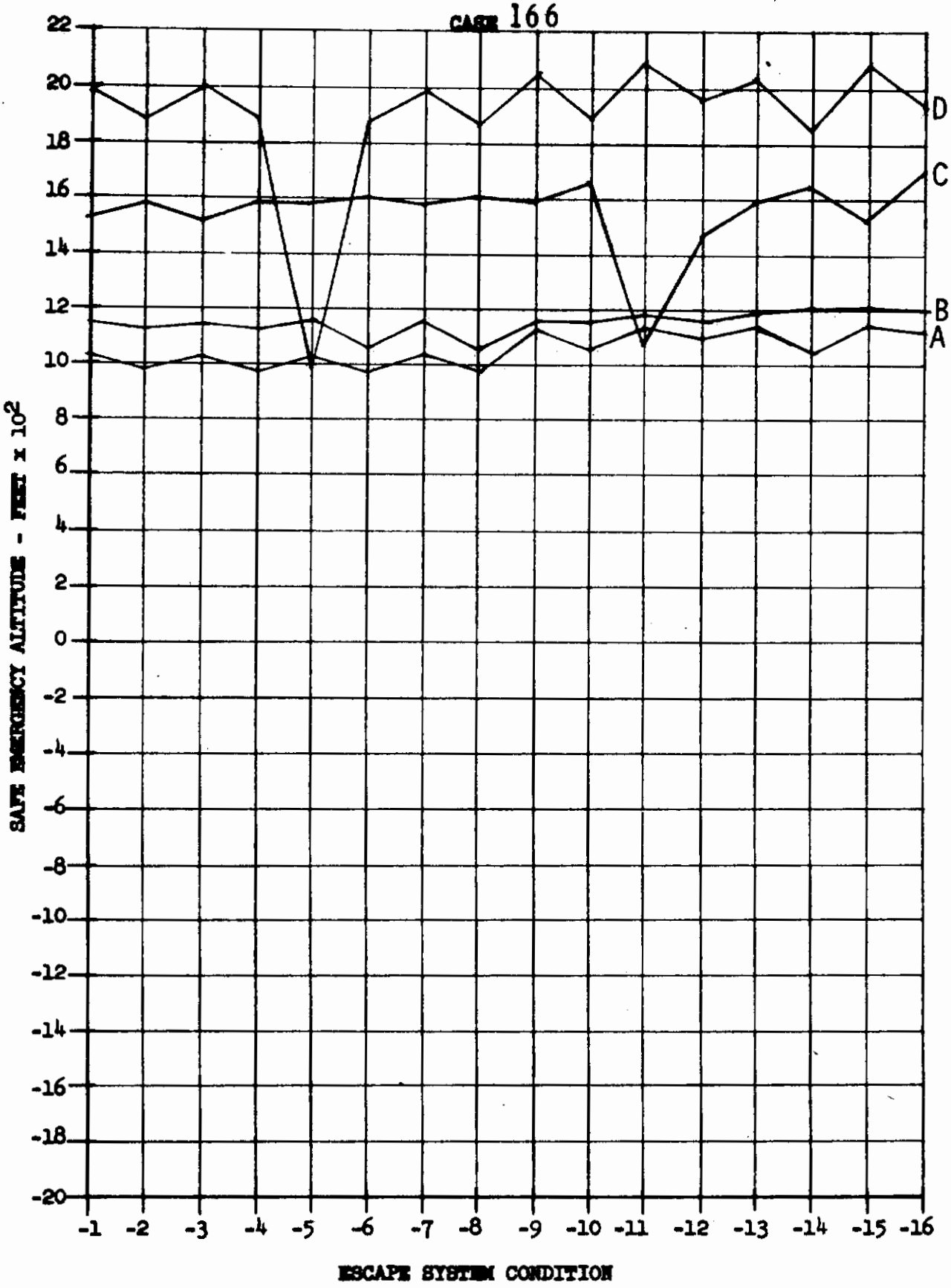

Approved for Public Release

Contrails

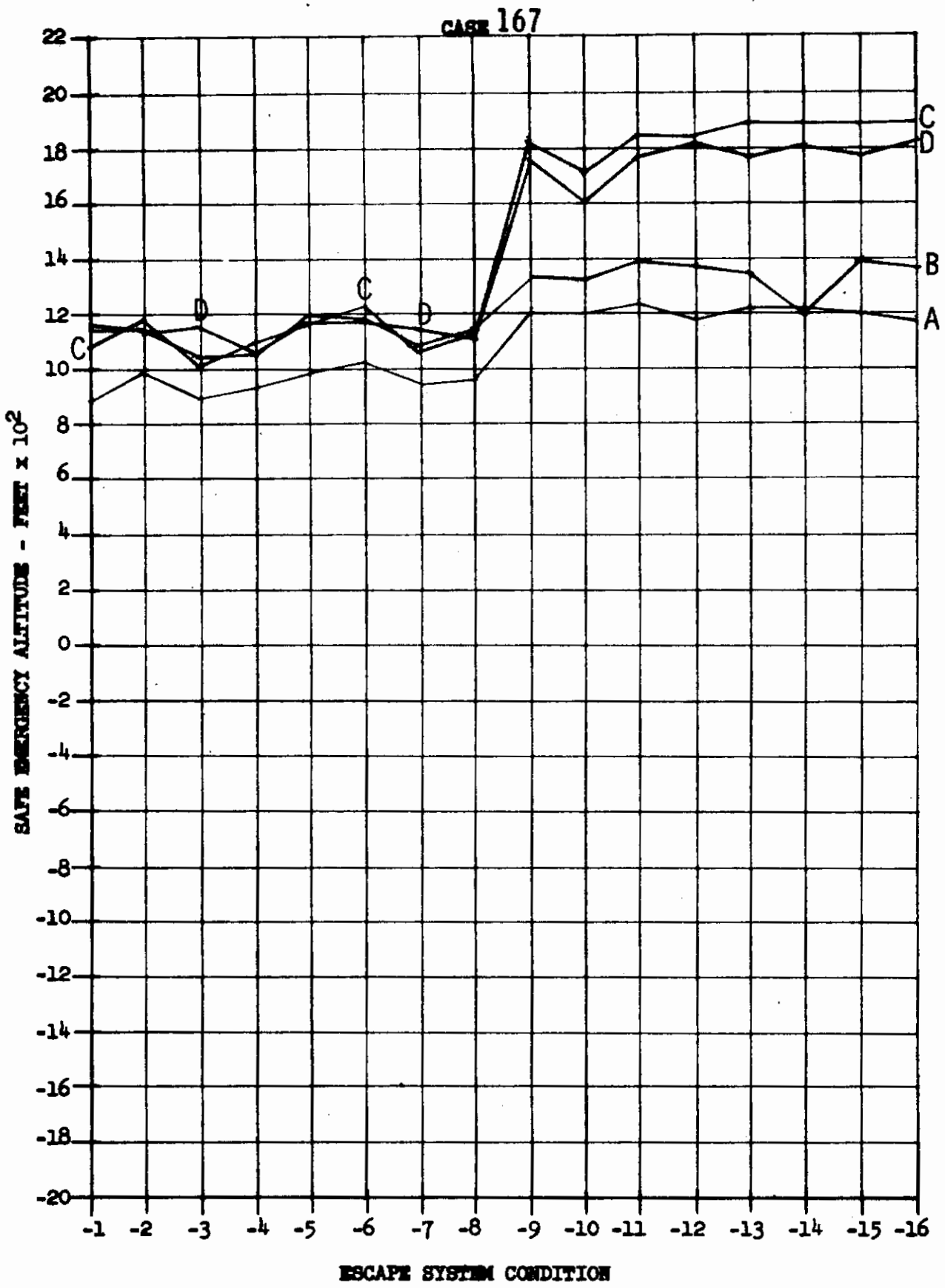

Approved for Public Release

Contrails

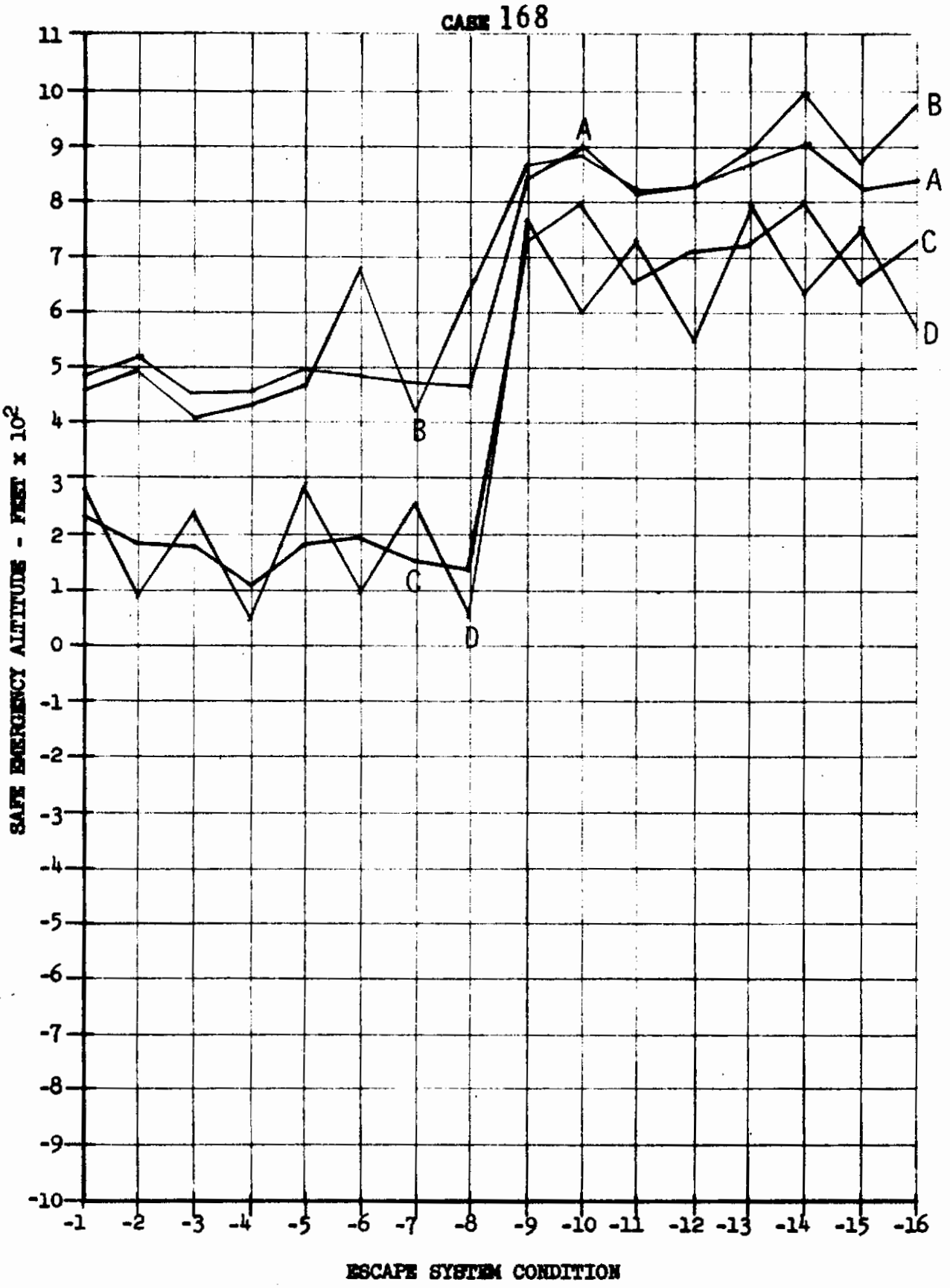

Approved for Public Release

Contrails

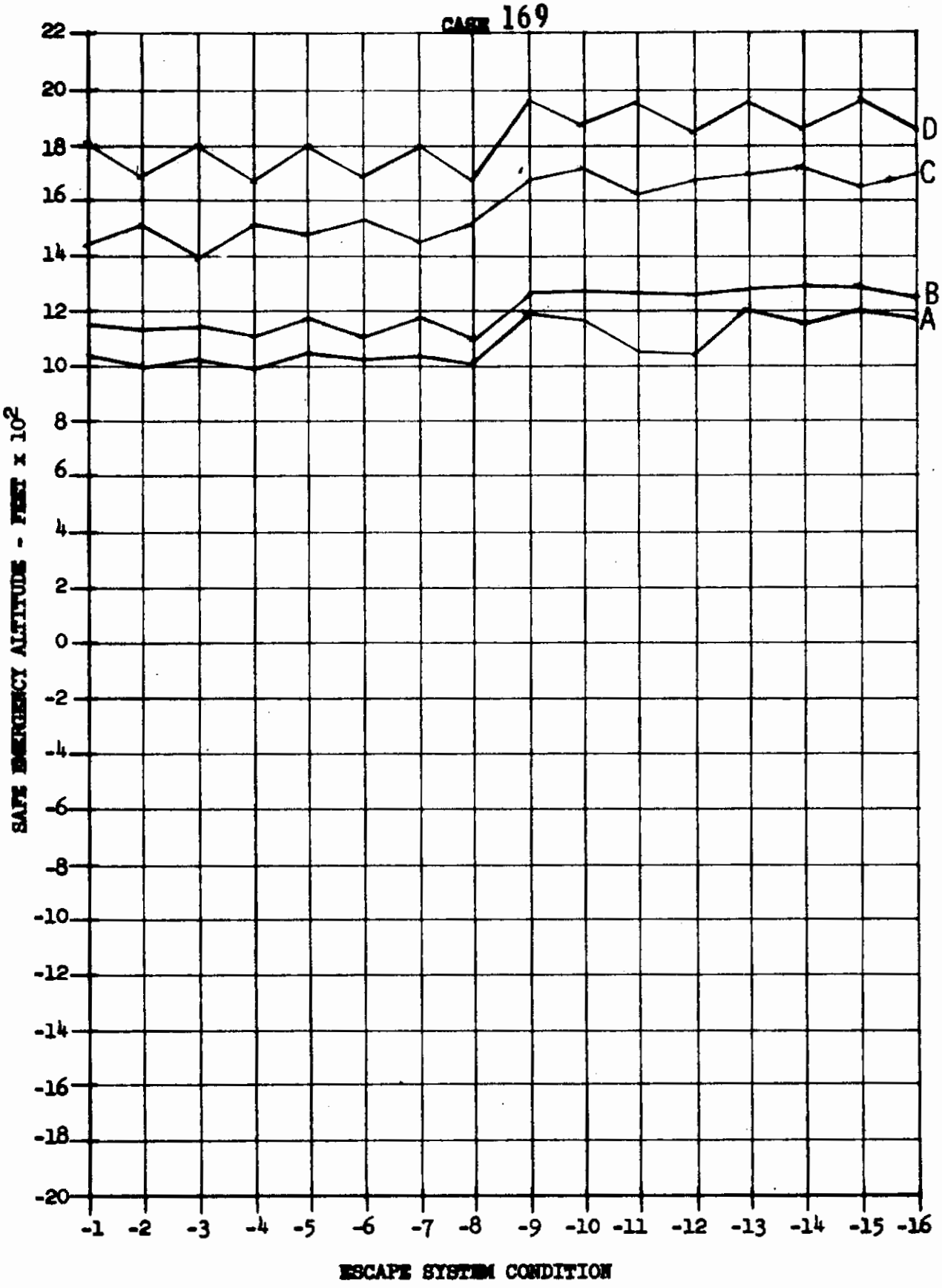

Approved for Public Release

Contrails

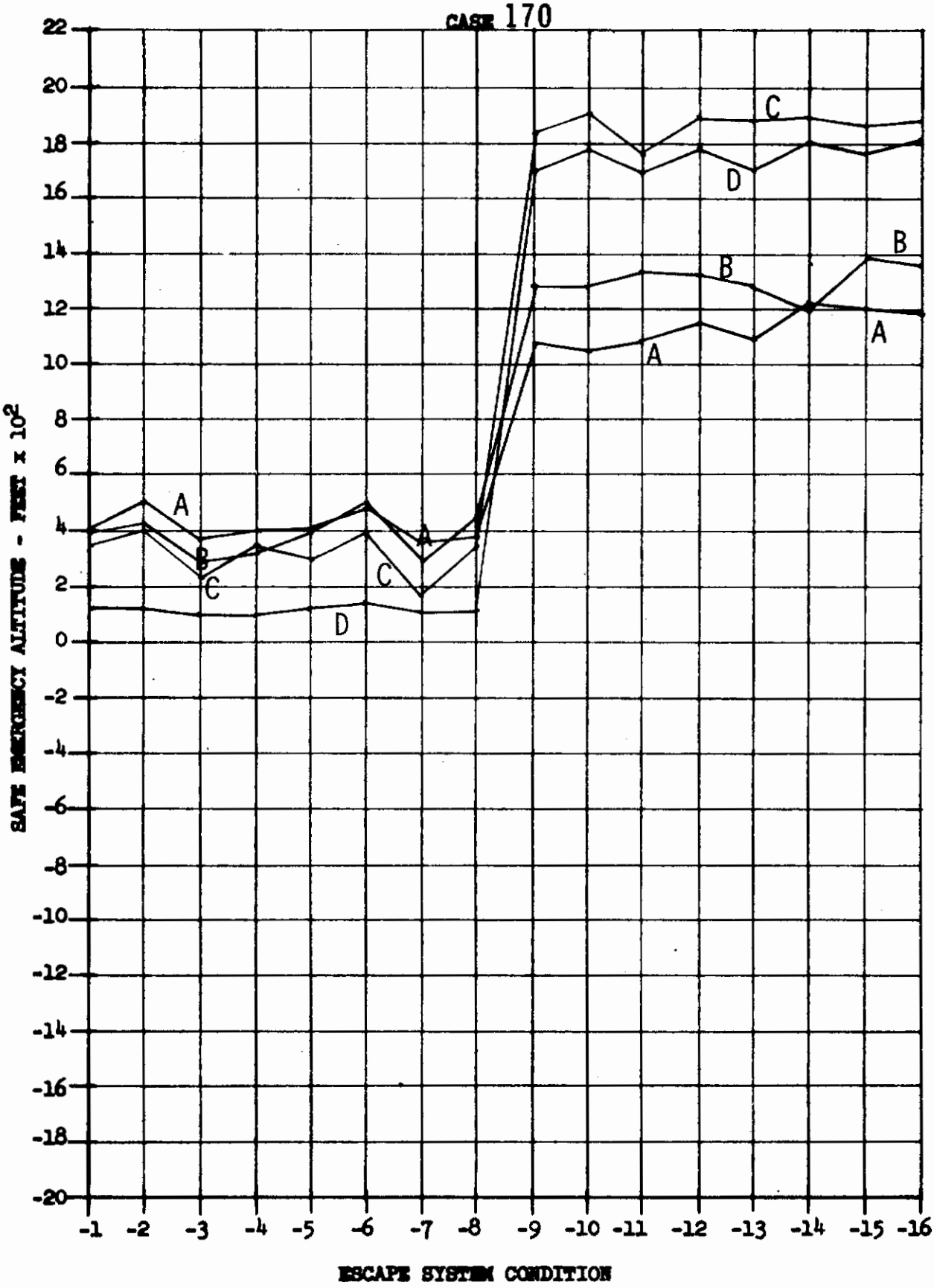

Approved for Public Release

Contrails

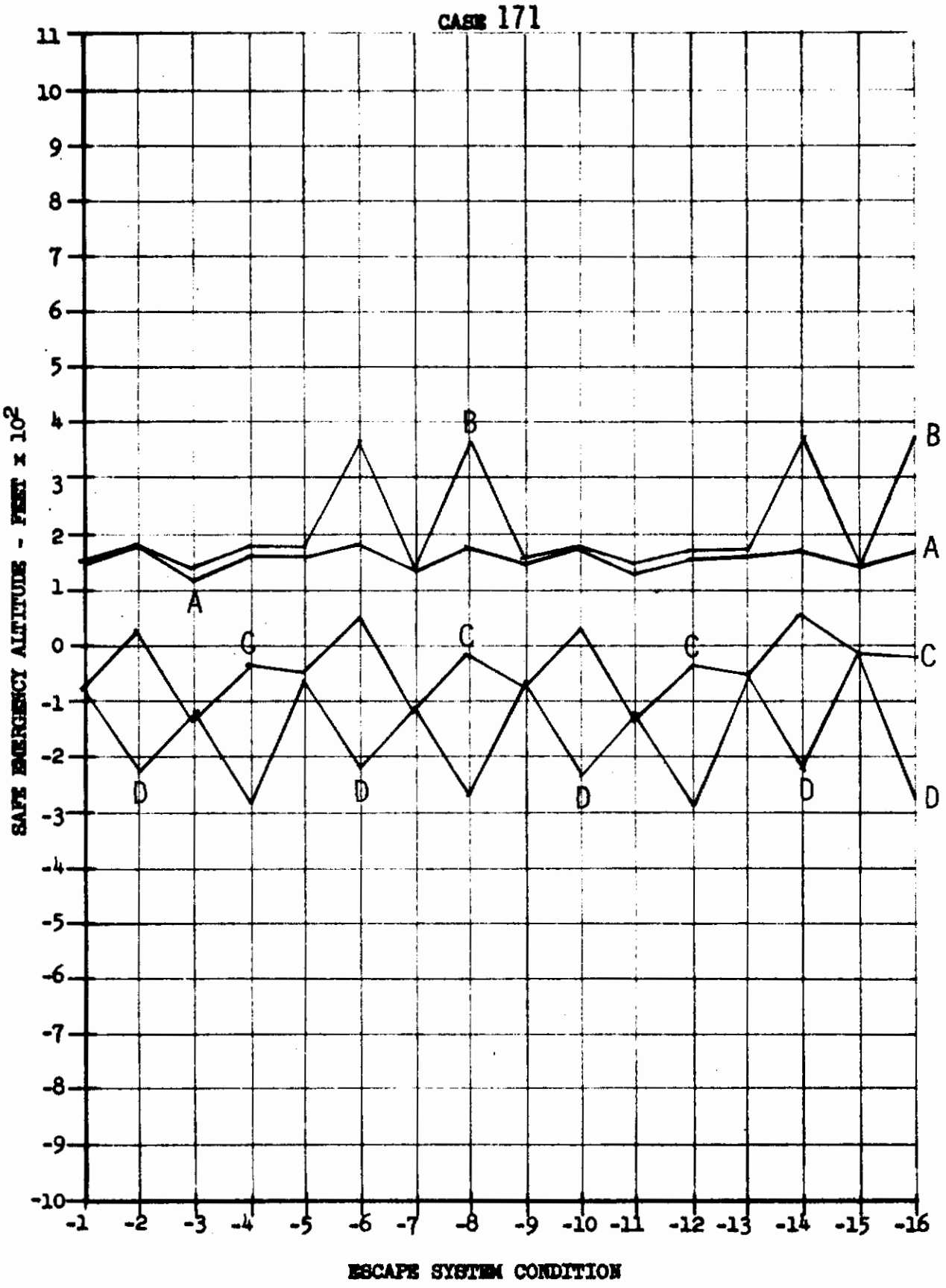

Approved for Public Release

Contrails

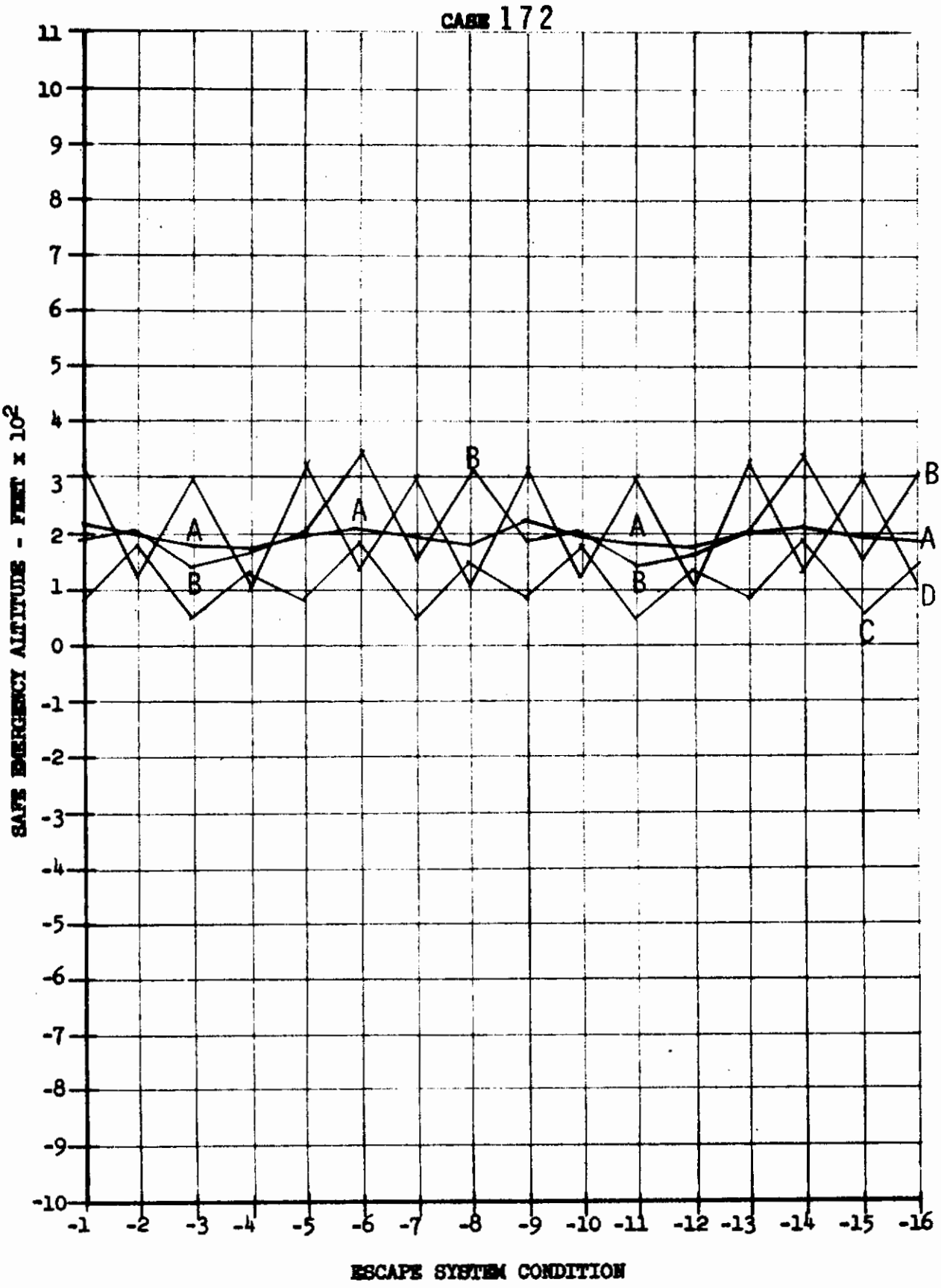

Approved for Public Release

Contrails

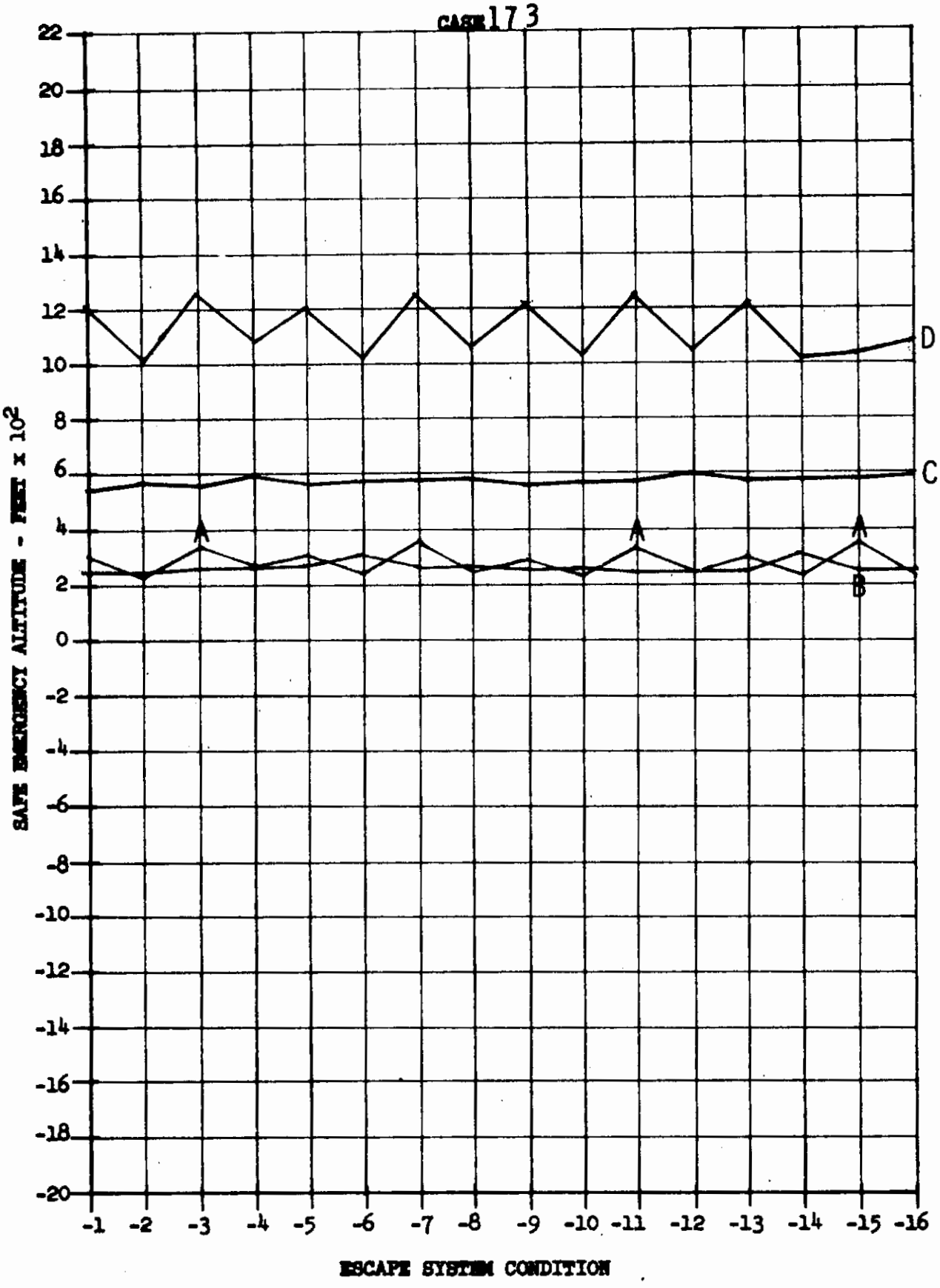

Approved for Public Release

Contrails

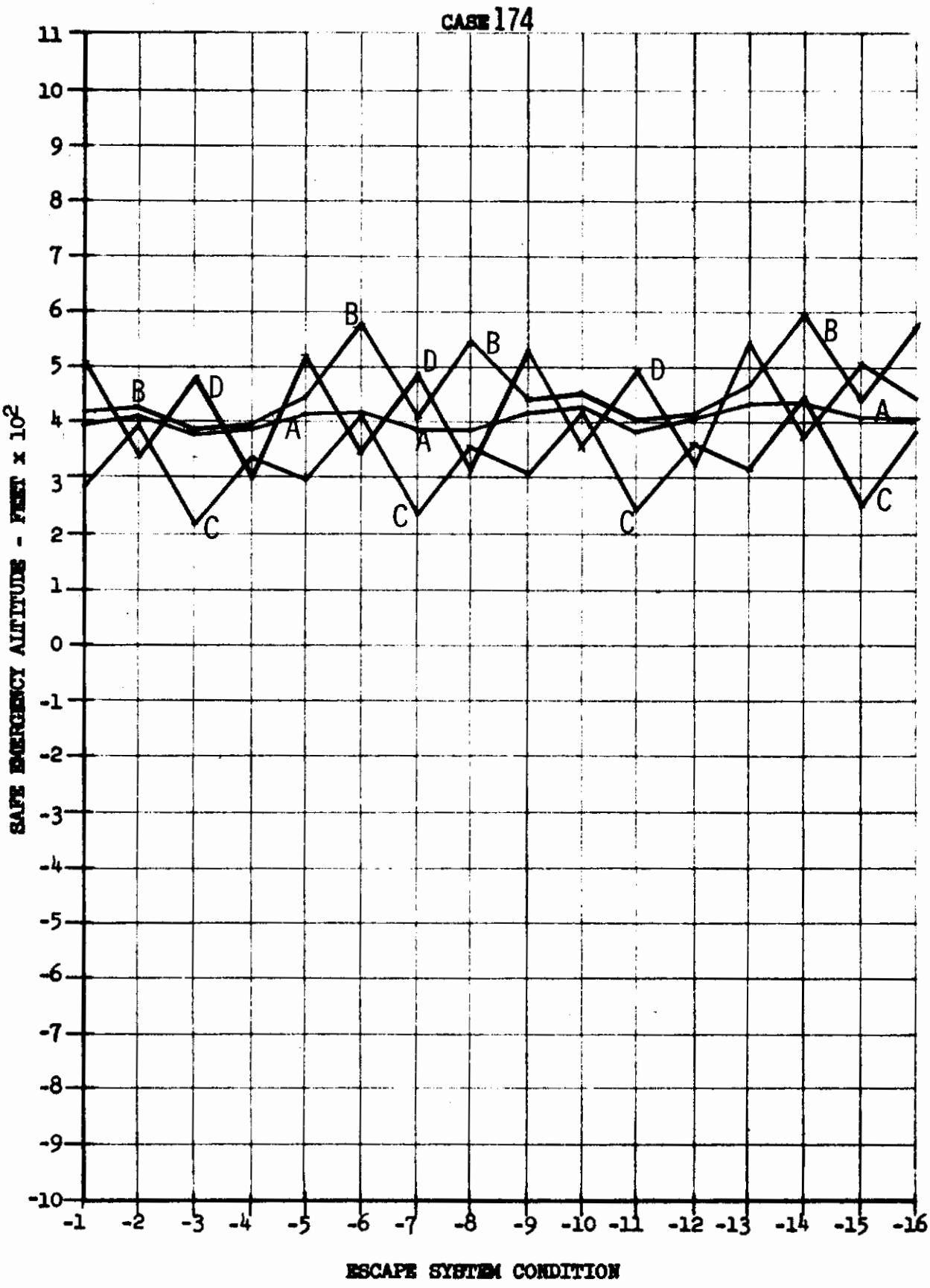

Approved for Public Release

Contrails

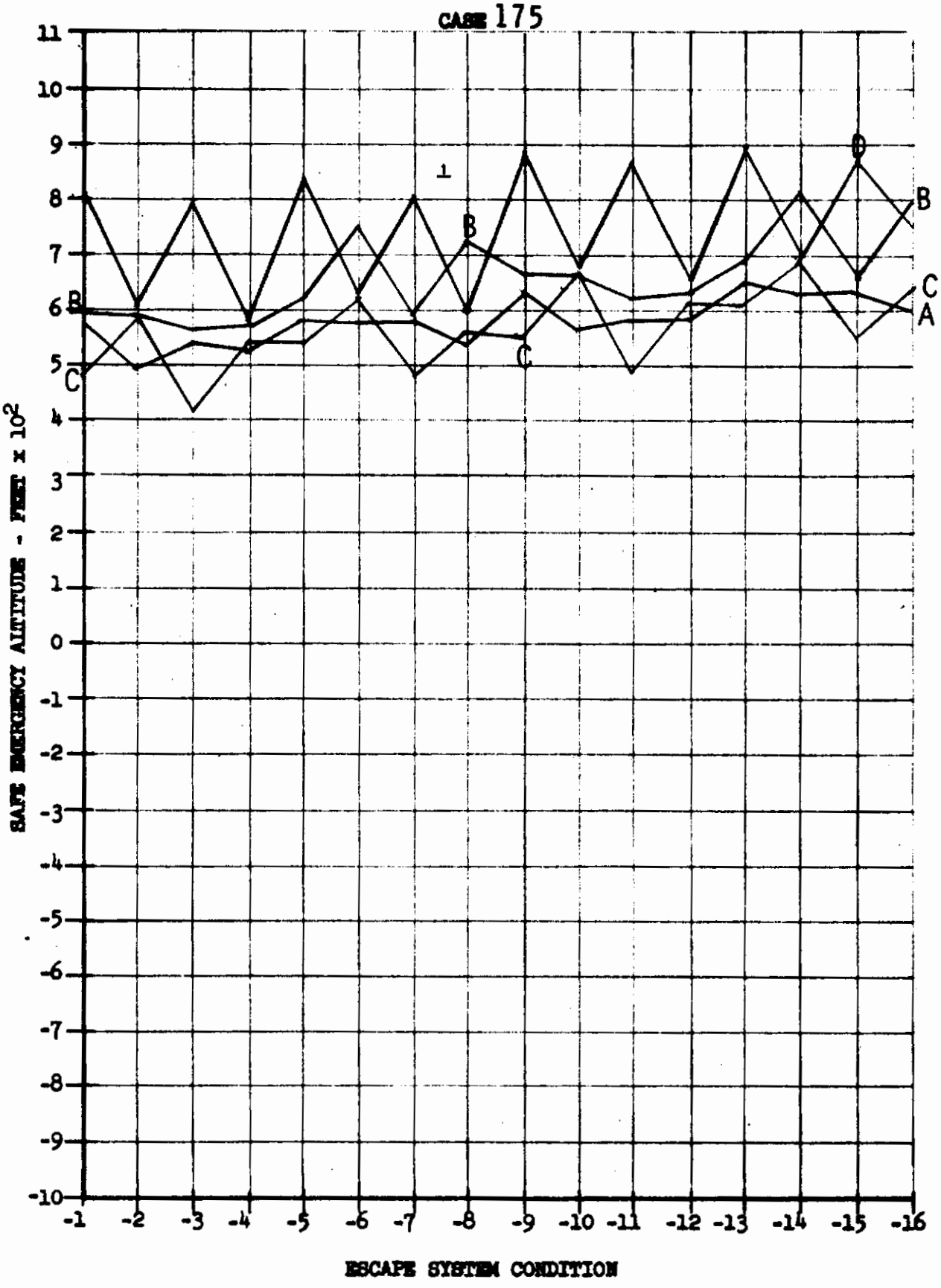

Approved for Public Release

Contrails

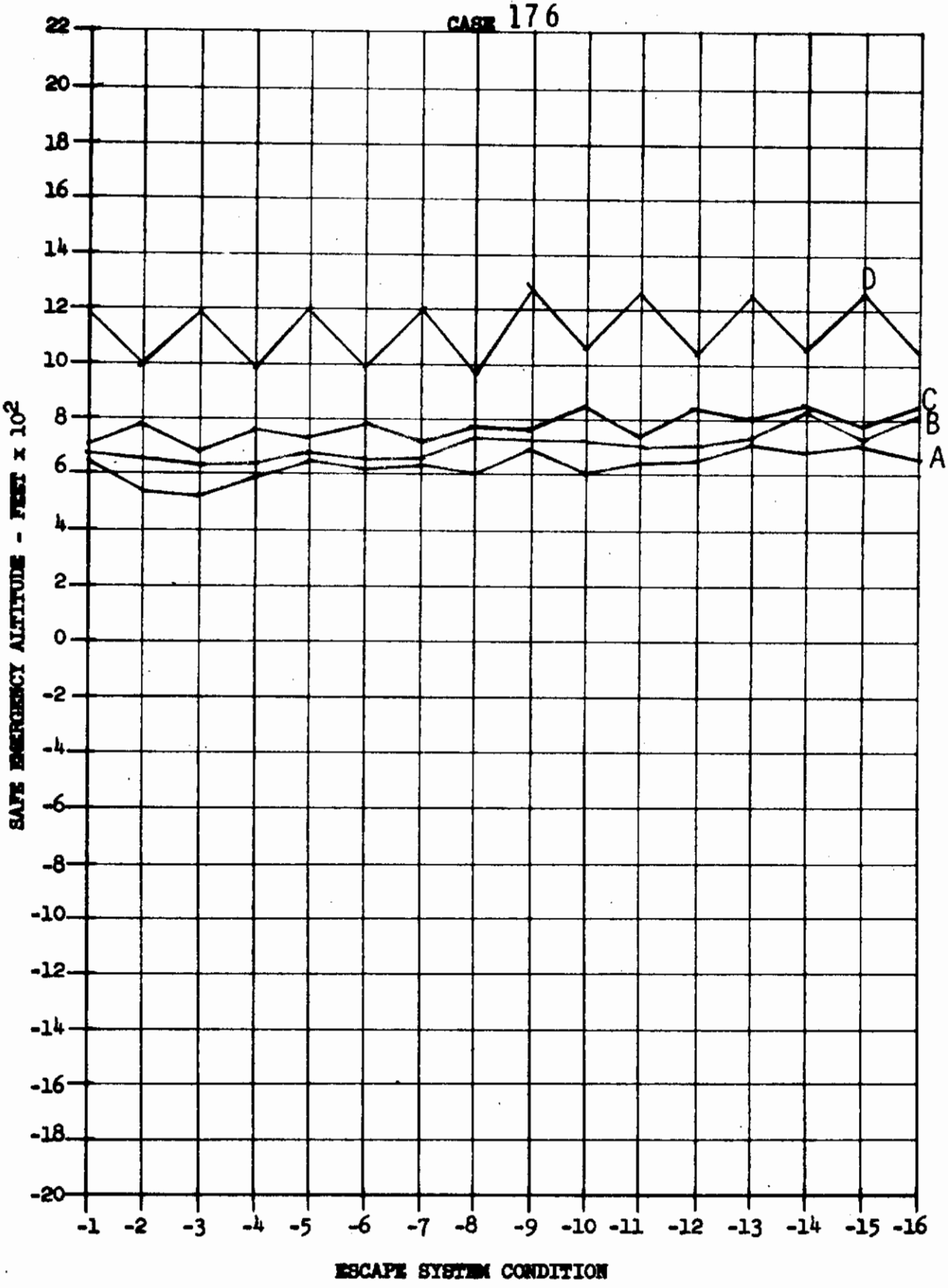

Approved for Public Release

Contrails

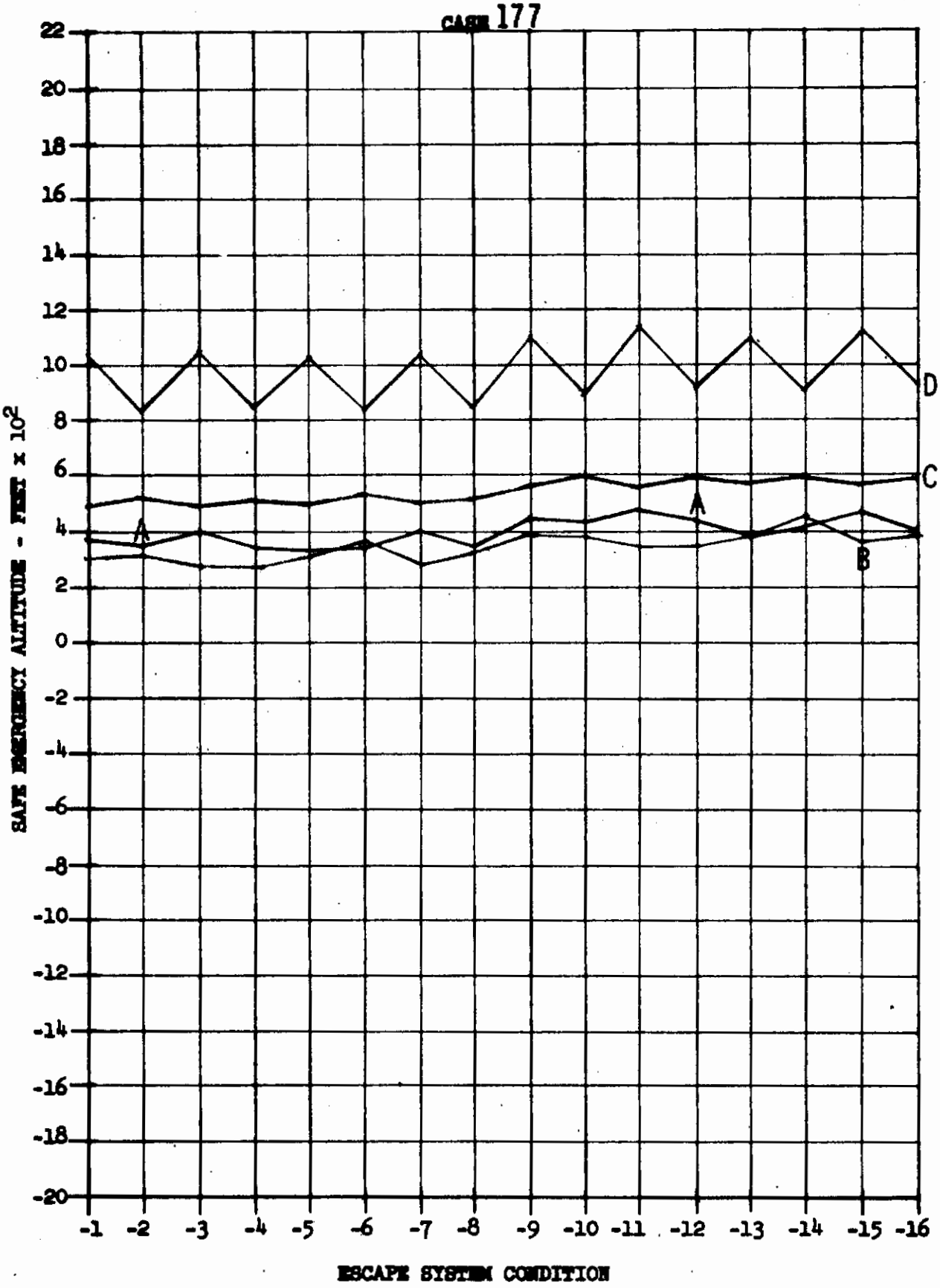

Approved for Public Release

Contrails

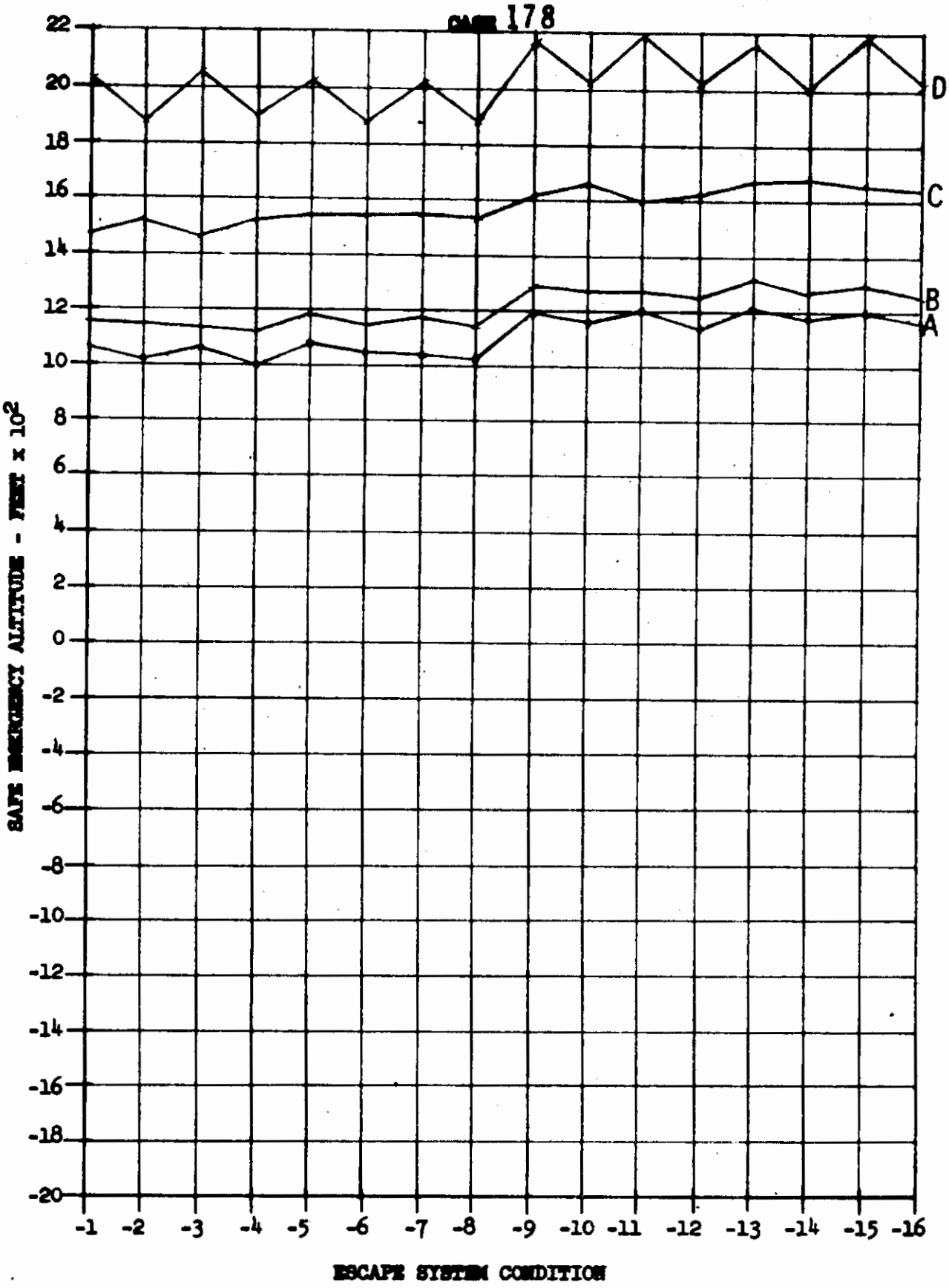

Approved for Public Release

Contrails

CASE 179

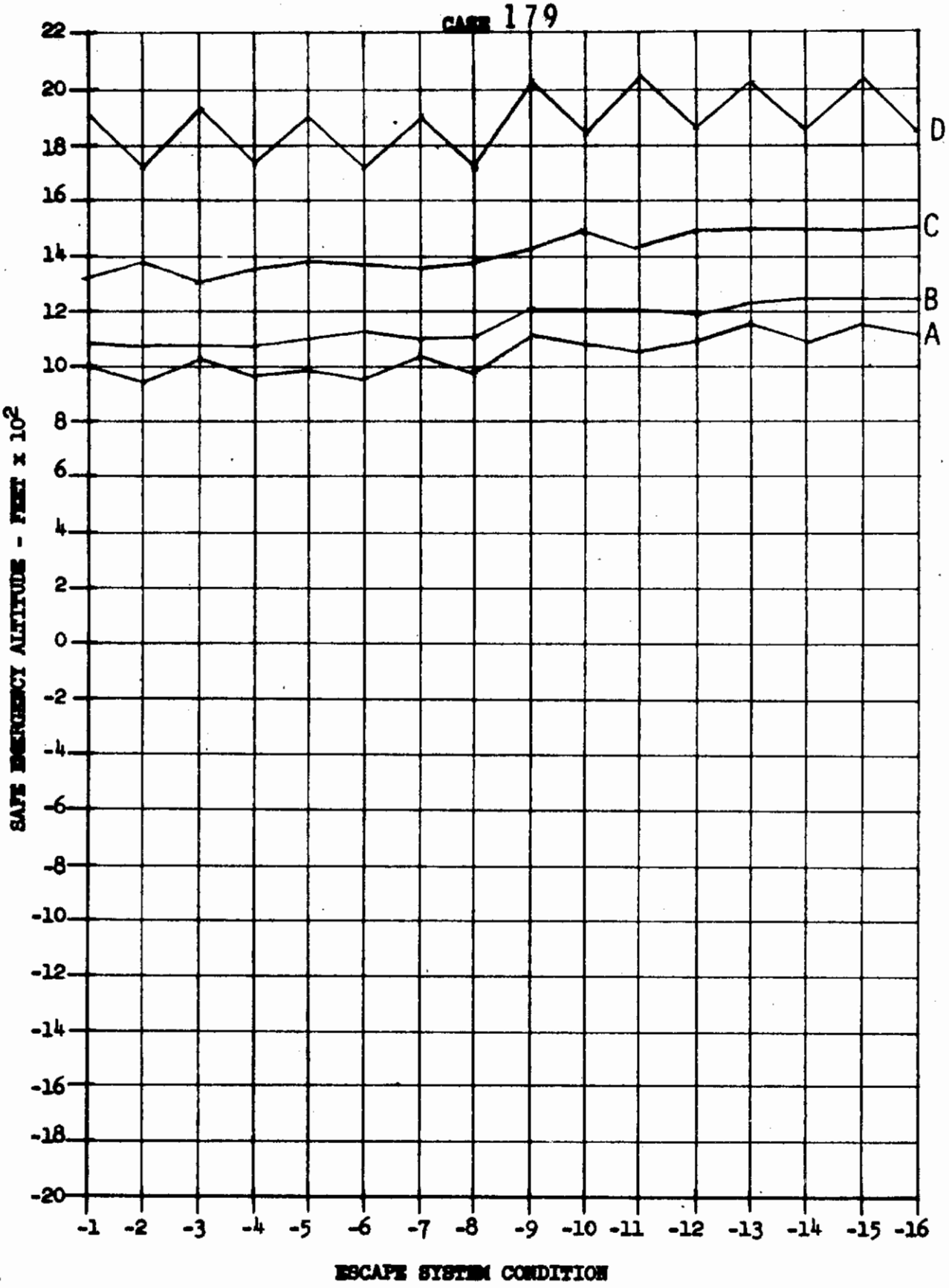

Approved for Public Release

Contrails

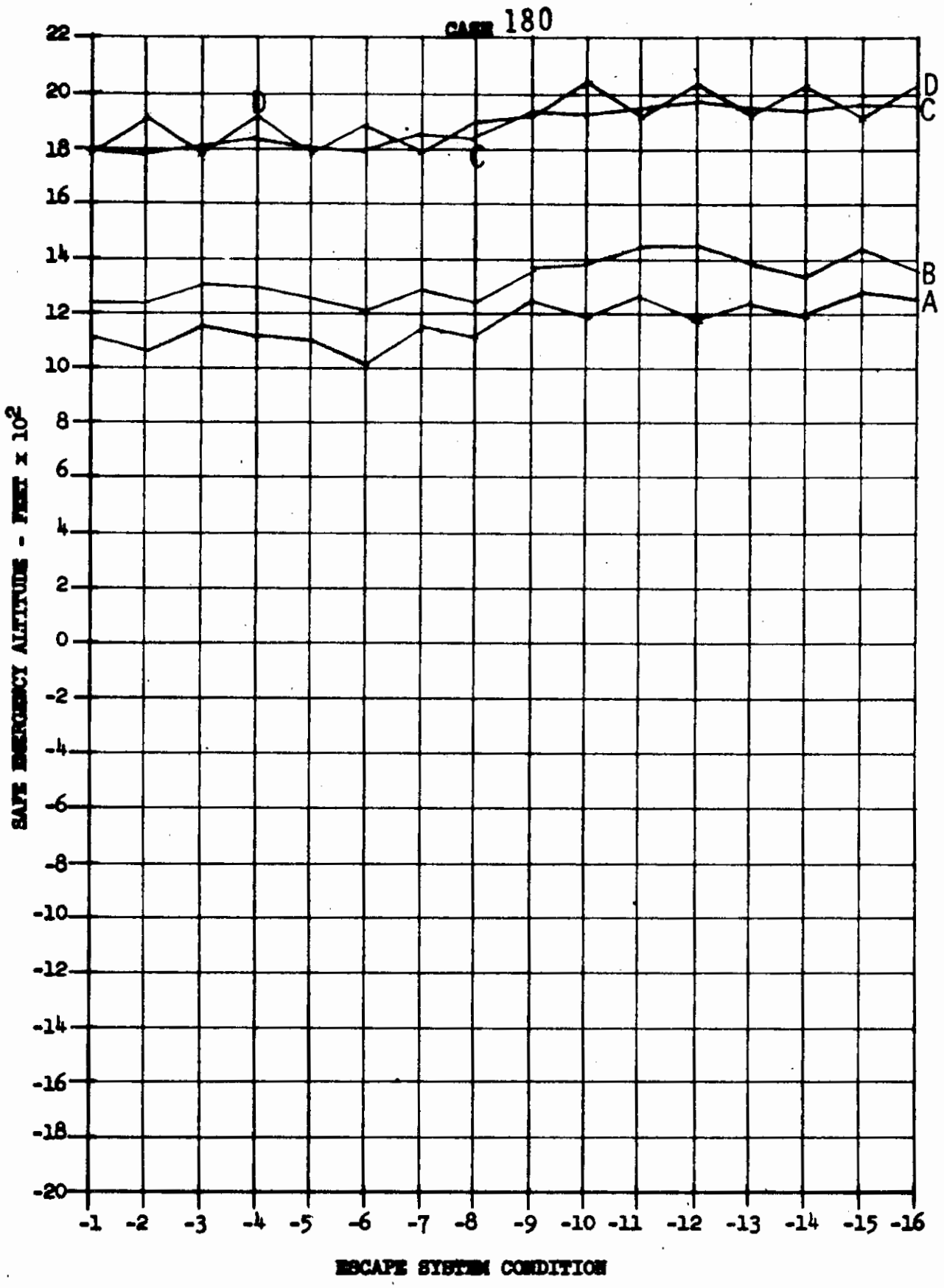

Approved for Public Release

Contrails

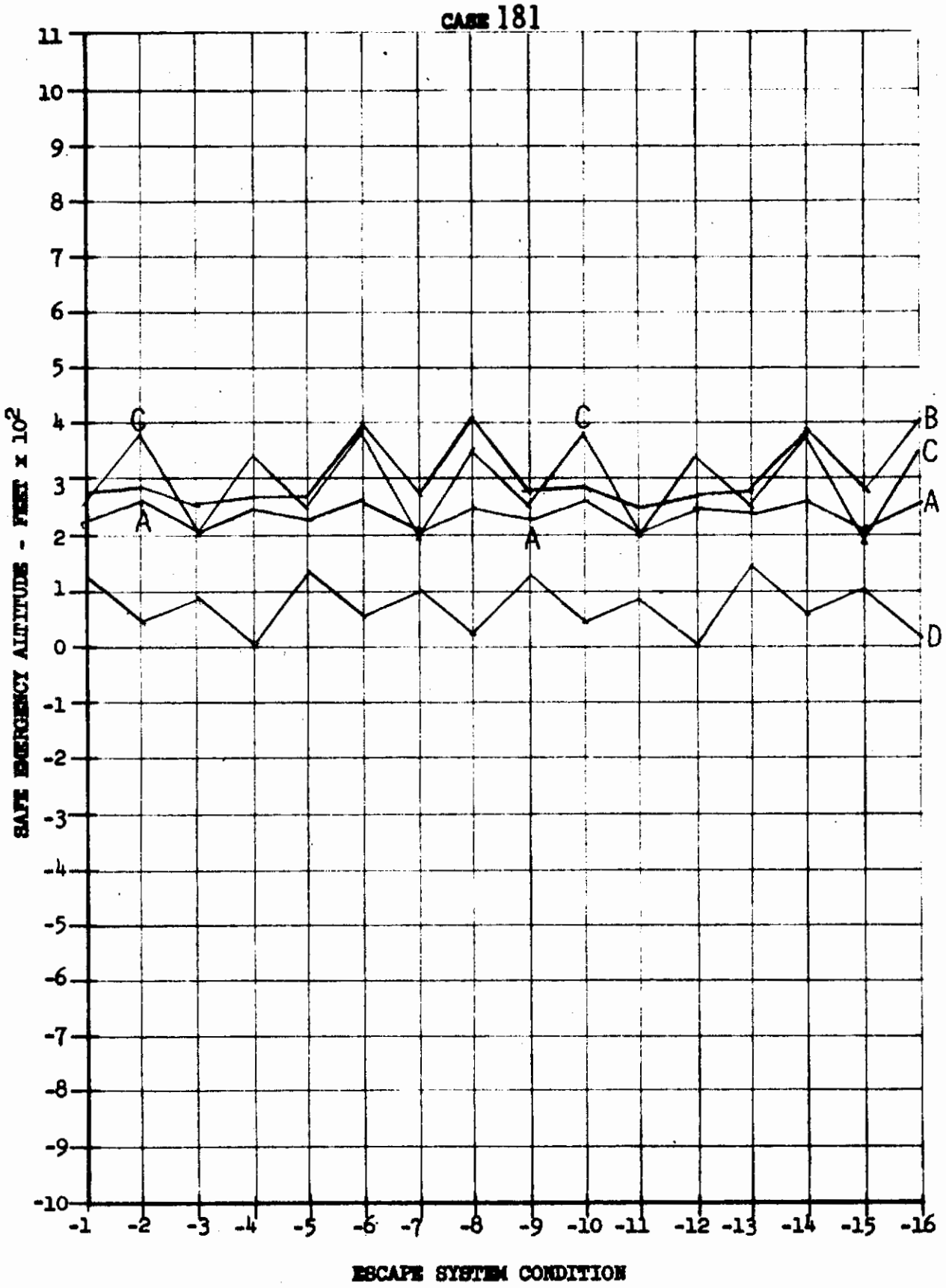

Approved for Public Release

Contrails

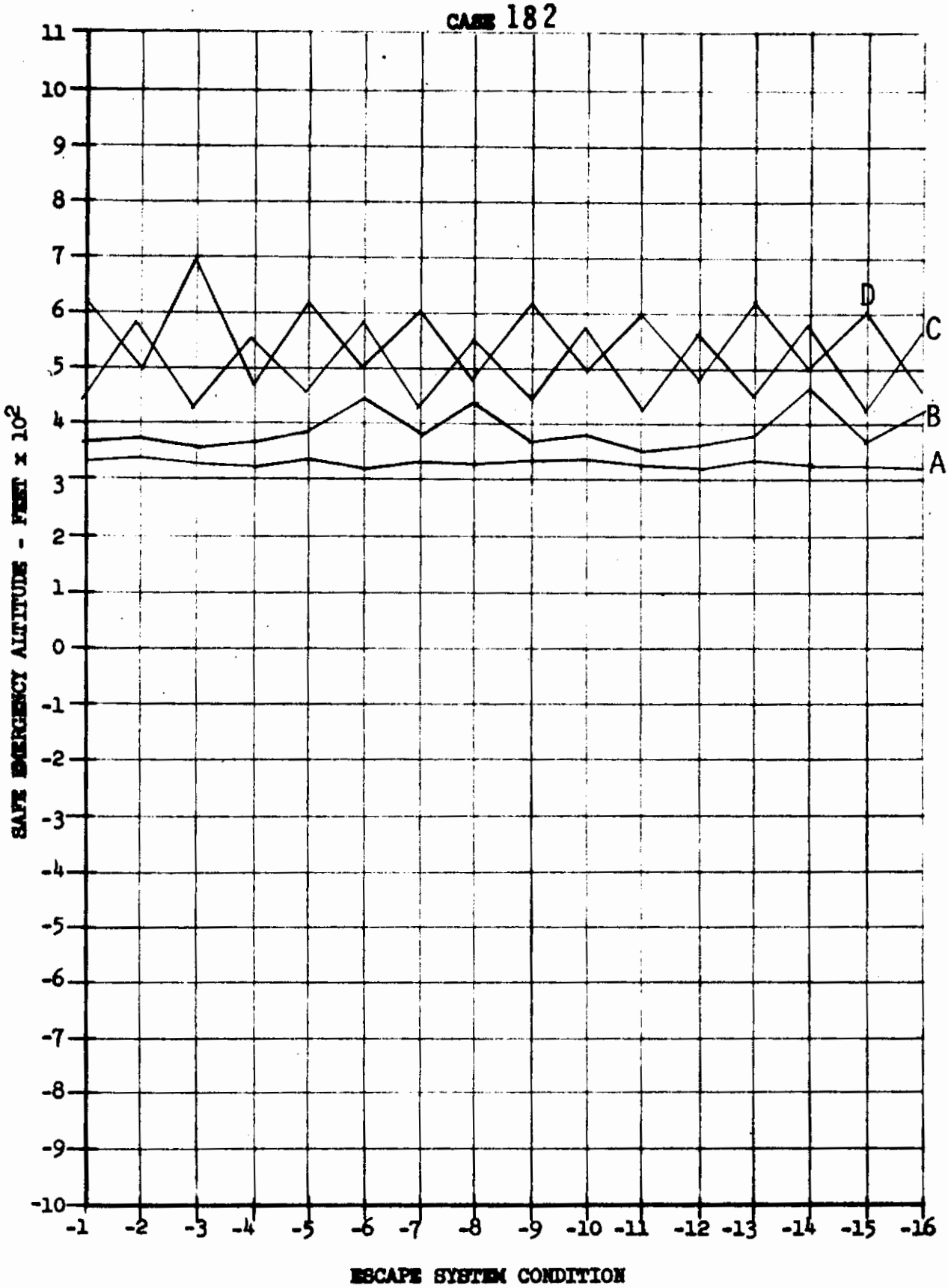

Approved for Public Release

Contrails

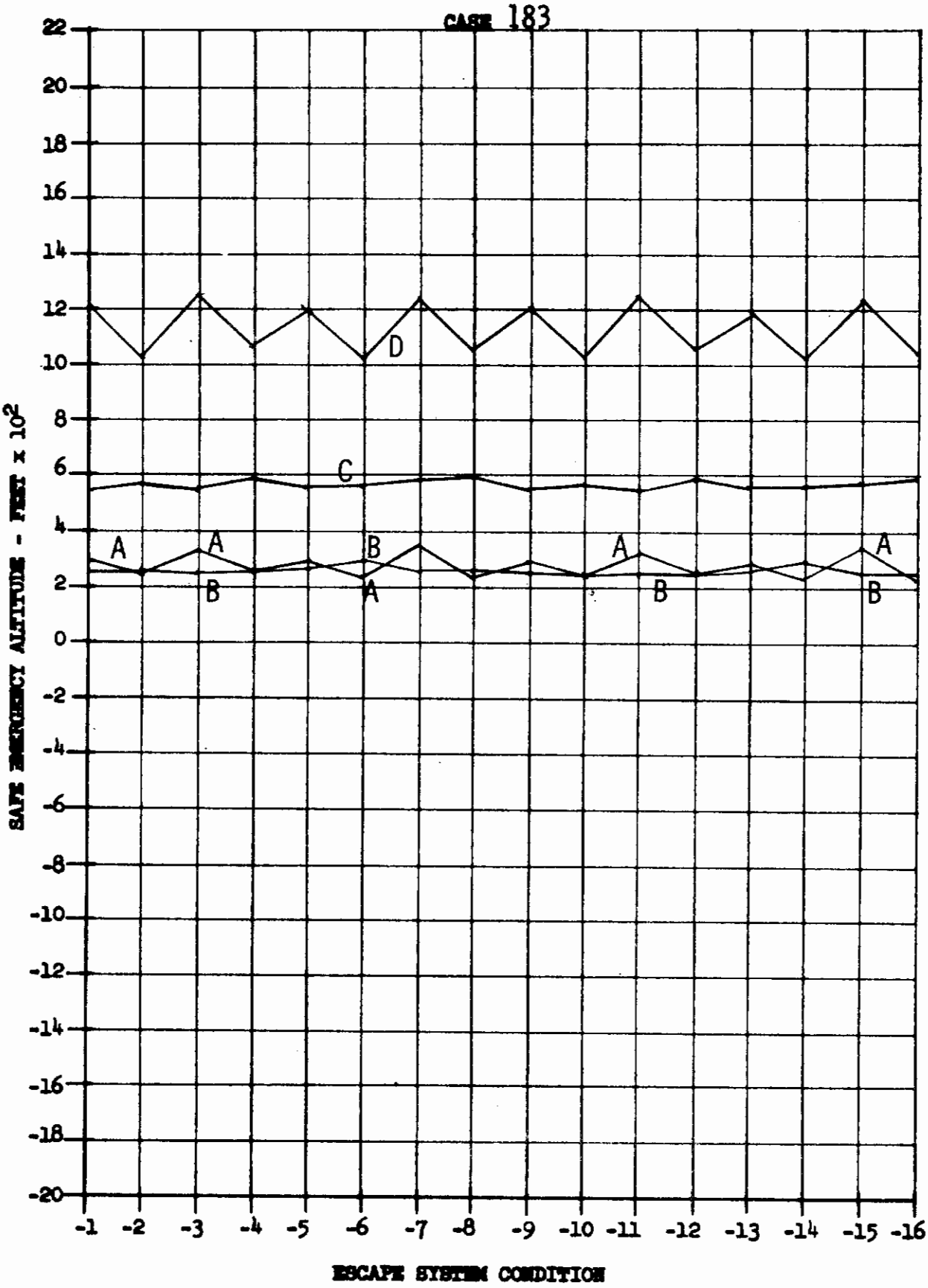

Approved for Public Release

Contrails

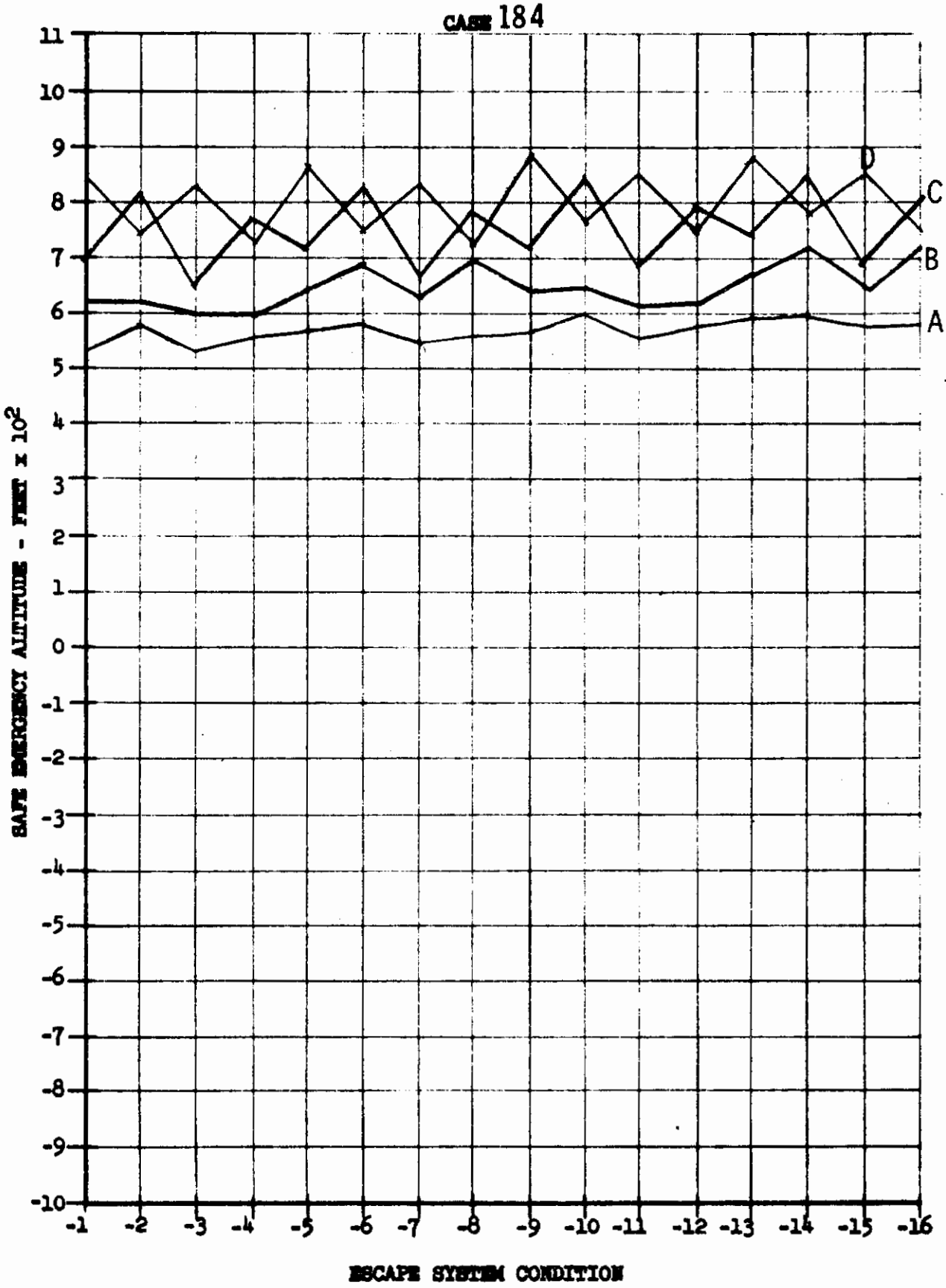

Approved for Public Release

Contrails

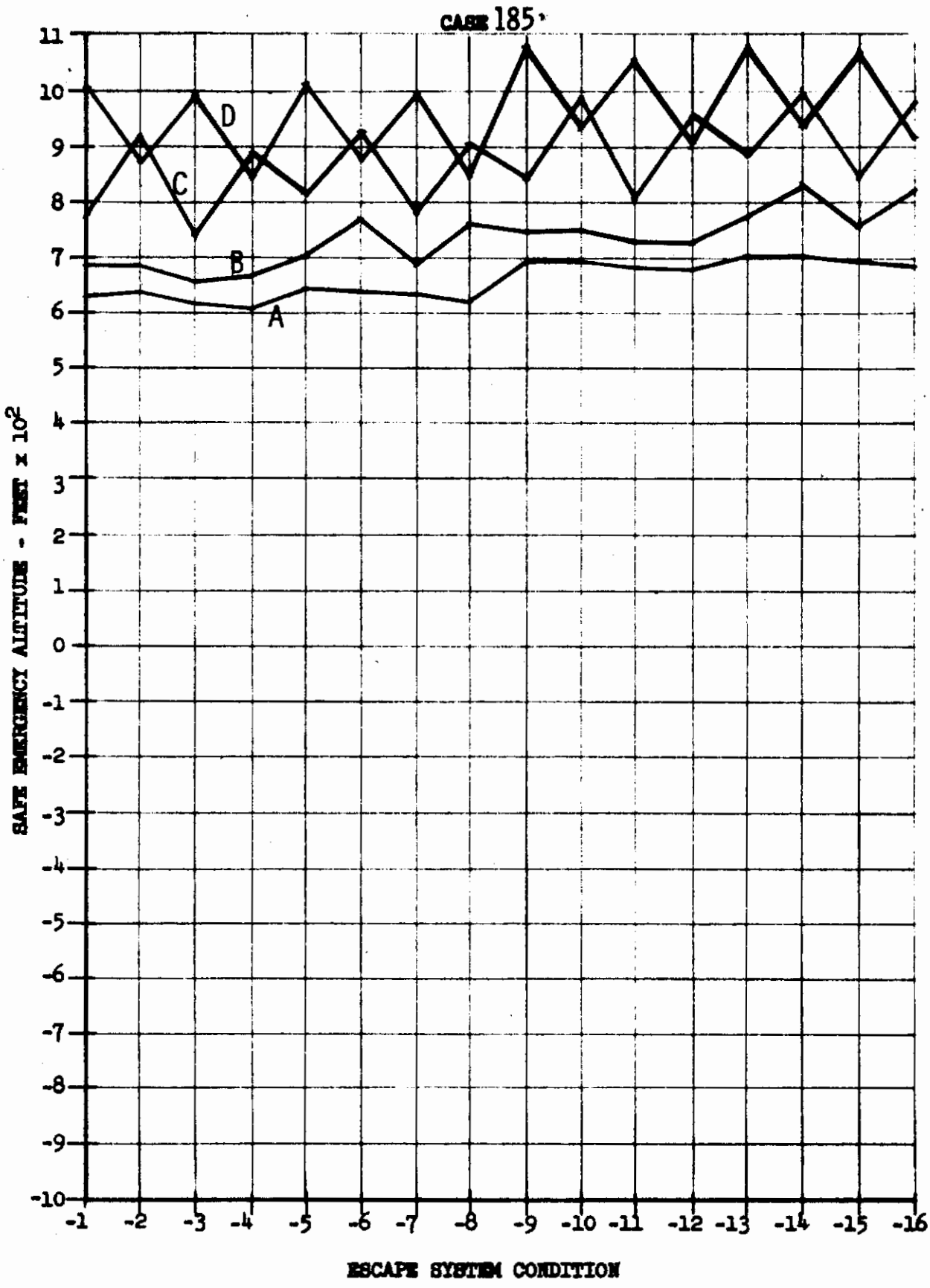

Approved for Public Release

Contrails

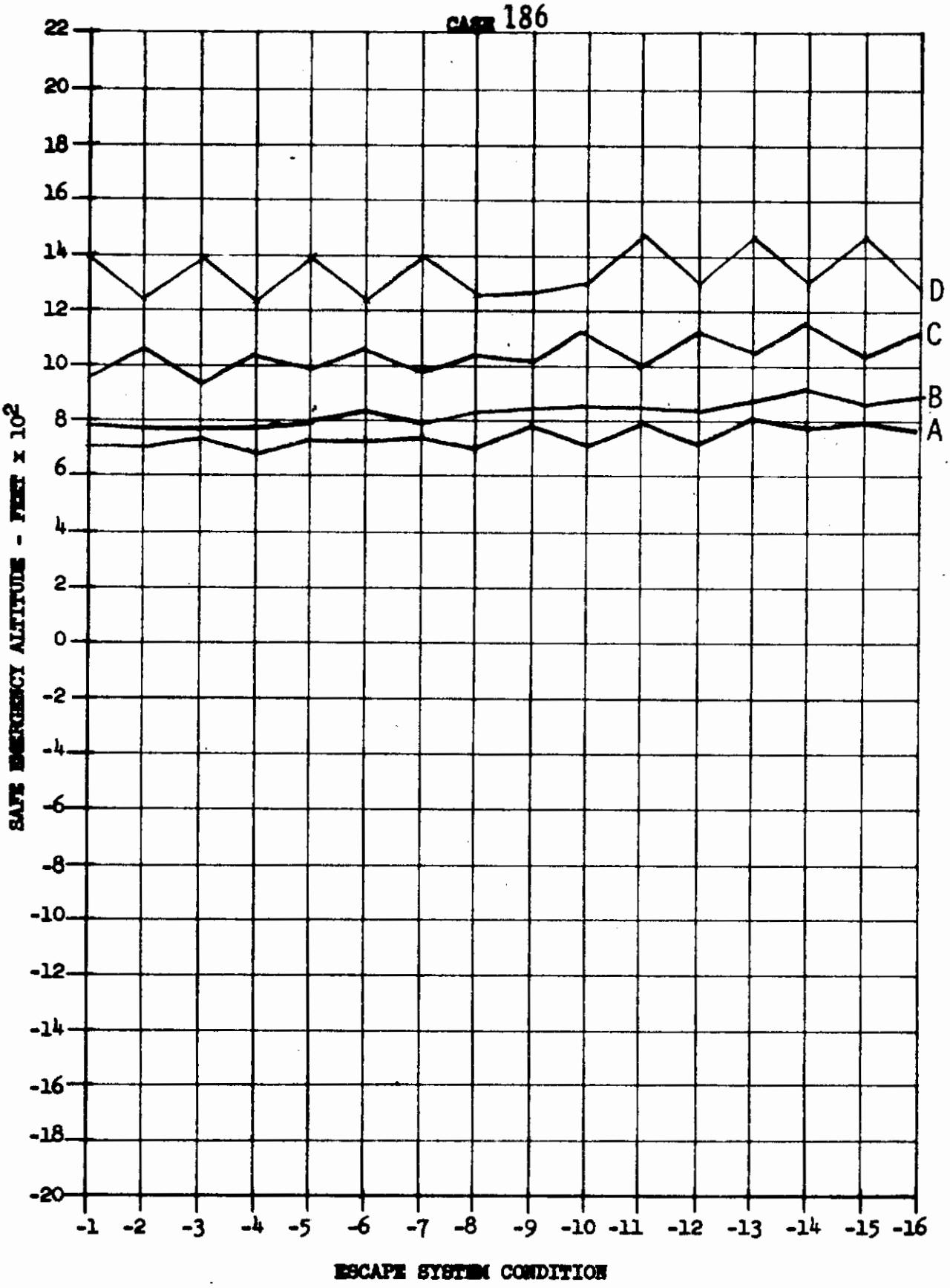

Approved for Public Release

Contrails

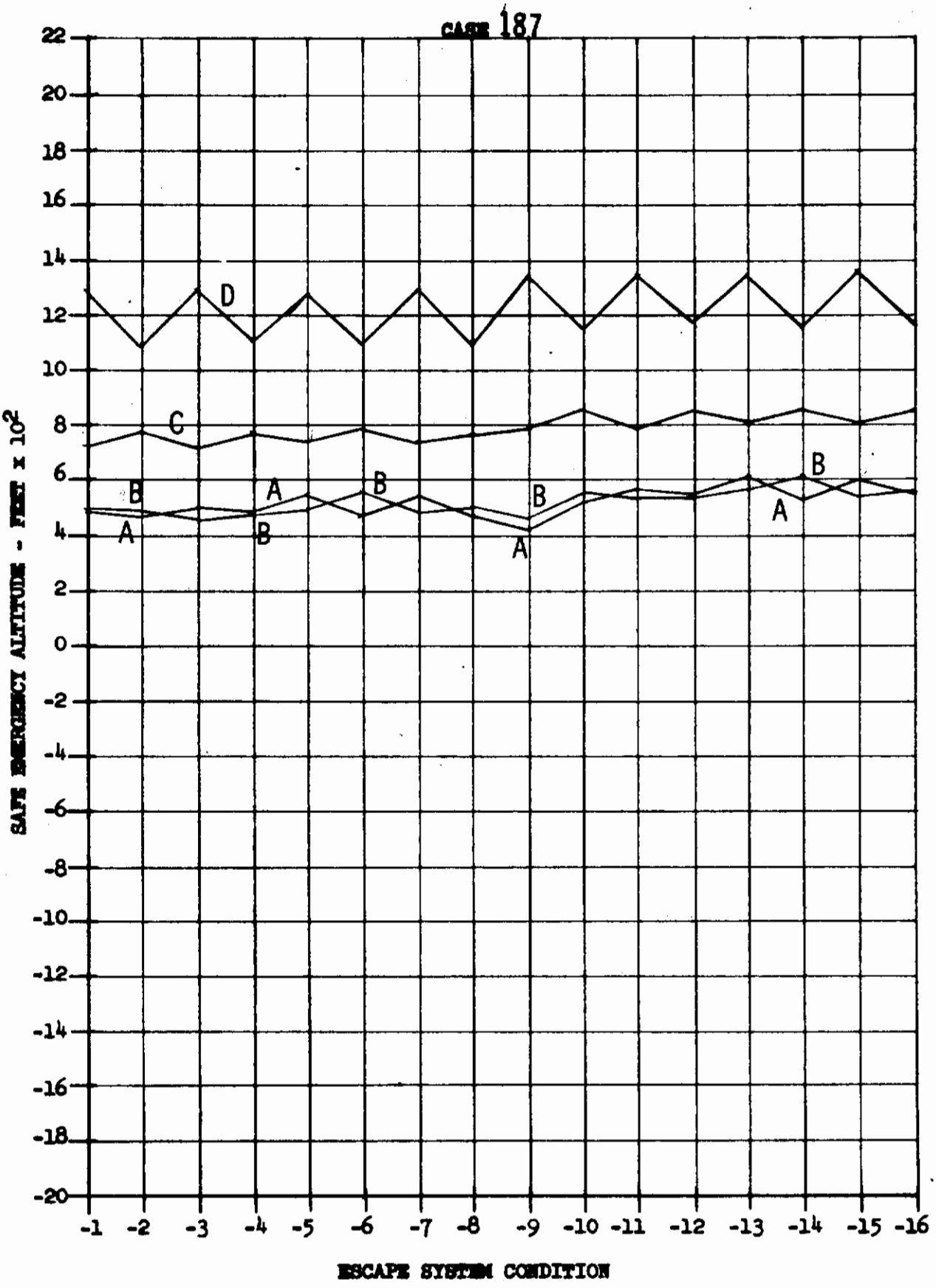

Approved for Public Release

Contrails

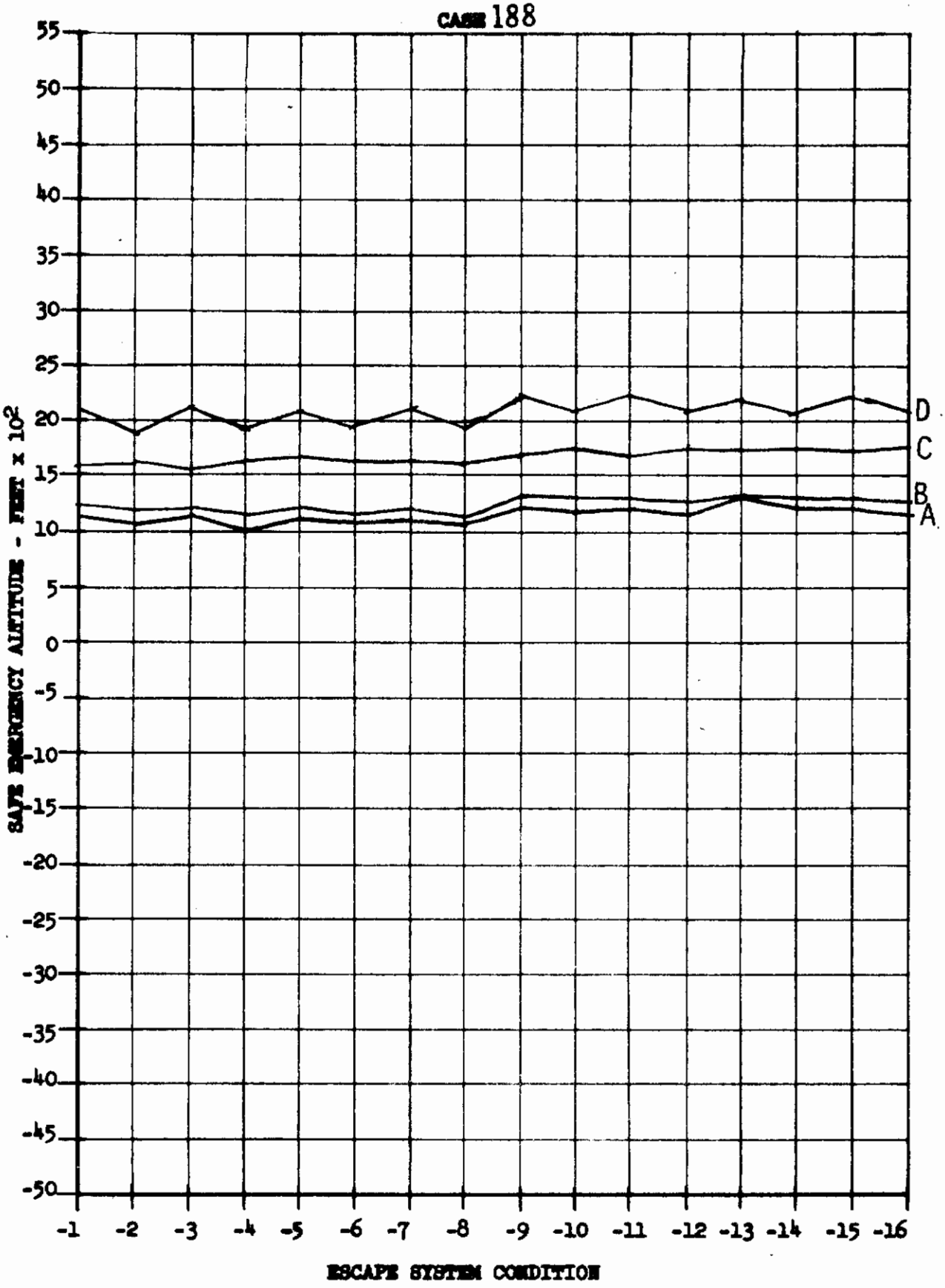

Approved for Public Release

Contrails

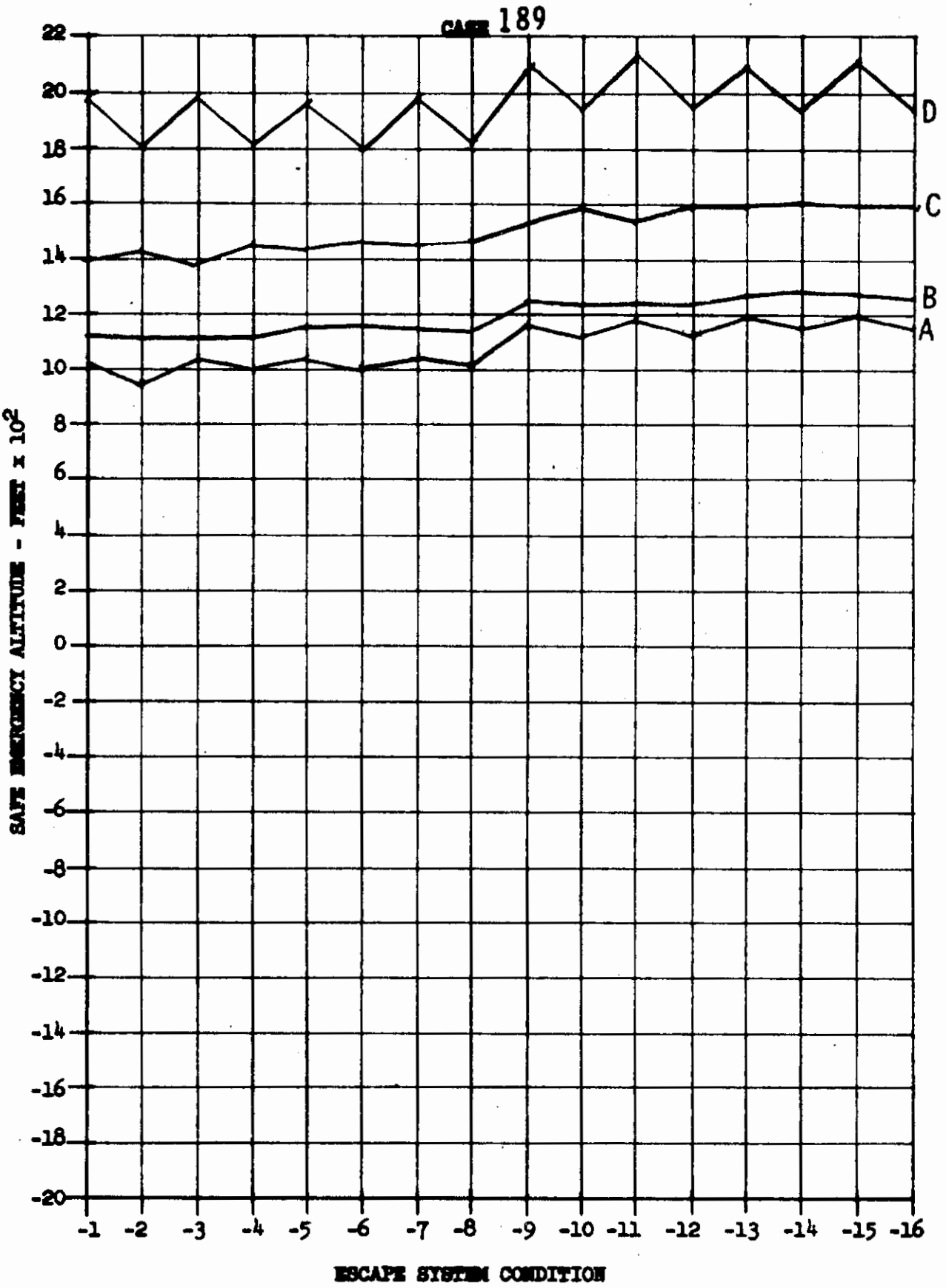

Approved for Public Release

Contrails

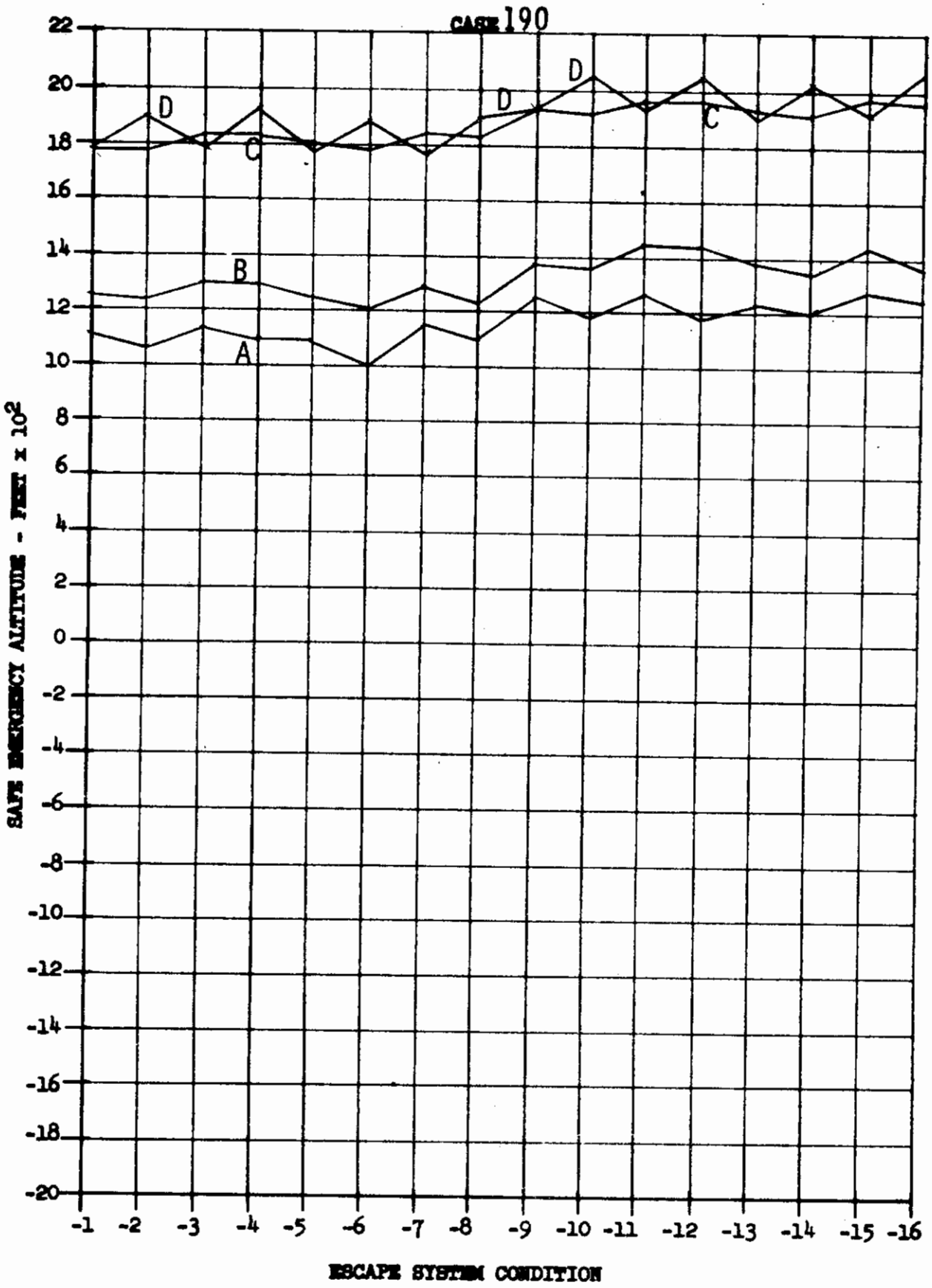

Approved for Public Release

Contrails

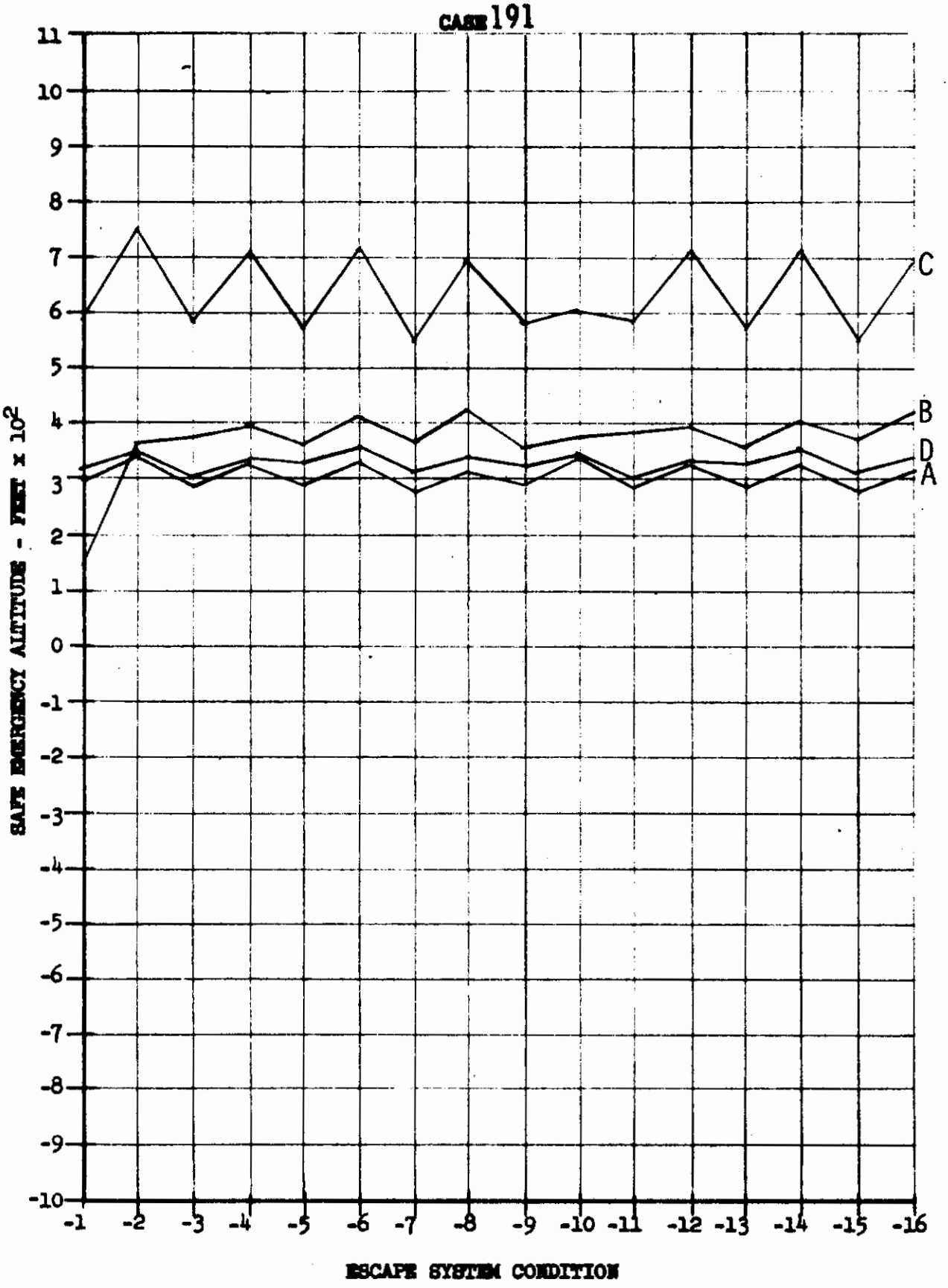

Approved for Public Release

Contrails

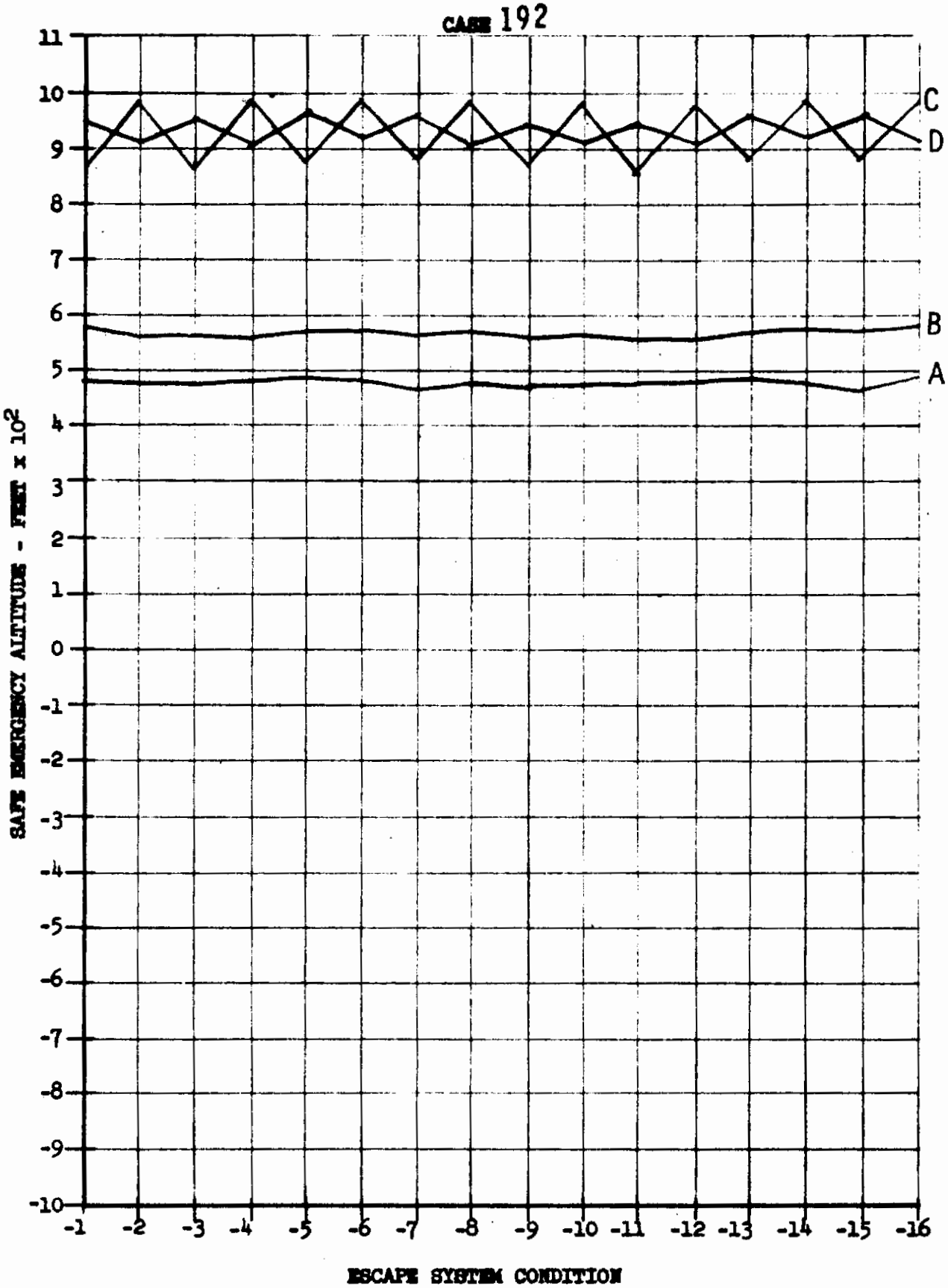

Approved for Public Release

Contrails

CASE 193

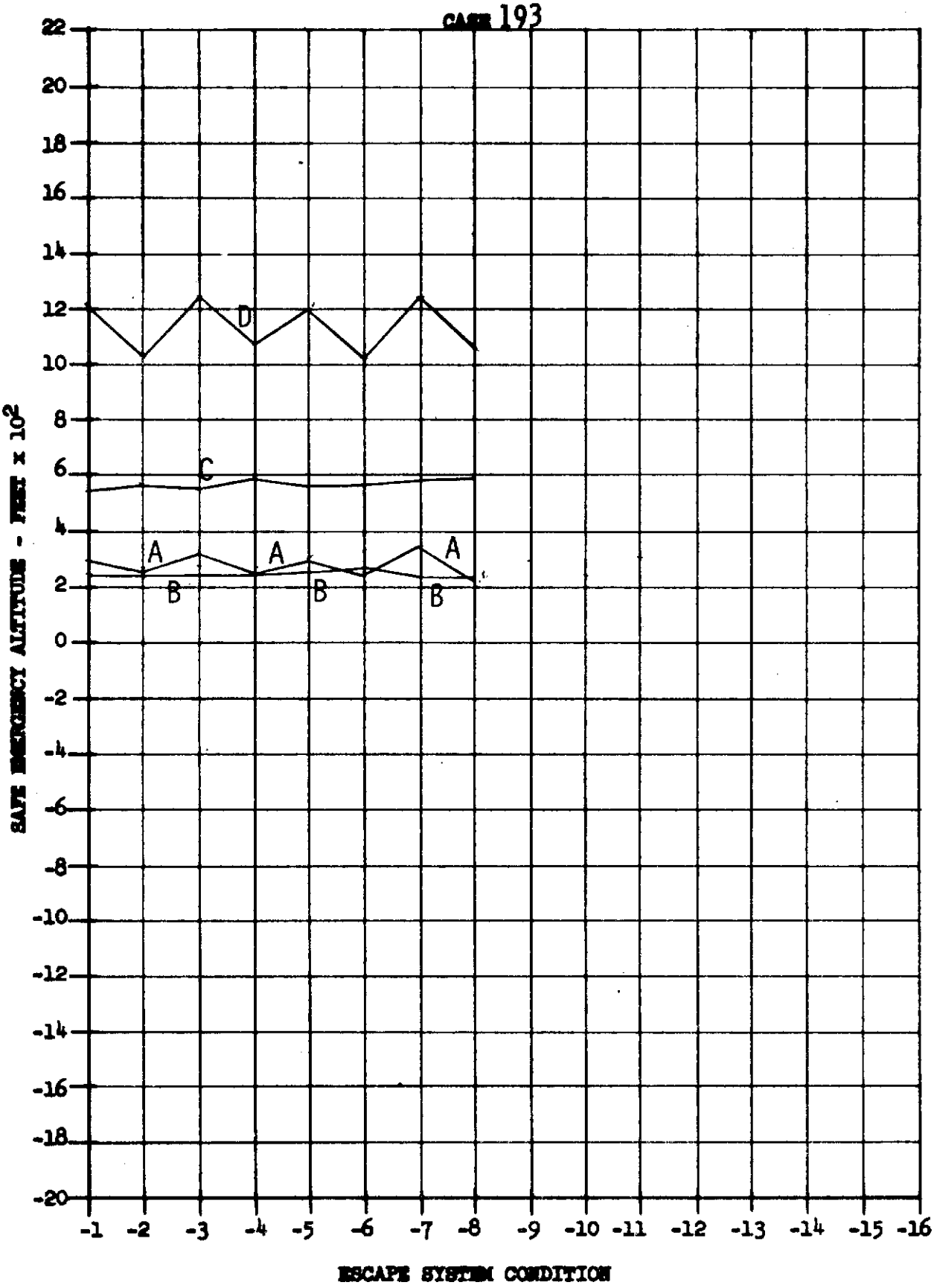

Approved for Public Release

Contrails

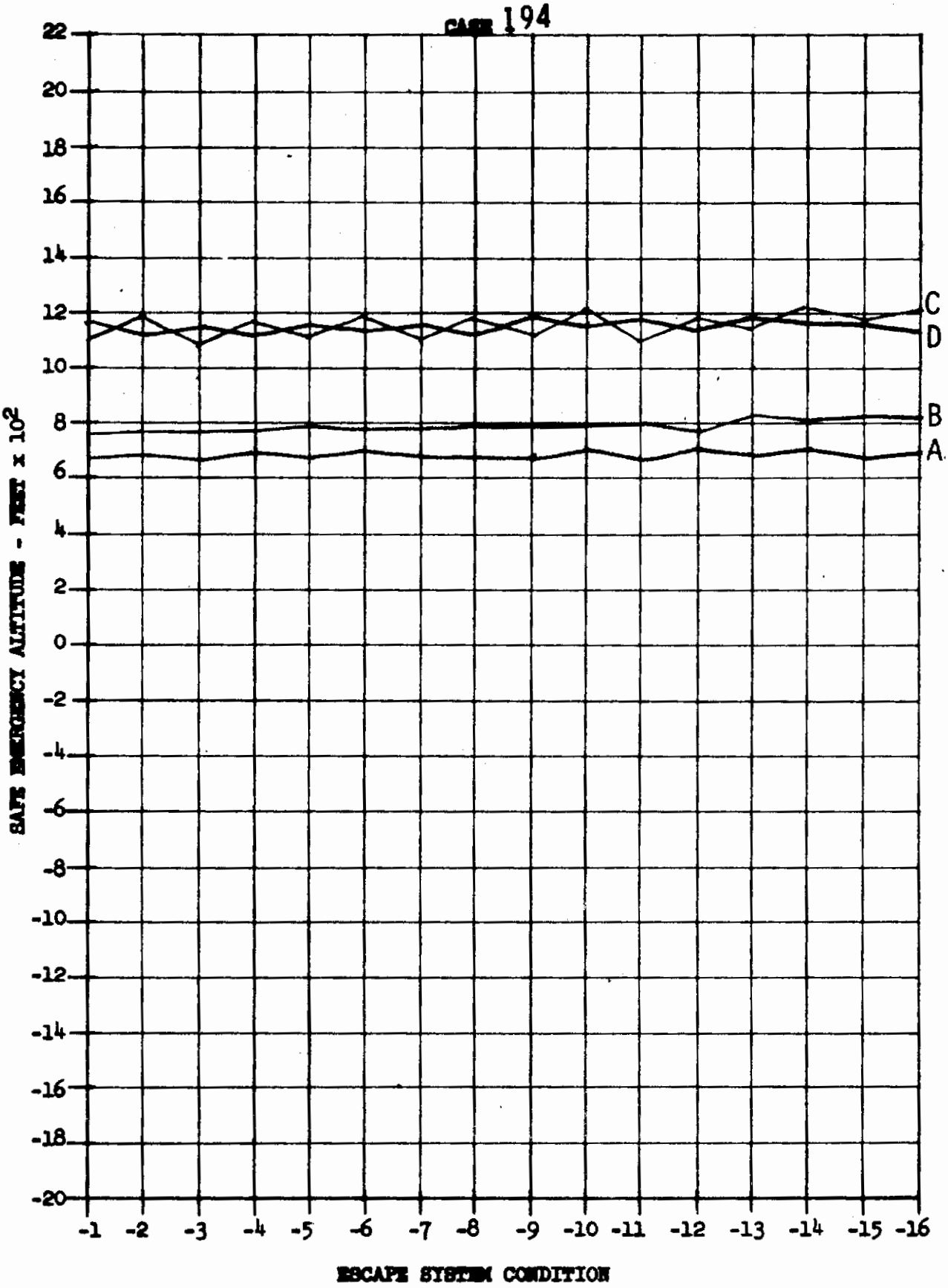

Approved for Public Release

Contrails

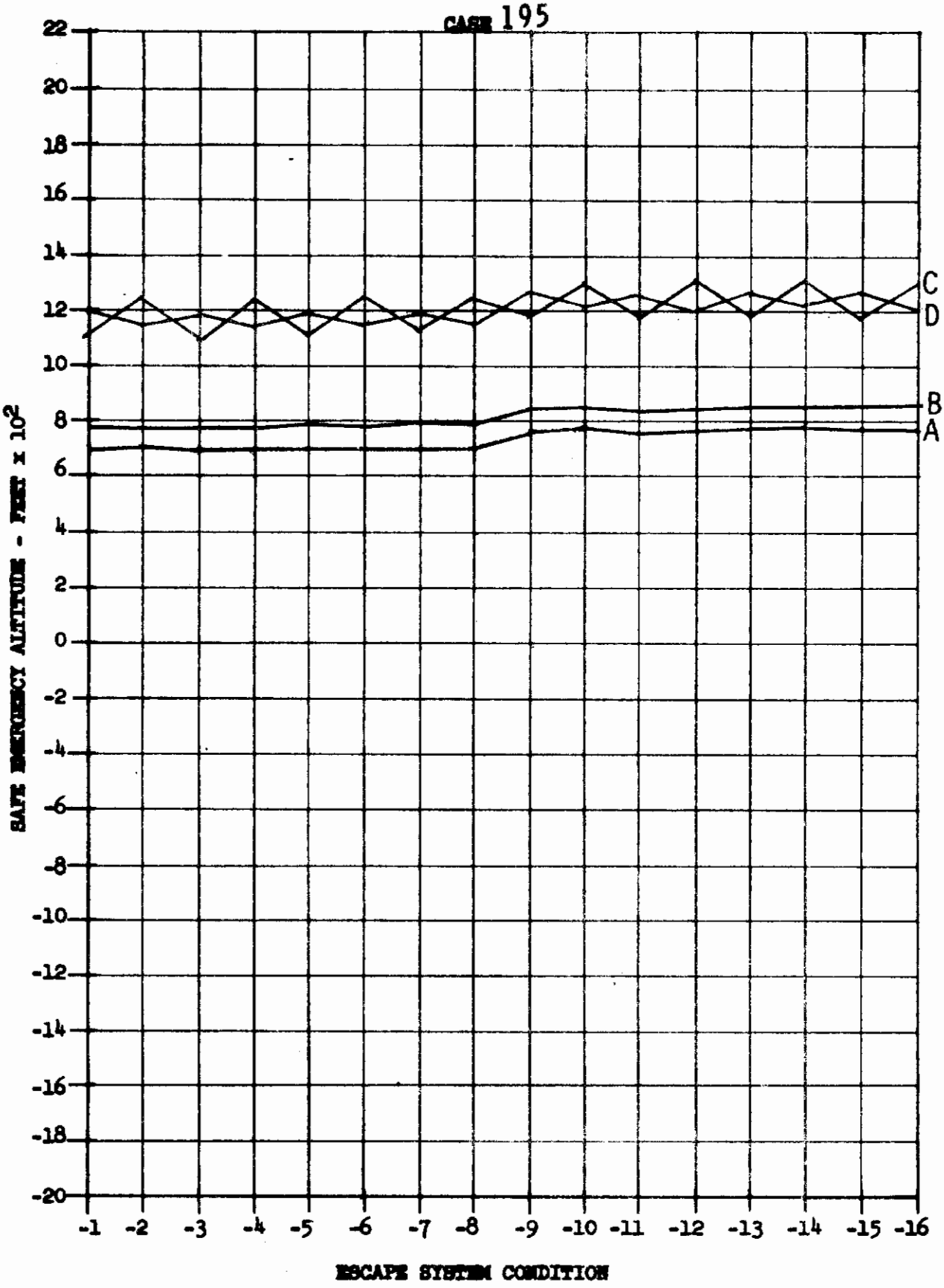

Approved for Public Release

Contrails

CASE 196

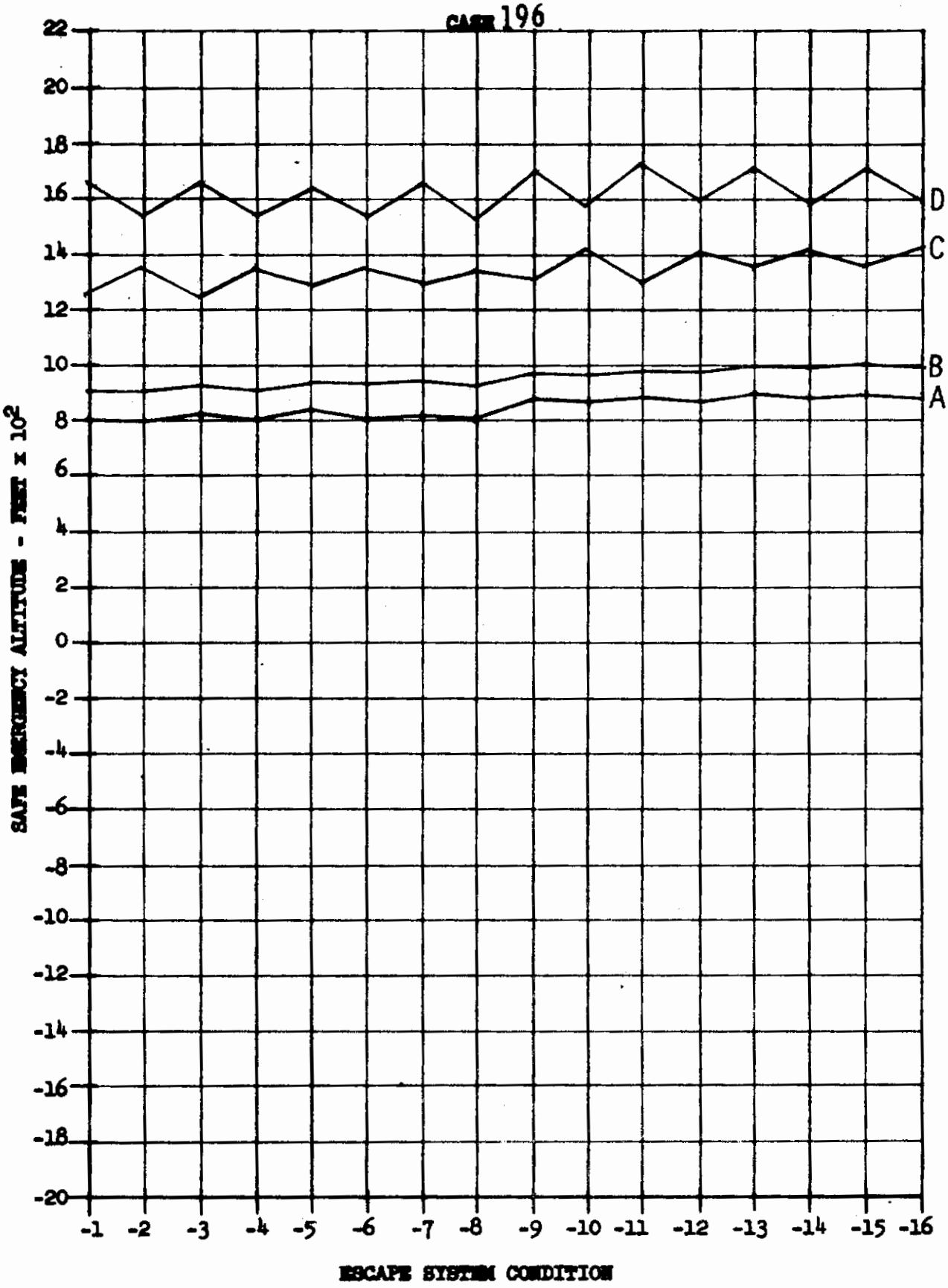

Approved for Public Release

Contrails

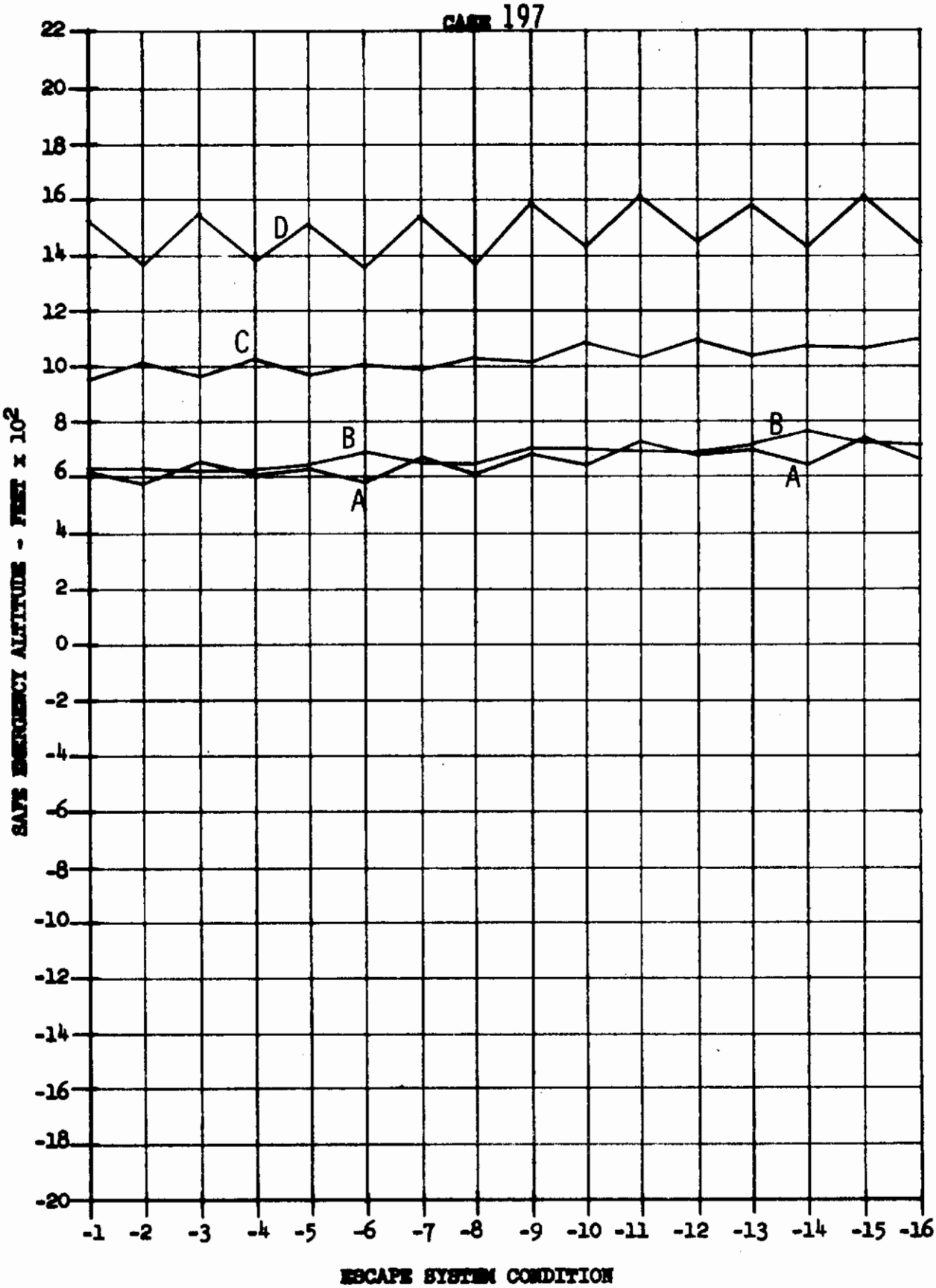

Approved for Public Release

Contrails

CASE 198

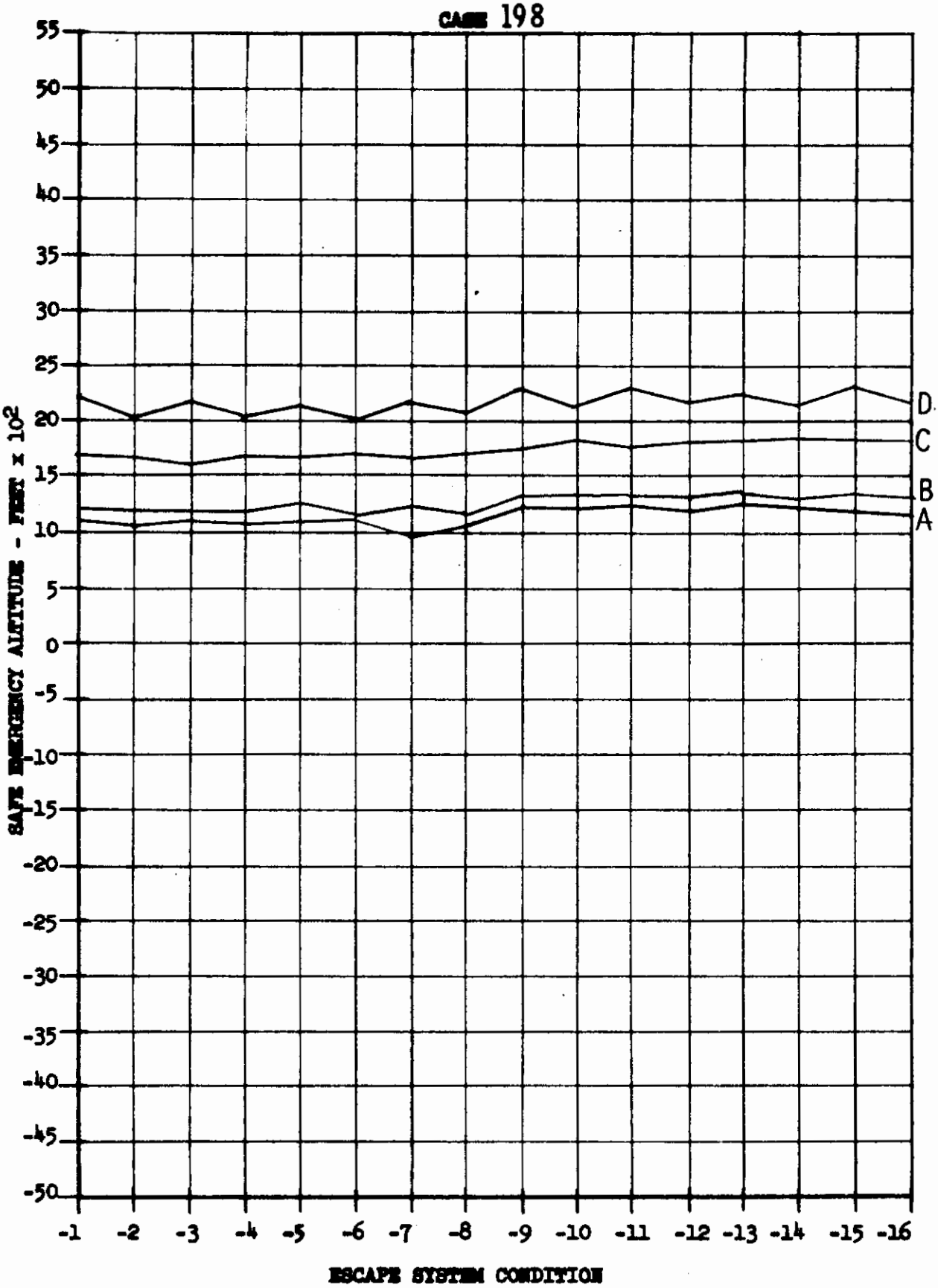

Approved for Public Release

Contrails

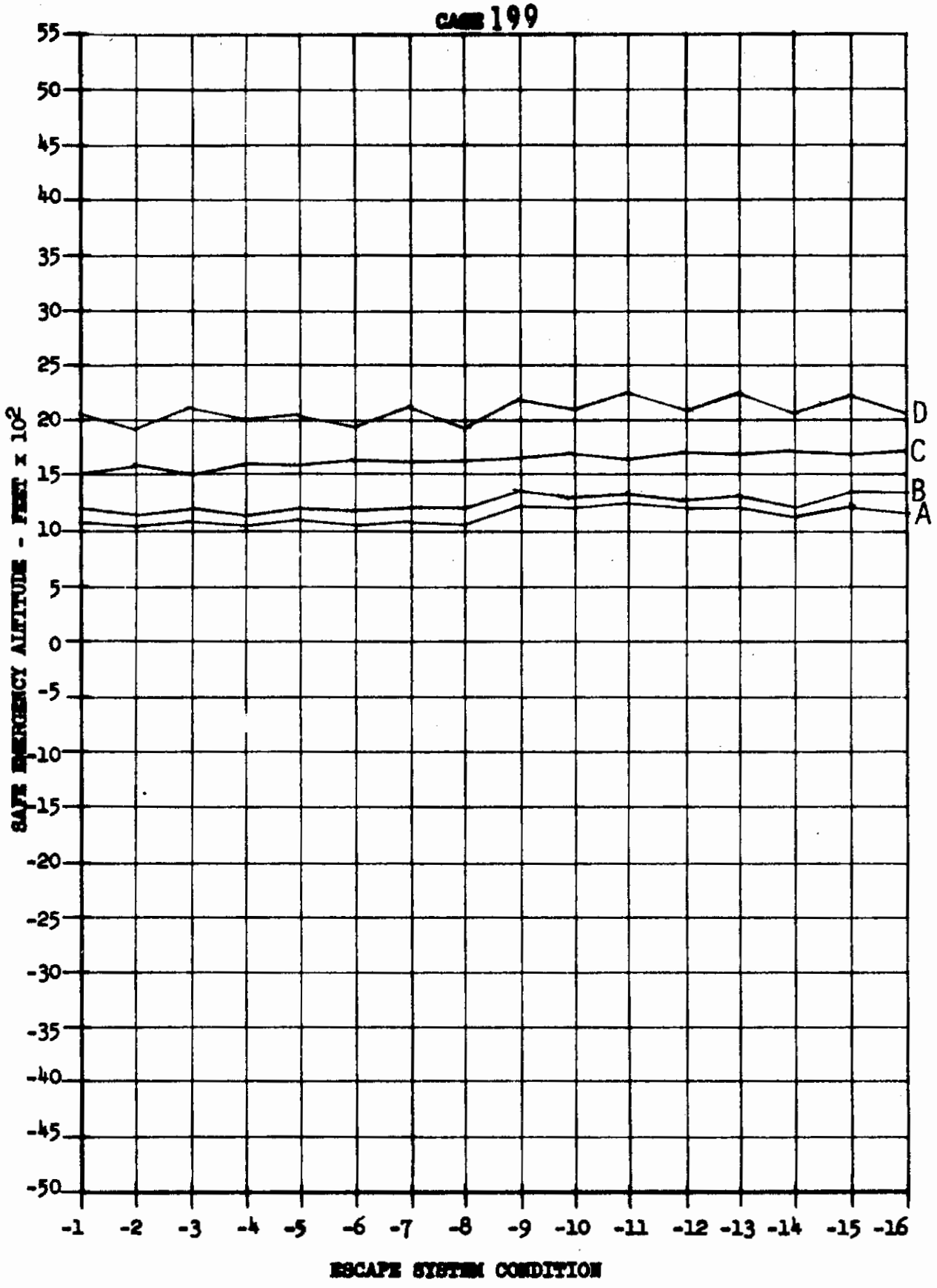

Approved for Public Release

Contrails

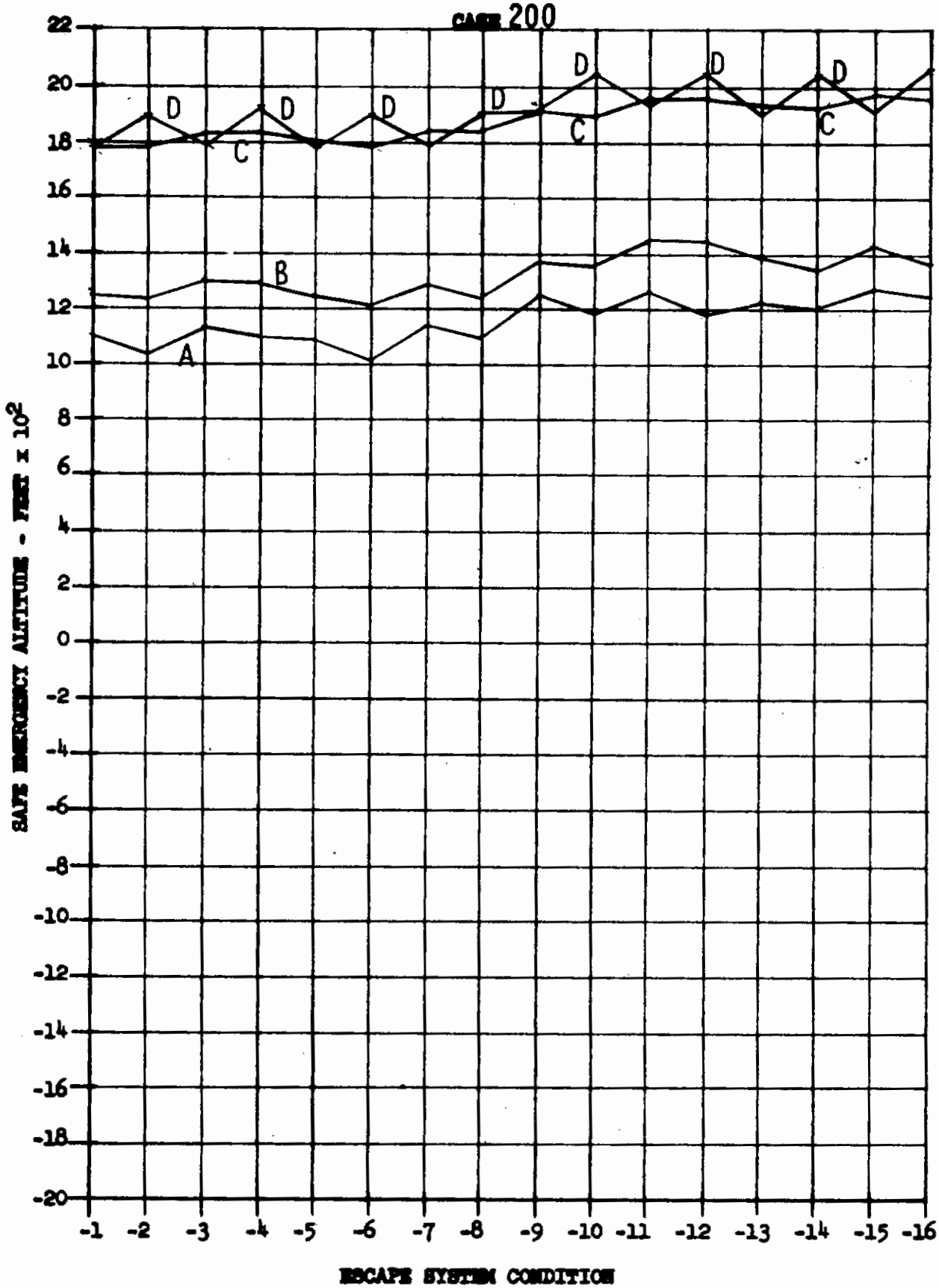

Approved for Public Release

Contrails

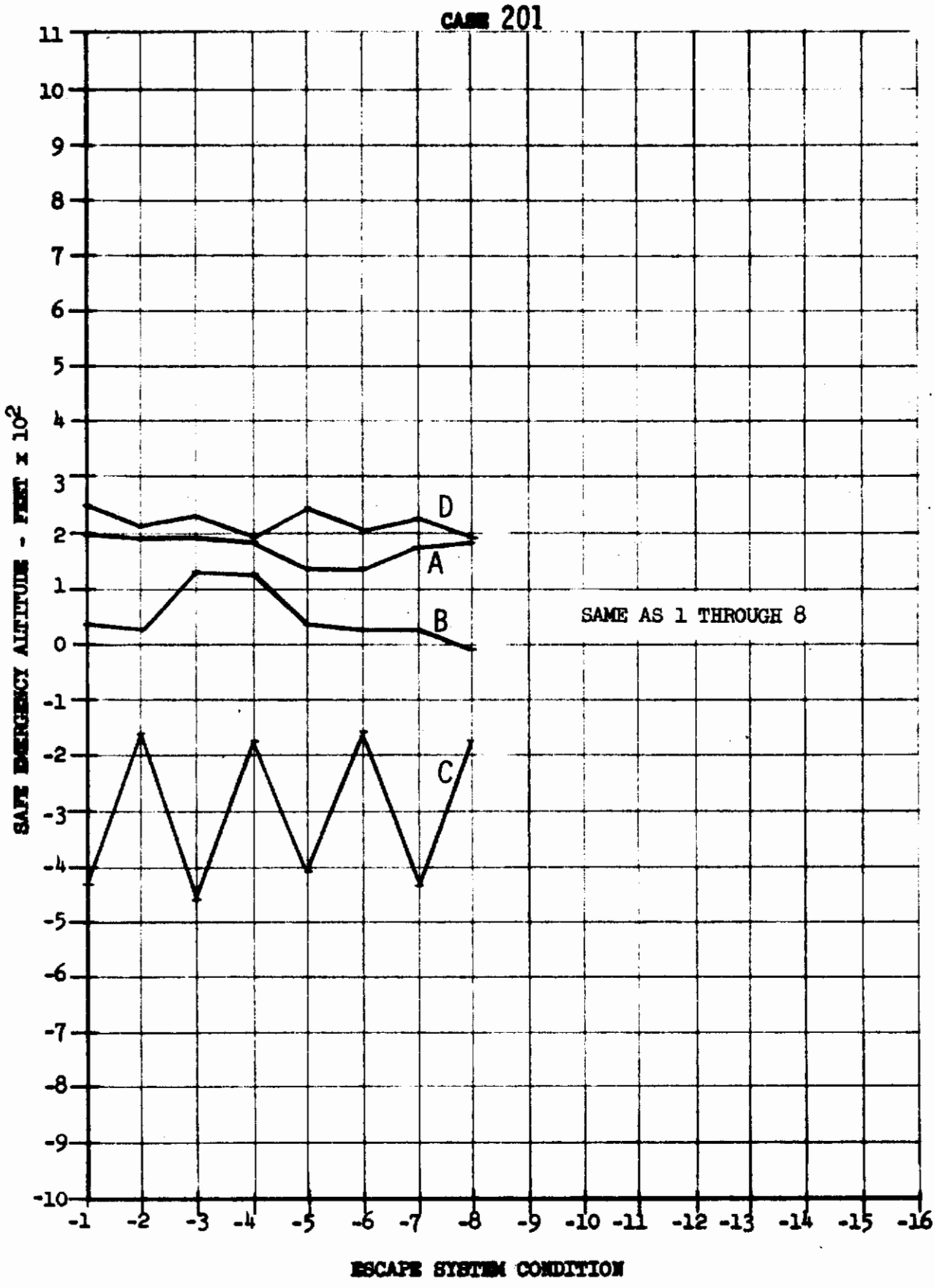

Approved for Public Release

Contrails

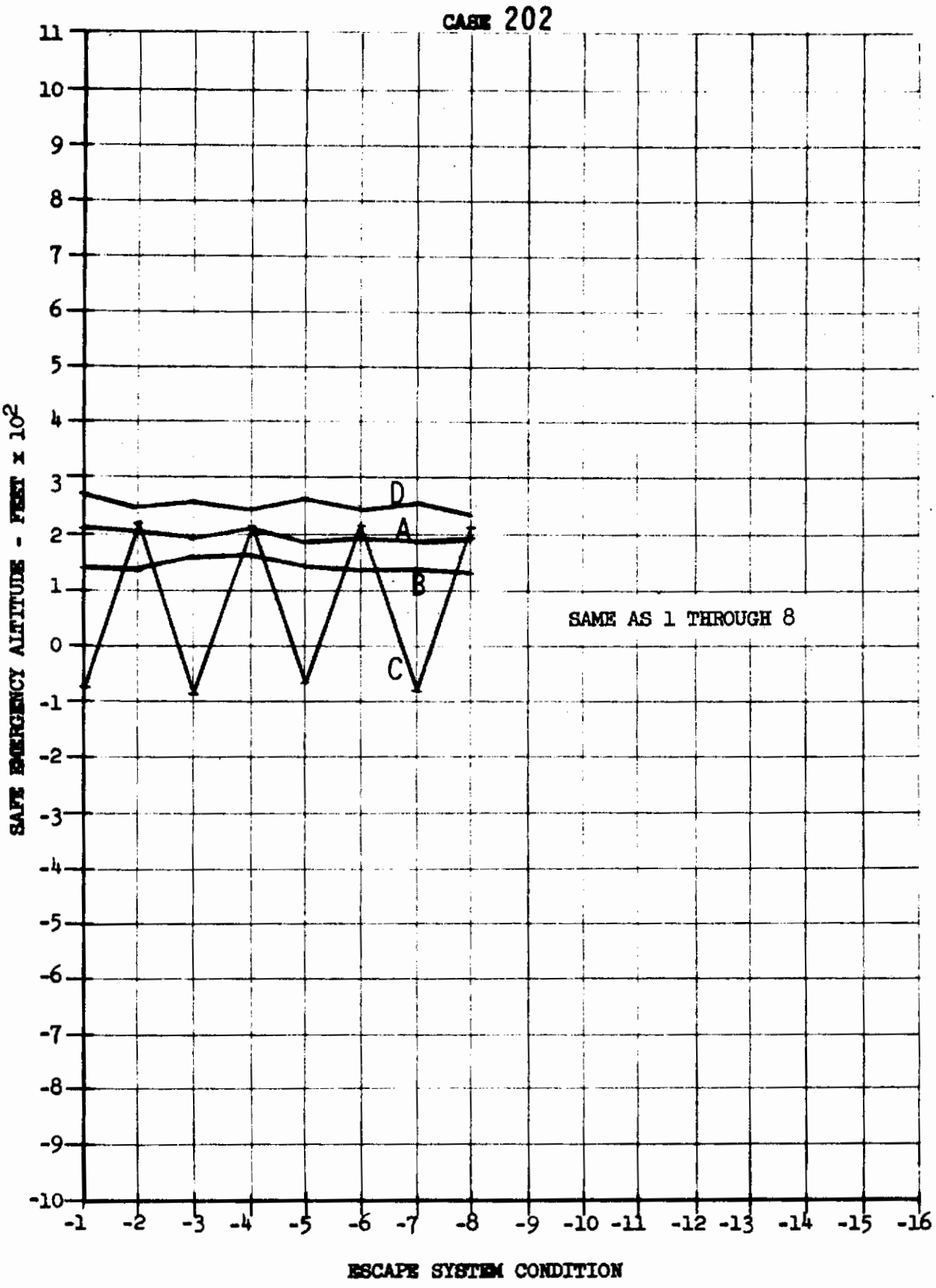

Approved for Public Release

Contrails

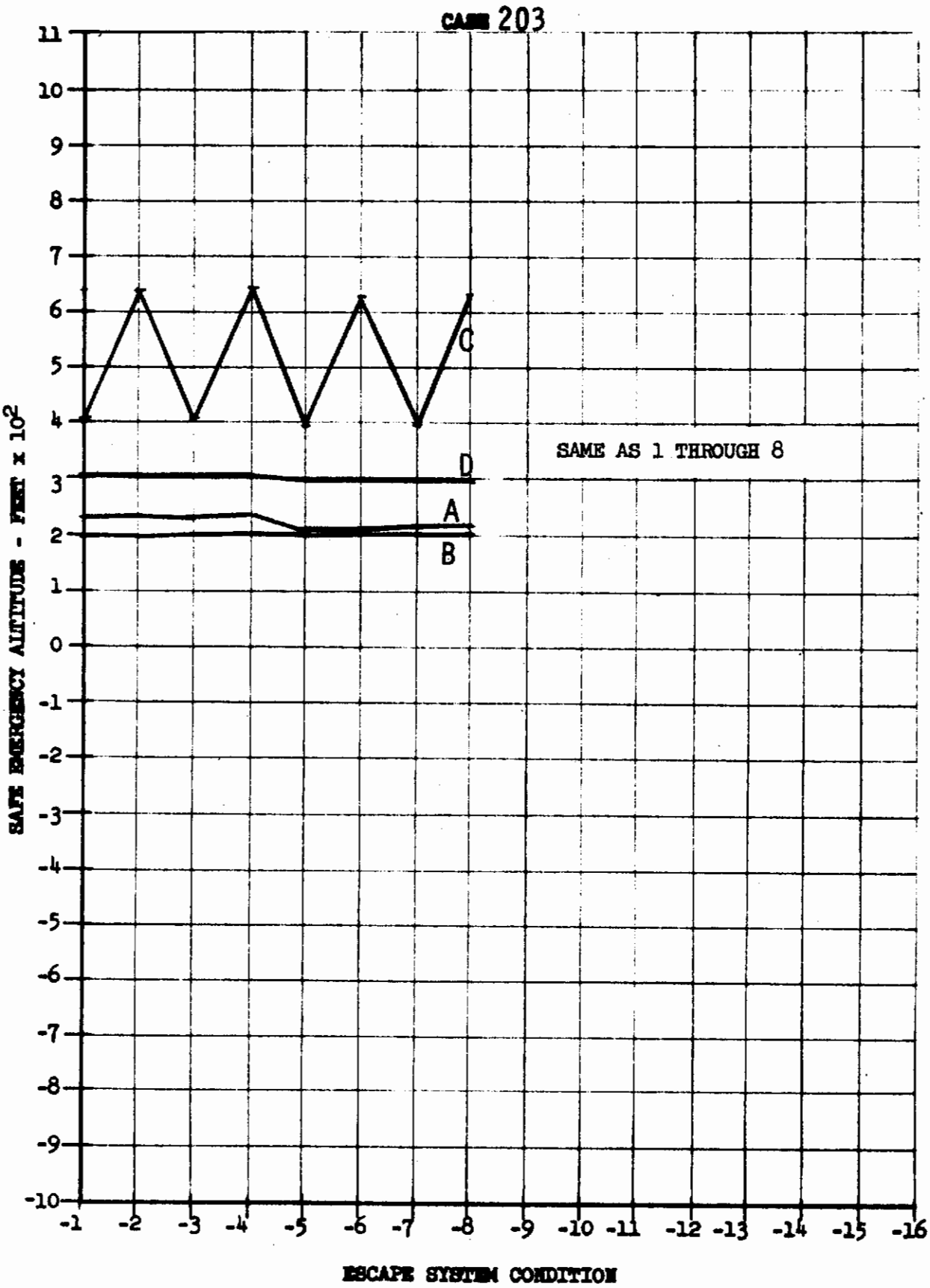

Approved for Public Release

Contrails

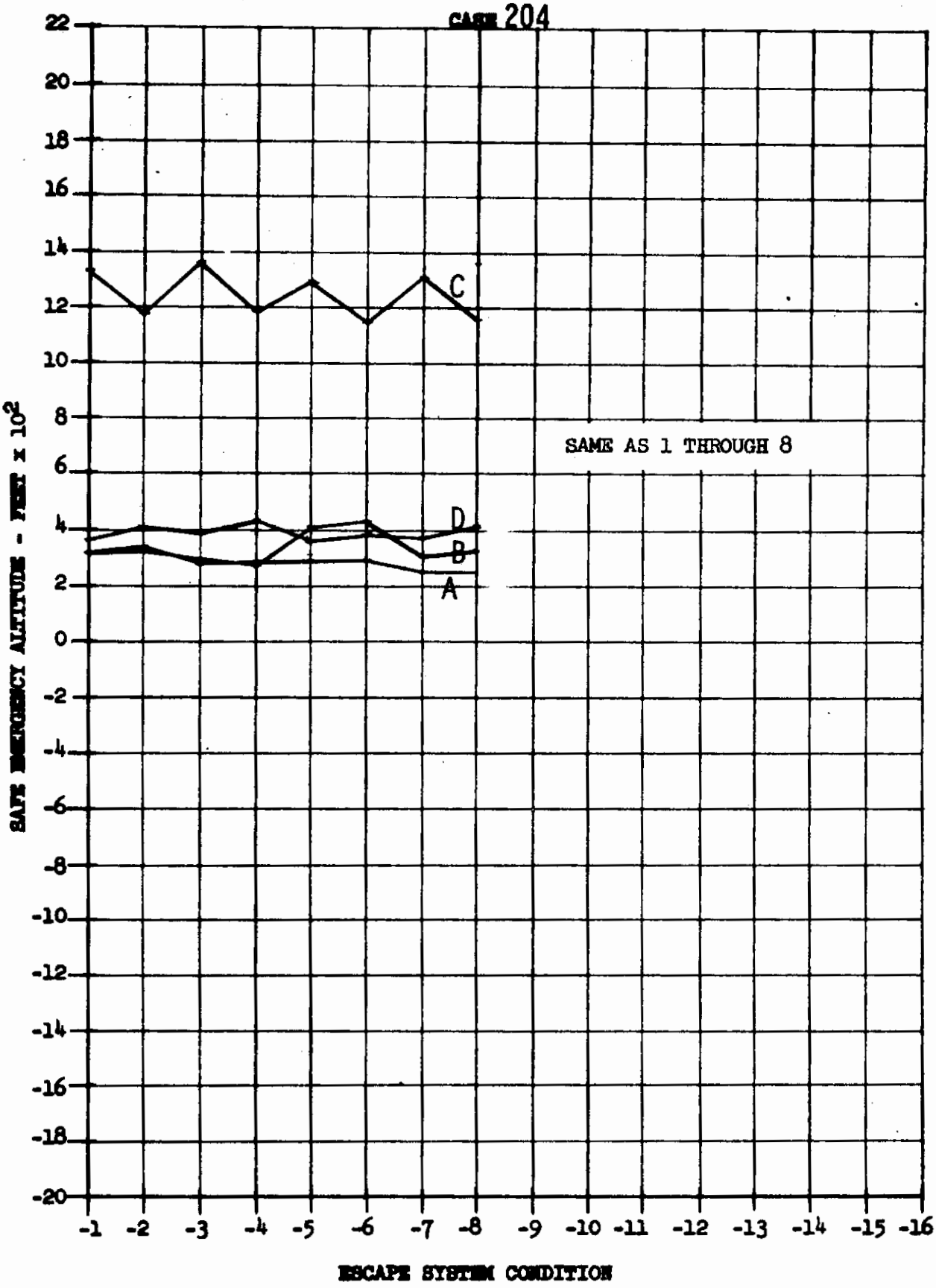

Approved for Public Release

Contrails

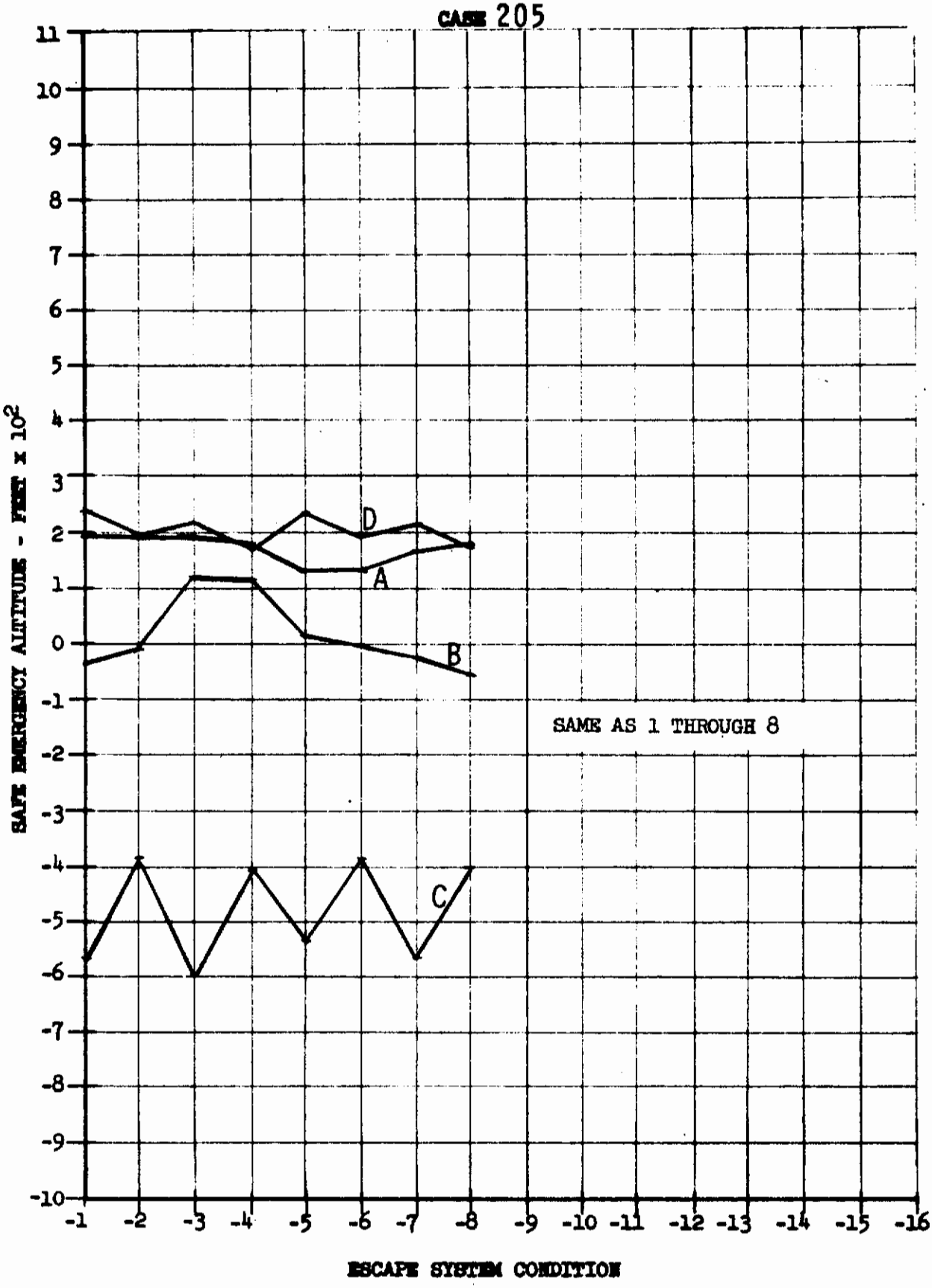

Approved for Public Release

Contrails

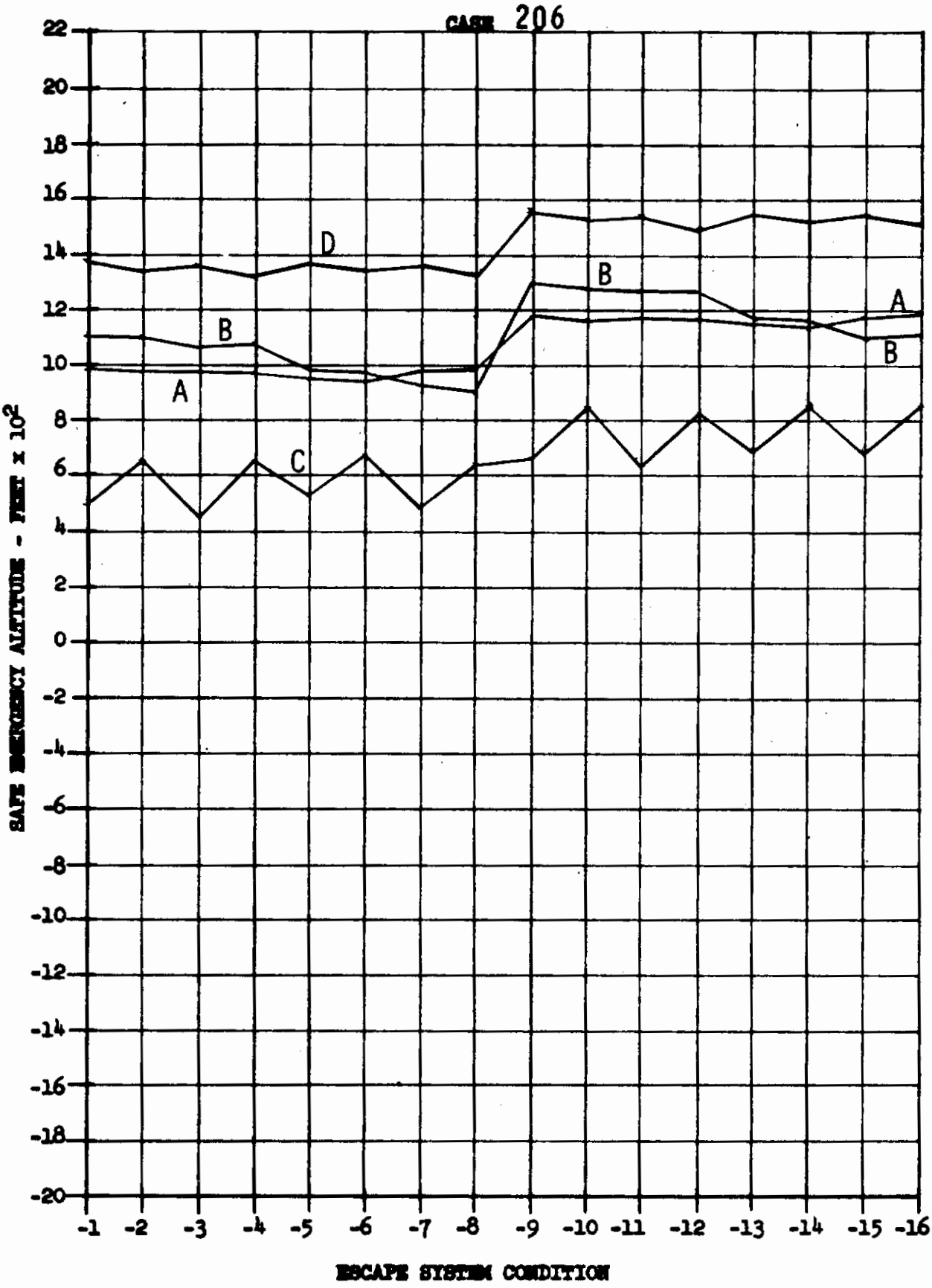

Approved for Public Release

Contrails

CASE 207

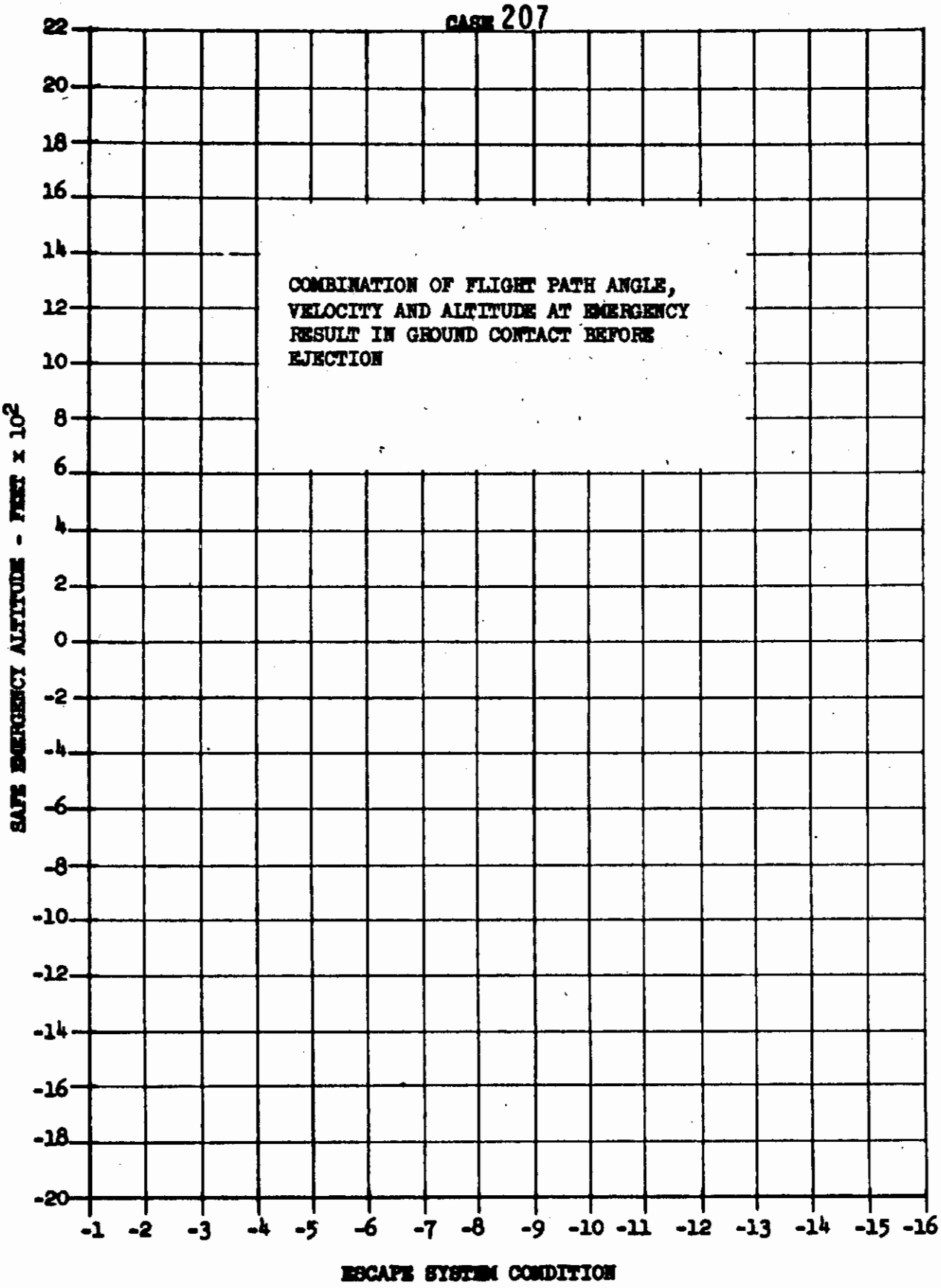

Approved for Public Release

Contrails

CASE 208

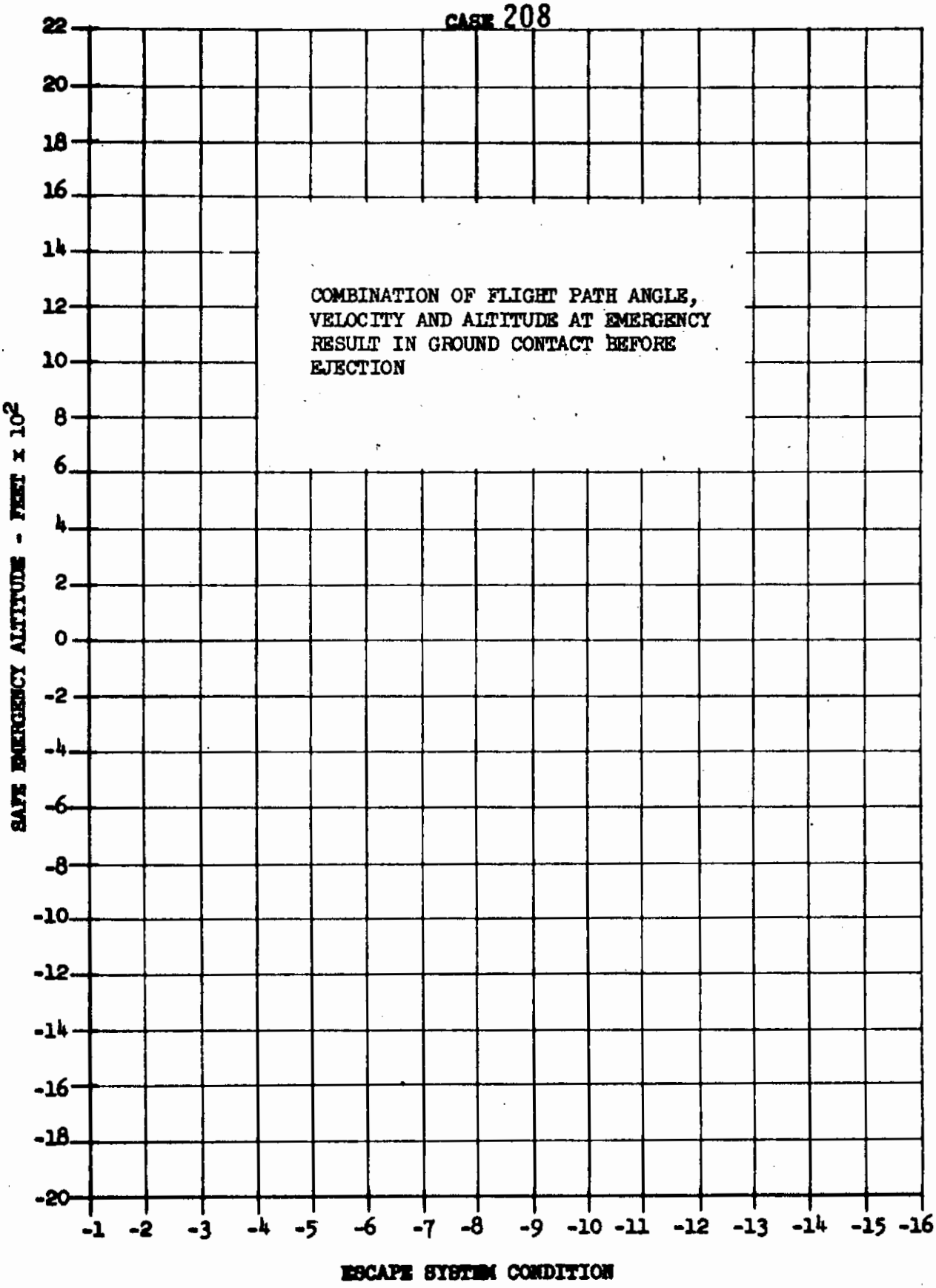

Approved for Public Release

Contrails

REFERENCES

1. Handbook of Instructions for Aircraft Design, AFSCM 80-1, Vol. I, Headquarters Air Force Systems Command, Andrews Air Force Base, Washington, D.C., 1 July 1967, (U)

2. K. E. French, "Inflation of a Parachute", AIAA Journal, Vol. I, No. 11, November 1963, (U)

3. Determination of Rocket Catapult Thrust Line for Escapac I-C-2, LB 32116, Douglas Aircraft Company, Inc., 23 February 1965. (U)

4. G. D. Horne and J. J. McDonnel, Studies to Determine Dynamic Displacement of Seat/Man Center of Gravity Due to Rocket, NAEC-ACEL-531, AD 474993, United States Naval Air Engineering Center, Philadelphia, Pennsylvania, 30 July 1965, (U)

5. E. A. Newquist and G. F. Zimmer, Development of Ejectable Nose Capsule Equipment for Feasibility Testing, ASD-TDR-62-752, Flight Dynamics Laboratory, Aeronautical Systems Division, Air Force Systems Command, Wright-Patterson Air Force Base, Ohio, January 1963, (U)

6. E. A. Newquist, M. D. Cassidy, C. W. Lindblom and P. J. Sullivan, Development of an Ejectable-Nose Escape Capsule, WADC TR 59-493, Lockheed Aircraft Corporation, Burbank, California, June 1959, (U)

7. H. H. Edwards, L. Oling and D. B. Taylor, Emergency Detection and Escape Initiation System, Part I. Liquid Propellant Boosters, ASD-TDR-62-276, Part I, Chance Vought Corporation, August 1962, (U)

8. J. F. Hegenwald, Jr. and D. W. Brown, Parametric Performance Analysis of Crew Escape Concepts in the VTOL and Conventional Takeoff and Landing Situations - Interim Technical Report, NA-66-1206, North American Rockwell Corporation, 5 November 1966, (U)

9. R. T. Smith, Transonic and Supersonic Wind Tunnel Tests on Five Percent and Twenty Percent Scale Models of the WADD Individual Escape Capsule, WADD-TN 60-79, Wright Air Development Division, Engineering Test Division, Wright-Patterson Air Force Base, Ohio, December 1960, (U)

10. R. Wendt and E. Hodder, Wind Tunnel Tests of a .25 Scale Model of an Encapsulated Seat at Mach Numbers from 0.6 to 1.4, NA-61-679, North American Rockwell Corporation, 23 June 1961, (U)

11. M. Kramer, Report on Additional Subsonic and Supersonic Wind Tunnel Tests of a 0.10 Scale Sting Mounted Ejection Seat Model for the North American (Los Angeles) 447L(X-15 Research Airplane) Weapon System, CWT-696, Southern California Cooperative Wind Tunnel, 13 January 1959, (U)

12. NAR/LAD Aerodynamic X-15 Project, Summary of Aerodynamic Development and Design of the Ejection Seat for the X-15 Research Airplane, NA-57-1455, North American Rockwell Corporation, 11 February 1958, (U)

Approved for Public Release

Contrails

13. NAR/LAD Research and Development, Low Speed Wind Tunnel Tests of a Modified 0.10 Scale Ejection Seat Model of Weapon System 447L(X-15 Research Airplane, NA-240) to Investigate the Effect of Booms, Fins, and Parachutes Upon Ejection Seat Stability, Volume I, NA-58-1660, North American Rockwell Corporation, 5 December 1958, (U)

14. N. B. Williams and O. E. Sipe, Wind Tunnel Tests of a High Speed Escape Capsule Model from M=.25 to 4.00, LAL 379, Lockheed Aircraft Corporation, 14 October 1958, (U)

15. L. M. Jenke, J. H. Jones and A. W. Myers, Force Tests on a Separable-Nose Crew Escape Capsule with Cold Flow Rocket Jet Simulation at Mach Numbers 1.5 through 6, AEDC-TR-66-74, Aro, Inc., April 1966, (U)

16. J. G. Brazier, Pilot Escape Study - Models D-558 and D-558-2, Part II High Speed Wind Tunnel Tests of 1/6 Scale Nose Section Models, E.S. 15379, ASTIA 171118, Douglas Aircraft Company, Inc., 21 September 1950, (U)

17. J. L. Hassell, Jr. and G. M. Ware, Investigation of the Low Subsonic Stability and Control Characteristics of a 0.34 Scale Free Flying Model of a Modified Half Cone Reentry Vehicle, TMX-665, National Aeronautics and Space Administration, January 1962, (U)

18. E. S. Cornett and H. L. Rubinson, Transonic Wind Tunnel Investigation of Effects of Windshield Shape and Canopy Body Combinations, RM L55G08, National Advisory Committee for Aeronautics, 20 September 1955, (U)

19. A. W. Robins, Force and Pressure Measurements on Several Canopy Fuselage Configurations at Mach Numbers 1.41 and 2.01, RM L55H23, National Advisory Committee for Aeronautics, December 1955, (U)

20. W. S. Sekscienski, Wind Tunnel Tests of a 25% Scale Model of the Glenn L. Martin Model 316 Escape Capsule, WTR 204, University of Maryland, October 1956, (U)

21. S. H. Scher and R. H. Goodwin, Wind Tunnel Investigation of the Stability of the Jettisonable Nose Section of the XS-2 Airplane, RM L8114, National Advisory Committee for Aeronautics, 14 October 1948, (U)

22. D. E. A. Reichenau, Static Stability Characteristics of the F-111 Crew Module With and Without a Stabilization Parachute at Mach Numbers of 0.5, 2.0, 2.5, 2.7, and 3.0 Phase II, AEDC-TR-65-147, ASTIA 465894, Aro, Inc., July 1965, (U)

23. D. B. Standish and R. R. Koehler, Parametric Performance Analysis of Crew Escape Concepts in the VTOL and Conventional Takeoff and Landing Situations-Computer Program Users Manual Including DART and STAPAC Subroutines, NA-67-894, North American Rockwell Corporation, 16 October 1967, (U)

24. S. G. Monroe, Parametric Performance Analysis of Crew Escape Concepts in the VTOL and Conventional Takeoff and Landing Situations-Benson-Lehner Plotting Program, NA-67-462, North American Rockwell Corporation, 22 May 1967, (U)

Approved for Public Release

Contrails

25. J. D. Mentzer and M. E. Wilfert, DART and STAPAC Computer Subroutines, DAC 33913, Douglas Aircraft Company, Inc., 17 August 1967, (U)

26. NASA Life Sciences Data Book, Webb Associates, Yellow Springs, Ohio, For Director of Aerospace Medicine, Office of Manned Space Flight Headquarters, National Aeronautics and Space Administration, June 1962, (U)

27. Handbook of Instructions for Aerospace Personnel Subsystems Designers, Part C Life Support, Chapter 13 Escape, Survival and Recovery, AFSCM 80-3 Headquarters, Air Force Systems Command, Andrews Air Force Base, Washington, D.C., 20331, Preliminary Draft Dated 15 December 1964, (U)

28. W. R. Santschi, J. DuBois and C. Omoto, Moments of Inertia and Centers of Gravity of the Living Human Body, AMRL-TDR-63-36, Aerospace Medical Division, 6570th Aerospace Medical Research Laboratories, Wright-Patterson Air Force Base, Ohio, May 1963, (U)

29. H. T. E. Hertzberg, G. S. Daniels and E. Churchill, Anthropometry of Flying Personnel - 1950, WADC-TR-52.321, Aero Medical Laboratory, Wright Air Development Center, Air Research and Development Command, USAF, Wright-Patterson Air Force Base, Ohio, September 1954, (U)

30. T. P. Lubinski and B. J. White, Feasibility Testing of the Ejectable Nose Capsule Crew Escape System ASRMDD-TM-62-41, Flight Dynamics Laboratory Aeronautical Systems Division, Air Force Systems Command USAF, Wright-Patterson Air Force Base, Ohio, April 1963, (U)

Approved for Public Release

Contrails

UNCLASSIFIED
Security Classification

DOCUMENT CONTROL DATA - R & D
(Security classification of title, body of abstract and indexing annotation must be entered when the overall report is classified)

1. ORIGINATING ACTIVITY (Corporate author)
Los Angeles Division of North American Rockwell Corp.
International Airport
Los Angeles, California 90009

2a. REPORT SECURITY CLASSIFICATION
UNCLASSIFIED

2b. GROUP

3. REPORT TITLE
PARAMETRIC PERFORMANCE ANALYSIS OF CREW ESCAPE CONCEPTS IN THE VTOL AND CONVENTIONAL TAKEOFF AND LANDING SITUATIONS

4. DESCRIPTIVE NOTES (Type of report and inclusive dates)
Final Report (August 1966 through January 1968)

5. AUTHOR(S) (First name, middle initial, last name)
Dean W. Brown and David B. Standish

6. REPORT DATE	7a. TOTAL NO. OF PAGES	7b. NO. OF REFS
January 1968	xiv & 362	30

8a. CONTRACT OR GRANT NO.
AF33(615)-5332
b. PROJECT NO.
412A
c.
d.

9a. ORIGINATOR'S REPORT NUMBER(S)
NA-67-1053

9b. OTHER REPORT NO(S) (Any other numbers that may be assigned this report)
AFFDL-TR-67-178

10. DISTRIBUTION STATEMENT
This document is subject to special export controls and each transmittal to foreign governments or foreign nationals may be made only with prior approval of the Air Force Flight Dynamics Laboratory (FDFR), Wright-Patterson Air Force Base, Ohio 45433.

11. SUPPLEMENTARY NOTES

12. SPONSORING MILITARY ACTIVITY
Air Force Flight Dynamics Laboratory
Research and Technology Division
Air Force Systems Command
Wright-Patterson Air Force Base, Ohio

13. ABSTRACT

The results of a parametric, performance analysis of four crew escape concepts are described. This analysis embodies investigation of aircraft, escape system and aerodynamic factors which influence the performance of crew escape concepts in the low altitude flight regime. A matrix of aircraft performance and maneuver conditions at the instant of emergency was developed from which representative ejection conditions were derived by allowing finite times for man-machine reactions. An existing six-degree-of-freedom computer program was modified to meet the study requirements and to conform to the Wright-Patterson Air Force Base computer and plotting system characteristics. The computer matrix consisted of 3328 ejection variations for each of the four escape concepts: A. Ejection Seat; B. Encapsulated Seat; C. Inset Capsule; and D. Nose Capsule. Of the total of 13,312 basic conditions, 1920 were conducted in three degrees of freedom and the remainder were in six degrees of freedom. The computer output consisted of both graphical and numerical data tapes. The graphical tapes were converted by a Stromberg-Carlson 4020 printer plotter, and FULFLO equipment produced cross plots of 42 output parameters for each six-degree-of-freedom run and 24 for each three-degree-of-freedom run. The numerical data tapes were analyzed by a computer program which determined the safe emergency altitude for each ejection condition and analyzed the effect of the accelerations imposed upon the crewman. A comprehensive investigation of the capabilities and limitations of the four escape concepts when subjected to the matrix ejection conditions was conducted.

This abstract is subject to special export controls and each transmittal to foreign governments or foreign nationals may be made only with the prior approval of the AF Flight Dynamics Laboratory (FDFR), Wright-Patterson AFB, Ohio.

DD FORM 1 NOV 1.5 1473

Approved for Public Release

UNCLASSIFIED
Security Classification

Contrails

14. KEY WORDS	LINK A		LINK B		LINK C	
	ROLE	WT	ROLE	WT	ROLE	WT
Crew Escape						
Ejection Seat						
Encapsulated Seat						
Escape Capsule						
VTOL Crew Escape						
Parachute Drag and Stability						
Safety Devices						

Approved for Public Release